Fluidization, Controllability and Control of Timed Continuous Petri Nets

Carlos Renato Vázquez Topete

Ph.D. THESIS

Advisor: Manuel Silva Suárez

Departamento de Informática e Ingeniería de Sistemas
Centro Politécnico Superior
Universidad de Zaragoza

April 2011

Resumen

En la literatura puede encontrarse una gran cantidad de resultados para el análisis de sistemas de eventos discretos utilizando modelos del paradigma de las redes de Petri (PN). Entre las aplicaciones se cuentan la validación en desarrollo de software, la implantación de controladores secuenciales, el análisis de protocolos de comunicación, de sistemas de manufactura, de cadenas de suministro, etc.

Una de las limitaciones más importantes en el análisis de sistemas de eventos discretos es la complejidad computacional que puede aparecer. En redes de Petri, tal complejidad se puede deber a una red (estructura) de gran tamaño, un marcado (población) grande y a la interconexión entre los nodos de la red. Frecuentemente, el conjunto de estados alcanzables de una red crece exponencialmente con respecto al marcado inicial, lo que es conocido como el problema de *explosión de estados*, haciendo prohibitivo el uso de técnicas de análisis por enumeración incluso para sistemas con estructuras pequeñas. Para evitar dicho problema, en la literatura se ha propuesto el análisis de sistemas de eventos discretos (y en particular de redes de Petri) por medio de modelos continuos que aproximan el comportamiento de los sistemas de eventos discretos originales. Este enfoque es conocido como *fluidificación*.

Este trabajo de Tesis concierne el estudio de redes de Petri continuas temporizadas (TCPN) bajo semántica de servidores infinitos, que han sido definidas como una aproximación potencial de redes de Petri estocásticas bajo una interpretación Markoviana. Las razones para esta selección son que las redes de Petri Markovianas (MPN, donde las transiciones disparan con retardos exponenciales y los conflictos se resuelven con política de carrera) tienen la propiedad de amnesia (por lo que el marcado representa toda la información necesaria para la futura evolución del sistema), y a que el análisis exacto, por medio de la Cadena de Markov isomorfa al grafo de alcanzabilidad, implica frecuentemente una complejidad computacional intratable, debido al problema de explosión de estados antes mencionado.

El uso de TCPNs, para el análisis de las correspondientes MPNs, está condicionado a la preservación de las propiedades bajo estudio, lo cual no siempre ocurre. Por otro lado, si una MPN admite una fluidificación razonable, el uso de modelos continuos conlleva una ventaja muy interesante: la posibilidad de aplicar técnicas y conceptos desarrollados en la Teoría de Control para sistemas continuos. Por ejemplo, la aplicación de técnicas para el análisis y síntesis de controladores que rechacen perturbaciones, para el análisis de la estabilidad, la observabilidad, etc. De esta forma, la fluidificación representa un puente entre unas clases particulares de sistemas de estados continuos y de eventos discretos.

En este trabajo se investigan algunos temas sobre el modelo TCPN. Primero, se aborda la aproximación que este modelo provee del comportamiento esperado de la red discreta estocástica original. Después, se considera la conexión entre vivacidad, acotación y temporización en las TCPNs. Mas adelante se analiza la controlabilidad de estos sistemas y se proponen tres estructuras de control diferentes. Finalmente, se describe como se pueden implantar dichos controladores en los modelos de red de Petri discretos originales.

Contents

Introduction . . . 1

1. Basic concepts and notation . . . 9
1.1 Basic notation . . . 9
1.2 Basic concepts on P/T net systems . . . 9
1.3 Markovian Petri nets . . . 12
1.4 Continuous and timed continuous Petri nets . . . 14
1.5 Properties of continuous PNs . . . 19
1.6 Basic concepts on continuous-state dynamic systems . . . 21

2. Fluidization . . . 25
2.1 Continuous PNs as relaxations of Markovian models . . . 25
2.2 On the approximation of MPNs by TCPNs: deterministic approximation . . . 26
2.3 Continuous models with noise: improving the approximation . . . 31
2.4 Approximation by partially relaxed models: Markovian hybrid Petri nets . . . 39
2.5 Improving by modifying the structure and semantics . . . 49
2.6 Conclusions on fluidization . . . 53

3. Timing-dependent properties . . . 55
3.1 Structural boundedness and repetitiveness in untimed Petri nets: discrete *vs* continuous . . . 56
3.2 Timing-dependent boundedness and repetitiveness in timed continuous PNs . . . 58
3.3 Existence of $\mathbf{w}$ and $\mathbf{v}$ for boundedness and repetitiveness . . . 59
3.4 Timing-dependent liveness: setting the problem . . . 66
3.5 Timing to avoid non-live markings . . . 70
3.6 Computing a timing for λ-Ct and λ-Cv . . . 76
3.7 Conclusions on timing-dependent properties . . . 81

4. Controllability . . . 83
4.1 Introduction . . . 83
4.2 State invariant and equilibrium sets . . . 86
4.3 Controllability definition . . . 88
4.4 Controllability if all the transitions are controllable . . . 89
4.5 Controllability with uncontrollable transitions . . . 92
4.6 Conclusions on controllability . . . 105

5. Control synthesis . . . 107
5.1 Preliminarily discussion of control methods found in the literature . . . 108
5.2 Affine control laws for TCPNs . . . 113
5.3 Coordinated control . . . 118
5.4 Pole-assignment centralized control for systems with uncontrollable transitions . . . 126
5.5 Conclusions on control laws . . . 135

6. Towards control applications in discrete systems . . . 137
6.1 Implementation of control laws for MPNs via TCPNs . . . 138
6.2 A stock level-control example . . . 143
6.3 Modeling and control of urban traffic systems . . . 148
6.4 Conclusions on control implementation . . . 157

General conclusions . . . 159

Appendix 171

A. ISS hybrid Petri nets simulator . . . 173
A.1 Simulation algorithm . . . 173
A.2 Simulator and interface . . . 175
A.3 HybNet block for Simulink . . . 180

B. Complementary results on fluidization . . . 183
B.1 Error introduced by $\Delta\tau$ . . . 183
B.2 Computation of the ultimate bound of the approximation error in Join-Free nets . . . 184
B.3 Lemmas for the approximation analysis . . . 186

C. Complementary results on controllability and control . . . 191
C.1 Algorithms for controllability analysis . . . 191
C.2 On the product $\mathbf{v}^T\mathbf{e}^{\mathbf{A}\tau}\mathbf{b}$ . . . 194
C.3 Additional algorithms for coordinated control . . . 200

List of Figures

0.1 A manufacturing system and its transient evolution. 4
0.2 Synthesis of controllers for stochastic PNs (MPN) via fluid models (TCPN). 6

1.1 A conservative and consistent Markovian Petri net. 11
1.2 A TCPN system and its $Class(\mathbf{m}_0)$ 17

2.1 A non ordinary Join-Free MPN system and its fluid relaxation. 29
2.2 Marked graph whose marking mainly evolves in two different regions. 30
2.3 Approximation of the transient behavior of the MPN of fig. 2.2. 38
2.4 A Non-monotonic MPN system and its stochastic fluid relaxation. 40
2.5 A MPN system whose fully relaxation is better than its partial relaxation. 42
2.6 A hybrid approximation of a MPN under condition 3. 45
2.7 A good hybrid approximation for the system of fig. 2.5(a). 47
2.8 A MPN system and its hybrid relaxations. 50
2.9 A PN that integrates a spurious deadlock. 51

3.1 a) A PN live as autonomous discrete but non-live under certain deterministic timing. b) A PN non live as autonomous, but live as timed. 56
3.2 a) λ-conservative but not λ-consistent TCPN. b) λ-consistent but not λ-conservative TCPN. 59
3.3 A Choice-Free (marked graph) PN that is conservative and consistent. 64
3.4 A conservative and consistent TEC net and its transformation into Choice-Free. 65
3.5 Deadlock system as autonomous, but deadlock-free for particular timings. 67
3.6 a) TCPN system with deadlock markings in two different regions. b) TCPN system with two independent T-semiflows. 73
3.7 a) TCPN system with two independent siphons. b) TEC unbounded TCPN model. 77

4.1 A Manufacturing cell and its Petri net model. 84
4.2 A TCPN system with its equilibrium set. 87
4.3 Two TCPN systems with identical P-flows but only being consistent and controllable. . . 92
4.4 Relation between BIC and null-controllability. 93
4.5 A TCPN system, with only one controllable transition, and its equilibrium set. 99
4.6 Unreachable makings for the system of fig. 4.5 104

5.1 Auxiliary figure for the proof of Proposition 5.2. 116
5.2 A consistent TCPN system and its evolution under an affine control law. 119
5.3 Modular-coordinated control scheme. 119
5.4 A modular view of a consistent and conservative TCPN system. 121
5.5 Marking of Module 1 and the buffers in the system of fig. 5.4 with local affine controllers. 121
5.6 Behavior of the system of fig. 5.4 under coordinated control. 126
5.7 TCPN system under pole-assignment control. 132
5.8 Controlling between regions. 134

6.1 Block diagram of a MPN under control. 140
6.2 Petri net model of one-part assembly in an automotive production system [Dub et al., 2002]. 144
6.3 Timed continuous Petri net relaxation of the model of fig. 6.2 145
6.4 Behavior of the system under control. 146

6.5 System under a $GMEC$ control. . . . 147
6.6 PN model of an intersection of two one-way streets. . . . 149
6.7 Queue lengths for the one-intersection model. . . . 150
6.8 PN model of an intersection of two one-way streets, the arrivals to the first queue occur in bursts. . . . 151
6.9 Computation of optimal switching delays. . . . 154
6.10 PN model of 2 intersections connected by a link. . . . 155
6.11 Marking of queues at the second intersection (fig. 6.10) under control. . . . 156

A.1 Introducing the parameters of the PN. . . . 176
A.2 Selecting the kind of PN and defining the timing of each transition. . . . 177
A.3 Plotting results after a simulation. . . . 179
A.4 Results obtained after simulating the system of fig. 5.7(a) as both MPN and TCPN. . . . 180
A.5 Simulink_HybPN model. . . . 181

List of Tables

2.1 Marking approximation of p_2 for the Join-Free MPN in fig. 2.1(a). 28
2.2 Marking approximation of p_3 for the MPN of fig. 2.2 29
2.3 Marking approximation of p_3 for the MPN of fig. 2.2 by the corresponding TnCPN 38
2.4 Approximation of p_5 in steady state for the MPN of fig. 2.4(a) 39
2.5 Average steady state markings at p_7 for the MPN and MHPN of fig. 2.6(a) 44
2.6 Average steady state markings at p_1 for the MPN and MHPN of fig. 2.5(a). 46
2.7 Average steady state markings at p_4 for the MPN and MnHPN of fig. 2.8(a). 49

3.1 General conditions for λ-conservativeness and λ-consistency. 62
3.2 Conditions for λ-conservativeness and λ-consistency for subclasses. 66

5.1 Qualitative characteristics of control laws. 111

Introduction

In order to logically model and analyze concurrency and synchronization in *discrete event dynamical systems* (DEDS), C.A. Petri introduced a certain kind of net formalism [Petri, 1962, Petri, 1966]. Later, as a result of the studies of A. Holt in the MAC Project of the MIT (during the second half of the 60's and the beginning of the 70's), those systems started to be known as *Petri nets* (PN). If the original PN model is event-driven (but fully non-deterministic), the introduction of temporal concepts were proposed several years later under different approaches. Firstly, introducing deterministic timings in order to deal with performance and real-time analysis (e.g., [Ramchandani, 1974, Merlin and Farber, 1976]). Later, stochastic timing extensions were introduced for performance evaluation purposes (e.g., [Molloy, 1982, Marsan et al., 1984, Florin and Natkin, 1985]). Other extensions to the untimed basic model have been proposed in order to provide compact representations of certain DEDS, leading to the class of high-level PNs (e.g., Coloured nets [Jensen, 1981], Predicate-Transition nets [Genrich and Lautenbach, 1981]). Finally, levels of abstractions and timed interpretations have been interleaved/mixed.

Nowadays, a large amount of results can be found in the literature regarding the analysis of DEDS by using different PN models. Applications involve the implementation of sequence controllers, validation in software development, analysis of communication protocols and networks, manufacturing systems, supply chains, etc.

Fluidization of Petri nets

It is well known that one of the most important limitations in the analysis (and synthesis problems) of DEDS is the computational complexity that may appear. The complexity in PNs appears due to a large net structure, a large marking population or a particular interconnection of the nodes (two PN systems whose nets have the same number of nodes and initially the same number of tokens may have far different number of states, due to the particular interconnection of their nodes). Frequently, the set of reachable markings increases exponentially w.r.t. the initial marking, what is known as the *state explosion problem*, making prohibitive the application of enumerative techniques even for net systems with a small structure (i.e., small number of places and transitions).

In this context, the *fluidization* or *continuization* (i.e., getting a continuous-state approximation) was proposed as a relaxation technique in order to overcome the state explosion problem. The idea consists in the analysis of the DEDS via a relaxed continuous approximation, i.e., a continuous-state system that behaves (or conserve certain interesting properties) in a similar way than the original model, reducing thus the computational efforts. In DEDS, fluidization has been explored in queueing networks (see, for instance, [Chen and Mandelbaum, 1991], [Dai, 1995], [Altman et al., 2001]), PNs ([David and Alla, 1987], [Silva and Recalde, 2002]) and more recently in Process Algebra [Hillston, 2005]. (The reader may think in hybrid automata, but this is not a relaxation of a (discrete) automata, on the contrary, it is an extension of such kind of models). The fluidization of stochastically timed DEDS can

be seen as particular cases of the approximation of discrete stochastic processes by differential equations, based on the functional central limit theorem (e.g., [Kurtz, 1970]), nevertheless, fluid versions of DEDS have been mainly developed following independent ways.

Regarding PNs, David and Alla firstly introduced fluid PNs with *constant* and *variable speeds* [David and Alla, 1987, David and Alla, 1990]. They did extensively work on this topic, motivated by the advantage of having a system that can be analyzed as a continuous one (technically, they can be seen as hybrid as well) and behaves (quantitatively) as an original T-timed PN model (examples can be found in [David and Alla, 2010]). This topic was revisited in [Recalde and Silva, 2001], making emphasis in the connection with the original discrete models. In fact, there the *infinite server semantics* (which happens to be the same that the variable speed) was derived as the approximation of the average behavior of a Markovian stochastic T-timed PN. From another approaches, in the 90's different authors proposed hybrid PN systems that can be used as models *per se*, rather than relaxations of discrete event systems. Some of them are the following:

- Trivedi and his group introduced the so called *fluid stochastic PNs* [Trivedi and Kulkarni, 1993]. This consists in a stochastically timed hybrid model defined as an extension of (discrete) stochastic PNs in which some places are allowed to have fluid tokens. The purpose of such model is the performance evaluation of complex stochastic systems.

- In the Valette and coworkers' approach [Champagnat et al., 1998], a hybrid system is defined as a combination of a discrete PN and a set of *differential and algebraic equations* (as a generalization of hybrid automata). Discrete places are associated to modes for the evolution of the continuous variables, while continuous guards activate the occurrence of discrete transitions. For example, this model becomes useful for modeling certain industrial processes under supervision.

- Demongodin and coworkers [Demongodin et al., 1993] extend the hybrid PN formalism of Alla and David (constant speed in the continuous, deterministic T-timed in the discrete) by adding two new nodes: *batch transitions* and *batch places*. The definition of this model is motivated by the need of a precise representation of the accumulation phenomena that frequently occurs in conveyors of certain production systems.

- Giua and coworkers introduced *first-order hybrid PNs* [Balduzzi et al., 2000]. This follows the basic definition of Alla and David with a few differences in the evolution rule. The continuous part is an autonomous continuous subnet where the firing speed of the transitions occurs with piecewise constant rates that can be chosen from a given set. The discrete part (a discrete subnet) evolves by the firing of discrete transitions or the emptying at continuous places. The authors have explored the application of this model for optimization purposes [Giua et al., 2000, Balduzzi et al., 2001].

These hybrid models enjoy a broad representativeness power. Nevertheless, the classical trade-off between expressiveness and complexity appears, and the analysis (and synthesis problems) in some of those hybrid systems becomes technically complex (at least, more complex than the analysis of the models introduced by David and Alla). There are other definitions of fluid and hybrid PN systems, several of them defined *ad hoc* for very particular problems. A detailed list of references (providing a wide overview, even if not updated) can be found in http://bode.diee.unica.it/ hpn/ (a bibliography on Hybrid PN systems elaborate by A. Giua).

This dissertation focus on the study of *timed continuous Petri nets* (TCPN) under infinite server semantics [Silva and Recalde, 2002] (equivalent to the *variable speed* fluid model [Alla and David, 1998]). In [Recalde and Silva, 2001] this model was proposed as a potential approximation of the *Markovian* timing interpretation of discrete PNs. The reason for this choice is that *Markovian (discrete) PNs* (MPN, where transitions fire with exponentially distributed random delays and conflicts are solved with a race policy) enjoy the time memoryless property. Therefore the current marking represents all the information required for the future evolution of the system. Moreover, MPNs are widely used for the analysis of performance evaluation [Molloy, 1982, Balbo and Silva, 1998], but the exact analysis of MPNs, via the underlying Markov Chain, frequently leads to untractable computational complexity, because of the already mentioned state explosion problem.

In order to use a TCPN for the analysis of the corresponding MPN, it is required that the relaxed model preserves the properties under study of the original discrete one. In PNs the fluidization seems a promising technique when the initial marking can be assumed as "large enough" (where the relative errors, and their consequences, tend to be small, because the rounding effects are relatively less significant). In fact, increasing the population does not affect the complexity of the analysis via fluid models, since, in the resulting continuous PN, the number of *state variables* is upper bounded by the number of places, being independent of the number of tokens in the net system (thus, the initial marking). Consider the following motivating example (the reader that is not familiar at all with PNs may first consult basics concepts and terminology in Chapter 1):

Example The PN of fig. 0.1(a) represents a simple manufacturing system, in which transitions represent stations (containing sets of machines: servers) and places represent intermediate buffers. Considering a Markovian timing interpretation with unitary rates and initial marking $\mathbf{M}_0 = [3, 2, 0, 1, 0, 1, 0]^T$, the transient evolution of the *expected value* of the marking of place 5 (a buffer) was obtained through several simulations and drawn in fig. 0.1(b) with a solid line (label $E\{\mathbf{M}\}$). The marking of the same place for the corresponding continuous approximation appears in fig. 0.1(b) as a dashed curve (label TCPN). It can be observed that the TCPN barely approximates the transient behavior of the discrete PN. The underlying Markov chain of the DEDS has 258 states. Next, both the MPN and the TCPN were simulated with initial markings $\mathbf{M}_0 = 5 \cdot [3, 2, 0, 1, 0, 1, 0]^T$ and $\mathbf{M}_0 = 10 \cdot [3, 2, 0, 1, 0, 1, 0]^T$. Fig. 0.1(c) and 0.1(d) show the corresponding trajectories thus obtained. Note that the approximation is good if the initial marking is multiplied by 5 (fig. 0.1(c)) but it is better if it is multiplied by 10 (fig. 0.1(d)). It can be said that (in this case) the approximation becomes better when the initial marking is increased. In fact, in Chapter 2 it will be proved that the quality of the approximation is related to the number of active servers (transitions' enabling degrees). In this way, since the net of this example is monotonic w.r.t. the initial marking, then the number of active servers becomes larger (and thus the approximation is better) when the initial marking is increased.

The Markov chain for the system with $\mathbf{M}_0 = 5 \cdot [3, 2, 0, 1, 0, 1, 0]^T$ has $100,000$ states, and more than 2.5 million when $\mathbf{M}_0 = 10 \cdot [3, 2, 0, 1, 0, 1, 0]^T$ (the state explosion problem). On the other hand, the continuous model has only 7 state variables in all the cases (one for each place, actually, two of them can be eliminated since they are linearly dependent), independently of the initial marking, i.e., the state explosion problem does not appear in the TCPN system by increasing the number of tokens in the initial marking.

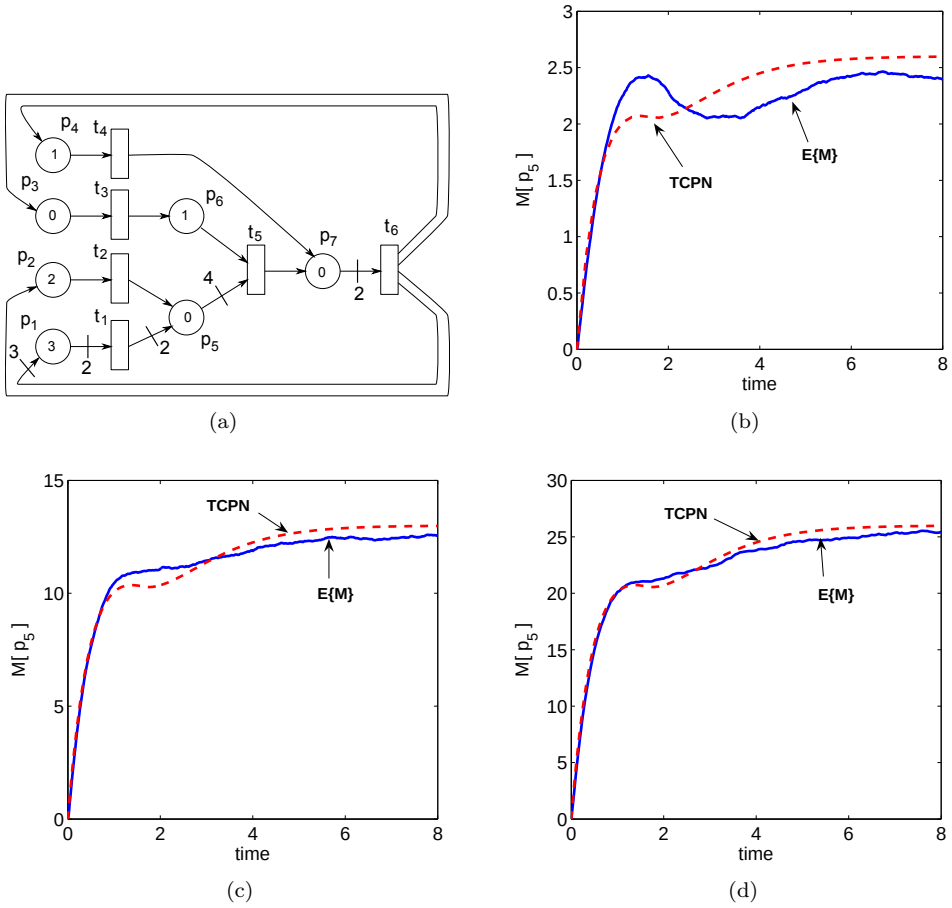

Fig. 0.1: (a) A manufacturing system and the transient evolution of the marking of place p_5 of the discrete PN (solid line) and the corresponding TCPN (dashed line) for (b) the initial marking $\mathbf{M}_0 = [3, 2, 0, 1, 0, 1, 0]^T$, (c) $\mathbf{M}_0 = [15, 10, 0, 5, 0, 5, 0]^T$ and (d) $\mathbf{M}_0 = [30, 20, 0, 10, 0, 10, 0]^T$.

Relaxations lead to loss of fidelity. Thus, as it may be expected, fluidization does not represent an universal and perfect tool. The first problem that may arise when using this technique is that the fluid model does not necessarily preserve the all the behavioral properties of the original DEDS model (for example, mutex properties are always lost). Thus, for certain cases, the analysis through fluidization may be useless. In other cases, the fluidization may provide only an educated guess. A second issue that may appear in the fluidization of PNs is the complexity generated by synchronizations. The model studied here, from a continuous-state dynamical systems' perspective, is a *piecewise linear* one. The number of embedded linear modes (sets of linear differential equations) increases exponentially w.r.t. the number of transitions representing rendez-vous (synchronizations). Thus, even if the behavior of a DEDS is preserved by its corresponding fluid relaxation, this could be too complex to be properly analyzed. Furthermore, large net structures may lead to continuous models with a large number of state variables, since one state variable is defined per each place (P-flows introduce linear dependencies between the state variables, then the number of these can be reduced, nevertheless, frequently most of the state variables are linearly independent and must be kept).

On the other hand, when a system admits a reasonable fluidization (in the sense that the fluid model preserves the desired properties of the discrete one), several advantages can be visualized by using continuous models: the first one is obviously the reduction of the complexity related to a large marking population, since in continuous models the state explosion problem does not appear, even more, certain problems can be analyzed by using algorithms with a polynomial-time complexity (thus, fluidization can be seen as analogous to the reduction of an integer programming problem into a linear one). Another interesting advantage is that, techniques and concepts developed in the Control Theory for continuous-sate systems can be applied to the continuous PN model. For instance, techniques for the analysis and application of performance controllers that reject perturbations, stability, observability, estimation, etc. In this way, fluidization represents a bridge between particular classes of continuous-state and discrete event systems.

State of the art of TCPNs and contributions

TCPNs under infinite server semantics can be seen as piecewise-linear hybrid systems (combining state-continuous and discrete event dynamics). On the other hand, they inherit concepts and properties from discrete PNs. In this way, the analysis of TCPNs is achieved by the application of a blend of concepts and techniques from the control and the PN theories.

In the literature, TCPNs have been mainly considered for modeling (e.g., [Alla and David, 1988, Amrah et al., 1997]) and control (e.g., [Hennequin et al., 1999, Kara et al., 2009, Lefebvre et al., 2007]). A particularly broad study of TCPNs have been addressed in the GISED research group at the University of Zaragoza (where the author developed this dissertation), frequently in collaboration with researches from other countries. Some contributions previously done by this group concern the approximation to discrete PN systems [Recalde and Silva, 2001, Mahulea et al., 2009], the study of qualitative properties [Júlvez et al., 2006], model checking [Kloetzer et al., 2010], performance evaluation [Júlvez et al., 2005], observability analysis [Júlvez et al., 2008, Mahulea et al., 2010], controllability analysis [Jiménez et al., 2005], [Mahulea et al., 2008b], control synthesis [Mahulea et al., 2008a], [Jing et al., 2008a], etc.

In this dissertation, the addressed problems are the approximation of stochastic (discrete) PNs (Chapter 2), the connection between liveness, boundedness and timing (Chapter 3), the analysis of controllability (Chapter 4) and synthesis of controllers (Chapter 5), and the implementation of these controllers into the original discrete PN models (Chapter 6). This last issue may be considered as the unifying point of the other problems addressed in this dissertation. Roughly speaking, given a MPN, if its behavior can be approximated by a TCPN, a controller for this can be synthesized (after a proper controllability analysis), and finally, such controller can be implemented into the original MPN, closing the loop of the synthesis of controllers via fluidization depicted in fig. 0.2.

Regarding the approximation of discrete PNs, few authors have addressed this problem for TCPNs. In [Zerhouni and Alla, 1990], deterministically timed PNs are considered as the reference models, and a criterion, based on simulations, is given for deciding if the fluid approximation is correct. Experimentally, it can be observed that most frequently, infinite server semantics provides a better approximation (but not necessarily a good one) than finite server semantics. This property was proved in [Mahulea et al., 2009]

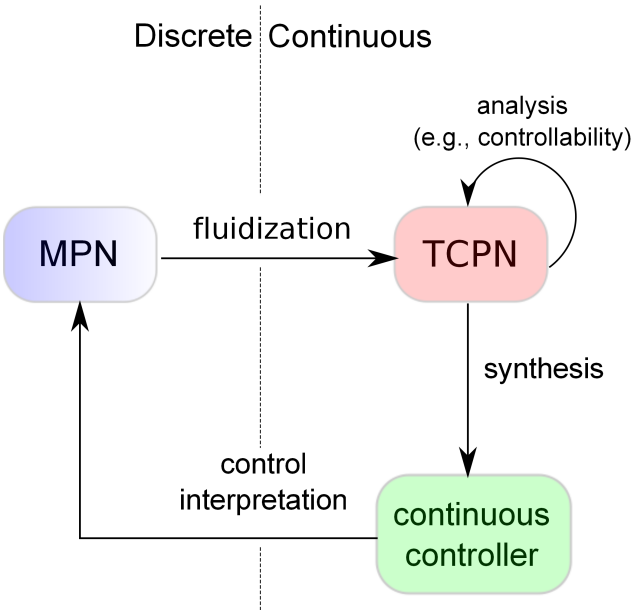

Fig. 0.2: Synthesis of controllers for stochastic PNs (MPN) via fluid models (TCPN).

for a relatively broad subclass of nets, named mono-T-semiflow reducible. From a different approach, in [Lefebvre et al., 2009] authors introduced a couple of new semantics in order to better approximate the steady state of a stochastic PN. Despite of these works, there is still a lack of results regarding this problem. In particular, it would be convenient to improve our understanding of when and why a TCPN approximates the behavior of the corresponding discrete PN.

Liveness and boundedness in continuous PNs were studied in [Recalde et al., 1999] for the autonomous model, providing necessary conditions (structural liveness and structural boundedness) for general classes of nets, and sufficent and necessary for a particular class (Equal Conflict, EQ). Regarding timed models, in [Júlvez et al., 2006] it was pointed out that if a continuous system reaches a non-live steady state as timed, it is also non-live as untimed. Nevertheless, the opposite is not true, and there may exist timings such that the timed model is live (bounded) while the untimed model is not live (unbounded). Then, some questions arise, e.g., for which structures and timings occur this timing-dependent liveness (boundedness)? what is the mechanism of such phenomenon?

Controllability and control in TCPNs have been addressed in the literature from a state-continuous systems approach (for instance, [Jiménez et al., 2005], [Lefebvre et al., 2007], [Mahulea et al., 2008b], [Kara et al., 2009]). In fact, the control objective frequently considered consists in driving the TCPN system towards a desired target marking, which is different from the control problems commonly addressed in DEDS (like disabling events for avoiding forbidden states). Regarding controllability, it is known that a continuous PN system is frequently not controllable in the sense of continuous-state systems (a continuous system is said controllable if all states in the state space can be reached from any other state in the sate space), due to the existence of state invariants [Mahulea et al., 2008b] (related to marking conservation laws imposed by P-flows). Nevertheless, when all the transitions are controllable (meaning that all the activities in the system can be arbitrarily slowed down), the set of reachable

markings and the set of nonnegative solutions for the fundamental equation are equivalent if the net is consistent. In case that there exist uncontrollable transitions (when some activities cannot be manipulated), the controllability analysis is much more complex. In a preliminary work [Jiménez et al., 2005], controllability was studied with uncontrollable transitions, adopting a local controllability notion, for the particular case of Join-Free net systems (which corresponds to linear systems that evolve in polytopes). Nevertheless, such controllability study cannot be easily extended to more general net subclasses.

Several authors have proposed control techniques for TCPN models under infinite server semantics, ranging from *fuzzy control* [Hennequin et al., 1999], the use of *linear matrix inequalities* for the synthesis of linear controllers [Kara et al., 2009], to *model predictive control* [Mahulea et al., 2008a]. A more detailed discussion about those control techniques is presented in Chapter 5. Despite the existence of several control laws, there is still a lack of control policies for systems in which the control actions cannot be applied to all the transitions (in most of the works it is assumed that all the activities in the system can be arbitrarily slowed down), or for systems having large net structures (that can be addressed by means of distributed control strategies).

Finally, an issue that remains as an intuitive idea, but have not been formally studied, is the application (or interpretation) of a control law, synthesized for a continuous PN, into the original discrete PN model. This idea has been considered by few authors, in the context of open and closed manufacturing lines [Amrah et al., 1998, Lefebvre, 1999, Kara et al., 2006]. For instance, in [Amrah et al., 1998] it was illustrated how a control law, derived for a variable speed continuous PN, can be applied to the original discrete PN model (a T-timed PN with constant firing delays). Nevertheless, such works do not provide a formal framework for such control implementation.

In this context, the contributions of this dissertation can be enumerated as follows:

- (Chapter 2) The approximation of the expected dynamical behavior of Markovian PNs by the corresponding TCPNs has been studied. Sufficient conditions for such approximations have been provided. Moreover, explanations at the net level for the existence of errors are given. In order to improve the approximation, a new stochastic continuous model TnCPN (defined by adding white noise to the flow of the TCPN system) and two hybrid PN models, MHPN and MnHPN, have been introduced and studied. Assuming ergodicity (i.e., the marking pdf when $\tau \to \infty$ is independent of the initial state, thus the limiting probabilities are unique) and liveness, it has been proved that the TnCPN and MnHPN models may approximate not only the expected value, but also the probability distribution of the marking of the Markovian PN when the number of active servers at the transitions is large. These results have been presented in [Vázquez et al., 2008b, Vázquez and Silva, 2009a].

- (Chapter 3) Regarding the connection between liveness, boundedness and the timing in continuous PNs, a couple of concepts (λ-Cv and λ-Ct) have been introduced in order to analyze the case where the timing allows a TCPN system to behave as conservative and/or consistent when the autonomous continuous PN does not exhibit those properties. Liveness in TCPNs has been studied in more detail. It has been shown that non-live steady-state markings are those at which siphons are unmarked. Later, it has been proven that λ-Ct is sufficient to guarantee that siphons remain marked (assuming they are initially marked), thus, it is a sufficient condition for timed-liveness. Finally, a couple of algorithms have been derived in order to compute a timing such that the TCPN

is λ-Ct or λ-Cv, enforcing thus liveness and boundedness, respectively. These results have been reported in [Vázquez et al., 2008, Vázquez and Silva, 2010, Vázquez and Silva, 2011].

- (Chapter 4) Controllability on TCPNs, under infinite server semantics, has been studied under a local controllability concept derived as a reformulation of the classical one (defined for linear time-invariant systems). For models in which control actions can be applied to all transitions, sufficient and necessary (structural) conditions for reachability and controllability have been obtained. For systems with uncontrollable transitions (whose flow cannot be arbitrarily reduced), sufficient and necessary conditions for controllability, over subsets of equilibrium markings (representing potential steady states of the system) that belong to a given region (related to a linear mode), have been derived. Moreover, a sufficient condition for controllability over the union of those subsets has been obtained. Preliminarily results have been published in [Vázquez et al., 2008a], but more mature results are presented in this dissertation.

- (Chapter 5) An affine control law has been proposed for TCPNs in which all the transitions are controllable, ensuring asymptotic stability and feasibility. Based on this affine control law, a modular-coordinated control strategy has been proposed in order to reduce the complexity during the synthesis. The resulting scheme consists of a set of affine local controllers and a coordinator that receives and sends information to the local controllers. Feasibility and convergence to the required marking have been proved. Finally, a centralized control law structure, for TCPN systems having uncontrollable transitions, has been proposed, by adapting the classical pole-assignment technique used in linear systems. Feasibility and closed-loop stability have been proved. These control proposals are presented in [Vázquez and Silva, 2009c, Vázquez et al., 2011].

- (Chapter 6) A control structure has been derived for the interpretation of a control law, designed for a TCPN system, into the corresponding MPN one. This control strategy has been applied to and application example: the stock level control of a Kanban-based automotive assembly line. The results obtained show the feasibility of the proposed control scheme. Moreover, a different control problem has been considered by introducing a hybrid PN model for intersections in an urban traffic network. The proposed model can be used for representing large urban traffic systems. The model thus obtained is so simple (but still captures key information) that it is possible to use it for the on-line optimization of the switching times of the traffic lights, by following a model predictive control procedure. These results have been reported in [Vázquez and Silva, 2009b, Vázquez et al., 2010].

- (Appendix A) Finally, a hybrid PN simulator has been developed for comparing, in a practical way, Markovian discrete PNs and their relaxations studied in this work.

This list of contributions clearly presents the structure of this document. In fact, note that the chapters correspond (excepting Chapter 3) to the activities (arcs) depicted in fig. 0.2. It is just required to mention here Chapter 1, where basic concepts on discrete and continuous PNs, and from the Control Theory, are recalled. Finally, a couple of appendices are also included, providing some algorithms and useful results that will be referred along the document.

Chapter 1

Basic concepts and notation

1.1 Basic notation

In the sequel, the following notation is adopted: vectors and matrices are bold, the first in lower case, the last in uppercase. Given a matrix $\mathbf{A}$ of dimension $n \times m$ and sets of ordered indexes $I = \{i_1, ..., i_r\}$ and $J = \{j_1, ..., j_s\}$, with $i_r \leq n$ and $j_s \leq m$, it will be denoted as $\mathbf{A}[I, J]$ the matrix built with the elements in the rows indicated by I and the columns indicated by J. A similar notation will be used with vectors. Then, given a vector $\mathbf{a}$, $\mathbf{a}[I]$ represents the vector built with the entries of $\mathbf{a}$ indicated in I. In particular, a_j is used to denote the j-th entry of vector $\mathbf{a}$. In case of the product of a matrix $\mathbf{A}$ and a column vector $\mathbf{b}$, $[\mathbf{Ab}]_j$ is used to denote the j-th entry of the vector resulting from the product $\mathbf{A} \cdot \mathbf{b}$. Moreover, given a matrix $\mathbf{A}$, $[\mathbf{A}]_j$ denotes the j-th row of $\mathbf{A}$, while $[\mathbf{A}]^j$ denotes its j-th column. Given column vectors $\mathbf{a}$ and $\mathbf{b}$, $diag(\mathbf{a}, \mathbf{b})$ denotes a diagonal matrix whose diagonal entries are those of vector $[\mathbf{a}^T, \mathbf{b}^T]$. This is extended to matrices, and $diag(\mathbf{A}, \mathbf{B})$ denotes a matrix diagonal by blocks, whose diagonal blocks are the square matrices $\mathbf{A}$ and $\mathbf{B}$. Finally, $\mathbf{1}$ usually denotes a vector whose entries are unitary and whose size is determined by the context.

Relation operators applied on vectors and matrices are interpreted component-wise. For instance, given a matrix $\mathbf{A}$ of dimension $n \times m$, the notation $\mathbf{A} \geq \mathbf{0}$ is equivalent to $\mathbf{A}[i, j] \geq 0 \; \forall i \in \{1, .., n\}, \forall j \in \{1, .., m\}$. The support of a vector $\mathbf{a}$ is denoted as $||\mathbf{a}||$ and is defined as the indices of the non-null entries of $\mathbf{a}$.

The conventional notation $a \sim Normal(\mu, \sigma)$ will be used to denote that the random variable (r.v.) a has a normal probability distribution function (pdf) with mean μ and variance σ. Similarly, the notation $a \sim Poisson(\eta)$ will be used to denote that the r.v. a has a Poisson pdf with parameter η. This notation can be extended to vectors of r.v.'s. For instance, $\mathbf{a} \sim Normal(\boldsymbol{\mu}, \boldsymbol{\sigma})$ denotes a vector in which each entry a_j is a normally distributed r.v. with mean μ_j and variance σ_j.

1.2 Basic concepts on P/T net systems

Let us provide here a few of basic concepts on Petri nets. A detailed introduction can be found in [Murata, 1989, Silva, 1993].

Definition 1.1. A place/transition (P/T) net is a bipartite oriented graph defined by the tuple $\mathcal{N} = \langle P, T, \mathbf{Pre}, \mathbf{Post} \rangle$, where P and T are disjoint sets of *places* and *transitions*, respectively. **Post** and

Pre are *incidence* matrices, natural valued with dimension $|P| \times |T|$, that describe the connection from the nodes T to those of P, and from P to T, respectively.

For instance, $\mathbf{Post}[p,t] = w$ means that there is an arc connecting the place $p \in P$ to the transition $t \in T$ with a weight (multiplicity) w, while $\mathbf{Pre}[p,t] = w$ means that there is an arc connecting the transition $t \in T$ to the place $p \in P$. On the contrary, $\mathbf{Post}[p,t] = 0$ (resp. $\mathbf{Pre}[p,t] = 0$) means that there does not exist an arc connecting $p \in P$ to $t \in T$ (resp. $t \in T$ to $p \in P$).

Definition 1.2. A P/T system is a discrete event system described by the pair $\langle \mathcal{N}, \mathbf{M}_0 \rangle$, where $\mathcal{N}$ is a P/T net and $\mathbf{M}_0 \in \mathbb{N}^{|P|}$ is a vector, named *initial marking*, that has the information about the number of marks or tokens that are initially in the places of the net, i.e., the initial marking distribution. The state in a P/T system is defined as the distribution of marks in the places, codified in the marking vector $\mathbf{M} \in \mathbb{N}^{|P|}$. The evolution of the P/T system is described as follows:

I. A transition $t \in T$ is said *enabled* at the marking $\mathbf{M} \in \mathbb{N}^{|P|}$ iff $\mathbf{M} \geq \mathbf{Pre}[P,t]$.

II. The occurrence or *firing* of an enabled transition leads to a new marking distribution $\mathbf{M'} \in \mathbb{N}^{|P|}$ that can be computed by using $\mathbf{M'} = \mathbf{M} + \mathbf{C}[P,t] = \mathbf{M} + \mathbf{C} \cdot \mathbf{e}_t$, where $\mathbf{C} = \mathbf{Post} - \mathbf{Pre}$ is named the token flow matrix or *incidence matrix*, and $\mathbf{e}_t$ denotes the t-th column vector of the unity matrix of dimension T.

Given a sequence of occurrences (or firings) $\sigma = t_1 ... t_k$, the marking reached is given by the so called *fundamental equation*

$$\mathbf{M'} = \mathbf{M} + \mathbf{C} \cdot \boldsymbol{\sigma} \tag{1.1}$$

where $\boldsymbol{\sigma} = \sum_{i \in \{1,\ldots,k\}} \mathbf{e}_i$ is called the *firing count vector*. Every reachable marking must agree with the fundamental equation, i.e., given $\mathbf{M'}$ reachable $\exists \boldsymbol{\sigma} \geq \mathbf{0}$ that fulfills (1.1). Nevertheless, the opposite does not hold in general in the sense that, given a vector $\exists \boldsymbol{\sigma} \geq \mathbf{0}$, the solution $\mathbf{M'}$ of (1.1) may not be a reachable marking, because there is not information about the fireability of a sequence represented by $\boldsymbol{\sigma}$.

The set of all the reachable markings, from the initial one $\mathbf{M}_0$, is called *reachability set*, and it is denoted as $RS(\mathbf{M}_0)$. The reachability relation can be represented by a *reachability graph*, where the nodes are the reachable markings and there is an arc from a node $\mathbf{M}$ to another $\mathbf{M'}$ iff there exists a transition t whose firing transfers the system from $\mathbf{M}$ to $\mathbf{M'}$.

Given a P/T net, the set of the input (output) nodes of a node v will be denoted as ${}^\bullet v$ ($v^\bullet$). For instance, given a place $p \in P$, ${}^\bullet p$ denotes the set of input transitions of p.

In the sequel, given a P/T net, it will be assumed that it is connected, i.e., for every pair of nodes there is a path connecting them (may be just in one direction), and that every place has a successor, i.e., $|p^\bullet| \geq 1$.

1.2.1 Structural components

Interesting results can be found about the behavior of a P/T system by studying particular sets of nodes (components) in the graph. Such components can be equivalently analyzed from the incidence matrices **Post** and **Pre**. This approach is known as *structural analysis* [Silva et al., 1998]. Among the interesting

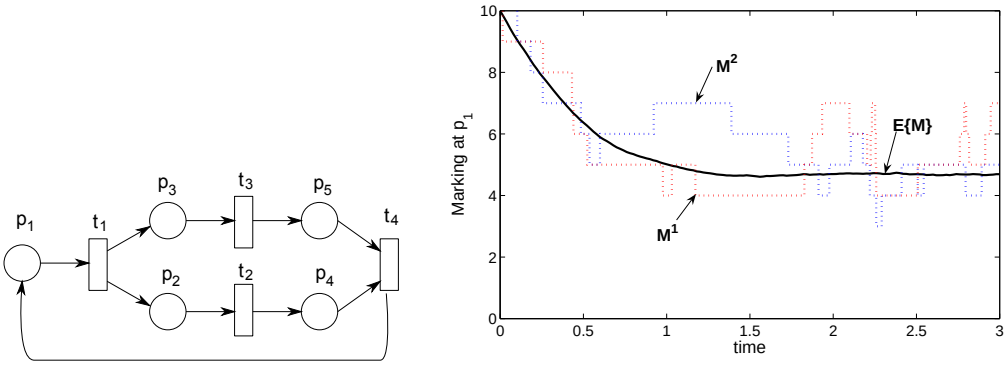

(a) (b)

Fig. 1.1: a) A conservative and consistent P/T net. b) Evolution of the corresponding MPN for the marking in p_1, with $\mathbf{M}_0 = [10, 0, 0, 0, 0]^T$ and $\boldsymbol{\lambda} = [1, 2, 2, 2]^T$.

components, let us introduce P- and T- components and siphons, which will be useful in the rest of this document.

Definition 1.3. Left and right annulers of the incidence matrix $\mathbf{C}$ are called $P-flows$ and $T-flows$, respectively. If these are nonnegative they are called $P-semiflows$ or $T-semiflows$. Basis for right and left annulers of $\mathbf{C}$ are denoted as $\mathbf{B}_y$ and $\mathbf{B}_x$, respectively. If there exists a positive right annuler, i.e., $\exists \mathbf{y} > \mathbf{0}$ s.t. $\mathbf{y}^T \cdot \mathbf{C} = \mathbf{0}$, then the net is said to be *conservative* (denoted as Cv). Similarly, if $\exists \mathbf{x} > \mathbf{0}$ s.t. $\mathbf{C} \cdot \mathbf{x} = \mathbf{0}$ the net is said *consistent* (denoted as Ct).
A P/T system is said *structurally bounded* and *structurally repetitive* if there exist $\mathbf{y} > \mathbf{0}$ and $\mathbf{x} > \mathbf{0}$ s.t. $\mathbf{y}^T \cdot \mathbf{C} \leq \mathbf{0}$ and $\mathbf{C} \cdot \mathbf{x} \geq \mathbf{0}$, respectively.
A set of places Σ is named a *siphon* iff ${}^\bullet\Sigma \subseteq \Sigma^\bullet$ (the set of input transitions is included in the corresponding output one), and it is *minimal* if it does not contain another *siphon*.

A T-semiflow $\mathbf{x}$ is defined at an algebraical level. At the net level, the support of $\mathbf{x}$ defines a set of transitions, called T-component, that may describe a cyclic sequence $\sigma_{\mathbf{x}}$ (if such a sequence is fireable), i.e., the marking reached after the occurrence of $\sigma_{\mathbf{x}}$ is equal to the initial marking since $\mathbf{M}' = \mathbf{M}_0 + \mathbf{C} \cdot \mathbf{x} = \mathbf{M}_0$. Analogously, given a P-semiflow $\mathbf{y}$, defined at an algebraical level, its support defines a set of places, called P-component, involved in a marking conservation law, i.e., for every reachable marking $\mathbf{M}'$ it holds $\mathbf{y}^T\mathbf{M}' = \mathbf{y}^T\mathbf{M}_0 + \mathbf{y}^T\mathbf{C} \cdot \boldsymbol{\sigma} = \mathbf{y}^T\mathbf{M}_0$, so the weighted sum of the marking in the places of $||\mathbf{y}||$ remains constant.

Example 1.1. Consider the PN model of fig. 1.1(a). The incidence matrix of this net model is given by

$$\mathbf{C} = \begin{bmatrix} -1 & 0 & 0 & 1 \\ 1 & -1 & 0 & 0 \\ 1 & 0 & -1 & 0 \\ 0 & 1 & 0 & -1 \\ 0 & 0 & 1 & -1 \end{bmatrix}$$

The vector $\mathbf{x} = [1, 1, 1, 1]^T$ is a T-semiflow, meaning that by firing all the transitions one time, the marking

reached is equal to the initial one. Furthermore, since $\mathbf{x} > \mathbf{0}$, the net is consistent. On the other hand, $\mathbf{y} = [2, 1, 1, 1, 1]^T$ is a P-semiflow, meaning that the sum $\mathbf{y}^T \cdot \mathbf{m} = 2\mathbf{m}[p_1] + \mathbf{m}[p_2] + \mathbf{m}[p_3] + \mathbf{m}[p_4] + \mathbf{m}[p_5]$ remains constant during the evolution of the system. The set of places, $\{p_1, p_2, p_3, p_4\}$ defines a *minimal siphon*.

Let us introduce now a few of structural definitions. A net is said *ordinary* if all the arcs have a weight equal to one, i.e., $\forall i, \forall j$: $\mathbf{Pre}[i, j] \in \{0, 1\}$ and $\mathbf{Post}[i, j] \in \{0, 1\}$. A net is said *strongly connected* (resp. *P-strongly connected*) iff for every pair of nodes (resp. places) x and y, there is a path leading from x to y.

Two transitions t and t' are said to be in conflict if ${}^\bullet t \cap {}^\bullet t' \neq \emptyset$. A conflict $\{t, t'\}$ is said to be topologically equal (equivalently, t and t' are in topological equal conflict relation) if $\exists \gamma > 0$ s.t. $Pre[P, t] = \gamma Pre[P, t']$.

Definition 1.4. Subclasses of nets are defined according to their structure:

I. $\mathcal{N}$ is Choice-free (CF) if $\forall p \in P : |p^\bullet| \leq 1$.

II. $\mathcal{N}$ is Join-free (JF) if $\forall p \in T : |{}^\bullet t| \leq 1$.

III. $\mathcal{N}$ is Fork-Attribution (FA) if it is CF and JF.

IV. $\mathcal{N}$ is Topologically Equal Conflict (TEC) if all the conflicts are topologically equal.

1.3 Markovian Petri nets

In this section, the Markovian stochastic (discrete) Petri net model is introduced (for more details see, for instance, [Marsan et al., 1995]), together with a difference equation that describes its transient behavior, obtained via the fundamental equation. This difference equation description will be particularly useful in the Chapter 2, in order to compare this system with its continuous relaxation.

1.3.1 The Markovian stochastic Petri net model

Definition 1.5. A *Markovian stochastic Petri net* system *(MPN)* is a stochastically T-timed Petri net system in which the transitions fire at independent exponentially distributed random time delays, and conflicts are solved with a race policy (given two enabled transitions having a common input place, it fires the one having the lowest associated delay). In this way, a MPN is the tuple $\langle \mathcal{N}, \boldsymbol{\lambda}, \mathbf{M}_0 \rangle$, where $\boldsymbol{\lambda} \in \mathbb{R}_{>0}^{|T|}$ represents the transition rates, i.e., the average delays associated to each server of the corresponding transitions.

In this work, *infinite server semantics* (ISS) will be assumed for all the transitions. Accordingly, the firing time of an enabled transition t_i, from a given marking $\mathbf{M}$, is given by an exponentially distributed random variable with parameter $\lambda_i \cdot Enab(t_i, \mathbf{M})$, where the integer *enabling degree* is $Enab(t_i, \mathbf{M}) = \min_{p \in {}^\bullet t_i} \{\lfloor \mathbf{M}[p] / \mathbf{Pre}[p, t_i] \rfloor\}$.

Note that, while a P/T net system is an event-driven dynamic system, a MPN is a time-driven one, i.e., its evolution (the occurrence of the events) is determined by the time, not by *decisions* taken over the events. Stochastic PNs are useful for the modeling and analysis of discrete event systems having an stochastic behavior, in particular, for performance evaluation [Marsan et al., 1995]. According to its definition, the reachability graph of a MPN system is isomorphous to a Markov Chain [Molloy, 1982], which is commonly used for analysis purposes. A problem frequently found when using that approach is the complexity involved in the analysis of a Markov Chain, when the size of this may be too large.

Example 1.2. Consider the MPN model given by the net $\mathcal{N}$ of fig. 1.1(a), with rates $\boldsymbol{\lambda} = [1, 2, 2, 2]^T$ and initial marking $\mathbf{M}_0 = [10, 0, 0, 0, 0]^T$. Fig. 1.1(b) shows the results after some simulations of this system. First, if the system is simulated once, the marking at every place takes integer values in a random way. If a new simulation is achieved, the marking evolution will be different. This can be seen in fig. 1.1(b), where the dashed curves (labeled $\mathbf{M}^1$ and $\mathbf{M}^2$) represent the marking at p_1 for two different simulations during 3 time units. Nevertheless, if several simulations are achieved, an *average evolution* can be obtained. The solid curve in fig. 1.1(b) (labeled $E\{\mathbf{M}\}$) represents such average evolution for the marking at p_1, which was computed from 3000 simulations.
The number of nodes in the reachability graph of this system is 506 nodes, meaning that the underlying Markov Chain is a dynamical system with 506 state-variables (a state-variable is associated to each node, representing the probability that the system is in the corresponding state marking). The large size of the Markov Chain makes difficult the exact computation of the average trajectories. For this reason, curve $E\{\mathbf{M}\}$ in fig. 1.1(b) was obtained through simulations in this example.

In performance evaluation analysis, it is commonly required the computation (or estimation) of average values in the *steady state*, e.g., average markings or throughputs (expected firing frequency). Through this dissertation, it will be frequently considered not only the expected marking in steady state, but also during the transient evolution of the system.

A MPN system is said to be ergodic if the underlying Markov chain is ergodic, which occurs if the Markov chain process $\mathbf{X}(\tau)$ is irreducible and has an unique stationary probability distribution $\{\pi_j\}$, with all $\pi_j > 0$. The stationary distribution $\{\pi_j\}$ is equal to both the long run probability of finding the process $\mathbf{X}(\tau)$ (the marking of the MPN) in state j and the long run fraction of time it spends in j, independently of the starting state (initial marking) i. Intuitively speaking, an ergodic Markov chain (thus an ergodic MPN) will always enter its steady state probability distribution $\{\pi_j\}$ when it has been run long enough. It is known that a MPN system is ergodic if $\mathbf{M}_0$ is a home state. For more details, the reader may consult [Marsan et al., 1995].

In the sequel, given a MPN system, we suppose that a unique steady-state behavior exists. Even more, we restrict our study to bounded in average and reversible (i.e., whose initial marking is a home state) PN systems, therefore, the stochastic process is ergodic.

1.3.2 Difference equation for the MPN system

Given a MPN $\langle \mathcal{N}, \boldsymbol{\lambda}, \mathbf{M}_0 \rangle$, define a discrete-time stochastic system $\langle \mathcal{N}, \boldsymbol{\lambda}, \boldsymbol{\mu}_0 \rangle$, where the initial state is given by $\boldsymbol{\mu}_0 = \mathbf{M}_0$ and whose state $\boldsymbol{\mu}_k \in \mathbb{N}^{|P|}$ (denoting the state at time $\tau_0 + k\Delta\tau$, where $\Delta\tau$ is a

constant sampling period) evolves according to the difference equation:

$$\boldsymbol{\mu}_{k+1} = \boldsymbol{\mu}_k + \mathbf{C} \cdot \Delta\boldsymbol{\sigma}(\mathbf{F}_k \Delta\tau) \tag{1.2}$$

where $\Delta\boldsymbol{\sigma}(\mathbf{F}_k\Delta\tau)$ is a column vector of length $|T|$ defined by elements as $\Delta\sigma_i(F_{k,i}\Delta\tau) \sim Poisson(F_{k,i}\Delta\tau)$ with $F_{k,i} = \lambda_i \cdot Enab(t_i, \boldsymbol{\mu}_k)$.

Proposition 1.6. *Assuming a small enough sampling $\Delta\tau$, the transient marking evolution $\mathbf{M}$ of the MPN system $\langle \mathcal{N}, \boldsymbol{\lambda}, \mathbf{M}_0 \rangle$ is approximated by the state $\boldsymbol{\mu}$ of the system described by (1.2), i.e., $\forall k$, the probability distribution of $\mathbf{M}(\tau_0 + k\Delta\tau)$ is similar to that of $\boldsymbol{\mu}_k$.*

Proof. Denote the initial time as τ_0 and consider a particular transition t_i. By definition of the MPN, the time delay of the next firing of each active server of t_i is characterized by a random variable having an exponential pdf with parameter λ_i. Now, consider a fixed time interval $\Delta\tau$. If a server of t_i is always active during $\Delta\tau$, then the number of its firings (the number of accomplished jobs) during $\Delta\tau$ is characterized by a r.v. having a Poisson pdf with parameter $\lambda_i \cdot \Delta\tau$ (see [Papoulis, 1984]). Furthermore, since we are considering infinite server semantics, the number of firings of t_i during $\Delta\tau$ is the sum of the number of firings of each of its servers during this time interval. If $\Delta\tau$ is small enough then the number of active servers of t_i during this time interval remains almost constant. Therefore, the number of firings of t_i, during the time interval $(\tau_0, \tau_0 + \Delta\tau)$, can be approximated by a r.v. $\Delta\sigma_i(F_i(\tau_0)\Delta\tau)$ having a Poisson pdf with parameter $F_i(\tau_0)\Delta\tau = \lambda_i \cdot Enab(t_i, \mathbf{M}_0)\Delta\tau$, where $Enab(t_i, \mathbf{M}_0)$ is the number of active servers of t_i at $\mathbf{M}_0$ (the sum of independent Poisson distributed r.v.'s is also a Poisson distributed r.v., whose parameter is the sum of the parameters of the summands).

Now, considering the firing count vector $\Delta\boldsymbol{\sigma}(\mathbf{F}(\tau_0)\Delta\tau)$, whose elements are the corresponding r.v.'s $\Delta\sigma_i(F_i(\tau_0)\Delta\tau)$ defined for each transition, the marking at time $\tau_0 + \Delta\tau$ can be approximated by using the fundamental equation, i.e.

$$\boldsymbol{\mu}(\tau_0 + \Delta\tau) = \mathbf{M}_0 + \mathbf{C}\Delta\boldsymbol{\sigma}(\mathbf{F}(\tau_0)\Delta\tau) \tag{1.3}$$

where $\boldsymbol{\mu}(\tau_0 + \Delta\tau)$ is a random variable that represents the approximation of the marking of the MPN at time $\tau_0 + \Delta\tau$. Finally, (1.2) is obtained by generalizing the previous equation for future time steps. ∎

In the previous proposition, the sampling $\Delta\tau$ must be small enough so the probability that $Enab(t_i, \boldsymbol{\mu}_k)$ remains constant during a sampling time $\Delta\tau$, is almost 1, for every time instant k.

This assumption may lead to approximation errors. Nevertheless, in the Appendix B it is proved that it can be imposed an arbitrary bound for these errors, by choosing a suitable value for $\Delta\tau$. Therefore, in the sequel, (1.2) will be considered as a valid difference equation for the MPN system, i.e., it will be assumed that (1.2) holds when $\boldsymbol{\mu}_k$ and $\boldsymbol{\mu}_{k+1}$ are replaced by $\mathbf{M}_k$ and $\mathbf{M}_{k+1}$, respectively.

1.4 Continuous and timed continuous Petri nets

In this section, the continuous and timed continuous PN models will be presented. More details about these models can be found in the literature, for instance [Silva and Recalde, 2004, David and Alla, 2010].

1.4.1 Continuous Petri nets

Definition 1.7. A *continuous PN* system is a pair $\langle \mathcal{N}, \mathbf{m}_0 \rangle$ where $\mathcal{N}$ is a P/T net (like in a P/T system) and $\mathbf{m}_0 \in \mathbb{R}_{\geq 0}^{|P|}$ is the initial marking. The evolution rule is different to the case of discrete P/T systems, since in continuous PNs the firing is not restricted to integer amounts, and so the marking $\mathbf{m} \in \mathbb{R}_{\geq 0}^{|P|}$ is not forced to be integer. Instead, a transition t_i is *enabled* at $\mathbf{m}$ iff for every $p_j \in {}^\bullet t_i$, $\mathbf{m}[p_i] > 0$; and its *enabling degree* is $enab(t_i, \mathbf{m}) = \min_{p_j \in {}^\bullet t_i}\{\mathbf{m}[p_j]/\mathbf{Pre}[p_j, t_i]\}$. The firing of t_i in a certain amount $\alpha \leq enab(t_i, \mathbf{m})$ leads to a new marking $\mathbf{m}' = \mathbf{m} + \alpha \cdot \mathbf{C}[P, t_i]$.

The usual PN system, $\langle \mathcal{N}, \mathbf{M}_0 \rangle$ with $\mathbf{M}_0 \in \mathbb{N}^{|P|}$, will be said to be *discrete* so as to distinguish it from a *continuous* PN system $\langle \mathcal{N}, \mathbf{m}_0 \rangle$, in which $\mathbf{m}_0 \in \mathbb{R}_{\geq 0}^{|P|}$. In the following, the marking of a continuous PN will be denoted in lower case $\mathbf{m}$, while the marking of the corresponding *discrete* one will be denoted in upper case $\mathbf{M}$. Observe that $Enab(t_i, \mathbf{M}) \in \mathbb{N}$ in discrete PNs, while $enab(t_i, \mathbf{m}) \in \mathbb{R}_{\geq 0}$ in continuous PNs.

Here, we always consider continuous net systems whose initial marking marks all *P-semiflows*, which can be verified by solving the following Linear Programming Problem (LPP):

Algorithm 1.1. Verification of marking at P-semiflows.

Compute $z = min\{\mathbf{y}^T \mathbf{m}_0\}$ s.t.

$$\mathbf{y}^T \mathbf{C} = \mathbf{0}$$
$$\mathbf{y} \geq \mathbf{0}$$
$$\mathbf{y}^T \cdot \mathbf{1} = 1$$

If $z > 0$ **then** there are not unmarked P-semiflows.

1.4.2 Timed continuous Petri nets

Definition 1.8. A *timed continuous Petri net (TCPN)* is a time-driven continuous-state system described by the tuple $\langle \mathcal{N}, \boldsymbol{\lambda}, \mathbf{m}_0 \rangle$, where $\langle \mathcal{N}, \mathbf{m}_0 \rangle$ is a *continuous* PN and the vector $\boldsymbol{\lambda} \in \mathbb{R}_{>0}^{|T|}$ represents the transitions rates that determine the temporal evolution of the system. Transitions fire according to certain speed, which generally is a function of the rates and the instantaneous marking. Like in Markovian *discrete* PNs, under *infinite server semantics* the *flow* (the firing speed, denoted as $\mathbf{f}(\mathbf{m})$) through a transition t_i is defined as the product of the rate, λ_i, and $enab(t_i, \mathbf{m})$, the instantaneous enabling of the transition, i.e., $f_i(\mathbf{m}) = \lambda_i \cdot enab(t_i, \mathbf{m}) = \lambda_i \cdot \min_{p \in {}^\bullet t_i}\{\mathbf{m}[p]/\mathbf{Pre}[p, t_i]\}$.

For the flow to be well defined, every continuous transition must have at least one input place, hence in the following we will assume $\forall t \in T, |{}^\bullet t| \geq 1$. The "min" in the above definition leads to the concept of *configurations*:

Definition 1.9. A *configuration* is a set of pairs $\mathcal{C} = \{(t_1, p^1), (t_2, p^2), ..., (t_{|T|}, p^{|T|})\}$ where $\forall t_k \in T$, $p^k \in {}^\bullet t_k$ is a place that, for some markings, provides the minimum ratio $\mathbf{m}[p^k]/\mathbf{Pre}[p^k, t_j]$. In such case, it is said that p^k *constrains* t_k. An upper bound for the number of configurations is $\prod_{t \in T} |{}^\bullet t|$.

For each possible configuration $\mathcal{C}_i$, a configuration matrix of dimension $|T| \times |P|$ is defined, denoted as $\mathbf{\Pi}_i$, in the following way:

$$\forall j \in \{1,..,|T|\}, k \in \{1,..,|P|\}, \qquad [\mathbf{\Pi}_i]_{j,k} = \begin{cases} \frac{1}{[\mathbf{Pre}]_{k,j}} & \text{if } p_k \text{ is constraining } t_j \text{ in } \mathcal{C}_i \\ 0 & \text{otherwise} \end{cases}$$

The set of all configuration matrices of the net system is denoted as $\{\mathbf{\Pi}\}$. Given a marking $\mathbf{m}$, the configuration operator $\mathbf{\Pi}(\mathbf{m})$ is defined as: $\mathbf{\Pi}(\mathbf{m}) = \mathbf{\Pi}_i$ where $\mathcal{C}_i$ is associated to $\mathbf{m}$, i.e., if $\mathbf{\Pi}_i\mathbf{m} = \mathbf{enab}(\mathbf{m})$. If $\mathbf{m}$ can be associated to more than one configuration, i.e., if $\exists \mathbf{\Pi}_i, \mathbf{\Pi}_j$ s.t. $\mathbf{\Pi}_i\mathbf{m} = \mathbf{\Pi}_j\mathbf{m} = \mathbf{enab}(\mathbf{m})$, and a particular configuration is not specified in the context, then any of them can be taken. For convention, let us take the one with the lowest index.

In this way, the flow through the transitions can be written in a vectorial form as $\mathbf{f}(\mathbf{m}) = \mathbf{\Lambda\Pi}(\mathbf{m})\mathbf{m}$, where $\mathbf{\Lambda}$ is a diagonal matrix whose elements are those of $\boldsymbol{\lambda}$. The dynamical behavior of a PN system is described by its state equation:

$$\dot{\mathbf{m}} = \mathbf{C\Lambda\Pi}(\mathbf{m})\mathbf{m} \tag{1.4}$$

1.4.3 State invariant and marking regions

It is a fact well-known that, given a *P-flow* $\mathbf{y}$, for any reachable marking $\mathbf{m}$, it holds $\mathbf{y}^T\mathbf{m} = \mathbf{y}^T\mathbf{m}_0$. Then, whenever a TCPN system has *P-flows*, linear dependencies between marking variables appear, introducing *state invariants* (from a Control Theory perspective). The following definition characterizes such state invariant.

Definition 1.10. The set $Class(\mathbf{m}_0)$ is defined as the equivalence class of $\mathbf{m}_0$ under the relation $\beta \subseteq \mathbb{R}_{\geq 0}^{|P|} \times \mathbb{R}_{\geq 0}^{|P|}$ defined as: $(\mathbf{m}_1, \mathbf{m}_2) \in \beta$ iff $\mathbf{B}_y^T\mathbf{m}_1 = \mathbf{B}_y^T\mathbf{m}_2$, where $\mathbf{B}_y$ is a basis of P-flows, i.e., $Class(\mathbf{m}_0) = \{\mathbf{m} \in \mathbb{R}_{\geq 0}^{|P|} | \mathbf{B}_y^T\mathbf{m} = \mathbf{B}_y^T\mathbf{m}_0\}$.

Remark 1.11. For a general TCPN system, every reachable marking belongs to $Class(\mathbf{m}_0)$.

The set $Class(\mathbf{m}_0)$ can be partitioned (except on the borders) into subsets of markings associated to different configurations:

Definition 1.12. For each configuration $\mathcal{C}_i$ (equivalently, for each value $\mathbf{\Pi}_i$ that the configuration matrix can take), a marking *region* is defined as the set $\Re_i = \{\mathbf{m} \in Class(\mathbf{m}_0) | \mathbf{\Pi}_i\mathbf{m} \leq \mathbf{\Pi}_j\mathbf{m}, \forall \mathbf{\Pi}_j \in \{\mathbf{\Pi}\}\}$.

Such regions are convex sets and inside each one the state equation (1.6) is linear, i.e., $\mathbf{\Pi}(\mathbf{m})$ is constant. Consider the affine hull of $Class(\mathbf{m}_0)$ given by $\text{aff}\{Class(\mathbf{m}_0)\} = \{\mathbf{m} | \mathbf{m} = \mathbf{C}\boldsymbol{\alpha} + \mathbf{m}_0, \boldsymbol{\alpha} \in \mathbb{R}^{|T|}\})$. In the sequel, let us denote by $int\{Class(\mathbf{m}_0)\}$ and $int\{\Re_i\}$ the sets of interior markings of $Class(\mathbf{m}_0)$ and $\Re_i$, considering neighborhoods on $\text{aff}\{Class(\mathbf{m}_0)\}$. Otherwise stated, $\mathbf{m}^q \in int\{Class(\mathbf{m}_0)\}$ if there exists an open neighborhood $N(\mathbf{m}^q)$ about $\mathbf{m}^q$ s.t. $N(\mathbf{m}^q) \cap \text{aff}\{Class(\mathbf{m}_0\} \subseteq Class(\mathbf{m}_0)$. Similarly, $\mathbf{m}^q \in int\{\Re_i\}$ if $\exists N(\mathbf{m}^q)$ s.t. $N(\mathbf{m}^q) \cap \text{aff}\{Class(\mathbf{m}_0)\} \subseteq \Re_i$ (in fact, $int\{Class(\mathbf{m}_0)\}$ is the relative interior of $Class(\mathbf{m}_0)$ but $int\{\Re_i\}$ is not the relative interior of $\Re_i$).

Remark 1.13. For each configuration $\mathcal{C}_i$ (set of input arcs) there is an associated marking region $\Re_i$, in the set $Class(\mathbf{m}_0)$, where the configuration matrix $\mathbf{\Pi}(\mathbf{m})$ takes a fixed value $\mathbf{\Pi}_i$, leading to a constant

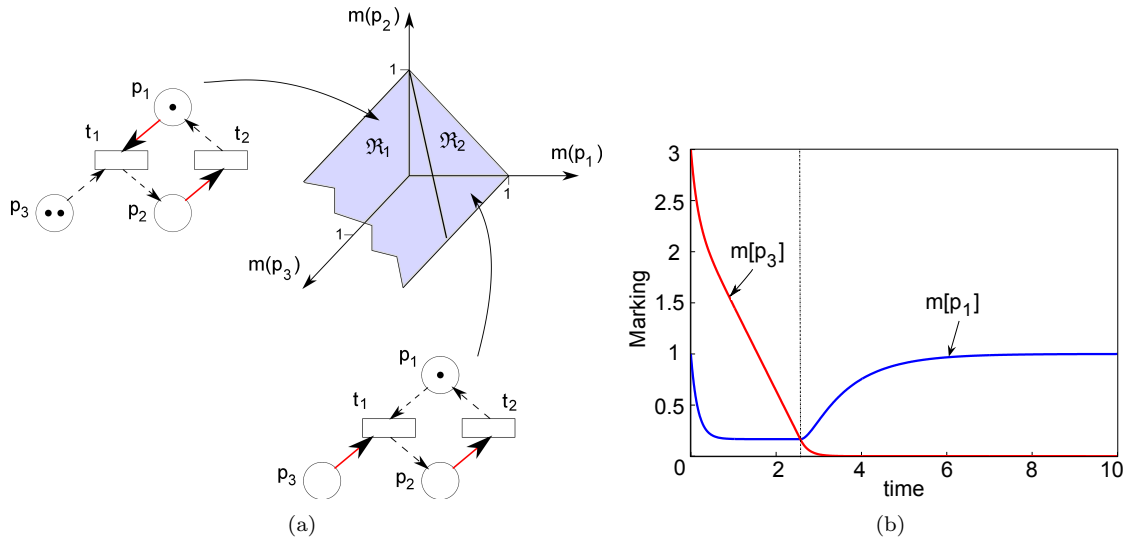

Fig. 1.2: a) A TCPN system and its $Class(\mathbf{m}_0)$. b) Transient evolution of markings at p_1 and p_3.

state matrix $\mathbf{C\Lambda\Pi}_i$ in the state equation (1.4) (equivalently, each configuration/region corresponds to a linear operation mode in the sense of piece-wise affine systems [Habets and van Schuppen, 2004]). In particular, *Join-Free* net systems are linear.

Example 1.3. Consider the TCPN defined by the net model depicted in fig. 1.2(a) with initial marking $\mathbf{m}_0 = [1, 0, 2]^T$ and $\boldsymbol{\lambda} = [5, 1]^T$. There is a synchronization at t_1, leading to two configurations: $\mathcal{C}_1 = \{(t_1, p_1), (t_2, p_2)\}$ and $\mathcal{C}_2 = \{(t_1, p_3), (t_2, p_2)\}$, whose corresponding arcs are depicted in solid line in fig. 1.2(a). These configurations define the corresponding configuration matrices:

$$\mathbf{\Pi}_1 = \begin{array}{c} \\ t_1 \\ t_2 \end{array} \begin{array}{c} \begin{array}{ccc} p_1 & p_2 & p_3 \end{array} \\ \begin{bmatrix} 1 & 0 & 0 \\ 0 & 1 & 0 \end{bmatrix} \end{array}, \qquad \mathbf{\Pi}_2 = \begin{array}{c} \\ t_1 \\ t_2 \end{array} \begin{array}{c} \begin{array}{ccc} p_1 & p_2 & p_3 \end{array} \\ \begin{bmatrix} 0 & 0 & 1 \\ 0 & 1 & 0 \end{bmatrix} \end{array}$$

A basis for the P-flows is given by $\mathbf{y} = [1, 1, 0]^T$, meaning that the sum of $\mathbf{m}[p_1] + \mathbf{m}[p_2]$ remains constant and equal to one. In this way, the set $Class(\mathbf{m}_0)$ is defined as the set $\{\mathbf{m} \geq \mathbf{0} | [1, 1, 0] \cdot \mathbf{m} = 1\}$, which is depicted in fig. 1.2(a) as a shadowed surface. This surface is divided into regions, according to the configurations, leading to the sets denoted as $\Re_1$ and $\Re_2$ in fig. 1.2(a). The bold line that separates both regions are actually markings belonging to both. While the system evolves in $\Re_1$, the configuration associated is $\mathcal{C}_1$, an the corresponding configuration matrix is given by $\mathbf{\Pi}(\mathbf{m}) = \mathbf{\Pi}_1$, thus, the system will evolve according to $\dot{\mathbf{m}} = \mathbf{C\Lambda\Pi}_1 \cdot \mathbf{m}$. Analogously, while the system evolves in $\Re_2$, the transient behavior is determined by $\dot{\mathbf{m}} = \mathbf{C\Lambda\Pi}_2 \cdot \mathbf{m}$. From a Control Theory perspective, the system is piecewise linear.

Finally, fig. 1.2(b) shows the transient evolution of the TCPN system for the marking at places p_1 and p_3. Note the abrupt change on the tendency of the marking p_1 when the curves cross each other (equivalently, when they cross the vertical dashed line), which corresponds to a change of configuration.

1.4.4 Discrete-time difference equation

Let us introduced a discrete time version of the state equation of a TCPN system. This will be particularly used in Chapter 2.

Given a TCPN system and its state equation (1.4), a discrete-time version of it, taking a sampling period $\Delta\tau$, is derived as (by using Taylor's series, for more details see [Phillips and Nagle, 1984]):

$$\begin{gathered}\mathbf{m}_{k+1} = \mathbf{A}_D \mathbf{m}_k \\ where\ \mathbf{A}_D = \sum_{r=0}^{\infty} \frac{(\mathbf{C}\boldsymbol{\Lambda}\boldsymbol{\Pi}(\mathbf{m}_k)\Delta\tau)^r}{r!}\end{gathered}$$

For a small enough $\Delta\tau$, $\mathbf{A}_D \simeq \mathbf{I} + \mathbf{C}\boldsymbol{\Lambda}\boldsymbol{\Pi}(\mathbf{m}_k)\Delta\tau$ (a first order approximation of the Taylor's series). Therefore, $\mathbf{m}_{k+1}$ is approximated by

$$\begin{aligned}\mathbf{m}_{k+1} &\simeq \mathbf{m}_k + \mathbf{C}\boldsymbol{\Lambda}\boldsymbol{\Pi}(\mathbf{m}_k)\mathbf{m}_k\Delta\tau \\ &= \mathbf{m}_k + \mathbf{C}\cdot\mathbf{f}_k\Delta\tau\end{aligned} \tag{1.5}$$

where $\mathbf{f}_k = \boldsymbol{\Lambda}\boldsymbol{\Pi}(\mathbf{m}_k)\mathbf{m}_k$.

It is important to remark that (1.5) is an approximation of the marking evolution of the TCPN. The smaller $\Delta\tau$ the better the approximation. It may occur the case that by simulating the difference equation (1.5), negative markings are obtained, when the system evolves near to a border of $Class(\mathbf{m}_0)$ and $\Delta\tau$ is not small enough. In such case, a smaller $\Delta\tau$ needs to be used (assuming liveness, it can be proved that it always exists a small enough $\Delta\tau$ that guarantees nonnegative markings). In this way, in the forthcoming analysis it is assumed that $\Delta\tau$ is small enough.

1.4.5 Control in TCPNs

Control actions in continuous PNs may only be a reduction of the flow through the transitions. That is, transitions (machines for example) cannot work faster than their nominal speeds. In the original discrete Petri net, such control action is analogous to impose additional delays (temporarily blocking) to the firing of the corresponding enabled transitions.

Definition 1.14. The control vector $\mathbf{u} \in \mathbb{R}^{|T|}$ is defined s.t. u_i represents the control action on t_i. The effective flow through a controlled transition is given by: $f_i(\tau) = \lambda_i \cdot enab_i(\tau) - u_i(\tau)$, where $0 \leq u_i(\tau) \leq \lambda_i \cdot enab_i(\tau)$.
Transitions in which a control action can be applied are called *controllable*. The set of all controllable transitions is denoted by T_c, and the set of uncontrollable transitions is $T_{nc} = T - T_c$. If t_i is not controllable then u_i must be null.

The behavior of a TCPN forced system is described by the state equation:

$$\begin{aligned}\dot{\mathbf{m}} &= \mathbf{C}\boldsymbol{\Lambda}\boldsymbol{\Pi}(\mathbf{m})\mathbf{m} - \mathbf{C}\mathbf{u} \\ \text{subject to} \quad & \mathbf{0} \leq \mathbf{u} \leq \boldsymbol{\Lambda}\boldsymbol{\Pi}(\mathbf{m})\mathbf{m}\end{aligned} \tag{1.6}$$

A control action that fulfills the required constraints, i.e., $\forall t_i \in T_{nc}\ u_i = 0$ and $\mathbf{0} \leq \mathbf{u} \leq \boldsymbol{\Lambda}\boldsymbol{\Pi}(\mathbf{m})\mathbf{m}$, is called *suitable bounded* (s.b.). If an input is not s.b. then it cannot be applied.

If all the transitions are controllable, i.e., $T_c = T$, the controlled state equation can be rewritten as a linear system without state-feedback:

$$\begin{aligned} \dot{\mathbf{m}} &= \mathbf{C}\mathbf{w} \\ \text{s.t. } \mathbf{0} &\leq \mathbf{w} \leq \mathbf{\Lambda\Pi}(\mathbf{m})\mathbf{m} \end{aligned} \tag{1.7}$$

where $\mathbf{w}$ represents the control action. The constraint $\mathbf{0} \leq \mathbf{w} \leq \mathbf{\Lambda\Pi}(\mathbf{m})\mathbf{m}$ is equivalent to $\mathbf{0} \leq \mathbf{u} = \mathbf{f}(\mathbf{m}) - \mathbf{w} \leq \mathbf{\Lambda\Pi}(\mathbf{m})\mathbf{m}$, i.e., $\mathbf{u}$ is s.b..

Definition 1.15. A marking $\mathbf{m}^q$ for which $\exists \mathbf{u}^q$ s.b. such that $\mathbf{C}(\mathbf{\Lambda\Pi}(\mathbf{m}^q)\mathbf{m}^q - \mathbf{u}^q) = \mathbf{0}$ is called *equilibrium marking*, while $\mathbf{u}^q$ and $\mathbf{w}^q = (\mathbf{\Lambda\Pi}(\mathbf{m}^q)\mathbf{m}^q - \mathbf{u}^q)$ are said to be its corresponding *equilibrium input* and *equilibrium flow*, respectively.

If no control is being applied, i.e., if $T_c = \emptyset$, then the equilibrium markings are simply nonnegative solutions for $\mathbf{C\Lambda\Pi}(\mathbf{m}^q)\mathbf{m}^q = \mathbf{0}$ and $\mathbf{B}_y^T(\mathbf{m}^q - \mathbf{m}_0) = \mathbf{0}$.

1.5 Properties of continuous PNs

In the following, a few useful definitions and properties for continuous PNs are presented.

1.5.1 Liveness definitions

Different concepts for liveness in untimed continuous Petri nets were introduced in [Recalde et al., 1999]. In this work, the concepts regarding to lim-reachability (reachability considering infinite firing sequences) will be used. Recalling from there:

Definition 1.16. An autonomous (untimed) continuous PN model $\langle \mathcal{N}, \mathbf{m}_0 \rangle$ is said *live* if for every transition t_j and for any marking $\mathbf{m}$ reachable from $\mathbf{m}_0$ (allowing infinite firing sequences), a successor $\mathbf{m}'$ exists such that $enab(t_j, \mathbf{m}') > \mathbf{0}$.
A net $\mathcal{N}$ is structurally live if $\exists \mathbf{m}_0$ such that $\langle \mathcal{N}, \mathbf{m}_0 \rangle$ is live.

Those concepts can be extended to timed continuous PNs. This was explored in [Júlvez et al., 2006], assuming that the TCPN model reaches a *steady state* $\mathbf{m}_{ss}$, i.e., the system reaches $\mathbf{m}_{ss}$ and remains at this for all future time. Accordingly,

Definition 1.17. A TCPN system $\langle \mathcal{N}, \boldsymbol{\lambda}, \mathbf{m}_0 \rangle$ that reaches a steady state $\mathbf{m}_{ss}$ is said *live* if the steady state flow is positive, which is expressed as $f(\mathbf{m}_{ss}) > \mathbf{0}$. The timed net $\langle \mathcal{N}, \boldsymbol{\lambda} \rangle$ is said *structurally live* if there exists an initial marking $\mathbf{m}_0$ such that $\langle \mathcal{N}, \boldsymbol{\lambda}, \mathbf{m}_0 \rangle$ is live. Finally, a system $\langle \mathcal{N}, \boldsymbol{\lambda}, \mathbf{m}_0 \rangle$ that reaches a steady state, deadlocks if the steady state flow is null, i.e., $f_{ss}(\mathbf{m}_{ss}) = \mathbf{0}$.

From an algebraic perspective, steady states in TCPN systems are *equilibrium* markings, i.e., solutions of $\dot{\mathbf{m}} = \mathbf{C\Lambda\Pi}(\mathbf{m})\mathbf{m} = \mathbf{0}$ with $\mathbf{m} \in Class(\mathbf{m}_0)$. Equilibrium markings can be classified according to its flow, independently if they are reachable or not, as follows:

Definition 1.18. An equilibrium marking $\mathbf{m}_{ss}$ can be classified as:

1) If $\mathbf{f}(\mathbf{m}_{ss}) = \mathbf{0}$ then $\mathbf{m}_{ss}$ is called *deadlock marking*. The configuration and region related to $\mathbf{m}_{ss}$ are called *deadlock configuration* and *deadlock region*, respectively.

2) If for some transition t_j, $[\mathbf{f}(\mathbf{m}_{ss})]_j = 0$ (where $[\mathbf{f}(\mathbf{m}_{ss})]_j$ denotes the j-th entry of $\mathbf{f}(\mathbf{m}_{ss})$) then $\mathbf{m}_{ss}$ is called *non-live marking*. The configuration and region related to $\mathbf{m}_{ss}$ are called *non-live configuration* and *non-live region*, respectively.

3) If $\mathbf{f}(\mathbf{m}_{ss}) > \mathbf{0}$ then $\mathbf{m}_{ss}$ is called *live marking*.
If in a given region $\Re_i$ there do not exist non-live equilibrium markings, then $\Re_i$ is called *live region*, and the associated configuration is said *live*.

Remark 1.19. According to the deadlock-freeness definition, a deadlock occurs when the system (asymptotically) reaches a deadlock marking. Similarly, the system becomes non-live when it (asymptotically) reaches a non-live marking. If the system reaches a live equilibrium marking, then it is live.

1.5.2 Eigenvalues of the state matrix for TCPNs

Regarding TCPNs, inside each region the state equation is linear, since $\mathbf{\Pi}(\mathbf{m})$ is constant. Thus, adopting a Control Theory perspective, the behavior of a TCPN can be analyzed *by regions* $\Re_i$ (or linear modes) through the knowledge of the eigenvalues and eigenvectors of the corresponding state matrices $\mathbf{C\Lambda\Pi}_i$. In particular, given a configuration matrix $\mathbf{\Pi}_i$, a number $s \in \mathbb{C}$ (in general, complex) is called *eigenvalue* if there exists a column vector $\mathbf{v} \in \mathbb{C}^{|P|}$ s.t.:

$$(s \cdot \mathbf{I} - \mathbf{C\Lambda\Pi}_i) \cdot \mathbf{v} = \mathbf{0} \tag{1.8}$$

Vector $\mathbf{v}$ is called *column eigenvector* related to s. Furthermore, if there exists such eigenvalue, there also exist a row vector $\mathbf{w}$, called *row eigenvector* related to s s.t.:

$$\mathbf{w} \cdot (s \cdot \mathbf{I} - \mathbf{C\Lambda\Pi}_i) = \mathbf{0} \tag{1.9}$$

Remark 1.20. Eigenvectors are related to P- and T-flows:

1) Given a P-flow $\mathbf{y}$, then $\forall \mathbf{\Lambda}, \mathbf{\Pi}_D$ it holds $\mathbf{y}^T \cdot \mathbf{C\Lambda\Pi}_D = \mathbf{0}$, which is equivalent to (1.9) with $\mathbf{w} = \mathbf{y}^T$ and $s = 0$. Therefore, *P-flows* are row eigenvectors related to a *zero valued eigenvalue* ($s = 0$), for any timing and any configuration (already shown in [Mahulea et al., 2008b]).

2) Given a column eigenvector $\mathbf{v}$ related to a *zero valued eigenvalue* (i.e., $\mathbf{v}$ that fulfills (1.8) with $s = 0$), then the vector $\mathbf{\Lambda\Pi}_D\mathbf{v}$ is a *T-flow*.

Nevertheless, neither all the row eigenvectors related to zero valued eigenvalues are associated to P-flows nor all the T-flows can be expressed as $\mathbf{\Lambda\Pi}_D\mathbf{v}$ with $\mathbf{v}$ being a column eigenvector (this is explored in detail in Chapter 3).

This perspective will be specially useful in Chapter 3 in order to study the connection between the timing and some behavioral properties. For that, a classification of the eigenvalues will be adopted.

- *Fixed eigenvalues* of $\mathbf{C\Lambda\Pi}_i$ are those that do not depend on $\mathbf{\lambda}$, i.e., they are timing independent.

- *Variable eigenvalues* of $\mathbf{C\Lambda\Pi}_i$ are those that depend on $\boldsymbol{\lambda}$.

In particular, zero valued eigenvalues related to P-flows are fixed (independently of $\boldsymbol{\lambda}$, every P-flow $\mathbf{y}$ fulfills $\mathbf{y}^T\mathbf{C\Lambda\Pi}_i = \mathbf{0}$). Similarly, a distinction will be made between *fixed* (timing independent) and *variable* poles.

1.6 Basic concepts on continuous-state dynamic systems

TCPN models are continuous-state systems, which are commonly studied in the Control Theory framework. In fact, TCPNs belong to a particular class of systems, called piecewise affine (in particular, piecewise linear without guard functions). Even more, if the net model exhibits a Join-Free structure, then the TCPN is a linear system, a class widely studied in the literature. In this way, through this dissertation, TCPNs will be frequently studied by adopting a Control Theory approach, in order to take advantage of the numerous results and techniques developed for these systems. In this section, a few of concepts, that will be used in the following chapters, are recalled from the literature.

The so called modern Control Theory is based on the concept of *state*, which is defined as the information required (together with the input applied to the system) to uniquely determine the future *evolution* of the system (see, for instance, [Chen, 1984]). Otherwise stated, the state represents the memory that the dynamical system has of its past [Levine, 1996]. This information is codified into a real valued vector, commonly denoted as $\mathbf{x}$, whose entries are called *state variables*.

In this way, the vector space $\mathbb{R}^n$, where n is the number of state variables (thus, the length of $\mathbf{x}$), is called *state space*, since any value that the state can take belongs to $\mathbb{R}^n$. The evolution of the state is described by its state equation

$$\begin{aligned} \dot{\mathbf{x}} &= \mathbf{f}(\mathbf{x}, \mathbf{u}, \tau) \\ \mathbf{y} &= \mathbf{h}(\mathbf{x}, \tau) \end{aligned} \tag{1.10}$$

where $\mathbf{u}$ and $\mathbf{y}$ represent the control actions (inputs) and the available observations (outputs), respectively, $\mathbf{f}(\cdot)$ and $\mathbf{g}(\cdot)$ are properly defined mappings and τ denotes the time. For the study of continuous-state systems, $\mathbf{f}(\cdot)$ and $\mathbf{g}(\cdot)$ are restricted to particular structures. For instance, if they do not dependent on τ, they are called *time invariant*. A more particular case occurs when $\mathbf{f}(\cdot)$ and $\mathbf{g}(\cdot)$ are linear operators, i.e.,

$$\begin{aligned} \dot{\mathbf{x}} &= \mathbf{A} \cdot \mathbf{x} + \mathbf{B} \cdot \mathbf{u} \\ \mathbf{y} &= \mathbf{O} \cdot \mathbf{x} \end{aligned} \tag{1.11}$$

In this case, the system is called *linear and time invariant* (denoted as *LTI*) [Chen, 1984].

The dynamic evolution of a continuous-state system can be studied through the function $\mathbf{f}(\mathbf{x}, \mathbf{u}, \tau)$, called *field vector*. If no control action is being applied (or such control is a fixed function of the state) and the system is time invariant, then it is said *autonomous*, since the evolution of its state only depends on this, i.e.,

$$\dot{\mathbf{x}} = \mathbf{f}(\mathbf{x}) \tag{1.12}$$

A solution $\mathbf{x}'$ for $\mathbf{f}(\mathbf{x}') = \mathbf{0}$ is called *equilibrium point*. In the case of LTI systems, the study of the mapping $\mathbf{f}(\cdot)$ becomes into the analysis of $\mathbf{A}$, which is commonly addressed by using the Theory of Linear Algebra.

Among different properties, some that are classically studied are *controllability*, *observability* and *stability*.

1.6.1 Basic stability concepts

Stability is a central concept in the study of dynamical systems. This is defined in different ways. In this work, the concept of stability refers to equilibrium points. An intuitive, and rough, definition is that, given an equilibrium point of a dynamic system, it is stable if all the trajectories of the system, starting in a neighborhood of the equilibrium point, stay nearby. Let us recalled a more formal definition from [Levine, 1996], about the Lyapunov stability

Definition 1.21. Given a continuous-state system (1.12) and an equilibrium point $\mathbf{x}'$, this is

- stable, if for each $\varepsilon > 0$, there is $\delta = \delta(\varepsilon) > 0$ such that $||\mathbf{x}(0) - \mathbf{x}'||_2 < \delta \Longrightarrow ||\mathbf{x}(\tau) - \mathbf{x}'||_2 < \varepsilon$, $\forall \tau \geq 0$.
- unstable if it is not stable.
- asymptotically stable if it is stable and δ can be chosen such that $||\mathbf{x}(0) - \mathbf{x}'||_2 < \delta \Longrightarrow lim_{\tau\rightarrow}\mathbf{x}(\tau) = \mathbf{x}'$

One of the main results in the study of stability is the so-called Lyapunov's stability theorem, which provides a sufficient condition for stability.

Theorem 1.22. *Let $\mathbf{x} = \mathbf{0}$ be an equilibrium point for (1.12) and $D \subset \mathbb{R}^n$ be a domain containing $\mathbf{x} = \mathbf{0}$. Let $V : D \rightarrow \mathbb{R}$ be a continuous differentiable function (commonly named Lyapunov function) such that: $V(\mathbf{0}) = 0$, $V(\mathbf{x}) > 0$ in $D - \{\mathbf{0}\}$ and $\dot{V}(\mathbf{x}) \leq \mathbf{0}$ in D. Then $\mathbf{x} = \mathbf{0}$ is stable. Moreover, if $\dot{V}(\mathbf{x}) < \mathbf{0}$ in $D - \{\mathbf{0}\}$ then $\mathbf{x} = \mathbf{0}$ is asymptotically stable.*

In linear systems, the stability can be decided from the eigenstructure of its sate matrix $\mathbf{A}$.

Theorem 1.23. *The equilibrium point $\mathbf{x} = \mathbf{0}$ of $\dot{\mathbf{x}} = \mathbf{A}\mathbf{x}$ is stable iff all the eigenvalues of $\mathbf{A}$ satisfy $Real\{s_i\} \leq 0$ and for every eigenvalue with $Real\{s_i\} = 0$ and algebraic multiplicity $r_i \geq 2$, $rank(\mathbf{A} - s_i\mathbf{I}) = n - r_i$, where n is the dimension of $\mathbf{x}$. The equilibrium point $\mathbf{x} = \mathbf{0}$ is (globally) asymptotically stable iff all eigenvalues satisfy $Real\{s_i\} < 0$ (in such case, $\mathbf{A}$ is called Hurwitz).*

Even if previous theorems consider $\mathbf{x}' = \mathbf{0}$ as the equilibrium point under study, these results can be applied when $\mathbf{x}' \neq \mathbf{0}$, just by defining the shifted variable $\mathbf{x}_{aux} = \mathbf{x} - \mathbf{x}'$ that evolves as $\dot{\mathbf{x}}_{aux} = \mathbf{g}(\mathbf{x}_{aux}) = \mathbf{f}(\mathbf{x}_{aux} + \mathbf{x}')$.

1.6.2 Basic controllability concepts

Controllability is a basic concept in dynamic systems related to the capability of these for being driven in a certain desirable way. In DEDS, the concept of controllability is related to the possibility of inducing an invariant set of trajectories, describing a safe behavior. Nevertheless, from a continuous-state systems perspective, the controllability concept is related to the capability for reaching state-points in the sate space. This topic will be studied in Chapter 4 for TCPNs by adopting a continuous-state systems approach, for this reason, here some basic concepts are recalled (see, for example, [Chen, 1984]).

Definition 1.24. A state equation is fully controllable if there exists an input such that for any two states $\mathbf{x}_1$ and $\mathbf{x}_2$ of the state space, it is possible to transfer the state from $\mathbf{x}_1$ to $\mathbf{x}_2$ in finite time.

Restricted to LTI systems, the controllability can be decided in a simple way. The fundamental idea is that the reachability set (from the origin) is determined by the span of $e^{\mathbf{A}\tau}\mathbf{B}$. This reachability set covers the complete state space (which in continuous-time LTI systems is equivalent to controllability) iff there do not exist state invariants (under any control action, i.e., $\nexists \mathbf{w} \neq \mathbf{0}$ s.t. $\mathbf{w}^T e^{\mathbf{A}\tau}\mathbf{B} = \mathbf{0}$), which can be stated in different ways (for more details, the reader may consult [Chen, 1984]):

Theorem 1.25. *Given an n-dimensional LTI system (1.11), it is controllable iff any of the following equivalent conditions is satisfied.*

I. all rows of $e^{\mathbf{A}\tau}\mathbf{B}$ are linearly independent on $[0, \infty)$ over $\mathbb{C}$, the field of complex numbers.

II. all rows of $(s\mathbf{I} - \mathbf{A})^{-1}\mathbf{B}$ are linearly independent over $\mathbb{C}$.

III. the controllability matrix $Contr(\mathbf{A}, \mathbf{B}) = [\mathbf{B}, \mathbf{AB}, ..., \mathbf{A}^{n-1}\mathbf{B}]$ has rank n.

IV. for every eigenvalue s of $\mathbf{A}$, the complex matrix $[s\mathbf{I} - \mathbf{A}, \mathbf{B}]$ has rank n.

In the previous theorem, there is no restriction on the control actions that can be applied to the system. Regarding that issue, Brammer [Brammer, 1972] addressed the *null-controllability* problem for LTI systems where the input is restricted to a convex set Ω. Let us firstly recall the null-controllability concept:

Definition 1.26. ([Brammer, 1972]) A linear state equation $\dot{\mathbf{x}} = \mathbf{Ax} + \mathbf{Bu}$ is *null-controllable* if there exists a small enough neighborhood $N(\mathbf{0})$ about the origin from which $\mathbf{x} = \mathbf{0}$ is reachable in finite time.

Furthermore, given a set S containing the origin, it is said that the system is null-controllable *over* S if there exists a small neighborhood $N(\mathbf{0})$ about the origin s.t. $\mathbf{x} = \mathbf{0}$ is reachable from any state in $N(\mathbf{0}) \cap S$.

The basic results of Brammer are recalled next:

Theorem 1.27 ((Brammer, 1972))**.** *Consider a LTI system (1.11) with the input constraint $\mathbf{u} \in \Omega$.*

I. If $\mathbf{u} = \mathbf{0}$ is an interior *point of Ω (meaning that all the inputs can be settled as either positive or negative), the system is null-controllable iff the controllability matrix $Contr(\mathbf{A}, \mathbf{B})$ has full rank.*

II. If $\exists \mathbf{u} \in \Omega$ s.t. $\mathbf{Bu} = \mathbf{0}$ and the convex hull of Ω has nonempty interior (useful if some inputs can only be positive or can only be negative), the system is null-controllable iff $Contr(\mathbf{A}, \mathbf{B})$ has full rank and there is no real eigenvector $\mathbf{v}$ of $\mathbf{A}^T$ satisfying $\mathbf{v}^T\mathbf{Bu} \leq \mathbf{0}$ $\forall \mathbf{u} \in \Omega$.

The first case amounts to the classical condition for linear unconstrained systems (because $\mathbf{u} = 0$ is in the interior of Ω). In the second case, the input constraints may disable some directions, which is captured by the additional condition (directions disabled have a positive projection on a vector $\mathbf{v}$, being a real eigenvector of $\mathbf{A}^T$ s.t. $\mathbf{v}^T\mathbf{Bu} \leq \mathbf{0}$ $\forall \mathbf{u} \in \Omega$).

In this way, a few basic concepts regarding Petri nets and state-continuous systems have been recalled through this chapter. This quick overview provides a ground material for the the analysis and

concepts that will be introduced in the following chapters. For more details, the reader may consult [Murata, 1989, Silva, 1993] for discrete, [Marsan et al., 1995] for stochastic, and [David and Alla, 2010, Silva and Recalde, 2004] for continuous PNs. Similarly, useful concepts and results for state-continuous systems can be found in [Chen, 1984, Khalil, 2002].

Chapter 2

Fluidization

2.1 Continuous PNs as relaxations of Markovian models

Timed continuous Petri nets, under infinite server semantics, were proposed [Recalde and Silva, 2001] by using the *Markovian* interpretation of discrete Petri nets as the reference (equivalent to the *variable speed* fluid model introduced by Alla and David [Alla and David, 1998]). The reasons for this choice are that Markovian (discrete) Petri nets (MPN, as defined in Subsection 1.3.1) enjoy the time memoryless property and the current marking represents all the information required for the future evolution of the system. MPN are widely used for the analysis of performance evaluation [Marsan et al., 1995, Balbo and Silva, 1998]. Furthermore, the exact analysis of MPNs, via the isomorphous Markov Chain [Molloy, 1982], frequently leads to an untractable computational complexity, because of the state explosion problem.

In this way, given a continuous net model, it is expected that this approximates the behavior of the corresponding original discrete PN. Nevertheless, such approximation does not always hold. Despite the relevance of this problem, there are just a few works in the literature addressing this. In particular, Zerhouni & Alla [Zerhouni and Alla, 1990] considered the approximation of deterministically timed Petri nets by variable speed continuous PN's. They proposed a criterion for validating the continuous model through simulations, but no formal analysis was achieved. Mahulea et al. [Mahulea et al., 2009] proved that for mono-T-semiflow nets (conservative and consistent nets with a unique minimal T-semiflow), a TCPN under infinite server semantics (ISS) provides a better approximation of the throughput of a stochastic PN than under finite server semantics, but this does not imply that the ISS actually provides a "good enough" approximation. Lefebvre et al. [Lefebvre et al., 2009] studied the throughput approximation of a subclass of stochastic PN's by fluid PN models, for which different semantics are introduced in order to provide a good steady state approximation. Nevertheless, there is still a lack of results regarding this problem. In particular, no formal analysis has been achieved for explaining when and why the approximation provided by a TCPN holds (or not).

In this framework, the approximation of MPNs by TCPN's is studied through this chapter. In some sense, here we deal with the *legitimization* of the so called infinite server semantics. According to the results obtained, under liveness and stability assumptions the marking of the TCPN approximates the *average* marking of the MPN if the system mainly evolves inside one region of the reachability set (a perfect match is obtain for ordinary Join Free nets). The approximation becomes better when the number

of active servers is large. Later, in order to improve the approximation when the system evolves through several regions, white gaussian noise is added to the transitions' flow, leading to a new stochastic model (denoted as TnCPN). The approximation provided by this model is also analyzed.

In a third step, a hybrid Petri net model MHPN is introduced as a *partial relaxation* of a MPN. It is shown that the approximation provided by such hybrid systems is not always better than that provided by full relaxations (given by fully continuous Petri nets). For this reason, different results are introduced, which may lead to provided sufficient conditions for an effective approximation. Finally, a couple of preliminarily ideas are advanced for the improvement of the approximation, by means of the modification of the structure and the semantics for particular transitions of the TCPN model.

2.2 On the approximation of MPNs by TCPNs: deterministic approximation

Through this section, it will be shown that the expected value of the marking of a MPN system can be approximated by the marking of the corresponding TCPN, under some particular assumptions. Let us remark that it is desirable to approximate not only the throughput, but also the complete marking during the transient behavior, because the marking represents the complete *state* of the system. Let us introduce first some useful definitions and notation.

Given a temporal variable, e.g. $\mathbf{M}_k$, the term $M_{k,j}$ will denote the j-th entry of the vector $\mathbf{M}_k$.

Definition 2.1. Given a MPN system and the corresponding TCPN one, the *marking approximation error* is defined as $\boldsymbol{\varepsilon}_k = \mathbf{m}_k - E\{\mathbf{M}_k\}$. Similarly, the *relative approximation error* of the marking is defined, for each $p_i \in P$, as $\epsilon_i = (m_{k,i} - E\{M_{k,i}\})/E\{M_{k,i}\}$ (assuming $E\{M_{k,i}\} > 0$).

2.2.1 Join-Free models

Proposition 2.2. *Consider an ergodic $MPN = \langle \mathcal{N}, \boldsymbol{\lambda}, \mathbf{M}_0 \rangle$, where $\mathcal{N}$ is Join-Free. Consider the corresponding $TCPN = \langle \mathcal{N}, \boldsymbol{\lambda}, \mathbf{m}_0 \rangle$, where $\mathbf{M}_0 = \mathbf{m}_0$.*
1) If $\mathcal{N}$ is ordinary then the marking of the TCPN is equal to the average value of the marking of the MPN, i.e., $\boldsymbol{\varepsilon}_k = \mathbf{0}$.
2) In non ordinary nets, approximation errors may appear. If the TCPN has a unique asymptotically stable equilibrium point in $Class(\mathbf{m}_0)$ then the approximation errors are ultimately bounded. The larger the average enabling degrees the lower the relative errors ($\boldsymbol{\epsilon}_k \to \mathbf{0}$), and thus, the better the approximation.

Proof. Assume that $\mathcal{N}$ is Join-Free, i.e., there are not synchronizations (rendez-vous). Then, the configuration matrix is constant $\boldsymbol{\Pi}$. According to this, the state equation of the TCPN (1.5) can be expressed as

$$\mathbf{m}_{k+1} \simeq [\mathbf{I} + \mathbf{C}\boldsymbol{\Lambda}\boldsymbol{\Pi}\Delta\tau]\,\mathbf{m}_k \tag{2.1}$$

Now, let us derive an expression for the expected value of the marking of the MPN system. According to (1.2), the expected value (average) of the marking at time step $k+1$ (denoted as $E\{\mathbf{M}_{k+1}\}$) can be

approximated by

$$E\{\mathbf{M}_{k+1}\} = E\{\mathbf{M}_k\} + \mathbf{C} \cdot E\{\Delta\boldsymbol{\sigma}(\mathbf{F}_k\Delta\tau)\} \tag{2.2}$$

By using the definitions of $\Delta\boldsymbol{\sigma}(\mathbf{F}_k\Delta\tau)$ and $\mathbf{F}_k$, and the fact that the average value of a Poisson distributed r.v. is equal to its parameter, it can be proved that $E\{\Delta\boldsymbol{\sigma}(\mathbf{F}_k\Delta\tau)\} = E\{\mathbf{F}_k\Delta\tau\} = \boldsymbol{\Lambda} \cdot E\{Enab(\mathbf{M}_k)\}\Delta\tau$, where $Enab(\mathbf{M}_k) = \lfloor\boldsymbol{\Pi}(\mathbf{M}_k)\mathbf{M}_k\rfloor$. Defining $\mathbf{b}_k = \boldsymbol{\Pi}(\mathbf{M}_k)\mathbf{M}_k - \lfloor\boldsymbol{\Pi}(\mathbf{M}_k)\mathbf{M}_k\rfloor$, it can be seen that $E\{\Delta\boldsymbol{\sigma}(\mathbf{F}_k\Delta\tau)\} = \boldsymbol{\Lambda} \cdot E\{\boldsymbol{\Pi}(\mathbf{M}_k)\mathbf{M}_k\}\Delta\tau - \boldsymbol{\Lambda} \cdot E\{\mathbf{b}_k\}\Delta\tau$. Substituting this into (2.2) we obtain:

$$E\{\mathbf{M}_{k+1}\} = E\{\mathbf{M}_k\} + \mathbf{C}\boldsymbol{\Lambda} \cdot E\{\boldsymbol{\Pi}(\mathbf{M}_k)\mathbf{M}_k\}\Delta\tau - \mathbf{C}\boldsymbol{\Lambda} \cdot E\{\mathbf{b}_k\}\Delta\tau \tag{2.3}$$

Note that $\mathbf{b}_k$ represents the difference between the function $\boldsymbol{\Pi}(\mathbf{M}_k)\mathbf{M}_k$ and the enabling degree. This variable is null for ordinary nets (because $\boldsymbol{\Pi}(\mathbf{M}_k)\mathbf{M}_k = \lfloor\boldsymbol{\Pi}(\mathbf{M}_k)\mathbf{M}_k\rfloor$ in those), but in general $\mathbf{0} \leq \mathbf{b}_k \leq \mathbf{1}$, where $\mathbf{1}$ denotes a vector whose entries are 1's.

Now, since the configuration matrix is constant in Join-Free nets, (2.3) can be expressed as

$$E\{\mathbf{M}_{k+1}\} = [\mathbf{I} + \mathbf{C}\boldsymbol{\Lambda}\boldsymbol{\Pi}\Delta\tau]\, E\{\mathbf{M}_k\} - \mathbf{C}\boldsymbol{\Lambda} \cdot E\{\mathbf{b}_k\}\Delta\tau \tag{2.4}$$

Comparing (2.4) with (2.1), it can be seen that both coincide if $E\{\mathbf{b}_k\} = \mathbf{0}$, which holds if $\mathcal{N}$ is ordinary. In such case, the marking trajectory of the TCPN system is equal to the trajectory described by the expected value of the marking of the corresponding MPN, thus statement 1 is proved.

For non ordinary nets the evolution of $E\{\mathbf{M}_k\}$ and $\mathbf{m}_k$ is not exactly the same, due to the term $\mathbf{C}\boldsymbol{\Lambda} \cdot E\{\mathbf{b}_k\}\Delta\tau$ that appears in (2.4) but not in (2.1). Nevertheless, it holds that $\mathbf{0} \leq \mathbf{b}_k \leq \mathbf{1}$. Therefore, the effect that the variable $\mathbf{b}_k$ introduces in the evolution of $E\{\mathbf{M}_k\}$ can be analyzed as a perturbation in the model without such term. Let us detail this idea:

Consider the approximation error $\boldsymbol{\varepsilon}_k = \mathbf{m}_k - E\{\mathbf{M}_k\}$. Then, according to (2.1) and (2.4), it is obtained:

$$\boldsymbol{\varepsilon}_{k+1} = [\mathbf{I} + \mathbf{C}\boldsymbol{\Lambda}\boldsymbol{\Pi}\Delta\tau]\, \boldsymbol{\varepsilon}_k + \mathbf{C}\boldsymbol{\Lambda} \cdot E\{\mathbf{b}_k\}\Delta\tau \tag{2.5}$$

In the sequel, the term $\mathbf{C}\boldsymbol{\Lambda} \cdot E\{\mathbf{b}_k\}\Delta\tau$ will be called *perturbation*. In this way, the evolution of the error can be seen as a nominal system, described by $\boldsymbol{\varepsilon}_{k+1} = [\mathbf{I} + \mathbf{C}\boldsymbol{\Lambda}\boldsymbol{\Pi}\Delta\tau]\, \boldsymbol{\varepsilon}_k$, under non-vanishing (it exists even if $\boldsymbol{\varepsilon}_k = \mathbf{0}$) but bounded perturbation. Now, let us assume that the origin ($\boldsymbol{\varepsilon} = \mathbf{0}$) is asymptotically stable in the nominal system, i.e., the TCPN system reaches the same steady state marking starting from any initial one inside $Class(\mathbf{m}_0)$ (equivalently, the eigenvalues of $[\mathbf{I} + \mathbf{C}\boldsymbol{\Lambda}\boldsymbol{\Pi}\Delta\tau]$, non related to P-flows, are inside the unity circle [Phillips and Nagle, 1984]). According to a well-known stability results (see, for example, [Khalil, 2002], Lemma 9.2, page 347), the asymptotic stability in the nominal error system implies that the error $\boldsymbol{\varepsilon}_k$ is ultimately bounded, i.e., there exists a bound β s.t. $\|\boldsymbol{\varepsilon}_k\| \leq \beta$ for all $k \geq \eta$, with $\tau_0 + \eta\Delta\tau$ being a finite time. Actually, it can be proved that such bound β depends on the structure and timing, but not on the initial marking. The computation of such bound is shown in Appendix B.

Finally, consider the relative approximation error ($\epsilon_i = \varepsilon_{k,i}/E\{M_{k,i}\}$, $\forall p_i \in P$). Since $\varepsilon_{k,i}$ is upper bounded by a constant value, then the larger $E\{M_{k,i}\}$, the lower ϵ_i. This can be seen directly in (2.4), by noting that if $\boldsymbol{\Pi} \cdot E\{\mathbf{M}\} >> \mathbf{1}$ then (2.4) is well approximated by (2.1), because in such case $|E\{\mathbf{b}_k\}| \leq \mathbf{1}$ is less significant; moreover, the errors are not accumulated because the nominal system is asymptotically

Tab. 2.1: Marking approximation of p_2 for the JF MPN in fig. 2.1(a), where $\mathbf{M}_0 = \mathbf{m}_0 = q \cdot [1,1,1]^T$

q	MPN	TCPN	error
1	0.600	0.75	25.0%
3	2.126	2.25	5.81%
4	2.878	3.00	4.25%
6	4.370	4.50	2.98%
10	7.422	7.50	1.04%
15	11.911	12.00	0.75%

stable. Roughly speaking, the larger the number of active servers (which is related to $\mathbf{\Pi} \cdot E\{\mathbf{M}_k\}$), the better the approximation. ∎

Example 2.1. Consider the Join-Free MPN of fig. 2.1(a) with firing rates $\lambda_1 = \lambda_2 = \lambda_3 = 1$. The TCPN system has been simulated, by using MatLab, and the steady-state results have been compared with those obtained for the MPN using TimeNET [Zimmermann and Knoke, 2007]. Table 2.1 resumes the results thus obtained. The first column represents the initial marking, given by $\mathbf{M}_0 = \mathbf{m}_0 = q \cdot [1,1,1]^T$. Second and third columns are the average marking of the MPN at the steady state, and the final value of the TCPN, respectively, for place p_2. The last column is the relative marking error.

This is a non ordinary Join-Free PN. Furthermore, in the TCPN model there exists only one equilibrium point (the steady state) which is asymptotically stable. Therefore, according to Proposition 2, it can be expected that, the larger the marking the lower the relative error, which is ultimately bounded. Note in table 2.1 that the relative error becomes lower as the average marking increases, which occurs for large values of q (this is a monotonic net, i.e., if the initial marking is increased, then the average marking at the steady state is also increased). Fig. 2.1(b) shows the evolution of both the marking of the TPCN and the expected value of the marking of the MPN, at place p_2, for $\mathbf{M}_0 = 10 \cdot [1,1,1]^T$. As it can be seen, not only the steady state but also the transient behavior of the MPN is well approximated by the TCPN.

2.2.2 Approximation in one region

In the previous subsection, the approximation of a MPN provided by the corresponding TCPN was analyzed for Join-Free nets. In general subclasses, the approximation may not hold even if the enabling degree of all the transitions is large. This is due to the change of marking regions during the evolution of the system, since this issue is not well captured by the flow definition in PNs. Let us illustrate this:

Example 2.2. Consider the MPN system of fig. 2.2, and its corresponding TCPN one, with initial marking $\mathbf{M}_0 = \mathbf{m}_0 = [5,5,55,5,6,4]^T$ and timing rates $\lambda_1 = \lambda_2 = \lambda_3 = 1$ for the first three transitions. Both the MPN and TCPN systems are simulated with different values for λ_4. The results are shown in Table 2.2. The values of the second and third columns correspond to the steady state marking of place p_3. The column denoted as $E\{Enab(t_4)\}$ is the average enabling degree of t_4 at the steady state. In all the experiments achieved, the average enabling degree of t_4 at the steady state was lower than those of the other transitions, thus, the larger this value, the larger the average enabling degrees of all the transitions. The value at the last column ($P.\mathbf{M} \in \Re_{ss}$) is the probability that the marking is inside

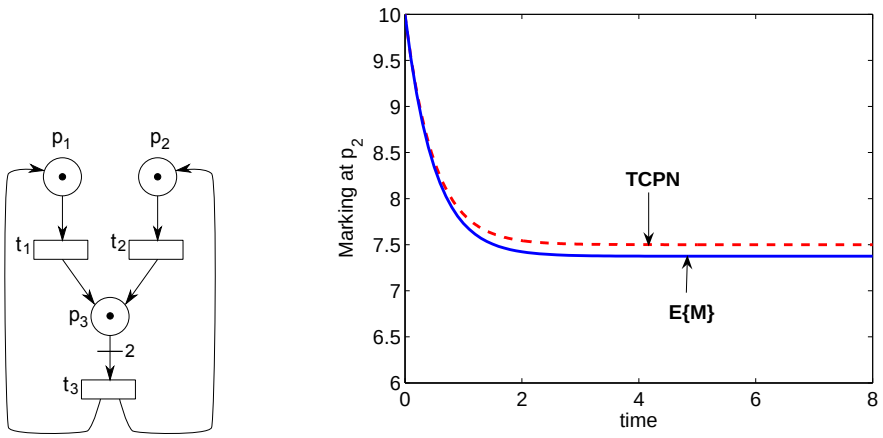

Fig. 2.1: (a) A JF, but non ordinary, net system. (b) For the initial marking $\mathbf{M}_0 = [10, 10, 10]^T$, the evolution of the average marking at p_2 is shown in solid line. In dashed line, the corresponding marking of the TCPN.

Tab. 2.2: Marking approximation of p_3 for the MPN of fig. 2.2

λ_4	MPN	TCPN	error	$E\{Enab(t_4)\}$	P. $\mathbf{M} \in \Re_{ss}$
2	54.62	55	0.7%	2.53	0.8433
1.5	53.87	55	2.1%	3.22	0.661
1.2	51.16	55	7.5%	3.88	0.413
1.1	46.65	55	17.9%	4.32	0.232
1.05	40.72	55	35.0%	4.56	0.115
1	29.97	55	83.5%	4.93	0.036

the region $\Re_{ss}$, which is the region associated to the steady state marking of the TCPN system, i.e., $\mathbf{m}_{ss} \in \Re_{ss}$. It can be observed that the lower the probability that $\mathbf{M}_k$ belongs to $\Re_{ss}$, the larger the relative error, even if the average enabling degrees increase.

Let us provide an intuitive explanation for this lack of approximation. If we consider the continuous model with $\lambda_4 = 1$ (when the approximation is worst), it can be proved that there exist *infinite equilibrium markings* in the configuration where t_2 is constrained by p_2 and t_3 is constrained by p_5, in fact, those equilibrium markings are characterized as $\{\mathbf{m} \in Class(\mathbf{m}_0) | \mathbf{m} = [5, 5, 5 + \alpha, 55 - \alpha, 5, 5]^T,\ 0 \leq \alpha \leq 50\}$. Then, the continuous system will reach one of those equilibrium markings, depending on the particular initial one (different steady states are reachable from different initial markings). On the contrary, the discrete net system is ergodic, then, independently of the initial marking (but belonging to $Class(\mathbf{m}_0)$), the steady state will be $[5, 5, 30, 30, 5, 5]^T$.

In the following, the approximation analysis is slightly extended, from the case of Join-Free nets, to systems in which the marking evolves inside a unique region with probability near to 1.

Proposition 2.3. *Consider a bounded in average and ergodic* $MPN = \langle \mathcal{N}, \boldsymbol{\lambda}, \mathbf{M}_0 \rangle$ *and the corresponding relaxation* $TCPN = \langle \mathcal{N}, \boldsymbol{\lambda}, \mathbf{m}_0 \rangle$*, with* $\mathbf{M}_0 = \mathbf{m}_0$*. If, for a given region* $\Re_j$*,* $Prob(\mathbf{M}_k \in \Re_j) \sim 1$*,* $\mathbf{m}_k \in \Re_j$ *during the time interval* $(\tau_0, \tau_0 + k\Delta\tau)$*, and the TCPN system has a unique asymptotically*

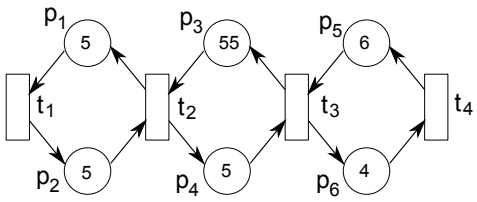

Fig. 2.2: Marked graph whose marking mainly evolves in two different regions.

stable equilibrium point in $\Re_j$, then the marking approximation error $\boldsymbol{\varepsilon}_k$ is ultimately bounded. The larger $Prob(\mathbf{M}_k \in \Re_j)$ and the average enabling degrees, the lower the relative approximation error $\boldsymbol{\epsilon}_k$.

Proof. Consider the equation (2.3) that appears in the proof of Proposition 2.2. This equation describes the dynamic evolution of the average marking of the MPN. Contrary to the previous case, in this one the system is not linear. Furthermore, (2.3) cannot be considered as a state equation of the average marking, since $E\{\mathbf{M}_{k+1}\}$ is not an *explicit* function of $E\{\mathbf{M}_k\}$, due to the term $E\{\mathbf{\Pi}(\mathbf{M}_k)\mathbf{M}_k\}$ (be aware that this is not equivalent to $\mathbf{\Pi}(E\{\mathbf{M}_k\})E\{\mathbf{M}_k\}$). Then, it is important to obtain an alternative representation of this term that leads to a proper state equation for $E\{\mathbf{M}_k\}$. By using conditional expected-value properties, it can be obtained

$$E\{\mathbf{\Pi}(\mathbf{M}_k)\mathbf{M}_k\} = \sum_{\forall \Re_i} \mathbf{\Pi}_i \cdot E\{\mathbf{M}_k | \mathbf{M}_k \in \Re_i\} Prob(\mathbf{M}_k \in \Re_i)$$

Assuming that the probability that $\mathbf{M}_k \in \Re_j$ is almost 1, for a particular $\Re_j$, then the previous equation can be substituted into (2.3), obtaining thus:

$$E\{\mathbf{M}_{k+1}\} = E\{\mathbf{M}_k\} + \mathbf{C}\mathbf{\Lambda}\mathbf{\Pi}_j \cdot E\{\mathbf{M}_k\}\Delta\tau + \mathbf{C}\mathbf{\Lambda}\left[\boldsymbol{\zeta}_k^j - E\{\mathbf{b}_k\}\right]\Delta\tau \tag{2.6}$$

where

$$\boldsymbol{\zeta}_k^j = \sum_{\forall \Re_i \neq \Re_j} \mathbf{\Pi}_i E\{\mathbf{M}_k | \mathbf{M}_k \in \Re_i\} Prob(\mathbf{M}_k \in \Re_i) + \mathbf{\Pi}_j \cdot [E\{\mathbf{M}_k | \mathbf{M}_k \in \Re_j\} Prob(\mathbf{M}_k \in \Re_j) - E\{\mathbf{M}_k\}] \tag{2.7}$$

Note that (2.6) is a state equation representation for $E\{\mathbf{M}_k\}$, so it can be used for analyzing the approximation provided by the corresponding TCPN system, as in the proof of Proposition 2.2. Before that, let us obtain a bound for $\boldsymbol{\zeta}_k^j$.

By hypothesis, $Prob(\mathbf{M}_k \in \Re_j) \sim 1$, then, let us assume that $E\{\mathbf{M}_k | \mathbf{M}_k \in \Re_j\} \simeq E\{\mathbf{M}_k\}$. Note that this assumption is much weaker than $\mathbf{M}_k \in \Re_j$, because even if the system does not evolve always inside $\Re_j$, for the *most probable* trajectories the marking belongs to $\Re_j$ (or at least close to the border of this region). In such case, $[E\{\mathbf{M}_k | \mathbf{M}_k \in \Re_j\} Prob(\mathbf{M}_k \in \Re_j) - E\{\mathbf{M}_k\}] \simeq E\{\mathbf{M}_k | \mathbf{M}_k \in \Re_j\}(Prob(\mathbf{M}_k \in \Re_j) - 1)$. Now, assume that the system is bounded in average, then, denoting as $\mathbf{M}_{max}$ the vector whose entries are the bounds for the average marking at the corresponding places, (2.7) can be relaxed as:

$$\begin{aligned} |\, \boldsymbol{\zeta}_k^j \,| \leq \quad & |\, \textstyle\sum_{\forall \Re_i \neq \Re_j} \mathbf{\Pi}_i \mathbf{M}_{max}(1 - Prob(\mathbf{M}_k \in \Re_j)) + \mathbf{\Pi}_j \mathbf{M}_{max}(Prob(\mathbf{M}_k \in \Re_j) - 1) \,| \\ & \leq \textstyle\sum_{\forall \Re_i} \mathbf{\Pi}_i \mathbf{M}_{max}(1 - Prob(\mathbf{M}_k \in \Re_j)) \end{aligned} \tag{2.8}$$

Therefore, given a lower bound for $Prob(\mathbf{M}_k \in \Re_j)$, the term $|\boldsymbol{\zeta}_k^j - E\{\mathbf{b}_k\}|$ in (2.6) is upper bounded by a constant value. Then, the approximation analysis in this case can be reduced to that used in the proof of Proposition 2.2. In detail, assuming that the TCPN evolves inside $\Re_j$, the evolution of the approximation error $\boldsymbol{\varepsilon}_k = \mathbf{m}_k - E\{\mathbf{M}_k\}$ is given by:

$$\boldsymbol{\varepsilon}_{k+1} = [\mathbf{I} + \mathbf{C}\boldsymbol{\Lambda}\boldsymbol{\Pi}_j\Delta\tau]\,\boldsymbol{\varepsilon}_k + \mathbf{C}\boldsymbol{\Lambda}\cdot\left[\boldsymbol{\zeta}_k^j - E\{\mathbf{b}_k\}\right]\Delta\tau \tag{2.9}$$

where $\left|\boldsymbol{\zeta}_k^j - E\{\mathbf{b}_k\}\right|$ can be seen as a perturbation whose magnitude is upper bounded by a function of $Prob(\mathbf{M}_k \in \Re_j)$. In this way, following an analysis similar to that used in the proof of Proposition 2.2 and assuming asymptotical stability of the the nominal system (in $\Re_j$), it can be proved that the approximation error is ultimately bounded by a function of $Prob(\mathbf{M}_k \notin \Re_j)$, thus, the larger $Prob(\mathbf{M}_k \in \Re_j)$ and the average marking, the lower the relative approximation error. ∎

Proposition 2.3 states that, in order to obtain an approximation by the $TCPN$ system, the following two conditions are sufficient:

- *Condition 1.* The enabling degree at the most probable markings of the MPN is large, i.e., $E\{Enab(t, \mathbf{M}_k)\} >> 1$, $\forall t \in T, \forall k$.
- *Condition 2.* The probability that the marking is inside the region $\Re_j$, where the TCPN evolves and has a unique asymptotically stable equilibrium point, is near to one, i.e., $Prob(\mathbf{M}_k \in \Re_j) \sim 1$, $\forall k$.

Remark 2.4. Even if the quality of the approximation decreases when the system changes of region (condition 2 does not hold temporarily) and/or the transitions are not enabled during certain period of time (condition 1), the approximation could be good enough for analysis and control purposes. Then, both conditions should be consider just as sufficient for the approximation.

Example 2.3. Consider again the MPN and the corresponding TCPN of fig. 2.2, and the results obtained from the simulations of these, shown in table 2.2. In this, it can be seen that, when the conditions of Proposition 2.3 are fulfilled, i.e., when the probability that the discrete marking is inside the region $\Re_{ss}$ is high like in the case $\lambda_4 = 2$, the approximation is good. This example shows the importance of the evolution inside a unique region.

2.3 Continuous models with noise: improving the approximation

In the previous section, it has been proved that the TCPN model can approximate the average marking of the corresponding MPN, if the probability that the MPN evolves inside a unique region (in which the TCPN also evolves) is near 1, i.e., condition 2. On the other hand, it was also shown through an example that if the MPN system evolves in different regions, the approximation may not be good. Through this section, a modification to the TCPN model is proposed in order to improve the approximation in such case. The modification consists in the addition of *white noise* to the transitions' flow of the TCPN model, obtaining thus a *continuous stochastic* system (TnCPN).

Definition 2.5. A *stochastic continuous* PN system, denoted as TnCPN, is defined as a TCPN $\langle \mathcal{N}, \boldsymbol{\lambda}, \mathbf{m}_0 \rangle$ in which the transitions' flow is stochastic, describing the following evolution (in discrete-time):

$$\begin{aligned} \mathbf{m}_{k+1} &= \mathbf{m}_k + \mathbf{C}\boldsymbol{\Lambda}\boldsymbol{\Pi}(\mathbf{m}_k)\mathbf{m}_k\Delta\tau + \mathbf{C}\mathbf{v}_k \\ &= \mathbf{m}_k + \mathbf{C}\cdot\Delta\mathbf{w}_k \end{aligned} \tag{2.10}$$

where $\Delta\mathbf{w}_k = \boldsymbol{\Lambda}\boldsymbol{\Pi}(\mathbf{m}_k)\mathbf{m}_k\Delta\tau + \mathbf{v}_k = \mathbf{f}_k\Delta\tau + \mathbf{v}_k$ and $\mathbf{v}_k$ is a noise column vector, of length $|T|$, whose elements are independent normally distributed r.v.'s with average value and covariance matrix:

$$\begin{aligned} E\{\mathbf{v}_k\} &= \mathbf{0} \\ \boldsymbol{\Sigma}_{\mathbf{v}_k} &= diag[\boldsymbol{\Lambda}\boldsymbol{\Pi}(\mathbf{m}_k)\mathbf{m}_k\Delta\tau] = diag[\mathbf{f}_k\Delta\tau] \end{aligned} \tag{2.11}$$

It may occur the case that by simulating the difference equation (2.10), negative markings are obtained. For this reason, for simulation purposes, the noise $\mathbf{v}_k$ is added only if $\mathbf{m}_{k+1} \geq \mathbf{0}$. This means that very close to boundaries the system may be kept as deterministic. In fact, if the system is crowded, i.e., $\mathbf{m}_0$ is large, the probability of getting $\mathbf{m}_{k+1} \ngeq \mathbf{0}$ is very low. On the other hand, in the forthcoming analysis it is always assumed that the system remains crowed, consequently, it will be assumed that the marking in (2.10) remains nonnegative.

In the sequel, it will be assumed that the MPN system is live an ergodic. Moreover, it will also assumed that there do not exist non-live equilibrium markings in $Class(\mathbf{m}_0)$ of the continuous Petri nets system (thus it is live).

2.3.1 Approximation of the expected value and covariance

The white noise added to the TCPN was defined in such a way that the expressions of the expected value and covariance of the MPN, and the resulting TnCPN, coincide. This will be shown through this section. First, let us obtain expressions for the moments of the marking of the MPN.

Proposition 2.6. *The expected value and covariance matrix of the marking of the MPN at time step $k+1$, denoted as $E\{\mathbf{M}_{k+1}\}$ and $\sum_{\mathbf{M}_{k+1}}$, can be expressed as functions of the moments of $\mathbf{M}_k$ and $\mathbf{F}_k\Delta\tau = \boldsymbol{\Lambda}\lfloor\boldsymbol{\Pi}(\mathbf{M}_k)\mathbf{M}_k\rfloor\Delta\tau$ as:*

$$E\{\mathbf{M}_{k+1}\} = \begin{bmatrix} \mathbf{I} & \mathbf{C} \end{bmatrix} \begin{bmatrix} E\{\mathbf{M}_k\} \\ E\{\mathbf{F}_k\Delta\tau\} \end{bmatrix} \tag{2.12}$$

$$\boldsymbol{\Sigma}_{\mathbf{M}_{k+1}} = \begin{bmatrix} \mathbf{I} & \mathbf{C} \end{bmatrix} \begin{bmatrix} \boldsymbol{\Sigma}_{\mathbf{M}_k} & \boldsymbol{\Sigma}_{\mathbf{M}_k,\boldsymbol{\Delta\sigma_k}} \\ \boldsymbol{\Sigma}_{\boldsymbol{\Delta\sigma_k},\mathbf{M}_k} & \boldsymbol{\Sigma}_{\Delta\boldsymbol{\sigma}(\mathbf{F}_k\Delta\tau)} \end{bmatrix} \begin{bmatrix} \mathbf{I} \\ \mathbf{C}^T \end{bmatrix} \tag{2.13}$$

where the covariance matrix $\boldsymbol{\Sigma}_{\Delta\boldsymbol{\sigma}(\Delta\mathbf{F}_k)}$ is given by:

$$\boldsymbol{\Sigma}_{\Delta\boldsymbol{\sigma}(\mathbf{F}_k\Delta\tau)} = \boldsymbol{\Sigma}_{\mathbf{F}_k\Delta\tau} + diag\left[E\{\mathbf{F}_k\Delta\tau\}\right] \tag{2.14}$$

and the cross covariance matrices $\mathbf{\Sigma}_{\mathbf{M}_k,\Delta\boldsymbol{\sigma}_k}$ *and* $\mathbf{\Sigma}_{\Delta\boldsymbol{\sigma}_k,\mathbf{M}_k}$ *can be computed by elements with:*

$$\begin{array}{ll}\forall i,j\in\{1,..,|P|\} & \mathbf{\Sigma}_{\mathbf{M}_k,\Delta\boldsymbol{\sigma}_k}[i,j]=cov\{M_{k,i},\Delta\sigma_j(F_{k,j}\Delta\tau)\}=cov\{M_{k,i},F_{k,j}\Delta\tau\}\\ & \mathbf{\Sigma}_{\Delta\boldsymbol{\sigma}_k,\mathbf{M}_k}[i,j]=cov\{\Delta\sigma_i(F_{k,i}\Delta\tau),M_{k,j}\}=cov\{F_{k,i}\Delta\tau,M_{k,j}\}\end{array}\tag{2.15}$$

Proof. First, by using the fact that $E\{\Delta\boldsymbol{\sigma}(\mathbf{F}_k\Delta\tau)\}=E\{\mathbf{F}_k\Delta\tau\}$ (proved in [Papoulis, 1984] and already used in the proof of Proposition 2.2), then (2.2) can be written as (2.12).

Now, according to (1.2), in order to compute the covariance matrix of $\mathbf{M}_{k+1}$ it is necessary to estimate the moments of $\Delta\boldsymbol{\sigma}(\mathbf{F}_k\Delta\tau)$. By definition, the firing count $\Delta\boldsymbol{\sigma}(\mathbf{F}_k\Delta\tau)$ is a vector of Poisson distributed r.v.'s whose parameters are the corresponding elements of $\mathbf{F}_k\Delta\tau$. However, these parameters are also r.v.'s, since they are function of $\mathbf{M}_{k+1}$ (also a vector of r.v.'s). Nevertheless, the covariance matrix of the firing count can be expressed in terms of the moments of its parameters. According to Poisson pdf properties (see, for instance, [Papoulis, 1984]), it can be proved that for any transition t_i,

$$var\{\Delta\sigma_i(F_{k,i}\Delta\tau)\}=var\{F_{k,i}\Delta\tau\}+E\{F_{k,i}\Delta\tau\}\tag{2.16}$$

Furthermore, using the total probability theorem and some properties of the conditional expected value, it can be demonstrated that, for any other transition t_j or place p_j it holds

$$cov\{\Delta\sigma_i(F_{k,i}\Delta\tau),\Delta\sigma_j(F_{k,j}\Delta\tau)\}=cov\{F_{k,i}\Delta\tau,F_{k,j}\Delta\tau\}\tag{2.17}$$

$$cov\{\Delta\sigma_i(F_{k,i}\Delta\tau),M_{k,j}\}=cov\{F_{k,i}\Delta\tau,M_{k,j}\}$$

Then, denoting the covariance matrices of $\mathbf{F}_k\Delta\tau$ and $\Delta\boldsymbol{\sigma}(\mathbf{F}_k\Delta\tau)$ as $\mathbf{\Sigma}_{\mathbf{F}_k\Delta\tau}$ and $\mathbf{\Sigma}_{\Delta\boldsymbol{\sigma}(\mathbf{F}_k\Delta\tau)}$, respectively, by using (2.16) and (2.17) it is obtained $\mathbf{\Sigma}_{\Delta\boldsymbol{\sigma}(\mathbf{F}_k\Delta\tau)}=\mathbf{\Sigma}_{\mathbf{F}_k\Delta\tau}+diag\,[E\{\mathbf{F}_k\Delta\tau\}]$. Finally, by combining these equations, (2.13) is obtained. ∎

Now, let us obtain similar expressions for the moments of the marking of the TnCPN.

Proposition 2.7. *The expected value and covariance matrix of the marking of the TnCPN at time step* $k+1$*, denoted as* $E\{\mathbf{m}_{k+1}\}$ *and* $\sum_{\mathbf{m}_{k+1}}$*, can be expressed as functions of the moments of* $\mathbf{m}_k$ *and* $\mathbf{f}_k\Delta\tau=\mathbf{\Lambda\Pi}(\mathbf{m}_k)\mathbf{m}_k\Delta\tau$ *as:*

$$E\{\mathbf{m}_{k+1}\}=\begin{bmatrix}\mathbf{I} & \mathbf{C}\end{bmatrix}\begin{bmatrix}E\{\mathbf{m}_k\}\\ E\{\mathbf{f}_k\Delta\tau\}\end{bmatrix}\tag{2.18}$$

$$\mathbf{\Sigma}_{\mathbf{m}_{k+1}}=\begin{bmatrix}\mathbf{I} & \mathbf{C}\end{bmatrix}\begin{bmatrix}\mathbf{\Sigma}_{\mathbf{m}_k} & \mathbf{\Sigma}_{\mathbf{m}_k,\Delta\mathbf{w}_k}\\ \mathbf{\Sigma}_{\Delta\mathbf{w}_k,\mathbf{m}_k} & \mathbf{\Sigma}_{\Delta\mathbf{w}_k}\end{bmatrix}\begin{bmatrix}\mathbf{I}\\ \mathbf{C}^T\end{bmatrix}\tag{2.19}$$

where

$$\mathbf{\Sigma}_{\Delta\mathbf{w}_k}=\mathbf{\Sigma}_{\mathbf{f}_k\Delta\tau}+diag\,[E\{\mathbf{f}_k\Delta\tau\}]\tag{2.20}$$

and the cross covariance matrices can be computed, by elements, with:

$$\begin{array}{ll}\forall i,j\in\{1,..,|P|\} & \mathbf{\Sigma}_{\mathbf{m}_k,\Delta\mathbf{w}_k}[i,j]=cov\{m_{k,i},\Delta w_{k,j}\}=cov\{m_{k,i},f_{k,j}\Delta\tau\}\\ & \mathbf{\Sigma}_{\Delta\mathbf{w}_k,\mathbf{m}_k}[i,j]=cov\{\Delta w_{k,i},m_{k,j}\}=cov\{f_{k,i}\Delta\tau,m_{k,j}\}\end{array}$$

Proof. First, since $\Delta\mathbf{w}_k = \mathbf{f}_k\Delta\tau + \mathbf{v}_k$ and $E\{\mathbf{v}_k\} = \mathbf{0}$ then $E\{\Delta\mathbf{w}_k\} = E\{\mathbf{f}_k\Delta\tau\}$. Substituting this into (2.10), it is obtained (2.18).

Now, for any transition t_i, t_j and place p_j, equalities analogous to (2.15-2.17) are obtained as:

$$\begin{aligned} &var\{\Delta w_{k,i}\} = var\{f_{k,i}\Delta\tau\} + E\{f_{k,i}\Delta\tau\} \\ &cov\{\Delta w_{k,i}, \Delta w_{k,j}\} = cov\{f_{k,i}\Delta\tau, f_{k,j}\Delta\tau\} \\ &cov\{\Delta w_{k,i}, m_{k,j}\} = cov\{f_{k,i}\Delta\tau, m_{k,j}\} \end{aligned}$$

Therefore, denoting the covariance matrices of $\mathbf{f}_k\Delta\tau$ and $\mathbf{w}_k$ as $\mathbf{\Sigma}_{\mathbf{f}_k\Delta\tau}$ and $\mathbf{\Sigma}_{\Delta\mathbf{w}_k}$, respectively, it is obtained $\mathbf{\Sigma}_{\Delta\mathbf{w}_k} = \mathbf{\Sigma}_{\mathbf{f}_k\Delta\tau} + diag\,[E\{\mathbf{f}_k\Delta\tau\}]$. Combining these equations, (2.19) is obtained. ∎

Remark 2.8. The moments of $\mathbf{m}_{k+1}$ as functions of $\mathbf{m}_k$ and $\mathbf{f}_k\Delta\tau$, are equal to those of $\mathbf{M}_{k+1}$ as functions of $\mathbf{M}_k$ and $\mathbf{F}_k\Delta\tau$. Furthermore, $\mathbf{F}_k = \mathbf{\Lambda}\lfloor\mathbf{\Pi}(\mathbf{M}_k)\mathbf{M}_k\rfloor$ is a function of $\mathbf{M}_k$ almost equivalent to $\mathbf{f}_k = \mathbf{\Lambda\Pi}(\mathbf{m}_k)\mathbf{m}_k$ for $\mathbf{m}_k$ (it is equal for ordinary nets, while for non-ordinary nets the difference is not relevant for large values of the enabling degree, i.e., $\lfloor\mathbf{\Pi}(\mathbf{M}_k)\mathbf{M}_k\rfloor \simeq \mathbf{\Pi}(\mathbf{M}_k)\mathbf{M}_k$). This likelihood is intentional, since the noise $\mathbf{v}_k$ added to the TCPN model was defined in order to obtain similar expressions for the moments.

Previous propositions lead to think about the possibility of moments approximation. Roughly speaking, if at some time step k, the moments of the marking $\mathbf{M}_k$ of the MPN are similar to those of the marking $\mathbf{m}_k$ of the TnCPN model, then the moments of the markings of both systems will be similar for the next time step $k+1$. Thus, following an inductive reasoning, it can be expected that the moments of the marking of the TnCPN approximates those of the MPN in the future time. Instead of formally proving such approximation, in the following subsection a stronger result will be introduced, according to which, assuming ergodicity and boundedness, if the enabling degree for the most probable values of $\mathbf{M}_k$ is large enough, then the pdf (not only the moments) of $\mathbf{M}_k$ is approximated by the pdf of $\mathbf{m}_k$.

2.3.2 Approximation of the marking's pdf by a TnCPN

Let us precise first the concept of approximation of the pdf For this, given the marking $\mathbf{m}_k$ of the TnCPN at time step k, the following function is defined:

$$Prob^c(\mathbf{m}_k = \mathbf{a}) = \int_{\mathbf{a}_{|P|}-1/2}^{\mathbf{a}_{|P|}+1/2} ... \int_{\mathbf{a}_1-1/2}^{\mathbf{a}_1+1/2} \phi_{\mathbf{m}_k}(\eta_{|P|}, ..., \eta_1)\partial\eta_1 ... \partial\eta_{|P|}$$

where $\phi_{\mathbf{m}_k}(\cdot)$ is the joint pdf of the entries of $\mathbf{m}_k$. Note that $Prob^c(\mathbf{m}_k = \mathbf{a})$ is actually the probability that $\mathbf{a} - (1/2)\cdot\mathbf{1} \leq \mathbf{m}_k \leq \mathbf{a} + (1/2)\cdot\mathbf{1}$. In the sequel, it will be said that the pdf of the marking of the MPN is *well* approximated by that of the TnCPN, at time step k, if $\forall\mathbf{a} \in [\mathbb{N}\cup\{0\}]^{|P|}$ the difference $Prob^c(\mathbf{m}_k = \mathbf{a}) - Prob(\mathbf{M}_k = \mathbf{a})$ is *small enough* (or at least, it is small for the values of $\mathbf{a}$ for which $Prob(\mathbf{M}_k = \mathbf{a})$ is meaningful). The lower the difference, the better the approximation.

In order to study the relation between the magnitude of the marking and the approximation provided by the TnCPN system, in the sequel, the initial marking of both the MPN and the TnCPN systems will be represented in parametric form as $\mathbf{M}_0 = q\cdot\mathbf{M}_0^r$ and $\mathbf{m}_0 = q\cdot\mathbf{m}_0^r$, where $q \in \mathbb{R}^+$ and $\mathbf{M}_0^r = \mathbf{m}_0^r > \mathbf{0}$ are deterministic values. For the evolution of both systems, it will be considered the use of a suitable

sampling $\Delta\tau = \Delta\tau^r/q$. It can be demonstrated that, if the sampling $\Delta^r\tau$ is small enough for the initial marking $\mathbf{M}_0^r$, then the sampling $\Delta\tau = \Delta^r\tau/q$ will be suitable for the scaled initial marking $\mathbf{M}_0 = q \cdot \mathbf{M}_0^r$, with $q > 1$ (this follows from the computation of the error introduced by $\Delta\tau$, provided in Appendix B). The same holds for the continuous system.

The following lemma introduces sufficient conditions leading to the approximation of the pdf after a finite number of time steps n. In order to follow the proof of this lemma, the reader must consider Lemmas B.2 and B.3 provided in Appendix B, which state that, the larger the initial marking, the better the approximation of $\sum_{i=0}^{k-1} \Delta\boldsymbol{\sigma}(\mathbf{F}_k\Delta\tau)$ to $Poisson(n \cdot \mathbf{F}_0^r\Delta^r\tau)$ and $\sum_{i=0}^{k-1} \mathbf{w}_k$ to $Normal(n \cdot \mathbf{f}_0\Delta\tau, n \cdot \mathbf{f}_0\Delta\tau)$, respectively (given an large enough number of time steps n). Later, the forthcoming Theorem 2.10 generalizes the approximation for future time, i.e., for $\tau > \tau_0 + n\Delta\tau$. For both Lemma 2.9 and Theorem 2.10, it will be assumed that the MPN system is live an ergodic, and that there do not exist non-live equilibrium markings in $Class(\mathbf{m}_0)$ of the continuous system (thus it is live).

Lemma 2.9. *Consider a MPN and the corresponding TnCPN. Consider the initial markings in parametric form $\mathbf{M}_0 = q \cdot \mathbf{M}_0^r$ and $\mathbf{m}_0 = q \cdot \mathbf{m}_0^r$, with $q \in \mathbb{R}^+$ and $\mathbf{M}_0^r = \mathbf{m}_0^r > \mathbf{0}$ deterministic. Consider the evolution of both systems with the sampling $\Delta\tau = \Delta\tau^r/q$ during a fix number of time steps n.*

1) For a large enough n, the probability distribution of $\mathbf{m}_n$ converges to that of $\mathbf{M}_n$ when $q \to \infty$. The larger q, the closer the pdf's of $\mathbf{M}_{k+n}$ and $\mathbf{m}_{k+n}$.

2) Assume that at some time step k the distribution of $\mathbf{m}_k$ approximates that of $\mathbf{M}_k$. Then, the larger the enabling degree for the most probable values of $\mathbf{M}_k$, the closer the pdf's of $\mathbf{M}_{k+n}$ and $\mathbf{m}_{k+n}$.

Proof. According to (2.10), the marking of the TnCPN at time step n, can be represented as:

$$\mathbf{m}_n = \mathbf{m}_0 + \mathbf{C}\sum_{k=0}^{n-1} \Delta\mathbf{w}_k \tag{2.21}$$

Similarly, according to (1.2), the marking of the MPN at time step n can be represented as:

$$\mathbf{M}_n = \mathbf{M}_0 + \mathbf{C}\sum_{k=0}^{n-1} \Delta\boldsymbol{\sigma}(\mathbf{F}_k\Delta\tau) \tag{2.22}$$

Comparing this equation with (2.21), it can be seen that the distribution of $\mathbf{m}_n$ approximates that of $\mathbf{M}_n$ if the pdf of $\sum_{k=0}^{n-1} \Delta\mathbf{w}_k$ approximates that of $\sum_{k=0}^{n-1} \Delta\boldsymbol{\sigma}(\mathbf{F}_k\Delta\tau)$.

According to the Lemmas B.2 and B.3 provided in Appendix B, the larger q (equivalently, the larger the initial marking) the better the approximation of $\sum_{i=0}^{k-1} \Delta\boldsymbol{\sigma}(\mathbf{F}_k\Delta\tau)$ to $Poisson(n \cdot \mathbf{F}_0^r\Delta^r\tau)$ and $\sum_{i=0}^{k-1} \Delta\mathbf{w}_k$ to $Normal(n \cdot \mathbf{f}_0\Delta\tau, n \cdot \mathbf{f}_0\Delta\tau)$, respectively. Note that $n \cdot \mathbf{F}_0^r\Delta^r\tau = n \cdot \mathbf{f}_0\Delta\tau$, since $\mathbf{F}_0^r\Delta^r\tau = \Lambda\Pi(\mathbf{M}_0^r)\mathbf{M}_0^r\Delta^r\tau = \Lambda\Pi(\mathbf{M}_0)\mathbf{M}_0\Delta\tau$ and $\mathbf{M}_0 = \mathbf{m}_0$. Furthermore, it is well know that a normal distribution approximates a Poisson one (see, for instance, [Papoulis, 1984]), i.e., $Normal(\eta, \eta) \simeq Poiss(\eta)$ for η large enough. The larger the parameter η the better the approximation (a typical value for this is $\eta = 10$, but it depends on the desired accuracy). In this way, if n is large enough s.t. $n \cdot \mathbf{f}_0\Delta\tau >> 10$ then the approximation of $\sum_{k=0}^{n-1} \Delta\boldsymbol{\sigma}(\mathbf{F}_k\Delta\tau)$ by $\sum_{k=0}^{n-1} \Delta\mathbf{w}_k$ follows. Thus, according to (2.21) and (2.22), the distribution of the continuous marking approximates that of the discrete marking at time step n. The first statement is thus proven.

Now, the second statement is a generalization of the first one, in which $\mathbf{M}_k$ is taken as the starting marking, i.e., it is analogous to $\mathbf{M}_0$. The difference appears in the fact that $\mathbf{M}_k$ is a vector of r.v.'s, while $\mathbf{M}_0$ is deterministic. Let us prove this statement in the following:

Suppose that at time step k the pdf of $\mathbf{M}_k$ is well approximated by that of $\mathbf{m}_k$. Thus, $\forall \mathbf{a} \in [\mathbb{N} \cup \{0\}]^{|P|}$ it holds $Prob^c(\mathbf{m}_k = \mathbf{a}) \simeq Prob(\mathbf{M}_k = \mathbf{a})$. Then, by the total probability theorem it can be obtained:

$$\begin{aligned} &Prob(\mathbf{M}_{k+n} = \mathbf{a}) - Prob^c(\mathbf{m}_{k+n} = \mathbf{a}) = \\ &\quad \textstyle\sum_{\forall \mathbf{b} \in [\mathbb{N} \cup \{0\}]^{|P|}} [Prob(\mathbf{M}_{k+n} = \mathbf{a} | \mathbf{M}_k = \mathbf{b}) - Prob^c(\mathbf{m}_{k+n} = \mathbf{a} | \mathbf{m}_k = \mathbf{b})] \cdot Prob(\mathbf{M}_k = \mathbf{b}) \end{aligned} \tag{2.23}$$

Note that $[Prob(\mathbf{M}_{k+n} = \mathbf{a} | \mathbf{M}_k = \mathbf{b}) - Prob^c(\mathbf{m}_{k+n} = \mathbf{a} | \mathbf{m}_k = \mathbf{b})]$ is the probability error after n time steps obtained by assuming that $\mathbf{M}_k = \mathbf{m}_k$ is deterministic an equal to $\mathbf{b}$. Thus, according to the first statement of this lemma (already proved), the larger $\mathbf{b}$ the smaller $[Prob(\mathbf{M}_{k+n} = \mathbf{a} | \mathbf{M}_k = \mathbf{b}) - Prob^c(\mathbf{m}_{k+n} = \mathbf{a} | \mathbf{m}_k = \mathbf{b})]$. In this way, by using (2.23) it can be concluded that the larger the enabling degree for the most probable values of $\mathbf{M}_k$ (i.e., the larger the values of $\mathbf{b}$ for which $Prob(\mathbf{M}_k = \mathbf{b})$ is relevant), the smaller the probability error $Prob(\mathbf{M}_{k+n} = \mathbf{a}) - Prob^c(\mathbf{m}_{k+n} = \mathbf{a})$. Finally, the second statement follows since previous reasoning is valid for each probable value $\mathbf{a}$. ∎

According to the previous lemma, if at some time step n the pdf of $\mathbf{M}_n$ is well approximated by that of $\mathbf{m}_n$, then the approximation holds at time step $2 \cdot n$. By following an inductive reasoning, it may be expected that the approximation will hold during the future evolution of both systems. Approximation errors do not accumulate if the stochastic processes are ergodic (which is analogous to asymptotic stability in the case of Join-Free models, used in the proof of Proposition 2.2). This is formalized in the following theorem.

Theorem 2.10. *Consider a MPN and the corresponding TnCPN, with large initial markings* $\mathbf{M}_0 = \mathbf{m}_0 > \mathbf{0}$. *Consider the evolution of both the MPN and the TnCPN systems during a large number of time steps* n. *Then, the probability approximation errors* $[Prob(\mathbf{M}_k = \mathbf{a}) - Prob^c(\mathbf{m}_k = \mathbf{a})]$, *for the most probable values of* $\mathbf{M}_k$, *are ultimately bounded. The larger the enabling degree for the most probable trajectories of the MPN system, the lower the bound for the approximation errors, thus, the better the approximation of the marking's pdf.*

Proof. Consider the underlying Markov chain of the MPN system [Molloy, 1982], whose evolution is given by $\dot{\boldsymbol{\pi}} = \mathbf{Q}\boldsymbol{\pi}$, where $\boldsymbol{\pi}$ is the probability vector and $\mathbf{Q}$ is the transitions rate matrix. The discrete-time version of this model is given by $\boldsymbol{\pi}_{k+1} = \mathbf{Q}_D \boldsymbol{\pi}_k$ (which can be obtained in a similar way that (1.5) for the TPCN model). Thus, after n time steps the probability vector is given by $\boldsymbol{\pi}_{k+n} = [\mathbf{Q}_D]^n \boldsymbol{\pi}_k$.

Now, by definition, for each $\mathbf{a} \in [\mathbb{N} \cup \{0\}]^{|P|}$ in the reachability set of the autonomous discrete PN, the variable $Prob(\mathbf{M}_k = \mathbf{a})$ corresponds to an entry of $\boldsymbol{\pi}_k$. It is possible to define a probability vector $\boldsymbol{\pi}_k^c$, whose entries correspond to the values $Prob^c(\mathbf{m}_k = \mathbf{a})$ for each $\mathbf{a} \in [\mathbb{N} \cup \{0\}]^{|P|}$. Thus, if the distribution of $\mathbf{m}_k$ approximates that of $\mathbf{M}_k$ then $\boldsymbol{\pi}_k^c \simeq \boldsymbol{\pi}_k$.

Let us define the *probability error* vector as $\boldsymbol{\varepsilon}_{\boldsymbol{\pi}_k} = \boldsymbol{\pi}_k - \boldsymbol{\pi}_k^c$. Suppose that the approximation holds at time step k, i.e., $\boldsymbol{\pi}_k^c \simeq \boldsymbol{\pi}_k$. This implies $[\mathbf{Q}_D]^n \boldsymbol{\pi}_k^c \simeq [\mathbf{Q}_D]^n \boldsymbol{\pi}_k = \boldsymbol{\pi}_{k+n} = \boldsymbol{\pi}_{k+n}^c + \boldsymbol{\varepsilon}_{\boldsymbol{\pi}_{k+n}}$. Thus, $\boldsymbol{\pi}_{k+n}^c \simeq [\mathbf{Q}_D]^n \boldsymbol{\pi}_k^c - \boldsymbol{\varepsilon}_{\boldsymbol{\pi}_{k+n}}$.

By using the previous expression, the evolution of the probability error can be represented as:

$$\boldsymbol{\varepsilon}_{\boldsymbol{\pi}_{k+n}} \simeq [\mathbf{Q}_D]^n \boldsymbol{\varepsilon}_{\boldsymbol{\pi}_k} + \boldsymbol{\varepsilon}^k_{\boldsymbol{\pi}_{k+n}} \tag{2.24}$$

where $\boldsymbol{\varepsilon}^k_{\boldsymbol{\pi}_{k+n}}$ is the approximation error introduced during the time interval $(k, k+n]$. Now, consider a lower bound for the enabling degree at the time step k (for the most probable values of $\mathbf{M}_k$) and an upper bound for $\boldsymbol{\varepsilon}^k_{\boldsymbol{\pi}_{k+n}}$. According to Lemma 2.9, the larger the lower bound for the enabling degree, the smaller the upper-bound for $\boldsymbol{\varepsilon}^k_{\boldsymbol{\pi}_{k+n}}$.

On the other hand, by hypothesis the MPN system is ergodic, meaning that there is only one solution for $\boldsymbol{\pi}_{ss} = [\mathbf{Q}_D]\boldsymbol{\pi}_{ss}$ s.t. $\mathbf{1} \cdot \boldsymbol{\pi}_{ss} = 1$, and for any initial probability vector $\boldsymbol{\pi}_0$ the system will converge to $\boldsymbol{\pi}_{ss}$. This implies that, given $\boldsymbol{\varepsilon}_{\boldsymbol{\pi}_0}$ s.t. $\mathbf{1} \cdot \boldsymbol{\varepsilon}_{\boldsymbol{\pi}_0} = 0$, the nominal probability error system $\boldsymbol{\varepsilon}_{\boldsymbol{\pi}_{k+n}} = [\mathbf{Q}_D]^n \boldsymbol{\varepsilon}_{\boldsymbol{\pi}_k}$ will converge to $\mathbf{0}$, i.e., the origin is asymptotically stable on the (invariant) subspace $\mathbf{1} \cdot \boldsymbol{\varepsilon}_{\boldsymbol{\pi}_k} = 0$.

Therefore, (2.24) can be seen as the nominal linear system $\boldsymbol{\varepsilon}_{\boldsymbol{\pi}_{k+n}} = [\mathbf{Q}_D]^n \boldsymbol{\varepsilon}_{\boldsymbol{\pi}_k}$, with the non-vanishing upper bounded perturbation $\boldsymbol{\varepsilon}^k_{\boldsymbol{\pi}_{k+n}}$. Thus, by following a similar analysis as in the case for Join-Free models (proof of Proposition 2.2), it can be concluded that, since the origin is the unique equilibrium point and it is asymptotically stable in the nominal error system, then $\boldsymbol{\varepsilon}_{\boldsymbol{\pi}_{k+n}}$ is ultimately bounded, i.e., the probability errors are ultimately bounded. Furthermore, the larger the enabling degree for the most probable trajectories of the system, the lower the upper bound for the non-vanishing perturbation, and so, the lower the ultimate bounded for the probability error. ∎

Example 2.4. Consider again the MPN of fig. 2.2. Simulations of the corresponding TnCPN were achieved, for the same values of initial marking and timing rates. The average markings at the steady state are shown in Table 2.3. Comparing the relative errors thus obtained (fourth column), with those of the TCPN (without noise, showed in table 2.2), it can be seen that the approximation provided by the TnCPN system is much better. The difference in both approximations is larger when the probability that the discrete system evolves inside a unique region is low (which occurs when $\lambda_4 \to 1$).

Furthermore, for timing rates $\lambda_1 = \lambda_2 = \lambda_3 = 1, \lambda_4 = 2$ and initial marking $\mathbf{M}_0 = [1, 9, 1, 59, 1, 9]^T$, the expected value of the marking of the MPN system was computed by using TimeNET. Also, the corresponding TnCPN was simulated with MatLab. Fig. 2.3 shows the average evolution of the marking of p_3. The smooth curves correspond to the expected value of the MPN (denoted as $E\{M\}$) and the original TCPN system. The other curve corresponds to the average trajectory obtained from 50 simulations of the TnCPN system. Vertical lines represent changes of regions. It can be seen that the average marking of the TnCPN system is close to the expected value of the marking of the MPN one ($E\{M\}$). On the other hand, the marking of the TCPN system shows a more significant error (of 8.8% at time $\tau = 32$), when the second change of region occurs. As expected, the addition of noise to the continuous model improves the approximation around this change of region.

Example 2.5. Consider now the MPN of fig. 2.4(a), with timing rates $\lambda_1 = 3, \lambda_2 = \lambda_3 = \lambda_4 = 1$ and initial marking $\mathbf{M}_0 = [0, 13, 20, 7, 8]^T$. The marking at the steady state was computed by using TimeNET, for different values of the initial marking at place p_5. Similarly, several simulations of the corresponding TnCPN systems were done in MatLab.

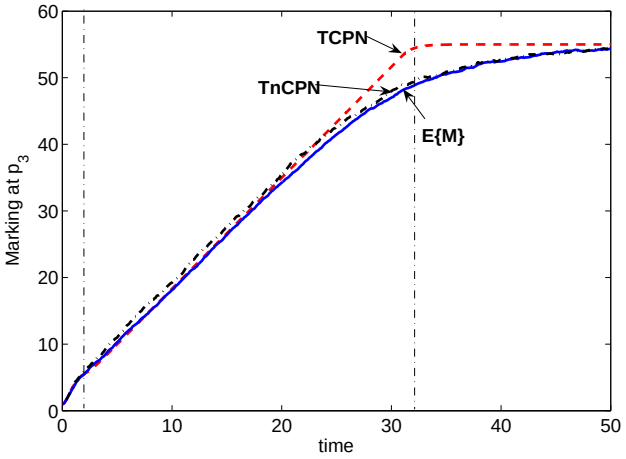

Fig. 2.3: Approximation of the transient behavior of the MPN of fig. 2.2 for $\lambda_1 = \lambda_2 = \lambda_3 = 1$ and $\lambda_4 = 2$.

Tab. 2.3: Marking approximation of p_3 for the MPN of fig. 2.2 by the corresponding TnCPN

λ_4	MPN	TnCPN	error
2	54.62	54.63	0.26%
1.5	53.87	53.88	0.22%
1.2	51.16	51.17	0.49%
1.1	46.65	46.66	1.52%
1.05	40.72	40.73	1.78%
1	29.97	30.73	2.54%

The average marking of the MPN, for place p_5 at the steady state, and the corresponding average values of the TnCPN are shown in table 2.4. The first column corresponds to the value of $\mathbf{M}_0(p_4)+\mathbf{M}_0(p_5)$ at the initial marking. The fourth column corresponds to the relative error and the last one ($E\{t_1\}$) is the average enabling degree of t_1 at the steady state (the average enabling degree of t_1 at the steady state is lower than those of the other transitions).

For this model, the corresponding TCPN (without noise) does not provide a good approximation of the MPN system. In this, the relation between the initial marking and the corresponding throughput is non monotonic. Nevertheless, in table 2.4 it can be seen that the TnCPN does provide a good approximation when the initial conditions for $\mathbf{M}_0(p_4) + \mathbf{M}_0(p_5)$ ranges from 15 to 30. As it is expected, the larger the enabling degree at the transitions (which can be seen from $E\{t_1\}$), the better the approximation.

Note that, the approximation does not improve when the initial marking, at only some places, is increased. Actually, the approximation does improve when the *enabling degree* of all the transitions, at the steady state, increases, since the data shown in table 2.4 correspond to the steady state. This example shows the role of the magnitude of the enabling degree in the approximation, as stated in Theorem 2.10, i.e., the larger the enabling degree, at the most probable values of $\mathbf{M}_k$, the better the approximation.

Furthermore, the transient behavior is also well approximated. Fig. 2.4(b) shows the average evolution of the marking of place p_1 during the first 3.5 seconds, for the initial marking $\mathbf{M}_0 = [0, 13, 20, 7, 8]^T$. The expected value of the MPN, obtained by several simulations using MatLab, is denoted by $E\{\mathbf{M}\}$.

Tab. 2.4: Approximation of p_5 in steady state for the MPN of fig. 2.4(a)

$\mathbf{M}_0(p_4)$ $+\mathbf{M}_0(p_5)$	MPN	TnCPN	error	$E\{t_1\}$
15	3.71	3.68	0.7%	3.43
20	4.41	4.22	4.2%	3.49
30	4.24	3.96	6.7%	2.80
40	3.65	3.21	11.9%	1.91
50	3.34	2.62	21.5%	1.25

The average trajectory of the TnCPN, obtained after 100 simulations, is also shown in fig. 2.4(b) (denoted as TnCPN). Note that the curve TnCPN is always close to the curve $E\{\mathbf{M}\}$, furthermore, the TnCPN provides a better approximation than the TCPN (the approximation by the TCPN is not so good because there are several changes of regions). Finally, fig. 2.4(c) shows the steady state probability distributions (obtained from several simulations) of the marking at p_1 of both, the MPN (square bars) and the TnCPN (solid curve, actually, this curve is the interpolation of the points $Prob^c(\mathbf{m}_{ss}(p_1) = a)$ for $a \in \{0, 1, ..., 40\}$). It can be seen that the marking probability distribution is also well approximated by the TnCPN.

2.4 Approximation by partially relaxed models: Markovian hybrid Petri nets

According to the results presented in Section 2.2, regarding the approximation of the average marking of a MPN by the marking of the corresponding TCPN, if the enabling degree of some transitions is not large enough then significant approximation errors may appear. In such case, it makes sense to fluidify only those transitions exhibiting large enabling degrees, obtaining thus a *hybrid* Petri net model.

2.4.1 Markovian hybrid Petri net model

Hybrid Petri nets were introduced by [Alla and David, 1998]. There, the *discrete* part of the *hybrid* PN model was defined as a timed PN (i.e., with constant delays at the transitions), while the *continuous* part is a *continuous* PN with constant speed (finite server semantics). In order to be consistent with the MPN model, the *hybrid* PN system considered in this section must include the random behavior of the MPN at the *discrete* transitions, and the infinite server semantics in the *continuous* part. Therefore, the following hybrid model is proposed as a *Markovian* timing for the autonomous hybrid PN already introduced in ([Silva and Recalde, 2004]).

Definition 2.11. A *Markovian hybrid* Petri net (MHPN), under infinite server semantics, is a tuple $\langle \mathcal{N}, \boldsymbol{\lambda}, \mathbf{M}_0^h \rangle$. $\mathcal{N}$ is the structure of the PN, in which the set of places P (transitions T) is partitioned into the set of continuous P^c (T^c) and discrete P^d (T^d) ones (i.e., $P = P^c \cup P^d$, $P^c \cap P^d = \emptyset$ and $T = T^c \cup T^d$, $T^c \cap T^d = \emptyset$). Since the fluidification is introduced through transitions then the fluid places are those neighboring fluid transitions, i.e., $P^c = {}^\bullet T^c \cup T^{c\bullet}$ (note that it is possible to make all the places fluid by fluidifying only some transitions). $\mathbf{M}_0^h \in \mathbb{N}^{|P|}$ represents the initial marking, and $\boldsymbol{\lambda} \in \mathbb{R}_{>0}^{|T|}$ represents the

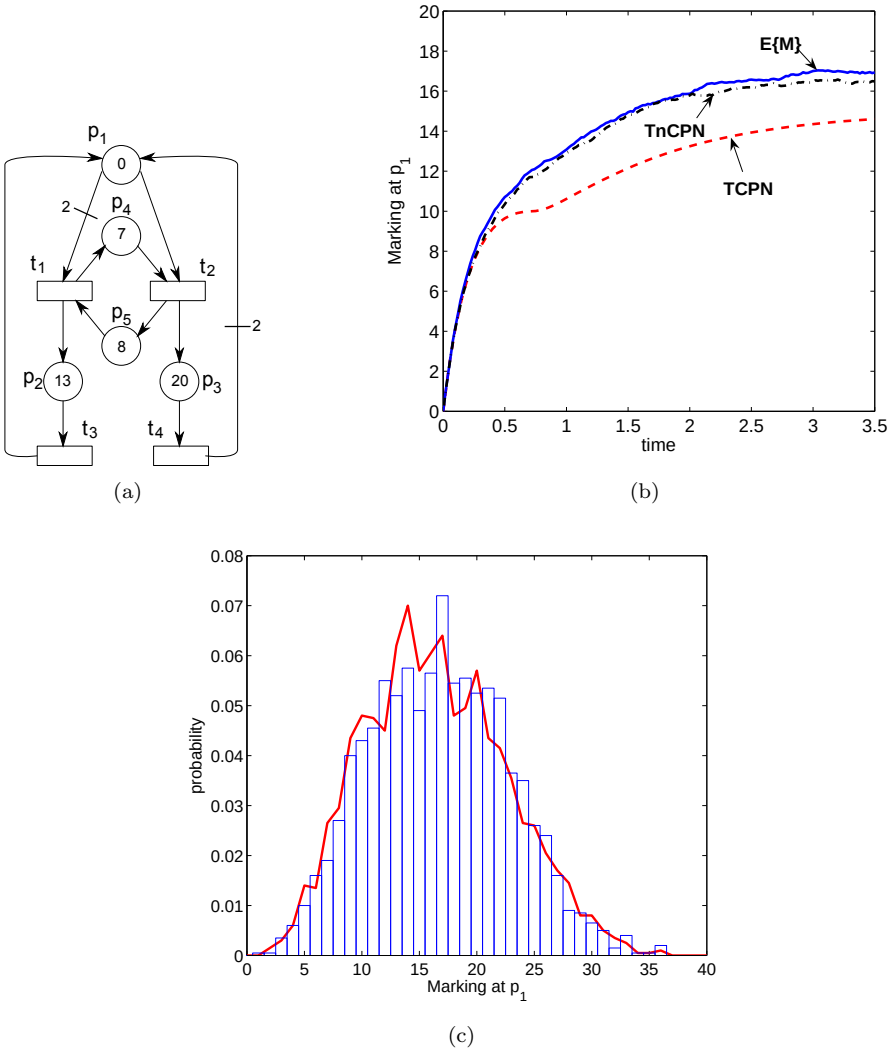

Fig. 2.4: (a) Non-monotonic MPN system. (b) Approximation of the transient behavior of the marking of place p_1. Region commutations in the TCPN occur at times 0.253, 0.715, 0.718 and 1.137. (c) Steady state probability distributions of the marking at p_1 of the MPN (bars) and TnCPN (solid line).

transition rates. Each discrete transition $t_i \in T^d$ fires in discrete amounts with exponentially distributed random time delays, with parameter $\lambda_i \cdot Enab(t_i, \mathbf{M}^h)$, as in the MPN model. Each continuous transition $t_i \in T^c$ fires according to the flow $f_i(\mathbf{M}^h) = \lambda_i \cdot enab(t_i, \mathbf{M}^h)$, as in the TCPN model.

Under this definition, the difference equation (1.2) can be used for representing the behavior of the discrete part of the system (the firing of discrete transitions), while (1.5) can be used for describing the behavior of the continuous part. Without loss of generality, let us suppose that the first columns of matrix $\mathbf{C}$ are related to the discrete transitions, while the last columns correspond to fluid ones. Then

the MHPN can be represented as:

$$\mathbf{M}_{k+1}^h \simeq \mathbf{M}_k^h + \mathbf{C} \cdot \begin{bmatrix} \Delta\boldsymbol{\sigma}(\mathbf{F}_k^d(\mathbf{M}_k^h)\Delta\tau) \\ \mathbf{f}(\mathbf{M}_k^h)\Delta\tau \end{bmatrix}$$

where $\mathbf{M}_k^h$ represents the whole marking. The firing vector $\Delta\boldsymbol{\sigma}(\mathbf{F}_k^d(\mathbf{M}_k^h)\Delta\tau) \sim Poisson(\mathbf{F}_k^d(\mathbf{M}_k^h)\Delta\tau)$ is defined just for the discrete transitions, while the flow function $\mathbf{f}(\mathbf{M}_k^h)$ is defined only for the continuous transitions.

Suppose that the first rows of the incidence matrix correspond to the discrete places, while the last rows to fluid ones. Let us divide the marking and the incidence, firing rate and configuration matrices according to the classification of places and transitions. Then, the marking is given by $\mathbf{M}_k^h = [\boldsymbol{\mu}_k^T \quad \mathbf{m}_k^T]^T$, where $\boldsymbol{\mu}_k$ and $\mathbf{m}_k$ correspond to the marking of the discrete and fluid places, respectively. The incidence matrices is divided into ${}^d\mathbf{C}^d = \mathbf{C}[P^d, T^d]$, ${}^d\mathbf{C}^c = \mathbf{C}[P^d, T^c]$, ${}^c\mathbf{C}^d = \mathbf{C}[P^c, T^d]$ and ${}^c\mathbf{C}^c = \mathbf{C}[P^c, T^c]$. The firing rate matrix is divided into $\boldsymbol{\Lambda}^d = \boldsymbol{\Lambda}[T^d, T^d]$ and $\boldsymbol{\Lambda}^d = \boldsymbol{\Lambda}[T^c, T^c]$. Similarly, for the configuration matrix, $\boldsymbol{\Pi}^d(\mathbf{M}_k^h) = \boldsymbol{\Pi}(\mathbf{M}_k^h)[T^d, P]$ and $\boldsymbol{\Pi}^c(\mathbf{M}_k^h) = \boldsymbol{\Pi}(\mathbf{M}_k^h)[T^c, P]$.

Since $P^d \cap ({}^\bullet T^c \cup T^{c\bullet}) = \emptyset$ then ${}^d\mathbf{C}^c = \mathbf{0}$. Therefore, the MHPN can be rewritten as two different but connected systems:

$$\begin{aligned} \boldsymbol{\mu}_{k+1} &\simeq \boldsymbol{\mu}_k +^d \mathbf{C}^d \cdot \Delta\boldsymbol{\sigma}(\mathbf{F}_k^d(\mathbf{M}_k^h)\Delta\tau) \\ \mathbf{m}_{k+1} &\simeq \mathbf{m}_k +^c \mathbf{C}^c \cdot \boldsymbol{\Lambda}^c\boldsymbol{\Pi}^c(\mathbf{m}_k)\mathbf{m}_k\Delta\tau +^c \mathbf{C}^d \cdot \Delta\boldsymbol{\sigma}(\mathbf{F}_k^d(\mathbf{M}_k^h)\Delta\tau) \end{aligned} \tag{2.25}$$

The flow of the fluid transitions only depends on the marking at the fluid places. On the contrary, the firing of discrete transitions depends on the marking of both discrete and fluid places, because discrete transitions can have input fluid places.

In this hybrid system, discrete transitions fire with random delays, while the continuous ones are deterministic w.r.t. the fluid marking. It is possible to add uncorrelated gaussian noise to the continuous transitions in order to improve the approximation of the flow at these (as done in the TCPN model).

Definition 2.12. A *Markovian hybrid* Petri net system with *noise* (MnHPN) is the tuple $\langle \mathcal{N}, \boldsymbol{\lambda}, \mathbf{M}_0^h \rangle$, defined in discrete-time as a MHPN system in which gaussian noise is added to the flow of the continuous transitions. Thus, each $t_j \in T^c$ fires according to $\Delta w_j = f_j(\mathbf{M}_k^h)\Delta\tau + v_j$, where the noise v_j is defined as $v_j \sim Normal(0, f_j(\mathbf{M}_k^h)\Delta\tau)$, i.e., like in TnCPNs.

The evolution of the MnHPN is given by:

$$\mathbf{M}_{k+1}^h \simeq \mathbf{M}_k^h + \mathbf{C} \cdot \begin{bmatrix} \Delta\boldsymbol{\sigma}(\mathbf{F}_k^d(\mathbf{M}_k^h)\Delta\tau) \\ \Delta\mathbf{w}_k \end{bmatrix} \tag{2.26}$$

An alternative representation, in which the marking at fluid and discrete places is separated, is given by:

$$\begin{aligned} \boldsymbol{\mu}_{k+1} &\simeq \boldsymbol{\mu}_k +^d \mathbf{C}^d \cdot \Delta\boldsymbol{\sigma}(\mathbf{F}_k^d(\mathbf{M}_k^h)\Delta\tau) \\ \mathbf{m}_{k+1} &\simeq \mathbf{m}_k +^c \mathbf{C}^c \cdot \Delta\mathbf{w}_k +^c \mathbf{C}^d \cdot \Delta\boldsymbol{\sigma}(\mathbf{F}_k^d(\mathbf{M}_k^h)\Delta\tau) \\ &= \mathbf{m}_k +^c \mathbf{C}^c \cdot \boldsymbol{\Lambda}^c\boldsymbol{\Pi}^c(\mathbf{m}_k)\mathbf{m}_k\Delta\tau +^c \mathbf{C}^c \cdot \mathbf{v}_k +^c \mathbf{C}^d \cdot \Delta\boldsymbol{\sigma}(\mathbf{F}_k^d(\mathbf{M}_k^h)\Delta\tau) \end{aligned} \tag{2.27}$$

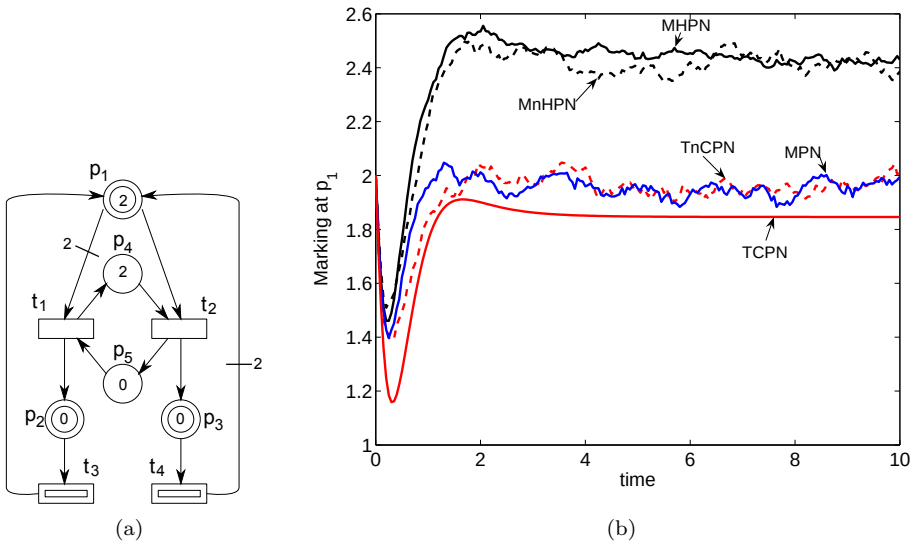

Fig. 2.5: a) A PN system with $\boldsymbol{\lambda} = [1, 3, 1, 2]^T$. b) Average marking trajectories obtained from 1000 simulations for the MPN and the different relaxations. As a hybrid model, nodes t_1, t_2, p_4 and p_5 are discrete.

2.4.2 Approximation of the MPN model by a MHPN

The MHPN model is defined as a partial relaxation of the MPN, so, one could think that the approximation provided by the *hybrid* system to the original *discrete* one should be better than that provided by the totally relaxed *continuous* model. However, that is not always the case.

Example 2.6. Consider the MPN system of fig. 2.5(a) with rates $\boldsymbol{\lambda} = [1, 3, 1, 2]^T$. This PN model was simulated 1000 times as a discrete, fluid and hybrid system, in order to obtain average trajectories of the marking at p_1. As a hybrid model, nodes $\{t_1, t_2, p_4, p_5\}$ are discrete, while others are continuous. Fig. 2.5(b) shows the resulting average trajectories for the marking at p_1. It can be seen that fluid models TCPN (1.5) and TnCPN (2.10) provide a better approximation to the MPN than hybrid models MHPN (2.25) and MnHPN (2.27), i.e., *a partial relaxation is not necessarily better than a full relaxation!*

Through this subsection, it will be shown that the expected value of the marking of a MPN system can be approximated by that of a MHPN, having the same structure, rates and initial markings, but under some particular conditions.

Let us introduce a structural condition for the net of the MHPN:

- *Condition 3.* Discrete transitions have only discrete input places, i.e., $\forall t_i \in T^d \; {}^\bullet t_i \subseteq P^d$.

Assuming this condition, the following proposition describes two particular cases in which the approximation of the average marking of a MPN is achieved.

Proposition 2.13. *Consider an ergodic* $MPN = \langle \mathcal{N}, \boldsymbol{\lambda}, \mathbf{M}_0 \rangle$ *and a* $MHPN = \langle \mathcal{N}, \boldsymbol{\lambda}, \mathbf{M}_0^h \rangle$, *with* $\mathbf{M}_0^h = \mathbf{M}_0$. *Assume that the MHPN fulfills the condition 3 and the continuous transitions are constrained by only one place, i.e., continuous transitions do not represent rendez-vous (synchronizations).*

1. *If the continuous subnet (the subnet $\langle P^c, T^c, \mathbf{Pre}[P^c, T^c], \mathbf{Post}[P^c, T^c]\rangle$) in the MHPN is ordinary then the approximation is achieved. In fact, $\boldsymbol{\varepsilon}_k = \mathbf{0}$.*

2. *If there exists a unique asymptotically stable equilibrium point in the system described by the continuous subnet, then $\boldsymbol{\varepsilon}_k$ is ultimately bounded. Moreover, the larger the average enabling degree of the continuous transitions, the lower $\boldsymbol{\epsilon}_k$.*

Proof. The evolution of the MHPN system is represented by (2.25), where the marking is splitted into the marking of discrete places P^d ($\boldsymbol{\mu}_k$) and continuous places P^c ($\mathbf{m}_k$). The same distinction can be applied to the marking of the MPN, i.e., we represent as $\mathbf{M}^d$ ($\mathbf{M}^c$) the marking of the MPN at the places that are kept as discrete (are fluidified) in the hybrid version, i.e., those in P^d (P^c). Similarly, we use the notation $\mathbf{F}_k^d(\cdot) = \mathbf{F}_k(\cdot)[T^d]$ and $\mathbf{F}_k^c(\cdot) = \mathbf{F}_k(\cdot)[T^c]$. By doing this and using (1.2), the evolution of the MPN system can be described as:

$$\begin{aligned}\mathbf{M}_{k+1}^d &= \mathbf{M}_k^d +^d \mathbf{C}^d \cdot \Delta\boldsymbol{\sigma}(\mathbf{F}_k^d(\mathbf{M}_k)\Delta\tau)\\ \mathbf{M}_{k+1}^c &= \mathbf{M}_k^c +^c \mathbf{C}^d \cdot \Delta\boldsymbol{\sigma}(\mathbf{F}_k^d(\mathbf{M}_k)\Delta\tau) +^c \mathbf{C}^c \cdot \Delta\boldsymbol{\sigma}(\mathbf{F}_k^c(\mathbf{M}_k)\Delta\tau)\end{aligned} \tag{2.28}$$

Since condition 3 holds, the firing of discrete transitions in the MHPN depends only on the marking at discrete places, i.e., $\Delta\boldsymbol{\sigma}(\mathbf{F}_k^d(\mathbf{M}_k^h)\Delta\tau)$ in (2.25) can be expressed as $\Delta\boldsymbol{\sigma}(\mathbf{F}_k^d(\mathbf{M}_k^h)\Delta\tau) = \Delta\boldsymbol{\sigma}(\Lambda^d \cdot Enab(\boldsymbol{\mu}_k)\Delta\tau)$. Similarly, the firing of transitions of the MPN, that are kept as discrete in the hybrid version, depends only on the marking $\mathbf{M}^d$, i.e., $\Delta\boldsymbol{\sigma}(\mathbf{F}_k^d(\mathbf{M}_k)\Delta\tau)$ in (2.28) is equal to $\Delta\boldsymbol{\sigma}(\Lambda^d \cdot Enab(\mathbf{M}_k^d)\Delta\tau)$. Substituting this into (2.28) and (2.25), it can be obtained, for the marking of places P^d:

$$\begin{aligned}\mathbf{M}_{k+1}^d &= \mathbf{M}_k^d +^d \mathbf{C}^d \cdot \Delta\boldsymbol{\sigma}(\Lambda^d \cdot Enab(\mathbf{M}_k^d)\Delta\tau) \qquad \text{for the MPN, and}\\ \boldsymbol{\mu}_{k+1} &= \boldsymbol{\mu}_k +^d \mathbf{C}^d \cdot \Delta\boldsymbol{\sigma}(\Lambda^d \cdot Enab(\boldsymbol{\mu}_k)\Delta\tau) \qquad \text{for the MHPN}\end{aligned} \tag{2.29}$$

Thus, the evolution of both $\mathbf{M}^d$ and $\boldsymbol{\mu}$ are ruled by similar equations. Furthermore, since $\mathbf{M}_0^h = \mathbf{M}_0$ then $E\{\mathbf{M}_k^d\} = E\{\boldsymbol{\mu}_k\}$, equivalently, $\boldsymbol{\varepsilon}_k[P^d] = \mathbf{0}$.

Now, let us analyze the approximation at the places that are fluidified. The average marking of $\mathbf{M}^c$, of the MPN (2.28), and the marking $\mathbf{m}$, of the MHPN (2.25), can be expressed as:

$$\begin{aligned}E\{\mathbf{M}_{k+1}^c\} &= E\{\mathbf{M}_k^c\} +^c \mathbf{C}^d \cdot E\{\Delta\boldsymbol{\sigma}(\mathbf{F}_k^d(\mathbf{M}_k)\Delta\tau)\} +^c \mathbf{C}^c \cdot E\{\Delta\boldsymbol{\sigma}(\mathbf{F}_k^c(\mathbf{M}_k)\Delta\tau)\}\\ E\{\mathbf{m}_{k+1}\} &= E\{\mathbf{m}_k\} +^c \mathbf{C}^d \cdot E\{\Delta\boldsymbol{\sigma}(\mathbf{F}_k^d(\mathbf{M}_k^h)\Delta\tau)\} +^c \mathbf{C}^c \cdot E\{\Lambda^c\boldsymbol{\Pi}^c(\mathbf{m}_k)\mathbf{m}_k\Delta\tau\}\end{aligned}$$

These equations can be used for representing the average approximation error at the continuous transitions, denoted as $\boldsymbol{\varepsilon}_k^c = \boldsymbol{\varepsilon}_k[P^c] = E\{\mathbf{M}_k^c\} - E\{\mathbf{m}_k\}$, as a linear system. Let us detail this. First, it has been shown that $\Delta\boldsymbol{\sigma}(\mathbf{F}_k^d(\mathbf{M}_k)\Delta\tau) = \Delta\boldsymbol{\sigma}(\Lambda^d \cdot Enab(\mathbf{M}^d)\Delta\tau)$ in the MPN, while $\Delta\boldsymbol{\sigma}(\mathbf{F}_k^d(\mathbf{M}_k^h)\Delta\tau) = \Delta\boldsymbol{\sigma}(\Lambda^d \cdot Enab(\boldsymbol{\mu})\Delta\tau)$ in the MHPN. Since $\boldsymbol{\mu}$ evolves like $\mathbf{M}^d$ (they behave according to the same difference equation (2.29)) then $E\{\Delta\boldsymbol{\sigma}(\mathbf{F}_k^d(\mathbf{M}_k)\Delta\tau)\} = E\{\Delta\boldsymbol{\sigma}(\mathbf{F}_k^d(\mathbf{M}_k^h)\Delta\tau\}$. On the other hand, let us define the vector $\mathbf{b}_k^c = \boldsymbol{\Pi}^c(\mathbf{M}_k^c)\mathbf{M}_k^c - \lfloor\boldsymbol{\Pi}^c(\mathbf{M}_k^c)\mathbf{M}_k^c\rfloor$, that represents the difference by rounding the enabling degree to the nearest lower integer. Thus, for the MPN, the average firing count of the transitions in T^c can be expressed as $E\{\Delta\boldsymbol{\sigma}(\mathbf{F}_k^c(\mathbf{M}_k)\Delta\tau)\} = \boldsymbol{\Lambda}^c E\{\lfloor\boldsymbol{\Pi}^c(\mathbf{M}_k^c)\mathbf{M}_k^c\}\rfloor\Delta\tau = \boldsymbol{\Lambda}^c E\{\boldsymbol{\Pi}^c(\mathbf{M}_k^c)\mathbf{M}_k^c\}\Delta\tau + \boldsymbol{\Lambda}^c\Delta\tau E\{\mathbf{b}_k^c\}$,

Tab. 2.5: Average steady state markings at p_7 for the MPN and MHPN of fig. 2.6(a)

q	MPN	MHPN	ϵ_{ss}
1	1.17	0.69	0.410
2	1.83	1.34	0.268
4	2.63	3.09	0.175
10	6.85	6.35	0.073
50	32.73	32.09	0.020

where $\mathbf{0} \leq \mathbf{b}_k^c \leq \mathbf{1}$. Furthermore, since each transition in T^c is constrained by only one place then $\mathbf{\Pi}^c(\mathbf{M}_k^c) = \mathbf{\Pi}^c$. Substituting these expressions into the previous equation, it is obtained:

$$E\{\mathbf{M}_{k+1}^c\} - E\{\mathbf{m}_{k+1}\} = \boldsymbol{\varepsilon}_{k+1}^c = [\mathbf{I} +^c \mathbf{C}^c \cdot \Lambda^c \mathbf{\Pi}^c \Delta\tau]\, \boldsymbol{\varepsilon}_k^c +^c \mathbf{C}^c \mathbf{\Lambda}^c \Delta\tau \mathbf{b}_k^c \tag{2.30}$$

If the continuous subnet of the MHPN is ordinary then $\mathbf{b}_k^c = \mathbf{0}$. Furthermore, since $\mathbf{M}_0 = \mathbf{M}_0^h$ then $\boldsymbol{\varepsilon}_0^c = \mathbf{0}$. Thus, according to (2.30), $\boldsymbol{\varepsilon}_k^c = \mathbf{0}$ for all future time k, i.e., the approximation is achieved. Statement 1 is thus proved.

Let us consider now the case in which the continuous subnet is non ordinary. The evolution of the error (2.30) can be seen as a nominal system, described by $\boldsymbol{\varepsilon}_{k+1}^c = [\mathbf{I} +^c \mathbf{C}^c \cdot \Lambda^c \mathbf{\Pi}^c \Delta\tau]\, \boldsymbol{\varepsilon}_k^c$, under non-vanishing but bounded perturbation ${}^c\mathbf{C}^c \mathbf{\Lambda}^c \Delta\tau \mathbf{b}_k^c$. Now, by hypothesis, the origin ($\boldsymbol{\varepsilon}_k^c = \mathbf{0}$) is asymptotically stable in the nominal system (equivalently, the eigenvalues of $[\mathbf{I} +^c \mathbf{C}^c \mathbf{\Lambda}^c \mathbf{\Pi}^c \Delta\tau]$, non related to P-flows, are inside the unity circle). By following the same reasoning used in the proof of Proposition 2.2, it can be proved that the asymptotic stability in the nominal error system implies that the error $\boldsymbol{\varepsilon}_k^c$ is ultimately bounded. In fact, the larger $E\{\mathbf{M}_k\}$ and the number of active servers, the lower the relative error $\boldsymbol{\epsilon}_k$ (because $\boldsymbol{\epsilon}_k = \boldsymbol{\varepsilon}_k ./ E\{\mathbf{M}_k\}$), thus, the better the approximation. ∎

Example 2.7. Consider the PN system of fig. 2.6(a) with $\boldsymbol{\lambda} = [1, 1, 1, 1, 1, 1, 1, 1, 1]^T$. This PN was simulated 1000 times as a discrete and a hybrid system, for different initial markings $\mathbf{M}_0 = \mathbf{M}_0^h = q \cdot [1, 0, 1, 0, 0, 0, 0, 0]^T$. As a hybrid model, nodes t_6, t_7, t_8, t_9, p_6, p_7 and p_8 are continuous, while others are kept as discrete. Table 2.5 shows the average steady state markings at place p_7. As it is expected, according to Proposition 2.13 (statement 2), the larger the average enabling degrees (which occurs for large average markings) the lower the relative approximation error ϵ_{ss}, which occurs for large values of q. Fig. 2.6(b) shows the average marking trajectories at the places p_1 and p_7, for the case $q = 50$. It can be seen that, not only the steady state but also the transient behavior is well approximated in this case.

Remark 2.14. Condition 3 implies that the marking at discrete places behave exactly in the same way in the MPN and the MHPN systems. This condition can be relaxed when the enabling degree of the discrete transitions is large, but it is critical in the case that the discrete transitions are barely enabled (like in the Example 2.6 of fig. 2.5, where the continuous place p_1 barely enables discrete transition t_1).

In the following proposition, the results of Proposition 2.13 are extended in two different senses: condition 3 is no longer required, and the continuous subnet of the MHPN is not assumed to be Join-Free. In this way, no restriction is assumed in the structure of the net, and the selection of discrete and

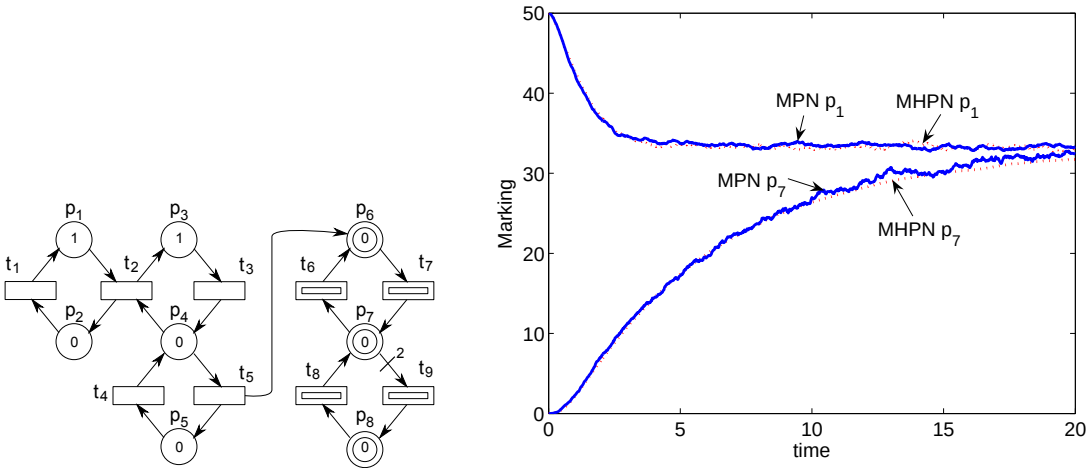

Fig. 2.6: a) A MPN system in which ${}^\bullet\{T^d\} \subseteq T^d$. As a hybrid model, nodes $t_6, t_7, t_8, t_9, p_6, p_7$ and p_8 are continuous, fulfilling condition 3.b) Average marking trajectories at places p_1 and p_7 for the case $q = 50$, obtained from 200 simulations. Solid curves correspond to MPN while dashed curves represent MHPN.

continuous transitions in the MHPN can be done freely (condition 3 constrains the selection of discrete and fluid transitions during the fluidization). Nevertheless, it is required that the enabling degrees of all the transitions in both systems be large, and that both systems evolve mainly in one region. This result can be seen as a generalization of Proposition 2.3 to hybrid systems.

Proposition 2.15. *Consider a bounded in average and ergodic* $MPN = \langle \mathcal{N}, \boldsymbol{\lambda}, \mathbf{M}_0 \rangle$ *and a* $MHPN = \langle \mathcal{N}, \boldsymbol{\lambda}, \mathbf{M}_0^h \rangle$*, with* $\mathbf{M}_0^h = \mathbf{M}_0$*. Assume that each transition in both systems is constrained by one place with a high probability, thus* $Prob(\mathbf{M}_k \in \Re_j) \simeq 1$ *and* $Prob(\mathbf{M}_k^h \in \Re_j) \simeq 1$*, for some region* $\Re_j$*. If the eigenvalues of* $[\mathbf{I} + \mathbf{C}\boldsymbol{\Lambda}\boldsymbol{\Pi}_j\Delta\tau]$ *(non-related to P-flows) are inside the unity circle, the marking approximation error* $\boldsymbol{\varepsilon}_k$ *is ultimately bounded. The larger* $Prob(\mathbf{M}_k \in \Re_j)$*,* $Prob(\mathbf{M}_k^h \in \Re_j)$ *and the enabling degrees (for the most probable trajectories), the lower the relative approximation error* $\boldsymbol{\epsilon}_k$*.*

Proof. In the proof of Proposition 2.13, the approximation error was described as the state of a linear system under a bounded perturbation. The same idea will be used in this proof. First, as shown in the proof of Proposition 2.3, by using the variable $\boldsymbol{\zeta}_k^j$ defined in (2.7), the enabling of the transitions of the MPN can be expressed as $E\{\lfloor \boldsymbol{\Pi}(\mathbf{M}_k)\mathbf{M}_k \rfloor\} = \boldsymbol{\Pi}_j E\{\mathbf{M}_k\} + \boldsymbol{\zeta}_k^j - E\{\mathbf{b}_k\}$. Now, the system is bounded in average, then, denoting as $\mathbf{M}_{max}$ the vector whose entries are the bounds for the average marking at the corresponding places, $\boldsymbol{\zeta}_k^j$ (2.7) is upperbounded as in (2.8). Accordingly, the firing count can be expressed as $E\{\Delta\boldsymbol{\sigma}(\mathbf{F}_k(\mathbf{M}_k)\Delta\tau)\} = \boldsymbol{\Lambda} \cdot \boldsymbol{\Pi}_j E\{\mathbf{M}_k\}\Delta\tau + \boldsymbol{\Lambda} \cdot (\boldsymbol{\zeta}_k^j - E\{\mathbf{b}_k\})\Delta\tau$, where $|E\{\mathbf{b}_k\}| \leq \mathbf{1}$ and $|\boldsymbol{\zeta}_k^j|$ is upper-bounded by a linear function of $(1 - Prob(\mathbf{M}_k \in \Re_j)$ (the larger $Prob(\mathbf{M}_k \in \Re_j)$ the lower the upper-bound for $\boldsymbol{\zeta}_k^j$ (2.8)).

Now, by using the difference equation (1.2) and the expression obtained for $E\{\Delta\boldsymbol{\sigma}(\mathbf{F}_k(\mathbf{M}_k)\Delta\tau)\}$, the expected value of the marking of the MPN can be expressed as:

$$E\{\mathbf{M}_{k+1}\} = [\mathbf{I} + \mathbf{C}\boldsymbol{\Lambda}\boldsymbol{\Pi}_j\Delta\tau]\, E\{\mathbf{M}_k\} + \mathbf{C}\boldsymbol{\Lambda} \cdot (\boldsymbol{\zeta}_k^j - E\{\mathbf{b}_k\})\Delta\tau \tag{2.31}$$

Tab. 2.6: Average steady state markings at p_1 for the MPN and MHPN of fig. 2.5(a). * In the first experiment, $\mathbf{M}_{ss}$ belongs to different regions with low probability.

$\mathbf{M}_0[p_1]$	MPN	MHPN	ϵ_{ss}	$Prob(\mathbf{M}_{ss} \in \Re_j)$
2	2.02	2.51	0.241	0.033*
4	3.29	3.86	0.173	0.442
6	4.81	1.35	0.123	0.734
8	6.70	7.05	0.052	0.894
10	8.54	8.68	0.016	0.966

Similarly, the expected value for the marking of the MHPN can be expressed as:

$$E\{\mathbf{M}_{k+1}^h\} = [\mathbf{I} + \mathbf{C}\boldsymbol{\Lambda}\boldsymbol{\Pi}_j\Delta\tau]\, E\{\mathbf{M}_k^h\} + \mathbf{C}\boldsymbol{\Lambda} \cdot (\boldsymbol{\zeta}_k^{j,h} - E\{\mathbf{b}_k^h\})\Delta\tau \tag{2.32}$$

where $\boldsymbol{\zeta}_k^{j,h}$ and $E\{\mathbf{b}_k^h\}$ are analogous to $\boldsymbol{\zeta}_k^j$ and $E\{\mathbf{b}_k\}$ for the MHPN, and their absolute values are also upper bounded. Moreover, $E\{\mathbf{b}_k^h\}[T^c] = \mathbf{0}$, because $\Delta\boldsymbol{\sigma}(\cdot)$ is defined only for the discrete transitions in the MHPN. Combining (2.31) and (2.32) it is obtained:

$$\boldsymbol{\varepsilon}_{k+1} = [\mathbf{I} + \mathbf{C}\boldsymbol{\Lambda}\boldsymbol{\Pi}_j\Delta\tau]\, \boldsymbol{\varepsilon}_k + \mathbf{C}\boldsymbol{\Lambda} \cdot (\boldsymbol{\zeta}_k^{j,h} - \boldsymbol{\zeta}_k^j - E\{\mathbf{b}_k^h\} + E\{\mathbf{b}_k\})\Delta\tau \tag{2.33}$$

Given lower bounds for $Prob(\mathbf{M}_k \in \Re_j)$ and $Prob(\mathbf{M}_k^h \in \Re_j)$, the term $|\boldsymbol{\zeta}_k^{j,h} - \boldsymbol{\zeta}_k^j - E\{\mathbf{b}_k^h\} + E\{\mathbf{b}_k|$ is upper bounded by a constant value. Then, the approximation analysis in this case can be reduced to that of the proof of Proposition 2.3, i.e., the error system (2.33) can be seen as a nominal system $\boldsymbol{\varepsilon}_{k+1} = [\mathbf{I} + \mathbf{C}\boldsymbol{\Lambda}\boldsymbol{\Pi}_j\Delta\tau]\, \boldsymbol{\varepsilon}_k$ under non-vanishing bounded perturbation $\mathbf{C}\boldsymbol{\Lambda}\cdot(\boldsymbol{\zeta}_k^{j,h} - \boldsymbol{\zeta}_k^j - E\{\mathbf{b}_k^h\} + E\{\mathbf{b}_k\})\Delta\tau$. Thus, assuming asymptotical stability of the the nominal system in $\Re_j$ (equivalently, the eigenvalues of $[\mathbf{I}+\mathbf{C}\boldsymbol{\Lambda}\boldsymbol{\Pi}_j\Delta\tau]$, non-related to P-flows, are inside the unity circle), it can be proved that the approximation error $\boldsymbol{\varepsilon}_k$ is ultimately bounded by a function of $Prob(\mathbf{M}_k \notin \Re_j)$ and $Prob(\mathbf{M}_k^h \notin \Re_j)$. Thus, the larger $Prob(\mathbf{M}_k \in \Re_j)$, $Prob(\mathbf{M}_k^h \in \Re_j)$ and the enabling degrees, the lower the relative approximation error $\boldsymbol{\epsilon}_k$. ∎

Example 2.8. Consider again the system of figure 2.5(a) with the same firing rates. The MPN and MHPN systems have been simulated 1000 times for different initial markings at p_1, while the initial markings for the other places remain as in fig. 2.5(a). Table 2.6 resumes the results thus obtained. The last column is the probability that $\mathbf{M}_k$ belongs to region $\Re_j$, in which t_1 and t_2 are constrained by p_5 and p_4, respectively. As expected, according to Proposition 2.15, the relative error is low when the probability that the marking belongs to an unique region is large, i.e., when $Prob(\mathbf{M}_{ss} \in \Re_j)$ is large. Fig. 2.7 shows the average marking trajectories at the places p_1 and p_2, for the case $\mathbf{M}_0[p_1] = 10$. It can be seen that, not only the steady state but also the transient behavior is well approximated.

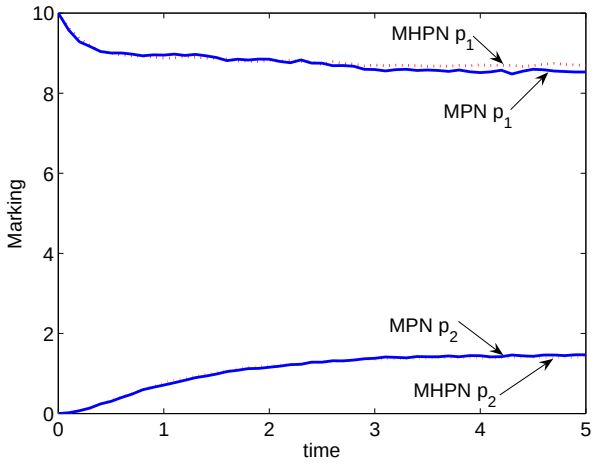

Fig. 2.7: Average marking trajectories of places p_1 and p_2 of the net model of fig. 2.5(a) with $\mathbf{M}_0[p_1] = 10$, obtained from 1000 simulations. Solid curves correspond to the MPN while dashed curves represent the MHPN.

2.4.3 Approximation of the pdf by a MnHPN

In the Subsection 2.3.2 it has been proved that the TnCPN system can approximate the pdf of the marking of the MPN when the expected enabling degree of all the transitions is large (Theorem 2.10). An analogous analysis is presented in this section, by proving that the pdf of the marking of the MPN can be approximated by that of a MnHPN.

The analysis in this section follows the same structure than that done for proving the $TnCPN$ approximation. First, consider the Lemma B.4 that appears in the Appendix B. This Lemma is the analogous result of Lemmas B.2 and B.3, but for MnHPNs. According to this, the larger the initial marking $\mathbf{M}_0^h$, the better the approximation of $\sum_{k=0}^{n} \Delta\boldsymbol{\sigma}(\mathbf{F}_k^d \Delta\tau)$ and $\sum_{k=0}^{n} \Delta\mathbf{w}_k$ by $Poisson(n\mathbf{F}_0^d\Delta\tau)$ and $Normal(n\mathbf{f}_0\Delta\tau)$, respectively, i.e., the sum of the firing counts of the discrete transitions is approximated by a Poisson r.v., while the sum of the flow at the continuous transitions with noise is approximated by a Normal r.v. By using this, the following result can be derived:

Lemma 2.16. *Consider a MPN and a MnHPN live and ergodics, having the same structure, rates and initial marking* $\mathbf{M}_0 = \mathbf{M}_0^h = q \cdot \mathbf{M}_0^r$. *Consider the evolution of both systems with the sampling* $\Delta\tau = \Delta^r\tau/q$ *during a fix number of time steps* n.

1. *For a large enough* n, *the probability distribution of* $\mathbf{M}_n^h$ *converges to that of* $\mathbf{M}_n$ *when* $q \to \infty$. *The larger* q, *the closer the pdf's of* $\mathbf{M}_n$ *and* $\mathbf{M}_n^h$.

2. *Assume that at some time step* k *the distribution of* $\mathbf{M}_k^h$ *approximates that of* $\mathbf{M}_k$. *Then, the larger the enabling degree for the most probable values of* $\mathbf{M}_k$, *the closer the pdf's of* $\mathbf{M}_{k+n}^h$ *and* $\mathbf{M}_{k+n}$.

Proof. According to (1.2), the marking of the MPN at time step n, is given by:

$$\mathbf{M}_n = \mathbf{M}_0 + \mathbf{C}\sum_{k=0}^{n-1} \Delta\boldsymbol{\sigma}(\mathbf{F}_k\Delta\tau) = \mathbf{M}_0 + \mathbf{C}\begin{bmatrix} \sum_{k=0}^{n-1} \Delta\boldsymbol{\sigma}(\mathbf{F}_k[T^d]\Delta\tau) \\ \sum_{k=0}^{n-1} \Delta\boldsymbol{\sigma}(\mathbf{F}_k[T^c]\Delta\tau) \end{bmatrix} \tag{2.34}$$

Similarly, according to (2.26), the marking of the MnHPN at time step n can be represented as:

$$\mathbf{M}_n^h = \mathbf{M}_0^h + \mathbf{C}\begin{bmatrix} \sum_{k=0}^{n-1} \Delta\boldsymbol{\sigma}(\mathbf{F}_k^d \Delta\tau) \\ \sum_{k=0}^{n-1} \Delta\mathbf{w}_k \end{bmatrix} \tag{2.35}$$

Comparing these equations it can be seen that the pdf of $\mathbf{M}_n^h$ approximates that of $\mathbf{M}_n$ if the pdfs of $\sum_{k=0}^{n-1} \Delta\boldsymbol{\sigma}(\mathbf{F}_k^d \Delta\tau)$ and $\sum_{k=0}^{n-1} \Delta\mathbf{w}_k$ approximate those of $\sum_{k=0}^{n-1} \Delta\boldsymbol{\sigma}(\mathbf{F}_k[T^d]\Delta\tau)$ and $\sum_{k=0}^{n-1} \Delta\boldsymbol{\sigma}(\mathbf{F}_k[T^c]\Delta\tau)$, respectively.

According to the Lemmas B.2 and B.4, the larger the initial marking the better the approximation of $\sum_{i=0}^{k-1} \Delta\boldsymbol{\sigma}(\mathbf{F}_k \Delta\tau)$ by $Poisson(n \cdot \mathbf{F}_0^r \Delta^r \tau)$ in the MPN, and $\sum_{k=0}^{n-1} \Delta\boldsymbol{\sigma}(\mathbf{F}_k^d \Delta\tau)$ by $Poisson(n\mathbf{F}_0^{d,r} \Delta^r \tau)$ in the MnHPN. Thus, since $\mathbf{F}_0^r[T^d]\Delta^r\tau = \mathbf{F}_0^{d,r}\Delta^r\tau$ then $\sum_{k=0}^{n-1} \Delta\boldsymbol{\sigma}(\mathbf{F}_k[T^d]\Delta\tau)$ and $\sum_{k=0}^{n-1} \Delta\boldsymbol{\sigma}(\mathbf{F}_k^d\Delta\tau)$ have similar pdfs for large initial markings.

On the other hand, note that $n \cdot \mathbf{F}_0^r[T^c]\Delta^r\tau = n \cdot \mathbf{f}_0\Delta\tau$, because $\mathbf{F}_0^r[T^c]\Delta^r\tau = \Lambda^c\Pi^c(\mathbf{M}_0^r)\mathbf{M}_0^r\Delta^r\tau = \Lambda^c\Pi^c(\mathbf{M}_0)\mathbf{M}_0\Delta\tau = \mathbf{f}_0\Delta\tau$ and $\mathbf{M}_0 = \mathbf{M}_0^h$. Furthermore, by Lemma B.4, $\sum_{k=0}^{n-1} \Delta\mathbf{w}_k$ is approximated by $Normal(n\mathbf{f}_0\Delta\tau)$ for large initial markings. Analogously, $\sum_{i=0}^{k-1} \Delta\boldsymbol{\sigma}(\mathbf{F}_k[T^c]\Delta\tau)$ is approximated by $Poisson(n \cdot \mathbf{F}_0^r[T^c]\Delta^r\tau)$ according to Lemma B.2. Moreover, as mentioned in the proof of Lemma 2.9, a normal distribution approximates a Poisson one, i.e., $Normal(\eta, \eta) \simeq Poiss(\eta)$ for η large enough. The larger the parameter η the better the approximation. Then, if n is large enough (let us say, $n \cdot \mathbf{f}_0\Delta\tau >> 10$) then the approximation of $\sum_{k=0}^{n-1} \Delta\boldsymbol{\sigma}(\mathbf{F}_k[T^c]\Delta\tau)$ by $\sum_{k=0}^{n-1} \Delta\mathbf{w}_k$ follows. Thus, according to (2.34) and (2.35), the distribution of the marking of the MnHPN approximates that of the marking of the MPN at time step n. The first statement is thus proven.

The second statement can be demonstrated by following the same reasoning used for proving the statement 2 of Lemma 2.9. ∎

According to the previous lemma, if at some time step n the pdf of $\mathbf{M}_n$ is well approximated by that of $\mathbf{M}_n^h$, then the approximation holds at time step $2 \cdot n$. By following an inductive reasoning, it may be expected that the approximation will hold during the future evolution of both systems. This reasoning is formalized in the following theorem:

Theorem 2.17. *Consider a MPN and a MnHPN, having the same structure, rates and initial markings* $\mathbf{M}_0 = \mathbf{M}_0^h >> \mathbf{0}$. *Consider the evolution of both the MPN and the MnHPN systems during a large number of time steps* n. *Then, the probability approximation errors* $[Prob(\mathbf{M}_k = \mathbf{a}) - Prob^c(\mathbf{M}_k^h = \mathbf{a})]$, *for the most probable values of* $\mathbf{M}_k$, *are ultimately bounded. The larger the enabling degree for the most probable trajectories of the MPN system, the lower the bound for the approximation errors, thus, the better the approximation of the marking's pdf.*

Proof. This theorem can be proved by following the same structure that for the proof of Theorem 2.10. We consider the underlying Markov chain of the MPN system in discrete-time $\boldsymbol{\pi}_{k+1} = \mathbf{Q}_D\boldsymbol{\pi}_k$. After n time steps, the probability vector is given by $\boldsymbol{\pi}_{k+n} = [\mathbf{Q}_D]^n\boldsymbol{\pi}_k$. On the other hand, for the hybrid model we define the probability vector $\boldsymbol{\pi}_k^h$, whose entries correspond to the values $Prob^c(\mathbf{M}_k^h = \mathbf{a})$ for each $\mathbf{a} \in [\mathbb{N} \cup \{0\}]^{|P|}$. Suppose that the approximation holds at time step k, i.e., $\boldsymbol{\pi}_k^h \simeq \boldsymbol{\pi}_k$. Then, the *probability error* $\boldsymbol{\varepsilon}_{\boldsymbol{\pi}_k} = \boldsymbol{\pi}_k - \boldsymbol{\pi}_k^h$ can be expressed as in (2.24), where $\boldsymbol{\varepsilon}_{\boldsymbol{\pi}_k+n}^k$ is the approximation error

Tab. 2.7: Average steady state markings at p_4 for the MPN and MnHPN of fig. 2.8(a).

$\mathbf{M}_0[p_5] = \mathbf{M}_0[p_7]$	MPN	MHPN	ϵ_{ss}
1	1.48	1.26	0.143
2	1.88	2.05	0.089
3	2.52	2.36	0.064
4	2.61	2.74	0.051
6	4.07	3.89	0.043

introduced during the time interval $(k, k+n]$. Consider a lower (resp. upper) bound for the enabling degree (reps. for $\boldsymbol{\varepsilon}^k_{\boldsymbol{\pi}_k+n}$) at the time step k. According to Lemma 2.16, the larger the lower-bound for the enabling degree, the smaller the upper-bound for $\boldsymbol{\varepsilon}^k_{\boldsymbol{\pi}_k+n}$.
On the other hand, ergodicity of the MPN implies that, given $\boldsymbol{\varepsilon}_{\boldsymbol{\pi}_0}$ s.t. $\mathbf{1} \cdot \boldsymbol{\varepsilon}_{\boldsymbol{\pi}_0} = 0$, the nominal error system $\boldsymbol{\varepsilon}_{\boldsymbol{\pi}_{k+n}} = [\mathbf{Q}_D]^n \boldsymbol{\varepsilon}_{\boldsymbol{\pi}_k}$ will converge to $\mathbf{0}$, i.e., the origin is asymptotically stable on the (invariant) subspace $\mathbf{1} \cdot \boldsymbol{\varepsilon}_{\boldsymbol{\pi}_k} = 0$. The error system (2.24) can be seen as the nominal linear system $\boldsymbol{\varepsilon}_{\boldsymbol{\pi}_{k+n}} = [\mathbf{Q}_D]^n \boldsymbol{\varepsilon}_{\boldsymbol{\pi}_k}$, with the non-vanishing upper bounded perturbation $\boldsymbol{\varepsilon}^k_{\boldsymbol{\pi}_k+n}$. Since the origin is the only equilibrium point and it is asymptotically stable, then $\boldsymbol{\varepsilon}_{\boldsymbol{\pi}_{k+n}}$ is ultimately bounded. The larger the enabling degree, the lower the upper-bound for the non-vanishing perturbation, and so, the lower the ultimate bounded for the probability error. ∎

Remark 2.18. Theorem 2.17 states that the pdf of the marking of a MnHPN can approximate that of the corresponding MPN, if the enabling degrees are large enough with a high probability. In practice, we have found that the approximation holds even for small enabling degrees (condition 1 barely fulfilled, e.g., with $E\{Enab(T)\} \sim 2 \cdot \mathbf{1}$). Thus, Theorem 2.17 only provides sufficient conditions for the approximation. The critical transitions, in which the enabling is strongly related to the accuracy of the approximation, are those representing synchronizations (rendez-vous) and constrained by continuous places, especially, discrete transitions barely enabled by continuous places.

Example 2.9. Consider the system of fig. 2.8(a) with rates $\boldsymbol{\lambda} = [30, 2, 30, 30, 30, 3.5, 10]^T$. The net system was simulated 1000 times as discrete and hybrid for different initial markings at places p_5 and p_7, while the initial marking at the other places are constant and equal to those shown in fig. 2.8(a). As hybrid, transitions t_6, t_7 and places p_4, p_5, p_6, p_7, p_8 and p_9 are continuous, while other transitions and places are discrete. In table 2.7, it is shown the average steady state marking at p_4. As expected, the larger the enabling degrees (corresponding to large markings at the steady state), the better the approximation (the lower the relative error). Fig. 2.8(b) shows the trajectories described by the average and variance of the marking at p_9, for both the MPN and the MnHPN for the case $\mathbf{M}_0[p_5] = \mathbf{M}_0[p_7] = 4$. It can be seen that not only the average, but also the variance of the marking is well approximated in this case.

2.5 Improving by modifying the structure and semantics

Since the approximation provided until now by a fluid or hybrid PN is not always accurate (even with the addition of noise), a question that may arise is the possibility of improving such approximation by

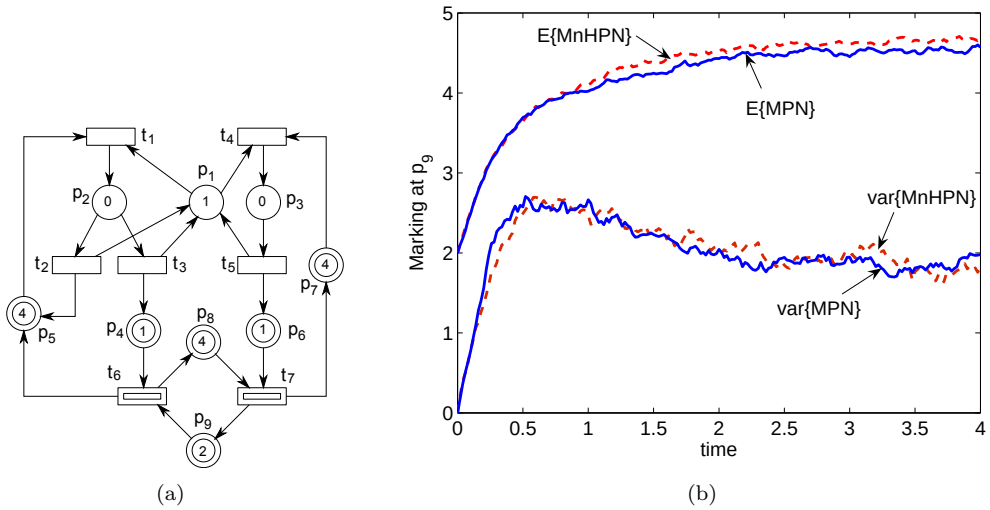

(a) (b)

Fig. 2.8: a) MPN system. As a hybrid PN, nodes t_6, t_7, p_4, p_5, p_6, p_7, p_8, p_9 are continuous while others are discrete. (b) Average and variance of the marking at p_9, for the MPN and the MnHPN, obtained from 1000 simulations.

means of modifying the continuous Petri net definition. Through this section, a couple of approaches, for such improvement, will be presented. Let us mention that these are just preliminarily ideas, that may lead to more developed techniques in the future.

2.5.1 Removing spurious solutions

In the field of discrete Petri nets, it is well known that the fundamental equation does not characterize the set of reachable markings, since it provides only a necessary condition for reachability, i.e., there may exist a marking $\mathbf{M'} = \mathbf{M}_0 + \mathbf{C} \cdot \boldsymbol{\sigma}$ with $\mathbf{M'} \in \mathbb{N}^{|P|}$ and $\boldsymbol{\sigma} \in \mathbb{N}^{|P|}$, but $\mathbf{M'}$ being unreachable (in the discrete PN). These markings are known as *spurious solutions* of the fundamental equation.

During the fluidization, spurious solutions become reachable markings in the autonomous continuous model, affecting the quality of the fluidization. This is specially undesirable when the spurious solutions represent deadlocks in the continuous PN, while the discrete system is live. The existence of such deadlock markings affects no only the steady state but also the dynamic behavior of the TCPN, even in the case that the spurious deadlock is not reachable in the timed model (i.e., it is reachable in the autonomous continuous PN, but not in the timed continuous).

Spurious deadlocks are related to traps. It is well known that initially marked traps cannot be completely emptied in discrete nets. Nevertheless, they can be emptied in continuous nets (in infinite time). Spurious deadlock markings can be computed in the following way:

Algorithm 2.1. Computation of spurious deadlocks.

Define $\mathbf{Pre}_\Theta$ and **$\mathbf{Post}_\Theta$** as $|P| \times |T|$ sized matrices such that:

I. $\mathbf{Pre}_\Theta[p,t] = 1$ if $\mathbf{Pre}[p,t] > 0$, $\mathbf{Pre}_\Theta[p,t] = 0$ otherwise.

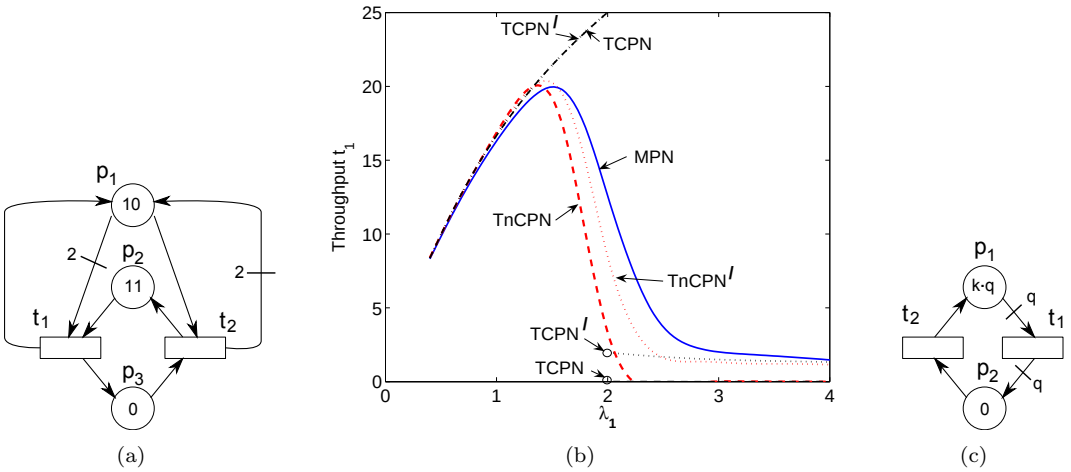

Fig. 2.9: a) A PN that integrates a spurious deadlock $\mathbf{M} = [0, 1, 10]^T$. b) Throughput for the MPN and its corresponding continuous relaxations, for $\lambda_1 \in [0.4, 4]$, $\lambda_2 = 1$ and initial marking $\mathbf{M}_0 = [10, 11, 0]^T$. c) Net model with weighted arcs.

II. $\mathbf{Post}_\Theta[p, t] = |{}^\bullet t|$ if $\mathbf{Post}[p, t] > 0$, $\mathbf{Post}_\Theta[p, t] = 0$ otherwise.

III. $\mathbf{C}_\Theta = \mathbf{Post}_\Theta - \mathbf{Pre}_\Theta$.

Compute a solution for the following linear inequalities system:

$$\begin{aligned}
&\mathbf{m} = \mathbf{m}_0 + \mathbf{C} \cdot \boldsymbol{\sigma},\ \mathbf{m}, \boldsymbol{\sigma} \geq 0, && \{\text{state equation}\}\\
&\mathbf{v}^T \cdot \mathbf{C}_\Theta = \mathbf{0},\ \mathbf{v} \geq \mathbf{0}, && \{\text{trap generator}\}\\
&\mathbf{v}^T \cdot \mathbf{m}_0 \geq 1, && \{\text{initially marked trap}\}\\
&\mathbf{v}^T \cdot \mathbf{m} = 0, && \{\text{trap empty at } \mathbf{m}\}
\end{aligned}$$

If there exists a solution **then** $\mathbf{m}$ is a spurious deadlock marking (w.r.t. the discrete net).

In this procedure, introduced in [Ezpeleta et al., 1993, Silva et al., 1998], equations $\mathbf{v}^T \cdot \mathbf{C}_\Theta = \mathbf{0}$ and $\mathbf{v} \geq \mathbf{0}$ define a generator of traps (Θ is a trap iff $\exists \mathbf{v} \geq \mathbf{0}$ such that $\Theta = ||\mathbf{v}||$ and $\mathbf{v}^T \cdot \mathbf{C}_\Theta = \mathbf{0}$). Thus, the above inequalities system directly imply that $||\mathbf{v}||$ is an initially marked trap that is empty at $\mathbf{m} \in Class(\mathbf{m}_0)$.

The approximation of the continuous model can be improved if the spurious solutions are *cut* from the state equation, by using the techniques introduced in [Colom and Silva, 1991]. In continuous systems, deadlock markings are always in the borders of the convex set of reachable markings and hence, spurious deadlocks can be cut by the addition of cutting implicit places (a place is said to be implicit if it is never the unique place that forbids the firing of its output transitions), increasing the number of P-semiflows and traps. Note that such an addition creates more traps that might be treated similarly (if they are the cause of spurious solutions). In any case, removing spurious solutions always represents an improvement of the fluidization, being specially important when those are deadlocks or represent non-live steady states.

Example 2.10. Consider the MPN given by the net of fig. 2.9(a) with initial marking $\mathbf{M}_0 = [10, 11, 0]^T$

and rates $\boldsymbol{\lambda} = [0.4, 1]$. This PN has a spurious deadlock $\mathbf{m} = [0, 1, 10]^T$, which can be cut by adding an *implicit* place. Since p_1 is an initially marked trap, its marking must satisfy $\mathbf{m}[p_1] \geq 1$. This equation together with the conservation law $\mathbf{m}[p_1] + \mathbf{m}[p_3] = 10$ leads to $\mathbf{m}[p_3] \leq 9$. This last inequality can be enforced in the state equation by adding a slack variable, i.e., a *cutting implicit place* q_3, such that $\mathbf{m}[p_3] + \mathbf{m}[q_3] = 9$. Thus q_3 is a place having t_2 as input transition, t_1 as output transition and 9 as initial marking. In the resulting net p_2 is implicit (structurally identical but with a higher marking) and therefore p_2 can be removed without affecting the system behavior. This is equivalent to consider $\mathbf{M}'_0 = [10, 9, 0]^T$ as the initial marking in the original net system of fig. 2.9(a). The MPN and the corresponding fluid model TCPN have been simulated for both initial markings $\mathbf{M}_0$ (with spurious deadlocks) and $\mathbf{M}'_0$, for different rates at t_1 ranging in $\lambda_1 \in [0.4, 4]$. The throughput at t_1, for both models, is shown if fig. 2.9(b). It can be seen that the MPN is live for any $\lambda_1 \in [0.4, 4]$, furthermore, the throughput seems as a smooth function of λ_1. On the other hand, the continuous model with the original $\mathbf{M}_0$ reaches the (spurious) deadlock for any $\lambda_1 \in (2, 4]$. Note the discontinuity at $\lambda_1 = 2$ for the TCPN model with both initial markings, i.e., the continuous model is neither monotonic nor smooth w.r.t the timing. Finally, it can be appreciated that the TCPN provides a much better approximation when the spurious deadlock is removed (with $\mathbf{M}'_0$), for any $\lambda_1 > 2$ (for $\lambda_1 \leq 2$ there is no change in the TCPN). Similarly, the continuous relaxation with noise TnCPN provides a better approximation when the spurious deadlock is removed. In fact, note in fig. 2.9(b) that the best fluid approximation is obtained with the combination of both improvements: removing spurious deadlocks and adding noise to the transitions.

2.5.2 Modification of the semantics

A semantics-modification approach has been proposed in [Lefebvre et al., 2009, Lefebvre et al., 2010]. There, in order to make the steady state of the continuous PN ($\mathbf{m}_{ss}$) to coincide with that of the MPN ($\mathbf{M}_{ss}$), the authors proposed a modification of the firing rates $\boldsymbol{\lambda}$ of the transitions in the continuous model. Two techniques are introduced: first, the firing rates are defined as *piecewise-constant*, i.e., $\boldsymbol{\lambda} \in \{\boldsymbol{\lambda}_1, ..., \boldsymbol{\lambda}_r\}$, depending on the configuration at which $\mathbf{m}(\tau)$ belongs, in the second approach (called *adaptive*) the firing rates are adjusted according to the instantaneous approximation error (in particular, $\dot{\boldsymbol{\lambda}} = \eta \cdot diag(\beta \mathbf{C}^T(\mathbf{M}_{ss} - \mathbf{m}(\tau)) + (1-\beta)(\boldsymbol{\chi}_{ss} - \mathbf{f}(\tau))$, with $\eta > 0$ and $\beta \in [0, 1]$ being decision parameters).

A different approach is considered here, consisting in the modification of the semantics but just for particular continuous transitions, which have weighted input arcs. In detail, as already mentioned, the existence of arc weights (a kind of synchronizations) affects the quality of the fluidization. A critical case occurs when there exists a transition t_j with a q-bounded input place $p_i \in {}^\bullet t_j$ and the weight of the arc connecting them is q as well (in any case, since liveness is assumed, the weight of the arcs cannot be larger than the bound of the corresponding input places). Consequently, the marking at p_i must be equal to its upper bound in order to enable t_j (the most basic example of this case is given in fig. 2.9(c) for $k = 1$, where the TCPN fails in approximating the throughput of t_1 when $q >> 1$). In this situation, transition t_j is enabled only at a few specific markings of the autonomous reachability set (in the example of fig. 2.9(c), the worst case is found because t_1 is enabled at *only one* marking). This enabling property is not captured by the continuous relaxation, where t_j is enabled whenever the places in ${}^\bullet t_j$ are marked, leading to significant approximation errors, i.e., $Enab(t_j) = \lfloor \mathbf{M}[p_i]/q \rfloor = 0$ for

almost all the markings, while in the TCPN $enab(t_j) = \mathbf{m}[p_i]/q > 0$ whenever $\mathbf{m}[p_i] > 0$. In order to improve the continuous approximation (for hybrid approximation other reasoning must be considered), the server semantics of the TCPN must be modified for t_j. A heuristic way for doing this, assuming $\{p_i\} = {}^\bullet t_j$, consists in the following expression: $\mathbf{f}[t_j] = \lambda_i(\mathbf{m}[p_i]/q)^q$ (this is obtained from a probabilistic relaxed view, in which the probability of a token to be in p_i is assumed as $E\{\mathbf{M}[p_i]\}/q$). This equation is equivalent to $\mathbf{f}[t_j] = \lambda_i \mathbf{m}[p_i] \cdot (\mathbf{m}[p_i]^{q-1}/q^q)$, which can be seen as the original ISS but multiplied by the marking-dependent function $(\mathbf{m}[p_i]^{q-1}/q^q)$. This modification may provide a better approximation. For instance, in the net of fig. 2.9(c) with $k = 1$ and $q = 4$, the throughput of t_1 obtained with this new semantic is 0.275, which is closer to the throughput of the MPN (0.32) than that obtained with the ISS (0.5). Nevertheless, further investigation is required in order to understand how and when the improvement is achieved.

2.6 Conclusions on fluidization

The approximation of the dynamical behavior of continuous PNs to that of the corresponding MPNs, has been studied in this paper. In order to improve the approximation, a new stochastic continuous model TCPN and two hybrid Petri net models, MHPN and MnHPN, are introduced and studied. The results obtained are listed in the following:

• The marking of a Join-Free TCPN model provides a good approximation of the average marking of the corresponding MPN, assuming asymptotic stability (Proposition 2.2). Errors may appear in non ordinary nets, but they are ultimately bounded. The larger the enabling degree, the better the approximation (condition 1). Those results are extended to non Join-Free nets, under the assumption that the system evolves inside one region with a high probability (condition 2, Proposition 2.3).

• In order to improve the approximation when the system evolves in several regions, a new stochastic continuous Petri net (TnCPN) is defined, by adding white gaussian *noise* to the transitions' flow of the TCPN model. Assuming liveness and ergodicity, it is formally demonstrated that the pdf (not only the expected value) of the marking of the TnCPN may approximate that of the MPN. The larger the enabling degrees during the most probable trajectories, the better the approximation (condition 1, Theorem 2.10).

• A hybrid Petri net model MHPN is introduced as a partial relaxation of a MPN. Such hybrid model is enriched by adding gaussian noise to the continuous transitions, leading to another hybrid system MnHPN. Nevertheless, the approximation provided by such hybrid systems is not always better than that provided by full relaxations (Example 2.6), in particular, when continuous places barely enable discrete transitions (thus condition 3 is not fulfilled). Proposition 2.15 states that the *average marking* of a MPN can be approximated by that of a MHPN if both systems mainly evolve inside a unique "stable" region (condition 2) and the enabling degrees are large enough (condition 1). Theorem 2.17 provides a stronger result: the *pdf of the marking* of the MPN can be approximated by that of the MnHPN if the enabling degree of the continuous transitions is large for the most probable trajectories of the MPN system (condition 1).

• Finally, a couple of preliminary ideas, for the improvement of the approximation of a continuous model by means of the modification of the structure and the semantics, are advanced.

Chapter 3

Timing-dependent properties

An interesting approach, when qualitative properties of discrete Petri nets are analyzed, is the so called *structural theory*. According to this, important information about the behavior of the system is obtained from the structure of the net, considering the initial marking as a parameter. For general models, structural techniques may give conditions, usually in one way (sufficient or necessary), for the properties under study. Obviously, if the analysis is restricted to particular subclasses, stronger results can be obtained. In the literature, a lot of results related to the computation of structural components can be found (e.g., [Brams, 1983], [Silva et al., 1998]). Among components that are important for the system's behavior are traps, siphons and (semi)flows. In some cases, these allow the verification of behavioral properties, like boundedness and liveness (see, for instance, [Silva et al., 1998]).

In this way, it seems interesting to extend the structural analysis to fluid Petri nets, in order to obtain information about its behavior. From this approach, in [Recalde et al., 1999] some results are provided for the autonomous model obtained from structural analysis. In [Júlvez et al., 2006], this kind of studies is advanced for the timed continuous system (under ISS). Since the integrality constraints are removed in the continuous nets, structural properties have a stronger meaning. Moreover, regarding TCPNs, timing rates can be also considered with the structural analysis, since it is characterized in a matricial form ($\mathbf{\Lambda}$).

Among the different structural (str.) properties, in this chapter str. boundedness and str. repetitiveness will be analyzed for timed continuous Petri nets. These properties are relevant for boundedness and liveness. In fact, by including the matricial characterization of the timing to this str. analysis, interesting results can be obtained concerning the relation between liveness (a behavioral property) and the timing.

Let us see this in more detail. It is in the folklore of the field that, for stochastic *discrete* models, liveness and non-liveness are preserved when the support of the stochastic functions associated to the firing of transitions is infinite. In particular, if a Markovian timing interpretation is considered, then the Markov chain and the reachability graph are isomorphous [Molloy, 1982]. Thus, any autonomous discrete net, and the result of timing it with arbitrary positive rates, are both simultaneously live or both equally non-live. On the other hand, it is well known that the addition of a deterministic timing to the firing of transitions (T-timed) in *discrete* Petri nets may not preserve liveness or non-liveness. Let us illustrate this with a couple of examples:

Example 3.1. The (discrete) net system in fig. 3.1(a), seen as autonomous (i.e., with no timing), is obviously live. On the opposite, the net system in fig. 3.1(b) is non-live as autonomous. If we consider a Markovian timing interpretation for both systems, the resulting stochastic discrete model of fig. 3.1(a)

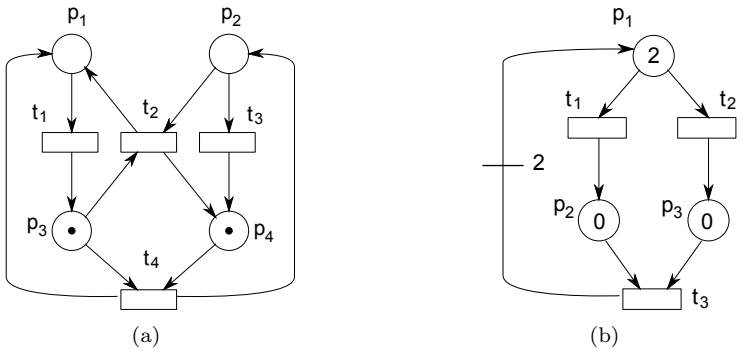

Fig. 3.1: (a) Live as autonomous *discrete* net system but non-live under certain deterministic timing: $\theta_1 > \theta_3$. (b) Non live as autonomous, but live as timed if $\theta_1 = \theta_2$.

is live and that of fig. 3.1(b) is non-live, for any positive exponential timing, i.e., liveness is preserved. Nevertheless, for the net of fig. 3.1(a), if we associate a deterministic timing θ_1 and θ_3 to transitions t_1 and t_3, respectively (i.e., t_1 (resp. t_3) fires after θ_1 (resp. θ_3) time units of being enabled), with θ_3 smaller (thus faster) than θ_1, t_2 will never be enabled, thus cannot be fired, and non liveness follows. On the other hand, for the net of fig. 3.1(b), if t_1 and t_2 are deterministically timed with $\theta_1 = \theta_2$, the system becomes live. Therefore, liveness of the discrete autonomous model is neither necessary nor sufficient for liveness of the (at least partially) deterministically-timed interpreted model. Regarding deadlock-freeness, things are a bit simpler: if a (discrete) system is deadlock-free as autonomous it will be deadlock-free if it is T-timed.

In this way, several questions may arise concerning continuous models, for instance, how the timing can affect the liveness property in continuous PN systems? what is the precise connection between str. boundedness and str. repetitiveness (structural properties) w.r.t. boundedness and liveness (behavioral properties) in the continuous model?

In this framework, through this chapter we will study the boundedness and repetitiveness properties for TCPN models, by following a structural approach but including the timing information. This will lead us to understand the connection between liveness and the timing of the continuous system. As a result of the analysis achieved, a couple of algorithms will be provided for computing timings that lead to bounded and live TCPN models, where the autonomous continuous net systems do not exhibit such properties.

3.1 Structural boundedness and repetitiveness in untimed Petri nets: discrete *vs* continuous

Some classical results related to boundedness, repetitiveness and liveness in untimed discrete and continuous Petri net models are here recalled. As it may be expected, by structural analysis stronger results can be obtained for continuous models .

The study of boundedness and repetitiveness in discrete Petri nets includes very well known results based on structural analysis. For instance, recalling from [Teruel et al., 1997]:

Property 3.1. Given a P/T net $\mathcal{N}$, the following three statements are equivalent:
1) $\mathcal{N}$ is structurally bounded, i.e., every place is bounded for every $\mathbf{M}_0$.
2) There exists $\mathbf{y} > \mathbf{0}$ s.t. $\mathbf{y}^T\mathbf{C} \leq \mathbf{0}$.
3) There does not exist $\mathbf{x} \geq \mathbf{0}$ s.t. $\mathbf{Cx} \gneq \mathbf{0}$.

Structural boundedness is sufficient but not necessary for boundedness. The dual concept of boundedness is repetitiveness. In [Teruel et al., 1997] a result is presented, analogous to Property 3.1, for repetitiveness.

Property 3.2. Given a P/T (discrete or continuous) net $\mathcal{N}$, the following three statements are equivalent:
1) $\mathcal{N}$ is structurally repetitive, i.e., every transition is repetitive for some $\mathbf{M}_0$.
2) There does not exist $\mathbf{y} > \mathbf{0}$ s.t. $\mathbf{y}^T\mathbf{C} \lneq \mathbf{0}$.
3) There exists $\mathbf{x} > \mathbf{0}$ s.t. $\mathbf{Cx} \geq \mathbf{0}$.

Properties 3.1 and 3.2 are also valid for continuous Petri net models. Moreover, stronger results can be obtained for these. This is stated in the following proposition, introduced in [Recalde et al., 1999]. Let us provide here an intuition for such result that will be useful in the following sections:

Proposition 3.3. *Consider a continuous PN system $\langle \mathcal{N}, \mathbf{m}_0 \rangle$. If all the transitions are fireable from $\mathbf{m}_0$ (otherwise stated, there are not empty siphons), then str. boundedness (str. repetitiveness) is sufficient and necessary for boundedness (repetitiveness) in the continuous model.*

Proof. In the proof of Properties 3.1 and 3.2 ([Teruel et al., 1997]), str. boundedness and str. repetitiveness are characterized with the following necessary reachability condition: if $\mathbf{M}'$ is reachable then $\mathbf{M}' \geq \mathbf{0}$ and $\exists \boldsymbol{\sigma} \geq \mathbf{0}$ s.t. $\mathbf{M}' = \mathbf{M} + \mathbf{C}\boldsymbol{\sigma}$. This reachability condition also holds for the continuous PNs, thus Properties 3.1 and 3.2 are still valid in these systems. Moreover, in continuous PNs, if all the transitions are fireable from $\mathbf{m}_0$, then $\mathbf{m}'$ is reachable *iff* $\exists \boldsymbol{\sigma} \geq \mathbf{0}$ s.t. $\mathbf{m}' = \mathbf{m} + \mathbf{C}\boldsymbol{\sigma} \geq \mathbf{0}$, i.e., the necessary condition for reachability used in the structural analysis becomes also sufficient for the continuous net. ∎

In a similar way, liveness in continuous systems may purely depend on structural components:

Proposition 3.4. *Consider a continuous PN system $\langle \mathcal{N}, \mathbf{m}_0 \rangle$ in which $\mathbf{m}_0 > \mathbf{0}$ (thus all transitions are fireable). The system is non-live* iff *there exists a siphon Σ and $\exists \mathbf{m}_f, \boldsymbol{\sigma} \geq \mathbf{0}$ s.t. $\forall p \in \Sigma, \mathbf{m}_f(p) = 0$ and $\mathbf{m}_f = \mathbf{m}_0 + \mathbf{C}\boldsymbol{\sigma}$.*

Proof. It is known that a continuous PN system fall into non-liveness *iff* a marking, in which a siphon is empty, is reached. On the other hand, it is known that if all the transitions are fireable from $\mathbf{m}_0$, it holds that $\mathbf{m}'$ is reachable *iff* $\exists \boldsymbol{\sigma} \geq \mathbf{0}$ s.t. $\mathbf{m}' = \mathbf{m} + \mathbf{C}\boldsymbol{\sigma} \geq \mathbf{0}$. Thus, the proposition follows by combining these two properties. ∎

In the general case, i.e., $\mathbf{m}_0 \not> \mathbf{0}$, this condition is still necessary for non-liveness, as proved in [Recalde et al., 1999] (Theorem 9).

3.2 Timing-dependent boundedness and repetitiveness in timed continuous PNs

Contrary to the case of autonomous models, for TCPN systems there is not available any algebraic characterization of the reachability property, due to the technical complexity involved. Thus, str. properties provide information only in one sense (necessity or sufficiency), just like in the discrete case.

Nevertheless, considering an analysis by regions (in which the system behaves linearly), more information can be obtained from an algebraic approach.

Proposition 3.5. *Given a TCPN system* $\langle \mathcal{N}, \boldsymbol{\lambda}, \mathbf{m}_0 \rangle$*, while it evolves inside a region* $\Re_i$*, the following three statements are equivalent:*
I.1) The system behaves as structurally bounded, i.e., every place is bounded for every $\mathbf{m}_0 \in \Re_i$*.*
I.2) There exists $\mathbf{w} > \mathbf{0}$ *s.t.* $\mathbf{w}^T \mathbf{C}\boldsymbol{\Lambda}\boldsymbol{\Pi}_i \leq \mathbf{0}$*.*
I.3) There does not exist $\mathbf{v} \geq \mathbf{0}$ *s.t.* $\mathbf{C}\boldsymbol{\Lambda}\boldsymbol{\Pi}_i \mathbf{v} \gneq \mathbf{0}$*.*
Similarly, while the system evolves inside a region $\Re_i$ *the following three statements are equivalent:*
II.1) The system behaves as structurally repetitive, i.e., every transition is repetitive for some $\mathbf{m}_0 \in \Re_i$*.*
II.2) There does not exist $\mathbf{w} > \mathbf{0}$ *s.t.* $\mathbf{w}^T \mathbf{C}\boldsymbol{\Lambda}\boldsymbol{\Pi}_i \lneq \mathbf{0}$*.*
II.3) There exists $\mathbf{v} > \mathbf{0}$ *s.t.* $\mathbf{C}\boldsymbol{\Lambda}\boldsymbol{\Pi}_i \mathbf{v} \geq \mathbf{0}$*.*

Proof. First, a necessary condition for reachability inside a region is obtained: If $\mathbf{m}' \geq \mathbf{0}$ is reachable trough a trajectory inside $\Re_i$, then there exists $\boldsymbol{\sigma} \geq \mathbf{0}$ s.t. $\mathbf{m}' = \mathbf{m}_0 + \mathbf{C}\boldsymbol{\Lambda}\boldsymbol{\Pi}_i\boldsymbol{\sigma}$. This condition is trivially obtained by integrating the state equation (1.4), thus: $\mathbf{m}(\tau) = \mathbf{m}_0 + \mathbf{C}\boldsymbol{\Lambda}\boldsymbol{\Pi}_i \int_0^\tau \mathbf{m}(\eta)d\eta$, where $\int_0^\tau \mathbf{m}(\eta)d\eta \geq \mathbf{0}$, and substituting $\int_0^\tau \mathbf{m}(\eta)d\eta = \boldsymbol{\sigma}$. Note that this necessary reachability condition is similar to that of discrete nets (but in this $\mathbf{C}\boldsymbol{\Lambda}\boldsymbol{\Pi}_i$ appears instead of $\mathbf{C}$). Thus, the proof can be completed by proceeding in a way similar to the structural analysis for discrete nets (Properties 3.1 and 3.2, whose proofs are in [Teruel et al., 1997]). ∎

In this case, *repetitive* means that the structure and timing allow the existence of a non-smaller marking, i.e., $\mathbf{m}(\tau) - \mathbf{m}_0 = \mathbf{C}\boldsymbol{\Lambda}\boldsymbol{\Pi}_i \int_0^\tau \mathbf{m}(\eta)d\eta \geq \mathbf{0}$. Furthermore, as in the discrete case, given a TCPN system that reaches a steady state $\mathbf{m}_{ss}$ in a region $\Re_i$, condition II.3 is necessary for timed-liveness.

Remark 3.6. It is often required that a system behaves as bounded and live. Therefore, it is desirable that Properties I.2 and II.3 be fulfilled for any reachable configuration, since one is sufficient for boundedness while the other is necessary for timed-liveness.

It is not difficult to prove that, given a configuration $\boldsymbol{\Pi}_i$, if I.2 and II.3 are simultaneously fulfilled then

$$\mathbf{w}^T \mathbf{C}\boldsymbol{\Lambda}\boldsymbol{\Pi}_i = \mathbf{0} \tag{3.1}$$

$$\mathbf{C}\boldsymbol{\Lambda}\boldsymbol{\Pi}_i \mathbf{v} = \mathbf{0} \tag{3.2}$$

Definition 3.7. If there exist $\mathbf{w} > \mathbf{0}$ and $\mathbf{v} > \mathbf{0}$ solutions for (3.1) and (3.2), it will be said that the timed model $\langle \mathcal{N}, \boldsymbol{\lambda} \rangle$ is λ-*conservative* (λ-Cv) and λ-*consistent* (λ-Ct) at $\boldsymbol{\Pi}_i$, respectively.

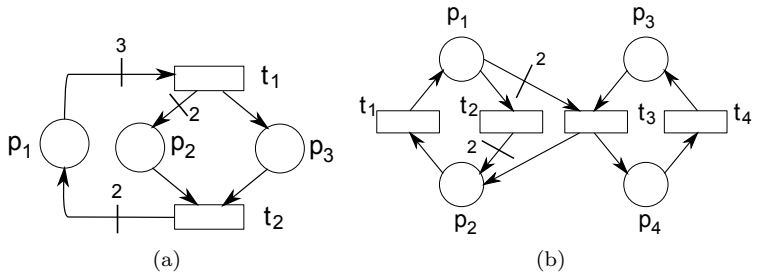

Fig. 3.2: (a) λ-Cv but not λ-Ct TCPN. (b) λ-Ct but not λ-Cv TCPN

Remark 3.8. The Property λ-Cv implies that the system is bounded while evolves in the corresponding region.

These two properties are important, since a TCPN system with $\mathbf{m}_0 \in \Re_i \cap \mathbb{R}_{>0}^{|P|}$ behaves as *bounded and timed-live* (this will be proved in Subsection 3.5.1) if the timed model is λ-Cv and λ-Ct at $\mathbf{\Pi}_i$, while it evolves inside $\Re_i$. Note that these properties depend not only on the structure (including the particular configuration matrix), but also on the timing. Then, several questions may arise, e.g.,: How must be the timing in order to fulfill with these conditions? If these hold for one configuration, are they also fulfilled for the others, or at least, for configurations related to stationary states? Are there net subclasses for which λ-Cv or λ-Ct always hold for any timing, or any configuration? This will be investigated in the forthcoming sections.

3.3 Existence of w and v for boundedness and repetitiveness

In untimed models, a net is conservative (consistent) iff the dual net (the net obtained by interchanging places and transitions) is consistent (conservative), since the incidence matrix of the dual net is the transpose of that of the primal one (times -1). This dual equivalence does not hold for λ-conservativeness and λ-consistency, at least for general cases (it holds for FA models), because the timing is also involved. Nevertheless, since $\mathbf{C\Lambda\Pi}_i$ is a square matrix, the dimension of its right and left annulers (nullity) is the same, then, there exists a bijection between vectors $\mathbf{w} \neq \mathbf{0}$ and $\mathbf{v} \neq \mathbf{0}$ in (3.1) and (3.2). In particular, $\exists \mathbf{w} \neq \mathbf{0}$ s.t. $\mathbf{w}^T\mathbf{C\Lambda\Pi}_i = \mathbf{0}$ iff $\exists \mathbf{v} \neq \mathbf{0}$ s.t. $\mathbf{C\Lambda\Pi}_i\mathbf{v} = \mathbf{0}$. Nevertheless, $\exists \mathbf{w} > \mathbf{0}$ (i.e., λ-Cv) is neither sufficient nor necessary for $\exists \mathbf{v} > \mathbf{0}$ (i.e., λ-Ct).

Example 3.2. The timed model of fig. 3.2(a) is conservative, thus λ-Cv for any timing and configuration, but $\nexists \boldsymbol{\lambda}$ s.t. it is λ-Ct at any configuration (a deadlock can be reached while t_2 is constrained by p_3). On the contrary, the model of fig. 3.2(b) is λ-Ct but not λ-Cv, $\forall \boldsymbol{\lambda}$ at the configuration in which t_3 is constrained by place p_3. Nevertheless, with $\boldsymbol{\lambda} = [1, 1, 2, 1]^T$ the system is both λ-Cv and λ-Ct at the configuration in which t_3 is constrained by p_1.

3.3.1 Existence of **w**

Proposition 3.9. *Consider a timed net* $\langle \mathcal{N}, \boldsymbol{\lambda} \rangle$.
1) If $\mathcal{N}$ *is conservative, then* $\langle \mathcal{N}, \boldsymbol{\lambda} \rangle$ *is* λ*-Cv for any timing and configuration.*

2) If $\langle \mathcal{N}, \boldsymbol{\lambda} \rangle$ is λ-Cv at a configuration $\boldsymbol{\Pi}_i$ and $\exists \mathbf{w} > \mathbf{0}$ s.t. $\mathbf{w}^T \mathbf{C} \boldsymbol{\Lambda} \boldsymbol{\Pi}_i = \mathbf{0}$ but $\mathbf{w}^T \mathbf{C} \neq \mathbf{0}$, then $\boldsymbol{\Pi}_i$ has left annulers.

Proof. For the first statement, note that any positive P-semiflow ($\mathbf{y} > \mathbf{0}$ s.t. $\mathbf{y}^T \cdot \mathbf{C} = \mathbf{0}$) fulfills (3.1), thus, conservativeness is a sufficient condition for λ-conservativeness. In such case, the timed net is λ-Cv for any timing and configuration.
Now let us prove the second statement. Denote as $\mathbf{B}_z^i$ a basis for the left annuler of $\boldsymbol{\Pi}_i$, i.e., $\forall \mathbf{z}$ s.t. $\mathbf{z}\boldsymbol{\Pi}_i = \mathbf{0}$, $\exists \boldsymbol{\eta}$ s.t. $\mathbf{z} = \boldsymbol{\eta}^T \mathbf{B}_z^i$. In this way, a solution $\mathbf{w}$ for (3.1) s.t. $\mathbf{w}^T \mathbf{C} \neq \mathbf{0}$ implies

$$\exists \boldsymbol{\eta} \neq \mathbf{0} \quad \text{s.t.} \quad \mathbf{w}^T \mathbf{C} \boldsymbol{\Lambda} = \boldsymbol{\eta}^T \mathbf{B}_z^i \tag{3.3}$$

By hypothesis, $\mathbf{w}^T \mathbf{C} \boldsymbol{\Lambda} \neq \mathbf{0}$ because $\boldsymbol{\Lambda}$ is always a full rank matrix. Therefore, if there exists such $\mathbf{w}$ then $\boldsymbol{\Pi}_i$ has left annulers. ∎

Property 3.10. A configuration matrix $\boldsymbol{\Pi}_i$ has left annulers (it is not full row rank) iff there are places constraining more than one transition (thus there are choices) at $\boldsymbol{\Pi}_i$.

Note that vectors $\mathbf{w} > \mathbf{0}$ that fulfill (3.3) are not P-flows. Nevertheless, such vectors also define marking conservation laws like P-flows, i.e., given an initial marking $\mathbf{m}_0 \in \Re_i$, for any marking $\mathbf{m}$ reached while the system evolves inside $\Re_i$, it holds $\mathbf{w}^T \mathbf{m} = \mathbf{w}^T \mathbf{m}_0$. Positiveness of $\mathbf{w}$ will depend on the structure and the particular timing. Thus, the timed model may be λ-Cv, but just for particular timings at such particular configuration.

Example 3.3. Consider the configuration matrices for the PN of fig. 3.2(b):

$$\boldsymbol{\Pi}_1 = \begin{bmatrix} 0 & 1 & 0 & 0 \\ 1 & 0 & 0 & 0 \\ 1/2 & 0 & 0 & 0 \\ 0 & 0 & 0 & 1 \end{bmatrix}, \qquad \boldsymbol{\Pi}_2 = \begin{bmatrix} 0 & 1 & 0 & 0 \\ 1 & 0 & 0 & 0 \\ 0 & 0 & 1 & 0 \\ 0 & 0 & 0 & 1 \end{bmatrix}$$

Matrix $\boldsymbol{\Pi}_2$ has full row rank. It means that there is not left annuler $\mathbf{B}_z^2$ for $\boldsymbol{\Pi}_2$, then, there is not a solution for (3.3). Thus, $\forall \boldsymbol{\lambda}$, $\forall \mathbf{w} \neq \mathbf{0}$, $\mathbf{w}^T \mathbf{C} \boldsymbol{\Lambda} \boldsymbol{\Pi}_2 \neq \mathbf{0}$, meaning that the model is λ-Cv at $\boldsymbol{\Pi}_2$ only if the net is conservative (but it is not). On the other hand, $\boldsymbol{\Pi}_1$ has not full row rank. Rows 2 and 3 are linearly dependent. Those rows mean that t_2 and t_3 are both constrained by p_1 at $\boldsymbol{\Pi}_1$. In this case, a basis for the left annuler of $\boldsymbol{\Pi}_1$ can be computed as $\mathbf{B}_z^1 = [0, -1, 2, 0]$. Then, if $\boldsymbol{\lambda}$ is s.t. $\exists \mathbf{w} > \mathbf{0}$ that fulfills (3.3), then the timed model is λ-Cv. This occurs for $\boldsymbol{\lambda} = [1, 1, 2, 1]^T$ with $\mathbf{w} = [1, 1, 1, 1]^T$. Actually, the model is not λ-Cv for any possible timing, but positive solutions for (3.1) exist whenever $[\boldsymbol{\lambda}_2, \boldsymbol{\lambda}_3]^T = \beta \cdot [1, 2]^T$ with $\beta \in \mathbb{R}^+$.

Note in previous example that *only the rates of transitions in conflict are meaningful for fulfilling* (3.3). In order to generalize this, let us introduce a new concept:

Definition 3.11. A transition t_k is said *exclusively constrained* (*exc*) by p_j at $\boldsymbol{\Pi}_i$, iff p_j constrains t_k and only t_k at this configuration.

Structurally persistent transitions, i.e., that are not in conflict, are always *exc* for any configuration. The rows of $\mathbf{\Pi}_i$ related to *exc* transitions are linearly independent of the other rows. Then, the columns of $\mathbf{B}_z^i$ related to these transitions are null. This leads to the following proposition:

Proposition 3.12. *Consider a TCPN system that is λ-Cv at a given configuration $\mathbf{\Pi}_i$. Suppose that there exists $\mathbf{w} > \mathbf{0}$ solution for (3.1) s.t. $\mathbf{w}^T\mathbf{C} \neq \mathbf{0}$. Then, the timing of the* exc *transitions does not affect the λ-conservativeness property, i.e., if the rate of t_j* exc *is changed then $\mathbf{w}$ will continue being a solution and so the system remains as λ-Cv. Furthermore, for each t_j* exc*, $\mathbf{w}^T[\mathbf{C}]^j$ is zero.*

Example 3.4. In the model of fig. 3.2(b), t_2 and t_3, which are in conflict, are *exc* at $\mathbf{\Pi}_2$ by p_1 and p_3, respectively. Nevertheless, both transitions are constrained by the same place (p_1) at $\mathbf{\Pi}_1$, i.e., they are not *exc* at this configuration.

3.3.2 Existence of $\mathbf{v}$

Proposition 3.13. *Consider a timed net $\langle \mathcal{N}, \boldsymbol{\lambda} \rangle$.*
1) If $\langle \mathcal{N}, \boldsymbol{\lambda} \rangle$ is λ-Ct at a configuration $\mathbf{\Pi}_i$, then $\mathcal{N}$ is consistent.
2) If $\mathcal{N}$ is consistent and all the transitions are exc *at a configuration $\mathbf{\Pi}_i$, i.e., it does not have left annulers, then $\langle \mathcal{N}, \boldsymbol{\lambda} \rangle$ is λ-Ct at $\mathbf{\Pi}_i$.*

Proof. First statement: condition (3.2) can be rewritten as

$$\exists \boldsymbol{\eta} \neq \mathbf{0}, \exists \mathbf{v} > \mathbf{0} \quad \text{s.t.} \quad \mathbf{B}_x \boldsymbol{\eta} = \mathbf{\Lambda \Pi}_i \mathbf{v} \tag{3.4}$$

where $\mathbf{B}_x$ is a basis for the T-flows. Thus, the timed model is λ-Ct at $\mathbf{\Pi}_i$ iff $\exists \mathbf{v} > \mathbf{0}$ that fulfills (3.4). Note that $\mathbf{v} > \mathbf{0}$ implies that $\mathbf{\Lambda \Pi}_i \mathbf{v}$ is a positive T-semiflow. Therefore, consistency is a necessary condition for (3.4), and thus for λ-Ct at any $\mathbf{\Pi}_i$.
For the second statement: if all the transitions are *exc* at $\mathbf{\Pi}_i$, then $\mathbf{\Pi}_i$ is a full row rank matrix. In such case, for any $\mathbf{x} > \mathbf{0}$ there always exists a vector $\mathbf{v} > \mathbf{0}$ s.t. $\mathbf{\Lambda \Pi}_i \mathbf{v} = \mathbf{x}$. Therefore, if the net is consistent and all the transitions are *exc*, there exists a solution for (3.4), and thus the model is λ-Ct at $\mathbf{\Pi}_i$. ∎

Statement 2 of Proposition 3.13 establishes a sufficient (but not necessary) condition for λ-Ct. In this way, if the net is consistent and there are transitions not *exc* ($\mathbf{\Pi}_i$ is not full row rank) then $\boldsymbol{\lambda}$ may (or may not) lead to the existence of a solution $\mathbf{v} > \mathbf{0}$ for (3.4), i.e., to λ-consistency. In such case, it can be proved that *the timing of the* exc *transitions does not affect the λ-consistency property*, as happens for the λ-Cv property.

Example 3.5. For $\mathbf{\Pi}_1$ in fig. 3.2(b), with $\boldsymbol{\lambda} = [1, 1, 2, 1]^T$, $\mathbf{v} = [1, 3, 1, 1]^T$ is a solution for (3.2). Nevertheless, for $\boldsymbol{\lambda} = [1, 1, 1, 1]^T$, $\nexists \mathbf{v} > \mathbf{0}$. Note that only the rate at t_3, which is in conflict and not *exc* at $\mathbf{\Pi}_1$, has been changed.

Remark 3.14. There is a relevant asymmetry between the annulers related to λ-Ct and λ-Cv: when the rank of $\mathbf{C\Lambda \Pi}_i$ is lower than that of $\mathbf{C}$, new place invariants (related to annulers $\mathbf{w}$) appear w.r.t. to the autonomous net, while the transition invariants (related to annulers $\mathbf{x} = \mathbf{\Lambda \Pi}_i \mathbf{v}$) remain unchanged, i.e., additional T-flows are not created.

Tab. 3.1: Conditions for λ-Cv and λ-Ct, where $\rho(\mathbf{\Pi}_i)$ denotes the rank of $\mathbf{\Pi}_i$ ($\mathbf{\Pi}_i$ is has full row rank iff $\rho(\mathbf{\Pi}_i) = |T|$).

I	Cv $\Longrightarrow \forall \boldsymbol{\lambda}, \mathbf{\Pi}_i$, $\langle \mathcal{N}, \boldsymbol{\lambda} \rangle$ is λ-Cv
II	Ct $\Longleftarrow \exists \boldsymbol{\lambda}, \mathbf{\Pi}_i$ s.t. $\langle \mathcal{N}, \boldsymbol{\lambda} \rangle$ is λ-Ct
III	Not Cv, $\rho(\mathbf{\Pi}_i) = \lvert T \rvert \Longrightarrow \langle \mathcal{N}, \boldsymbol{\lambda} \rangle$ is not λ-Cv at $\mathbf{\Pi}_i$
IV	Ct, $\rho(\mathbf{\Pi}_i) = \lvert T \rvert \Longrightarrow \forall \boldsymbol{\lambda}$, $\langle \mathcal{N}, \boldsymbol{\lambda} \rangle$ is λ-Ct at $\mathbf{\Pi}_i$
V	Cv, Ct, $\rho(\mathbf{\Pi}_i) = \lvert T \rvert \Longrightarrow \forall \boldsymbol{\lambda}$, $\langle \mathcal{N}, \boldsymbol{\lambda} \rangle$ is λ-Ct, λ-Cv at $\mathbf{\Pi}_i$
VI	$\rho(\mathbf{\Pi}_i) = \lvert T \rvert \Longrightarrow \forall \mathbf{w}$ solution of (3.1), $\mathbf{w}^T\mathbf{C} = \mathbf{0}$
VII	Ct $\Longrightarrow \forall \mathbf{\Pi}_i \; \exists \boldsymbol{\lambda}$ s.t. $\langle \mathcal{N}, \boldsymbol{\lambda} \rangle$ is λ-Ct
VIII	If $\rho(\mathbf{\Pi}_i) < \lvert T \rvert$ then it may exist $\mathbf{w} > \mathbf{0}$ solution for (3.1) s.t. $\mathbf{w}^T\mathbf{C} \neq \mathbf{0}$ for particular $\boldsymbol{\lambda}$ at the transitions not *exc*
IX	If Ct & $\rho(\mathbf{\Pi}_i) < \lvert T \rvert$ then it may exist $\mathbf{v} > \mathbf{0}$ solution for (3.2) for particular $\boldsymbol{\lambda}$ at the transitions not *exc*

Proposition 3.15. *Consider a timed net $\langle \mathcal{N}, \boldsymbol{\lambda} \rangle$. If the net is consistent then for any $\mathbf{\Pi}_i$ there exists $\boldsymbol{\lambda}$ s.t. $\langle \mathcal{N}, \boldsymbol{\lambda} \rangle$ is λ-Ct.*

Proof. If the net is consistent then $\exists \boldsymbol{\eta}$ s.t. $\mathbf{B}_x\boldsymbol{\eta} > \mathbf{0}$. Next, consider an arbitrary vector $\mathbf{v} \in \mathbb{R}^{|T|}_{>0}$, so, for an arbitrary $\mathbf{\Pi}_i$, $\mathbf{\Pi}_i\mathbf{v} > \mathbf{0}$. In this way, it is always possible to find a timing $\boldsymbol{\lambda}$ s.t. (3.4) is fulfilled, i.e., that leads to λ-Ct. ∎

Finally, Table 3.1 resumes the existence conditions shown through the previous subsections: Proposition 3.9 proves statements I, III and VI; Proposition 3.13 proves statements II and IV; and Proposition 3.15 provides the proof of statement VII.

Through the following subsections, conditions for λ-Cv and λ-Ct are analyzed for particular subclasses of PNs: Fork-Attribution, Choice-Free, Join-Free and Topologically Equal-Conflict nets; obtaining thus stronger results.

3.3.3 Choice-Free and Fork-Attribution nets

Proposition 3.16. *Consider a Choice-Free timed net $\langle \mathcal{N}, \boldsymbol{\lambda} \rangle$. The model is λ-Cv, $\forall \boldsymbol{\lambda}, \mathbf{\Pi}_i$, iff the net is conservative. Similarly, the model is λ-Ct, $\forall \boldsymbol{\lambda}, \mathbf{\Pi}_i$, iff the net is consistent.*

If additionally there are not synchronizations in the net (thus, it is Fork-Attribution) and it is strongly connected, then, $\forall \boldsymbol{\lambda}$, it is λ-Ct iff it is λ-Cv.

Proof. CF nets allow attributions, forks and synchronizations but not choices. Then, each configuration matrix $\mathbf{\Pi}_i$ has full row rank (all transitions are *exc*). Therefore, according to Table 3.1, $\forall \boldsymbol{\lambda}, \mathbf{\Pi}_i$ the model is λ-Cv iff the net is conservative (statements I and III), and $\forall \boldsymbol{\lambda}, \mathbf{\Pi}_i$ the model is λ-Ct iff the net is consistent (statements IV and II).
A Fork-Attribution net is a Choice-Free without synchronizations (there is only one configuration). Furthermore, a strongly connected FA net is consistent iff it is conservative ([Teruel et al., 1997]), thus, $\forall \boldsymbol{\lambda}$ it is λ-Ct iff it is λ-Cv. ∎

For FA nets, closed-form expressions can be obtained for basis of P- and T-semiflows (these basis have dimension 1). For this, define a matrix $\mathbf{\Pi}^{e1}$ as equal to $\mathbf{\Pi}$, excepting the first row which is null. Then, basis for P- and T-semiflows for a conservative and consistent FA net are given by:

$$\mathbf{x} = \sum_{k=0}^{|T|} \left[\mathbf{\Pi}^{e1} \cdot \mathbf{Post}\right]^k \cdot \mathbf{e}_1 \tag{3.5}$$

$$\mathbf{y}^T = \mathbf{e}_j^T \cdot \sum_{k=0}^{|T|} \left[\mathbf{Post} \cdot \mathbf{\Pi}^{e1}\right]^k \tag{3.6}$$

where $\mathbf{e}_1$ (resp. $\mathbf{e}_j$) denotes the first column (resp. j-th column) vector of the unity matrix of order $|T|$, and $p_j \in^\bullet t_1$. A basis for the solutions $\mathbf{v}$ for (3.2) can be computed as:

$$\mathbf{v} = \left[\mathbf{\Lambda\Pi}\right]^{-1} \cdot \mathbf{x} \tag{3.7}$$

Previous equations can be used for computing right annulers $\mathbf{v}$ for CF nets as follows:

Procedure 3.1. Computation of right annulers $\mathbf{v}$ for CF nets.

Define the P-subnet $\mathcal{N}^P$ with the places that are constraining transitions at $\mathbf{\Pi}_i$ (denoted as P^P). Thus, $\mathcal{N}^P$ is a FA model.
Use (3.5), (3.6) and (3.7) for computing $\mathbf{w}^P > \mathbf{0}$ and $\mathbf{v}^P > \mathbf{0}$ s.t. $(\mathbf{w}^P)^T\mathbf{C}^P\mathbf{\Lambda\Pi}_i^P = \mathbf{0}$ and $\mathbf{C}^P\mathbf{\Lambda\Pi}_i^P\mathbf{v}^P = \mathbf{0}$, where $\mathbf{C}^P$ (resp. $\mathbf{\Pi}_i^P$) are the restrictions of $\mathbf{C}$ (resp. $\mathbf{\Pi}_i$) to the rows (resp. columns) related to the places in P^P.
Let us suppose, without loss of generality, that the first columns of $\mathbf{\Pi}_i$ are related to the places in P^P, i.e., $\mathbf{\Pi}_i = [\mathbf{\Pi}_i^P, \mathbf{0}]$. Then, a **general solution** $\mathbf{v} > \mathbf{0}$ for (3.2) is given by:

$$\mathbf{v} = \begin{bmatrix} \mathbf{v}^P & \mathbf{0} \\ \mathbf{0} & \mathbf{I} \end{bmatrix} \cdot \boldsymbol{\eta} \quad \forall \boldsymbol{\eta} > \mathbf{0} \tag{3.8}$$

where $\mathbf{I}$ is the unity matrix of order $|P| - |P^P|$.

If the original CF net is consistent then the subnet $\mathcal{N}^P$ is consistent too. On the other hand, conservativeness of $\mathbf{C}^P$ is not necessary for conservativeness of $\mathbf{C}$. Therefore, even if there does not exist $\mathbf{w}^P > \mathbf{0}$ s.t. $(\mathbf{w}^P)^T\mathbf{C}^P\mathbf{\Lambda\Pi}_i^P = \mathbf{0}$, it may exist $\mathbf{w} > \mathbf{0}$ solution for (3.1).

Example 3.6. Consider the CF model of fig. 3.3. Let $\mathbf{\Pi}_1$ be the configuration matrix in which t_4 is constrained by p_4. The subnet $\mathcal{N}^P$ obtained by removing p_5 with its input and output arcs is FA. Although the original model is conservative (e.g., $\mathbf{y} = [2, 1, 1, 1, 1]^T$ is a P-semiflow), and thus λ-Cv (I in Table 3.1), $\mathbf{C}^P$ is not. On the other hand, since the original net is consistent (thus λ-Ct, since it is a CF model and IV in Table 3.1 applies) then $\mathbf{C}^P$ is consistent too. By using (3.5) and (3.7), the vector $\mathbf{v}^P = [1/\lambda_1, 1/\lambda_2, 1/\lambda_3, 1/\lambda_4]^T$ that fulfills $\mathbf{C}^P\mathbf{\Lambda\Pi}_i^P\mathbf{v}^P = \mathbf{0}$ is computed. Therefore, according to (3.8),

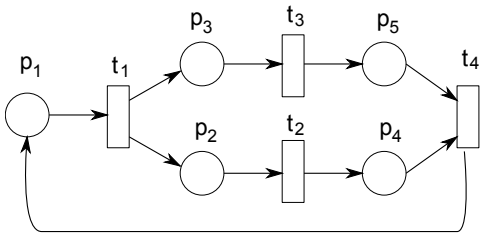

Fig. 3.3: A Choice-Free (marked graph) PN that is conservative and consistent.

a general solution $\mathbf{v} > \mathbf{0}$ for (3.2) is given by

$$\mathbf{v} = \begin{bmatrix} 1/\lambda_1 & 1/\lambda_2 & 1/\lambda_3 & 1/\lambda_4 & 0 \\ 0 & 0 & 0 & 0 & 1 \end{bmatrix}^T \boldsymbol{\eta} \quad \forall \boldsymbol{\eta} > \mathbf{0}$$

Note that $v_5 = \eta_2$ can be freely settled, since p_5 is not constraining any transition at $\mathbf{\Pi}_1$. On the other hand, the other entries of $\mathbf{v}$ must be settled according to certain proportions in such a way that $\mathbf{\Lambda\Pi}_1\mathbf{v}$ be a T-semiflow.

3.3.4 Join-Free and Equal-Conflict nets

The next proposition resumes the statements of Table 3.1 that can be applied to Join-Free nets.

Proposition 3.17. *Consider a Join-Free timed net $\langle \mathcal{N}, \boldsymbol{\lambda} \rangle$. If the net is conservative then $\forall \boldsymbol{\lambda}$ it is λ-Cv (statement I). Independently of the conservativeness of the net, for particular rates $\boldsymbol{\lambda}$ at the transitions in conflict, it may exist $\mathbf{w} > \mathbf{0}$ solution for (3.1) s.t. $\mathbf{w}^T\mathbf{C} \neq \mathbf{0}$ (statement VIII). On the other hand, if the net is consistent, it may exist $\mathbf{v} > \mathbf{0}$ solution for (3.2) for particular rates $\boldsymbol{\lambda}$ at the transitions in conflict (statement IX).*

Given a firing rate vector $\boldsymbol{\lambda}$, it is possible to merge the transitions in conflict of a JF model, obtaining thus a FA one $\langle \mathcal{N}^R, \boldsymbol{\lambda}^R \rangle$, whose marking describes the same trajectory, i.e., $\mathbf{C}^R\mathbf{\Lambda}^R\mathbf{\Pi}^R = \mathbf{C\Lambda\Pi}$, where $\mathbf{C}^R$ is the incidence matrix of $\mathcal{N}^R$. For this:

Procedure 3.2. Transformation of a JF TCPN to a FA one, given a timing $\boldsymbol{\lambda}$.

For each place p_j that is constraining more than one transition, **compute** its output flow when its marking is 1, i.e., $f^j = [1, .., 1] \cdot [\mathbf{\Lambda\Pi}]_j$.
Compute the column of $\mathbf{C}^R$ related to the new transition, obtained by merging those in $p_j^\bullet$, as $\mathbf{c}^j = \frac{1}{f^j}[\mathbf{C\Lambda\Pi}]_j$.
Build $\mathbf{C}^R$ with the columns of $\mathbf{C}$ related to the transitions that are *exc* and the column vectors $\mathbf{c}^j$ defined for each place that is constraining more than one transition.
Define $\mathbf{\Lambda}^R$ by keeping the same rates at the transitions that are *exc*, while the new merged transitions have a rate equal to the corresponding f^j.

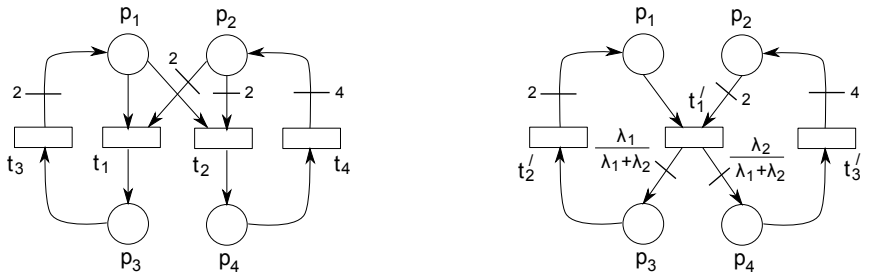

Fig. 3.4: (a) A conservative and consistent TEC net, and (b) its transformation.

According to this procedure, the corresponding $\mathbf{\Pi}^R$ has the rows of $\mathbf{\Pi}$ related to the transitions *exc*, while the others are elementary and linearly independent, thus $\mathbf{\Pi}^R$ has full rank. In this way, it is not difficult to see that $\mathbf{C}^R\mathbf{\Lambda}^R\mathbf{\Pi}^R = \mathbf{C\Lambda\Pi}$, i.e., the resulting FA system evolves exactly as the original JF one. Be aware that the net model thus obtained depends on $\boldsymbol{\lambda}$.

Remark 3.18. Since the resulting net $\mathbf{C}^R$ is FA then (3.5), (3.6) and (3.7) can be used for computing $\mathbf{w}^R > \mathbf{0}$ and $\mathbf{v}^R > \mathbf{0}$ s.t. $(\mathbf{w}^R)^T\mathbf{C}^R\mathbf{\Lambda}^R\mathbf{\Pi}^R = \mathbf{0}$ and $\mathbf{C}^R\mathbf{\Lambda}^R\mathbf{\Pi}^R\mathbf{v}^R = \mathbf{0}$. Furthermore, since $\mathbf{C}^R\mathbf{\Lambda}^R\mathbf{\Pi}^R = \mathbf{C\Lambda\Pi}$, the original model is λ-Cv (resp. λ-Ct) iff $\mathbf{C}^R$ is conservative (resp. consistent).

This transformation can be applied to TEC nets, obtaining a CF model $\langle \mathcal{N}^R, \boldsymbol{\lambda}^R \rangle$ (choices are eliminated, but synchronizations remain), so the results obtained in the previous subsection also hold for this. In the following proposition, it is shown that λ-Cv and λ-Ct are independent of the configurations for TEC nets.

Proposition 3.19. *Given a Topological Equal Conflict TCPN system, for any two different configurations $\mathbf{\Pi}_i$ and $\mathbf{\Pi}_j$, the timed model is λ-Cv (resp. λ-Ct) at $\mathbf{\Pi}_i$ iff it is λ-Cv (resp. λ-Ct) at $\mathbf{\Pi}_j$. Furthermore, $\mathbf{w}$ is a solution for (3.1) at $\mathbf{\Pi}_i$ iff it is also a solution at $\mathbf{\Pi}_j$. Similarly, $\mathbf{v}$ is a solution for (3.2) at $\mathbf{\Pi}_i$ iff $\mathbf{P}_i^j\mathbf{v}$ is a solution at $\mathbf{\Pi}_j$, where $\mathbf{P}_j^i$ is a matrix s.t. $\mathbf{\Pi}_i = \mathbf{\Pi}_j\mathbf{P}_i^j$.*

Proof. In TEC nets, given two different configurations $\mathbf{\Pi}_i$ and $\mathbf{\Pi}_j$, there exists a square full rank matrix $\mathbf{P}_j^i \geq \mathbf{0}$ s.t. $\mathbf{\Pi}_i = \mathbf{\Pi}_j\mathbf{P}_i^j$ (since $\forall t_j, t_k$ in conflict $\mathbf{Pre}[P, t_j] = \gamma\mathbf{Pre}[P, t_k]$, each configuration matrix is a scaled column permutation of any other, which is equivalent to the product of elementary matrices, i.e., $\mathbf{P}_j^i$). ∎

Example 3.7. Consider the TEC model of fig. 3.4(a). Transitions t_1 and t_2 are in TEC relation. Denote as $\mathbf{\Pi}_1$ (resp. $\mathbf{\Pi}_2$) the configuration in which p_1 (resp. p_2) constrains both. By previous proposition, $\langle \mathcal{N}, \boldsymbol{\lambda} \rangle$ is λ-Cv and λ-Ct at $\mathbf{\Pi}_2$ iff it is λ-Cv and λ-Ct at $\mathbf{\Pi}_1$. Let us focus on $\mathbf{\Pi}_1$. Given a timing $\boldsymbol{\lambda}$, t_1 and t_2 can be merged, obtaining thus a Choice-Free model. For that, the output flow of p_1 is computed when it has a marking equal to one, i.e., $f^1 = [1,1,1,1,1] \cdot [\mathbf{\Lambda\Pi}]_1 = \lambda_1 + \lambda_2$. Then, the new transition, resulting from merging t_1 and t_2, is defined. Its corresponding column at $\mathbf{C}^R$ is computed as $\mathbf{c}^1 = \frac{1}{f^1}[\mathbf{C\Lambda\Pi}]_1$, obtaining thus the model (fig. 3.4(b)):

$$\mathbf{C}^R = \begin{array}{c} \\ p_1 \\ p_2 \\ p_3 \\ p_4 \end{array} \begin{array}{c} \begin{array}{ccc} t_1 \wedge t_2 & t_3 & t_4 \end{array} \\ \begin{bmatrix} -1 & 2 & 0 \\ -2 & 0 & 4 \\ \frac{\lambda_1}{\lambda_1+\lambda_2} & -1 & 0 \\ \frac{\lambda_2}{\lambda_1+\lambda_2} & 0 & -1 \end{bmatrix} \end{array}, \qquad \mathbf{\Lambda}^R = \begin{array}{c} \begin{array}{ccc} t_1 \wedge t_2 & t_3 & t_4 \end{array} \\ \begin{bmatrix} \lambda_1+\lambda_2 & 0 & 0 \\ 0 & \lambda_3 & 0 \\ 0 & 0 & \lambda_4 \end{bmatrix} \end{array}$$

Note that $\mathbf{C}^R$ is consistent, and then λ-Ct (IV in Table 3.1 applies), iff $\lambda_1 = \lambda_2$. Assuming this, $\langle \mathcal{N}, \boldsymbol{\lambda} \rangle$ is λ-Ct at $\mathbf{\Pi}_1$ and thus, at $\mathbf{\Pi}_2$. It is already λ-Cv in both configurations since $\mathbf{C}$ is conservative (statement I).

Tab. 3.2: Conditions for λ-conservativeness and λ-consistency for subclasses.

CF	Cv $\iff \forall \boldsymbol{\lambda}$ $\langle \mathcal{N}, \boldsymbol{\lambda} \rangle$ is λ-Cv Ct $\iff \forall \boldsymbol{\lambda}$ $\langle \mathcal{N}, \boldsymbol{\lambda} \rangle$ is λ-Ct If the net is strongly connected and FA: $\langle \mathcal{N}, \boldsymbol{\lambda} \rangle$ is λ-Cv $\iff$ it is λ-Ct and (3.5) and (3.7) provide a basis for $\mathbf{v} > \mathbf{0}$. If $\mathcal{N}$ is Cv FA, (3.6) provide a basis for $\mathbf{w} > \mathbf{0}$.
TEC	Cv $\implies \forall \boldsymbol{\lambda}$ $\langle \mathcal{N}, \boldsymbol{\lambda} \rangle$ is λ-Cv Ct $\implies \exists \boldsymbol{\lambda}$ s.t. $\langle \mathcal{N}, \boldsymbol{\lambda} \rangle$ is λ-Ct Given $\boldsymbol{\lambda}$, it may exist $\mathbf{w} > \mathbf{0}$ solution for (3.1) s.t. $\mathbf{w}^T\mathbf{C} \neq \mathbf{0}$. Given $\boldsymbol{\lambda}$, the model can be transformed into CF, if the net is JF the resulting model is FA. λ-Ct (λ-Cv) at $\mathbf{\Pi}_i \iff \lambda$-Ct ($\lambda$-Cv) at $\mathbf{\Pi}_j$.
Siphons	$\langle \mathcal{N}, \boldsymbol{\lambda} \rangle$ λ-Ct at $\mathbf{\Pi}_i \implies$ each minimal siphon that may be emptied at $\mathbf{\Pi}_i$ is λ-Cv.

Table 3.2 summarizes the results found in this section, concerning λ-Cv and λ-Ct in net subclasses.

3.4 Timing-dependent liveness: setting the problem

Let us concentrate now in the liveness property. Regarding autonomous (untimed) *continuous* net systems, it has been proved that deadlock-freeness and liveness are decidable [Recalde et al., 2010]. If a system reaches a deadlock as timed, it also deadlocks as untimed (already stated for a subclass of nets in [Júlvez et al., 2006]). This clearly holds also for liveness since the evolution of a timed system just gives a particular trajectory of the untimed model.

Proposition 3.20. *If the contPN system $\langle \mathcal{N}, \mathbf{m}_0 \rangle$ is live, then for any $\lambda > \mathbf{0}$, $\langle \mathcal{N}, \lambda, \mathbf{m}_0 \rangle$ is live.*

On the contrary, a contPN that deadlocks as autonomous can be live as timed for particular timings. The next example shows a simple case.

Example 3.8. The system of fig. 3.1(b) deadlocks as untimed, but the timed system is live if $\lambda_1 = \lambda_2$. It may seem that the set of rates for which this kind of things occurs has to be of null measure, i.e., a smaller dimension manifold, but it is not so. For instance, the contPN system in fig. 3.5(a) deadlocks

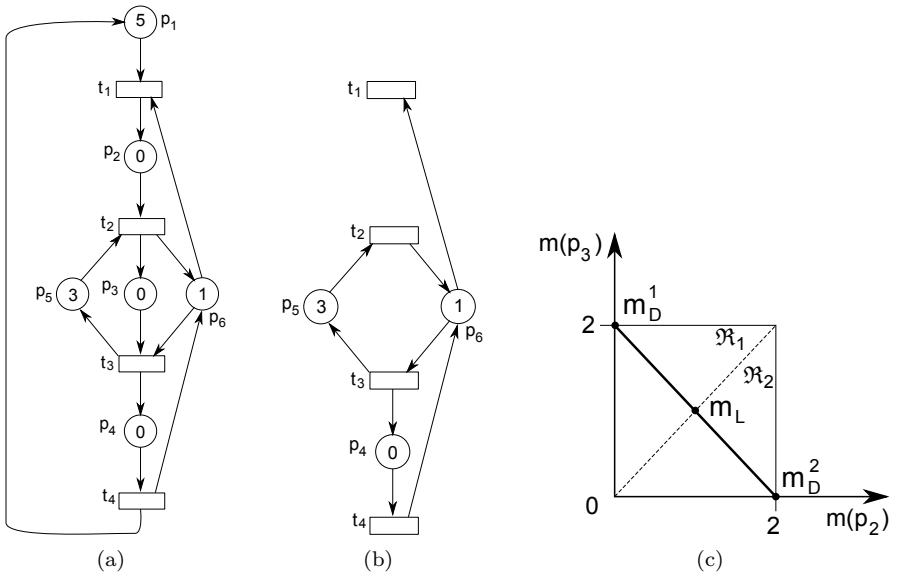

Fig. 3.5: (a) Deadlock system as autonomous, but deadlock-free as timed if $\lambda_3 > \lambda_1$. (b) Minimal siphon of the net. (c) Autonomous reachability set of the net system of fig. 3.1(b) with its equilibrium markings.

as autonomous. The deadlock occurs because the siphon $\Sigma_D = \{p_4, p_5, p_6\}$ empties. Nevertheless, the timed system is deadlock-free if $\lambda_3 > \lambda_1$. Let us prove this by showing that under such timing Σ_D will never empty. First, the deadlock belongs to a configuration in which $\mathbf{m}[p_6] \leq \mathbf{m}[p_3]$, because $\mathbf{m}[p_6] = 0$ at the deadlock. Nevertheless, inside this configuration, the marking of the siphon is always increasing, since $\mathbf{m}[p_4] + \mathbf{m}[p_5] + \mathbf{m}[p_6] = \mathbf{m}_0[p_4] + \mathbf{m}_0[p_5] + \mathbf{m}_0[p_6] + \int(\mathbf{f}[t_3] - \mathbf{f}[t_1])d\tau$, and $\int(\mathbf{f}[t_3] - \mathbf{f}[t_1])d\tau = \int(\lambda_3 - \lambda_1) \cdot \mathbf{m}[p_6] \cdot d\tau > 0$. Clearly, if $\lambda_3 \geq \lambda_1$ the siphon never empties and the system is deadlock-free (sooner or later the deadlock configuration is left). In particular, if $\lambda_1 = \lambda_3$ the total marking of the siphon will remain constant. In any case, no deadlock occurs if the initial marking at p_1 is 3 instead of 5. That is, deadlock-freeness is non monotonic with respect to the marking: increasing the number of resources ($\mathbf{m}_0[p_1] > 3$) can kill the system!

Nevertheless, for some nets there do not exist rates that make the system deadlock-free.

Example 3.9. Consider the system in fig. 3.1(b) but with a weight of 1 at arc (t_3, p_1). Here the reasoning is purely structural: the net is structurally bounded but not consistent so it is non live for any timing.

In the following subsections, it will be investigated the existence of a timing that makes a non-live contPN system to be live as timed. If it is assumed that the timed system reaches a steady state marking, liveness can be studied from the flow at such marking. In the sequel, consider the definitions of *deadlock, live and non-live markings* introduced in Subsection 3.5.1.

Since deadlock markings are particular cases of non-live ones, only non-live markings will be studied in the sequel. In this way, liveness can be studied by using the following approach:

1) Given a TCPN system $\langle \mathcal{N}, \lambda, \mathbf{m}_0 \rangle$, compute non-live equilibrium markings in $Class(\mathbf{m}_0)$.

2) For a particular initial marking or a set of them, solve the reachability of the non-live markings.

The advantage of this approach is that the first problem can be solved by adopting an algebraic perspective, which will be done through the next subsection. The second problem can be studied by using results from the Control Theory, which will be investigated in forthcoming subsections.

3.4.1 Live and non-live equilibrium markings

Let us present in this subsection some basic results about the existence of live and non-live equilibrium markings in a given region $\Re_D$. Non-live markings can be easily computed by using the following LPP.

Algorithm 3.3. Computation of non-live markings.

Let $\mathbf{\Pi}_D$ be a given configuration matrix, and let T_D be a set of transitions. The following LPP computes an equilibrium marking $\mathbf{m}_D \in \Re_D$, if it exists, at which all the transitions in T_D are dead.

max	$[1,...,1] \cdot \mathbf{m}_D$ subject to	
	$\mathbf{m}_D \geq \mathbf{0}$	
	$\mathbf{B}_y^T(\mathbf{m}_D - \mathbf{m}_0) = \mathbf{0}$	{in $Class(\mathbf{m}_0)$}
	$\mathbf{C\Lambda\Pi}_D\mathbf{m}_D = \mathbf{0}$	{equilibrium marking}
	$\mathbf{\Pi}_D\mathbf{m}_D \leq \mathbf{\Pi}_j\mathbf{m}_D \quad \forall \mathbf{\Pi}_j$	{belongs to $\Re_D$}
	$[\mathbf{\Pi}_D]_i\,\mathbf{m}_D = 0 \quad \forall t_i \in T_D$	{non-live}

Proof. Since $\mathbf{m}_D \geq \mathbf{0}$ and $\mathbf{B}_y^T(\mathbf{m}_D - \mathbf{m}_0) = \mathbf{0}$ then, by definition, $\mathbf{m}_D \in Class(\mathbf{m}_0)$. Furthermore, $\mathbf{\Pi}_D\mathbf{m}_D \leq \mathbf{\Pi}_j\mathbf{m}_D\ \forall \mathbf{\Pi}_j$ implies that $\mathbf{m}_D \in \Re_D$. The marking $\mathbf{m}_D$ is an equilibrium one because $\mathbf{C\Lambda\Pi}_D\mathbf{m}_D = \mathbf{0}$. Finally, since $\mathbf{\Lambda}$ is a diagonal matrix, $[\mathbf{\Pi}_D]_i\mathbf{m}_D = 0$ implies $[\mathbf{f}(\mathbf{m}_D)]_i = [\mathbf{\Lambda\Pi}_D\mathbf{m}_D]_i = 0$. Then, $\forall t_i \in T_D\ [\mathbf{f}(\mathbf{m}_D)]_i = 0$. Therefore, $\mathbf{m}_D$ is a non-live equilibrium marking in $\Re_D$ in which all the transitions in T_D are dead. ∎

Non-live markings can appear in different regions. In general, when more than one non-live marking appear, they can be isolated or connected in $Class(\mathbf{m}_0)$, but even in this case they may not describe a convex set. Nevertheless, if in a given region there exist two non-live equilibrium markings $\mathbf{m}_1$ and $\mathbf{m}_2$, at which transition t_i is dead, then all markings in the linear segment defined by $\mathbf{m}_1$ and $\mathbf{m}_2$ are also non-live equilibrium markings with t_i dead. This is proven in the following:

Proposition 3.21. *Given a TCPN system, consider a marking region $\Re_D \subseteq Class(\mathbf{m}_0)$ with an equilibrium marking $\mathbf{m}_D \in \Re_D$. If there exists $\boldsymbol{\eta} \geq \mathbf{0}$ s.t.*

$$\begin{bmatrix} \mathbf{\Pi}_D \\ \mathbf{B}_y^T \end{bmatrix} \boldsymbol{\eta} = \mathbf{0} \tag{3.9}$$

then all the markings in $S = \{\mathbf{m} \in \Re_D | (\mathbf{m} - \mathbf{m}_D) = \boldsymbol{\eta} \cdot \alpha, \alpha \in \mathbb{R}\}$ are also equilibrium markings having the same flow, i.e., $\forall \mathbf{m} \in S$ it holds $\mathbf{f}(\mathbf{m}) = \mathbf{f}(\mathbf{m}_D)$. If $\mathbf{m}_D$ is in the int$\{\Re_D\}$ then $\{S/\mathbf{m}_D\} \neq \emptyset$. In this way, if $\mathbf{m}_D$ is a non-live marking in which all the transitions in T_D are dead, then $\forall \mathbf{m} \in S$, $\mathbf{m}_D$ is non-live and all the transitions in T_D are dead at this marking.

Proof. Consider a marking $\mathbf{m} \in S$. Then, $\mathbf{f}(\mathbf{m}) - \mathbf{f}(\mathbf{m}_D) = \mathbf{\Lambda\Pi}_D\mathbf{m} - \mathbf{\Lambda\Pi}_D\mathbf{m}_D = \mathbf{\Lambda\Pi}_D(\mathbf{m} - \mathbf{m}_D)$. Since $\mathbf{m} \in S$ then $\exists\alpha$ s.t. $(\mathbf{m} - \mathbf{m}_D) = \boldsymbol{\eta}\alpha$. According to (3.9), $\mathbf{\Pi}_D(\mathbf{m} - \mathbf{m}_D) = \mathbf{\Pi}_D\boldsymbol{\eta}\alpha = \mathbf{0}$. Therefore, $\mathbf{f}(\mathbf{m}) - \mathbf{f}(\mathbf{m}_D) = \mathbf{\Lambda\Pi}_D(\mathbf{m} - \mathbf{m}_D) = \mathbf{0}$, meaning that $\mathbf{f}(\mathbf{m}) = \mathbf{f}(\mathbf{m}_D)$. In this way, since both markings have the same flow, if $\mathbf{m}_D$ is an equilibrium marking at which all the transitions in T_D are dead then $\mathbf{m}$ is also an equilibrium marking in which all the transitions in T_D are dead.
Now, assume that $\mathbf{m}_D$ is in $int\{\Re_D\}$. Then $\mathbf{m}_D > \mathbf{0}$, which implies that for a small enough $\alpha \in \mathbb{R}$ the marking $\mathbf{m}' = \mathbf{m}_D + \boldsymbol{\eta}\alpha > \mathbf{0}$. Furthermore, $\mathbf{B}_y^T\boldsymbol{\eta} = \mathbf{0}$ implies that $\mathbf{B}_y^T\mathbf{m}' = \mathbf{B}_y^T\mathbf{m}_D$, thus $\mathbf{m}' \in Class(\mathbf{m}_0)$. Moreover, since $\mathbf{m}_D$ is in $int\{\Re_D\}$ then, for a small enough α, $\mathbf{m}' \in \Re_D$, thus $\{S/\mathbf{m}_D\} \neq \emptyset$. ∎

Live markings may exist in non-live regions. This is interesting since, if the timing is s.t. a live marking is attractive, i.e., it is asymptotically stable, then the system will avoid the non-live markings, and thus liveness follows. Conditions for the existence of such live markings, in function of the eigenvectors associated to null eigenvalues, are introduced next:

Proposition 3.22. *Let $\langle \mathcal{N}, \boldsymbol{\lambda}, \mathbf{m}_0 \rangle$ be a TCPN system. Let $\mathbf{m}_D$ be a non-live marking and let $\mathbf{\Pi}_D$ and $\Re_D$ be its associated configuration matrix and region, respectively.*

1) If all the eigenvalues of $\mathbf{C\Lambda\Pi}_D$ non associated to P-flows *are not null then $\forall\mathbf{v}$ s.t. $\mathbf{C\Lambda\Pi}_D\mathbf{v} = \mathbf{0}$ and $\mathbf{B}_y^T\mathbf{v} = \mathbf{0}$, $\mathbf{v} = \mathbf{0}$ is fulfilled. As a consequence, $\mathbf{m}_D$ is the only equilibrium marking in $\Re_D$.*

2) If there exists an eigenvector $\mathbf{v}$, associated to a variable *zero valued eigenvalue, s.t. $\mathbf{\Lambda\Pi}_D\mathbf{v}$ is a T-semiflow, $\mathbf{B}_y^T\mathbf{v} = \mathbf{0}$, $dim(\Re_D) = rank(\mathbf{C})$, and $\mathbf{m}_D$ is associated to only one configuration, then there exist infinite non deadlock equilibrium markings in $\Re_D$, at which the transitions related to positive entries of $\mathbf{\Lambda\Pi}_D\mathbf{v}$ are live.*

Proof. First, in order to separate the null eigenvalues related to *P-flows* from the others, let us define a similarity transformation $[\mathbf{Z}^T, \mathbf{B}_y]^T$, where $\mathbf{B}_y^T$ is a basis for *P-flows* and $\mathbf{Z}$ is a suitable matrix for completing the rank. Denoting by $[\mathbf{A}, \mathbf{B}]$ the inverse transformation, the transformed state matrix is described by

$$\begin{bmatrix} \mathbf{Z} \\ \mathbf{B}_y^T \end{bmatrix} \mathbf{C\Lambda\Pi}_D \begin{bmatrix} \mathbf{A} & \mathbf{B} \end{bmatrix} = \begin{bmatrix} \mathbf{ZC\Lambda\Pi}_D\mathbf{A} & \mathbf{ZC\Lambda\Pi}_D\mathbf{B} \\ \mathbf{0} & \mathbf{0} \end{bmatrix}$$

since $\mathbf{B}_y^T\mathbf{C} = \mathbf{0}$. According to this transformation, the eigenvalues of $\mathbf{ZC\Lambda\Pi}_D\mathbf{A}$ are those of $\mathbf{C\Lambda\Pi}_D$ non associated to *P-flows*.
Statement 1). By hypothesis, all the eigenvalues, non associated to the *P-flows*, are not null. Then, all the eigenvalues of $\mathbf{ZC\Lambda\Pi}_D\mathbf{A}$ are not null, which implies that it has full rank. Let $\mathbf{v}$ be a vector s.t $\mathbf{C\Lambda\Pi}_D\mathbf{v} = \mathbf{0}$ and $\mathbf{B}_y^T\mathbf{v} = \mathbf{0}$. Applying the similarity transformation:

$$\begin{bmatrix} \mathbf{ZC\Lambda\Pi}_D\mathbf{A} & \mathbf{ZC\Lambda\Pi}_D\mathbf{B} \\ \mathbf{0} & \mathbf{0} \end{bmatrix} \begin{bmatrix} \mathbf{Zv} \\ \mathbf{B}_y^T\mathbf{v} \end{bmatrix} = \mathbf{0}$$

Now, since $\mathbf{B}_y^T\mathbf{v} = \mathbf{0}$ and $\mathbf{ZC\Lambda\Pi}_D\mathbf{A}$ has full rank then $\mathbf{v} = \mathbf{0}$. Finally, since every equilibrium marking $\mathbf{m}_1 \in \Re_D$ must satisfy $\mathbf{C\Lambda\Pi}_D(\mathbf{m}_1 - \mathbf{m}_D) = \mathbf{0}$ and $\mathbf{B}_y^T(\mathbf{m}_1 - \mathbf{m}_D) = \mathbf{0}$, then $(\mathbf{m}_1 - \mathbf{m}_D)$ is null, so $\mathbf{m}_1 = \mathbf{m}_D$.

Statement 2). By hypothesis, there exists $\mathbf{v} \neq \mathbf{0}$ such that $\mathbf{C\Lambda\Pi}_D\mathbf{v} = \mathbf{0}$, $\mathbf{B}_y^T\mathbf{v} = \mathbf{0}$ and $\mathbf{\Lambda\Pi}_D\mathbf{v}$ is a T-semiflow. Now, consider a vector $\mathbf{m}_1 = \mathbf{m}_D + \mathbf{v}\alpha$, note that it is nonnegative for a small enough $\alpha \geq 0$ ($\forall p_j$ s.t. $\mathbf{m}_D[p_j] = 0$ it fulfills that $v_j \geq 0$, because p_j is constraining a transition and $\mathbf{\Lambda\Pi}_D\mathbf{v} \geq \mathbf{0}$). Furthermore, since $\mathbf{B}_y^T\mathbf{m}_1 = \mathbf{B}_y^T\mathbf{m}_D$, $dim(\Re_D) = rank(\mathbf{C})$ and $\mathbf{m}_D$ is related to only one configuration, there always exists a small enough $\alpha \geq 0$ s.t. $\mathbf{m}_1 \in \Re_D$. Moreover, $\mathbf{C\Lambda\Pi}_D\mathbf{m}_1 = \mathbf{0}$ and $\mathbf{\Lambda\Pi}_D\mathbf{v} \neq 0$ (which implies that $\mathbf{\Lambda\Pi}_D\mathbf{m}_1 \neq \mathbf{\Lambda\Pi}_D\mathbf{m}_D = \mathbf{0}$), i.e., $\mathbf{m}_1$ is a non deadlock marking in which the transitions related to positive entries of $\mathbf{\Lambda\Pi}_D\mathbf{v}$ are live. Finally, by linearity, every marking in the convex described by $\mathbf{m}_1$ and $\mathbf{m}_D$ is also a non deadlock equilibrium marking, and the flow at those markings is positive at those transitions related to positive entries of $\mathbf{\Lambda\Pi}_D\mathbf{v}$, i.e., they are live. ∎

Remark 3.23. A particular case of statement 2 of previous proposition occurs when the eigenvector $\mathbf{v}$ is s.t. $\mathbf{\Lambda\Pi}_D\mathbf{v} > \mathbf{0}$. In such case there exist infinite live equilibrium markings in $\Re_D$. Note that this occurs if the system is λ-Ct in $\Re_D$ (such $\mathbf{v}$ fulfills (3.2)), then, this property is a sufficient condition for the existence of live equilibrium markings in non-live regions.

Example 3.10. Consider the net system of fig. 3.1(b). Fig. 3.5(c) shows the projection of the autonomous reachability set $Class(\mathbf{m}_0)$ (since $\mathbf{m}[p_1] + \mathbf{m}[p_2] + \mathbf{m}[p_3] = 2$ due to the P-semiflow $\mathbf{y}^T = [1, 1, 1]$, the markings at p_2 and p_3 are sufficient to univocally describe every reachable marking). As mentioned in the Example 3.8, this system deadlocks as untimed, but it is timed-live if $\lambda_1 = \lambda_2$. In fact, this continuous model has two deadlock markings, $\mathbf{m}_D^1 = [0, 2, 0]^T$ and $\mathbf{m}_D^1 = [0, 0, 2]^T$, belonging to two different configurations: $\mathbf{\Pi}_1$ for that in which p_2 constraints t_3, and $\mathbf{\Pi}_2$ when p_3 constraints t_3. By setting $\boldsymbol{\lambda} = [1, 1, 2]^T$, the vector $\mathbf{v} = [1, 0.5, 0.5]^T$ fulfills with $\mathbf{C\Lambda\Pi}_1\mathbf{v} = \mathbf{C\Lambda\Pi}_2\mathbf{v} = \mathbf{0}$ and $\mathbf{B}_y^T\mathbf{v} = \mathbf{0}$ (in this case, such $\mathbf{v}$ implies λ-Ct in both configurations). Then, according to the second statement of Proposition 3.22, there exist infinite live equilibrium markings in both regions. These are depicted in fig. 3.5(c) as a bold line that connects $\mathbf{m}_D^1$ and $\mathbf{m}_D^2$, i.e., all these markings excepting $\mathbf{m}_D^1$ and $\mathbf{m}_D^2$ are live. Note the existence of a live equilibrium marking belonging to both configurations $\mathbf{m}_L = [1, 0.5, 0.5]^T$ (in this case, $\mathbf{m}_L = \mathbf{v}$ because $\mathbf{B}_y^T\mathbf{v} = \mathbf{0}$, but in general, $\mathbf{v}$ fulfilling (3.2) is not an equilibrium marking).

3.5 Timing to avoid non-live markings

In this section, a sufficient condition for avoiding non-live markings, by suitably choosing the timing $\boldsymbol{\lambda}$, will be provided.

3.5.1 $\boldsymbol{\lambda}$-Ct as a sufficient condition for liveness

Firstly, let us show the connection between non-live markings and siphons.

Proposition 3.24. *Let $\langle \mathcal{N}, \boldsymbol{\lambda}, \mathbf{m}_0 \rangle$ be a TCPN system. Consider an equilibrium marking $\mathbf{m}_D \in Class(\mathbf{m}_0)$. There are empty siphons at $\mathbf{m}_D$ iff it is a non-live marking.*

Proof. Suppose that the system is at an equilibrium marking $\mathbf{m}_D$ at which there are empty siphons. Since empty siphons never gain marks, then the places belonging to supports of those empty siphons remain unmarked, so, their output transitions never become enabled and thus they are dead. For the other implication, suppose that the system is at a non-live equilibrium marking $\mathbf{m}_D$. Then, at least

one input place of each dead transition is empty at $\mathbf{m}_D$, and they remain empty for future time (it is an equilibrium marking). If there exists a place p_i that always remains unmarked, then for each input transition t_j to this place, it must exist an input place p_k to t_j, which remains also unmarked for all time. Repeating this reasoning, it can be seen that p_i should belong to an unmarked siphon. ∎

Let us start the analysis from a dynamic systems' perspective. Recalling from Subsection 1.5.2, *P-flows* are related to null eigenvalues that do not depend on the timing $\boldsymbol{\lambda}$ (equivalently, *P-flows* are related to fixed null poles [Mahulea et al., 2008b]). Nevertheless, not all the null poles are related to P-flows.

Definition 3.25. Null poles can be:

1) Fixed and related to P-flows, i.e., $\exists \mathbf{w} \neq \mathbf{0}$ s.t. $\mathbf{w}^T\mathbf{C} = \mathbf{0}$, then $\forall \boldsymbol{\lambda}$, $\forall \boldsymbol{\Pi}_i$, $\mathbf{w}^T\mathbf{C}\boldsymbol{\Lambda}\boldsymbol{\Pi}_i = \mathbf{0}$.

2) Fixed but not related to P-flows, i.e., $\forall \boldsymbol{\lambda}\ \exists \mathbf{w} \neq \mathbf{0}$ s.t. $\mathbf{w}^T\mathbf{C}\boldsymbol{\Lambda}\boldsymbol{\Pi}_i = \mathbf{0}$ but $\mathbf{w}^T\mathbf{C} \neq \mathbf{0}$. These null poles appear in particular configurations, when $rank(\boldsymbol{\Pi}_i) < rank(\mathbf{C})$.

3) Variable, i.e., $\exists \boldsymbol{\lambda}\ \exists \mathbf{w} \neq \mathbf{0}$ s.t. $\mathbf{w}^T\mathbf{C}\boldsymbol{\Lambda}\boldsymbol{\Pi}_i = \mathbf{0}$ with $\mathbf{w}^T\mathbf{C} \neq \mathbf{0}$. These null poles appear even if $rank(\boldsymbol{\Pi}_i) = rank(\mathbf{C})$, but in this case, the span of $\boldsymbol{\Lambda}\boldsymbol{\Pi}_i$ includes T-flows, i.e., $span(\Lambda\boldsymbol{\Pi}_i) \cap span(\mathbf{B}_x) \neq \emptyset$, where $\mathbf{B}_x$ is a basis of T-flows (right annuller of $\mathbf{C}$).

Remark 3.26. A particular case of null poles of the kind 2) and 3) occurs when $\mathbf{w} > \mathbf{0}$, making the system to be λ-Cv at $\boldsymbol{\Pi}_i$. These zero valued poles are related to marking conservation laws that are not *P-flows*, i.e., $\mathbf{w}$ s.t. $\mathbf{w}^T\dot{\mathbf{m}} = \mathbf{w}^T\mathbf{C}\boldsymbol{\Lambda}\boldsymbol{\Pi}_i = \mathbf{0}$ but $\mathbf{w}^T\mathbf{C} \neq \mathbf{0}$. From a dynamic systems' point of view, this marking conservation laws are state invariants, i.e., the evolution of the system is restricted to the manifold where $\mathbf{w}^T\mathbf{m} = \mathbf{w}^T\mathbf{m}_0$ (until a change of configuration occurs). In this way, this property can affect the reachability of non-live markings in TCPNs: if the marking conservation law involves the support of a siphon, this will never empty, thus the non-live markings at which this siphon is empty are not reachable.

Proposition 3.27. *Consider a non-live marking $\mathbf{m}_D \in \Re_D$, in which a minimal siphon Σ_D is empty. If the timing $\boldsymbol{\lambda}$ is s.t. there exists an eigenvector $\mathbf{w} \geq \mathbf{0}$, related to a variable zero valued pole of $\mathbf{C}\boldsymbol{\Lambda}\boldsymbol{\Pi}_D$, whose support is equal to Σ_D (i.e., $\forall j$, $w_j > 0$ iff $p_j \in \Sigma_D$), then the siphon Σ_D cannot be emptied (assuming it is initially marked) while the system evolves inside $\Re_D$. Consequently, $\mathbf{m}_D$ is not reachable from any $\mathbf{m}_0 \in \Re_D$ s.t. $\mathbf{w}^T\mathbf{m}_0 > 0$ (i.e., that marks Σ_D), through a trajectory inside $\Re_D$.*

Proof. First, since $\mathbf{w} \geq \mathbf{0}$ is s.t. $\mathbf{w}^T\mathbf{C}\boldsymbol{\Lambda}\boldsymbol{\Pi}_D = \mathbf{0}$, then, premultiplying the state equation, $\mathbf{w}^T\dot{\mathbf{m}} = \mathbf{w}^T\mathbf{C}\boldsymbol{\Lambda}\boldsymbol{\Pi}_D = \mathbf{0}$. Denote as $\mathbf{m}(\tau)$ the marking reached after τ time units (assuming that the system evolves inside $\Re_D$). By integrating previous equation, it is obtained $\int_0^\tau \mathbf{w}^T\dot{\mathbf{m}}d\tau = \mathbf{w}^T(\mathbf{m}(\tau) - \mathbf{m}_0) = \mathbf{0}$, equivalently $\mathbf{w}^T\mathbf{m}(\tau) = \mathbf{w}^T\mathbf{m}_0$. Next, assume that the siphon is initially marked, i.e., $\exists j$ s.t. $[\mathbf{m}_0]_j > 0$ and $p_j \in \Sigma_D$. Thus, according to the definition of $\mathbf{w}$, $p_j \in \Sigma_D$ implies $w_j > 0$, then $\mathbf{w}^T\mathbf{m}_0 > 0$. In this way, $\mathbf{w}^T\mathbf{m}(\tau) > 0$. Furthermore, since $\mathbf{w} \geq \mathbf{0}$ and $\mathbf{m}(\tau) \geq \mathbf{0}$ then $\exists k$ s.t. $w_k > 0$ and $[\mathbf{m}(\tau)]_k > 0$. Finally, $w_k > 0$ implies that $p_k \in \Sigma_D$, thus, the siphon is not empty at $\mathbf{m}(\tau)$ (at least p_k is marked). Since this reasoning holds for any marking $\mathbf{m}(\tau)$ reached through a trajectory inside $\Re_D$, the proof is completed. ∎

The existence of $\mathbf{w} \neq \mathbf{0}$ involving a siphon, as mentioned in the Proposition 3.27, can be understood as the λ-Cv property for such siphon. In the proof of the following theorem, it will be shown that the property λ-Ct in the net ensures λ-Ct in each minimal siphon, and for these, both λ-Cv and λ-Ct are equivalent. In this way, λ-Ct implies that every minimal siphon is λ-Cv, and so, for each of these $\exists\mathbf{w}$ as in Proposition 3.27, leading to a sufficient condition for liveness as a generalization of the Proposition 3.27.

Theorem 3.28. *Consider a TCPN system. If the timed net is λ-Ct at a given $\mathbf{\Pi}_i$, and the initial marking $\mathbf{m}_0 \in \Re_i$ marks all the minimal siphons, then the system is timed-live while evolves in $\Re_i$.*

Proof. Assume that the system is λ-Ct at $\mathbf{\Pi}_i$. Let Σ be a minimal siphon that may be emptied at $\mathbf{\Pi}_i$, i.e., $\exists\mathbf{m}' \in \Re_i$ s.t. $\mathbf{m}'[\Sigma] = \mathbf{0}$. If $\mathbf{m}'$ does not belong to any other region, then every place in Σ is constraining its output transitions at $\mathbf{\Pi}_i$ (otherwise, if each $\mathbf{m}'$ s.t. $\mathbf{m}'[\Sigma] = \mathbf{0}$ belongs to another region, it can be proved that there exists a minimal siphon Σ' whose places constrain their output transitions at $\mathbf{\Pi}_i$ and that empties iff Σ empties). In this way, the P-subnet $\langle \mathcal{N}^\Sigma, \boldsymbol{\lambda}^\Sigma \rangle$, defined by keeping the places in Σ and the transitions in $\Sigma^\bullet$, is a JF model. Let us suppose, without loss of generality, that the first rows of $\mathbf{C}$ correspond to places of Σ. In such case, $\mathbf{C\Lambda\Pi}_i$ can be written by blocks as:

$$\mathbf{C\Lambda\Pi}_i = \begin{bmatrix} \mathbf{C}^\Sigma\mathbf{\Lambda}^\Sigma\mathbf{\Pi}_i^\Sigma & \mathbf{0} \\ [\mathbf{C\Lambda\Pi}_i]_{2,1} & [\mathbf{C\Lambda\Pi}_i]_{2,2} \end{bmatrix}$$

Thus, since $\exists\mathbf{v} > \mathbf{0}$ annuler of $\mathbf{C\Lambda\Pi}_i$, i.e., the timed net is λ-Ct, the restriction of $\mathbf{v}$ to the places in Σ, denoted as $\mathbf{v}^\Sigma$, fulfills with $\mathbf{v}^\Sigma > \mathbf{0}$ and $\mathbf{C}^\Sigma\mathbf{\Lambda}^\Sigma\mathbf{\Pi}_i^\Sigma\mathbf{v}^\Sigma = \mathbf{0}$. Therefore, $\langle \mathcal{N}^\Sigma, \boldsymbol{\lambda}^\Sigma \rangle$ is λ-Ct.
On the other hand, as shown in Subsection 3.3.4, it is possible to transform $\langle \mathcal{N}^\Sigma, \boldsymbol{\lambda}^\Sigma \rangle$ into an equivalent FA model $\langle \mathcal{N}^R, \boldsymbol{\lambda}^R \rangle$. Furthermore, since Σ is minimal then it is P-strongly connected, thus the transformed net $\mathcal{N}^R$ is a FA strongly connected net. In this way, $\langle \mathcal{N}^R, \boldsymbol{\lambda}^R \rangle$ is λ-Ct iff it is λ-Cv. Since the same properties hold for $\langle \mathcal{N}^\Sigma, \boldsymbol{\lambda}^\Sigma \rangle$ and this is λ-Ct, then it is λ-Cv. Thus, $\exists\mathbf{w}^\Sigma > \mathbf{0}$ s.t. $\mathbf{w}^\Sigma \cdot \mathbf{C}^\Sigma\mathbf{\Lambda}^\Sigma\mathbf{\Pi}_i^\Sigma = \mathbf{0}$. This implies that $\exists\mathbf{w} \geq \mathbf{0}$ that fulfills $\mathbf{w}^T\mathbf{C\Lambda\Pi}_i = \mathbf{0}$ and $w_j > 0$ iff $p_j \in \Sigma$. The existence of such $\mathbf{w} \geq \mathbf{0}$ means that the siphon Σ is conservative ($\mathbf{w}^T\mathbf{m} = \mathbf{w}^T\mathbf{m}_0$), then, it never empties while the system evolves in $\Re_i$. Finally, since this holds for each minimal siphon, then the system is timed-live while evolves in $\Re_i$ (assuming that minimal siphons are initially marked). ∎

Example 3.11. Consider the model of fig. 3.5(a). This PN is non-live as autonomous. Places $\Sigma = \{p_4, p_5, p_6\}$ describe the minimal siphon, shown in fig. 3.5(b), that can be emptied at the configuration $\mathbf{\Pi}_i$ in which t_1 and t_3 are constrained by p_6 and t_2 is constrained by p_5. Denote the P-subnet defined by the siphon as $\mathcal{N}^\Sigma$. This is a JF model, in which transitions in conflict (t_1 and t_3) can be merged, obtaining thus the following FA timed model $\langle \mathcal{N}^R, \boldsymbol{\lambda}^R \rangle$:

$$\mathbf{C}^R = \begin{array}{c} \\ p_4 \\ p_5 \\ p_6 \end{array} \begin{array}{c} \begin{array}{ccc} t_2 & t_1 \wedge t_3 & t_4 \end{array} \\ \begin{bmatrix} 0 & \frac{\lambda_3}{\lambda_1+\lambda_3} & -1 \\ -1 & \frac{\lambda_3}{\lambda_1+\lambda_3} & 0 \\ 1 & -1 & 1 \end{bmatrix} \end{array}, \qquad \mathbf{\Lambda}^R = \begin{array}{c} \begin{array}{ccc} t_2 & t_1 \wedge t_3 & t_4 \end{array} \\ \begin{bmatrix} \lambda_2 & 0 & 0 \\ 0 & \lambda_1+\lambda_3 & 0 \\ 0 & 0 & \lambda_4 \end{bmatrix} \end{array}$$

Note that $\mathbf{C}^R$ becomes consistent (and thus conservative, since it is a strongly connected FA net) iff $\lambda_1 = \lambda_3$. In such case, $\mathbf{w}^R = [1, 1, 1]^T$ is a basis for the left annuler of $\mathbf{C}^R\mathbf{\Lambda}^R\mathbf{\Pi}^R = \mathbf{C}^\Sigma\mathbf{\Lambda}^\Sigma\mathbf{\Pi}^\Sigma$. By using

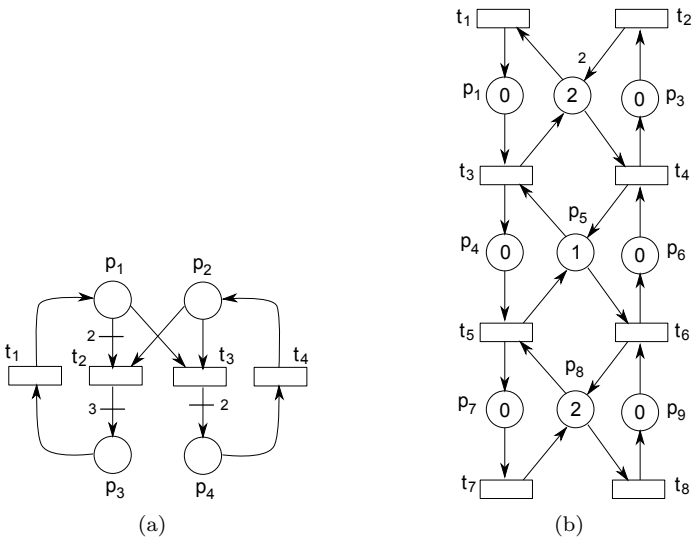

Fig. 3.6: (a) TCPN system with deadlock markings in two different regions. (b) TCPN system with two independent T-semiflows.

$\mathbf{w}^R$, a left annuler of the original model is computed as $\mathbf{w} = [0,0,0,1,1,1]^T \geq \mathbf{0}$. This vector implies that the total marking in the siphon $\mathbf{w}^T\mathbf{m} = \mathbf{m}[p_4] + \mathbf{m}[p_5] + \mathbf{m}[p_6]$ remains constant, while the system evolves in this configuration (Proposition 3.27). Finally, since Σ is the unique minimal siphon and it can be emptied only at this configuration, the timed system is timed-live. According to Theorem 3.28, the same conclusion can be obtained just by proving that the timed model is λ-Ct with $\lambda_1 = \lambda_3$.

Remark 3.29. If the net system is consistent, it is possible to compute a timing s.t. the system is λ-Ct at a given configuration $\Re_D$ (Proposition 3.15), inducing thus liveness in the considered region (Theorem 3.28). Nevertheless, consistency is no longer sufficient to guarantee the existence of a timing $\boldsymbol{\lambda}$ for simultaneously avoiding non-live markings in several regions (but consistency is still necessary).

Example 3.12. Consider the net system of fig. 3.6(a) that has two deadlocks, $\mathbf{m}_D^1 = [0,6,0,0]^T$ and $\mathbf{m}_D^2 = [6,0,0,0]^T$. The corresponding deadlock configurations are $\mathcal{C}_D^1 = \{(t_1,p_1),(t_2,p_1),(t_3,p_3),(t_4,p_4)\}$ and $\mathcal{C}_D^2 = \{(t_1,p_2),(t_2,p_2),(t_3,p_3),(t_4,p_4)\}$, respectively. Since this net is consistent, according to Proposition 3.15, for each configuration it is possible to find a timing for avoiding the corresponding deadlock marking. Nevertheless, for this net it does not exist a timing that simultaneously induces the λ-Ct property in *both* regions. In order to prove this, note that a basis for T-flows is given by $\mathbf{x} = [1,1,1,1]^T$, then, if there exist a positive vector $\mathbf{v}^1$ and $\mathbf{v}^2$ for each configuration they must fulfill $\boldsymbol{\Lambda\Pi}_D^1\mathbf{v}^1 = \beta\boldsymbol{\Lambda\Pi}_D^2\mathbf{v}^2$ for some $\beta > 0$. This equality can be written by elements as $[0.5\lambda_1 v_1^1, \lambda_2 v_1^1, \lambda_3 v_3^1, \lambda_4 v_4^1]^T = \beta[\lambda_1 v_2^2, \lambda_2 v_2^2, \lambda_3 v_3^2, \lambda_4 v_4^2]^T$ (where v_j^i means the $j-th$ entry of $\mathbf{v}^i$). Therefore $0.5v_1^1 = \beta v_2^2$ and $v_1^1 = \beta v_2^2$, but such equalities do not have positive simultaneous solutions, so, there does not exist a timing $\boldsymbol{\lambda}$ that induces live equilibrium markings in all deadlock regions. Nevertheless, it does not mean that the timed system is dead for all timing (e.g., with $\boldsymbol{\lambda} = [1,2,1,1]^T$ the timed system converges to $\mathbf{m}_1 = [0.75, 1.5, 2.25, 1.5]^T$, which is live).

3.5.2 Stability of non-live equilibrium markings

From a control theory perspective, non-live equilibrium markings are equilibrium points, so, the knowledge of the value of the poles (in each non-live configuration) is useful to decide if, given a particular timing, a non-live marking will be reached or will not. This idea is captured in the following propositions.

Proposition 3.30. *Let $\langle \mathcal{N}, \boldsymbol{\lambda}, \mathbf{m}_0 \rangle$ be a TCPN system. Given a non-live marking $\mathbf{m}_D$ that belongs to a unique region $\Re_D$, then*

1) *If the real parts of the poles of $\mathbf{C\Lambda\Pi}_D$, non associated to the P-flows, are* negative, *then $\mathbf{m}_D$ is locally asymptotically stable, i.e., there exists a neighborhood of $\mathbf{m}_D$, named $N(\mathbf{m}_D)$, s.t. if $\mathbf{m}_0 \in N(\mathbf{m}_D)$ then the system* inevitably *reaches $\mathbf{m}_D$.*

2) *If $\mathbf{C\Lambda\Pi}_D$ has* a zero valued *pole, non associated to the P-flows, and the real parts of the others are* negative, *then $\mathbf{m}_D$ is stable (nevertheless $\mathbf{m}_D$ could be reached or not).*

3) *If there exists a* variable *null eigenvalue of $\mathbf{C\Lambda\Pi}_D$, with an associated eigenvector $\mathbf{v}$ s.t. $\mathbf{B}_y^T\mathbf{v} = \mathbf{0}$ and $\mathbf{\Lambda\Pi}_D\mathbf{v}$ is a T-flow with positive entries at those transitions that are dead at $\mathbf{m}_D$ (particularly, if the system is λ-Ct), then $\mathbf{m}_D$ is not reachable from a positive marking $\mathbf{m}_0 \in \Re_D$, through a trajectory in $\Re_D$.*

4) *If there exists a pole of $\mathbf{C\Lambda\Pi}_D$ having a positive real part, then $\mathbf{m}_D$ is unstable, so it is not reachable from another marking, through a trajectory in $\Re_D$.*

Proof. By using the similarity transformation introduced in the proof of Proposition 3.22, the dynamical behavior of the TCPN in $\Re_D$ can be described by a reduced order system $\dot{\boldsymbol{\mu}} = \mathbf{A}_r\boldsymbol{\mu} + \mathbf{b}_r$, where $\mathbf{A}_r = \mathbf{ZC\Lambda\Pi}_D\mathbf{A}$, $\mathbf{b}_r = \mathbf{ZC\Lambda\Pi}_D\mathbf{B}\mathbf{B}_y^T\mathbf{m}_0$ and $\mathbf{m} = \mathbf{A}\boldsymbol{\mu} + \mathbf{B}\mathbf{B}_y^T\mathbf{m}_0$. In this reduced system, only the poles of $\mathbf{C\Lambda\Pi}_D$ non associated to P-flows are present. Now, if the condition of statement 1) is fulfilled, then, according to Proposition 3.22, $\mathbf{m}_D$ is the only equilibrium marking in $\Re_D$. Thus, statements 1), 2) and 4) are immediate from Theorem 1.23.

If the hypothesis of Statement 3) is fulfilled, then it is possible to define a vector $\mathbf{v}' = \mathbf{m}_D + \beta\mathbf{v}$ that is positive for a small enough β. Furthermore, $\mathbf{C\Lambda\Pi}_D\mathbf{v}' = \mathbf{0}$, then the system is λ-Ct at $\mathbf{\Pi}_D$, thus, according to Theorem 3.28, $\mathbf{m}_D$ is not reachable through a trajectory in $\Re_D$. ∎

The stability analysis of a non-live marking $\mathbf{m}_D$, which is related to more than one configuration, is more complex, since it is a stability problem of a piecewise linear system. Nevertheless, it is possible to know what could happen for particular cases.

Proposition 3.31. *Let $\langle \mathcal{N}, \boldsymbol{\lambda}, \mathbf{m}_0 \rangle$ be a TCPN system. Given a non-live marking $\mathbf{m}_D$ that belongs to different regions $\Re_D^1$,...,$\Re_D^k$, then*

1) *If for every region $\Re_D^i$, to which $\mathbf{m}_D$ belongs, the poles of $\mathbf{C\Lambda\Pi}_D^i$ are real and negative, then $\mathbf{m}_D$ is locally asymptotically stable, i.e., there exists a neighborhood of $\mathbf{m}_D$, named $N(\mathbf{m}_D)$, s.t. if $\mathbf{m}_0 \in N(\mathbf{m}_D)$ then the system inevitably reaches $\mathbf{m}_D$.*

2) If for all regions $\Re_D^i$*, there exists an eigenvector* $\mathbf{v}^i$*, associated to a* variable *zero eigenvalue of* $\mathbf{C\Lambda\Pi}_D^i$*, s.t.* $\mathbf{B}_y^T\mathbf{v}^i = \mathbf{0}$ *and* $\mathbf{\Lambda\Pi}_D^i\mathbf{v}^i > \mathbf{0}$*, then* $\mathbf{m}_D$ *is not reachable from* $\mathbf{m}_0 > \mathbf{0}$ *through a trajectory in* $\bigcup \Re_D^i$*.*

Proof. As in the proof of previous proposition, for every configuration $\mathcal{C}_D^i$ related to $\mathbf{m}_D$, there exists a reduced order system that describes the dynamical behavior of the system in $\Re_D^i$. If the condition of statement 1) is fulfilled, then every linear subsystem has real and negative poles. It is well known in the Control Theory (see for instance [Chen, 1984]) that in such case the state is decreasing for all time. Then, the marking, and thus the flow, is decreasing while the system stay in $\Re_D^i$. Since that happens for every system associated to $\mathbf{m}_D$, then for a small enough neighborhood of $\mathbf{m}_D$, named $N(\mathbf{m}_D)$, the flow is decreasing, consequently, the system inevitably will reach $\mathbf{m}_D$. Statement 2) is an immediate generalization of the statement 3) of Proposition 3.30, i.e., the condition of Statement 2) implies that the system cannot approximate to $\mathbf{m}_D$ in any of the configurations at which $\mathbf{m}_D$ belongs. ∎

The first statement of previous proposition can be extended by using the classical Common Lyapunov Function (CLF) criterion (see, for instance, [Liberzon, 2004]), i.e., there exists a neighborhood of $\mathbf{m}_D$ from where the system inevitably reaches $\mathbf{m}_D$ if there exist symmetric positive definite matrices $\mathbf{P}$ and $\mathbf{Q}^i$ s.t. $(\mathbf{ZC\Lambda\Pi}_D^i\mathbf{A})^T\mathbf{P} + \mathbf{P}(\mathbf{ZC\Lambda\Pi}_D^i\mathbf{A}) = -\mathbf{Q}^i$ for each $\Re_D^i$ to which $\mathbf{m}_D$ belongs, where $\mathbf{Z}$ and $\mathbf{A}$ are the matrices introduced in the proof of Proposition 3.22.

3.5.3 Examples: towards a dynamic interpretation of liveness

Through this section, a few examples will be analyzed in order to illustrate the potential application of the results introduced through this section.

In the sequel, given a non-live configuration $\mathcal{C}_D$, the possibility of choosing $\boldsymbol{\lambda}$ s.t. *variable* zero valued poles are induced will firstly be analyzed through the characteristic polynomial of $\mathbf{C\Lambda\Pi}_D$.

Property 3.32. Consider the characteristic polynomial of $\mathbf{C\Lambda\Pi}_D$, where $\mathbf{\Lambda}$ is in parametric form. The order of the lowest order term is equal to the number of *fixed* zero valued poles, and a particular $\mathbf{\Lambda}$ that makes this lowest order term to be zero leads to a *variable* zero valued pole. In such case, statement 3 of Proposition 3.30 may follow.

Example 3.13. Consider the TCPN system of fig. 3.5(a). In this case, there exists a unique deadlock $\mathbf{m}_D = [1, 1, 3, 0, 0, 0]^T$, belonging to a unique configuration $\Re_D$. The lowest order term of the characteristic polynomial of $\mathbf{C\Lambda\Pi}_D$ is $s^3(\lambda_4\lambda_1\lambda_2 - \lambda_4\lambda_2\lambda_3)$. It means that there exist 3 *fixed* zero valued poles (related to 3 P-semiflows), and that a timing $\boldsymbol{\lambda}$ s.t $\lambda_2\lambda_4(\lambda_1 - \lambda_3) = 0$ creates an additional zero valued pole. Then, a timing $\boldsymbol{\lambda}$ s.t. $\lambda_1 = \lambda_3$ fulfills that condition, in which case, according to Proposition 3.30, $\mathbf{m}_D$ is not reachable from any $\mathbf{m}_0 > \mathbf{0}$ through a trajectory in $\Re_D$. Moreover, since $\mathbf{m}_D$ belongs only to $\Re_D$, then the TCPN system is deadlock-free. Such $\boldsymbol{\lambda}$ establishes an "equilibrium" between the flow going into the siphon $\Sigma = \{p_4, p_5, p_6\}$ and the flow going out of it, as it was shown in the Example 3.8. Furthermore, if $\lambda_3 > \lambda_1$, then the coefficient of this term becomes negative and it can be demonstrated, through the Routh-Hurwitz criterion (see, for instance, [Chen, 1984]), that $\mathbf{m}_D$ is unstable (at leats one pole becomes positive), then the system is deadlock-free (Proposition 3.30). Since this system has only

one elementary T-semiflow, deadlock-freeness implies liveness (equivalently, $\mathbf{m}_D$ is the unique non-live equilibrium marking).

Example 3.14. Now, consider the system of fig. 3.6(b). It has 16 configurations but only three with deadlocks:

$$\mathcal{C}_1 = \{(t_3, p_5), (t_4, p_6), (t_5, p_8), (t_6, p_5)\}$$
$$\mathcal{C}_2 = \{(t_3, p_5), (t_4, p_2), (t_5, p_8), (t_6, p_5)\}$$
$$\mathcal{C}_3 = \{(t_3, p_5), (t_4, p_2), (t_5, p_4), (t_6, p_5)\}$$

(the arcs that constrain transitions t_1, t_2, t_7 and t_8 are not written because they are the same for all the configurations). Configuration $\mathcal{C}_2$ has infinite deadlocks ($\exists \boldsymbol{\eta} \neq 0$ satisfying (3.9)). All deadlocks in the system are connected. Computing the lowest order terms of the characteristic polynomial for the three cases we obtain

$$\begin{aligned}
\mathcal{C}_1: &\quad s^3\lambda_1\lambda_2\lambda_7\lambda_4(\lambda_3\lambda_8 - \lambda_5\lambda_6) \\
\mathcal{C}_2: &\quad s^4\left[\lambda_1\lambda_2\lambda_7(\lambda_3\lambda_8 - \lambda_5\lambda_6) + \lambda_2\lambda_7\lambda_8(\lambda_1\lambda_6 - \lambda_3\lambda_4)\right] \\
\mathcal{C}_3: &\quad s^3\lambda_2\lambda_7\lambda_8\lambda_5(\lambda_1\lambda_6 - \lambda_3\lambda_4)
\end{aligned}$$

For any timing $\boldsymbol{\lambda}$ s.t. $\lambda_3\lambda_8 = \lambda_5\lambda_6$ and $\lambda_1\lambda_6 = \lambda_3\lambda_4$, a *variable* zero valued pole is added to every deadlock configuration. In this system, every possible non-live equilibrium marking $\mathbf{m}_D$ is actually a deadlock one, i.e., $\Sigma_D^{\bullet} = T$. Nevertheless, if a variable zero valued eigenvalue is added then there exists an eigenvector $\mathbf{v} \neq \mathbf{0}$ s.t. $[\boldsymbol{\Lambda}\boldsymbol{\Pi}_D\mathbf{v}]_i > 0$ for some t_i, so, according to Proposition 3.31, non live markings in which t_i is dead are not reachable from a positive initial marking. Finally, since every non-live marking is a deadlock one, then the system is live.

Example 3.15. The system of fig. 3.7(a) has two different minimal T-semiflows, whose supports are covered, independently, by siphons $\Sigma_1 = \{p_4, p_5, p_6\}$ and $\Sigma_2 = \{p_9, p_{10}, p_{11}\}$. That means that there exist non-live equilibrium markings that are not deadlocks. Now, if the timing $\boldsymbol{\lambda}$ is s.t. $\lambda_1 = \lambda_3$, the siphon Σ_1 conserves its total marking (as in the system of figure 3.5(a)). But, if $\lambda_5 > \lambda_7$ then the siphon Σ_2 will empty, so, the system does not reach a deadlock, but it becomes non live. Nevertheless, if $\boldsymbol{\lambda}$ is s.t. $\lambda_1 = \lambda_3$ and $\lambda_5 = \lambda_7$, both siphons remain marked, for all time, i.e., the timed system is live.

3.6 Computing a timing for λ-Ct and λ-Cv

In this section, it will be computed a timing in order to enforce λ-Ct (thus timed-liveness) in the corresponding region (λ-Ct is sufficient for this, assuming $\mathbf{m}_0 > \mathbf{0}$, according to Theorem 3.28). Similarly, an algorithm for computing a timing that leads to λ-Cv, thus boundedness, will be provided.

In order to cope with different constraints, given some *nominal rates* $\boldsymbol{\lambda}_N$ the transitions are classified as:

1) *Uncontrollable*, whose set is denoted as T_{nc}. The rates of these must be equal to the nominal ones.
2) *Weakly controllable*, whose set is denoted as T_{wc}. The rates of these can be decreased (but not

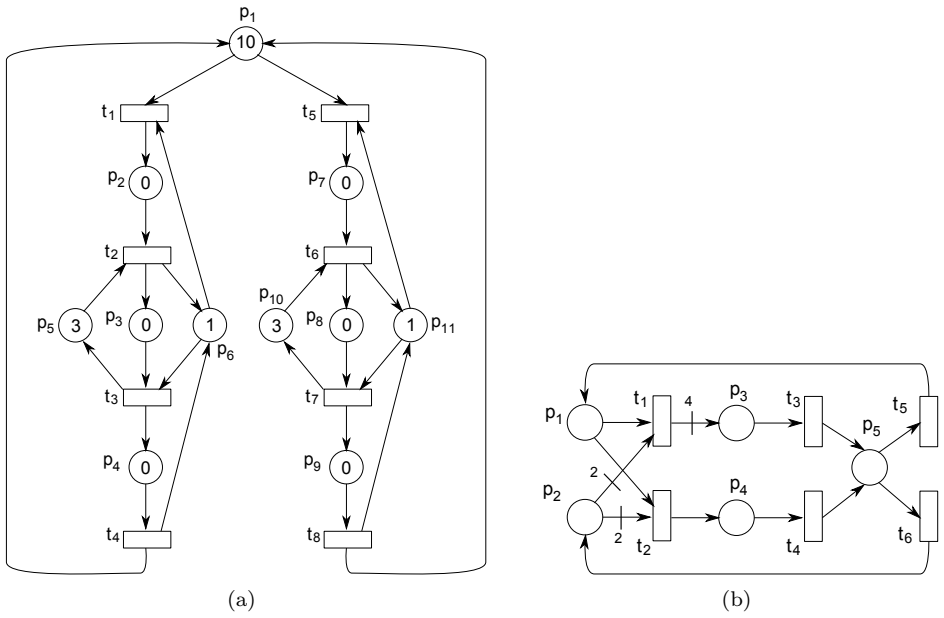

Fig. 3.7: (a) TCPN system with two independent siphons. (b) EQ unbounded TCPN model.

increased) with respect to their nominal values.

3) *Freely controllable* (T_{fc}). The rates of these can be modified freely, but they must be positive.

Note that controllable and uncontrollable transitions were defined in Subsection 1.4.5 in a different way. Nevertheless, the use of the same terms for the classification introduced above obeys to the control interpretation that will be introduced in the following subsection, where the equivalence of these definitions will be explained.

Without loss of generality, let us suppose that the first columns of $\mathbf{C}$ correspond to transitions in T_{fc}, the following columns are related to transitions in T_{wc}, while the last columns are related to transitions in T_{nc}. In this way, matrices $\mathbf{C}$, $\mathbf{\Lambda}$ and $\mathbf{\Pi}_i$ have the following structure:

$$\mathbf{C} = \left[\begin{array}{ccc} \mathbf{C}^{fc} & \mathbf{C}^{wc} & \mathbf{C}^{nc} \end{array} \right]$$

$$\mathbf{\Lambda} = \left[\begin{array}{ccc} \mathbf{\Lambda}^{fc} & \mathbf{0} & \mathbf{0} \\ \mathbf{0} & \mathbf{\Lambda}^{wc} & \mathbf{0} \\ \mathbf{0} & \mathbf{0} & \mathbf{\Lambda}^{nc} \end{array} \right], \quad \mathbf{\Pi}_i = \left[\begin{array}{c} \mathbf{\Pi}_i^{fc} \\ \mathbf{\Pi}_i^{wc} \\ \mathbf{\Pi}_i^{nc} \end{array} \right]$$

where $\mathbf{C}^{fc}$ (resp. $\mathbf{\Pi}^{fc}$, $\mathbf{\Lambda}^{fc}$), $\mathbf{C}^{wc}$ (resp. $\mathbf{\Pi}^{wc}$, $\mathbf{\Lambda}^{wc}$) and $\mathbf{C}^{nc}$ (resp. $\mathbf{\Pi}^{nc}$, $\mathbf{\Lambda}^{nc}$) correspond to the columns (resp. rows, columns & rows) of $\mathbf{C}$ (resp. $\mathbf{\Pi}$, $\mathbf{\Lambda}$) related to transitions in T_{fc} (resp. T_{wc}, T_{nc}). Similarly, matrix $\mathbf{B}_x$ can be written as $[(\mathbf{B}_x^{fc})^T, (\mathbf{B}_x^{wc})^T, (\mathbf{B}_x^{nc})^T]^T$.

The following algorithm computes a timing (if it exists) that enforces λ-consistency at a configuration $\mathbf{\Pi}_i$, fulfilling the constraints imposed to the transitions.

Algorithm 3.4. Computation of a timing for inducing λ-Ct.

Compute vectors $\mathbf{v}$ and $\boldsymbol{\eta}$ that fulfill the following linear constraints:

$$\left[\begin{array}{cc} \boldsymbol{\Lambda}^{nc}\boldsymbol{\Pi}_i^{nc}, & -\mathbf{B}_x^{nc} \end{array}\right] \cdot \left[\begin{array}{c} \mathbf{v} \\ \boldsymbol{\eta} \end{array}\right] = \mathbf{0}$$

$$\left[\begin{array}{cc} \mathbf{I} & \mathbf{0} \\ \mathbf{0} & \mathbf{B}_x^{fc} \\ \boldsymbol{\Lambda}_N^{wc}\boldsymbol{\Pi}_i^{wc}, & -\mathbf{B}_x^{wc} \end{array}\right] \cdot \left[\begin{array}{c} \mathbf{v} \\ \boldsymbol{\eta} \end{array}\right] \geq \left[\begin{array}{c} \mathbf{1} \\ \mathbf{1} \\ \mathbf{0} \end{array}\right] \epsilon \quad \text{with } \epsilon \in \mathbb{R}^+$$

Define the rates of the transitions in $T_{fc} \cup T_{wc}$ as: $\lambda_j = [\mathbf{B}_x\boldsymbol{\eta}]_j / [\boldsymbol{\Pi}_i\mathbf{v}]_j$.

Proof. Consider (3.4) which is equivalent to λ-Ct. This can be expressed as three simultaneous equalities: $\boldsymbol{\Lambda}^{fc}\boldsymbol{\Pi}_i^{fc}\mathbf{v} = \mathbf{B}_x^{fc}\boldsymbol{\eta}$, $\boldsymbol{\Lambda}^{wc}\boldsymbol{\Pi}_i^{wc}\mathbf{v} = \mathbf{B}_x^{wc}\boldsymbol{\eta}$ and $\boldsymbol{\Lambda}^{nc}\boldsymbol{\Pi}_i^{nc}\mathbf{v} = \mathbf{B}_x^{nc}\boldsymbol{\eta}$.
Since $\boldsymbol{\Lambda}^{nc}$ is fixed, the third equality is equivalent to $[\boldsymbol{\Lambda}^{nc}\boldsymbol{\Pi}_i^{nc}, -\mathbf{B}_x^{nc}] \cdot [\mathbf{v}, \boldsymbol{\eta}]^T = \mathbf{0}$. Since $\boldsymbol{\Lambda}^{fc}$ can be freely defined, then, given $[\mathbf{v}, \boldsymbol{\eta}]$ with $\mathbf{v} > \mathbf{0}$, $\boldsymbol{\Lambda}^{fc}$ can always be computed by elements: $\lambda_j = [\mathbf{B}_x\boldsymbol{\eta}]_j / [\boldsymbol{\Pi}_i\mathbf{v}]_j$ $\forall t_j \in T_{fc}$. By using these expressions, the timing for transitions in $T_{fc} \cup T_{nc}$ can be computed. Now, the rates of the transitions in T_{wc} must fulfill $\lambda_j \leq \lambda_{N,j}$. This is equivalent to $\boldsymbol{\Lambda}^{wc}\boldsymbol{\Pi}_i^{wc}\mathbf{v} \leq \boldsymbol{\Lambda}_N^{wc}\boldsymbol{\Pi}_i^{wc}\mathbf{v}$ (where $\boldsymbol{\Lambda}_N^{wc}$ denotes the firing rate matrix of $\boldsymbol{\lambda}_N$ restricted to T_{wc}), since $\boldsymbol{\Pi}_i^{wc}\mathbf{v} > \mathbf{0}$. Therefore, given $[\mathbf{v}, \boldsymbol{\eta}]$ s.t. $\boldsymbol{\Lambda}_N^{wc}\boldsymbol{\Pi}_i^{wc}\mathbf{v} \geq \mathbf{B}_x^{wc}\boldsymbol{\eta}$, the rates of $\boldsymbol{\Lambda}^{wc}$ can be always computed by elements: $\lambda_j = [\mathbf{B}_x\boldsymbol{\eta}]_j / [\boldsymbol{\Pi}_i\mathbf{v}]_j$ $\forall t_j \in T_{wc}$. These conditions can be combined in order to obtain the given algorithm. ∎

Example 3.16. Consider the TCPN system of fig. 3.6(a) with nominal rates $\boldsymbol{\lambda}_N = [2, 1, 3, 3]^T$, $T_{nc} = \{t_1, t_2\}$ and $T_{wc} = \{t_3, t_4\}$. This net is not TEC, but it is consistent. There are two minimal siphons ($\Sigma_1 = \{p_1, p_3\}$ and $\Sigma_2 = \{p_2, p_4\}$) that can be emptied in the untimed model. This occurs at $\mathbf{m}_D^1 = [0, 6, 0, 0]^T$ and $\mathbf{m}_D^2 = [6, 0, 0, 0]^T$, which are related to configurations $\boldsymbol{\Pi}_1$ in which p_1 constraints t_1 and t_2, and $\boldsymbol{\Pi}_2$ in which p_2 constraints both, respectively. Since this net is not live as untimed, the goal is to compute a timing s.t. the timed system is timed-live.

Let us compute, for each configuration, a timing that enforces λ-consistency, by using the previous algorithm (as shown in Example 3.12, there do not exist a timing that simultaneously enforce λ-Ct at both configurations). For $\boldsymbol{\Pi}_1$, since $T_{nc} = \{t_1, t_2\}$, the first and second rows of $\boldsymbol{\Pi}_1$ and $\mathbf{B}_x^1$ correspond to $\boldsymbol{\Pi}_1^{nc}$ and $\mathbf{B}_x^{nc}$, respectively. The third and fourth rows of $\boldsymbol{\Pi}_1$ and $\mathbf{B}_x^1$ correspond to $\boldsymbol{\Pi}_1^{wc}$ and $\mathbf{B}_x^{wc}$. In this case, vectors $\mathbf{v}^T = [1.12, 1, 0.84, 1]$ and $\boldsymbol{\eta}^T = [0.56]$ were obtained (with $\epsilon = 0.1$). Now, λ_1 and λ_2 are fixed since $t_1, t_2 \in T_{nc}$, then, only t_3 and t_4 are computed in the second step of the algorithm. In this way, firing rates $\boldsymbol{\lambda}_A^1 = [2, 1, 0.5, 1.12]^T$ were obtained. Similarly, firing rates $\boldsymbol{\lambda}_A^2 = [2, 1, 1, 1.5384]^T$ were obtained for $\boldsymbol{\Pi}_2$. Thus, according to Theorem 3.28, the net system with the timing $\boldsymbol{\lambda}_A^1$ is timed-live while evolves inside $\Re_1$. On the other hand, the net system with the timing $\boldsymbol{\lambda}_A^2$ is timed-live while evolves inside $\Re_2$.

The problem of finding $\boldsymbol{\lambda}$ for enforcing λ-Cv is more difficult. This can be reduced by assuming $T_{fc} = \emptyset$ (for this, consider each $t \in T_{fc}$ as weakly controllable with a large nominal rate). Thus, $\mathbf{B}_z^i = [\mathbf{B}_z^{i,wc}, \mathbf{B}_z^{i,nc}]$. Denote as T_{nec}^i the set of transitions that are not *exc* at $\boldsymbol{\Pi}_i$. A timing (if it exists) that enforces λ-Cv at $\boldsymbol{\Pi}_i$, fulfilling the constraints imposed to the transitions, can be computed as follows:

Algorithm 3.5. Computation of a timing for inducing λ-Cv.

Compute vectors $\mathbf{v}$ and $\boldsymbol{\eta}$ that fulfill the following bilinear constraints:

$$\left[\begin{array}{c} \mathbf{w}^T\boldsymbol{\eta}^T \end{array}\right] \cdot \left[\begin{array}{c} \mathbf{C}^{nc}\mathbf{\Lambda}^{nc} \\ -\mathbf{B}_z^{i,nc} \end{array}\right] = \mathbf{0}$$
$$\left[\begin{array}{cc} \mathbf{w}^T & \boldsymbol{\eta}^T \end{array}\right] \cdot \left[\begin{array}{c} \mathbf{I} \\ \mathbf{0} \end{array}\right] \geq \mathbf{1}\cdot\epsilon \qquad \text{with } \epsilon \in \mathbb{R}^+$$

$$\begin{array}{ll} \forall t_j \in T_{wc}\cap T^i_{nec}: & \boldsymbol{\eta}^T\left[\mathbf{B}^i_z\right]^j\left(\left[\mathbf{C}\right]^j\right)^T\mathbf{w} \geq 0 \\ \forall t_j \in T_{wc}\cap T^i_{nec}: & \mathbf{w}^T\left[\mathbf{C}\mathbf{\Lambda}_N\right]^j\left(\left[\mathbf{C}\mathbf{\Lambda}_N\right]^j\right)^T\mathbf{w} \geq \boldsymbol{\eta}^T\left[\mathbf{B}^i_z\right]^j\left(\left[\mathbf{B}^i_z\right]^j\right)^T\boldsymbol{\eta} \\ \forall t_j \in T_{wc}/T^i_{nec}: & \mathbf{w}^T\left[\mathbf{C}\right]^j = 0 \end{array}$$

Define the rates of the transitions in $T_{wc}\cap T^i_{nec}$ as: $\lambda^{wc}_j = \left[\boldsymbol{\eta}^T\mathbf{B}_z\right]_j / \left[\mathbf{w}^T\mathbf{C}\right]_j$.
Define the rates of transitions in T_{wc}/T^i_{nec} can be defined arbitrarily but fulfilling $\lambda_{N,j} \geq \lambda_j \geq 0$.

Proof. Condition (3.3) can be expressed as: $\mathbf{w}^T\mathbf{C}^{wc}\mathbf{\Lambda}^{wc} = \boldsymbol{\eta}^T\mathbf{B}^{i,wc}_z$ and $\mathbf{w}^T\mathbf{C}^{nc}\mathbf{\Lambda}^{nc} = \boldsymbol{\eta}^T\mathbf{B}^{i,nc}_z$. Given $[\mathbf{w}^T, \boldsymbol{\eta}^T]$, $\mathbf{\Lambda}^{wc}$ can be computed by elements as: $\lambda_j = [\boldsymbol{\eta}^T\mathbf{B}^i_z]_j/[\mathbf{w}^T\mathbf{C}]_j$, whenever $[\mathbf{w}^T\mathbf{C}]_j \neq 0$, $\forall t_j \in T_{wc}$. Nevertheless, in order to obtain nonnegative rates, it is required either $[\boldsymbol{\eta}^T\mathbf{B}^i_z]_j > 0 \wedge [\mathbf{w}^T\mathbf{C}]_j > 0$, or $[\boldsymbol{\eta}^T\mathbf{B}^i_z]_j < 0 \wedge [\mathbf{w}^T\mathbf{C}]_j < 0$, or $[\boldsymbol{\eta}^T\mathbf{B}^i_z]^j = 0$, for all $t_j \in T_{wc}$. These constraints can be expressed as $\boldsymbol{\eta}^T[\mathbf{B}^i_z]^j([\mathbf{C}]^j)^T\mathbf{w} \geq 0$ and $\mathbf{w}^T[\mathbf{C}]^j = 0 \rightarrow \boldsymbol{\eta}^T[\mathbf{B}^i_z]^j = 0$. Moreover, in order to fulfill with $\lambda_j \leq \lambda_{N,j}$ $\forall t_j \in T_{wc}$, it is required that $|[\mathbf{w}^T\mathbf{C}\mathbf{\Lambda}_N]_j| \geq |[\boldsymbol{\eta}^T\mathbf{B}^i_z]_j|$ for all $t_j \in T_{wc}$. This last condition can be expressed as: $\mathbf{w}^T[\mathbf{C}\mathbf{\Lambda}_N]^j([\mathbf{C}\mathbf{\Lambda}_N]^j)^T\mathbf{w} \geq \boldsymbol{\eta}^T[\mathbf{B}^i_z]^j([\mathbf{B}^i_z]^j)^T\boldsymbol{\eta}$. Note that this last inequality also implies $\mathbf{w}^T[\mathbf{C}]^j = 0 \rightarrow \boldsymbol{\eta}^T[\mathbf{B}^i_z]^j = 0$. Furthermore, if t_j is a *exc* transition, then $[\mathbf{B}^i_z]^j = \mathbf{0}$, thus, all the previous conditions are fulfilled at this. Nevertheless, it is required that $\mathbf{w}^T[\mathbf{C}]^j = 0$ for each *exc* t_j. Combining these conditions, the current algorithm is obtained. ∎

Example 3.17. Consider the TEC model of fig. 3.7(b), with $T_{nc} = \{t_1, t_5\}$ and $T_{wc} = \{t_2, t_3, t_4, t_6\}$. Denote as $\mathbf{\Pi}_1$ the configuration in which p_1 constraints both t_1 and t_2, and $\mathbf{\Pi}_2$ the other. Consider the nominal rates as $\boldsymbol{\lambda}_N = [1, 3, 5, 5, 1, 3]$. This net model is consistent but not bounded, thus, the goal in this example is to obtain a timing for enforcing λ-conservativeness, and thus boundedness. Consider first the model at $\mathbf{\Pi}_1$. By using previous algorithm, a timing for making the system λ-Cv at $\mathbf{\Pi}_1$ can be computed. For this, a basis for the left annuler of $\mathbf{\Pi}_1$ is given by:

$$\mathbf{B}^1_z = \left[\begin{array}{cccccc} 1 & -1 & 0 & 0 & 0 & 0 \\ 0 & 0 & 0 & 0 & 1 & -1 \end{array}\right]$$

Since $T_{nc} = \{t_1, t_5\}$, the first and fifth columns of $\mathbf{C}$ and $\mathbf{B}^1_z$ correspond to $\mathbf{C}^{nc}$ and $\mathbf{B}^{1,nc}_z$. In this way, vectors $\mathbf{w}^T = [1, 1, 1, 1, 1]$ and $\boldsymbol{\eta}^T = [1, 0]$ were obtained (with $\epsilon = 0.1$). Now, λ_1 and λ_5 are fixed

since $T_{nc} = \{t_1, t_5\}$, while t_3 and t_4 are *exc*, so, λ_3 and λ_4 are settled with the nominal values. Only t_2 and t_6 are computed in the second step of the algorithm. In this way, the following rates, with which the model is λ-Cv at $\mathbf{\Pi}_1$, were obtained $\boldsymbol{\lambda}_A = [1, 0.5, 5, 5, 2.741]^T$. Furthermore, since the net is TEC, then the model with the same timing is also λ-Cv at $\mathbf{\Pi}_2$ (Proposition 3.19). Therefore, the TCPN with the rates $\boldsymbol{\lambda}_A$ is bounded.

These algorithms can also be used for enforcing λ-Ct and λ-Cv in more than one configuration with the same timing, just by adding the corresponding constraints at step 1. Nevertheless, it may occur the case that a single timing cannot enforce λ-Ct or λ-Cv in more than one region, as shown in the Example 3.12.

3.6.1 Control interpretation

A timing that makes a TCPN model bounded and/or live can be interpreted as a control action applied to a TCPN with different nominal rates. This will be explained through this subsection.

As introduced in Subsection 1.4.5, given a TCPN system having (nominal) rates $\boldsymbol{\lambda}_N$, a control action is defined as a modification of the flow through the controllable transitions. In this subsection a distinction between two kind of controllable transitions, named *weekly* and *freely* controllable, is made. The flow of a weakly controllable transition can only be reduced from its nominal value, while the flow of a freely controllable transition can be either increased or decreased with respect to this value. In this way, the control vector $\mathbf{u} \in \mathbb{R}^{|T|}$ must fulfill ($u_j = 0$ if $t_j \in T_{nc}$), ($u_j \geq 0$ if t_j is weakly controllable), and, in any case, ($\lambda_j \cdot enab_j(\tau) \geq u_j$), so the effective flow is nonnegative. The results introduced in this chapter can be interpreted as the solution of the following control problems:

Definition 3.33. Consider a TCPN system $\langle \mathcal{N}, \boldsymbol{\lambda}_N, \mathbf{m}_0 \rangle$.

P.I Suppose that the system is unbounded as untimed. Then, compute a control law $\mathbf{u}(\mathbf{m})$ s.t. the controlled timed system is bounded.

P.II Suppose that there exists a marking $\mathbf{m}_D \in Class(\mathbf{m}_0)$ reachable in the autonomous model, at which some transitions are dead. Then, compute a control law $\mathbf{u}(\mathbf{m})$ s.t. the marking $\mathbf{m}_D$ is avoided in the controlled timed system.

Furthermore, the control action must fulfill the required constraints:

- The effective flow must be non negative, i.e., $\forall t_j \ [\mathbf{\Lambda}_N \mathbf{\Pi}(\mathbf{m})\mathbf{m}]_j \geq u_j$.
- The effective flow of weakly controllable transitions can only be reduced from its nominal value, i.e., $u_j \geq 0 \ \forall t_j \in T_{wc}$.
- Control action cannot be applied to uncontrollable transitions, thus $u_j = 0 \ \forall t_j \in T_{nc}$.

Proposition 3.34. *Given a TCPN with nominal rates $\boldsymbol{\lambda}_N$ and the problem P.I. (resp. P.II), consider a timing $\boldsymbol{\lambda}_A$ s.t. the system $\langle \mathcal{N}, \boldsymbol{\lambda}_A, \mathbf{m}_0 \rangle$ is bounded (resp. $\mathbf{m}_D$ is avoided), at a given configuration, fulfilling $\lambda_{A,j} \geq 0 \ \forall t_j$, $\lambda_{A,j} = \lambda_{N,j} \ \forall t_j \in T_{nc}$ and $\lambda_{A,j} \leq \lambda_{N,j} \ \forall t_j \in T_{wc}$.*

Then, the nominal system $\langle \mathcal{N}, \boldsymbol{\lambda}_N, \mathbf{m}_0 \rangle$ will be bounded (resp. $\mathbf{m}_D$ will be avoided) under the control law:

$$\mathbf{u}_A = [\mathbf{\Lambda}_N - \mathbf{\Lambda}_A] \, \mathbf{\Pi}(\mathbf{m})\mathbf{m} \tag{3.10}$$

Proof. The flow of the system with the timing $\boldsymbol{\lambda}_A$ is equivalent to the flow of the system with the original nominal rates $\boldsymbol{\lambda}_N$ but under a control action $\mathbf{u}_A$, i.e., $\boldsymbol{\Lambda}_A\boldsymbol{\Pi}(\mathbf{m})\mathbf{m} = \boldsymbol{\Lambda}_N\boldsymbol{\Pi}(\mathbf{m})\mathbf{m} - \mathbf{u}_A$. On the other hand, note that, $\forall t_j \in T_{nc}$, since $\lambda_{A,j} = \lambda_{N,j}$ then $u_{A,j} = 0$. Similarly, $\forall t_j \in T_{wc}$, $u_{A,j} \geq 0$ because $\lambda_{N,j} \geq \lambda_{A,j}$. Furthermore, since $\lambda_{A,j} \geq 0\ \forall t_j$ then $[\boldsymbol{\Lambda}_N\boldsymbol{\Pi}(\mathbf{m})\mathbf{m}]_j \geq u_{A,j}$. Therefore, all the required constraints are fulfilled. ∎

Example 3.18. Consider the TCPN system of fig. 3.6(a) with the parameters described in Example 3.16. In that example, two firing rates, $\boldsymbol{\lambda}_A^1 = [2, 1, 0.5, 1.12]^T$ and $\boldsymbol{\lambda}_A^2 = [2, 1, 1, 1.5384]^T$, were obtained in order to induce λ-Ct in two deadlock configurations, $\boldsymbol{\Pi}_2$ and $\boldsymbol{\Pi}_2$. Thus, the original TCPN with the nominal rates is timed-live while the control law (3.10) is being applied, where $\boldsymbol{\lambda}_A = \boldsymbol{\lambda}_A^1$ while the system is in $\boldsymbol{\Pi}_1$, $\boldsymbol{\lambda}_A = \boldsymbol{\lambda}_A^2$ while the system is in $\boldsymbol{\Pi}_2$ and $\boldsymbol{\lambda}_A = \boldsymbol{\lambda}_N$ in other configurations.

Consider now the TEC model of fig. 3.7(b) with the parameters described in Example 3.17. There, the timing $\boldsymbol{\lambda}_A = [1, 0.5, 5, 5, 2.741]^T$ was computed in such a way that the system $\langle \mathcal{N}, \boldsymbol{\lambda}_A, \mathbf{m}_0 \rangle$ is bounded in all the configurations. Therefore, according to Proposition 3.34, the TCPN with the nominal rates $\boldsymbol{\lambda}_N$ is bounded while the control law (3.10) is being applied.

3.7 Conclusions on timing-dependent properties

The concepts of λ-Cv and λ-Ct were introduced in this chapter, in order to analyze the case where the timing $\boldsymbol{\lambda}$ allows a TCPN system to behave as conservative and/or consistent when the autonomous contPN do not exhibit these properties. The existence of a timing for enforcing such properties was analyzed first for the general case (Table 3.1) and later for particular net subclasses (Table 3.2).

Liveness of TCPN was studied in more detail, by splitting the problem into two different ones: the existence of non-live equilibrium markings, and the reachability of them. The first problem is an algebraic one that can be easily solved in polynomial time (LPP in Subsection 3.4.1). It was shown that non-live markings are strongly related to unmarked siphons (Proposition 3.24). Later, it was proved that λ-Ct is sufficient for timed-liveness (Theorem 3.28, assuming $\mathbf{m}_0 > \mathbf{0}$), while the system evolves inside the corresponding region. From a dynamic systems' perspective, λ-Ct implies that each minimal siphon in the net is λ-Cv, while this property means the existence of proper state invariants, i.e., the system evolves on a manifold on which the minimal siphons cannot be emptied, thus liveness follows (Subsection 3.5.1). By using some classical results on stability in linear systems, a couple of sufficient conditions for avoiding non-live equilibrium markings, and sufficient conditions for reaching them, have been introduced (Propositions 3.30 and 3.31). Some illustrative examples were presented in order to interpret the obtained results at the net level.

Finally, algorithms, devoted to compute $\boldsymbol{\lambda}$ s.t. the TCPN is λ-Ct or λ-Cv, enforcing thus liveness and boundedness, respectively, were provided.

Chapter 4

Controllability

4.1 Introduction

Timed continuous Petri nets are essentially continuous-state systems (in fact, they are piecewise-linear hybrid systems, but the discrete state or mode is implicit on the continuous state). In this way, regarding control, it seems natural to consider two different approaches: 1) the extension of control techniques used in discrete PN's, as the supervisory-control theory (for instance, [Holloway et al., 1997b, Iordache and Antsaklis, 2006]); and 2) the application of control techniques developed in the Control Theory for continuous-state systems. Most frequently, the control objective in the first approach is to meet some safety specifications, like avoiding *forbidden* states (deadlocks, mutual exclusions or imposing boundedness), by means of disabling transitions (events) at particular discrete states. A particular objective of the second approach consists in driving the system, by means of a (usually) continuous control action, towards a desired steady state (stabilization at a set-point), or state trajectory (tracking, see for instance [Chen, 1984]).

Through this dissertation, the second approach is considered. In particular, the control objective consists in driving a TCPN system towards a desired target marking (the marking of the TCPN represents the *state* of the system and approximates the average marking in the original discrete PN), most frequently a potential steady state. As already explained in Subsection 1.4.5, the only control action that is allowed in continuous Petri nets is the reduction of the *flow* or *instantaneous throughput* at certain transitions, named *controllable* (equivalently, a reduction of the average frequency of occurrence of certain events in the original PN). Increasing such flow (frequency of occurrence) is not allowed since the systems that are frequently modeled evolve according to a consumption/production logic (e.g., manufacturing systems, supply chains, traffic systems) in which the events (machines for instance) have nominal speeds that cannot be increased. This control problem has been addressed by different authors in the field of TCPNs, proposing control techniques ranging from fuzzy logic control [Hennequin et al., 1999], gradient-based controllers [Lefebvre et al., 2007], model predictive control [Mahulea et al., 2008a], feedback control synthesis based on linear matrix inequalities [Kara et al., 2009], etc. A discussion on control techniques for TCPNs is provided in Chapter 5.

Assuming that the continuous model approximates the discrete one, enforcing a desired target marking in the continuous PN is analogous to enforcing an *average marking* in the original discrete model, which may be interesting in several kinds of systems. For instance, this idea has been illustrated for

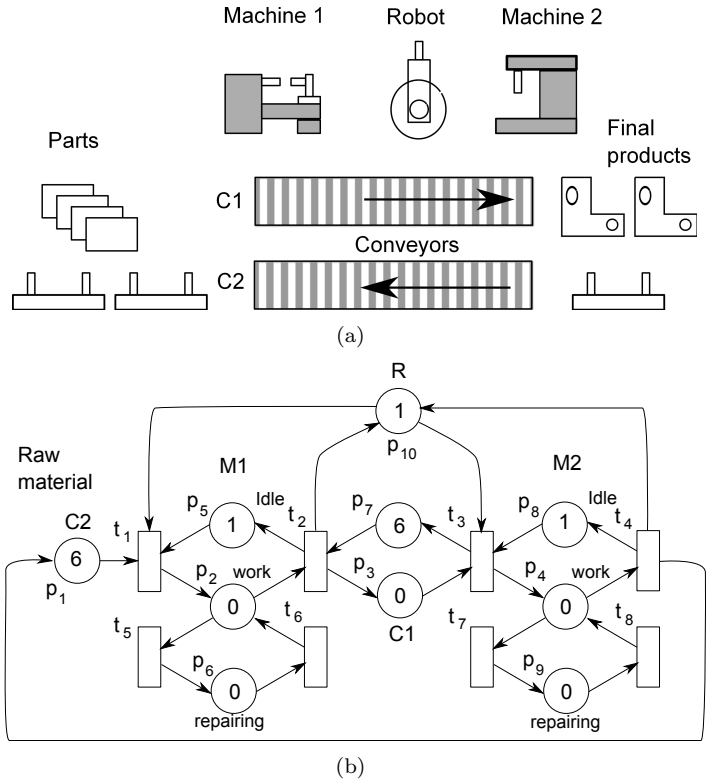

Fig. 4.1: (a) Manufacturing cell, and (b) its Petri net model.

deterministically timed models of manufacturing lines [Amrah et al., 1997] and for the stock-level control of a stochastically timed automotive assembly line model [Vázquez and Silva, 2009b] (explained in detail in Chapter 6).

In TCPNs it is frequently assumed that the target marking is reachable, however, this may be difficult to verify. In fact, it is known that TCPN systems are most frequently not *controllable* in the classical continuous-state sense, i.e., not any marking can be reached from any other [Mahulea et al., 2008b]. For this reason, a deeper understanding on the controllability of TCPNs is required.

Let us illustrate, with an example, the controllability notion that will be studied through this chapter.

Example 4.1. Consider the manufacturing cell of fig. 4.1(a) and its PN model depicted on fig. 4.1(b). This is composed of two process machines M1 and M2, a robot R that loads and unloads both machines, and two conveyors, one intermediate for transferring partially processed material from M1 to M2 (denoted as C1), and the other (C2) for taking back the empty pallets from M2 to M1. Let us consider the corresponding TCPN model with certain rates for the transitions (the average frequency with which the events naturally occur if they are enabled). Let us assume that the only allowed control action consists in reducing the speed (frequency) with which the robot unload the material from M2, i.e., transition t_4 is the only controllable one. Observe that the speed of unloading material cannot be increased w.r.t. its nominal value. Suppose that the most efficient operation is obtained if C1 has an *average* number of pieces of 1.8 (equivalently, if $\mathbf{m}[p_3] = 1.8$ in the TCPN). Such stationary operating point (a forced equilibrium point in the state space) corresponds to a particular target marking, which

can be reached from the initial state by delaying the unloading of M2 (i.e., by reducing the firing speed of t_4 in a certain degree). Now, suppose that, after some time, it is decided to set the operating point in such a way that the average number of pieces in C1 is one, i.e., $\mathbf{m}[p_3] = 1$ in the TCPN. It can be proved that, by reducing the speed at t_4, it is not possible to drive the system towards such a steady state from the current one (from the marking in which $\mathbf{m}[p_3] = 1.8$). In this way, this system exhibits a lack of *controllability* in the classical continuous-state sense.

From a continuous-state systems perspective, a TCPN system is a piecewise-linear one, in which the control actions must be *nonnegative* (because it is allowed to reduce, but not to increase, the activity of some of the events in the system) and *upper bounded* by a piecewise-linear function of the state (because the maximum amount of reduction is limited by the amount of existing activity), i.e., the state equation has the form:

$$\dot{\mathbf{m}} = \mathbf{A}_i\mathbf{m} + \mathbf{B}\mathbf{u}$$

where $\mathbf{u}$ is subject to $\mathbf{0} \leq \mathbf{u} \leq \mathbf{L}_i\mathbf{m}$ and $i \in \{1, ..., r\}$ depends on the value of $\mathbf{m}$, the state

The reachability and controllability problems for such kind of continuous-state systems is not trivial (for instance, as pointed out by [Bemporad et al., 1999]). Despite the fact that a lot of works can be found in the literature addressing the controllability problem for hybrid systems, they mostly focus on very particular classes, due to the complexity involved in the analysis. For instance, for particular cases of switching systems [Ezzine and Haddad, 1989, Sun and Zheng, 2001, Xie and Wang, 2002], for linear complementarity systems [Camlibel, 2007], for planar (bi-dimensional) bimodal piecewise linear systems [Xu and Xie, 2005] and for general piecewise-affine systems [Habets and van Schuppen, 2001]. A more detailed discussion is provided in Section 4.3. Nevertheless, in the general case (when there are transitions-events that cannot be controlled), TCPN systems are *frequently not controllable*. Moreover, the non negativeness of the input, required by TCPNs, adds complexity to the controllability analysis (e.g., for linear systems, the controllability with nonnegative inputs depends on the eigen-structure of the state matrix [Brammer, 1972]). Furthermore, the existence of marking conservation laws in these systems (e.g., $\mathbf{y}^T\mathbf{m} = constant$) leads to the existence of *state invariants* (under any control action), destroying in this way the controllability property even for the case in which all the transitions-events can be controlled [Mahulea et al., 2008b].

By taking advantage of the particular structure of TCPN systems, in [Jiménez et al., 2005] it was proved that for the particular subclass of Join-Free TCPNs there exists an interesting set of markings in which the system exhibits the controllability property, i.e., a TCPN can be "locally" controllable. Such idea will be extended here in order to consider any TCPN, by studying the controllability *over* sets of interesting markings (in particular, over equilibrium markings, i.e., "potential steady states" where the system can be stabilized).

The *reachability* and *controllability* properties are studied through this chapter for general TCPN systems. Firstly, the notion of controllability used in this work is provided and compared with other controllability definitions introduced in the literature for related hybrid systems. Later, the controllability is analyzed for the case in which all the transitions are controllable, providing a polynomial time characterization. Finally, the controllability is studied for systems with uncontrollable transitions.

4.2 State invariant and equilibrium sets

In this section, a few useful concepts will be introduced regarding equilibrium markings.

Given a P-flow $\mathbf{y}$, for any reachable marking $\mathbf{m}$, $\mathbf{y}^T\mathbf{m} = \mathbf{y}^T\mathbf{m}_0$. Then, whenever a TCPN system has *P-flows*, linear dependencies between marking variables appear, introducing *state invariants* (so, under any control action, the evolution of the system is restricted to the manifold where $\mathbf{y}^T\mathbf{m} = \mathbf{y}^T\mathbf{m}_0$). Therefore, systems with P-flows are not controllable in the classical sense [Mahulea et al., 2008b]. Nevertheless, we are interested in the study of controllability "over" this invariant, which happens to be the set $Class(\mathbf{m}_0)$ defined in Subsection 1.4.3.

Equilibrium markings represent the "stationary operating points" of the modeled system. For this reason, the study of controllability over sets of these markings is particularly interesting, since controllers are frequently designed in order to drive the system towards a desired stationary operating point. The following definitions will be useful for the study of controllability for systems with uncontrollable transitions.

Definition 4.1. The set of *equilibrium markings* is defined as:

$$\mathbb{E} = \{\mathbf{m} \in Class(\mathbf{m}_0) | \exists \mathbf{u} \text{ s.t. } \mathbf{\Lambda\Pi}(\mathbf{m})\mathbf{m} \geq \mathbf{u} \geq \mathbf{0},\ \mathbf{u}[T_{nc}] = \mathbf{0} \text{ and } \mathbf{C}(\mathbf{\Lambda\Pi}(\mathbf{m})\mathbf{m} - \mathbf{u}) = \mathbf{0}\}$$

The set of equilibrium markings in the i-th region is defined as:

$$E_i = \{\mathbf{m} | \mathbf{m} \in \mathbb{E} \cap \Re_i\}$$

Note that, if all the transitions are controllable then $\mathbb{E} = Class(\mathbf{m}_0)$ (by defining $\mathbf{u} = \mathbf{\Lambda\Pi}(\mathbf{m})\mathbf{m}$). By definition, sets E_i are convex. A useful matricial representation of a given set E_i is introduced next:

Definition 4.2. A full column rank matrix $\mathbf{G}_i$ is called *Generator* of $E_i \neq \emptyset$ if it fulfills:

a) $\forall \mathbf{m}_1, \mathbf{m}_2 \in E_i$, the vector $(\mathbf{m}_1 - \mathbf{m}_2)$ is in the range of $\mathbf{G}_i$ (it is a linear combination of the columns of $\mathbf{G}_i$).

b) $\mathbf{G}_i$ is minimal (if one of its columns is removed then **a** is false).

A generator $\mathbf{G}_i$ is a kind of basis of $E_i \neq \emptyset$ (formally speaking, it is not a basis because E_i is not a vector space). Observe that, by definition, the columns of $\mathbf{G}_i$ are linear combinations of those of $\mathbf{C}$, the incidence matrix, since the span of $\mathbf{G}_i$ is a subset of the span of $\mathbf{C}$. In the following, an algorithm for computing this matrix, whose proof is given in the Appendix C, is provided.

Algorithm 4.1. Computation of a generator $\mathbf{G}_i$.

For each $t_j \in T_c = \{t_{c_1}, ..., t_{c_{|T_c|}}\}$ do

Compute a solution $\mathbf{d}_j$ for:

$$\begin{bmatrix} \mathbf{C\Lambda\Pi}_i \\ \mathbf{B}_y^T \end{bmatrix} \mathbf{d}_j = \begin{bmatrix} [\mathbf{C}]^j \\ \mathbf{0} \end{bmatrix} \tag{4.1}$$

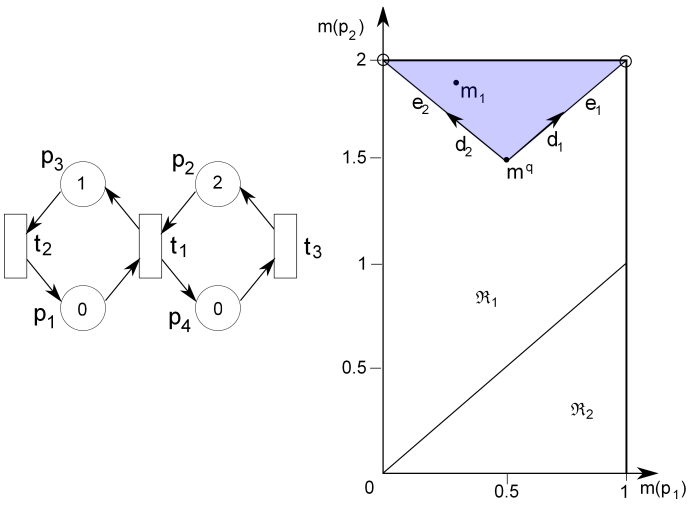

Fig. 4.2: A TCPN system with $\lambda = [1,1,1]^T$ and $T_c = \{t_1, t_2\}$. Since there are two P-semiflows, which impose the marking invariants $\mathbf{m}[p_1] + \mathbf{m}[p_3] = 1$ and $\mathbf{m}[p_2] + \mathbf{m}[p_3] = 2$, the markings at p_1 and p_2 are enough to represent $Class(\mathbf{m}_0)$. There are two different regions. The equilibrium set is the shadowed area.

If there exists such a solution $\mathbf{d}_j$ **then** add it as a column of $\mathbf{G}_i$

end for

Compute a basis $\mathbf{D}$ for the right annuler of

$$\begin{bmatrix} \mathbf{C}\boldsymbol{\Lambda}\boldsymbol{\Pi}_i \\ \mathbf{B}_y^T \end{bmatrix} \mathbf{D} = \mathbf{0} \tag{4.2}$$

If $\mathbf{D} \neq \mathbf{0}$ then add the columns of $\mathbf{D}$ to $\mathbf{G}_i$ (i.e., $\mathbf{G}_i$ has the form $[\mathbf{d}_{c_1}, ..., \mathbf{d}_{c_{|T_c|}}, \mathbf{D}]$).

If $\mathbf{G}_i$ does not have full column rank, **then** remove linearly dependent columns until obtaining a full column rank matrix.

If the only solution for (4.2) is $\mathbf{D} = \mathbf{0}$ then $[(\mathbf{C}\boldsymbol{\Lambda}\boldsymbol{\Pi}_i)^T, \mathbf{B}_y]^T$ has full column rank. In such case, for each $t_j \in T_c$ there exists $\mathbf{d}_j$ solution for (4.1). This algebraic property is interesting for controllability, as will be shown in Subsection 4.5.3.

The following example illustrates some definitions given in this section.

Example 4.2. Consider the system of fig. 4.2 with $\boldsymbol{\Lambda} = \mathbf{I}$ and $T_c = \{t_1, t_2\}$. Fig. 4.2 shows the projection of $Class(\mathbf{m}_0)$ on the plane defined by the marking at places p_1 and p_2. There are two configurations in this system: $\mathcal{C}_1 = \{(p_1, t_1), (p_3, t_2), (p_4, t_3)\}$ and $\mathcal{C}_2 = \{(p_2, t_1), (p_3, t_2), (p_4, t_3)\}$. $\Re_1$ and $\Re_2$ are the regions related to $\mathcal{C}_1$ and $\mathcal{C}_2$, respectively. The shadowed triangle with all its edges and vertices corresponds to E_1. Actually, in this example $E_1 = \mathbb{E}$ and $E_2 = \emptyset$. A generator of E_1 is computed by using Algorithm 4.1 as (in this case, a right annuler $\mathbf{D}$ in (4.2) does not exist):

$$\mathbf{G}_1 = \begin{bmatrix} \mathbf{d}_1 & \mathbf{d}_2 \end{bmatrix} = \begin{bmatrix} 0.5, & 0.5, & -0.5, & -0.5 \\ -0.5, & 0.5, & 0.5, & -0.5 \end{bmatrix}^T$$

The restriction of vectors $\mathbf{d}_1$ and $\mathbf{d}_2$ to the places p_1 and p_2 is also drawn in fig. 4.2.

4.3 Controllability definition

The classical linear systems controllability definition (recalled in Subsection 1.6.2) cannot be applied to TCPN systems because the set of reachable markings never compose a vector space (all reachable markings are nonnegative and belong to $Class(\mathbf{m}_0)$). Moreover, in TCPN systems the input must be s.b., i.e., $\mathbf{0} \leq \mathbf{u} \leq \mathbf{\Lambda\Pi}(\mathbf{m})\mathbf{m}$, $u_i = 0\, \forall t_i \in T_{nc}$. Therefore, the following reformulation of the classical controllability definition is proposed.

Definition 4.3. The TCPN system $\langle \mathcal{N}, \boldsymbol{\lambda}, \mathbf{m}_0 \rangle$ *is controllable with bounded input* (BIC) *over* $S \subseteq Class(\mathbf{m}_0)$ if for any two markings $\mathbf{m}_1, \mathbf{m}_2 \in S$ there exists an input $\mathbf{u}$ that transfers the system from $\mathbf{m}_1$ to $\mathbf{m}_2$ in finite or infinite time, and it is suitably bounded, i.e., $\mathbf{0} \leq \mathbf{u} \leq \mathbf{\Lambda\Pi}(\mathbf{m})\mathbf{m}$, and $\forall t_i \in T_{nc}$ $u_i = 0$ along the marking trajectory.

It is important to remark that controllability depends on the structure and timing of the system, independently of the particular initial marking.

From the control theory perspective, the TCPN model under ISS is a hybrid system. In particular, it is a *piecewise linear* system with nonnegative and dynamically upper bounded (constrained) input.

In the literature, a lot of results can be found on the controllability analysis for particular classes of hybrid systems. Nevertheless, the peculiarities of TCPN systems, like the particular constraints on the input and the state invariants, are not usually considered. For instance, in [Sun and Zheng, 2001] and [Xie and Wang, 2002] sufficient and necessary conditions for controllability of 3-dimensional switched linear systems and single switching sequence systems were provided, respectively, but always under the assumption of unconstrained inputs. In [Ezzine and Haddad, 1989] it was studied the controllability for switching linear systems with a deterministic sequence. The classical work of Brammer [Brammer, 1972], regarding to controllability in linear systems with bounded inputs, has been extended in [Camlibel, 2007] to a particular class of piecewise linear systems known as *linear complementarity systems* (dynamical extensions of the linear complementarity problem that can model interesting physical systems), but they are not close to general TCPNs.

Authors in [Bemporad et al., 1999] and [Habets and van Schuppen, 2001] studied the controllability for *Piecewise Affine Systems* (PWA), which is a more general class of hybrid system that includes the TCPNs under ISS. The controllability of planar (bi-dimensional) bimodal piecewise linear systems was studied in [Xu and Xie, 2005]. This last work is very particular and the analysis is based on the study of the entries of the matrices of the system, which is an approach difficult to generalize for TCPNs having more than two places. In [Bemporad et al., 1999] the controllability for PWA systems was addressed as the capability of the system for reaching any state of the final-set from any initial state contained in the initial-set. There, it was shown that observability and controllability properties for these systems can be very complex and counterintuitive. Furthermore, controllability tests, based on Mixed-Integer Linear Programming, were provided. Nevertheless, they exhibit an exponential complexity in the reachability-time, then, its application becomes particularly prohibitive for TCPNs, where it is frequent to find systems with a significant number of state variables.

In [Habets and van Schuppen, 2001] a sufficient condition for "reachability"(that is also extended to controllability) was provided for PWA systems. There, it is considered that the continuous subsystem

evolves inside polytopes (convex sets of states), each one related to a discrete state. Recalling from there, any continuous state and any discrete state can be reached if: 1) for each polytope, any continuous state is reachable from any other through a trajectory inside the polytope; and 2) any discrete state is reachable. In TCPNs those conditions would mean: 1) for each region, any marking is reachable from any other through a trajectory inside the region, and 2) a marking inside each region is reachable. Nevertheless, this notion of "reachability"is too strong for TCPNs. In fact, TCPN systems with uncontrollable transitions are frequently not controllable over full regions, and subsets of these must be considered. Even in such case, considering convex subsets of regions as the polytopes, while in [Habets and van Schuppen, 2001] it is required that the system must remain inside the given subset (polytope), that is not required in our controllability notion, allowing thus more trajectories.

Regarding continuous Petri nets, controllability was firstly studied in [Amer-Yahia et al., 1996] for Join-Free nets, pointing out that the classical rank condition is not sufficient for controllability (which will be explained in Subsection 4.5.1). From a different perspective, in [Jiménez et al., 2005] the controllability for Join-Free TCPNs under ISS with uncontrollable transitions was studied. There it was characterized an interesting invariant set, named Controllability Space (CS), in which the system exhibits the controllability property. Nevertheless, since this CS set is marking dependent, the results of [Jiménez et al., 2005] become difficult to extend to general subclasses of nets, where the existence of several regions makes the general reachability problem untractable.

In this way, the introduction of the controllability definition provided here is motivated by the need of a precise notion of controllability that considers the peculiarities of TCPNs and a set-point control objective. Let us remark that the forthcoming analysis is not restricted to particular subclasses of PN's and it is based on a blend of the classical techniques from state-continuous control theory and the general Petri nets one.

4.4 Controllability if all the transitions are controllable

In this section, the reachability and controllability properties are studied assuming that all the transitions are controllable. The results introduce necessary and sufficient conditions for reachability and controllability over $Class(\mathbf{m}_0)$.

Proposition 4.4. *Let $\langle \mathcal{N}, \boldsymbol{\lambda}, \mathbf{m}_0 \rangle$ be a TCPN system in which $T_c = T$. A marking $\mathbf{m}_1 \in Class(\mathbf{m}_0)$ is reachable from $\mathbf{m}_0 \in int\{Class(\mathbf{m}_0)\}$ iff $\exists \boldsymbol{\sigma} \geq \mathbf{0}$ such that $\mathbf{C}\boldsymbol{\sigma} = (\mathbf{m}_1 - \mathbf{m}_0)$.*

Proof. Let us prove first the sufficiency. Consider $\boldsymbol{\sigma} \geq \mathbf{0}$ such that $\mathbf{C}\boldsymbol{\sigma} = (\mathbf{m}_1 - \mathbf{m}_0)$ with $\mathbf{m}_1 \in Class(\mathbf{m}_0)$. If $\mathbf{m} \in int\{Class(\mathbf{m}_0)\}$ then $\boldsymbol{\Lambda\Pi}(\mathbf{m})\mathbf{m} > \mathbf{0}$. In this case, since all the transitions are controllable, it is always possible to compute the input $\mathbf{u} = (\boldsymbol{\Lambda\Pi}(\mathbf{m})\mathbf{m} - \alpha\boldsymbol{\sigma})$, where $\alpha > 0$ is a small enough scalar. This input is s.b. since $\alpha\boldsymbol{\sigma} \geq \mathbf{0}$ implies $\mathbf{u} \leq \boldsymbol{\Lambda\Pi}(\mathbf{m})\mathbf{m}$, moreover, $\mathbf{u} \geq \mathbf{0}$ for a small enough α. Substituting $\alpha\boldsymbol{\sigma} = (\boldsymbol{\Lambda\Pi}(\mathbf{m})\mathbf{m} - \mathbf{u})$ into the state equation (1.6) we obtain $\dot{\mathbf{m}} = \mathbf{C}\alpha\boldsymbol{\sigma}$. Thus, according to the hypothesis, $\dot{\mathbf{m}} = \alpha(\mathbf{m}_1 - \mathbf{m}_0)$. Therefore, it is always possible to direct the field vector in all $\mathbf{m} \in int\{Class(\mathbf{m}_0)\}$, including the line connecting $\mathbf{m}_0$ with $\mathbf{m}_1$ denoted as $L = \{\mathbf{m} | \mathbf{m} = \beta\mathbf{m}_0 + (1-\beta)\mathbf{m}_1\}$, to the direction $(\mathbf{m}_1 - \mathbf{m}_0)$, and thus to reach $\mathbf{m}_1$ through a trajectory in L.

For the necessity, suppose that $\mathbf{m}_1$ is reachable, at time τ_1, from $\mathbf{m}_0$ by means of a s.b. input $\mathbf{u}(\tau)$.

Then, integrating the state equation, it is obtained:

$$\int_0^{\tau_1} \dot{\mathbf{m}}(\tau)d\tau = (\mathbf{m}_1 - \mathbf{m}_0) = \mathbf{C} \cdot \int_0^{\tau_1} (\mathbf{\Lambda\Pi}(\mathbf{m}(\tau))\mathbf{m}(\tau) - \mathbf{u}(\tau))d\tau$$

Now, since $\mathbf{u}(\tau)$ is s.b., then $(\mathbf{\Lambda\Pi}(\mathbf{m}(\tau))\mathbf{m}(\tau) - \mathbf{u}(\tau)) \geq \mathbf{0}$ for all τ. Thus, defining $\boldsymbol{\sigma} = \int_0^{\tau_1}(\mathbf{\Lambda\Pi}(\mathbf{m}(\tau))\mathbf{m}(\tau) - \mathbf{u}(\tau))$, it is obtained that $(\mathbf{m}_1 - \mathbf{m}_0) = \mathbf{C}\boldsymbol{\sigma}$ and $\boldsymbol{\sigma} \geq \mathbf{0}$. ∎

Lemma 4.5. *Let $\langle \mathcal{N}, \boldsymbol{\lambda}, \mathbf{m}_0 \rangle$ be a TCPN system in which all the transitions are controllable. The system $\langle \mathcal{N}, \boldsymbol{\lambda}, \mathbf{m}_0 \rangle$ is BIC over $int\{Class(\mathbf{m}_0)\}$ iff the net is* consistent.

Proof. Consider two markings $\mathbf{m}_1 \in int\{Class(\mathbf{m}_0)\}$ and $\mathbf{m}_2 \in Class(\mathbf{m}_0)$. Since both markings belong to $Class(\mathbf{m}_0)$, then there exists $\mathbf{v}$ s.t. $\mathbf{Cv} = (\mathbf{m}_2 - \mathbf{m}_1)$. Furthermore, since the net is consistent, then $\exists \mathbf{x} > \mathbf{0}$ s.t. $\mathbf{Cx} = \mathbf{0}$. In this way, for a large enough scalar $\beta > 0$, the vector $\boldsymbol{\sigma} = \mathbf{v} + \beta\mathbf{x}$ fulfills $\boldsymbol{\sigma} > \mathbf{0}$. Then, according to Proposition 4.4, $\mathbf{m}_2$ is reachable from $\mathbf{m}_1$. Therefore, if the net is consistent then any marking in $Class(\mathbf{m}_0)$ is reachable from any other in $int\{Class(\mathbf{m}_0)\}$.

Now, for the other implication, consider any vector $\mathbf{d} \in span(\mathbf{C})$ and a marking $\mathbf{m}_1 \in int\{Class(\mathbf{m}_0)\}$. Then, there exists a scalar $\beta > 0$ such that $\mathbf{m}_1 + \beta\mathbf{d} \geq \mathbf{0}$. Let $\mathbf{m}_2 = \mathbf{m}_1 + \beta\mathbf{d}$, then $\mathbf{m}_2 \in Class(\mathbf{m}_0)$. Since the system is BIC over the interior of $Class(\mathbf{m}_0)$, $\mathbf{m}_2$ is a particular solution of the fundamental equation, so $(\mathbf{m}_2 - \mathbf{m}_1) = \beta\mathbf{d} = \mathbf{C}\boldsymbol{\sigma}$, where $\boldsymbol{\sigma} \geq \mathbf{0}$. Therefore, $\forall \mathbf{d} \in span(\mathbf{C}), \exists \boldsymbol{\sigma}$ such that $\mathbf{C}\boldsymbol{\sigma} = \mathbf{d}$. Finally, it can be proved that this property implies that $\exists \mathbf{x} > \mathbf{0}$ such that $\mathbf{Cx} = \mathbf{0}$, i.e., the net is consistent. ∎

Remark 4.6. The reachability and controllability over $int\{Class(\mathbf{m}_0)\}$, when all the transitions are controllable, depends only on the structure of the net and can be verified in polynomial time. The timing $\boldsymbol{\lambda}$ only affects the time required for reaching the desired markings.

Next, the previous result regarding the controllability over $int\{Class(\mathbf{m}_0)\}$ is extended to the complete $Class(\mathbf{m}_0)$, by including the border markings of this set in the analysis.

Theorem 4.7. *Let $\langle \mathcal{N}, \boldsymbol{\lambda}, \mathbf{m}_0 \rangle$ be a TCPN system in which all the transitions are controllable. The system $\langle \mathcal{N}, \boldsymbol{\lambda}, \mathbf{m}_0 \rangle$ is BIC over $Class(\mathbf{m}_0)$ iff the net is* consistent *and there do not exist* empty siphons *at any marking in $Class(\mathbf{m}_0)$.*

Proof. First, according to lemma 4.5, consistency is sufficient and necessary for controllability in the interior of $Class(\mathbf{m}_0)$. Furthermore, consistency also implies that any marking at the border of $Class(\mathbf{m}_0)$ is reachable from any other in the interior. Then, the proof is completed if we demonstrate that, a marking $\mathbf{m}_f \in int\{Class(\mathbf{m}_0)\}$ is reachable from a marking $\mathbf{m}_0$ at the border iff there are not empty siphons at $\mathbf{m}_0$.

If there exists an empty siphon at $\mathbf{m}_0$ then $\nexists \mathbf{u}$ that transfers the system to some $\mathbf{m}_f > \mathbf{0}$, because empty siphons can never gain marks. For the other implication, consider an input $\mathbf{u}$ such that for any enabled transition t_j, $u_j < [\mathbf{\Lambda\Pi}(\mathbf{m})\mathbf{m}]_j$. Suppose that such input is being applied from $\mathbf{m}_0$. If there exists a place p_i that remains unmarked for all time, then for each input transition t_j to this place, there exists an input place p_k to t_j, which remains unmarked for all time. Repeating this reasoning, it can be seen that p_i remains unmarked for all time iff it belongs to an unmarked siphon, so, if there are not

empty siphons at $\mathbf{m}_0$ then p_i will eventually get marked, and the same applies for all empty places (i.e., such input transfers the system to some $\mathbf{m}_f > \mathbf{0}$). ∎

Remark 4.8. The controllability of a TCPN over $Class(\mathbf{m}_0)$, when all the transitions are controllable, depends on the structure of the net, but it is independent of the timing and initial marking (this property does not depend on the particular value of $\mathbf{m}_0$, since it holds for any marking inside $Class(\mathbf{m}_0)$). Furthermore, the BIC property can be verified in polynomial time by using the following algorithm:

Algorithm 4.2. Controllability when all the transitions are controllable.

Solve $\mathbf{C} \cdot \mathbf{x} = \mathbf{0}$, s.t. $\mathbf{x} > \mathbf{0}$
If there is not solution for $\mathbf{x}$ **then** the system is not BIC over $Class(\mathbf{m}_0)$
else
Solve the following inequalities for $\mathbf{m}$ and $\mathbf{y}$:

$$\begin{array}{ll} \mathbf{m} \geq \mathbf{0} & \\ \mathbf{B}_y^T \mathbf{m} = \mathbf{B}_y^T \mathbf{m}_0 & \{\mathbf{m} \text{ belongs to } Class\{\mathbf{m}_0\}\} \\ \mathbf{y} \geq \mathbf{0} & \\ \mathbf{y}^T \mathbf{C}' \leq \mathbf{0} & \{||\mathbf{y}|| \text{is a siphon}\} \\ \mathbf{y}^T \mathbf{m} = \mathbf{0} & \{\text{the siphon is empty at } \mathbf{m}\} \end{array} \tag{4.3}$$

where $\mathbf{C}' = \mathbf{Post} - \mathbf{Pre}'$ with $\mathbf{Pre}'$ defined by elements as:
$\forall t \in T$, $\forall p \in^\bullet t\, \mathbf{Pre}'(p,t) \geq \mathbf{Pre}(p,t) \cdot \sum_{p' \in t^\bullet} \mathbf{Post}(p',t)$.
If there is a solution **then** the system is not BIC over $Class(\mathbf{m}_0)$,
else the system is BIC over $Class(\mathbf{m}_0)$.

Proof of Algorithm 4.2: First, consistency, which is necessary for BIC (Theorem 4.7), is equivalent to $\exists \mathbf{x} > \mathbf{0}$ s.t. $\mathbf{Cx} = \mathbf{0}$, i.e., the first part of Algorithm 4.2. Next, according to the results introduced in [Ezpeleta et al., 1993] (Proposition 3.4 and Subsection 3.2), given a vector $\mathbf{y}$, $||\mathbf{y}||$ is a siphon iff $\mathbf{y} \geq \mathbf{0}$ and $\mathbf{y}^T\mathbf{C}' \leq \mathbf{0}$, where $\mathbf{C}' = \mathbf{Post} - \mathbf{Pre}'$ with $\mathbf{Pre}'$ defined by elements as: $\forall t \in T$, $\forall p \in^\bullet t$ $\mathbf{Pre}'(p,t) \geq \mathbf{Pre}(p,t) \cdot \sum_{p' \in t^\bullet} \mathbf{Post}(p',t)$. Thus the condition of the Theorem 4.7: $\exists \mathbf{m} \in Class(\mathbf{m}_0)$ and a siphon Σ s.t. $\mathbf{m}(\Sigma) = \mathbf{0}$, is equivalent to $\exists \mathbf{m}, \mathbf{y}$ that fulfill $\mathbf{m} \geq \mathbf{0}$, $\mathbf{B}_y^T\mathbf{m} = \mathbf{B}_y^T\mathbf{m}_0$ (i.e., $\mathbf{m} \in Class(\mathbf{m}_0)$), $\mathbf{y} \geq \mathbf{0}$, $\mathbf{y}^T\mathbf{C}' \leq \mathbf{0}$ (i.e., $||\mathbf{y}||$ is a siphon) and $\mathbf{y}^T\mathbf{m} = \mathbf{0}$ (i.e., the siphon is empty at $\mathbf{m}$), i.e., the inequalities (4.3). Note that, the existence of solutions $\mathbf{m}$ and $\mathbf{y}$ can be decided in polynomial time. ∎

The following example illustrates the application of previous results.

Example 4.3. Consider the TCPN systems of fig. 4.3, where $\mathbf{m}_0 = [2,3,1,1]^T$, $\mathbf{m}_1 = [1,3,2,1]^T$ and $\mathbf{m}_2 = [2,1,1,3]^T$. For the system in fig. 4.3(a), $\exists \boldsymbol{\sigma} \geq \mathbf{0}$ such that $\mathbf{C}\boldsymbol{\sigma} = (\mathbf{m}_1 - \mathbf{m}_0)$, but $\nexists \boldsymbol{\sigma} \geq \mathbf{0}$ such that $\mathbf{C}\boldsymbol{\sigma} = (\mathbf{m}_2 - \mathbf{m}_0)$, then, according to Proposition 4.4, $\mathbf{m}_1$ is reachable but $\mathbf{m}_2$ is not. Therefore it is not BIC over $Class(\mathbf{m}_0)$. The same conclusion can be obtained by using Theorem 4.7. The shadowed area in fig. 4.3(a) corresponds to the set of reachable markings. Note that it is the intersection of $Class(\mathbf{m}_0)$ and the convex cone (originated from $\mathbf{m}_0$) defined by vectors $\mathbf{c}'_1$ and $\mathbf{c}'_2$, which represent the columns of $\mathbf{C}$ restricted to p_1 and p_2. Now, consider the system of fig. 4.3(b). In this, the convex

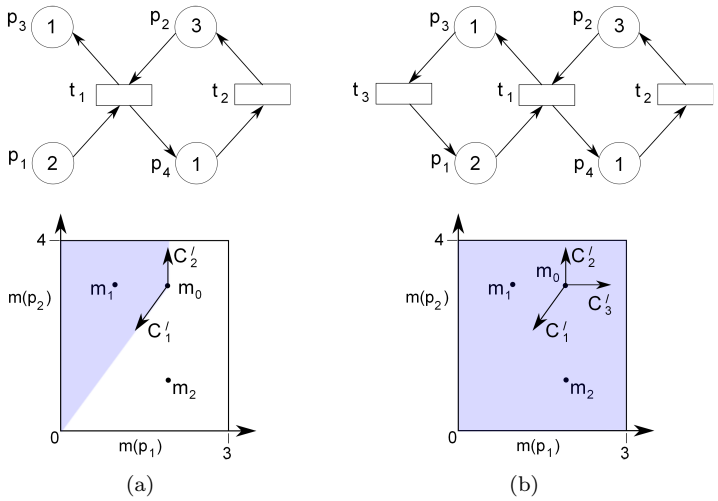

Fig. 4.3: Two TCPN systems with identical P-flows. The shadowed areas correspond to the sets of reachable markings. Only the system (b) is consistent and controllable over $Class(\mathbf{m}_0)$.

cone defined by the vectors $\mathbf{c}'_1$, $\mathbf{c}'_2$ and $\mathbf{c}'_3$ covers all $Class(\mathbf{m}_0)$, thus, according to Proposition 4.4, any marking in $Class(\mathbf{m}_0)$ can be reached from any other in $int\{Class(\mathbf{m}_0)\}$. The property that the convex cone of $\mathbf{c}'_1$, $\mathbf{c}'_2$ and $\mathbf{c}'_3$ covers $Class(\mathbf{m}_0)$ is equivalent to consistency. Thus, according to Lemma 4.5, the same result can be obtained, i.e., the system is BIC over the interior of $Class(\mathbf{m}_0)$. Moreover, since at the border markings of $Class(\mathbf{m}_0)$ there are not unmarked siphons (what can be verify by using the Algorithm 4.2) then, according to Theorem 4.7, the system is BIC over $Class(\mathbf{m}_0)$.

4.5 Controllability with uncontrollable transitions

In general, systems with uncontrollable transitions are not controllable over $int\{Class(\mathbf{m}_0)\}$, even if their nets are consistent. In this case, a smaller set of markings need to be considered. For practical reasons, the controllability will be studied here over sets of *equilibrium markings*. These sets are particularly interesting, since controllers are frequently designed in order to drive the system towards a desired *stationary operating point*, which corresponds to a point in the state space where the system can be stabilized. Furthermore, since the system is linear inside each region, the controllability will be first investigated over each E_i (equilibrium markings in $\Re_i$).

In the following subsection, it will be shown that the BIC property is related to the concept of *null-controllability* (Definition 1.26). Based on this, the main result, regarding the controllability in a single region, will be presented in Subsection 4.5.2. Later, in Subsection 4.5.3, a few of particular but interesting results will be derived, whose application will be illustrated through some examples. Finally, in Subsection 4.5.4 those results are extended in order to consider several regions.

4.5.1 BIC and null controllability

Inside a given region $\Re_i$, a TCPN model is linear and time-invariant (LTI). Accordingly, the analysis developed in this subsection is inspired by the work of Brammer [Brammer, 1972], who first addressed

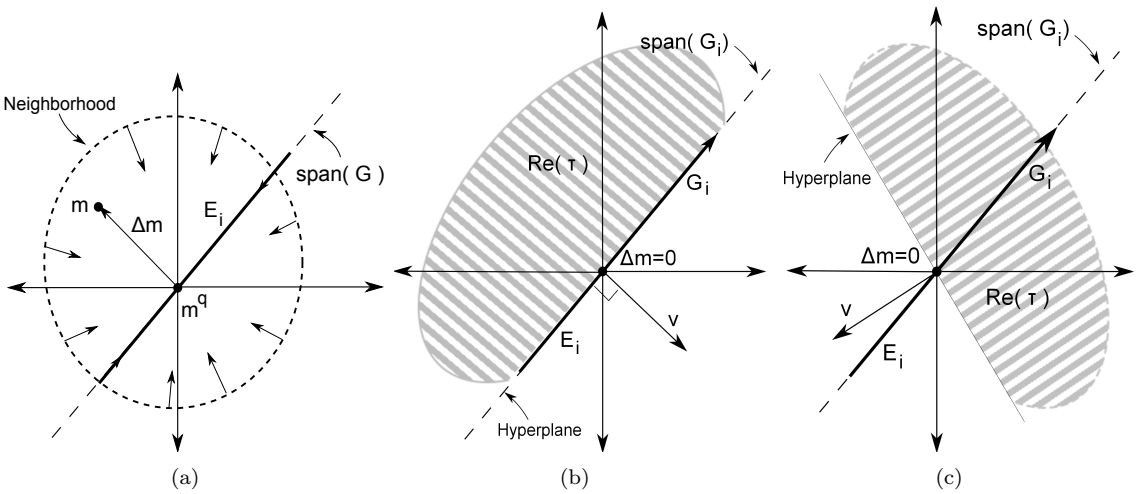

Fig. 4.4: a) BIC around a neighborhood as a null-controllability problem. b) Case in which $\exists \mathbf{v}$ s.t. $\mathbf{v}^T \Delta\mathbf{m}(\tau) \leq \mathbf{0}$ but $\mathbf{v}^T\mathbf{G} = \mathbf{0}$, the system is not null-controllable but still BIC. c) Case in which $\exists \mathbf{v}$ s.t. $\mathbf{v}^T \Delta\mathbf{m}(\tau) \leq \mathbf{0}$ and $\mathbf{v}^T\mathbf{G} \neq \mathbf{0}$, the system is not null-controllable and not BIC.

the null-controllability problem for LTI systems where the input is restricted to a convex set Ω. The main Brammer's result has been recalled as Theorem 1.27 in Subsection 1.6.2. According to that result, the controllability with input constraints cannot be decided (in general) from the rank of the controllability matrix.

The BIC property in TCPNs (Definition 4.3) can be reformulated as a null-controllability problem (around equilibrium markings) as follows:

Property 4.9. Consider an equilibrium marking $\mathbf{m}^q \in int\{\Re_i\}$. The evolution of the marking increment $\Delta\mathbf{m} = \mathbf{m} - \mathbf{m}^q$ is described by the state equation:

$$\dot{\Delta\mathbf{m}} = \mathbf{A}_i \Delta\mathbf{m} - [\mathbf{C}]^{T_c} \Delta\mathbf{u} \tag{4.4}$$

where $\mathbf{A}_i = \mathbf{C}\mathbf{\Lambda}\mathbf{\Pi}_i$, and $[\mathbf{C}]^{T_c}$ (resp. $\Delta\mathbf{u}$) results by eliminating from $\mathbf{C}$ its columns (resp. eliminating from $(\mathbf{u} - \mathbf{u}^q)$ its entries) related to uncontrollable transitions, thus $\mathbf{C}(\mathbf{u} - \mathbf{u}^q) = [\mathbf{C}]^{T_c}\Delta\mathbf{u}$. Then, $\mathbf{m}^q$ is reachable from any *equilibrium marking* in a small enough neighborhood iff the incremental system (4.4) is null-controllable *over* the subspace generated by the columns of $\mathbf{G}_i$, the generator of E_i (see, for instance, fig. 4.4(a)).

Remark 4.10. Since the set E_i is convex, the TCPN is BIC over $E_i \cap int\{\Re_i\}$ if the incremental system (4.4) is null-controllable *over* the span of $\mathbf{G}_i$, for any $\mathbf{m}^q$ in $E_i \cap int\{\Re_i\}$.

The restriction of controllability over $span(\mathbf{G}_i)$ is required in our case, since it may happen that $\mathbf{m}^q \in E_i$ is reachable from all of the *equilibrium* markings, but not from all of the non-equilibrium ones, in any neighborhood. In such case, the TCPN would be still BIC over E_i but not null-controllable (see for instance fig. 4.4(b), where the set from which $\Delta\mathbf{m} = \mathbf{0}$ is reachable is denoted as $Re(\tau)$, which does not include any neighborhood about $\Delta\mathbf{m} = \mathbf{0}$ but it does include all the equilibrium markings).

Now, let us analyze the constraints imposed to the incremental input $\Delta\mathbf{u}$ (i.e., the corresponding

Ω). Remember the constraint $\mathbf{0} \leq \mathbf{u} \leq \mathbf{\Lambda\Pi}_i\mathbf{m}$. In the sequel, in order to simplify the analysis, the controllability analysis will be focused on the equilibrium markings having a positive equilibrium flow, i.e., $\mathbf{0} < \mathbf{\Lambda\Pi}_i\mathbf{m}^q - \mathbf{u}^q$. Those markings represent the most interesting equilibrium markings, since all the transitions have activity at them. This leads to two possibilities for each controllable transition:

- If for a given $t_j \in T_c$ the entry u_j^q fulfills $0 = u_j^q < [\mathbf{\Lambda\Pi}_i\mathbf{m}^q]_j$ then the corresponding entry in $\Delta\mathbf{u}$, which is equal to $(u_j - u_j^q)$, can only be settled as nonnegative (because $u_j \geq 0$), leading to the controllability issues pointed out by Brammer.
- If $0 < u_j^q < [\mathbf{\Lambda\Pi}_i\mathbf{m}^q]_j$ then the corresponding entry in $\Delta\mathbf{u}$ can be settled as either positive or negative (by making u_j greater or lower than u_j^q), at least in a small neighborhood of $\mathbf{m}^q$. If this occurs for all the controllable transitions, then the controllability can be decided by a rank criterion as in the first statement of the Theorem 1.27.

In this way, it becomes useful to characterize the set of markings and transitions at which the input can be "arbitrarily" controlled, i.e., where the entries of $\Delta\mathbf{u}$ can be settled as positive or negative.

Definition 4.11. A transition $t_j \in T_c$ is said to be *fully controllable* at E_i if there exists an equilibrium marking $\mathbf{m}^q \in E_i$ with an equilibrium input $\mathbf{u}^q$ such that $0 < u_j^q < [\mathbf{\Lambda\Pi}_i\mathbf{m}^q]_j$ (so, the corresponding entry in $\Delta\mathbf{u}$ can be settled as either positive or negative in a neighborhood of $\mathbf{m}^q$). Otherwise, t_j is said to be *partially controllable* (since the corresponding entry in $\Delta\mathbf{u}$ can only be settled as nonnegative). The set of fully (partially) controllable transitions at E_i is denoted as T_{cf}^i (T_{cp}^i).

Definition 4.12. Sets E_i^+ and E_i^* are defined as follows:

- $E_i^+ = \{\mathbf{m}^q \in E_i | \exists \mathbf{u}^q \text{ s.t. } \mathbf{u}^q < \mathbf{\Lambda\Pi}_i\mathbf{m}^q\}$ is the set of equilibrium markings $\mathbf{m}^q \in \Re_i$ with a positive equilibrium flow $\mathbf{0} < \mathbf{\Lambda\Pi}_i\mathbf{m}^q - \mathbf{u}^q$.
- The subset $E_i^* = \{\mathbf{m}^q \in E_i^+ | \exists \mathbf{u}^q \text{ s.t. } 0 < u_j^q, \forall t_j \in T_{cf}^i\}$ is defined as the set of equilibrium markings at which all the inputs related to the transitions in T_{cf}^i can be arbitrarily controlled, i.e., where $0 < u_j^q < [\mathbf{\Lambda\Pi}_i\mathbf{m}^q]_j$.

Accordingly, given a marking $\mathbf{m}^q \in E_i^*$, there exists a small enough neighborhood of $\mathbf{m}^q$ where the input of the incremental system $\Delta\mathbf{u}$ can be settled as positive or negative, for those entries related to the transitions in T_{cf}^i. On the other hand, the entries of $\Delta\mathbf{u}$ related to the transitions in T_{cp}^i can only be settled as nonnegative.

Remark 4.13. In general, $E_i^* \subseteq E_i^+ \subseteq E_i$. The sets E_i^*, E_i^+ and E_i are convex. Furthermore, every $\mathbf{m} \in \{E_i^+ - E_i^*\}$ is on one "border"of E_i^+. By definition, if $T_{cf}^i = \emptyset$ then $E_i^* = E_i^+$.

Example 4.4. Consider for instance the system of fig. 4.2. In this, the interior of the triangle corresponds to E_1^*, while the union of E_1^* and the edges e_1 and e_2 (without the circled points) corresponds to E_1^+. Furthermore, $T_{cf}^1 = T_c$ and $T_{cp}^1 = \emptyset$. In this way, for any marking $\mathbf{m}$ in the interior of E_1 its equilibrium input fulfills $0 < u_j < [\mathbf{\Lambda\Pi}_1\mathbf{m}]_j$ for any $t_j \in T_{cf}^1 = T_c$. On the other hand, for $\mathbf{m}^q$ in fig. 4.2 its associated input $\mathbf{u}^q = \mathbf{0}$ and $\mathbf{\Lambda\Pi}_1\mathbf{m}^q - \mathbf{u}^q > \mathbf{0}$, then $\mathbf{m}^q \in \{E_1^+ - E_1^*\}$.

In the sequel, let us denote as $\mathbf{C}_c$, $\mathbf{C}_{cf}^i$ and $\mathbf{C}_{cp}^i$ the matrices built with the columns of $\mathbf{C}$ related to transitions in T_c, T_{cf}^i and T_{cp}^i, respectively. This notation helps to rewrite, in a more convenient way, the incremental system (4.4).

Property 4.14. Consider an equilibrium marking $\mathbf{m}^q \in E_i^*$. The incremental system (4.4), with $\mathbf{m} \in \Re_i$ being in a small enough neighborhood about $\mathbf{m}^q$, can be reformulated as

$$\dot{\Delta\mathbf{m}} = \mathbf{A}_i\Delta\mathbf{m} + \mathbf{B}_i\Delta\mathbf{u}^*, \qquad \text{subject to } \Delta\mathbf{u}^* \in \Omega$$
$$\text{where } \mathbf{A}_i = \mathbf{C}\boldsymbol{\Lambda}\boldsymbol{\Pi}_i, \quad \mathbf{B}_i = [-\mathbf{C}_{cf}^i, \mathbf{C}_{cf}^i, -\mathbf{C}_{cp}^i], \quad \text{and } \Omega = \{\Delta\mathbf{u}^* \geq \mathbf{0} | \Delta\mathbf{u}^* \leq \Delta\mathbf{u}^{max}\}, \tag{4.5}$$
$$\text{for some } \Delta\mathbf{u}^{max} > \mathbf{0} \text{ (meaning that the interior set of } \Omega \text{ is not empty).}$$

The null-controllability of system (4.5) is equivalent to that of system (4.4) because, on one hand, for any input $\mathbf{u}$ that is s.b. at a neighbor marking $\mathbf{m}$, $\exists\Delta\mathbf{u}^* \geq \mathbf{0}$ s.t. $\mathbf{C}(\mathbf{u}-\mathbf{u}^q) = [\mathbf{C}_{cf}^i, -\mathbf{C}_{cf}^i, \mathbf{C}_{cp}^i]\Delta\mathbf{u}^*$. On the other hand, given any $\Delta\mathbf{u}^* \geq \mathbf{0}$, $\exists\alpha > 0$ small enough s.t. an input $\mathbf{u}$, fulfilling $\mathbf{C}(\mathbf{u}-\mathbf{u}^q) = [\mathbf{C}_{cf}^i, -\mathbf{C}_{cf}^i, \mathbf{C}_{cp}^i] \cdot \alpha\Delta\mathbf{u}^*$, is s.b. at any marking in a small enough neighborhood about $\mathbf{m}^q$. In this way, no additional distinction between partially and fully controllable transitions is required.

4.5.2 Controllability in one region

The following lemma, which is a slight extension of the Lemma 3.1 introduced in [Brammer, 1972], provides a geometric interpretation for non null-controllability over the subspace of $\mathbf{G}_i$ (Brammer did not consider the controllability problem over subspaces). This lemma will be used in Theorem 4.16, which is the central result of this section, providing sufficient and necessary conditions for controllability over a set E_i^*.

Lemma 4.15. *Consider a given equilibrium marking $\mathbf{m}^q \in E_i^* \cap int\{\Re_i\}$. The incremental system $\dot{\Delta\mathbf{m}} = \mathbf{A}_i\Delta\mathbf{m} + \mathbf{B}_i\Delta\mathbf{u}^*$ (described in (4.5)) is null-controllable over the subspace generated by $\mathbf{G}_i$ (otherwise stated, $\mathbf{m}^q$ is reachable from every equilibrium marking in a small enough neighborhood) iff the columns of $\mathbf{G}_i$ belong to the span of the controllability matrix $Contr(\mathbf{A}_i, \mathbf{B}_i) = [\mathbf{B}_i, \mathbf{A}_i\mathbf{B}_i, ..., \mathbf{A}_i^{n-1}\mathbf{B}_i]$ and $\nexists\mathbf{v}$ s.t. $\mathbf{v}^T\mathbf{G}_i \neq \mathbf{0}$ and $\mathbf{v}^T\mathbf{e}^{\mathbf{A}_i\tau}\mathbf{B}_i\Delta\mathbf{u}^* \leq \mathbf{0}$ $\forall\tau \geq 0$ and for all admissible input $\Delta\mathbf{u}^* \in \Omega$.*

Proof. The proof follows the same structure as the Lemma 3.1 of [Brammer, 1972]. First, the incremental system (4.5) is null-controllable iff the reachable set from the origin at time step τ, denoted as $Re(\tau)$, contains an open set about the origin for some τ. In our case, we only require that $Re(\tau)$ contains all the states over the intersection of a small enough neighborhood and the subspace generated by $\mathbf{G}_i$ (otherwise stated, every equilibrium marking in a small enough neighborhood is reachable from $\mathbf{m}^q$). For this it is required that the columns of $\mathbf{G}_i$ belong to the span of the controllability matrix $Contr(\mathbf{A}_i, \mathbf{B}_i)$ (remember that the analysis is restricted to equilibrium markings, the rest of markings are not interesting). In order to show this, consider the solution of the incremental system $\Delta\mathbf{m}(\tau) = \int_0^\tau \mathbf{e}^{\mathbf{A}_i(\tau-\varsigma)}\mathbf{B}_i\Delta\mathbf{u}^*(\varsigma)d\varsigma$, where it is assumed that the initial condition is $\Delta\mathbf{m}(\tau) = \mathbf{0}$. By expanding $\mathbf{e}^{\mathbf{A}_i(\tau-\varsigma)}$ in Taylor series, it can be obtained $\Delta\mathbf{m}(\tau) = \sum_{j=0}^\infty \mathbf{A}_i^j\mathbf{B}_i \int_0^\tau (\tau-\varsigma)^j/j!\Delta\mathbf{u}^*(\varsigma)d\varsigma$, which can be rewritten as $\Delta\mathbf{m}(\tau) = \sum_{j=0}^\infty \mathbf{A}_i^j\mathbf{B}_i \cdot \boldsymbol{\alpha}_j(\tau, \Delta\mathbf{u}^*)$, for some proper vectors $\boldsymbol{\alpha}_j(\tau, \Delta\mathbf{u}^*)$. Next, according to the Cayley-Hamilton Theorem, for any $(\tau, \Delta\mathbf{u}^*)$ the vector $\sum_{j=0}^\tau \mathbf{A}_i^j\mathbf{B}_i\boldsymbol{\alpha}_j(\tau, \Delta\mathbf{u}^*)$ is in the span of $Contr(\mathbf{A}_i, \mathbf{B}_i) = [\mathbf{B}_i, \mathbf{A}_i\mathbf{B}_i, ..., \mathbf{A}_i^{n-1}\mathbf{B}_i]$, thus any reachable incremental state $\Delta\mathbf{m}(\tau)$ is in the span of the controllability matrix. Now let us consider a vector $\mathbf{d}$ that does not belong to the span of the controllability matrix. Then, $\forall\beta \neq 0$, $\beta\mathbf{d}$ is not reachable in the incremental system, equivalently, $\forall\beta \neq 0$, $\mathbf{m}^q + \beta\mathbf{d}$ is not reachable from $\mathbf{m}^q$. If $\mathbf{d}$ were a column of $\mathbf{G}_i$ then the set $\{\mathbf{m}^q + \beta\mathbf{d} | \beta \neq 0\}$ would

include equilibrium markings in any neighborhood of $\mathbf{m}^q$, in such case, these would not be reachable. Therefore, a necessary condition for controllability over equilibrium markings is that the columns of $\mathbf{G}_i$ are in the span of $Contr(\mathbf{A}_i, \mathbf{B}_i)$.

Additionally, under the hypothesis that the admissible input's set Ω is compact and contains the origin, the reachable set $Re(\tau)$ is convex (Lemma 2.6 of [Brammer, 1972]). Therefore, assuming that $\mathbf{G}_i$ belongs to the span of $Contr(\mathbf{A}_i, \mathbf{B}_i)$, if the system is not null-controllable then there exists a hyperplane through the origin, normal to a vector $\mathbf{v}$, satisfying $\mathbf{v}^T \Delta\mathbf{m}(\tau, \Delta\mathbf{u}^*) \leq \mathbf{0}\ \forall\tau$ and for all admissible $\Delta\mathbf{u}^*$, i.e., the complete reachable set is on one half of the space divided by the hyperplane (see, for instance, fig. 4.4(b) and 4.4(c)). In our case, since we are interested in the states that lie on the subspace generated by $\mathbf{G}_i$, an additional condition for non null-controllability is required: such hyperplane must transverse such subspace, i.e., $\mathbf{v}^T\mathbf{G}_i \neq \mathbf{0}$. Now, by taking $\mathbf{m}^q$ as the initial marking, the solution of the incremental system is given by $\Delta\mathbf{m}(\tau) = \int_0^\tau \mathbf{e}^{\mathbf{A}_i(\tau-s)}\mathbf{B}_i\Delta\mathbf{u}^*(s)ds$. Finally, by continuity and special choices of the input, it follows that $\mathbf{v}^T\Delta\mathbf{m}(\tau, \Delta\mathbf{u}^*) \leq \mathbf{0}$ is fulfilled iff $\mathbf{v}^T\mathbf{e}^{\mathbf{A}_i\tau}\mathbf{B}_i\Delta\mathbf{u}^* \leq \mathbf{0}\ \forall\tau$ and admissible $\Delta\mathbf{u}^*$ (for instance, by choosing impulse functions $\Delta\mathbf{u}^*(\tau) = \delta(\tau - \tau')[0, .., 0, 1, 0, .., 0]$, for each input variable Δu_i and $\tau' \geq 0$). ∎

Previous lemma introduces an algebraic characterization for null-controllability for a given equilibrium marking $\mathbf{m}^q$. This result is extended in the following theorem, leading to the BIC property in one region. Furthermore, the condition $\mathbf{v}^T\mathbf{e}^{\mathbf{A}_i\tau}\mathbf{B}_i\Delta\mathbf{u}^* \leq \mathbf{0}\ \forall\Delta\mathbf{u}^* \in \Omega$ is relaxed by assuming that Ω has non-empty interior and $\Delta\mathbf{u}^* \geq \mathbf{0}$, $\forall\Delta\mathbf{u}^* \in \Omega$.

Theorem 4.16. *Let $\langle \mathcal{N}, \boldsymbol{\lambda}, \mathbf{m}_0 \rangle$ be a TCPN system. Consider E_i^* such that $E_i^* \cap int\{\Re_i\} \neq \emptyset$ and let $\mathbf{G}_i$ be a generator of it. The system is BIC over E_i^*, considering all marking trajectories in $\Re_i$, iff $\mathbf{G}_i$ in the span of $Contr(\mathbf{A}_i, \mathbf{B}_i) = [\mathbf{B}_i, \mathbf{A}_i\mathbf{B}_i, ..., \mathbf{A}_i^{n-1}\mathbf{B}_i]$ and $\nexists\mathbf{v}$ s.t. $\mathbf{v}^T\mathbf{G}_i \neq \mathbf{0}$ and $\mathbf{v}^T\mathbf{e}^{\mathbf{A}_i\tau}\mathbf{B}_i \leq \mathbf{0}\ \forall\tau \geq 0$.*

Proof. First, $\mathbf{G}_i \in span\{Contr(\mathbf{A}_i, \mathbf{B}_i)\}$ is a necessary condition for null controlability, as shown in Lemma 4.15. Therefore, in the sequel it is assumed that $\mathbf{G}_i \in span\{Contr(\mathbf{A}_i, \mathbf{B}_i)\}$.

Part 1. Let us firstly prove that conditions: $\mathbf{G}_i$ belongs to the span of $Contr(\mathbf{A}_i, \mathbf{B}_i)$ and $\nexists\mathbf{v}$ s.t. $\mathbf{v}^T\mathbf{G}_i \neq \mathbf{0}$ and $\mathbf{v}^T\mathbf{e}^{\mathbf{A}_i\tau}\mathbf{B}_i \leq \mathbf{0}\ \forall\tau \geq 0$ are sufficient and necessary for BIC over $E_i^* \cap int\{\Re_i\}$.

Since we are dealing with controllability around a neighborhood, the exact value of the upper bound for $\Delta\mathbf{u}^*$ is not relevant, but just the restriction that it must be nonnegative and the property that the interior of Ω is not empty (as pointed out by Brammer). Thus, the inequality constraint of the controllability condition of Lemma 4.15, i.e., $\mathbf{v}^T\mathbf{e}^{\mathbf{A}_i\tau}\mathbf{B}_i\Delta\mathbf{u}^* \leq \mathbf{0}\ \forall\tau\ \forall\Delta\mathbf{u}^* \in \Omega = \{\Delta\mathbf{u}^* \geq \mathbf{0} | \Delta\mathbf{u}^* < \Delta\mathbf{u}^{max}\}$, is relaxed to $\mathbf{v}^T\mathbf{e}^{\mathbf{A}_i\tau}\mathbf{B}_i \leq \mathbf{0}\ \forall\tau$. Note that this inequality does not depend on the particular value of the equilibrium marking. Thus, if $\nexists\mathbf{v}$ s.t. $\mathbf{v}^T\mathbf{G}_i \neq \mathbf{0}$ and $\mathbf{v}^T\mathbf{e}^{\mathbf{A}_i\tau}\mathbf{B}_i \leq \mathbf{0}\ \forall\tau$ then every equilibrium marking in $E_i^* \cap int\{\Re_i\}$ is reachable from any other equilibrium marking in a small-enough neighborhood. Accordingly, if such $\mathbf{v}$ does not exists, since the set $E_i^* \cap int\{\Re_i\}$ is convex, then any equilibrium marking in $E_i^* \cap int\{\Re_i\}$ is reachable from any other equilibrium marking in $E_i^* \cap int\{\Re_i\}$, thus the system is BIC over this set.

On the other hand, suppose that it exists such $\mathbf{v}$. So, for any $\mathbf{m}^q \in E_i^* \cap int\{\Re_i\}$ the corresponding incremental system is not null-controllable over the subspace of $\mathbf{G}_i$. Otherwise stated, given a particular $\mathbf{m}^q \in E_i^* \cap int\{\Re_i\}$, any neighborhood of it contains equilibrium markings from which it is not reachable. Thus, the system is not BIC (considering all the trajectories inside $\Re_i$).

Part 2. Let us demonstrate that the system is controllable over E_i^* iff it is controllable over $E_i^* \cap int\{\Re_i\}$, considering all the trajectories inside $\Re_i$.

Suppose that the system is controllable over $E_i^* \cap int\{\Re_i\}$. Consider any marking $\mathbf{m}^r \in E_i^* - (E_i^* \cap int\{\Re_i\})$ and the markings $\mathbf{m}^q, \mathbf{m}^{r\prime}, \mathbf{m}^{q\prime} \in E_i^* \cap int\{\Re_i\}$, such that $(\mathbf{m}^r - \mathbf{m}^q) = \alpha(\mathbf{m}^{r\prime} - \mathbf{m}^{q\prime})$ with $\alpha > 0$. Since the system is BIC over $E_i^* \cap int\{\Re_i\}$, then $\exists \mathbf{u}'$ that transfers the state from $\mathbf{m}^{r\prime}$ to $\mathbf{m}^{q\prime}$. So, by linearity, an input $\mathbf{u}$ such that $(\mathbf{u} - \mathbf{u}^q) = \alpha(\mathbf{u}' - \mathbf{u}^{q\prime})$ transfers the state from $\mathbf{m}^r$ to $\mathbf{m}^q$. Actually, $(\mathbf{m}(\tau) - \mathbf{m}^q) = \alpha(\mathbf{m}'(\tau) - \mathbf{m}^{q\prime})$, where $\mathbf{m}(\tau)$ (resp. $\mathbf{m}'(\tau)$) is the marking at time τ if $\mathbf{m}_0 = \mathbf{m}^q$ (resp. $\mathbf{m}_0 = \mathbf{m}^{q\prime}$) and $\mathbf{u}$ (resp. $\mathbf{u}'$) is applied. Then, by choosing a suitable trajectory for $\mathbf{m}'(\tau)$, we can make $\mathbf{m}(\tau)$ to stay always inside $\Re_i$ (such trajectory exists, otherwise, if all the trajectories from $\mathbf{m}^r$ leave the region, then the reachability set is on one half of the space divided by the hyperplane that separates region $\Re_i$ from another one, so the system is not BIC).

In the sequel, it must be proved that such input is s.b. Since $\mathbf{0} \leq \mathbf{u}' \leq \mathbf{\Lambda\Pi}_i\mathbf{m}'$ then $-\alpha\mathbf{u}^{q\prime} \leq \alpha(\mathbf{u}' - \mathbf{u}^{q\prime}) \leq \alpha(\mathbf{\Lambda\Pi}_i\mathbf{m}' - \mathbf{u}^{q\prime})$. Now, substituting $\mathbf{u}'$ and $\mathbf{m}'$ and arranging the terms, we obtain: $(\mathbf{u}^q - \alpha\mathbf{u}^{q\prime}) \leq \mathbf{u} \leq \mathbf{\Lambda\Pi}_i\mathbf{m} - (\mathbf{w}^q - \alpha\mathbf{w}^{q\prime})$. Since $\mathbf{w}^q > \mathbf{0}$ and $(\mathbf{u}_j^{q\prime} > 0 \Rightarrow \mathbf{u}_j^q > 0)$, then $\exists\alpha > 0$ small enough such that $\mathbf{u}^q \geq \alpha\mathbf{u}^{q\prime}$ and $\mathbf{w}^q \geq \alpha\mathbf{w}^{q\prime}$, so, $\mathbf{0} \leq \mathbf{u} \leq \mathbf{\Lambda\Pi}_i\mathbf{m}$, i.e., $\mathbf{u}$ is s.b.. Therefore, for any $\mathbf{m}^r \in E_i^* - (E_i^* \cap int\{\Re_i\})$ there exists $\mathbf{m}^q \in E_i^* \cap int\{\Re_i\}$ reachable from $\mathbf{m}^r$. Furthermore, since the points of $E_i^* - (E_i^* \cap int\{\Re_i\})$ are limit points of $E_i^* \cap int\{\Re_i\}$, then every marking in $E_i^* - (E_i^* \cap int\{\Re_i\})$ can be reached (in finite time, since the flow in a neighborhood of such marking is positive) from any marking in $E_i^* \cap int\{\Re_i\}$. Therefore, the system is BIC over E_i^* if it is BIC over $E_i^* \cap int\{\Re_i\}$. Finally, by definition, if the system is not controllable over $E_i^* \cap int\{\Re_i\}$, considering all marking trajectories in $\Re_i$, then it is not BIC over E_i^*. ∎

The inequality $\mathbf{v}^T\mathbf{e}^{\mathbf{A}_i\tau}\mathbf{B}_i \leq \mathbf{0}\ \forall\tau \geq 0$, presented in the previous theorem, seems difficult to verify due to the exponential matrix $\mathbf{e}^{\mathbf{A}_i\tau}$. Brammer [Brammer, 1972] introduced an equivalent condition in terms of the eigenvectors of $\mathbf{A}^T$. Nevertheless, Brammer's condition does not provide the specific value of such $\mathbf{v}$, but just information about its existence. This represents a problem in our case since, in order to apply the Theorem 4.16, we require more information about the value of every $\mathbf{v}$ fulfilling $\mathbf{v}^T\mathbf{e}^{\mathbf{A}_i\tau}\mathbf{B}_i \leq \mathbf{0}$ $\forall\tau \geq 0$, in order to verify if one of them fulfills $\mathbf{v}^T\mathbf{G} \neq \mathbf{0}$. Therefore, a complete analysis for evaluating the full condition of Theorem 4.16 has been achieved. This is provided in detail in Appendix C. The results of such analysis are resumed in the following *polynomial-time* algorithm:

Algorithm 4.3. Controllability over a region.

Solve $\mathbf{G}_i = Contr(\mathbf{A}_i, \mathbf{B}_i) \cdot \mathbf{Z}$
If there is not solution for $\mathbf{Z}$ **then** the system is not BIC over E_i^*
else
Consider the following inequalities system:

$$
\begin{array}{ll}
\mathbf{S}\mathbf{Q}^T \cdot \mathbf{v} = diag([1,-1]) \cdot \mathbf{v}'' & \{\text{auxiliary variable}\} \\
\mathbf{v}'' \geq \mathbf{0} & \{\text{condition for auxiliary variable}\} \\
\mathbf{v}^T \cdot \mathbf{B}_i \leq \mathbf{0} & \{\text{for } \mathbf{v}^T \mathbf{e}^{\mathbf{A}_i \tau} \mathbf{B}_i \leq \mathbf{0} \text{ at } \tau = 0\} \\
\forall jth \text{ column of } \mathbf{B}_i & \\
\mathbf{H}(\mathbf{Q}, [\mathbf{B}_i]^j) \cdot \mathbf{v}'' \leq \mathbf{0} & \{\text{for } \mathbf{v}^T \mathbf{e}^{\mathbf{A}_i \tau} \mathbf{B}_i \leq \mathbf{0} \text{ at } \tau \to \infty\} \\
 & \\
\text{where } \mathbf{Q}, \mathbf{S} \text{ and } \mathbf{H}(\mathbf{Q}, [\mathbf{B}_i]^j) & \text{are constant matrices defined in Appendix C}
\end{array}
\tag{4.6}
$$

If $\mathbf{v}^T \mathbf{G}_i = \mathbf{0}$ is a redundant constraint in (4.6) **then** the system is BIC over E_i^*,
else the system is not BIC over E_i^*, considering all the trajectories in $\Re_i$.

Proof of Algorithm 4.3: Let us provide first a sketch of the analysis reported in the Appendix C, that leads to Proposition C.3, that states the equivalence of $\mathbf{v}^T \mathbf{e}^{\mathbf{A}_i \tau} \mathbf{B} \leq \mathbf{0}\ \forall \tau \geq 0$ with the set of inequalities (4.6). The property $\exists \mathbf{v}$ s.t. $\mathbf{v}^T \mathbf{e}^{\mathbf{A}_i \tau} \mathbf{B}_i \leq \mathbf{0}\ \forall \tau \geq 0$ can be reduced to $\exists \mathbf{v}$ s.t. $\mathbf{v}^T \mathbf{e}^{\mathbf{A}_i \tau} \mathbf{B}_i \leq \mathbf{0}$ for $\tau = 0$ and in the limit $\tau \to \infty$. For $\tau = 0$, the inequality $\mathbf{v}^T \mathbf{e}^{\mathbf{A}_i \tau} \mathbf{B}_i \leq \mathbf{0}$ is equivalent to $\mathbf{v}^T \mathbf{B}_i \leq \mathbf{0}$, which is included in (4.6). Later, by transforming $\mathbf{A}_i$ into a Jordan block form, it is possible to represent $lim_{\tau \to \infty} \mathbf{v}^T \mathbf{e}^{\mathbf{A}_i \tau} [\mathbf{B}_i]^j \leq \mathbf{0}$ as a linear inequality, for each column $[\mathbf{B}_i]^j$ of matrix $\mathbf{B}_i$. This is possible since any $\mathbf{v}$ can be expressed as a linear combination of the generalized eigenvectors of $\mathbf{A}_i$, while the projection of $\mathbf{e}^{\mathbf{A}_i \tau} [\mathbf{B}_i]^j$ on each of these eigenvectors is a particular weighted sum of exponential terms (of the kind $c_i \tau^{m_j} e^{s_j \tau}$ if real or $c_i \tau^{m_j} e^{s_j \tau} sin(\tau - h_i)$ if complex). In detail, for an eigenvector related to a real eigenvalue, the projection of $\mathbf{e}^{\mathbf{A}_i \tau} [\mathbf{B}_i]^j$ on it keeps a constant sign during the evolution of the system (the sign of $c_i \tau^{m_j} e^{s_j \tau}$ only depends on c_i, so this can be determined from $\mathbf{A}_i$ and $[\mathbf{B}_i]^j$). On the other hand, if the eigenvector is related to a complex eigenvalue, the projection periodically becomes positive and negative (the sign of $c_i \tau^{m_j} e^{s_j \tau} sin(\tau - h_i)$ is periodically positive and negative, due to the sin function). Thus, $lim_{\tau \to \infty} \mathbf{v}^T \mathbf{e}^{\mathbf{A}_i \tau} [\mathbf{B}_i]^j < \mathbf{0}$ holds iff the projection associated to the largest of those exponential functions, when $\tau \to \infty$ (the term $c_i \tau^{m_j} e^{s_j \tau}$ with the largest exponents), is related to a real eigenvector, is negative (resp. positive) and the corresponding component in $\mathbf{v}$ is positive (resp. negative). This is represented by the inequality $\mathbf{H}(\mathbf{Q}, [\mathbf{B}_i]^j) \cdot \mathbf{v}'' \leq \mathbf{0}$, where the auxiliary variable $\mathbf{v}''$ is used, being nonnegative and equivalent (in certain way) to $\mathbf{v}$. This leads to the inequalities (4.6).

Now let us prove the algorithm. If there does not exist a solution for $\mathbf{G}_i = Contr(\mathbf{A}_i, \mathbf{B}_i) \cdot \mathbf{Z}$ then $\mathbf{G}_i$ is not in the span of the controllability matrix, thus, according to Theorem 4.16, the system is not BIC over E_i^* considering all the trajectories in $\Re_i$.

Now, assume that there exists a solution for $\mathbf{G}_i = Contr(\mathbf{A}_i, \mathbf{B}_i) \cdot \mathbf{Z}$, thus $\mathbf{G}_i$ is in the span of the controllability matrix. If $\mathbf{v}^T \mathbf{G}_i = \mathbf{0}$ is redundant in (4.6) then, according to Proposition C.3, $\nexists \mathbf{v}$ s.t. $\mathbf{v}^T \mathbf{G}_i \neq \mathbf{0}$ and $\mathbf{v}^T \mathbf{e}^{\mathbf{A}_i \tau} \mathbf{B}_i \leq \mathbf{0}\ \forall \tau \geq 0$, thus, by Theorem 4.16, the system is BIC over E_i^*. On the contrary, if $\mathbf{v}^T \mathbf{G}_i = \mathbf{0}$ is not redundant then, by Proposition C.3, $\exists \mathbf{v}$ s.t. $\mathbf{v}^T \mathbf{G}_i \neq \mathbf{0}$ and $\mathbf{v}^T \mathbf{e}^{\mathbf{A}_i \tau} \mathbf{B}_i \leq \mathbf{0}$ $\forall \tau \geq 0$, thus, according to Theorem 4.16, the system is not BIC over E_i^* considering all the trajectories in $\Re_i$. ∎

Remark 4.17. The controllability inside a region with uncontrollable transitions depends not only on the structure of the net but also on the timing $\boldsymbol{\lambda}$ of the system. On the contrary, it is independent of the initial marking (the particular value of $\mathbf{m}_0$ is irrelevant, since the controllability property is equivalent

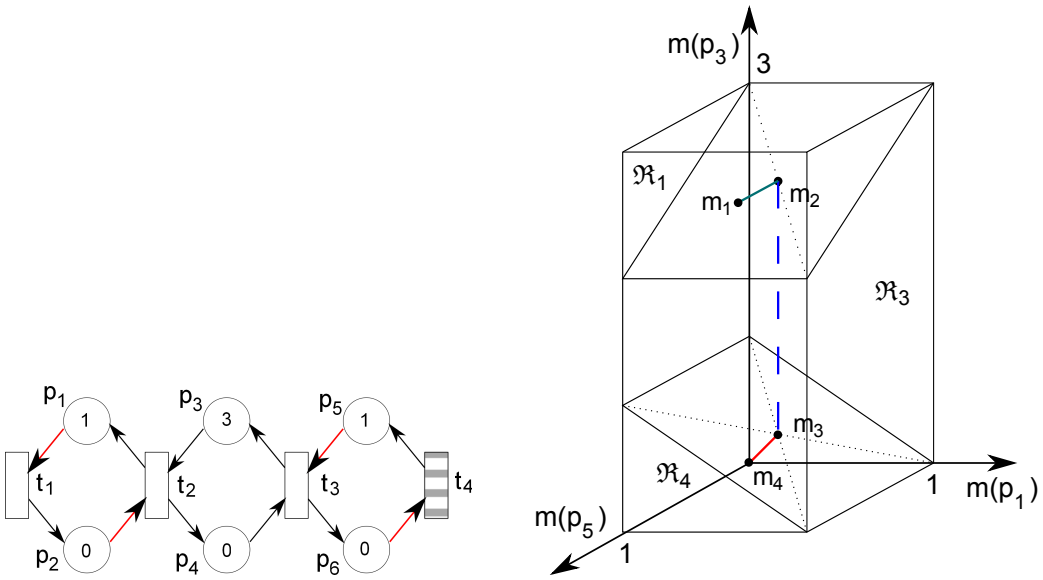

Fig. 4.5: a) A TCPN system. Transition t_4 is the only controllable one. b) The set $Class(\mathbf{m}_0)$ and its $\mathbb{E}$

for any system having the same net, timing and any initial marking in $Class(\mathbf{m}_0)$). Previous algorithm provides a polynomial-time procedure for the verification of the BIC property, since redundancy of a constraint in a set of inequalities can be decided in polynomial time (for computation methods see, for instance, [Paulraj and Sumathi, 2010]).

Example 4.5. Consider the system of fig. 4.5 with $T_c = \{t_4\}$ and $\lambda_1 = \lambda_2 = \lambda_3 = \lambda_4 = 1$. The four configurations are characterized by: $\mathcal{C}_1 = \{(p_2, t_2), (p_4, t_3)\}$, $\mathcal{C}_2 = \{(p_3, t_2), (p_4, t_3)\}$, $\mathcal{C}_3 = \{(p_2, t_2), (p_5, t_3)\}$ and $\mathcal{C}_4 = \{(p_3, t_2), (p_5, t_3)\}$. The arcs (p_1, t_1) and (p_6, t_4) are also present in all the configurations. Nevertheless, given the initial marking of this system, $\mathcal{C}_2$ cannot occur because p_3 and p_4 cannot constrain t_2 and t_3 at the same time (for this, it would be necessary that $\mathbf{m}[p_3] \leq \mathbf{m}[p_2] \leq 1$ and $\mathbf{m}[p_4] \leq \mathbf{m}[p_5] \leq 1$, which implies $\mathbf{m}[p_3] + \mathbf{m}[p_4] \leq 2$ but, according to the P-semiflows and the initial marking, $\mathbf{m}[p_3] + \mathbf{m}[p_4] = 3$). The polytope shown in fig. 4.5 corresponds to the projection of $Class(\mathbf{m}_0)$ on the markings at p_1, p_3 and p_5 (markings of p_2, p_4 and p_6 are redundant because of the invariants $\mathbf{m}[p_1] + \mathbf{m}[p_2] = 1$, $\mathbf{m}[p_3] + \mathbf{m}[p_4] = 3$ and $\mathbf{m}[p_5] + \mathbf{m}[p_6] = 1$). The markings in the segments $[\mathbf{m}_2, \mathbf{m}_3]$ and $[\mathbf{m}_3, \mathbf{m}_4)$ correspond to E_3^* and E_4^*, respectively. The marking $\mathbf{m}_2$ also belongs to E_1^* (the segment $(\mathbf{m}_1, \mathbf{m}_2]$ shown in fig. 4.5 corresponds to E_1^* for the system with another timing, which will be explained in a forthcoming example). Let us focus on E_3^*. In this case, $T_{cf}^3 = \emptyset$, $T_{cp}^3 = \{t_4\}$, and

$$\mathbf{G}_3 \quad = \quad [\quad 0, \quad 0, \quad -1, \quad 1, \quad 0, \quad 0 \quad]^T$$

The matrices of the incremental system (as in (4.5)) are given by:

$$\mathbf{A}_3 = \mathbf{C}\boldsymbol{\Lambda}\boldsymbol{\Pi}_3 = \begin{bmatrix} -1 & 1 & 0 & 0 & 0 & 0 \\ 1 & -1 & 0 & 0 & 0 & 0 \\ 0 & -1 & 0 & 0 & 1 & 0 \\ 0 & 1 & 0 & 0 & -1 & 0 \\ 0 & 0 & 0 & 0 & -1 & 1 \\ 0 & 0 & 0 & 0 & 1 & -1 \end{bmatrix}, \quad \mathbf{B}_3 = -\mathbf{C}_{cp}^3 = \begin{bmatrix} 0 \\ 0 \\ 0 \\ 0 \\ -1 \\ 1 \end{bmatrix}$$

Let us investigate the controllability over E_3^*. First, it is easy to verify that $\mathbf{G}_3$ is in the span of $Contr(\mathbf{A}_3, \mathbf{B}_3)$. Then, let us compute the matrices required by the Algorithm 4.3 (defined in Appendix C). The transformation of $\mathbf{A}_3$ into the Jordan block form leads to:

$$\mathbf{Q} = \begin{bmatrix} 0 & 1 & 0.5 & 0 & 0 & -0.5 \\ 0 & 1 & 0.5 & 0 & 0 & 0.5 \\ -0.5 & 0.25 & 0 & 0 & -0.25 & 0 \\ 0.5 & 0.75 & 1 & -1 & 0.25 & 0 \\ 0 & 0.5 & 0.5 & 0 & 0.5 & 0.5 \\ 0 & 0.5 & 0.5 & 0 & -0.5 & -0.5 \end{bmatrix}, \quad \mathbf{J} = \begin{bmatrix} \begin{bmatrix} 0 & 1 \\ 0 & 0 \end{bmatrix} & 0 & 0 & 0 & 0 \\ 0 & 0 & [0] & 0 & 0 & 0 \\ 0 & 0 & 0 & [0] & 0 & 0 \\ 0 & 0 & 0 & 0 & [-2] & 0 \\ 0 & 0 & 0 & 0 & 0 & [-2] \end{bmatrix}$$

$$\mathbf{B}' = \mathbf{Q}^{-1}\mathbf{B}_3 = \begin{bmatrix} 1 \\ 0 \\ 0 \\ 0 \\ -2 \\ 0 \end{bmatrix}$$

There are five different blocks in $\mathbf{J}$: three blocks related to eigenvalue 0, the first of them associated to two generalized eigenvectors, and two other (1-dimension) blocks associated to eigenvalues -2. This leads to the following matrices $\overline{\mathbf{b}_j}$:

$$\overline{\mathbf{b}_1} = \begin{bmatrix} 0 & 0 \\ 1 & 0 \end{bmatrix}, \quad \overline{\mathbf{b}_2} = \overline{\mathbf{b}_3} = [0], \quad \overline{\mathbf{b}_4} = [-2], \quad \overline{\mathbf{b}_5} = [0]$$

Since there are blocks associated to repetitive eigenvalues, a matrix S, as described in Appendix C, is required to be computed:

$$\begin{array}{l} \boldsymbol{\alpha}(\tau) = [\ \tau \quad 1 \quad 1 \quad 1 \quad e^{-2\tau} \quad e^{-2\tau}\ ] \\ \widehat{\boldsymbol{\alpha}}(\tau) = [\ \tau \quad 1 \quad e^{-2\tau}\ ] \end{array} \longrightarrow \quad \mathbf{S} = \begin{bmatrix} 1 & 0 & 0 & 0 & 0 & 0 \\ 0 & 1 & 1 & 1 & 0 & 0 \\ 0 & 0 & 0 & 0 & 1 & 1 \end{bmatrix}$$

leading to the following vectors:

$$\mathbf{S} \cdot diag[\overline{\mathbf{b}_1}, .., \overline{\mathbf{b}_5}] \cdot \mathbf{S}^T = \begin{bmatrix} 0 & 0 & 0 \\ 1 & 0 & 0 \\ 0 & 0 & -2 \end{bmatrix}$$
$$\mathbf{a} = \begin{bmatrix} 1 & 0 & -2 \end{bmatrix}, \quad \hat{\mathbf{a}} = \begin{bmatrix} 1 & -1 & 0 & 0 & -2 & 2 \end{bmatrix}$$

Finally, we obtain the matrix required by Algorithm 4.3:

$$\mathbf{H}(\mathbf{Q}, \mathbf{B}_3) = \begin{bmatrix} 1 & 0 & 0 & 0 & 0 & 0 \\ 0 & -\infty & 0 & 0 & 0 & 1 \end{bmatrix}$$

It is easy to see that $\mathbf{v}'' = [0, 1, 0, 0, 0, 0]^T \geq \mathbf{0}$ fulfills with the inequality $\mathbf{H}(\mathbf{Q}, \mathbf{B}_3)\mathbf{v}'' \leq \mathbf{0}$ of Algorithm 4.3. Furthermore, vector $\mathbf{v}^T = [0, -1, 2, 0, 1, 0]$ fulfills with $\mathbf{S}\mathbf{Q}^T \cdot \mathbf{v} = (diag([1, -1])\mathbf{v}''$ and the inequality $\mathbf{v}^T\mathbf{B}_3 \leq \mathbf{0}$, thus, such $\mathbf{v}''$ and $\mathbf{v}$ are a solution of (4.6). Finally, $\mathbf{v}^T\mathbf{G}_3 = 2 \neq \mathbf{0}$, i.e., $\mathbf{v}^T\mathbf{G}_3 = \mathbf{0}$ is not redundant in (4.6). Then, according to Proposition C.3, $\mathbf{v}$ is s.t. $\mathbf{v}^T\mathbf{G}_3 \neq \mathbf{0}$ and $\mathbf{v}^T e^{\mathbf{A}_3\tau}\mathbf{B}_3 \leq \mathbf{0}$ $\forall\tau$, thus, according to Theorem 4.16, the system is not BIC over E_3^*. Vector $\mathbf{v}$ and the corresponding normal hyperplane are represented in fig. 4.6(a). This divides $\Re_3$ in two parts. Then, $\mathbf{v}^T e^{\mathbf{A}_3\tau}\mathbf{B}_3 \leq \mathbf{0}$ $\forall\tau$ implies that the system cannot reach, from $\mathbf{m}_0$, any marking in the half of $\Re_3$ being pointed out by $\mathbf{v}$ (for instance, $\mathbf{m}_2$ is not reachable from $\mathbf{m}_0$).

4.5.3 Other derived results for one region

In this subsection, a few of interesting controllability results will be introduced. They provide simple tools for checking controllability in special cases. Moreover, a few examples will be presented in order to illustrate their application.

The next corollary splits the condition of Theorem 4.16 into a necessary and a sufficient one.

Corollary 4.18. *Let $\langle \mathcal{N}, \boldsymbol{\lambda}, \mathbf{m}_0 \rangle$ be a TCPN system. Consider some E_i^* such that $E_i^* \cap int\{\Re_i\} \neq \emptyset$, as previously defined, and let $\mathbf{G}_i$ be a generator of it. Then:*

1. *If $\mathbf{G}_i$ is in the span of $Contr(\mathbf{A}_i, \mathbf{C}_{cf}^i)$ then the system is controllable over E_i^*. Furthermore, if $T_{cf}^i = T_c$ then it is also a necessary condition for controllability over E_i^*, considering all the marking trajectories in $\Re_i$.*

2. *If $\mathbf{G}_i$ is not in the span of $Contr(\mathbf{A}_i, \mathbf{C}_c)$ then the system is not controllable over E_i^*, considering all the marking trajectories in $\Re_i$.*

Proof. Statement 1). Suppose that $\mathbf{G}_i$ is in the span of $Contr(\mathbf{A}_i, \mathbf{C}_{cf}^i)$. In this case, since $\mathbf{B}_i = [-\mathbf{C}_{cf}^i, \mathbf{C}_{cf}^i, -\mathbf{C}_{cp}^i]$, $\mathbf{G}_i$ is in the span of $Contr(\mathbf{A}_i, \mathbf{B}_i)$. Then, according to Theorem 4.16, the system would be BIC iff $\nexists\mathbf{v}$ s.t. $\mathbf{v}^T\mathbf{G}_i \neq \mathbf{0}$ and $\mathbf{v}^T e^{\mathbf{A}_i\tau}\mathbf{B}_i \leq \mathbf{0}$ $\forall\tau$. Let us consider now just the inputs related to the transition in T_{cf}^i, i.e., as if $\mathbf{B}_i = [-\mathbf{C}_{cf}^i, \mathbf{C}_{cf}^i]$. Then, $\mathbf{v}^T e^{\mathbf{A}_i\tau}\mathbf{B}_i = [-\mathbf{v}^T e^{\mathbf{A}_i\tau}\mathbf{C}_{cf}^i, \mathbf{v}^T e^{\mathbf{A}_i\tau}\mathbf{C}_{cf}^i] \leq \mathbf{0}$ $\forall\tau$ iff $\mathbf{v}^T e^{\mathbf{A}_i\tau}\mathbf{B}_i = \mathbf{0}$, i.e., $\mathbf{v}$ is orthogonal to $e^{\mathbf{A}_i\tau}\mathbf{B}_i$, $\forall\tau$. Furthermore, the space defined by $e^{\mathbf{A}_i\tau}\mathbf{B}_i$ $\forall\tau$ is equal to the span of $Contr(\mathbf{A}_i, \mathbf{C}_{cf}^i)$ (easy to show by expanding $e^{\mathbf{A}_i\tau}\mathbf{B}_i$ in Taylor series and applying the Cayley-Hamilton Theorem). Thus, if $\mathbf{v}^T \cdot Contr(\mathbf{A}_i, \mathbf{C}_{cf}^i) = \mathbf{0}$ and $\mathbf{G}_i$ is in the span of $Contr(\mathbf{A}_i, \mathbf{C}_{cf}^i)$

then $\mathbf{v}^T\mathbf{G}_i = \mathbf{0}$. Therefore, according to Theorem 4.16, the system is BIC over E_i^*.
On the other hand, suppose that $T_c = T_{cf}^i$, so $\mathbf{C}_{cf} = \mathbf{C}_c$. If $\mathbf{G}_i$ is not in the span of $Contr(\mathbf{A}_i, \mathbf{C}_{cf}^i)$ then it is not in the span of $Contr(\mathbf{A}_i, \mathbf{C}_c)$. This condition is equal to that of statement 2.

Statement 2). Since $\mathbf{B}_i = [-\mathbf{C}_{cf}^i, \mathbf{C}_{cf}^i, -\mathbf{C}_{cp}^i]$ then the columns of $\mathbf{B}_i$ are the columns of $\mathbf{C}_c$ but with different signs. Then, if $\mathbf{G}_i$ is not in the span of $Contr(\mathbf{A}_i, \mathbf{C}_c)$ then it is not in the span of $Contr(\mathbf{A}_i, \mathbf{B}_i)$, thus, according to Theorem 4.16, the system is not BIC over E_i^*. ∎

Previous corollary provides controllability conditions that are simple and useful in particular cases. In our experience, those are very frequent. Nevertheless, by using this, the controllability of the system cannot be decided if $\mathbf{G}_i$ is in the range of $Contr(\mathbf{A}_i, \mathbf{C}_c)$ but not in the range of $Contr(\mathbf{A}_i, \mathbf{C}_{cf}^i)$. In such case, Algorithm 4.3 must be used in order to decide the controllability over E_i^* (like in example 4.5), still in polynomial time.

The next corollary provides a controllability rank-condition, according to which a system is BIC for *any set of controllable transitions*, over the corresponding E_i^*. Roughly speaking, such rank condition (4.7) means the existence of a bijection between the markings in $\Re_i$ and their field vectors ($\dot{\mathbf{m}}$). Such bijection implies that each column of $\mathbf{G}_i$ is associated to one controllable transition (see the Algorithm 4.1 for the computation of $\mathbf{G}_i$) and this is included in the range of the controllability matrix. Thus, since $T_c = T_{cf}^i$ (a consequence of the encountered bijection), according to the first statement of Corollary 4.18 the system is controllable.

Corollary 4.19. *Let $\langle \mathcal{N}, \boldsymbol{\lambda}, \mathbf{m}_0 \rangle$ be a TCPN system. Consider a given region $\Re_i$, If*

$$rank\left(\begin{bmatrix} \mathbf{C}\boldsymbol{\Lambda}\boldsymbol{\Pi}_i \\ \mathbf{B}_y^T \end{bmatrix}\right) = |P| \tag{4.7}$$

then, for any set of controllable transitions T_c s.t. $E_i^* \cap int\{\Re_i\} \neq \emptyset$, the system is BIC over E_i^*.

Proof. For this proof consider the Algorithm 4.1 for the computation of $\mathbf{G}_i$. Note that $\mathbf{C}\boldsymbol{\Lambda}\boldsymbol{\Pi}_i = \mathbf{A}_i$, according to the definition of the incremental system (4.5). First, let us prove that condition (4.7) implies that $\forall t_j \in T_c$ there exists a solution $\mathbf{d}_j$ for (4.1), i.e., $\mathbf{A}_i\mathbf{d}_j = \mathbf{C}^j$ and $\mathbf{B}_y^T\mathbf{d}_j = \mathbf{0}$. This implies that, according to the procedures for the computation of $\mathbf{G}_i$ and T_{cf}^i (Algorithm C.1 provided in the Appendix C), $\mathbf{G}_i$ is composed of such vectors $\mathbf{d}_j$ and $T_{cf}^i = T_c$.

For that, consider a particular $t_j \in T_c$. Define a matrix $\mathbf{K}_{|P|\times m}$ as a basis of the right annuller of $\mathbf{B}_y^T$, then $\forall \mathbf{d}_j$ s.t. $\mathbf{B}_y^T\mathbf{d}_j = \mathbf{0}$, $\exists \delta_j$ s.t $\mathbf{d}_j = \mathbf{K}\delta_j$. Therefore, $\exists \mathbf{d}_j$ that fulfills (4.1) iff $\exists \delta_j$ s.t. $\mathbf{A}_i\mathbf{K}\delta_j = \mathbf{C}^j$. Now, condition (4.7) implies that $\mathbf{A}_i\mathbf{K}$ has full column rank, i.e., $rank(\mathbf{A}_i\mathbf{K}) = m$. Consider the matrix $\mathbf{P}$ s.t. $\mathbf{P}\mathbf{K} = \mathbf{I}$, then, the matrix $[\ \mathbf{P}^T,\ \ \mathbf{B}_y\ ]^T$ is non singular. Premultiplying the transpose of this matrix to $\mathbf{A}_i\mathbf{K}$ and considering $\mathbf{B}_y^T\mathbf{C} = \mathbf{0}$, it is easy to see that $rank(\mathbf{A}_i\mathbf{K}) = rank(\mathbf{P}\mathbf{A}_i\mathbf{K}) = m$, i.e., $\mathbf{P}\mathbf{A}_i\mathbf{K}$ is non singular. In the same way, premultiplying the transpose of the same matrix to the equality $\mathbf{A}_i\mathbf{K}\delta_j = \mathbf{C}^j$ and considering $\mathbf{B}_y^T\mathbf{C} = \mathbf{0}$ and $\mathbf{B}_y^T\mathbf{C}^j = \mathbf{0}$, it is easy to see that $\exists \delta_j$ s.t. $\mathbf{A}_i\mathbf{K}\delta_j = \mathbf{C}^j$ iff $\exists \delta_j$ s.t. $\mathbf{P}\mathbf{A}_i\mathbf{K}\delta_j = \mathbf{P}\mathbf{C}^j$, moreover, since $\mathbf{P}\mathbf{A}_i\mathbf{K}$ is non singular, then such δ_j exists, which implies that $\exists \mathbf{d}_j$ that fulfills (4.1), and this reasoning is valid $\forall t_j \in T_c$.

Now, let us demonstrate that $\mathbf{G}_i$ belongs to the span of $Contr(\mathbf{A}_i, \mathbf{C}_{cf}^i)$. Since $\forall t_j \in T_c$ $\exists \mathbf{d}_j$ that fulfills (4.1), according to the Algorithm 4.1 for the computation of $\mathbf{G}_i$, $\mathbf{G}_i = [\mathbf{d}_1, ..., \mathbf{d}_{|T_c|}]$ (if $\mathbf{G}_i$ has not full column rank, the linearly dependent columns are eliminated, but the present proof is still valid),

and according to the Algorithm C.1 for computing T^i_{cf}, $T^i_{cf} = T_c$. Then, consider a particular column of $\mathbf{G}_i$, i.e., a particular $\mathbf{d}_j$. According to the Cayley-Hamilton Theorem, there exist coefficients $\alpha_1, ..., \alpha_{|P|}$ s.t. $\mathbf{I} + \mathbf{A}_i\alpha_1 + ... + (\mathbf{A}_i)^{|P|}\alpha_{|P|} = \mathbf{0}$. Postmultiplying $\mathbf{d}_j$ to this equation, substituting $\mathbf{A}_i\mathbf{d}_j = [\mathbf{C}]^j$ and rearranging the terms, we obtain $[[\mathbf{C}]^j, ..., (\mathbf{A}_i)^{|P|-1}[\mathbf{C}]^j] \cdot [\alpha_1, ..., \alpha_{|P|}]^T = -\mathbf{d}_j$, i.e., $\mathbf{d}_j$ is in the span of $Contr(\mathbf{A}_i, [\mathbf{C}]^j)$. Moreover, since this reasoning can be applied $\forall \mathbf{d}_j$ of $\mathbf{G}_i$, then $\mathbf{G}_i$ is in the span of $Contr(\mathbf{A}_i, \mathbf{C}^i_{cf})$, and according to Corollary 4.18, the system is BIC over E^*_i. ∎

Finally, from Theorem 4.16, a necessary condition for reachability can also be derived.

Corollary 4.20. *Let $\langle \mathcal{N}, \boldsymbol{\lambda}, \mathbf{m}_0 \rangle$ be a TCPN system. If the marking $\mathbf{m}_1 \in \Re_i$ is reachable from another $\mathbf{m}_0 \in \Re_i$, through a trajectory in $\Re_i$, then $\exists \mathbf{b}$ s.t. $Contr(\mathbf{A}_i, \mathbf{C}_c) \cdot \mathbf{b} = (\mathbf{m}^q - \mathbf{m}_0)$.*

Proof. First, for the incremental system defined from $\mathbf{m}_0$, i.e., $\Delta\mathbf{m} = (\mathbf{m} - \mathbf{m}_0)$, the reachability set is a subset of the span of $Contr(\mathbf{A}_i, \mathbf{B}_i)$ (as explained in the proof of Lemma 4.15). Now, let us proceed by contradiction. Suppose that $\nexists \mathbf{b}$ such that $Contr(\mathbf{A}_i, \mathbf{C}_c) \cdot \mathbf{b} = (\mathbf{m}^q - \mathbf{m}_0)$, thus $(\mathbf{m}^q - \mathbf{m}_0)$ is not in the span of $Contr(\mathbf{A}_i, \mathbf{C}_c)$, which is equal to the span of $Contr(\mathbf{A}_i, \mathbf{B}_i)$. Therefore, $(\mathbf{m}^q - \mathbf{m}_0)$ is not reachable in the incremental system, thus $\mathbf{m}^q$ is not reachable from $\mathbf{m}_0$. ∎

Example 4.6. Consider again the system of fig. 4.5 with $T_c = \{t_4\}$, but with a different timing: $\lambda_1 = \lambda_2 = \lambda_3 = 1$ and $\lambda_4 = 2$. In this case, the sets E^*_3 and E^*_4 remain unchanged (w.r.t. the Example 4.5), but E^*_1 becomes the segment $(\mathbf{m}_1, \mathbf{m}_2]$ shown in fig. 4.5. Moreover, for this system $T^1_{cf} = T^3_{cf} = T^4_{cf} = \{t_4\}$, and

$$\begin{array}{rcl} \mathbf{G}_1 & = & [\ \ 0,\ \ 0,\ \ 0,\ \ 0,\ -1/2,\ 1/2\ ]^T \\ \mathbf{G}_3 & = & [\ \ 0,\ \ 0,\ -1,\ \ 1,\ \ 0,\ \ 0\ ]^T \\ \mathbf{G}_4 & = & [\ -1/3,\ 1/3,\ -1/3,\ 1/3,\ -1/3,\ 1/3\ ]^T \end{array}$$

Since $T^i_{cf} = T_c$ for the three configurations, the first statement of Corollary 4.18 provides sufficient and necessary conditions for controllability over each E^*_i. In this case the system fulfills that condition for the three E^*_i, so, it is BIC over each one.

Note that the system is controllable over E^*_3 with $\boldsymbol{\lambda} = [1, 1, 1, 2]^T$ but not with $\boldsymbol{\lambda} = [1, 1, 1, 1]^T$ (as shown in Example 4.5), i.e., the controllability depends not only in the structure but also on the timing.

Example 4.7. There is an easy alternative for verifying the controllability over E^*_1 and E^*_4 in the system of fig. 4.5 with $T_c = \{t_4\}$ and $\boldsymbol{\lambda} = [1, 1, 1, 2]^T$. By verifying

$$rank\left(\begin{bmatrix} \mathbf{C}\boldsymbol{\Lambda}\boldsymbol{\Pi}_1 \\ \mathbf{B}_y^T \end{bmatrix}\right) = rank\left(\begin{bmatrix} \mathbf{C}\boldsymbol{\Lambda}\boldsymbol{\Pi}_4 \\ \mathbf{B}_y^T \end{bmatrix}\right) = |P|$$

it can be concluded, according to Corollary 4.19, that for any set of controllable transitions T_c, the system is BIC over the corresponding sets E^*_1 and E^*_4, whenever $E^*_1 \cap int\{\Re_1\} \neq \emptyset$ and $E^*_4 \cap int\{\Re_4\} \neq \emptyset$, respectively.

Example 4.8. Now, let us investigate the reachability of this system in $\Re_3$. Consider the markings $\mathbf{m}_5 = [1,\ 0,\ 2,\ 1,\ 0.5,\ 0.5]^T$ and $\mathbf{m}_3 = [0.5,\ 0.5,\ 0.5,\ 2.5,\ 0.5,\ 0.5]^T$ (they are drawn in fig. 4.6(b)). A

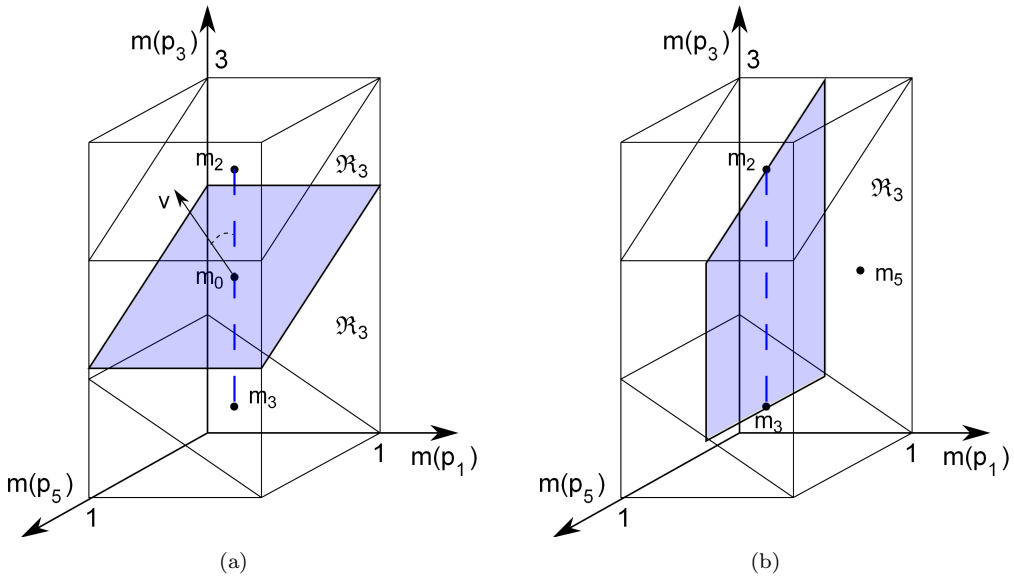

Fig. 4.6: Region $\Re_3$ and set E_3^* for the system of fig. 4.5. a) With $\boldsymbol{\lambda} = [1,1,1,1]^T$, the shadowed area represents the hyperplane that divides $\Re_3$. Vector $\mathbf{v}$, normal to the hyperplane, is pointing upwards. b) The shadowed area represents the span of the controllability matrix for the system with timing $\boldsymbol{\lambda} = [1,1,1,2]^T$.

basis for the range of the controllability matrix of $\Re_3$, i.e., $Contr(\mathbf{C\Lambda\Pi}_3, \mathbf{C}_c)$, is given by

$$\begin{bmatrix} 0 & 0 & 0 & 0 & -1 & 1 \\ 0 & 0 & 1 & -1 & 0 & 0 \end{bmatrix}^T$$

Since $(\mathbf{m}_5 - \mathbf{m}_3) = [0.5, -0.5, 1.5, -1.5, 0, 0]^T$ is not in the range of $Contr(\mathbf{C\Lambda\Pi}_3, \mathbf{C}_c)$ then, according to Corollary 4.20, $\mathbf{m}_1$ is not reachable from $\mathbf{m}_3$, through a trajectory inside $\Re_3$. From a geometrical point of view, the shadowed surface in fig. 4.6 represents the range of $Contr(\mathbf{C\Lambda\Pi}_3, \mathbf{C}_c)$ from $\mathbf{m}_3$, therefore, every marking reachable from $\mathbf{m}_3$, through a trajectory inside $\Re_3$, must belong to this, but it does not mean that all markings in the shadowed surface are reachable.

4.5.4 Controllability over several regions

In our experience, we have always found (but it has not been proved) that the equilibrium set $\mathbb{E}$ is connected. In such case, the following proposition, which introduces a sufficient condition for controllability over the union of connected equilibrium sets, would be the generalization of the results introduced in the previous subsection in order to consider several regions.

Proposition 4.21. *Let $\langle \mathcal{N}, \boldsymbol{\lambda}, \mathbf{m}_0 \rangle$ be a TCPN system. Consider some equilibrium sets E_1^*, E_2^*,..., E_j^* related to different regions $\Re_1$, $\Re_2$,..., $\Re_j$. If the system is BIC over each E_1^* and their union (i.e., $\bigcup_{i=1}^{j} E_i^*$) is connected, then the system is BIC over the union.*

Proof. Consider two of those sets E_1^*, E_2^* such that $E_1^* \cap E_2^* \neq \emptyset$. Let $\mathbf{m}^q$ be a marking such that $\mathbf{m}^q \in E_1^* \cap E_2^*$. Since the system is controllable over E_1^* and E_2^*, there exists a marking $\mathbf{m}_2 \in E_2^* - E_1^*$

that is reachable, in finite time, from another marking in $\mathbf{m}_1 \in E_1^+ - E_2^+$, due to the fact that both are reachable from $\mathbf{m}^q$, in finite time, and to the continuity and positiveness of the flow function (and thus the field vector) in a neighborhood of $\mathbf{m}^q$. Then, any marking of E_2^* is reachable from any marking of E_1^*, via $\mathbf{m}_1$ and $\mathbf{m}_2$. Following a similar reasoning, it can be concluded that the system is controllable over $\bigcup_{i=1}^{j} E_i^*$. ∎

Algorithm C.2 (introduced in Appendix C) can be used to compute an equilibrium marking that belongs to two given equilibrium sets E_1^* and E_2^*, if it exists. In this way, it can be investigated wether E_1^* and E_2^* are connected.

Example 4.9. Consider the system of fig. 4.5, where $T_c = \{t_4\}$, $\lambda_1 = \lambda_2 = \lambda_3 = 1$ and $\lambda_4 = 2$. It has been previously shown that the system is controllable over each E_i^*. Now, since the union of E_1^*, E_3^* and E_4^* is connected, then, according to Proposition 4.21, the system is BIC over $E_1^* \cup E_3^* \cup E_4^*$. For instance, it is possible to transfer the system from $\mathbf{m}_3$ to a marking arbitrarily close to $\mathbf{m}_1$ ($\mathbf{m}_1 \notin E_1^*$, but any marking $\mathbf{m}_1'$ in the open interval $(\mathbf{m}_1, \mathbf{m}_2]$ belongs to E_1^*) and in the opposite direction. Note that, in this case, the union of those sets is almost the entire $\mathbb{E}$. Actually, $E_1^* \cup E_3^* \cup E_4^* = \mathbb{E} - \{\mathbf{m}_1, \mathbf{m}_4\}$ ($\mathbf{m}_4 \notin E_4^*$ because at this marking the flow at transitions $\{t_1, t_2, t_3\}$ is null).

4.6 Conclusions on controllability

A local controllability concept has been introduced in this chapter as a reformulation of the classical one defined for linear systems. Accordingly, controllability over a subset S implies reachability of S, assuming $\mathbf{m}_0 \in S$. For models in which control actions can be applied to all transitions, sufficient and necessary conditions for reachability and controllability has been provided. In this case the controllability over $int\{Class(\mathbf{m}_0)\}$ is guaranteed iff the system is consistent, obtaining thus a purely structural characterization of controllable models.

For systems with uncontrollable transitions, sufficient and necessary conditions for controllability, over subsets of equilibrium markings that belong to a given region, have been introduced. Moreover, a sufficient condition for controllability over the union of those subsets has been derived. It has been shown that the controllability with uncontrollable transitions depends not only on the structure of the net but also on the timing.

Chapter 5

Control synthesis

Continuous Petri nets are relaxations of discrete Petri nets, but at the same time, they are continuous-state systems (in fact, they are technically hybrid). In this way, it seems natural to consider two different approaches for the control concept: 1) at the discrete level, the extension of control techniques used in discrete PN's, as the supervisory-control theory (for instance, [Holloway et al., 1997b, Iordache and Antsaklis, 2006]) and 2) at the fluidized level, the application of control techniques developed for continuous-state systems. Usually, the control objective in the first approach is to meet some safety specifications, like avoiding *forbidden* states (e.g., deadlocks or markings that unavoidable lead to a deadlock, markings that violate mutual exclusion specifications, etc.), by means of disabling transitions at particular states. The objective of the second approach consists in driving the system, by means of a (usually) continuous control action, towards a desired steady state, or state trajectory (see, for instance, [Chen, 1984]). Regarding control on continuous Petri nets, most of the specific works that can be found in the literature deals with the second control approach applied to the *infinite* server semantics model. Accordingly, the same approach will be considered in this Chapter, as already adopted in Chapter 5 for the controllability analysis.

Enforcing a desired steady state or target marking in a continuous PN is analogous to reaching an average marking in the original discrete model (assuming that the continuous model approximates the discrete one), which may be interesting in several kinds of systems. This idea has been illustrated by different authors and will be discussed in detail in Chapter 6.

Through this chapter, three techniques will be proposed for the control of TCPNs, under infinite server semantics, in order to reach a desired target marking. In the first one (Section 5.2), a centralized *affine* control strategy is introduced, assuming that all the transitions are controllable. An extension of this will be introduced in Section 5.3, by decomposing the net system into an interconnected set of subsystems leading to a decentralized control strategy, reducing thus the complexity involved in the synthesis procedure. Finally, a centralized pole-assignment control technique will be presented in Section 5.4, in which the existence of uncontrollable transitions is considered. Before that, in the following subsections a few of control techniques will be recalled from the literature, in order to provide a wider perspective of the control problem in TCPN systems.

5.1 Preliminarily discussion of control methods found in the literature

Through the following paragraphs, a few of control techniques, proposed in the literature for continuous Petri nets, will be recalled. Similar to the *set-point* control problem in state-continuous systems, the control objective here consists in driving the system towards a desired target marking (a steady state, here denoted as $\mathbf{m}_d$). This desired marking can be selected, in a preliminarily planning stage, according to some optimality criterion [Silva and Recalde, 2004], e.g., maximizing the flow. Most of the work done on this issue is devoted to centralized dynamic control assuming that all the transitions are controllable. It will be firstly presented those control techniques that require to control all the transitions, while a couple of techniques (gradient-base and pole assignment), where uncontrollable transitions are considered, will be presented at the end of this subsection.

Fuzzy control [Hennequin et al., 1999]- The authors showed that the flow of a fluid transition, under infinite server semantics with an implicit self-loop, can be represented as the output of two fuzzy rules under the Sugeno model. It was proved that if the integral of the output of each fuzzy rule converges to a finite value then the resulting global fuzzy system (that represents the controlled flow) converges as well. Moreover, upper and lower bounds of this convergence were derived. Based on that, it was proposed a *proportional fuzzy control*, proving convergence of the system to the desired output (the marking of a place $p_j \in P$, i.e., $\mathbf{m}_d[p_j]$), assuming that this is smaller than the initial upstream marking, i.e., $\mathbf{m}_d[p_j] \leq \mathbf{m}_0[p_i], \forall p_i \in {}^\bullet p_j$, which is not the general case.

Control for a piecewise-straight marking trajectory - Dealing with the tracking control problem of a mixed ramp-step reference signal, this approach was firstly explored in [Jing et al., 2008a] for Join-Free nets and extended to general PNs in [Jing et al., 2008b]. There, a high & low gain proportional controller is synthesized, while a polygonal trajectory, as a sort of *path-planning* problem at a higher level, is computed. Let us detail a related synthesis procedure introduced in [Apaydin-Ozkan et al., 2009]. Consider the line l connecting $\mathbf{m}_0$ and $\mathbf{m}_d$, and the markings in the intersection of l with the region's borders, denoted as $\mathbf{m}_c^1$, $\mathbf{m}_c^2$, ..., $\mathbf{m}_c^n$. Define $\mathbf{m}_c^0 = \mathbf{m}_0$ and $\mathbf{m}_c^{n+1} = \mathbf{m}_d$. Then, $\forall k \in \{0, n\}$ compute τ_k by solving the linear programming problem (LPP):

$$\begin{array}{ll} min\, \tau_k & \\ s.t.: & \mathbf{m}_c^{i+1} = \mathbf{m}_c^i + \mathbf{C} \cdot \mathbf{x} \\ & 0 \leq x_j \leq \lambda_j [\mathbf{\Pi}_j^z]_i \, min\{\mathbf{m}_c^i, \mathbf{m}_c^{i+1}\}\tau_k \\ & \forall j \in \{1, ..., |T|\} \text{ where i satisfies } [\mathbf{\Pi}_j^z]_i \neq \mathbf{0} \end{array} \tag{5.1}$$

The control law to be applied is thus $\mathbf{w} = \mathbf{x}/\tau_k$ (the model is represented as $\dot{\mathbf{x}} = \mathbf{C}\mathbf{w}$, where $\mathbf{w} = \mathbf{\Lambda\Pi}(\mathbf{m})\mathbf{m} - \mathbf{u}$), when the system is between the markings $\mathbf{m}_c^k$ and $\mathbf{m}_c^{k+1}$. The time required for reaching the desired marking is given by $\tau_f = \sum_{k=0}^{n} \tau_k$. *Feasibility* and *convergence* to $\mathbf{m}_f$ were proved in [Apaydin-Ozkan et al., 2009].

In order to obtain faster trajectories, intermediate states, not necessarily on the line connecting the initial and the target marking, can be computed by means of a *bilinear* programming problem (BPP). The idea is to currently compute the intermediate markings $\mathbf{m}_c^k$, on the borders of the regions, that minimizes the total time $\tau_f = \sum_{k=0}^{n} \tau_k$ with some additional monotonicity constraints. Finally, the same

algorithm can be adapted in order to recursively compute intermediate markings in the interior of the regions, obtaining thus faster trajectories.

Model predictive control (MPC) [Mahulea et al., 2008a] - Here, two solutions were considered based on the *implicit* and *explicit* methods (see, for instance, [Bemporad et al., 2002]). The evolution of the timed continuous Petri net model, in *discrete-time*, is represent by the difference equation: $\mathbf{m}_{k+1} = \mathbf{m}_k + \Delta\tau \cdot \mathbf{C} \cdot \mathbf{w}_k$, subject to the constraints $\mathbf{0} \leq \mathbf{w}_k \leq \mathbf{f}_k$ with $\mathbf{f}_k$ being the flow without control, which is equivalent to $\mathbf{P} \cdot [\mathbf{w}_k^T, \mathbf{m}_k^T]^T \leq \mathbf{0}$, for a particular matrix $\mathbf{P}$. The sampling $\Delta\tau$ must be chosen small enough in order to avoid spurious markings, in particular, for ensuring the positiveness of the markings. For that, the following condition is required to be fulfilled $\forall\, p \in P \;:\; \sum_{t_j \in p^\bullet} \lambda_j \Delta\tau < 1$.

The goal of the MPC control scheme introduced in [Mahulea et al., 2008a] is to drive the system towards a desired marking $\mathbf{m}^d$, while minimizing the quadratic performance index $J(\mathbf{m}_k, N) = (\mathbf{m}_{k+N} - \mathbf{m}_d)^T \mathbf{Z} (\mathbf{m}_{k+N} - \mathbf{m}_d) + \sum_{j=0}^{N-1} [(\mathbf{m}_{k+j} - \mathbf{m}_d)^T \mathbf{Q} (\mathbf{m}_{k+j} - \mathbf{m}_d) + (\mathbf{w}_{k+j} - \mathbf{w}_d)^T \mathbf{R} (\mathbf{w}_{k+j} - \mathbf{w}_d)]$, where $\mathbf{Z}$, $\mathbf{Q}$ and $\mathbf{R}$ are positive definite matrices and N is a given time horizon. This leads to the following optimization problem that needs to be solved in each time step:

$$\begin{aligned} &\min J(\mathbf{m}_k, N) \\ &\text{s.t.} : \forall j \in \{0, ..., N-1\}, \qquad \mathbf{m}_{k+j+1} = \mathbf{m}_{k+j} + \Delta\tau \cdot \mathbf{C} \cdot \mathbf{w}_{k+j} \\ &\qquad\qquad\qquad\qquad\quad \mathbf{P} \cdot \begin{bmatrix} \mathbf{w}_{k+j} \\ \mathbf{m}_{k+j} \end{bmatrix} \leq \mathbf{0} \\ &\qquad\qquad\qquad\qquad\quad \mathbf{w}_{k+j} \geq \mathbf{0} \end{aligned} \tag{5.2}$$

In [Mahulea et al., 2008a] it was shown that the standard techniques used for ensuring converge in linear/hybrid systems, i.e., terminal constraints or terminal cost, cannot be applied in continuous nets. Nevertheless, a particular control law, guaranteeing *asymptotic stability* for all possible initial and final states, was proposed. Simulations showed that the horizon N is not required to be too large (actually, it is well known in classical systems' theory that $\exists \bar{N}$ s.t. $\forall \mathbf{m}_0$ and $\forall N \geq \bar{N}$, the finite and the infinite horizon controllers are equal). Nevertheless, sometimes N is such that the computational time needed to solve the optimization problem becomes larger than the sampling period, making the implementation unfeasible.

An alternative MPC approach for this problem is the *explicit* solution [Bemporad et al., 2002], where the set of all states that are controllable is split into polytopes. In each polytope the control command is defined as a piecewise affine function of the state. The closed-loop *stability* is guaranteed with this approach. On the contrary, when either the order of the system or the length of the prediction horizon are not small, the *complexity* of the explicit controller becomes quickly prohibitive. Furthermore, the computation of the polytopes sometimes is unfeasible.

Proportional control synthesis with LMI [Kara et al., 2009]- The proposed control scheme consists of a set of proportional (affine) control laws, one for each region. In detail, the controlled flow is represented, in discrete time, by $\mathbf{w}_k = \mathbf{F}^r(\mathbf{m}_k - \mathbf{m}^d) + \mathbf{R}$, where $\mathbf{R}$ is a vector and $\mathbf{F}^r$ is a gain matrix computed for each region (the superindex r denotes the $r-th$ region). In each region, the control and the marking are required to fulfill:

1. the input constraints: $\mathbf{0} \leq \mathbf{w}_k \leq \mathbf{f}_k$, where $\mathbf{f}_k$ represents the flow without control,

2. the region membership: $\mathbf{m}_k \in \mathcal{P}(\mathbf{S}^r, \mathbf{g}^r)$, where $\mathcal{P}(\mathbf{S}^r, \mathbf{g}^r) = \{\mathbf{m} | \mathbf{S}^r\mathbf{m} \leq \mathbf{g}^r\}$ is the inequality representation of the r-th region (a polyhedral),

3. the existence of a contractive invariant set (in order to prove closed-loop stability), which is stated as: $\mathbf{x}_k \in \mathcal{P}(\mathbf{Q}, \boldsymbol{\mu}) \rightarrow \mathbf{x}_{k+1} \in \mathcal{P}(\mathbf{Q}, \alpha\boldsymbol{\mu})$, where $\mathbf{x}_k = (\mathbf{m}_k - \mathbf{m}_d)$ is the current error, $\alpha < 1$ and $\mathcal{P}(\mathbf{Q}, \alpha\boldsymbol{\mu}) = \{\mathbf{x} | \mathbf{Q}\mathbf{x} \leq \alpha\boldsymbol{\mu}\}$ is the contractive set (so, the absolute error is monotonic decreasing).

The methodology consists in expressing the previous conditions as sets of linear matrix inequalities (LMI), one set for each region. The solution of a LMI can be achieved in polynomial time. Furthermore, *converge* to the desired marking $\mathbf{m}_d$ is guaranteed. The main drawback of this approach is that a LMI must be solved for each region, but the number of these increases exponentially w.r.t. the number of synchronizations (joins).

ON-OFF (minimum-time) control for persistent nets [Wang et al., 2010] - Stronger results may be obtained when the problem is restricted to particular net subclasses. Accordingly, the minimum-time control problem was solved in this work for *persistent continuous Petri nets* (i.e., net systems where the enabling of any transition t_j cannot decrease by the firing of any other transition $t_i \neq t_j$). First, a minimal firing count vector $\boldsymbol{\sigma}$ s.t. $\mathbf{m}_d = \mathbf{m}_0 + \mathbf{C}\boldsymbol{\sigma}$ is computed ($\boldsymbol{\sigma}$ is minimal if for any T-semiflow $\mathbf{x}$, $||\mathbf{x}|| \not\subseteq ||\boldsymbol{\sigma}||$, where $||\cdot||$ stands for the support of a vector). Later, the control law is defined, for each transition t_j, as:

$$\mathbf{u}[t_j] = \begin{cases} 0 & \text{if } \int_0^{\tau^-} \mathbf{w}[t_j]d\tau < \boldsymbol{\sigma}[t_j] \\ \mathbf{f}[t_j] & \text{if } \int_0^{\tau^-} \mathbf{w}[t_j]d\tau = \boldsymbol{\sigma}[t_j] \end{cases}$$

This means that if t_j has not been fired an amount of $\boldsymbol{\sigma}[t_j]$, then t_j is completely ON. Otherwise, t_j is completely OFF (it is blocked). It is proved that this ON-OFF control policy drives the system towards $\mathbf{m}_d$ in *minimum time*. An intuitive reason for this is that, for persistent nets, the firing order is irrelevant for reaching a marking. Thus, what only matters is the amount of firings required, which is provided by $\boldsymbol{\sigma}$.

Gradient-base control with uncontrollable transitions [Lefebvre et al., 2007]- Here, the input control actions consist in reducing the rates of the controllable transitions from their nominal maximum values, which is equivalent to reduce the flow, as considered along this dissertation. Nevertheless, the goal of the control problem is slightly different, since it is no longer required to drive the whole marking of the system to a desired value, but only the marking of a subset of places (the *output* of the system). The analysis is achieved in discrete time. Let us provide the basic idea for the case of a single-output system. Firstly, a cost function is defined as $v_k = 1/2\epsilon_k^2$, where ϵ_k denotes the output error. The control proposed has an structure like: $\mathbf{u}_k = \mathbf{u}_{k-1} - (\mathbf{s}_k\mathbf{s}_k^T + \alpha\mathbf{I})^{-1}\mathbf{s}_k\epsilon_k$, where the input $\mathbf{u}_k$ is the rate of the controllable transitions and $\mathbf{s}_k$ is the output sensitivity function vector with respect to the input (the gradient vector $\nabla_{\mathbf{u}}\, y$). The factor $\alpha > 0$ is a small term added to avoid ill conditioned matrix computations. The gradient is computed by using a first order approximation method. One of the advantages of this approach is that the change of regions (or configurations) is not explicitly taken into account during the computation of the gradient. Furthermore, a sufficient *condition for stability* is provided.

Pole assignment control with uncontrollable transitions [Vázquez and Silva, 2009b] - This control technique will be discussed in detail in Section 5.4. In a first step, it is assumed that the initial and desired markings are equilibrium ones and belong to the same region. The control approach considered

Tab. 5.1: Qualitative characteristics of control laws. The following abbreviations are used: conf. (configuration), min. (minimize), func. (function), exp. (exponential), comp. (complexity) and pol. (polynomial).

Technique	Computational issues	Optimality criterion	Subclass	T_{nc}	Stability
PW-straight trajectory	a LPP for each conf.	heuristic for min. time	all	no	yes
MPC	exp. comp. on $\|T\|, N$	min. quadratic or linear func. of $\mathbf{m}, \mathbf{u}$	all	no	under suf. conditions
LMI	a LMI for each conf.	none	all	no	yes
ON-OFF	linear comp. on $\|T\|$	minimum time	structurally persistent	no	yes
Gradient-based	pol. comp. on # outputs	min. quadratic error	all	yes	under a suf. condition
Pole-assignment	a pole-assignment for each conf.	none	all	yes	yes

has the following structure: $\mathbf{u} = \mathbf{u}'_d + \mathbf{K}(\mathbf{m} - \mathbf{m}'_d)$, where $(\mathbf{m}'_d, \mathbf{u}'_d)$ is a suitable intermediate equilibrium marking. The gain matrix $\mathbf{K}$ is computed, by using any pole-assignment technique, in such a way that the controllable poles are settled as distinct, real and negative. Intermediate markings $\mathbf{m}'_d$, with their corresponding input $\mathbf{u}'_d$, are computed during the application of the control law (either at each sampling period or just at an arbitrary number of them) by using a given LPP with linear complexity that guarantees that the required input constraints are fulfilled. Later, those results are extended in order to consider several regions. For this, it is required that the initial and desired markings belong to a connected union of equilibrium sets, i.e., $\mathbf{m}_0 \in E_1^*$, $\mathbf{m}_d \in E_n^*$ and $\cup_{i=1}^n E_i^*$ is connected. Thus, there exist equilibrium markings $\mathbf{m}_1^q, ..., \mathbf{m}_{n-1}^q$ on the borders of consecutive regions, i.e., $\mathbf{m}_j^q \in E_j^* \cap E_{j+1}^*$, $\forall j \in \{1, .., j-1\}$. A gain matrix $\mathbf{K}_j$, satisfying the previously mentioned conditions, is computed for each region. Then, inside each jth region, the control action $\mathbf{u} = \mathbf{u}'_d + \mathbf{K}_j(\mathbf{m} - \mathbf{m}'_d)$ is applied, where $\mathbf{m}'_d$ is computed, belonging to the segment $[\mathbf{m}_j^q, \mathbf{m}_{j+1}^q]$, by using a similar LPP. It was proved that this control law can always be computed and applied (*feasibility*). Furthermore, *convergence* to the desired $\mathbf{m}_d$ was also demonstrated, whenever the conditions for controllability are fulfilled and $\cup_{i=1}^n E_i^*$ is connected (see Chapter 4). The main drawback of this technique is that a gain matrix and a LPP have to be derived for each region in the marking path.

5.1.1 Preliminary comparison of control methods under infinite server semantics

Having several control methods available for timed continuous PNs, a question that may arise concerns the selection of the most appropriate technique for a given particular system and purpose, and the necessity for deriving more of them. There are several properties that may be taken into account, like feasibility, closed-loop stability, robustness, computational complexity (for the synthesis and during the application), etc.

Table 5.1 resumes a few qualitative properties of some of the control methods described above. Accordingly, provided a structurally persistent PN, the natural choice will be an $ON - OFF$ control law, since it does not exhibit computational problems, ensures convergence an provides the minimum-time transient behavior. For no-persistent nets, MPC ensures converge and minimizes a quadratic criterion. Nevertheless, when the number of transitions grows, the complexity may become untractable. In such case, control synthesis based on LMI or enforcing piecewise-straight trajectories would be more appropriated. Finally, control laws based on gradient-descendent and pole assignment methods are developed in order to deal with uncontrollable transitions. The synthesis of this last technique becomes tedious (but automatizable) when several configurations appear in the system, since a pole assignment is required for each configuration. This problem does not appear for the gradient based controller; on the contrary, this technique does not guarantee convergence for the general case, while the pole assignment does it.

Given a system with just a few configurations and transitions, all of them being controllable, most of the described control laws could be synthesized and applied to it, ensuring convergence. In such case, the criterion for selecting one of them may be a quantitative one, like minimizing either a quadratic optimization criterion or the time spent for reaching the desired marking. At the present moment, such quantitative comparison has not systematically been made, but it is our intuition that the transient response of the mentioned techniques should be comparable (of the same order of magnitude), i.e., one technique could be the best for a TCPN system, while another technique could be better for a slightly different model.

In general, there does not exist a control technique that can deal with general net subclasses having large net structures, ensuring stability and, at the same time, minimizing an optimization criterion. This lack of techniques is specially remarkable when uncontrollable transitions are considered. For this reason, through this chapter a couple of control law structures will be derived, in order to deal with systems with a large net structure 5.3 and systems with uncontrollable transitions 5.4.

5.1.2 Towards decentralized control

In the literature, there is lack of techniques for the efficient synthesis of controllers for systems with large net structures (with many places and transitions). For this topic, it seems natural to consider decentralized and distributed control strategies.

In a completely distributed approach, the model can be considered as composed of several subsystems that share information through *communication channels*, modeled by places. For each subsystem, a controller is designed. The mission of each local controller is to drive its corresponding subsystem from its initial marking to a required one, taking into account the interaction with the other subsystems. For this, it is required that neighboring local controllers share information. This problem has been addressed in [Apaydin-Ozkan et al., 2010] for a system composed of two MTS subsystems asynchronously connected (through places: channels or buffers). The key point is related to the coordination among local controllers and the possibility of concurrently reaching the target marking in every subsystem. A *consensus* algorithm is proposed in order to coordinate the local controllers, sharing information about the tokens sent and required by each subsystem. Feasibility and concurrent convergence are demonstrated.

A second approach will be discussed in detail in Section 5.3, in which the existence of an upper-level controller, named *coordinator*, is allowed [Vázquez et al., 2011]. This coordinator may receive and send information to the local controllers, but it cannot apply control actions directly to the TCPN system. The existence of such coordinator increases the capability of the local controllers, allowing to consider wider classes for the net subsystems. Subsystems are assumed to be (separately) live and consistent, but they are not restricted to particular net subclasses. Each local controller is defined as a properly-scaled affine control law, while the coordinator is an agent that receives, processes (with a linear-complexity algorithm) and sends information to the local controllers. Feasibility and concurrent convergence to the required markings are proved.

5.2 Affine control laws for TCPNs

Through this section, an affine control strategy will be derived for TCPN systems, assuming that all the transitions are controllable and the net system is consistent, thus controllable over the interior of $Class(\mathbf{m}_0)$ (Lemma 4.5).

The control scheme proposed here is based on the work reported in [Habets and van Schuppen, 2004], [Habets et al., 2006], regarding the control synthesis for piecewise-affine hybrid systems, which can be seen as a wider hybrid class that includes TCPNs. Nevertheless, TCPNs represent a complex case when using the techniques developed in [Habets et al., 2006], because of the existence of state-dependent input constraints (that are not considered in [Habets and van Schuppen, 2004, Habets et al., 2006]), and the fact that TCPN systems mainly evolve in high dimension polytopes (which significantly increases the complexity during the control synthesis). In this way, the techniques introduced there will be slightly extended here in order to synthesize affine controllers for TCPN models in a different way. For this purpose, let us recall a few results through the following subsection.

5.2.1 Affine control laws for simplices in affine systems

Let us start with a few definitions. A *polyhedral* set is a subset of $\mathbb{R}^m$, described by a finite number of linear inequalities. A bounded polyhedral set is called a *polytope*. Alternatively, a polytope can be characterized as the convex hull of a finite number of points: the *vertices* of the polytope. A *face* of a polyhedral set is the intersection of the set with one of its supporting hyperplanes. If a polyhedral set $\mathcal{P}$ has dimension m, the faces of $\mathcal{P}$ of dimension $m-1$ are called *facets*. A description of several problems encountered during the synthesis and analysis in polyhedrals and several algorithms for their resolution, including the computation of the vertices, are provided by [Fukuda, 2000]. An m-dimensional polytope with exactly $m+1$ vertices is called a *simplex*. The number of facets in a simplex is equal to the number of its vertices, i.e., $m+1$.

Definition 5.1. An *affine system* in a polytope $\mathcal{X}$ is:

$$\dot{\mathbf{x}} = \mathbf{A}\mathbf{x} + \mathbf{B}\mathbf{u} + \mathbf{a} \tag{5.3}$$

with the restrictions $\mathbf{x} \in \mathcal{X}$ and $\mathbf{u} \in \mathcal{U}$, where $\mathcal{U}$ is a polytope of admissible inputs.

An admissible *affine control law* is an affine function $\mathbf{u} : \mathcal{X} \to \mathcal{U}$ characterized by $\mathbf{u}(\mathbf{x}) = \mathbf{F}\mathbf{x} + \mathbf{g}$.

Let $\mathcal{S}$ denote a closed full-dimensional simplex in $\mathbb{R}^m$ with vertices $\mathbf{v}_1, ..., \mathbf{v}_{m+1}$. Let $F_1, ..., F_{m+1}$ denote the facets of S, and assume that the facets are numbered in such a way that for $i = 1, .., m+1$, $\mathbf{v}_i$ is the only vertex not belonging to facet F_i. For $i = 1, .., m+1$, let $\mathbf{n}_i$ denote the outward unit normal vector of facet F_i. Considering an affine control law $\mathbf{u}(\mathbf{x}) = \mathbf{F}\mathbf{x} + \mathbf{g}$, the evaluation of this at the vertices of S will be denoted as $\mathbf{u}_j = \mathbf{u}(\mathbf{v}_j)$, $\forall j \in \{1, ..., m+1\}$.

Due to the linearity of both the system and the control law inside $\mathcal{S}$, the evaluation of the control law, at the vertices of $\mathcal{S}$, must fulfill

$$[\mathbf{F}, \mathbf{g}] \cdot \begin{bmatrix} \mathbf{v}_1 & ... & \mathbf{v}_{m+1} \\ 1 & ... & 1 \end{bmatrix} = [\mathbf{u}_1, ..., \mathbf{u}_{m+1}] \tag{5.4}$$

Since $\mathcal{S}$ is a full-dimensional simplex then the matrix $\begin{bmatrix} \mathbf{v}_1 & ... & \mathbf{v}_{m+1} \\ 1 & ... & 1 \end{bmatrix}$ is square and has full rank. Therefore, there is a bijection between $(\mathbf{F}, \mathbf{g})$ and the set of values $\mathbf{u}_j$ (with $j \in \{1, ..., m+1\}$). In the sequel, for the synthesis of a control law, the values of the input $\mathbf{u}_j$ at the vertices are first computed. Once these are obtained, the pair $(\mathbf{F}, \mathbf{g})$ can be computed by using (5.4).

Consider the following conditions for the values $\mathbf{u}_j$:

Condition 1. From Theorem 4.12 in [Habets et al., 2006], a facet F_i is *disabled* by the control action $\mathbf{u}(\mathbf{m}) = \mathbf{F}\mathbf{x} + \mathbf{g}$, whose valuation at vertices $\mathbf{v}_1, ..., \mathbf{v}_{m+1}$ is given by $\mathbf{u}_1, ..., \mathbf{u}_{m+1}$, iff

$$\forall j \in \{1, ..., m+1\} \backslash \{i\} \quad \mathbf{n}_i^T (\mathbf{A}\mathbf{v}_j + \mathbf{B}\mathbf{u}_j + \mathbf{a}) \leq 0 \tag{5.5}$$

Condition 2. Let $\mathbf{x}_f \in S$, and $(\mu_1, ..., \mu_{m+1})$ be s.t. $\sum_{j=1}^{m+1} \mu_j \mathbf{v}_j = \mathbf{x}_f$. According to Theorem 4.19 in [Habets et al., 2006], $\mathbf{x}_f$ is the *unique equilibrium point* in $\mathcal{S}$ (in closed loop) iff

$$i)\, \mathbf{B} \sum_{j=1}^{m+1} \mu_j \mathbf{u}_j = -\mathbf{A}\mathbf{x}_f - \mathbf{a} \qquad \{\text{i.e., } \dot{\mathbf{x}}_f = \mathbf{0}\} \tag{5.6}$$

$$ii)\, span(\{\mathbf{A}\mathbf{v}_j + \mathbf{B}\mathbf{u}_j | j = 1, ..., m+1\}) = \mathbb{R}^m \tag{5.7}$$

According to Theorems 4.18-4.19 in [Habets et al., 2006], conditions (5.5-5.7) can be combined in order to compute a control law that fulfills different requirements. Here, we are interested in two particular problems:

Problem 1.a) Find an admissible affine control law such that for every initial state $\mathbf{x}_0 \in S$, the corresponding state trajectory $\mathbf{x}(t, \mathbf{x}_0)$ of the closed-loop system satisfies $\forall t \geq 0$, $\mathbf{x}(t, \mathbf{x}_0) \in S$, i.e., the system remains inside $\mathcal{S}$.

Problem 1.b) Additionally, it holds $lim_{t \to \infty} \mathbf{x}(t, \mathbf{x}_0) = \mathbf{x}_f$.

Solution: Problem 1.a is solved by computing values for the control law at the vertices $\mathbf{u}_j$ in such a way that (5.5) is fulfilled for all the facets of $\mathcal{S}$. Problem 1.b is solved if additionally *condition 2* is fulfilled, i.e., (5.6) and (5.7). Note that (5.5) and (5.6) are linear inequalities (only the values of $\mathbf{u}_j$ are unknown, while other vectors and parameters are known) then the computation of values $\mathbf{u}_j$ satisfying (5.5) and (5.6) can be done in polynomial time. Once these are computed, it must be checked wether (5.7) holds or not, in a negative case, $\mathbf{u}_j$ should be computed again (the set of solutions $\mathbf{u}_j$ that do not fulfill (5.7) is on a smaller dimension manifold, so, it is improbable to obtain such values during the

computation). Finally, the control law, i.e., the pair $(\mathbf{F}, \mathbf{g})$, can be obtained by solving (5.4).

Through the next subsection, the results previously recalled will be extended to polytopes, which are mostly encountered during the synthesis of controllers for TCPN systems ($Class(\mathbf{m}_0)$ is, in general, a polytope).

5.2.2 Affine control on polytopes

A possible solution for the synthesis of affine controllers in polytopes consists in decomposing the polytope into simplices and synthesizing an affine control law for each of them [Habets and van Schuppen, 2004]. In this subsection, a different approach will be introduced, by synthesizing a unique (global) affine control law for the complete polytope. The resulting control scheme is more conservative, but it will be demonstrated that such control law can always be computed for TCPN systems.

In polytopes, the matrix $\begin{bmatrix} \mathbf{v}_1 & ... & \mathbf{v}_{m+1} \\ 1 & ... & 1 \end{bmatrix}$ in (5.4) has, in general, more columns than rows, i.e., the number of vertices is larger than the dimension of the polytope plus 1. Therefore, computing the values $\mathbf{u}_j$ that fulfill the required conditions may not be sufficient for obtaining a control law, since the existence of a pair $(\mathbf{F},\mathbf{g})$ that satisfies (5.4), for the obtained values $\mathbf{u}_j$, is not guaranteed. In this case, it is additionally required that the same linear dependencies that involve the vertices $\mathbf{v}_j$ be also effective for the values $\mathbf{u}_j$.

Proposition 5.2. *Consider a polytope of dimension $k-1$ with m vertices, and the values for the input at those ($\mathbf{u}_j$, $j \in \{1,...,m\}$). Assume, without loss of generality, that the first k vertices define a simplex of dimension $k-1$. Thus, for each vertex $\mathbf{v}_j \neq \mathbf{v}_1$ there exists a unique column vector $\boldsymbol{\gamma}_i$ s.t. $\mathbf{v}_j - \mathbf{v}_1 = [\mathbf{v}_2 - \mathbf{v}_1, \mathbf{v}_3 - \mathbf{v}_1, ..., \mathbf{v}_k - \mathbf{v}_1]\boldsymbol{\gamma}_j$.*

There exists a pair $(\mathbf{F}, \mathbf{g})$ that fulfills (5.4) iff:

$$\forall j \in \{k+1, ..., m\}, \qquad (\mathbf{u}_j - \mathbf{u}_1) = [(\mathbf{u}_2 - \mathbf{u}_1), (\mathbf{u}_3 - \mathbf{u}_1), ..., (\mathbf{u}_k - \mathbf{u}_1)]\, \boldsymbol{\gamma}_j \tag{5.8}$$

Proof. By hypothesis, the first k vertices define a simplex of dimension $k-1$, the same dimension of the whole polytope. Therefore, all the vertices belong to the hyperplane defined by the first k vertices (see fig. 5.1). Then, for each $\mathbf{v}_j \neq \mathbf{v}_1$ it must exist a vector $\boldsymbol{\gamma}_j$ s.t. $(\mathbf{v}_j - \mathbf{v}_1) = [(\mathbf{v}_2 - \mathbf{v}_1), ..., (\mathbf{v}_k - \mathbf{v}_1)]\boldsymbol{\gamma}_j$. Furthermore, the matrix $[(\mathbf{v}_2 - \mathbf{v}_1), ..., (\mathbf{v}_k - \mathbf{v}_1)]$ has full column rank, which implies that $\boldsymbol{\gamma}_j$ is unique. Now, (5.4) is equivalent to $\forall j\ \mathbf{u}_j = \mathbf{F}\mathbf{v}_j + \mathbf{g}$. Since the first k vertices define a full-dimensional simplex then there always exists a unique pair $(\mathbf{F}, \mathbf{g})$ that fulfills $\mathbf{u}_j = \mathbf{F}\mathbf{v}_j + \mathbf{g}$, $\forall j \in \{1, .., k\}$. Such pair also fulfills $\mathbf{u}_j = \mathbf{F}\mathbf{v}_j + \mathbf{g}$, $\forall j \in \{k+1, .., m\}$, iff $(\mathbf{u}_j - \mathbf{u}_1) = \mathbf{F}(\mathbf{v}_j - \mathbf{v}_1)$, $\forall j \in \{k+1, .., m\}$. Substituting $(\mathbf{v}_j - \mathbf{v}_1)$ by the expression previously obtained, it results $(\mathbf{u}_j - \mathbf{u}_1) = \mathbf{F}[(\mathbf{v}_2 - \mathbf{v}_1), ..., (\mathbf{v}_k - \mathbf{v}_1)]\boldsymbol{\gamma}_j$. Finally, this equation is equivalent to $(\mathbf{u}_j - \mathbf{u}_1) = [(\mathbf{u}_2 - \mathbf{u}_1), ..., (\mathbf{u}_k - \mathbf{u}_1)]\boldsymbol{\gamma}_j$. ∎

For polytopes, the indices of the vertices in (5.5) need to be reconsidered. If F_i is a facet that must be disabled (*condition 1*) then, denoting as $\mathcal{I}_{F_i}$ the indices of the vertices related to F_i, (5.5) is rewritten as

$$\forall j \in \mathcal{I}_{F_i} \quad \mathbf{n}_i^T(\mathbf{A}\mathbf{v}_j + \mathbf{B}\mathbf{u}_j + \mathbf{a}) \leq 0 \tag{5.9}$$

Similarly, (5.6) can be rewritten, by describing $\mathbf{x}_f$ as a linear combination of linearly independent

vertices. Assume, without loss of generality, that the first k vertices define a simplex having the same dimension of the polytope. Then, define $(\mu_1, ..., \mu_k)$ such that $\sum_{j=1}^{k} \mu_j \mathbf{v}_j = \mathbf{x}_f$. Thus, (5.6) is transformed into

$$\mathbf{B} \sum_{j=1}^{k} \mu_j \mathbf{u}_j = -\mathbf{A}\mathbf{x}_f - \mathbf{a} \tag{5.10}$$

In this way, the results recalled in Subsection 5.2.1, regarding the control problems 1.a and 1.b, are extended to polytopes.

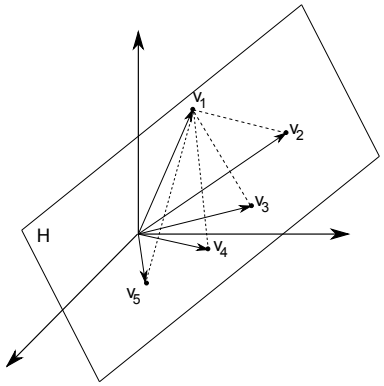

Fig. 5.1: Figure for the proof of Proposition 5.2. Vertices belong to the hyperplane H. Dashed lines represent vectors ($\mathbf{v}_j$-$\mathbf{v}_1$).

5.2.3 Affine control laws for TCPN systems

Consider a TCPN system, controllable over the interior of $Class(\mathbf{m}_0)$ (thus, according to Lemma 4.5, the net is consistent). Define the set $int_\epsilon\{Class(\mathbf{m}_0)\} = \{\mathbf{m} \in Class(\mathbf{m}_0) | \mathbf{m} \geq \mathbf{1} \cdot \epsilon\}$, for an arbitrarily small $\epsilon > 0$.

This subsection is devoted to the following control problem:

Problem 2. Find a s.b. control law for driving the TCPN system towards the desired marking $\mathbf{m}_f$, assuming $\mathbf{m}_f, \mathbf{m}_0 \in int_\epsilon\{Class(\mathbf{m}_0)\}$.

Procedure 5.1. Synthesis of a s.b. centralized control law for driving the system towards $\mathbf{m}_f$.

Synthesis of the control law (off-line):

I . **Compute** the vertices $\{\mathbf{v}_1, ..., \mathbf{v}_m\}$ of $int_\epsilon\{Class(\mathbf{m}_0)\}$ and **enumerate** them s.t. the first k define a simplex having the same dimension of the polytope.

II . **Compute** the vectors $\mathbf{n}_i$ normal to the corresponding facets of $Class(\mathbf{m}_0)$ and pointing outwards this.

III. For the system $\dot{\mathbf{m}} = \mathbf{C}\mathbf{w}$ where $\mathbf{w}$ is the control input, **compute** some values $\mathbf{w}_j$ for the input at the vertices (i.e., with $\mathbf{w}_j$ instead $\mathbf{u}_j$) simultaneously fulfilling:

- $\mathbf{w}_j \geq \mathbf{0}$,
- equation (5.8),
- equation (5.9) for all the facets,
- equation (5.10) with $\mathbf{x}_f = \mathbf{m}_f$.

IV. **Compute** $\mathbf{F}$ and $\mathbf{g}$ that fulfill (5.4).

V . **Verify** that $\mathbf{m}_f$ is the unique equilibrium point in the closed-loop system that belongs to $Class(\mathbf{m}_0)$, by using (5.7) (the condition (5.6) is already fulfilled, since it was transformed into (5.10)). Otherwise, compute another values $\mathbf{u}_j$ and ($\mathbf{F}$,$\mathbf{g}$).

Application of the control law (on-line):

I . **Define** $\eta(\mathbf{m}) = min(\mathbf{f}(\mathbf{m})./(\mathbf{F}\mathbf{m} + \mathbf{g}))$, where ./ denotes the element-wise division operator.

II. **Apply** the control law:

$$\mathbf{u}(\mathbf{m}) = \mathbf{f}(\mathbf{m}) - \eta(\mathbf{m}) \cdot (\mathbf{F}\mathbf{m} + \mathbf{g}) \tag{5.11}$$

Step I of the synthesis procedure corresponds to the *vertex enumeration problem*. A description of this problem and algorithms for its resolution are provided by [Fukuda, 2000]. Vectors $\mathbf{n}_i$ computed in step II are also normal to the facets of $int_\epsilon\{Class(\mathbf{m}_0)\}$. The computation of these as stated in step II has the advantage that it depends only on the original polytope $Class(\mathbf{m}_0)$. All the constraints for the values $\mathbf{w}_j$ in step III are linear. Then, step III can be achieved in polynomial time. In particular, consider the quadratic problem: $min \sum(\mathbf{f}(\mathbf{v}_j) - \mathbf{w}_j)^T(\mathbf{f}(\mathbf{v}_j) - \mathbf{w}_j)$, subject to the constraints in step III. This will usually lead to a fast control law, since the values $\mathbf{w}_j$ thus computed will be close to their upper bounds $\mathbf{f}(\mathbf{v}_j)$, i.e., values that allow the maximum flow. In any case, the scalar function $\eta(\mathbf{m})$ ensures that the control action is always s.b.

Proposition 5.3. *It is always possible to synthesize a control law (5.11) by using Procedure 5.1.*

Proof. Let us construct a particular control law. Consider the polytope $int_\epsilon\{Class(\mathbf{m}_0)\}$. Enumerate its vertices s.t. the first k define a simplex $\mathcal{S}$, having the same dimension of the polytope, that includes $\mathbf{m}_f$.
First, for the vertices of such simplex (i.e., $\{\mathbf{v}_1, ..., \mathbf{v}_k\}$), define the vectors $\mathbf{d}_j = \mathbf{m}_f - \mathbf{v}_j$. Since the net is consistent then, for each $\mathbf{d}_j$ there exists $\mathbf{w}_j$ s.t. $\mathbf{d}_j = \mathbf{C} \cdot \mathbf{w}_j$ and $\mathbf{w}_j \geq \mathbf{0}$. These $\mathbf{w}_j$ define an affine control law ($\mathbf{F}$,$\mathbf{g}$) according to (5.4). Note that, considering the system as $\dot{\mathbf{m}} = \mathbf{C}\mathbf{w}$, such values $\mathbf{w}_j$ fulfill with (5.9), since the field vector at the vertices $\{\mathbf{v}_1, ..., \mathbf{v}_k\}$ points towards $\mathbf{m}_f$, i.e., inside the simplex, thus the polytope. Furthermore, by linearity of the model ($\dot{\mathbf{m}} = \mathbf{C}\mathbf{w}$), the field vector at $\mathbf{m}_f$ is null, so, the condition (5.10) holds. Moreover, (5.7) also holds since the field vector at the vertices of the simplex constitutes a basis (by definition, $span\{\mathbf{d}_1, ..., \mathbf{d}_k\} = span\{\mathbf{v}_1, ..., \mathbf{v}_k\}$).
Given such $\mathbf{w}_j$ for $j \in \{1, ..., k\}$, the values of $\mathbf{w}_j$ for $j \in \{k+1, ..., N\}$ are uniquely determined according to (5.8). Let us show that these also fulfill (5.9).

For each vertex $\mathbf{v}_j \in \{\mathbf{v}_{k+1}, ..., \mathbf{v}_m\}$, define $\mathbf{v}'_j$ as the intersection of the segment ($\mathbf{m}_f$,$\mathbf{v}_j$) with the frontier of the simplex $\mathcal{S}$. In this way, there must exist $\boldsymbol{\gamma} \geq \mathbf{0}$ s.t. $[\mathbf{v}_1, ..., \mathbf{v}_k]\boldsymbol{\gamma} = \mathbf{v}'_j$ and $\mathbf{1} \cdot \boldsymbol{\gamma} = 1$. According to this, by linearity, $\mathbf{d}'_j = \mathbf{m}_f - \mathbf{v}'_j = [\mathbf{d}_1, ..., \mathbf{d}_k]\boldsymbol{\gamma}$. Similarly, by linearity, the value of the input at $\mathbf{v}'_j$, denoted as $\mathbf{w}'_j$, is s.t. $\mathbf{w}'_j = [\mathbf{w}_1, ..., \mathbf{w}_k]\boldsymbol{\gamma} \geq \mathbf{0}$ and $\mathbf{d}'_j = \mathbf{C} \cdot \mathbf{w}'_j$, i.e., the field vector at $\mathbf{v}'_j$ points towards $\mathbf{m}_f$. Finally, since $\mathbf{v}'_j$ is in the segment ($\mathbf{m}_f$,$\mathbf{v}_j$) and the field vector at $\mathbf{m}_f$ is null, then the field vector at $\mathbf{v}_j$ is also pointing towards $\mathbf{m}_f$ and the input at this fulfills $\mathbf{w}_j \geq \mathbf{0}$. Thus, the input at this vertex also fulfills (5.9). Therefore, all the constraints enumerated in steps I-V in Procedure 5.1 are fulfilled. ∎

Proposition 5.4. *Control law (5.11) drives the system towards the required marking* $\mathbf{m}_f$ *while the control action is s.b. along the trajectory.*

Proof. Consider the state equation of the TCPN system as $\dot{\mathbf{m}} = \mathbf{Cw}$, where $\mathbf{w} = \boldsymbol{\Lambda\Pi}(\mathbf{m})\mathbf{m} - \mathbf{u}$. This model is linear, then the current control problem is similar to the problem 1.b of Subsection 5.2.2 with $\mathbf{x}_f = \mathbf{m}_f$, but in a polytope instead a simplex, and with the input constraint $\mathbf{0} \leq \mathbf{w} \leq \mathbf{f}(\mathbf{m})$ instead $\mathbf{u} \in U$. Therefore, according to the results shown in the previous subsections, the control law $\mathbf{w}(\mathbf{m}) = \mathbf{Fm}+\mathbf{g}$ (equivalently, $\mathbf{u} = \mathbf{f}(\mathbf{m})-(\mathbf{Fm}+\mathbf{g})$), where $(\mathbf{F}, \mathbf{g})$ are obtained through the steps I-V of the previous procedure, would drive the system towards $\mathbf{m}_f$ through a trajectory inside $int_\epsilon\{Class(\mathbf{m}_0)\}$. Since the closed-loop system is affine, then convergence to $\mathbf{m}_f$ means asymptotic stability.
The closed-loop system with such input is equivalent to the closed-loop system with (5.11) and $\eta = 1$. In such case, since $\mathbf{m}_f$ is asymptotically stable, there exists a quadratic Lyapunov function $V(\mathbf{m}) = (\mathbf{m} - \mathbf{m}_f)^T\mathbf{P}(\mathbf{m} - \mathbf{m}_f)$ whose derivative is negative, i.e., $\dot{V}(\mathbf{m}) = -(\mathbf{m} - \mathbf{m}_f)^T\mathbf{Q}(\mathbf{m} - \mathbf{m}_f) < 0$, where the matrix $\mathbf{Q} = -[(\mathbf{CF})^T\mathbf{P} + \mathbf{P}(\mathbf{CF})]$ is positive definite ($\mathbf{x}^T\mathbf{Qx} > 0\ \forall \mathbf{x} \neq \mathbf{0}$). By using the same Lyapunov function for the closed-loop system under (5.11) (thus $\eta \neq 1$), its derivative can be computed as $\dot{V}(\mathbf{m}) = -\eta(\mathbf{m})(\mathbf{m} - \mathbf{m}_f)^T\mathbf{Q}(\mathbf{m} - \mathbf{m}_f)$. This is negative (meaning that the system will be driven towards $\mathbf{m}_f$) whenever $\eta(\mathbf{m}) > 0$. This holds since $\mathbf{f}(\mathbf{m}) > \mathbf{0}$ (because the close-loop system remains inside $int\{Class(\mathbf{m}_0)\}$) and $\mathbf{Fm} + \mathbf{g} \geq \mathbf{0}$ (due to the constraint $\mathbf{w}_j \geq \mathbf{0}$).
Finally, since $\eta(\mathbf{m}) \cdot (\mathbf{Fm} + \mathbf{g}) \geq \mathbf{0}$ (so $\mathbf{f}(\mathbf{m}) \geq \mathbf{u}(\mathbf{m})$) and $\eta(\mathbf{m}) = min(\mathbf{f}(\mathbf{m})./(\mathbf{Fm} + \mathbf{g}))$ implies $\eta(\mathbf{m})\dot{(}\mathbf{Fm} + \mathbf{g}) \leq \mathbf{f}(\mathbf{m})$ (so $\mathbf{u}(\mathbf{m}) \geq \mathbf{0}$), then the input is s.b. ∎

Example 5.1. Consider the TCPN system depicted in fig. 5.2(a), with initial marking $\mathbf{m}_0 = [0.1, 1.8, 0.1, 0.1, 0.8, 0.1,\ 0.1, 2.8, 0.1]^T$ and timing $\boldsymbol{\lambda} = [1, 1, 1, 1, 1, 1, 1, 1]^T$. It is desired to drive this system towards $\mathbf{m}_f = [0.3, 0.3, 1.4, 0.2,\ 0.6, 0.2, 1.4, 1.1, 0.5]^T$. This TCPN can be seen as a piecewise-linear system with 16 distinct modes (configurations), according to its state equation. Nevertheless, by following Procedure 5.1, a unique affine control was obtained (5.11), by computing a gain matrix $\mathbf{F}$, of order 9×8, and a vector $\mathbf{g} = \mathbf{0}$. This control law was applied to the system. Fig. 5.2(b) shows the resulting marking trajectories. It can be observed that the control law successfully drives the system towards the desired marking.

5.3 Coordinated control

In the previous section, an affine control structure was proposed for the control of TCPN systems in which all the transitions are controllable. The main drawback of this technique is the complexity involved in

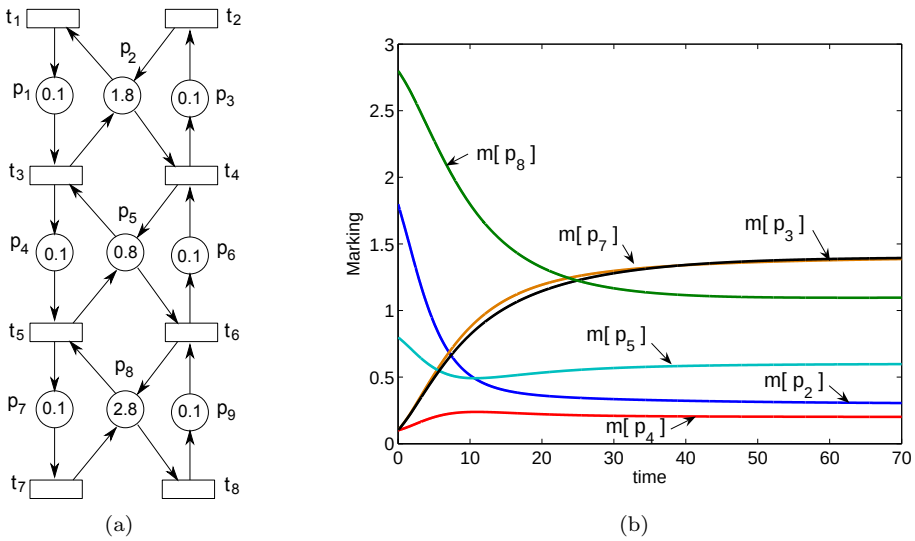

Fig. 5.2: (a) A consistent TCPN system, and (b) its evolution when an affine control law is being applied.

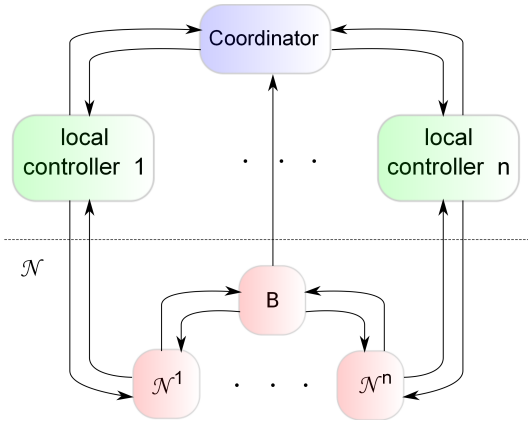

Fig. 5.3: Modular-coordinated control scheme.

the vertex and facets computation. Even if there exist efficient tools for such computations (for instance, [Fukuda, 2000]), for systems having a large structure the synthesis of a controller may be untractable. In such case, one way for dealing with such complexity consists in decomposing the system into a set of interconnected subsystems, i.e., a modular view of the model. In this way, a controller can be computed for each subsystem, reducing thus the complexity involved in the synthesis procedure. Though this section, a particular proposal for such a control strategy will be considered, as an extension of the affine control laws introduced before.

Definition 5.5. Given a PN $\mathcal{N} = \langle P, T, \mathbf{Pre}, \mathbf{Post}\rangle$, a *modular view* of this is a set of n PNs, named *modules*, denoted as $\mathcal{N}^i = \langle P^i, T^i, \mathbf{Pre}^i, \mathbf{Post}^i, \mathbf{m}_0^i\rangle$, where $\mathbf{m}_0^i = \mathbf{m}_0[P^i]$, $\mathbf{Pre}^i = \mathbf{Pre}[P^i, T^i]$ and $\mathbf{Post}^i = \mathbf{Post}[P^i, T^i]$, for each $i \in \{1, ..., n\}$. These modules are interconnected by places, called buffers B, so P is the disjoint union of $P^1, ..., P^n$ and B, and T is the disjoint union of $T^1, ..., T^n$. We assume that the following conditions hold:

1. For every $i, j \in \{1, ..., n\}$, if $i \neq j$ then $\mathbf{Pre}[P^i, T^j] = \mathbf{Post}[P^i, T^j] = \mathbf{0}$.
2. For each buffer $b \in B$, $|b^\bullet| \geq 1$.
3. For every $i \in \{1, ..., n\}$, the module $\mathcal{N}^i$ is consistent.
4. The net model $\mathcal{N}$ is consistent.

In the sequel, it will be assumed, without loss of generality, that the incidence matrix of the modular net model has a structure like:

$$\mathbf{C} = \begin{bmatrix} \mathbf{C}^1 & \mathbf{0} & ... & \mathbf{0} \\ \mathbf{0} & \mathbf{C}^2 & ... & \mathbf{0} \\ \vdots & \vdots & ... & \vdots \\ \mathbf{0} & \mathbf{0} & ... & \mathbf{C}^n \\ \mathbf{C}_B^1 & \mathbf{C}_B^2 & ... & \mathbf{C}_B^n \end{bmatrix}$$

where $\mathbf{C}^i = \mathbf{C}[P^i, T^i]$ and $\mathbf{C}_B^i = \mathbf{C}[B, T^i]$. In this way, the marking is represented as $\mathbf{m} = [(\mathbf{m}^1)^T, .., (\mathbf{m}^n)^T, (\mathbf{m}^B)^T]^T$, where $(\mathbf{m}^i)^T$ is the transpose of $\mathbf{m}^i = \mathbf{m}[P^i]$, and similarly $\mathbf{m}^B = \mathbf{m}[B]$. Furthermore, $\mathbf{B}_x^i \geq \mathbf{0}$ represents a basis for the T-semiflows of $\mathbf{C}^i$. In this section, we are interested in the following control problem:

Problem 3. Given a TCPN system $\langle \mathcal{N}, \boldsymbol{\lambda}, \mathbf{m}_0 \rangle$, where $\mathcal{N}$ is a modular PN, find a *coordinated-control scheme* for driving concurrently each module $\mathcal{N}^i$ of $\mathcal{N}$ towards a desired marking $\mathbf{m}_f^i \in Class(\mathbf{m}_0^i)$ by means of s.b. control actions, assuming they are concurrently reachable while the buffers remain marked.

Fig. 5.3 shows the structure of a coordinated-control scheme. This consists of a set of local controllers and an upper-level controller, named *coordinator*. A local controller is synthesized for each module, receiving information from the coordinator and having local information: the marking of the corresponding module and the neighboring buffers. The coordinator receives and sends minimum information from and to the local controllers, but it does not apply control actions into the system. Furthermore, the coordinator can observe the marking of the buffers.

5.3.1 The need for coordination

By hypothesis, a modular TCPN system is consistent, thus controllable over $int\{Class(\mathbf{m}_0)\}$. The same holds for each of the modules $\mathcal{N}^i$. Thus, if the initial marking of the buffers were large enough, i.e., if $\mathbf{m}_0^B >> \mathbf{0}$, each module could be driven towards its corresponding desired marking $\mathbf{m}_f^i \in Class(\mathbf{m}_0^i)$ by means of a *local control law* like (5.11), using only local information, i.e., $\mathbf{m}^i$. In such case, it would be obtained a completely decentralized control scheme with neither communication between local controllers nor with the coordinator.

Example 5.2. Consider the modular TCPN system depicted in fig. 5.4, consisting of three modules interconnected by four buffers. The rates for the transitions are $\boldsymbol{\lambda}^1 = [4, 1, 1, 1]$ for $\mathcal{N}^1$, $\boldsymbol{\lambda}^2 = [1, 1, 1]$ for $\mathcal{N}^2$ and $\boldsymbol{\lambda}^3 = [1, 1, 1, 1]$ for $\mathcal{N}^3$. The initial markings are $\mathbf{m}_0^1 = [9.7, 0.1, 0.1, 0.1]^T$ for $\mathcal{N}^1$, $\mathbf{m}_0^2 = [0.1, 0.1, 4.8]^T$ for $\mathcal{N}^2$ and $\mathbf{m}_0^3 = [4.8, 0.1, 0.1]^T$ for $\mathcal{N}^3$. The initial marking at the buffers is $\mathbf{m}_0^B = [0.1, 0.1, 2.5, 4]^T$. Consider the control problem of transferring the modules towards $\mathbf{m}_f^1 = [1, 1, 1, 7]$, $\mathbf{m}_f^2 = [0.5, 3, 1.5]$ and $\mathbf{m}_f^3 = [1.5, 0.5, 3]$, respectively. For each module, gain matrices $\mathbf{F}^i$ and vectors

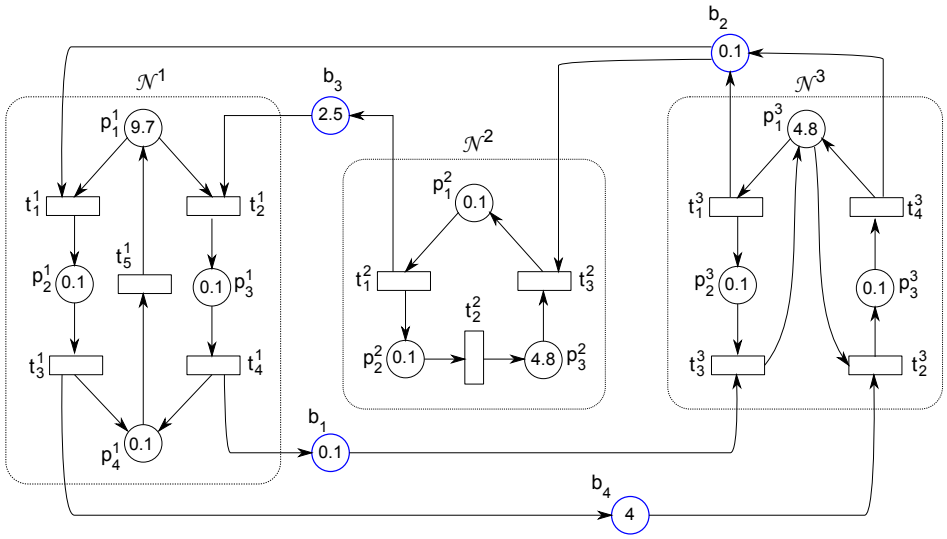

Fig. 5.4: A consistent and conservative TCPN system. Buffer b_2 is not output private (it supplies tokens to $\mathcal{N}^1$ and $\mathcal{N}^2$).

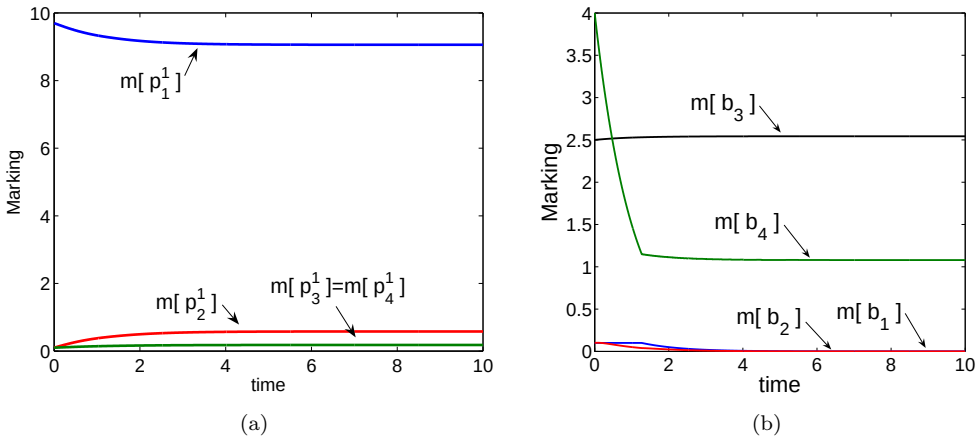

Fig. 5.5: (a) Marking of Module 1 in closed-loop. (b) Marking in the buffers.

$\mathbf{g}^i$ were computed, by using Procedure 5.1. Later, the resulting control laws (5.11) were simultaneously applied to the corresponding modules. Fig. 5.5(a) shows the obtained trajectories for the marking of $\mathcal{N}^1$. It can be observed that the module got stuck at a marking different than the desired one. The same has occurred to the other modules, because the buffers b_1 and b_2 were emptied, as shown in fig. 5.5(b) ($\mathcal{N}^3$ requires marking from b_1 while $\mathcal{N}^1$ and $\mathcal{N}^2$ require marking from b_2). Thus, although the net system is live (without control), the applied control scheme stops the activity in all the modules.

In general, the marking at the buffers is limited (frequently, they are part of a *P-component*), and so, they impose constraints to the control actions that are not taken into account during the synthesis of the local controllers, e.g., a module $\mathcal{N}^i$ has the constraint $\mathbf{w}^i \leq \mathbf{f}^i(\mathbf{m}^i, \mathbf{m}^B)$, where $\mathbf{m}^B$ represents the marking at the buffers, but the control law obtained with Procedure 5.1 is synthesized only for fulfilling $\mathbf{w}^i \leq \mathbf{f}^i(\mathbf{m}^i)$. In the worst case, a set of buffers may empty, consequently, the local controllers will

stop the activity of the modules that require tokens from them. This does not mean that the system is actually in a deadlock, on the contrary, it might be possible to recover the system. Nevertheless, the local controllers are not synthesized in order to increase the marking at the buffers. Therefore, it is important to have a certain *coordination* between the local controllers, in order to make the modules to evolve with a suitable speed so that the buffers do not empty, i.e., imposing a *fairness* relation between modules. This will be the task of the *coordinator*.

5.3.2 Modular-coordinated control

In this Subsection, a modular-coordinated control strategy will be introduced. In general, different kinds of control techniques can be considered for the local controllers. Nevertheless, PWA control laws will be used in this case, as a generalization of the control strategy introduced in Section 5.2.

In sequel, it will be assumed that both the initial and the final markings belong to $int_\epsilon\{Class(\mathbf{m}_0)\}$ for a given small $\epsilon > 0$. Similarly, it will be assumed that the operation of each local controller and the coordinator are ruled by a global clock and they always receive and send the required information without loss or delays.

As shown in the previous subsection, certain coordination is required in order to make the buffers to remain marked. This can be achieved by applying a modular control scheme, like the one shown in fig. 5.3, that drives the system through a linear (straight) trajectory (due to the convexity of $Class(\mathbf{m}_0)$, it is always possible to drive the system to any reachable marking, through a straight trajectory). Let us describe this in an informal way. Compute firstly a proper final marking for the buffers $\mathbf{m}_f^B > \mathbf{1}\epsilon$ such that $\mathbf{m}_f = [(\mathbf{m}_f^1)^T, ..., (\mathbf{m}_f^n)^T, (\mathbf{m}_f^B)^T]^T$ is reachable (such marking exists by hypothesis). Next, compute for each module (task for the local controllers) a vector $\mathbf{d}^i > \mathbf{0}$ s.t. $(\mathbf{m}_f^i - \mathbf{m}^i) = \mathbf{C}^i\mathbf{d}^i$. Furthermore, compute (task for the coordinator) a vector $\boldsymbol{\gamma} > \mathbf{0}$ s.t. $(\mathbf{m}_f^B - \mathbf{m}^B) = \sum \mathbf{C}_B^i\mathbf{d}^i + [\mathbf{C}_B^1\mathbf{B}_x^1, ..., \mathbf{C}_B^n\mathbf{B}_x^n]\boldsymbol{\gamma}$. In this way, if each local controller applies $\mathbf{w}^i = \mathbf{d}^i + \mathbf{B}_x^i\boldsymbol{\gamma}[T^i]$ then the closed-loop behavior of each module will be $\dot{\mathbf{m}}^i = \mathbf{C}^i\mathbf{d}^i + \mathbf{C}^i\mathbf{B}_x^i\boldsymbol{\gamma}[T^i] = (\mathbf{m}_f^i - \mathbf{m}^i)$, i.e., each field vector will be pointing towards the corresponding $\mathbf{m}_f^i$, consequently, the modules will be concurrently driven towards their final states describing linear trajectories. Moreover, the closed-loop behavior of the marking of the buffers will be $\dot{\mathbf{m}}^B = \sum \mathbf{C}_B^i\mathbf{d}^i + [\mathbf{C}_B^1\mathbf{B}_x^1, ..., \mathbf{C}_B^n\mathbf{B}_x^n]\boldsymbol{\gamma} = (\mathbf{m}_f^B - \mathbf{m}^B)$, thus, the marking of the buffers will converge to $\mathbf{m}_f^B$ describing a linear trajectory, so, the buffers will remain marked.

This control scheme can be extended by adding an affine control element to the local control laws. This is formalized in the forthcoming Procedure 5.2, nevertheless, let us provide here an intuition for such control procedure. First, define $\mathbf{w}'^i = \mathbf{F}^i\mathbf{m}^i + \mathbf{g}^i$, where $(\mathbf{F}^i, \mathbf{g}^i)$ is a proper affine control law computed (for each module) by using Procedure 5.1. Defining a *linearizing factor* $\psi \in [0, 1]$, the following local control law is proposed for each module: $\mathbf{w}^i = \mathbf{d}^i\psi + \mathbf{w}'^i(1 - \psi) + \mathbf{B}_x^i\boldsymbol{\gamma}^i$. Note that, if $\psi = 1$ then the local controllers will drive their modules toward the corresponding $\mathbf{m}_f^i$ describing linear trajectories (it is actually the control scheme described in the previous paragraph). On the other hand, with $\psi = 0$ the control laws obtained are the evaluations of the affine control laws $\mathbf{w}'^i$, which corresponds to the decentralized scheme with local affine controllers used in Example 5.2. In order to make the buffers to remain marked, the linearizing factor must be properly computed. One possibility is to impose the constraint $\dot{\mathbf{m}}^B = \sum \mathbf{C}_B^i[\mathbf{d}^i\psi + \mathbf{w}'^i(1-\psi) + \mathbf{B}_x^i\boldsymbol{\gamma}^i] > \mathbf{1}\epsilon - \mathbf{m}^B$. In this way, the field vector of the marking of the buffers is always pointing towards a positive marking $> \mathbf{1}\epsilon$ (given the definition of $\boldsymbol{\gamma}$, previous

constraint is equivalent to $\sum \mathbf{C}_B^i(\mathbf{w}'^i - \mathbf{d}^i)(1-\psi) > \mathbf{1}\epsilon - \mathbf{m}_f^B$).

Finally, in order to make the control laws to be s.b., i.e., $\mathbf{w}^i \leq \mathbf{f}^i(\mathbf{m}^i, \mathbf{m}^B)$, a proper global scale factor η may be applied to the control actions, i.e., each local controller would apply $\mathbf{w}^i = [\mathbf{d}^i\psi + \mathbf{w}'^i(1-\psi) + \mathbf{B}_x^i\boldsymbol{\gamma}^i]\eta$, where $\eta > 0$ is the maximum scalar s.t. $\mathbf{w}^i \leq \mathbf{f}^i(\mathbf{m}^i, \mathbf{m}^B)$ for all the modules. The factor must be the same for all the local controllers, so the direction of the global field vector is not modified. Then, η must be computed by the coordinator by using information from the local controllers, regarding the maximum control action allowed with respect to each of the three components $\mathbf{d}_i$, $\mathbf{B}_x^i$ and $\mathbf{w}'^i$ (these are codified in three factors η_d^i, $\eta_{x_j}^i$ and η_w^i, respectively). Combining all these issues, the following control scheme is proposed:

Procedure 5.2. Synthesis of a coordinated control scheme.

Synthesis of local control laws (planing step):

- *Coordinator:* **Compute** a suitable desired marking for the buffers s.t. all of them are marked $\mathbf{m}_f^B > \mathbf{1}\epsilon$ and $\mathbf{m}_f = [(\mathbf{m}_f^1)^T, ..., (\mathbf{m}_f^n)^T, (\mathbf{m}_f^B)^T]^T$ is reachable. **Compute** a T-semiflow $\mathbf{0} \leq \mathbf{x} \leq \mathbf{f}(\mathbf{m}_f)$.

- *Each local controller:* **Compute** an affine control law $(\mathbf{F}^i, \mathbf{g}^i)$, by using Procedure 5.1, for driving the module $\mathcal{N}^i$ to the corresponding $\mathbf{m}_f^i$, with the additional constraint $\mathbf{w}(\mathbf{m}_f^i) = \mathbf{x}[T^i]$.

Dynamic control (on-line, in discrete time):

Coordinator:

- ***Receive*** *from the local controllers the values* $\eta_{x_j}^i$, η_d^i, η_w^i, $\mathbf{C}_B^i\mathbf{d}^i$ *and* $\mathbf{C}_B^i \cdot (\mathbf{w}'^i - \mathbf{d}^i)$.

I . **Compute** a vector $\boldsymbol{\gamma} > \mathbf{0}$ solution for

$$(\mathbf{m}_f^B - \mathbf{m}^B) - \sum \mathbf{C}_B^i\mathbf{d}^i = [\mathbf{C}_B^1\mathbf{B}_x^1, ..., \mathbf{C}_B^n\mathbf{B}_x^n]\boldsymbol{\gamma} \tag{5.12}$$

II . **Compute** $\psi = min\ \alpha$ s.t. $\alpha \in [0,1]$ and $\sum \mathbf{C}_B^i(\mathbf{w}'^i - \mathbf{d}^i)(1-\alpha) > \mathbf{1}\epsilon - \mathbf{m}_f^B$.

III. **Define**, for each module, $\boldsymbol{\gamma}^i = \boldsymbol{\gamma}[T^i]$ and $\eta^i = 1/((1-\psi)/\eta_w^i + \psi/\eta_d^i + \sum \boldsymbol{\gamma}^i[j]/\eta_{x_j}^i)$.

IV. **Evaluate** $\eta = min(\eta^1, ..., \eta^n)$.

- ***Send****, to each local controller, the values* η, ψ *and* $\boldsymbol{\gamma}^i$.

For each local controller:

- ***Receive*** *from the coordinator the new values for* ψ, η *and* $\boldsymbol{\gamma}^i$.

I . **Compute** a vector $\mathbf{d}^i > \mathbf{0}$ s.t. $(\mathbf{m}_f^i - \mathbf{m}^i) = \mathbf{C}^i\mathbf{d}^i$.

II . **Evaluate** the affine control action: $\mathbf{w}'^i = \mathbf{F}^i\mathbf{m}^i + \mathbf{g}^i$.

III. **Apply** the control action:

$$\mathbf{u}^i = \mathbf{f}^i(\mathbf{m}^i, \mathbf{m}^B) - \left[\mathbf{w}'^i(1-\psi) + \mathbf{d}^i\psi + \mathbf{B}_x^i\boldsymbol{\gamma}^i\right]\eta \tag{5.13}$$

IV. **Compute** the values:

- $\eta_d^i = max\,\alpha$ s.t. $\mathbf{d}^i\alpha \leq \mathbf{f}^i(\mathbf{m}^i, \mathbf{m}^B)$,
- $\eta_w^i = max\,\alpha$ s.t. $\mathbf{w}'^i\alpha \leq \mathbf{f}^i(\mathbf{m}^i, \mathbf{m}^B)$,
- $\eta_{x_j}^i = max\,\alpha$ s.t. $\mathbf{x}_j\alpha \leq \mathbf{f}^i(\mathbf{m}^i, \mathbf{m}^B)$, for each column (T-semiflow) $\mathbf{x}_j$ of $\mathbf{B}_x^i$.

- ***Send*** *the values* $\eta_{x_j}^i$, η_d^i, η_w^i, $\mathbf{C}_B^i \cdot \mathbf{d}^i$ *and* $\mathbf{C}_B^i \cdot (\mathbf{w}'^i - \mathbf{d}^i)$ *to the coordinator.*

In Section C.3 in the appendix, a simple algorithm for the computation of $\mathbf{m}_f^B$ is provided. The computation of $\mathbf{d}^i$, achieved by each local controller at step I at each sampling, and $\boldsymbol{\gamma}$ achieved by the coordinator at step I, can be done with Algorithm C.3 (in Section C.3), having a linear complexity. Similarly, an efficient algorithm for the computation of values $\eta_{x_j}^i$, η_w^i, η_d^i, η_T^i and ψ is also provided in Section C.3.

Proposition 5.6. *Procedure 5.2 is well defined, i.e., all the required information is available and all the conditions for the computation are satisfied.*

Proof. Since the net $\mathcal{N}$ is consistent and $\mathbf{m}_f$ is assumed reachable, then $\exists\boldsymbol{\sigma} > \mathbf{0}$ s.t. $(\mathbf{m}_f^i - \mathbf{m}^i) = \mathbf{C}^i\boldsymbol{\sigma}[T^i]$, for each module, and $(\mathbf{m}_f^B - \mathbf{m}^B) = \sum \mathbf{C}_B^i\boldsymbol{\sigma}[T^i]$. Consider a module $\mathcal{N}^i$. Since this is consistent, then there always exists a particular solution $\mathbf{d}^i > \mathbf{0}$ for $(\mathbf{m}_f^i - \mathbf{m}^i) = \mathbf{C}^i\mathbf{d}^i$. Furthermore, the general solution for $\boldsymbol{\sigma}[T^i]$ is given by $\boldsymbol{\sigma}[T^i] = \mathbf{d}^i + \mathbf{B}_x^i\boldsymbol{\gamma}^i$, with $\boldsymbol{\gamma}^i > \mathbf{0}$. Then, given particular solutions $\mathbf{d}^i$ for each module, there always exists $\boldsymbol{\gamma}$ s.t. $(\mathbf{m}_f^B - \mathbf{m}^B) = \sum \mathbf{C}_B^i\mathbf{d}^i + \sum \mathbf{C}_B^i\boldsymbol{\gamma}[T^i]$, i.e., solution for (5.12). Therefore, it is always possible to compute vectors $\mathbf{d}^i$ and $\boldsymbol{\gamma}$ according to the control procedure.
On the other hand, note that $\psi = 1$ is a trivial solution for $\sum \mathbf{C}_B^i(\mathbf{w}'^i - \mathbf{d}^i)(1-\psi) > \mathbf{1}\epsilon - \mathbf{m}_f^B$. Moreover, the step III for the operation of the local controllers implies that the buffers remain marked (this is proven in detail in the proof of Proposition 5.7). Thus, $\mathbf{f}^i(\mathbf{m}^i, \mathbf{m}^B) > \mathbf{0}$ for each module. Since $\mathbf{d}^i > \mathbf{0}$ and $\boldsymbol{\gamma} > \mathbf{0}$, then scalars η_w^i, η_d^i, $\eta_{x_j}^i$, η^i and η can always be computed and they are positive.
Finally, η is computed in such a way that each local control action is s.b., so it can be applied. Let us prove this by showing that η is computed in such a way that $\mathbf{w}^i = [\mathbf{w}'^i(1-\psi) + \mathbf{d}^i\psi + \mathbf{B}_x^i\boldsymbol{\gamma}^i]\eta \leq \mathbf{f}^i(\mathbf{m}^i, \mathbf{m}^B)$ ($\mathbf{w}^i \geq \mathbf{0}$ already since $\mathbf{w}'^i > \mathbf{0}$, $\mathbf{d}^i > \mathbf{0}$, $\mathbf{B}_x^i \geq \mathbf{0}$ and $\boldsymbol{\gamma}^i > \mathbf{0}$). By using the definitions of η_d^i, η_w^i and $\eta_{x_j}^i$, computed by the local controllers, and η^i computed by the coordinator, it can be proved that $[\mathbf{w}'^i(1-\psi) + \mathbf{d}^i\psi + \mathbf{B}_x^i\boldsymbol{\gamma}^i]\eta^i \leq \mathbf{f}^i(\mathbf{m}^i, \mathbf{m}^B)$. Later, since $0 < \eta \leq \eta^i$, then $\mathbf{w}^i \leq \mathbf{f}^i(\mathbf{m}^i, \mathbf{m}^B)$ for all the modules. ∎

Proposition 5.7. *If the coordinated control scheme of Procedure 5.2 is applied, each module will be driven towards the corresponding* $\mathbf{m}_f^i$.

Proof. For the sake of simplicity, the analysis is achieved in continuous-time, but an analogous reasoning can be used for the discrete-time case. Firstly let us show that the buffers remain marked. Consider a module $\mathcal{N}^i$. By definition of ψ, $\sum \mathbf{C}_B^i(\mathbf{w}'^i - \mathbf{d}^i)(1-\psi) > \mathbf{1}\epsilon - \mathbf{m}_B^f$. Combining this equation with (5.12), it is obtained $\mathbf{m}^B + \sum \mathbf{C}_B^i[\mathbf{w}'^i(1-\psi) + \mathbf{d}^i\psi + \mathbf{B}_x^i\boldsymbol{\gamma}^i] > \mathbf{1}\epsilon$. Substituting (5.13) it is obtained $\mathbf{m}_B + (1/\eta)\sum \mathbf{C}_B^i[\mathbf{f}^i(\mathbf{m}^i, \mathbf{m}^B) - \mathbf{u}^i] > \mathbf{1}\epsilon$. Furthermore, substituting $\dot{\mathbf{m}}^B = \sum \mathbf{C}_B^i[\mathbf{f}^i(\mathbf{m}^i, \mathbf{m}^B) - \mathbf{u}^i]$ (given by definition) into the previous equation, it is obtained $(1/\eta)\dot{\mathbf{m}}^B > \mathbf{1}\epsilon - \mathbf{m}^B$. This means that, in case $\mathbf{m}_j^B \leq \epsilon$ for some buffer b_j, the field vector of the marking of b_j points towards a marking $\mathbf{m}[b_j] > \epsilon$, i.e., ψ is computed in such a way that the buffers remain marked (the analysis can also be achieved in discrete-time, obtaining the analogous expression $(1/\eta)(\mathbf{m}_{\tau+1}^B - \mathbf{m}_\tau^B)/\Delta\tau > \mathbf{1}\epsilon - \mathbf{m}_\tau^B$, having the same interpretation).

Now, suppose that $\psi = 0$. Then, as shown for the centralized affine control scheme, there exists a quadratic Lyapunov function $V(\mathbf{m}^i) = (\mathbf{m}^i - \mathbf{m}_f^i)^T\mathbf{P}(\mathbf{m}^i - \mathbf{m}_f^i)$ whose derivative is negative, i.e., the matrix $\mathbf{Q} = -[(\mathbf{CF})^T\mathbf{P} + \mathbf{P}(\mathbf{CF})]$ is positive definite and so $\dot{V}(\mathbf{m}^i) = -\eta(\mathbf{m}^i - \mathbf{m}_f^i)^T\mathbf{Q}(\mathbf{m}^i - \mathbf{m}_f^i) < 0$, $\forall \mathbf{m}^i \neq \mathbf{m}_f^i$. In general, independently of the values received from the coordinator, the derivative of the same Lyapunov function with $\psi \neq 0$ can be computed as $\dot{V}(\mathbf{m}^i) = -\eta(1-\psi)(\mathbf{m}^i - \mathbf{m}_f^i)^T\mathbf{Q}(\mathbf{m}^i - \mathbf{m}_f^i) - \eta\psi(\mathbf{m}^i - \mathbf{m}_f^i)^T\mathbf{P}(\mathbf{m}^i - \mathbf{m}_f^i)$. Since $\mathbf{P}$ and $\mathbf{Q}$ are definite positive and $\eta > 0$, then the derivative of the Lyapunov function is negative for $\psi \in [0, 1]$, and so the module will asymptotically converge to $\mathbf{m}_f^i$ (a similar result can be obtained for the discrete-time case, by using the Lyapunov function $\Delta V(\mathbf{m}_\tau^i) = (\mathbf{m}_{\tau+1}^i - \mathbf{m}_f^i)^T\mathbf{P}(\mathbf{m}_{\tau+1}^i - \mathbf{m}_f^i) - (\mathbf{m}_\tau^i - \mathbf{m}_f^i)^T\mathbf{P}(\mathbf{m}_\tau^i - \mathbf{m}_f^i)$ and assuming $\Delta\tau << 1$). ∎

Example 5.3. Consider again the TCPN system depicted in fig. 5.4 with the same rates and initial marking. The desired markings for the modules are given by $\mathbf{m}_f^1 = [1, 1, 1, 7]$, $\mathbf{m}_f^2 = [0.5, 3, 1.5]$ and $\mathbf{m}_f^3 = [1.5, 0.5, 3]$, respectively. Consider a desired marking for the buffers $\mathbf{m}_f^B = [0.5, 0.5, 0.5, 0.5]^T$. For each module, gain matrices $\mathbf{F}^i$ and vectors $\mathbf{g}^i$ were computed according to Procedure 5.1. Later, the coordinated control strategy of Procedure 5.2 was applied. Fig. 5.6(a) shows the trajectories for the marking of $\mathcal{N}^1$. It can be observed that the module was successfully driven to the desired marking $\mathbf{m}_f^1$. Similarly, modules $\mathcal{N}^2$ and $\mathcal{N}^3$ were driven towards $\mathbf{m}_f^2$ and $\mathbf{m}_f^3$, respectively. Fig. 5.6(b) shows the marking evolution of the buffers. Note that the control makes the buffers to remain marked by converging to $\mathbf{m}_f^B > \mathbf{1}\epsilon$. Later, the control scheme was slightly modified and applied by forcing $\psi = 1$ during all the time. As expected, the control was successful in this case as well. Fig. 5.6(c) shows the marking at place p_3^1 vs. p_4^1 (a projection of the phase portrait). The solid curve corresponds to the system with the coordinated control as defined in Procedure 5.2 ($\psi(\mathbf{m})$), while the dashed curve represents the closed-loop system but with $\psi = 1$ for all the time. Note that in this second case, the trajectory described is linear, showing thus the meaning of ψ.

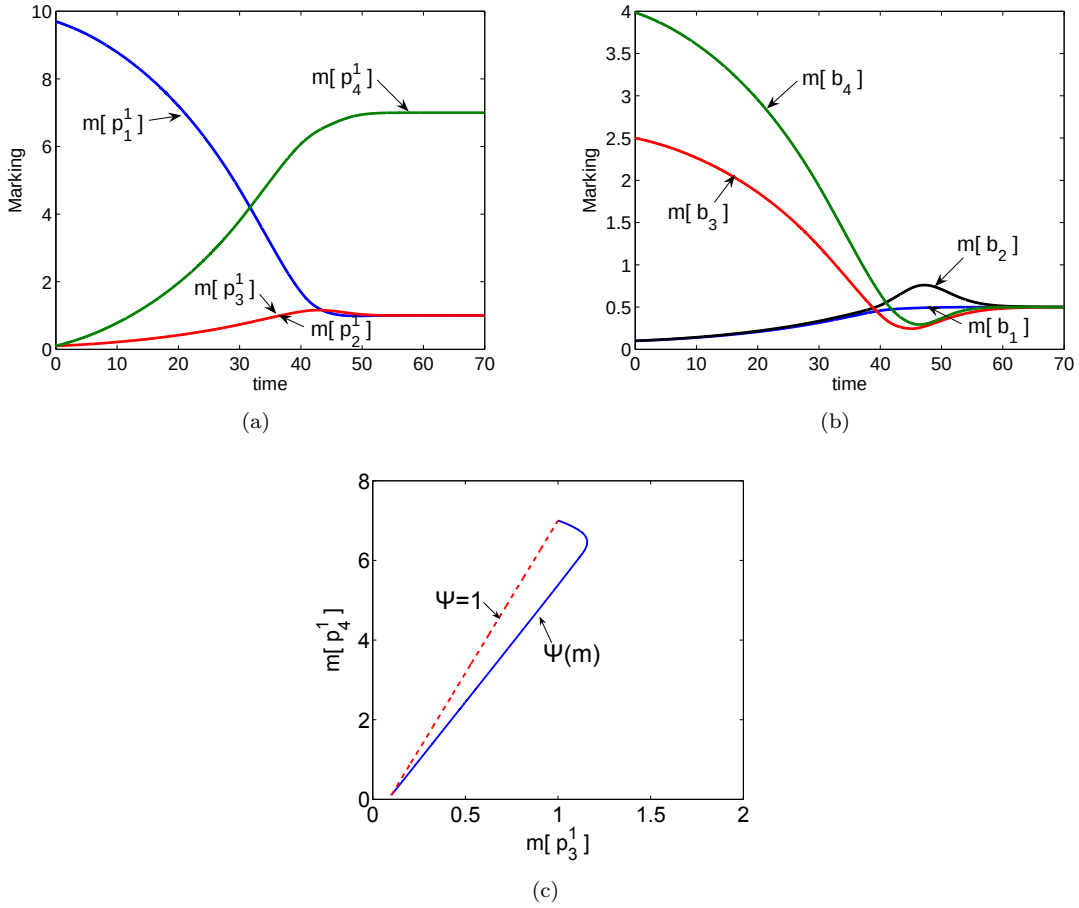

Fig. 5.6: a) Marking of Module 1 of the system of fig. 5.4 in closed-loop behavior, under the coordinated control of Procedure 5.2. b) Marking in the buffers. c) Phase portrait. Solid curve corresponds to the original coordinated control strategy. Dashed curve is obtained by forcing $\psi = 1$.

5.4 Pole-assignment centralized control for systems with uncontrollable transitions

In this section, a centralized control law structure is proposed for the case in which the system has uncontrollable transitions. As explained in Chapter 4, the controllability is much more complex in this case. There, a few of results regarding the controllability over sets of equilibrium markings ($E_i = \{\mathbf{m} \in \Re_i | \exists \mathbf{u}$ s.b. at $\mathbf{m}$ s.t. $\mathbf{C}(\mathbf{\Lambda\Pi}(\mathbf{m})\mathbf{m} - \mathbf{u}) = 0\}$) were provided. Remmeber that equilibrium markings represent "stationary operating points" in the original discrete system, then, the resulting control law will transfer the system from one operating point to another required one. For this, the controllable transitions were classified, in each region $\Re_i$, as fully controllable T_{cf}^i and partially controllable T_{cp}^i.

The analysis achieved though this section is made under the assumption that the system is controllable under the corresponding sets E_i^* by means of the fully controllable transitions, i.e., the system fulfills the first statement of Corollary 4.18 in the corresponding configurations.

5.4.1 Controlling inside one region

In this subsection, a control law structure is proposed for the case in which the initial and desired markings, denoted as $\mathbf{m}_0$ and $\mathbf{m}_d$ respectively, belong to a common region $\Re_i$ and both are equilibrium markings.

In the sequel it is assumed that the system fulfills the sufficient condition for controllability of Corollary 4.18, so the system is controllable over E_i^* using only fully controllable transitions T_{cf}^i. According to this, control will be applied by means of these transitions, while other controllable ones (those in T_{cp}^i) will be considered as uncontrollable.

Now, the classical feedback control law (for instance see [Chen, 1984]) is given by

$$\mathbf{u} = \mathbf{u}_d + \mathbf{K} \cdot \mathbf{e} \tag{5.14}$$

where $\mathbf{K}$ is a gain matrix, $\mathbf{u}_d$ is the input related to the desired marking $\mathbf{m}_d$ and $\mathbf{e} = \mathbf{m} - \mathbf{m}_d$ is the marking error.

Under these assumptions, if a negative and unbounded input could be applied to the system then $\mathbf{m}_d$ would be reachable by means of a control law like (5.14), but this is not the case because the input must be suitably bounded. Nevertheless, as it will be proved next, given a stabilizing feedback gain matrix $\mathbf{K}$ it is possible to compute an *intermediate* desired marking $\mathbf{m}'_d$, in the segment defined by $\mathbf{m}_0$ and $\mathbf{m}_d$ but close enough to $\mathbf{m}_0$, s.t. the input thus defined is suitably bounded along the trajectory, which remains in $\Re_i$. Computing several of these *intermediate* markings, $\mathbf{m}_d$ can be reached by jumping through them. Based on this idea, a control procedure is proposed, whose effectiveness and feasibility are formally proved through this section.

Now, let us introduce some useful notation. Let $\mathbf{u}_0$ and $\mathbf{u}_d$ ($\mathbf{w}_0$ and $\mathbf{w}_d$) be the equilibrium inputs (equilibrium flows) of $\mathbf{m}_0$ and $\mathbf{m}_d$, respectively ($\mathbf{m}_0$ and $\mathbf{m}_d$ are equilibrium markings). Define the constant vectors $\mathbf{e}_0 = \mathbf{m}_0 - \mathbf{m}_d$ and $\Delta\mathbf{u} = \mathbf{u}_0 - \mathbf{u}_d$, and consider the error $\mathbf{e} = \mathbf{m} - \mathbf{m}_d$. Consider a given *intermediate* target marking $\mathbf{m}'_d$ in the segment defined by $\mathbf{m}_0$ and $\mathbf{m}_d$. This marking can be expressed as $\mathbf{m}'_d = \mathbf{m}_d + \beta\mathbf{e}_0$, where β is a scalar that belongs to $[0, 1]$. By linearity, $\mathbf{m}'_d$ is an equilibrium marking and one of its equilibrium inputs is given by $\mathbf{u}'_d = \mathbf{u}_d + \beta\Delta\mathbf{u}$. The equilibrium flow of $\mathbf{m}'_d$ and the error defined from it are given by $\mathbf{e}' = \mathbf{m} - \mathbf{m}'_d = \mathbf{e} - \beta\mathbf{e}_0$ and $\mathbf{w}'_d = \mathbf{w}_d + \beta(\mathbf{w}_0 - \mathbf{w}_d) = \Lambda\mathbf{\Pi}_i\mathbf{m}'_d - \mathbf{u}'_d$, respectively.

Procedure 5.3. Synthesis of a centralized pole-assignment control law for systems with uncontrollable transitions.

Synthesis of control law (planing step)

I . **Compute** a stabilizing feedback gain matrix $\mathbf{K}$ s.t. the controllable eigenvalues of the closed-loop state matrix ($\mathbf{C}\Lambda\mathbf{\Pi}_i - \mathbf{CK}$) are distinct, real and negative, and the rows of $\mathbf{K}$, non related with transitions in T_{cf}^i, are null.

II . Given $\mathbf{m}_0$ **compute** a *intermediate* desired marking $\mathbf{m}'_d$, which belongs to the segment defined by $\mathbf{m}_0$ and $\mathbf{m}_d$, as follows

$$\mathbf{m}'_d = \mathbf{m}_d + \beta \mathbf{e}_0 \tag{5.15}$$

where β is obtained by solving the following LPP

$$\begin{array}{ll} \beta = min\ \gamma & \text{subject to} \\ \mathfrak{c}_1 + neg(\mathbf{A})\mathbf{T}_i^{-1}\mathbf{e} + \gamma\left(\mathfrak{c}_2 - neg(\mathbf{A})\mathbf{T}_i^{-1}\mathbf{e}_0\right) \geq \mathbf{0} & \\ \gamma \geq 0 & \end{array} \tag{5.16}$$

$\mathbf{T}_i$ is a similarity transformation matrix s.t. the transformed error $\mathbf{T}_i^{-1}\mathbf{e}$ is nonnegative and decreasing in the closed-loop system, i.e., $\dot{\mathbf{e}} = (\mathbf{C}\Lambda\mathbf{\Pi}_i - \mathbf{C}\mathbf{K})\mathbf{e}$, the function $neg(A)$ is defined by elements as

$$neg(\mathbf{A})_{i,j} = \begin{cases} A_{ij} & \text{if } A_{ij} < 0 \\ 0 & \text{otherwise} \end{cases} \tag{5.17}$$

and the constants are defined as

$$\mathbf{A} = \begin{bmatrix} \mathbf{K} \\ \Lambda\mathbf{\Pi}_i - \mathbf{K} \\ \mathbf{\Pi}_j^1 - \mathbf{\Pi}_i \\ \vdots \\ \mathbf{\Pi}_j^r - \mathbf{\Pi}_i \end{bmatrix} \mathbf{T}_i, \qquad \mathfrak{c}_1 = \begin{bmatrix} \mathbf{u}_d \\ \mathbf{w}_d \\ \left(\mathbf{\Pi}_j^1 - \mathbf{\Pi}_i\right)\mathbf{m}_d \\ \vdots \\ \left(\mathbf{\Pi}_j^r - \mathbf{\Pi}_i\right)\mathbf{m}_d \end{bmatrix}, \qquad \mathfrak{c}_2 = \begin{bmatrix} \Delta\mathbf{u} \\ \mathbf{w}_0 - \mathbf{w}_d \\ \left(\mathbf{\Pi}_j^1 - \mathbf{\Pi}_i\right)\mathbf{e}_0 \\ \vdots \\ \left(\mathbf{\Pi}_j^r - \mathbf{\Pi}_i\right)\mathbf{e}_0 \end{bmatrix} \tag{5.18}$$

considering all the configurations $\mathbf{\Pi}_j^1$,..., $\mathbf{\Pi}_j^r$ whose corresponding regions $\Re_j^1$,...,$\Re_j^r$ are neighbors of $\Re_i$. Roughly speaking, first constant terms ($\mathbf{K}$, $\mathbf{u}_d$ and $\Delta\mathbf{u}$) ensure that $\mathbf{u} > \mathbf{0}$, second terms ensure that $\mathbf{w} > \mathbf{0}$ and last terms guarantee that the trajectory lies in $\Re_i$.

Dynamic control (on-line)

III. **Apply** the following control law, which will transfer the system towards $\mathbf{m}'_d$ describing a trajectory in $\Re_i$ with a s.b. control action,

$$\mathbf{u} = \mathbf{u}'_d + \mathbf{K}\left(\mathbf{m} - \mathbf{m}'_d\right) \tag{5.19}$$

IV. At any time, **compute** a new intermediate marking $\mathbf{m}'_d$, closer to $\mathbf{m}_d$ than the previous one, by solving again the LPP (5.16). **Iterate** this step, while the control law (5.19) is being applied, until the *intermediate* desired marking be computed as $\mathbf{m}_d$, i.e., $\mathbf{m}'_d = \mathbf{m}_d$.

In order to prove the effectiveness of this control approach, we proceed as follows: in Proposition 5.8 the existence of $\mathbf{K}$ and $\mathbf{T}_i$, as they were previously defined, is proved. In Proposition 5.9 it is proved that

the LPP (5.16) actually provides the next *intermediate* target marking, i.e., $\mathbf{m}'_d$ is reached by means of (5.19) and this input is s.b.. Finally, in Proposition 5.10 it is proved that this LPP has always a solution, and this converges to $\beta = 0$, i.e., $\mathbf{m}'_d = \mathbf{m}_d$.

Proposition 5.8. *Consider a given $\mathbf{m}'_d \in int(\Re_i)$. The controllable poles of the closed-loop system can be arbitrarily assigned by means of a proper gain matrix $\mathbf{K}$, whose rows non related to transitions of T^i_{cf} are null. If such poles are real, distinct and negative then the system converges asymptotically to the marking $\mathbf{m}'_d$. Moreover, there exists a similarity transformation $\mathbf{T}_i$ s.t. the transformed error $\mathbf{T}_i^{-1}\mathbf{e}'$ is nonnegative and decreasing.*

Proof. Assume $T_c = T^i_{cf}$. Denoting as $\mathbf{K}^i_{cf}$ the matrix built with the rows of $\mathbf{K}$ related to the transitions in T^i_{cf}, then $\mathbf{CK} = \mathbf{C}^i_{cf}\mathbf{K}^i_{cf}$ and $\mathbf{K}^i_{cf}$ fully determines $\mathbf{K}$ (other rows of $\mathbf{K}$ are null). Applying the control law expressed in (5.19), the following closed-loop state equation is obtained

$$\dot{\mathbf{e}}' = (\dot{\mathbf{m}} - \dot{\mathbf{m}}'_d) = (\mathbf{C}\boldsymbol{\Lambda}\boldsymbol{\Pi}_i - \mathbf{C}^i_{cf}\mathbf{K}^i_{cf})\mathbf{e}' \tag{5.20}$$

Consider the Kalman decomposition $\mathbf{T}_{kal}$ (see, for instance, [Chen, 1984]), so

$$\mathbf{T}_{kal}^{-1}\mathbf{C}\boldsymbol{\Lambda}\boldsymbol{\Pi}_i\mathbf{T}_{kal} = \begin{bmatrix} \mathbf{A}_{11} & \mathbf{A}_{12} \\ \mathbf{0} & \mathbf{A}_{22} \end{bmatrix} \qquad \mathbf{T}_{kal}^{-1}\mathbf{C}^i_{cf} = \begin{bmatrix} \mathbf{B} \\ \mathbf{0} \end{bmatrix}$$

and the pair $(\mathbf{A}_{11}, \mathbf{B})$ is controllable in the classical sense. Then, the eigenvalues of $(\mathbf{A}_{11} - \mathbf{B}\mathbf{K}_{kal})$ can be arbitrarily assigned by a proper choice of a gain matrix $\mathbf{K}_{kal}$. Assume that $\mathbf{K}_{kal}$ places those eigenvalues as real, distinct and negative. Consider the gain matrix of the original system s.t. $\mathbf{K}^i_{cf} = \begin{bmatrix} \mathbf{K}_{kal}, & \mathbf{0} \end{bmatrix} \mathbf{T}_{kal}^{-1}$, so the controllable eigenvalues of $(\mathbf{C}\boldsymbol{\Lambda}\boldsymbol{\Pi}_i - \mathbf{CK})$ are equal to those assigned by $\mathbf{K}_{kal}$. The transformed closed-loop system is given by

$$\dot{\boldsymbol{\epsilon}}' = \mathbf{T}_{kal}^{-1}\dot{\mathbf{e}}' = \begin{bmatrix} (\mathbf{A}_{11} - \mathbf{B}\mathbf{K}_{kal}) & \mathbf{A}_{12} \\ \mathbf{0} & \mathbf{A}_{22} \end{bmatrix} \boldsymbol{\epsilon}' \qquad \boldsymbol{\epsilon}'_0 = \begin{bmatrix} \boldsymbol{\epsilon}'_{10} \\ \boldsymbol{\epsilon}'_{20} \end{bmatrix}$$

where $\boldsymbol{\epsilon}'_0 = \mathbf{T}_{kal}^{-1}\mathbf{e}'_0$. Now, by controllability hypothesis $\mathbf{G}_i \in Span\{Contr(\mathbf{C}\boldsymbol{\Lambda}\boldsymbol{\Pi}_i, \mathbf{C}^i_{cf})\}$, so $\mathbf{T}_{kal}^{-1}\mathbf{G}_i \in Span\{Contr(\mathbf{T}_{kal}^{-1}\mathbf{C}\boldsymbol{\Lambda}\boldsymbol{\Pi}_i\mathbf{T}_{kal}, \mathbf{T}_{kal}^{-1}\mathbf{C}^i_{cf})\}$, which is equivalent to

$$\mathbf{T}_{kal}^{-1}\mathbf{G}_i \in Span\left\{ \begin{bmatrix} \mathbf{B} & \mathbf{A}_{11}\mathbf{B} & ,..., & \mathbf{A}_{11}^{|P|-1}\mathbf{B} \\ \mathbf{0} & \mathbf{0} & ,..., & \mathbf{0} \end{bmatrix} \right\}$$

Since $\mathbf{T}_{kal}^{-1}\mathbf{e}'_0 \in Span\{\mathbf{T}_{kal}^{-1}\mathbf{G}_i\}$ then $\boldsymbol{\epsilon}'_{20} = \mathbf{0}$, i.e., the transformed initial error is null at the uncontrollable part. Now, consider a modal decomposition of $(\mathbf{A}_{11} - \mathbf{B}\mathbf{K}_{kal})$, i.e., a modal matrix $\mathbf{V}$ s.t. $\mathbf{V}^{-1}(\mathbf{A}_{11} - \mathbf{B}\mathbf{K}_{kal})\mathbf{V} = \mathbf{D}$ where $\mathbf{D}$ is diagonal, and compute a diagonal matrix $\mathbf{S}$ whose elements are in $\{-1, 1\}$ (so $\mathbf{S} = \mathbf{S}^{-1}$) in such a way that $\mathbf{S}\mathbf{V}^{-1}\boldsymbol{\epsilon}'_{10} \geq \mathbf{0}$. Then, defining the similarity transformation

$$\mathbf{T}_i = \mathbf{T}_{kal} \begin{bmatrix} \mathbf{VS} & \mathbf{0} \\ \mathbf{0} & \mathbf{I} \end{bmatrix} \tag{5.21}$$

the original closed-loop system (5.20) can be transformed as

$$\begin{aligned}\mathbf{T}_i^{-1}\overset{\bullet}{\mathbf{e}'} &= \begin{bmatrix} \overset{\bullet}{\boldsymbol{\varepsilon}'_1} \\ \boldsymbol{\varepsilon}'_2 \end{bmatrix} = \begin{bmatrix} \mathbf{D} & (\mathbf{VS})^{-1}\mathbf{A}_{12} \\ \mathbf{0} & \mathbf{A}_{22} \end{bmatrix} \begin{bmatrix} \boldsymbol{\varepsilon}'_1 \\ \boldsymbol{\varepsilon}'_2 \end{bmatrix} \\ \mathbf{T}_i^{-1}\mathbf{e}'_0 &= \boldsymbol{\varepsilon}'_0 = \begin{bmatrix} \boldsymbol{\varepsilon}'_{10} \\ \boldsymbol{\varepsilon}'_{20} \end{bmatrix} \geq \mathbf{0}\end{aligned} \tag{5.22}$$

Since $\boldsymbol{\varepsilon}'_{20} = \boldsymbol{\epsilon}'_{20} = \mathbf{0}$, the solution of such equation is

$$\begin{aligned}\boldsymbol{\varepsilon}'_1(\tau) &= e^{\mathbf{D}\tau}\boldsymbol{\varepsilon}'_{10} \\ \boldsymbol{\varepsilon}'_2(\tau) &= \boldsymbol{\varepsilon}'_{20} = \mathbf{0}\end{aligned}$$

Finally, since $\mathbf{D}$ is a diagonal matrix with negative diagonal entries (which correspond to the eigenvalues of the closed-loop system), then $\boldsymbol{\varepsilon}'_0 \geq \boldsymbol{\varepsilon}'(\tau) \geq \mathbf{0}\ \forall\tau$, and the error converges to zero. ∎

In the sequel, let us assume that $\mathbf{K}$ is s.t. the controllable poles of the closed-loop system are real, distinct and negative.

Proposition 5.9. *Consider the initial and desired markings $\mathbf{m}_0, \mathbf{m}_d \in int\{\Re_i\}$. Suppose that at some time τ_1, $\mathbf{m}(\tau_1) \in int\{\Re_i\}$ and a solution β for the LPP (5.16) is computed. Consider the* intermediate *desired marking as in (5.15). If the input (5.19) is being applied then $\mathbf{m}'_d$ will be reached through a trajectory inside $\Re_i$. Moreover, such input will be suitable bounded along the marking trajectory.*

Proof. According to (5.16) and denoting $\mathbf{e}'(\tau_1) = \mathbf{e}(\tau_1) - \beta\mathbf{e}_0$

$$\mathfrak{c}_1 + \beta\mathfrak{c}_2 + neg(\mathbf{A})\mathbf{T}_i^{-1}\mathbf{e}'(\tau_1) \geq \mathbf{0} \tag{5.23}$$

Now, since the control law (5.19) is being applied, according to Proposition 5.8 the error of the closed-loop system fulfills $\mathbf{T}_i^{-1}\mathbf{e}'(\tau_1) \geq \mathbf{T}_i^{-1}\mathbf{e}'(\tau) \geq \mathbf{0}$ for $\tau \geq \tau_1$, so, $neg(\mathbf{A})\mathbf{T}_i^{-1}\mathbf{e}'(\tau_1) \leq neg(\mathbf{A})\mathbf{T}_i^{-1}\mathbf{e}'(\tau)$ (because $neg(\mathbf{A}) \leq \mathbf{0}$ by definition). Furthermore, since $\mathbf{T}_i^{-1}\mathbf{e}'(\tau) \geq \mathbf{0}$ then $neg(\mathbf{A})\mathbf{T}_i^{-1}\mathbf{e}'(\tau) \leq \mathbf{A}\mathbf{T}_i^{-1}\mathbf{e}'(\tau)$. Therefore $neg(\mathbf{A})\mathbf{T}_i^{-1}\mathbf{e}'(\tau_1) \leq \mathbf{A}\mathbf{T}_i^{-1}\mathbf{e}'(\tau)$, so, substituting this into (5.23) we obtain

$$\mathfrak{c}_1 + \beta\mathfrak{c}_2 + \mathbf{A}\mathbf{T}_i^{-1}\mathbf{e}'(\tau) \geq \mathbf{0}, \qquad \forall\tau \geq \tau_1$$

Substituting the constants (5.18) and using the definitions of $\mathbf{e}'$, $\mathbf{w}'_d$ and $\mathbf{m}'_d$, the previous inequality is transformed into

$$\begin{gathered}\mathbf{u}(\tau) \geq \mathbf{0} \\ \Lambda\boldsymbol{\Pi}_i\mathbf{m}(\tau) - \mathbf{u}(\tau) \geq \mathbf{0} \\ \left(\boldsymbol{\Pi}_j^1 - \boldsymbol{\Pi}_i\right)\mathbf{m}(\tau) \geq \mathbf{0} \\ \vdots \\ \left(\boldsymbol{\Pi}_j^r - \boldsymbol{\Pi}_i\right)\mathbf{m}(\tau) \geq \mathbf{0} \\ \forall\tau \geq \tau_1\end{gathered}$$

Then, $\mathbf{u}(\tau)$ is s.b. for all time and the system lies in $\Re_i$. ∎

The LPP (5.16) can be solved very efficiently on-line, because it can be reduced to the problem of finding the minimum entry of a properly computed vector (illustrated for a similar problem in Section C.3). Furthermore, some of the inequalities are always fulfilled and can be eliminated (those involving uncontrollable transitions and null constants).

Proposition 5.10. *Suppose that the initial and desired markings ($\mathbf{m}_0$ and $\mathbf{m}_d$) belong to $int(\Re_i) \cap E_i^*$, and that the entries of $\mathbf{u}_0$ and $\mathbf{u}_d$ are positive for all the fully controllable transitions. Then, there exists solution β for the LPP (5.16) at $\mathbf{m}_0$. Moreover, if the control Procedure 5.3 is being applied then there will exist solution β at all future markings. Furthermore, the closer the marking is to $\mathbf{m}_d$, the lower is this solution, until obtaining a value of 0.*

Proof. Consider the inequality of (5.16) but reorder it as

$$\mathfrak{c}_1 + \gamma \mathfrak{c}_2 + neg(\mathbf{A})\mathbf{T}_i^{-1}(\mathbf{e} - \gamma \mathbf{e}_0) \geq \mathbf{0} \tag{5.24}$$

First consider a given $\gamma \in [0, 1]$. In this way, the marking $\mathbf{m}'_d = \mathbf{m}_d + \gamma \mathbf{e}_0$ is in the segment defined by $\mathbf{m}_0$ and $\mathbf{m}_d$, so, it belongs to $int(\Re_i)$ and the vector

$$\mathfrak{c}_1 + \gamma \mathfrak{c}_2 = \begin{bmatrix} \mathbf{u}'_d \\ \mathbf{w}'_d \\ \left(\mathbf{\Pi}_j^1 - \mathbf{\Pi}_i\right) \mathbf{m}'_d \\ \vdots \\ \left(\mathbf{\Pi}_j^r - \mathbf{\Pi}_i\right) \mathbf{m}'_d \end{bmatrix}$$

is positive at the relevant entries (those that correspond to non null rows of $\mathbf{A}$). Therefore, for a small enough value of $(\mathbf{e} - \gamma \mathbf{e}_0) = \mathbf{e}'$, i.e., for $\mathbf{m}$ close enough to $\mathbf{m}'_d$, the corresponding γ is a solution for (5.24). A particular case occurs at $\mathbf{m}_0$, in which $(\mathbf{e} - \gamma \mathbf{e}_0) = (1 - \gamma)\mathbf{e}_0 = \mathbf{e}'$ (i.e., a value of γ close enough to 1 makes $\mathbf{e}'$ be small enough, and then such γ is a solution for (5.24) and the LPP).

Now, suppose that at time τ_1 a solution β_1 is computed. Substituting $\gamma = \beta_1 - \Delta\gamma$ into (5.24) and reordering the terms

$$\mathfrak{c}_1 + \beta_1 \mathfrak{c}_2 + neg(\mathbf{A})\mathbf{T}_i^{-1}(\mathbf{e} - \beta_1 \mathbf{e}_0) - \Delta\gamma(\mathfrak{c}_2 - neg(\mathbf{A})\mathbf{T}_i^{-1}\mathbf{e_0}) \geq \mathbf{0} \tag{5.25}$$

Consider a future time $\tau_2 > \tau_1$. If the control law (5.19) is being applied (with $\beta = \beta_1$) then $\mathbf{T}_i^{-1}\mathbf{e}'(\tau_2) \leq \mathbf{T}_i^{-1}\mathbf{e}'(\tau_1)$, which implies that $neg(\mathbf{A})\mathbf{T}_i^{-1}\mathbf{e}'(\tau_2) \geq neg(\mathbf{A})\mathbf{T}_i^{-1}\mathbf{e}'(\tau_1)$, so, at τ_2 there will exist $\Delta\gamma > 0$ that fulfills (5.25), i.e., as $\mathbf{m}$ approximates to $\mathbf{m}'_d$ a lower solution can be obtained.

Finally, note that a lower solution β_2 cannot be obtained only if either the current one is null or $\mathfrak{c}_1 + \beta_1 \mathfrak{c}_2$ has null elements at the relevant entries. Nevertheless, this last condition implies that $\mathbf{m}'_d = \mathbf{m}_d + \beta_1 \mathbf{e}_0$ belongs to the frontier of $\Re_i$ and/or there is a null entry of $\mathbf{u}'_d$ related to a transition in T_{cf}^i, but this never occurs under the hypothesis assumed. Therefore, the solution $\beta = 0$ will be eventually obtained. ∎

The computation of β can be done at every sampling or just at some of them. Any pole assignment technique can be used for computing $\mathbf{K}$. It can be proved that, in some cases, this control approach can

also be applied even if $\mathbf{m}_d$ or $\mathbf{m}_0$ belongs to the frontier of the region, and/or $\mathbf{u}_d$ or $\mathbf{u}_0$ have null entries related to fully controllable transitions.

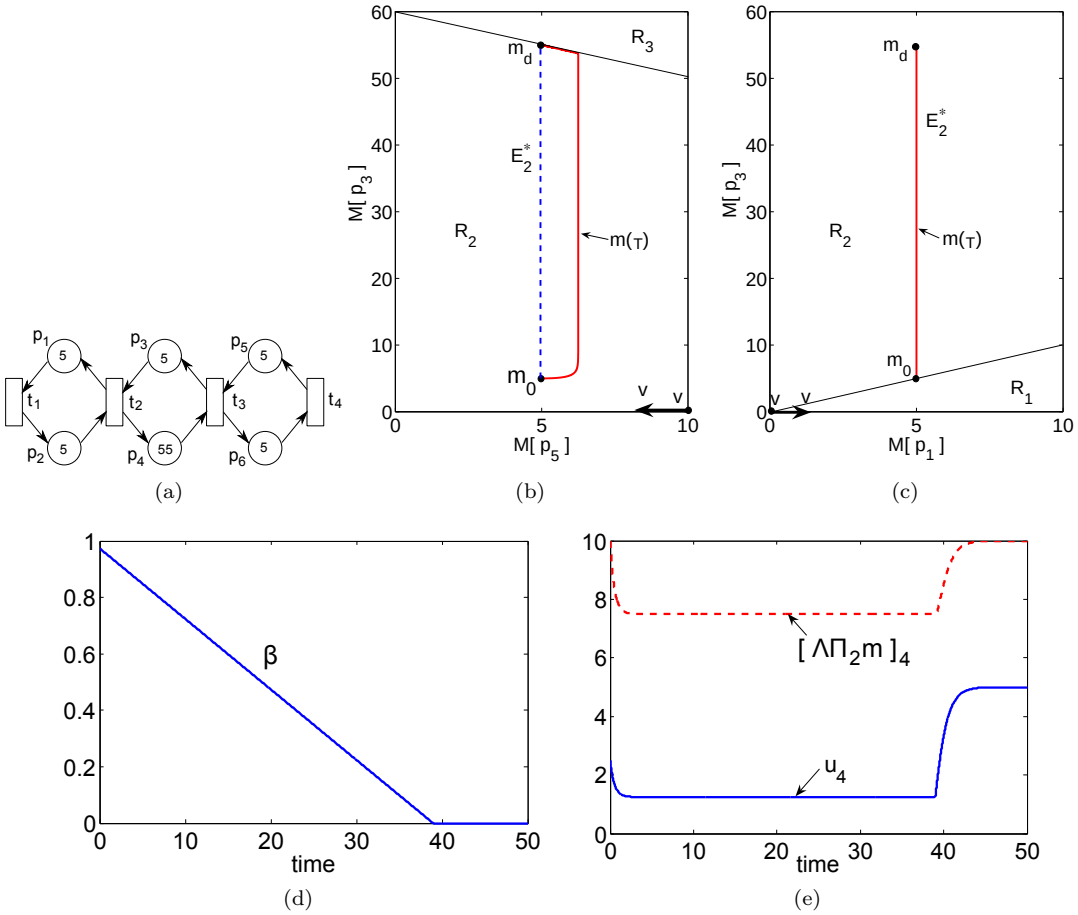

Fig. 5.7: a) TCPN system. b), c) Projections of $Class(\mathbf{m}_0)$ on the planes $[\mathbf{m}(p_5), \mathbf{m}(p_3)]$ and $[\mathbf{m}(p_1), \mathbf{m}(p_3)]$, the dashed line is E_2^* while the solid one is the trajectory of the closed-loop system (both coincide in the second projection). d) Computed value for β, e) input signal $\mathbf{u}$ and flow $(\Lambda\mathbf{\Pi}_2\mathbf{m})$ of t_4 during the closed-loop evolution.

Example 5.4. Consider the system of fig. 5.7(a) with $\lambda_1 = \lambda_2 = \lambda_3 = 1$ and $\lambda_4 = 2$. Let $T_c = \{t_4\}$. This system has two synchronizations and only 3 feasible regions. Projections of $Class(\mathbf{m}_0)$ on the planes $[\mathbf{m}(p_5), \mathbf{m}(p_3)]$ and $[\mathbf{m}(p_1), \mathbf{m}(p_3)]$ are shown in figs. 5.7(b) and 5.7(c) (the marking of only three places is required to defined a reachable marking, then two projections are sufficient for representing $Class(\mathbf{m}_0)$). The initial marking is $\mathbf{m}_0 = [5, 5, 5, 55, 5, 5]^T$ while the desired one is $\mathbf{m}_d = [5, 5, 55, 5, 5, 5]^T$. Both markings belong to the same region $\Re_2$.

The set of equilibrium markings in $\Re_2$, i.e., E_2^*, is shown in figs. 5.7(b) and 5.7(c) as a dashed line. A generator for it is given by $\mathbf{G}_2 = [0, 0, 1, -1, 0, 0]^T$. For this case, $T_c = T_{cf}^2$ and the system is controllable over E_2^* (already proven in the Example 4.6). The proposed control procedure was applied to this system. A gain matrix $\mathbf{K}$, that places the controllable poles of the closed-loop system at -1

and -2, was computed. Also, we computed the required similarity transformation matrix $\mathbf{T}_2$. The LPP was continuously solved (at each simulation time step). Fig. 5.7(d) shows the evolution of the value computed for β. The closed-loop trajectory is drawn in figs. 5.7(b) and 5.7(c) (solid line). It can be seen that this control law successfully transfered the state from $\mathbf{m}_0$ to $\mathbf{m}_d$ through a trajectory in $\Re_2$, moreover, it can be seen in fig. 5.7(e) that the input is s.b..

5.4.2 Controlling between neighbor regions

This section is devoted to advance the ideas leading to the generalization of the previously introduced control law structure. In particular, it is considered the problem of transferring the system from an equilibrium marking $\mathbf{m}_{01} \in \Re_1$ to another one $\mathbf{m}_{d2} \in \Re_2$, where $\Re_1$ and $\Re_2$ are *neighbor* regions. It is assumed that the system fulfills the sufficient conditions for controllability over E_1^* and E_2^* of Corollary 4.18. Also, it is assumed that there exists an equilibrium marking $\mathbf{m}_{int}$ that belongs to $E_1^* \cap E_2^*$ but not to another region.

Under these hypothesis, a control law for each region can be computed by using the control scheme introduced in Procedure 5.3. Then, a first idea is to compute and apply a control law that transfers the marking from $\mathbf{m}_{01} \in \Re_1$ to $\mathbf{m}_{int}$, through a trajectory in $\Re_1$, and another control law that transfers the marking from $\mathbf{m}_{int}$ to $\mathbf{m}_{d2} \in \Re_2$. Nevertheless, the first control law will transfer the marking towards $\mathbf{m}_{int}$ in infinite time, so the second control law will never be applied. Then, the problem can be reduced to the computation of a control law that transfers the marking from any $\mathbf{m} \in \Re_1$ in a neighborhood of $\mathbf{m}_{int}$, to an equilibrium marking $\mathbf{m}'_{d2} \in \Re_2 - \Re_1$. Such control law exists because the system fulfills the conditions of Proposition 4.21.

In order to solve this problem, consider the LPP (5.16) for $\Re_1$ with $\mathbf{m}_{int}$ as the desired marking, $\Delta\mathbf{u} = \mathbf{u}_{01} - \mathbf{u}_{int}$ and without the inequalities $\gamma \geq 0$ and that which involves $\mathbf{\Pi}_2 - \mathbf{\Pi}_1$. Then, this new LPP is obtained

$$\begin{aligned} \beta = min\ \gamma \qquad & \text{subject to} \\ & \mathfrak{c}_1 + neg(\mathbf{A})\mathbf{T}_1^{-1}\mathbf{e} + \gamma\left(\mathfrak{c}_2 - neg(\mathbf{A})\mathbf{T}_1^{-1}\mathbf{e}_0\right) \geq \mathbf{0} \end{aligned} \tag{5.26}$$

where $\mathfrak{c}_1$, $\mathfrak{c}_2$ and $\mathbf{A}$ are defined like in (5.18) with $i = 1$, $\mathbf{m}_d = \mathbf{m}_{int}$, $\mathbf{u}_d = \mathbf{u}_{int}$, $\mathbf{w}_d = \mathbf{w}_{int}$ and $\mathbf{\Pi}_j^1$,...,$\mathbf{\Pi}_j^r$ are related to all the neighbor regions of $\Re_1$ excepting $\mathbf{\Pi}_2$.

If at a given marking $\mathbf{m}(\tau_1)$, close enough to $\mathbf{m}_{int}$, a value of $\beta < 0$ were computed, then the target marking $\mathbf{m}'_d = \beta\mathbf{m}_{01} + (1-\beta)\mathbf{m}_{int}$ would belong to $\Re_2$. In such case, the control law (5.19) would transfer the system from $\mathbf{m}(\tau_1) \in \Re_1$ to some $\mathbf{m}(\tau_2) \in \Re_2 \cap \Re_1$, and once the marking would reach the frontier, a control law could be applied in order to finally reach $\mathbf{m}_{d2} \in \Re_2$. It is easy to prove that a value $\beta < 0$ can be computed if the entries of $\mathbf{u}_{int}$, related to transition of T_{cf}^1, are positive, i.e., $\mathbf{m}_{int} \in E_1^* \cap E_2^*$.

Denote the solution for the modified LPP (5.26) as β_1 and the solution for the LPP (5.16) defined for $\Re_2$ as β_2. A simple way to guarantee that a solution $\beta_2 < 1$ will be computed once the system reach the common frontier, consists in computing both, β_1 and β_2, simultaneously when the marking is approximating to the frontier, and adding a new rule:
if $\beta_1 < 0$ but $\beta_2 \geq 1$ then consider β_1 as zero for the computation of $\mathbf{m}'_d$.

In this way, an input for crossing the border is computed (i.e., $\beta_1 < 0$ is considered) only if $\beta_2 < 1$, otherwise, the system will be transferred towards $\mathbf{m}_{int}$ and it will remain in $\Re_1$, until reaching a neighborhood of $\mathbf{m}_{int}$ in which such values can be computed (such neighborhood exists because $\beta_2 < 1$

and $\beta_1 < 0$ can be obtained at $\mathbf{m}_{int}$). Finally, the system will probably cross the frontier at a non equilibrium marking, then the error of the uncontrollable part (for the system at $\Re_2$) may not be null, in such case, we have to ask for the non controllable poles (non related to P-flows) to have real negative parts (thus the uncontrollable dynamics are asymptotically stable).

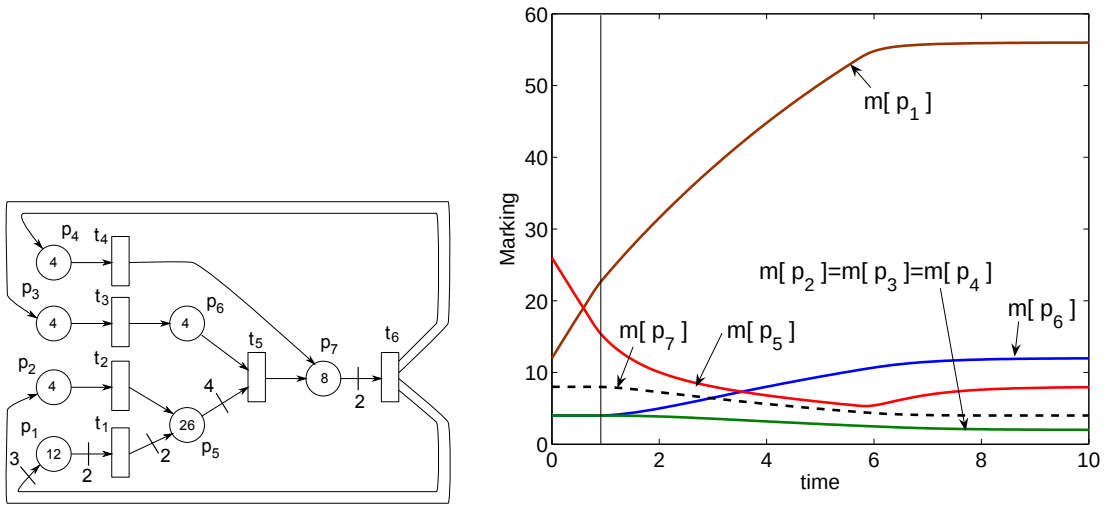

Fig. 5.8: a) TCPN system controllable over $E_1^+ \cup E_2^+$. b) Marking of places for the trajectory described by the closed-loop system.

Example 5.5. Consider the system of fig. 5.8(a) with $\mathbf{\Lambda} = \mathbf{I}$. Let $T_c = \{t_1\}$. This system has one synchronization, which leads to two regions that are denoted as $\Re_1$ (in which p_5 is constraining t_5) and $\Re_2$. The initial marking is $\mathbf{m}_0 = [12,\ 4,\ 4,\ 4,\ 26,\ 4,\ 8]^T$ which belongs to $\Re_2$. Consider a desired marking $\mathbf{m}_d = [56,\ 2,\ 2,\ 2,\ 8,\ 12,\ 4]^T$, which belongs to $\Re_1$. There exists an interface equilibrium marking $\mathbf{m}_{int} = [22,\ 4,\ 4,\ 4,\ 16,\ 4,\ 8]^T$ s.t. $\mathbf{m}_{int} \in E_1^* \cap E_2^*$. This system fulfills the conditions of Proposition 4.21 for the controllability over $E_1^* \cup E_2^*$. In this way, stabilizing gain matrices were computed for each region. The equilibrium input of $\mathbf{m}_{int}$ is given by $\mathbf{u}_{int} = [5,\ 0,\ 0,\ 0,\ 0,\ 0]^T$, i.e., it is positive at the entry related to t_1 (the only controllable transition), so, it is possible to transfer the system through the region's frontier. Applying the proposed scheme, the system is successfully transferred from $\mathbf{m}_0$ to $\mathbf{m}_d$ through a trajectory in which the input is s.b.. The marking trajectories are shown in fig. 5.8(b), where the vertical line denotes the change of region.

Finally, let us point out that, in our experience, it always has been found (but still not proved) that the union of sets E_i^* is connected. In such case, the synthesis of a control law for several regions is reduced to the problem of transferring the system between neighbor regions, which was studied in this subsection.

5.5 Conclusions on control laws

Different control laws, for TCPNs under infinite server semantics, have been proposed in the literature. This chapter starts with a quick overview of some representative techniques, and a preliminarily comparison between them. Nevertheless, there is a lack of control methods that can be used when the systems exhibit a large net structure of uncontrollable transitions are considered. Motivated by this, three different control structures are proposed through this chapter:

• First, an affine control law is considered in order to provide a simple synthesis procedure for systems in which all the transitions are controllable, ensuring asymptotic stability and feasibility. The complexity of the control synthesis does not depend on the number of configurations (like in other control laws) but on the number of vertices of the polytope (thus, the number of places).

• A modular-coordinated control strategy was proposed in order to reduce the complexity involved in the synthesis procedure. The resulting scheme consists of a set of affine local controllers and a coordinator that receives and sends information to the local controllers. Feasibility and convergence to the required markings have been proved. The application of the control scheme is achieved in polynomial time. Furthermore, the combined complexity involved in the synthesis of the local controllers (off-line) is lower than in the centralized case. It is left for a future research, to investigate the performance of the proposed control scheme under lost or delayed information conditions.

• Finally, a control law structure, for TCPN systems having uncontrollable transitions, has been proposed, by adapting the classical pole-assignment technique used in LTI systems [Chen, 1984]. The implementation of this control law consists of the computation of a suitable gain matrix for each region, and the resolution of a LPP during its application for computing suitable intermediate markings that guarantees the boundedness of the input. It is proved that such control law can always be computed and transfers the marking towards the desired one, whenever the conditions for controllability are fulfilled and there exist suitable interface markings between the regions. The main drawback of this control technique is that one controller has to be synthesized for each configuration. In this way, more efforts are required in order to investigate efficient synthesis techniques for systems having a large number of synchronizations.

Chapter 6

Towards control applications in discrete systems

In the literature, several works can be found providing different control strategies for (discrete) Petri nets. These can be classified into two different classes [Holloway et al., 1997a]: the *state feedback control*, which has been mainly studied by means of a particular model called controlled Petri nets, and the *event feedback control* that has been mainly considered in a formal language setting and the corresponding models are called labeled Petri nets. Extensions to timed systems can also be found in the literature. Most control strategies are defined for the same control objective: disabling transitions for avoiding forbidden markings, in accordance with the Supervisory-Control Theory.

From another perspective, the existence of fluid models that can approximate the behavior of discrete Petri nets leads to consider another kind of control goals, i.e., problems frequently addressed in the Control Theory for continuous-state systems, like the stabilization of the system, the tracking of a reference signal or the regulation of the output in order to follow another dynamic system [Chen, 1984, Khalil, 2002]. One of those control problems (a classical one) is the stabilization of the system at a desired/required steady state (set-point), which has been addressed in Chapter 5 for TCPNs.

Enforcing a desired target marking in a continuous PN is analogous to reaching an average marking in the original discrete model (assuming that the continuous model approximates the discrete one), which may be interesting in several kinds of systems. This idea has been considered by some authors. For instance, in [Amrah et al., 1998] it was proposed a methodology for the control of open and closed manufacturing lines. There, the control actions consist in the modification of the maximal firing speeds of the controllable transitions of the continuous model. It was illustrated how the control law can be applied to the original discrete Petri net model (a T-timed model with constant firing delays). This approach has been used in [Lefebvre, 1999] and [Kara et al., 2006] as well, in the same context of manufacturing lines.

In this framework, the results introduced in Chapters 3, 5 and 6, regarding the fluidization of Markovian PNs, the controllability analysis and the control synthesis for TCPNs, will be combined in this chapter in order to propose a control scheme for MPNs via its continuous relaxation. If in the TCPN system, the designed control law drives the marking towards a desired equilibrium one by means of a reduction of the flow of the controllable transitions, in the MPN the adaptation of the same control law

will drive the *average marking* towards a desired value, just by applying *additional delays* to the controllable transitions. This control approach is different to the control techniques that can be frequently found in the literature for DES. Furthermore, there are important differences w.r.t. the works reported in [Amrah et al., 1998, Lefebvre, 1999, Kara et al., 2006], these are : 1) here MPNs are considered as the original discrete model (instead of deterministically T-timed PNs), 2) the proposed structure is based on the results obtained by a formal analysis of the fluid approximation, controllability and control synthesis, introduced in chapters 3, 5 and 6, 3) general kinds of net structures and control techniques are considered. Here we are dealing with the interpretation of the control results, obtained for the continuous model, into the original discrete one, making a contribution to the bridge between continuous-state systems and DES ones. In other words, we are closing the loop of the control synthesis for DES by using fluid models (illustrated in fig. 0.2).

This control structure will be described in Section 6.1. Later, a stock-level control problem of an automotive assembly line system, originally modeled as a stochastically timed discrete Petri net [Dub et al., 2002], will be considered in Section 6.2. The resulting scheme will allow to control the average value of the marking at the places that represent the stock-level, by means of applying additional delays to a controllable transition, representing the action of sending a material request to the supplier.

Finally, in Section 6.3 a different control application for DES via fluidization is introduced: the coordination of the traffic signals in an urban traffic network. For this, a hybrid model for the traffic behavior at an intersection is obtained by relaxing a discrete PN model, capturing important aspects of the flow dynamics in urban networks. It is shown that this model can be used in order to obtain control policies that can improve the traffic flow at intersections, leading to the possibility of controlling several connected intersections in a distributed way.

6.1 Implementation of control laws for MPNs via TCPNs

In this section, the implementation of a control law designed for a TCPN system, into the corresponding MPN, will be described. This can be seen as the last step of a general procedure for the analysis and synthesis of DES through fluid models, which was depicted in fig. 0.2 and is described in the following steps:

Procedure 6.1. Synthesis and implementation of a controller for a MPN via its corresponding TCPN.

I. Consider a live and ergodic MPN.

II. Obtain the corresponding TCPN, verifying that it approximates the behavior of the MPN (as analyzed in Chapter 2).

IV. Compute, if it is not provided, the required steady state (for instance, by minimizing an optimization criterion, [Mahulea et al., 2008b]).

V. Verify the controllability of the TCPN system (as discussed in Chapter 4).

VI. Verify the observability of the TCPN system (this is discussed, in detail, in [Júlvez et al., 2008, Mahulea et al., 2010]).

VII. Synthesize a suitable controller (as discussed in Chapter 5).

VIII. Implement the controller into the MPN (the topic of this chapter)

In order to implement such a controller, it is required an interpretation, in one hand, for the "continuous" control input in terms of the MPN, and in the other hand, for the marking of the MPN in terms of the TCPN. Let us provide a preliminarily idea for these.

The control actions in the TCPN are defined as a reduction to the transition's flow. The flow represents the speed at which the transitions fire, which in the discrete PN can be understood as the firing frequency. In this way, the control actions will be interpreted in the MPN as a reduction of the firing frequency, which is equivalent to the addition of *external* (and controllable) delays. On the other hand, the results obtained in Chapter 3, regarding the fluidization of MPNs, provide an answer for the interpretation of the marking of the MPN into that of the TCPN, i.e., the *expected marking* of the discrete model can be approximated by that of the continuous one.

In fact, a better approximation is provided by the TnCPN model. Remember that the TnCPN is actually defined as the TCPN with the addition of gaussian white noise $\mathbf{v}_k$ (see, Section 2.3). In this way, the TnCPN model can be seen, from a Control Theory perspective (see, for instance, [Khalil, 2002]), as the nominal system TCPN (i.e., $\mathbf{m}_{k+1} = \mathbf{m}_k + \mathbf{C}\boldsymbol{\Lambda}\boldsymbol{\Pi}(\mathbf{m}_k)\mathbf{m}_k\Delta\tau$) under the state perturbation $\mathbf{C}\mathbf{v}_k$. The stabilization of this kind of systems is typically addressed in the control synthesis in continuous-state systems. For this, a control law is synthesized for the nominal system (in this case, the TCPN), while an estimation of the average state is obtained by using a filter. Such estimation is then used for the evaluation of the control law, obtaining thus a proper control implementation for the system with noise. This approach will be detailed in the following subsection.

6.1.1 Control architecture

A control structure for the application of a control law to a MPN, via its corresponding TCPN, is described in the Block Diagram of fig. 6.1. This is a typical structure of a closed-loop system under an estimation-based control.

Blocks in the upper dashed box (*Plant*) represent the original system (modeled by a MPN). In the Block diagram of fig. 6.1, it is considered a linear output function, i.e., the information that we have about the state of the MPN is:

$$\mathbf{Y}_k = \mathbf{H} \cdot \mathbf{M}_k \tag{6.1}$$

In order to ensure observability, it is assumed that the output has enough information to determine the current configuration and reconstruct the marking.

The lower dashed box (*TCPN+Control*) represents the corresponding TCPN system under a control law. The synthesis of controllers was discussed in detail in the Chapter 5. Here, it is assumed that the control law, designed for the TCPN, is properly "soft" (this and its derivatives do not exhibit

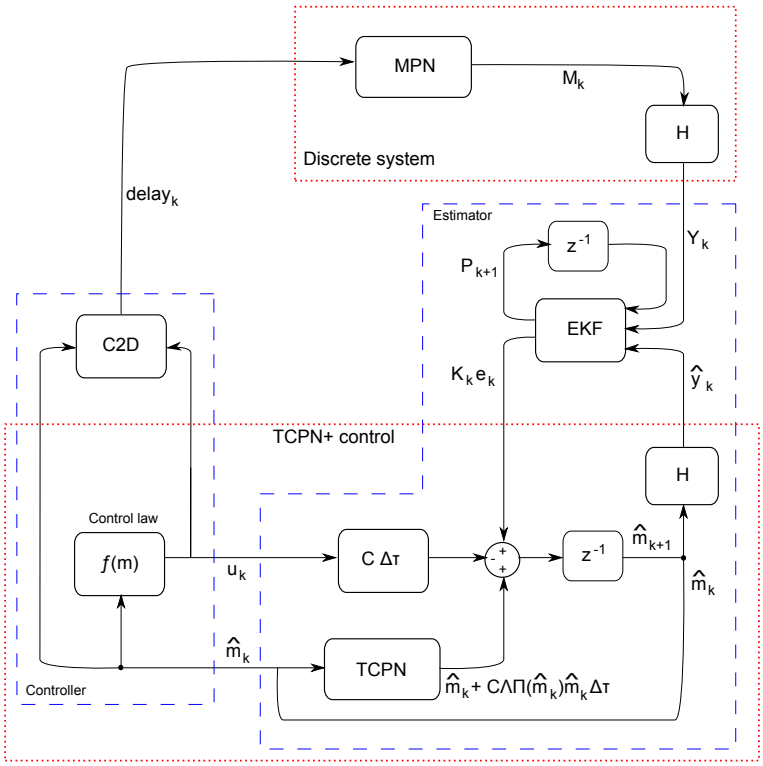

Fig. 6.1: Block diagram of a MPN under control.

discontinuities or stiffness) and suitably bounded. The same output function, considered for the MPN, is also applied to the continuous system. It is assumed that the TCPN is observable (a detailed discussion of observability in TCPNs can be found in [Júlvez et al., 2008, Mahulea et al., 2010]). Then, the output of the TCPN is:

$$\widehat{\mathbf{y}}_k = \mathbf{H} \cdot \widehat{\mathbf{m}}_k \tag{6.2}$$

Blocks *C2D* and *EKF* play the role of *interfaces* between the MPN and the TCPN systems. *C2D* transfers the information, about the control actions, from the TCPN system to the MPN one, while *EKF* do the same in the opposite direction, with the information of the outputs. The function of these blocks will be explained in detail in the following subsections. Let us point out that, if *C2D* and *EKF* were eliminated, only the MPN and the TCPN blocks would be present, i.e., blocks in dashed boxes *Discrete system* and *TCPN+Control*. In such case, two independent systems would be obtained, whose outputs would be linear functions on particular realizations (marking trajectories) of both systems, but no interaction between them would occur.

6.1.2 Interface block C2D

First, let us consider the Block Diagram in fig. 6.1 without the block *EKF*. As it was pointed out in Chapter 2, the expected value of the marking of the MPN may be approximated by the average marking of corresponding TnCPN, which can be seen as the nominal system TCPN under the state perturbation

$\mathbf{C}\mathbf{v}_k$. Then, let us suppose, at this moment, that such approximation holds.

Assume that a s.b. control law is being applied to the TCPN system. Consider the state equation of the continuous model. Given a controllable transition t_j, the controlled flow is equal to $w_j = \lambda_j \cdot enab(t_j, \mathbf{m}) - u_j$. Nevertheless, since the input is s.b., there exists a function $\alpha(u_j, \mathbf{m})$ that takes values in the interval $[0, 1]$ such that $u_j = \alpha(u_j, \mathbf{m}) \cdot \lambda_j \cdot enab(t_j, \mathbf{m})$, then $w_j = (1 - \alpha(u_j, \mathbf{m})) \cdot \lambda_j \cdot enab(t_j, \mathbf{m})$. This last equality means that each active server of t_j fires with an average delay of $((1-\alpha(u_j, \mathbf{m})) \cdot \lambda_j)^{-1}$ in the controlled TCPN system, instead of the average delay of λ_j^{-1} that would have without control. Then, the control law *imposes* to each active server of t_j an additional delay of:

$$delay[t_j] = \frac{1}{(1 - \alpha(u_j, \mathbf{m}))\lambda_j} - \frac{1}{\lambda_j} \tag{6.3}$$

If additional delays are defined for all the controllable transitions in the same way, and these are added to the corresponding average delays of the MPN system, then its average marking will be approximated by that of the TCPN in the closed-loop behavior as well. Block *C2D* computes such additional delays, so, according to (6.3) and substituting α, the output of *C2D* is defined as:

$$delay_k[t_j] = \frac{enab(t_j, \mathbf{m}_k)}{\lambda_j \cdot enab(t_j, \mathbf{m}_k) - \mathbf{u}_k[t_j]} - \frac{1}{\lambda_j} \tag{6.4}$$

Note that it is only required to compute the additional delays for the controllable transitions T_c. In order to exemplify the application of these additional delays into the MPN system, suppose that at some time step k the controllable transition t_j in the MPN is newly enabled, then the firing delay of t_j in the open-loop system would be given by a random variable having an exponential pdf with parameter $(1/\lambda_j) \cdot (1/Enab(t_j, \mathbf{M}_k))$, but, in order to apply the control law the parameter of the exponential pdf is considered as $(1/\lambda_j + delay_k[t_j]) \cdot (1/Enab(t_j, \mathbf{M}_k))$. In this way, t_j will fire with the required average delay, in agreement with the input applied to the TCPN system. This control interpretation is a particular one of many that can be defined, nevertheless, this is used for simplicity and because it has shown positive results.

6.1.3 Interface block EKF

Block *C2D* may be enough for applying the control law into the MPN, if the approximation holds and the MPN exhibits its expected behavior (otherwise stated, if each transition of the MPN fires at the expected delay). Nevertheless, note that the MPN does not receive any feedback in this way (remember that at this point, block *EKF* is not considered). Then, in order to improve the accuracy, an *Extended Kalman Filter* (EKF) is added in the Block Diagram of fig. 6.1 (for a detailed introduction to Kalman Filter see, for instance, [Grewal and Andrews, 2001]).

In order to analyze block *EKF*, suppose that no control law is being applied to both systems. Now, as it was pointed out in Subsection 2.3, the MPN can be approximated by the corresponding TnCPN. Then, by using the approximation error $\boldsymbol{\varepsilon}_k = \mathbf{M}_k - \mathbf{m}_k$, the evolution of the output of the MPN (the

evolution of the signal $\mathbf{Y}_k$ in fig. 6.1) can be described as:

$$\begin{aligned} \mathbf{m}_{k+1} &= [\mathbf{I} + \mathbf{C}\boldsymbol{\Lambda}\boldsymbol{\Pi}(\mathbf{m}_k)\Delta\tau]\,\mathbf{m}_k + \mathbf{C}\mathbf{v}_k \\ \mathbf{Y}_{k+1} &= \mathbf{H}\cdot\mathbf{M}_{k+1} = \mathbf{H}\cdot\mathbf{m}_{k+1} + \mathbf{H}\cdot\boldsymbol{\varepsilon}_{k+1} \end{aligned} \tag{6.5}$$

Note that $E\{\boldsymbol{\varepsilon}_k\} \simeq \mathbf{0}$ by the approximation hypothesis. Previous system is actually the corresponding TCPN one plus white gaussian noise at the state ($\mathbf{C}\mathbf{v}_k$, which is also uncorrelated in time) and the output ($\mathbf{H}\boldsymbol{\varepsilon}_{k+1}$). In this way, it seems obvious to use an EKF in order to obtain a noise-free estimation of the marking of the underlying TCPN model, i.e., an estimation of $E\{\mathbf{m}_k\} \simeq E\{\mathbf{M}_k\}$. Then, such an estimator can be defined as as:

$$\begin{aligned} \widehat{\mathbf{m}}_{k+1} &= [\mathbf{I} + \mathbf{C}\boldsymbol{\Lambda}\boldsymbol{\Pi}(\widehat{\mathbf{m}}_k)\Delta\tau]\,\widehat{\mathbf{m}}_k + \mathbf{K}_k\mathbf{e}_k \\ \widehat{\mathbf{y}}_{k+1} &= \mathbf{H}\cdot\widehat{\mathbf{m}}_{k+1} \end{aligned} \tag{6.6}$$

where $\mathbf{K}_k$ is the Kalman estimation gain matrix and $\mathbf{e}_k = \mathbf{Y}_k - \widehat{\mathbf{y}}_k$ is the output estimation error. In order to ensure convergence, it is assumed that the output $\mathbf{Y}_k$ has enough information to determine the current configuration, and the pair $(\mathbf{H}, \mathbf{C}\boldsymbol{\Lambda}\boldsymbol{\Pi}_i)$ is observable for all the visited configurations $\boldsymbol{\Pi}_i$ (a detailed discussion of observability in TCPNs can be found in [Júlvez et al., 2008, Mahulea et al., 2010]).

The gain introduced by the Kalman Filter ($\mathbf{K}_k\mathbf{e}_k$) is computed in the block *EKF* as (see, for instance, [Grewal and Andrews, 2001] pages 121 and 180):

$$\begin{aligned} \mathbf{P}'_{k+1} &= [\mathbf{I} + \mathbf{C}\boldsymbol{\Lambda}\boldsymbol{\Pi}(\widehat{\mathbf{m}}_k)\Delta\tau]\cdot\mathbf{P}_\mathbf{k}\cdot[\mathbf{I} + \mathbf{C}\boldsymbol{\Lambda}\boldsymbol{\Pi}(\widehat{\mathbf{m}}_k)\Delta\tau]^T + \mathbf{Q}_k \\ \mathbf{K}_k &= \mathbf{P}'_{k+1}\cdot\mathbf{H}^T\cdot\left[\mathbf{H}\cdot\mathbf{P}'_{k+1}\cdot\mathbf{H}^T + \mathbf{R}_k\right]^{-1} \\ \mathbf{P}_{k+1} &= [\mathbf{I} - \mathbf{K}_k\cdot\mathbf{H}]\,\mathbf{P}'_{k+1} \\ \mathbf{K}_k\mathbf{e}_k &= \mathbf{K}_k\cdot(\mathbf{Y}_k - \widehat{\mathbf{y}}_k) \end{aligned} \tag{6.7}$$

Matrix $\mathbf{Q}_k$ represents the covariance of the state perturbation, which according to the TnCPN approximation and the definition of $\mathbf{v}_k$, it should be close to $\mathbf{C}\cdot diag[\boldsymbol{\Lambda}\boldsymbol{\Pi}(\widehat{\mathbf{m}}_k)\widehat{\mathbf{m}}_k\Delta\tau]\cdot\mathbf{C}^T$. Matrix $\mathbf{R}_k$ represents the covariance of the output perturbation, i.e., the covariance of $\boldsymbol{\varepsilon}_k$. A reasonable estimation for such covariance is given by $\mathbf{R}_k = 0.5\cdot\mathbf{I}$ (assuming that the discrete marking follows a normal-multivariate distribution, such value for $\mathbf{R}$ means that the error between markings is less that 1.5 with probability close to 0.95). Since the covariance matrix of the error ($\mathbf{P}_{k+1}$) is used for the next time step, a feedback-loop with the unit delay z^{-1} is added in the Block Diagram.

Then, block *EKF* computes the gain $\mathbf{K}_k\mathbf{e}_k$, which is required in order to obtain the state estimation for the next time step $\widehat{\mathbf{m}}_{k+1}$, according to (6.6). In this way, with the output of the MPN system and the block *EKF*, it is possible to obtain an estimation for the average state as if it were a TCPN system, i.e., it is obtained $\widehat{\mathbf{m}}$ that evolves like the TCPN system but approximates the average marking of the MPN in agreement to its output values $\mathbf{Y}$.

Finally, consider the case that the net system is Join-Free, thus the TCPN is a linear system and the block *EKF* becomes a Kalman Filter. In such case, according to the *Separation Principle* (see, for instance, [Levine, 1996] part B, Subsection 37.5), a perfect interaction between the controller and the estimator can be expected (according to this principle, the optimal controller for the nominal system, together with a Kalman filter, will provide the optimal control for the system under perturbations). In

the general case, the evolution of the continuous system is not linear, but linear by *regions* (while the flow is continuous across them) and time invariant. In this way, it is still reasonable to integrate the *EKF* and the control law obtained in separated ways, leading to the control structure of fig. 6.1. Nevertheless, further research is required in order to provide sufficient conditions for close-loop stability (a related problem has been addressed for PWA systems in [Heemels et al., 2008]).

6.2 A stock level-control example

In this section, the control scheme introduced in Section 6.1 will be applied to a Kanban-based automotive assembly line (introduced in [Dub et al., 2002]) in order to control the stocks level.

6.2.1 The model

Authors in [Dub et al., 2002] proposed an stochastic Petri net model for an existing assembly line that produces cars. The production is based on a Kanban process. The assembly line is a self-moving transporter, which carries the car bodies through a number of quite similar production cells. The time that the car body spends in every production cell is equal for all productions cells and is given by the line rhythm, which is constant. Each production cell has some small stores (racks) where palettes with all parts, specific to the particular production cell, are to be found. In every cell there is a space to accommodate at maximum two palettes of each part type used there. One palette contains only the same kind of parts.

Fig. 6.2 shows the model proposed for describing the assembly of one part. Tokens in p_1 represents the Kanban-tickets in the local store. Tokens in p_2 represents the Ktickets in the space close to the production cell. Such number is limited by a conservative law imposed by p_3 ($\mathbf{M}[p_2]+\mathbf{M}[p_3] = 2$). Place p_4 represents the number of parts available in the palette that is being used for production. The number of parts in one palette is 60 (arc (t_3, p_4)), while the number of parts of the same kind required for one car production is 2 (arc (p_4, t_4)). Transition t_5 represents the assembly operation. Its delay is equal to the time interval between the production of two consecutive cars (given by the production speed or line rhythm). Place p_5 enables t_3 when the marking in p_4 is null, i.e., when no more parts are available in the palette that is being used. The container withdraw is described by the subnet defined by $\{p_9, p_{10}, p_{11}\}$, which works in the following way: transition t_8 models the waiting time before an order (orders are done just at some hours), after its firing p_{10} enables t_6 and t_7. A Kanban-ticket in p_8 means that an order must be done, in such case t_6 fires (its delay is considerably lower than that of t_7) and a token is transferred from p_8 to p_{12}, meaning that a supply order is ready to be sent. On the other hand, if there is a token in p_{10} but not in p_8 then t_7 fires, meaning that the Kanban container is withdrawn. Transition t_{11} represents the time from the moment of ordering to the moment of delivery, while a token in p_{14} represents the truck arrival. Transition t_{10} does not appear in the original model in [Dub et al., 2002]. In this work it is added for control purposes: its delay will be controlled meaning that orders (tokens in p_{12}) can be delayed before being sent.

Only some of the transitions' average delays are reported in [Dub et al., 2002]. Nevertheless, only three transitions exhibit significant, and almost constant, delays: t_5, t_8 and t_{11}. Furthermore, t_6 must fire faster than t_7 whenever both are enabled. For our purpose, average delays are defined as in fig.

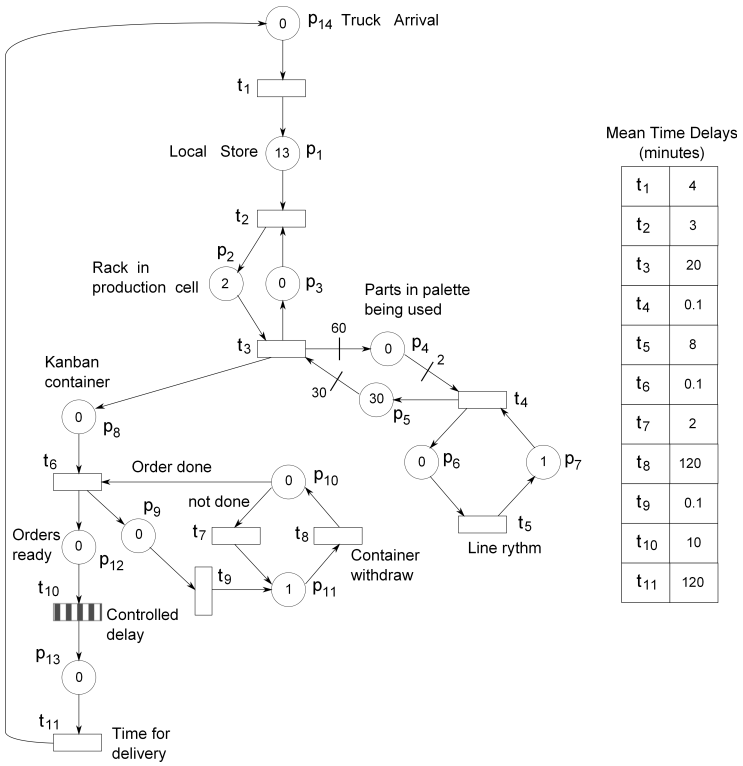

Fig. 6.2: Petri net model of one-part assembly in an automotive production system [Dub et al., 2002].

6.2. Transitions t_5, t_8 and t_{11} fire according to an Erlang-3 pdf (in order to reduce their coefficients of variation), transitions t_6 and t_7 fire with constant delays, while the other transitions fire with exponential pdf and infinite server semantics.

Fig. 6.3 shows the proposed TCPN model, in which some modifications w.r.t the original PN are introduced in order to obtain a better fluid approximation. In this model, the component representing the parts in the palette that is being used is substituted by the component of places $\{p_5^1, ..., p_5^4\}$, a token in p_5^4 means that the palette in use is empty. The container withdraw is modeled in a similar way, the difference is that, in order to reduce the coefficient of variation, t_8 of fig. 6.2 is now split in three transitions $\{t_8^1, t_8^2, t_8^3\}$ (classical simulation of an Erlang-3 by 3 exponentials). In a similar way, t_{11} of fig. 6.2 is split into $\{t_{11}^1, t_{11}^2, t_{11}^3\}$. Note that places $\{p_1, p_2, p_3, p_8, p_{10}, p_{12}, p_{14}\}$ keep the same meaning, in the same way that their corresponding output transitions do. All transitions fire according to an exponential pdf and infinite server semantics (t_6 and t_7 fire with constant delays in the original model, but their delays are very small w.r.t. the others so they can be well approximated by exponential delays). Average delays are defined as in fig. 6.3. Note that the delays of $\{t_5^1, t_5^2, t_5^3\}$ sum the total time required for emptying the palette that is being used, i.e., the sum of the delays for t_4 and t_5 of the original model (fig. 6.2) multiplied by 30. In the same way, the sum of delays of $\{t_8^1, t_8^2, t_8^3\}$ and $\{t_{11}^1, t_{11}^2, t_{11}^3\}$ of the TCPN are equal to the delays of t_8 and t_{11} of the original model, respectively.

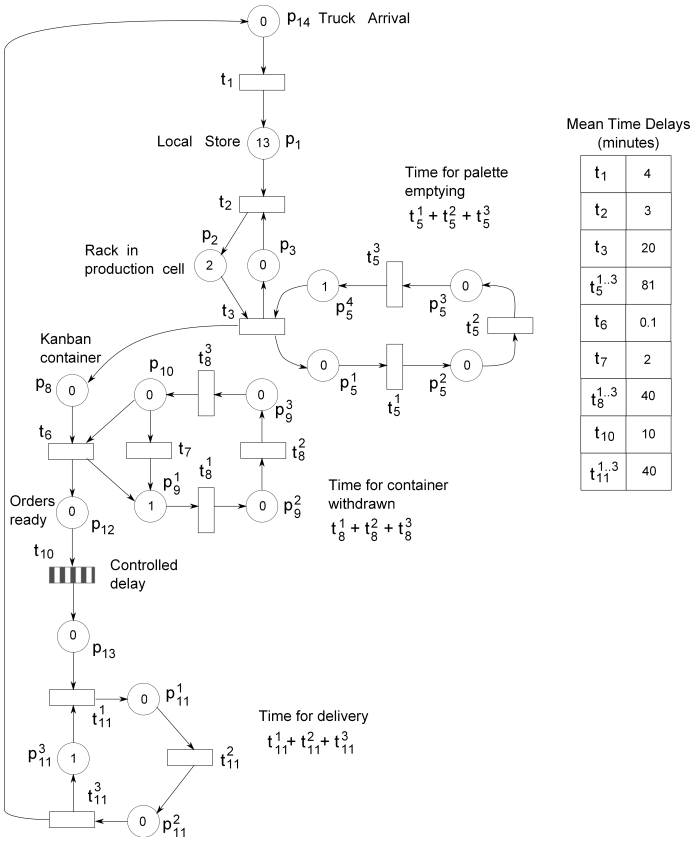

Fig. 6.3: Timed continuous Petri net relaxation of the model of fig. 6.2

6.2.2 Application of the control scheme

The goal in [Dub et al., 2002] is to propose a methodology for the optimization of the stock reserves, i.e., to control the sum of ($\mathbf{M}[p_1]$+$\mathbf{M}[p_2]$) in fig. 6.2. Having a large number of Kanbans in the store $\mathbf{M}[p_1]$ implies unnecessary costs, on the contrary, missing Kanbans might stop the whole production. Such Kanban missing can occur for unexpected delays in truck arrivals or lost orders. In that paper, the optimum number of K-Tickets (the optimum value for $\mathbf{M}[p_1]$+$\mathbf{M}[p_2]$) is computed based on simulation data. Nevertheless, during the operation, the level of the stock reserves can be far from its desired value, since the optimization is made in such a way that the stock reserves are in its optimal level *in average*, but not for all the time. This may lead to undesired problems, specially under unexpected perturbations (that were not considered during the optimization).

In the sequel, the control scheme introduced in the previous section will be applied to the system of fig. 6.2, in order to make this to keep a desired stock level. The PN of fig. 6.2 represents the original model or *Plant*, i.e., the upper dashed box MPN in the block diagram of fig. 6.1, while fig. 6.3 represents the model for the TCPN system (*TCPN+Control* in the block diagram), for which the control law is designed. Output functions are defined as $\mathbf{Y} = [\mathbf{M}[p_8], \mathbf{M}[p_{12}], \mathbf{M}[p_{14}], \mathbf{M}[p_1], \mathbf{M}[p_2], \mathbf{M}[p_{10}], \mathbf{M}[p_5]/30]$ for the original system and $\widehat{\mathbf{y}} = [\mathbf{m}[p_8], \mathbf{m}[p_{12}], \mathbf{m}[p_{14}], \mathbf{m}[p_1], \mathbf{m}[p_2], \mathbf{m}[p_{10}], \mathbf{m}[p_5^4]]$ for the estimator. Note that these expressions are equal, excepting the last output, which is required in order to know the

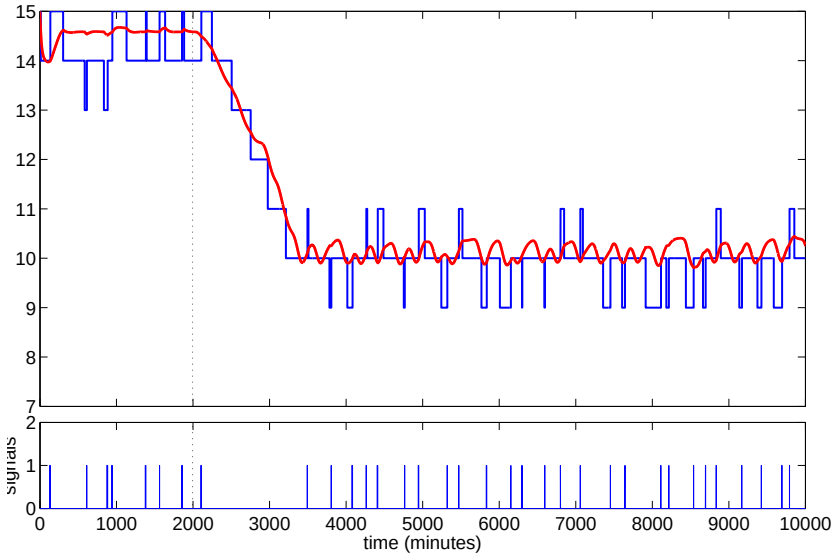

Fig. 6.4: Number of Kanban-Tickets in the local store and racks ($\mathbf{M}[p_1]+\mathbf{M}[p_2]$) in the closed-loop systems, and firing signals of the controllable transition t_{10} (an impulse means a firing). The control law is applied after time 2000 min.

arc that is constraining t_3. Now, following [Dub et al., 2002], let us suppose that the optimum value for the sum $\mathbf{M}[p_1]+\mathbf{M}[p_2]$ is computed as 10, then, our control law must impose additional delays in t_{10} such that the sum in the original system be as close to 10 as possible.

By using the techniques introduced in Section 5.4, a control law was designed for the TCPN system (fig. 6.3). Later, this was interpreted and applied to the original discrete PN model, according to the control scheme described in the previous section (fig. 6.1). The results are shown in fig. 6.4. Control law is applied after 2000 min. The continuous curve in fig. 6.4 corresponds to the *estimator* ($\widehat{\mathbf{m}}_k$), while the other one (square) represents the discrete original system. As it can be seen, the control law successfully drives the discrete system for obtaining the desired average marking at the local store and racks. Fig. 6.4 also shows the firing signals for the unique controllable transition t_{10} in the closed-loop system. A unit impulse means that t_{10} is fired, i.e., that an order is released and sent to the parts supplier.

For the estimator implementation it was required to adjust the values for the covariance matrices $\mathbf{Q}_k$ and $\mathbf{R}_k$ of the Kalman filter, in order to obtain a good closed-loop performance (final adjustments are commonly required when using Kalman filters). If the theoretical values provided in the previous section for $\mathbf{Q}_k$ and $\mathbf{R}_k$ are used, the estimated marking $\widehat{\mathbf{m}}_k$ will be close to the state of the MPN ($\mathbf{M}_k$). Therefore the control input $\mathbf{u}_k$ will be computed by using the noisy signal $\widehat{\mathbf{m}}_k$. Nevertheless, the control law was designed for the TCPN without noise, so, such input signal may result in a bad close-loop performance. On the other hand, by decreasing $\mathbf{Q}_k$, the trajectory of $\widehat{\mathbf{m}}_k$ will become soft enough, leading to a suitable (and expected) behavior of the closed-loop TCPN system. Nevertheless, a very low value for $\mathbf{Q}_k$ will make the estimator to obtain a poor estimation, in such case, the behavior of the continuous system could be different from that of the MPN. The best performance is obtained by

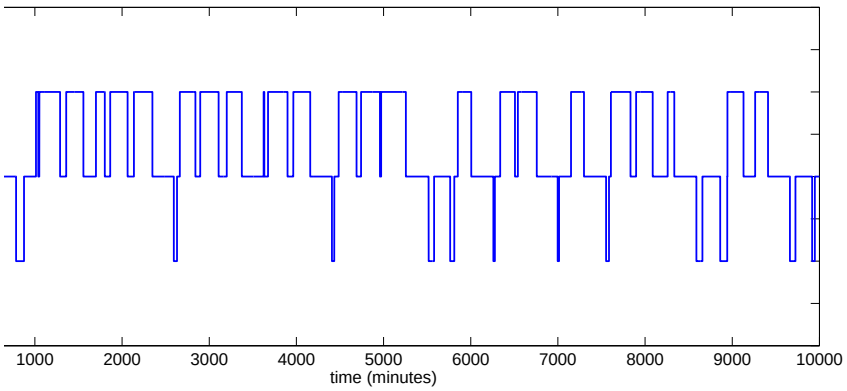

Fig. 6.5: Number of Kanbans in the local store and racks ($\mathbf{M}[p_1] + \mathbf{M}[p_2]$) with the $GMEC$ control.

decreasing $\mathbf{Q}_k$ from its theoretical value (obtaining thus a soft estimated trajectory) but, at the same time, decreasing the entries of $\mathbf{R}_k$ corresponding to the outputs whose approximation must be improved.

6.2.3 Comparing with GMECs

Finally, for comparison purposes, let us show the results obtained by using a control feedback with Generalized Mutual Exclusion Constraints (GMEC), introduced in [Giua et al., 1992]. Such approach is defined for safety specifications, according to which a weighted sum of markings must be limited. In our case, the specification could be defined with the following GMEC: $\mathbf{M}[p_1] + \mathbf{M}[p_2] \leq 10$. The controller that enforces the GMEC consists in the addition of a new place, called *Monitor*, having as input transition t_3 and output one t_1. Nevertheless, t_1 is not controllable, then t_{10} is taken as the Monitor's output transition, fulfilling in this way the GMEC. For the initial marking, p_1 should have 8 tokens (i.e., $10 - \mathbf{M}_0[p_2]$) and the new place, the Monitor, must have 5 tokens (i.e., total K-Tickets 15, minus $\mathbf{M}_0[p_1] + \mathbf{M}_0[p_2]$), while the other places remain marked as in fig. 6.2. The results are shown in fig. 6.5. As it can be seen, the GMEC control approach guarantees that the sum $\mathbf{M}[p_1] + \mathbf{M}[p_2]$ is not larger than 10. Nevertheless, this sum is not always close to the desired value, because the $GMEC$ is defined for imposing upper bounds to the marking but not for enforcing a desired marking.

In this example, the performance provided by the GMEC control for $\mathbf{M}[p_1] + \mathbf{M}[p_2]$ may still be considered as good enough (an average value of 9.46 was obtained), but it is not always the case. For instance, consider the same system (fig. 6.2) but with $\mathbf{M}[p_1] = 4$ at the initial marking. Suppose that a value of 4 is desired for the sum of $\mathbf{M}[p_1] + \mathbf{M}[p_2]$. After simulating $30,000$ minutes, by using a GMEC $\mathbf{M}[p_1] + \mathbf{M}[p_2] \leq 5$ an average value (for the sum) of 4.59 was obtained, while a value of 3.60 resulted with GMEC $\mathbf{M}[p_1] + \mathbf{M}[p_2] \leq 4$. They represent 14.75 and 9.9 percent error, respectively. On the other hand, the control strategy introduced through this chapter provides an average value of 4.02. Therefore, if a good accuracy for the average value is required, the method proposed in this chapter is more suitable. On the other hand, if a safety specification must be fulfilled, the GMEC control approach is a better choice. In any case, both methods can be combined obtaining the best properties of each one, for instance, if we would like that $\mathbf{M}[p_1] + \mathbf{M}[p_2] \leq 5$ but having an average value of 4.

6.3 Modeling and control of urban traffic systems

In this section, a new example, about the use of relaxed models for the control synthesis of DES, will be considered. In this case, the problem under study consists in the design of a control policy for the traffic lights at the intersections of an urban traffic network. For this, a T-timed PN, whose transitions have stochastic or deterministic delays, will be proposed for the traffic intersections, and later, this model will be partially relaxed obtaining thus a hybrid PN model. Next, a control law will be derived.

Let us provide first an overview of the problem. The objective is to obtain a coordinated control policy for the traffic lights in an urban network in order to reduce the total travel time of the vehicles, by selecting the red-to-green switching times of the traffic signals. There are several authors that have addressed this problem from different perspectives. For instance, by using heuristic optimization algorithms ([Bazzan, 2005], [Toshihiko, 2003]), or considering a formal model-based optimization approach [Porche et al., 1996], or dealing with the scalability problem, resulted from the complex behavior and the combinatorial nature of traffic networks, by adopting macroscopic models and distributed control and optimization techniques [Camponagara and Kraus, 2003, van den Berg et al., 2004]. In general, switching strategies for traffic lights [USDOT, 2005] can be classified according to how fast they respond to on-line traffic measurements.

Pre-timed controllers select a fixed period, called the cycle time, for all traffic lights in a given area, and select the fraction of green for each direction in each intersection. Moreover the relative time offsets (the phase shifts between the switching times at consecutive intersections) is selected so as to guarantee as much as possible a green wave of vehicles that do not have to stop. These pre-timed controllers may be adjusted during the day to adapt to different traffic patterns, but they only use the average traffic flow data, not the on-line measurements of queue sizes or of current traffic flows.

A different approach is adopted by allowing the actuated traffic signals to react to local measurements of queues of waiting vehicles (or detected oncoming traffic) by switching to green, if at all possible. This may reduce the local average delays significantly, but this strategy can destroy any advantage of a green wave. Traffic responsive systems therefore must try to adapt to instantaneous information on the local traffic intensity by a *coordinated* action for the different traffic lights in a given area. Examples of such strategies have been developed since the 1980s (for example the SCATS [Lowrie, 1982] and the SCOOT systems [Hunt et al., 1982]). These systems adjust from time to time the green fraction at each intersection, and/or the phase shifts, according to some heuristically developed rules.

Recently, the availability of on-line measured traffic data and the capabilities of road side control agents, have improved so much that it makes sense to develop model based on-line optimization algorithms for coordinated traffic responsive control systems. The first part of this section will consist in providing a model that can serve this purpose. As a result of a partial fluidization, a hybrid Petri net is obtained, representing the queueing behavior of vehicles at intersections. This model will allow to locally optimize the green-red periods of the corresponding traffic lights, but considering the control policies that are applied at upstream intersections. Moreover, by adding models that represent the traffic flow along the links connecting intersections, the behavior of a complete urban traffic network can be described. This idea is advanced in the last subsection.

Regarding traffic intersections, different Petri net models can be found in the literature. Among them, the model introduced in [Dotoli et al., 2006] is the closest to the one introduced in this section.

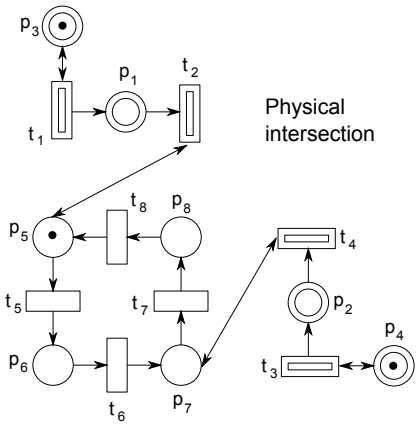

Fig. 6.6: PN model of an intersection of two one-way streets.

In that paper, the heavily populated discrete timed Petri net is aggregated into sets of piecewise linear equations. The model introduced here is different in that the heavily populated discrete event model is relaxed, while keeping the Petri net structure intact as much as possible.

It is important to mention that, the abstracted model introduced here and the results obtained in this section can be extended in order to obtain distributed control strategies for networks with more complicated signalized intersections. Nevertheless, such strategies are left for future research.

6.3.1 Fluidization of an intersection model

Consider the discrete timed PN system of fig. 6.6. This model represents the intersection of two one-way streets controlled by a traffic light, under *free-flow condition* (without congestion, the traffic flux is proportional to the traffic density). The subnet $\{p_1, p_2, p_3, p_4\}$ corresponds to the *physical intersection*: tokens in places p_1 and p_2 represent the cars at the queues waiting to enter the intersection while tokens at p_3 and p_4 are the servers at the input transitions (lanes upstream of the queues in p_1 and p_2, respectively). The subnet $\{p_5, p_6, p_7, p_8\}$ represents the *traffic light*. According to this model, the first queue (p_1) is served (t_2 is enabled) only if in the model of the traffic light there is a token at p_5. In a similar way, the second queue (p_2) is served only if in the model of the traffic light there is a token at p_7. A token at either place p_6 or p_8 represents a yellow period (yellow for one queue but red for the other), so, no queue is being served when there is a token in these places. Transitions $\{t_5, t_6, t_7, t_8\}$, representing the switching of the traffic light, are defined as having deterministic time delays. On the other hand, transitions $\{t_1, t_2, t_3, t_4\}$, corresponding to car arrivals and departures (services) at the intersection, are defined as having exponentially distributed random time delays.

The PN system of fig. 6.6 is relaxed into a *hybrid* PN model, in which transitions $\{t_1, t_2, t_3, t_4\}$, corresponding to car arrivals and departures (services), are relaxed into fluid, while other transitions remain discrete (traffic light). Average delays of transitions $\{t_1, t_2, t_3, t_4, t_5, t_6, t_7, t_8\}$ are defined as $(1, 1/3, 1, 1/3, 20, 5, 20, 5)$. Note that the *hybrid* model thus obtained is deterministic, since all the stochastic transitions have been fluidified. The marking trajectories of places p_1 and p_2 are shown in fig. 6.7 (solid curves). On the other hand, after 20 simulations of the original stochastic discrete model, the

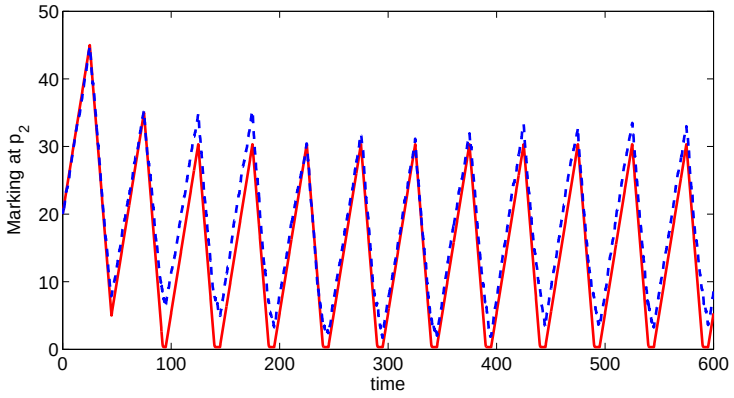

(a)

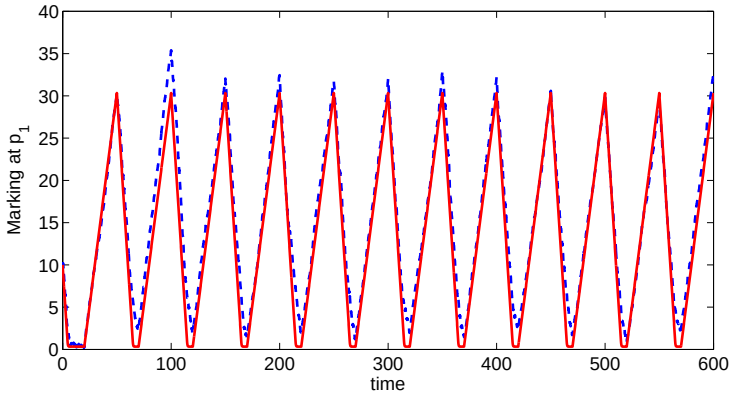

(b)

Fig. 6.7: Marking trajectories of the PN system of fig. 6.6. Dashed curves correspond to the average trajectory of the stochastic PN, while the continuous ones correspond to the hybrid PN. a) Curves of p_1, b) curves of p_2.

average trajectories for the same places were computed, and are also shown in fig. 6.7 (dashed curves). Note that the trajectories of both the hybrid PN and the average of the discrete PN models coincide almost perfectly. Hence, the hybrid PN can be used for a quantitative analysis of the original discrete system, with the advantage that this model is deterministic and that the state explosion problem does not appear in this.

Lefeber & Rooda [Lefeber and Rooda, 2006] studied a mathematical model similar to the hybrid version of fig. 6.6. The results of [Lefeber and Rooda, 2006] characterize the optimal steady state periodic orbit that minimizes the cost

$$J = \frac{1}{\mathcal{T}_{ss}} \int_0^{\mathcal{T}_{ss}} [x_1(\tau) + x_2(\tau)] \cdot d\tau \tag{6.8}$$

where x_1 and x_2 denote the queues (markings at $\{p_1, p_2\}$ in fig. 6.6) and $\mathcal{T}_{ss}$ denotes the period of the orbit. Furthermore, they also provide a feedback control law that guarantees the convergence of the system to that orbit.

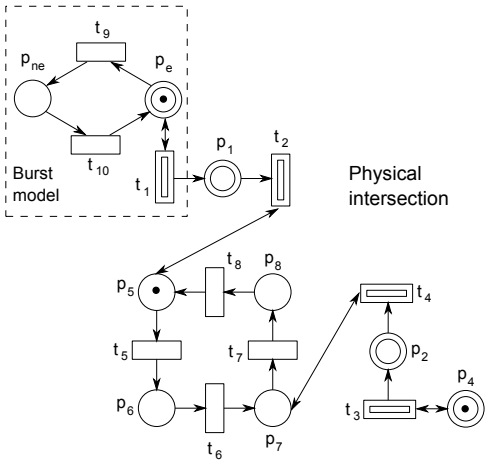

Fig. 6.8: PN model of an intersection of two one-way streets, the arrivals to the first queue occur in bursts.

An important assumption made in the model of fig. 6.6 (and in [Lefeber and Rooda, 2006]) is that the arrival rates are *constant*. Nevertheless, in an urban traffic network, the cars departing one intersection are the arrivals to the neighboring ones. Since each intersection is being controlled by a traffic light, the departures do not have constant flow rates, and so the arrivals to downstream intersections do not occur with a constant flow rate but in *bursts* (the intensity of the traffic flow is higher during short periods, like *batches* of cars moving closely together). In order to consider those burst arrivals, the PN of fig. 6.6 is modified, leading to the system of fig. 6.8.

In this new model, the arrivals to the first queue occur in bursts. A token in place p_e enables t_1, meaning cars arriving with a rate λ_1. After some given delay θ_9, transition t_9 fires (which is discrete and deterministically timed) removing the token at p_e and putting it in p_{ne}, in this way, t_1 is no longer enabled meaning that no cars can arrive. After a given delay θ_{10}, transition t_{10} fires and the token returns to p_e, enabling again t_1. In this way, the time during which a burst is arriving at the first queue is θ_9, the number of cars that arrive during that time is $\theta_9 \cdot \lambda_1$, the time between the arrival of two consecutive bursts (between the car leading a burst and the car leading the next burst) is $\theta_9 + \theta_{10}$. Therefore, transitions t_9, t_{10} and places p_e and p_{ne} characterize the bursts that arrive to the first queue. In this model, the arrivals to the second queue still occur with a constant rate. Those arrivals can also be generalized in order to consider bursts. Nevertheless, for the sake of simplicity, they will be kept as constant in this report.

The results obtained in [Lefeber and Rooda, 2006] do not provide the optimal behavior for the system of fig. 6.8, since the arrivals to the first queue do not occur with a constant rate. Furthermore, in the case studied in this work, the discrete subnet (the subnet described by transitions $\{t_5, t_6, t_7, t_8, t_9, t_{10}\}$) does not describe a sequential process but a concurrent one, i.e., there are many possible trajectories in the untimed subnet. For instance, in the PN model of fig. 6.6, the discrete subnet always evolves with the sequence $t_5, t_6, t_7, t_8, t_5, ...$; but in the model of fig. 6.8 the discrete subnet can evolve as $t_5, t_9, t_6, t_7, t_8, t_{10}, ..$ or $t_5, t_9, t_6, t_{10}, t_7, t_8, ..$ etc.; the trajectory or sequence that occurs in the timed model depends on the delays of t_5 and t_7, i.e., the parameters to optimize. For this reason, the optimal periodic orbit for this new model is difficult to characterize, because it is not possible to obtain an

analytical expression (as a function of the delays t_5 and t_7) of the cost J (6.8).

6.3.2 Optimization for one intersection

In this subsection, a parameter optimization problem is introduced and solved for the 1-intersection model of fig. 6.8, obtaining thus the optimal switching delays for the traffic light. Note that, since the yellow periods are fixed a priori for safety reasons, by defining the switching delays for the green signals (a green signal for one queue means red for the other), the timing of the traffic light is completely defined.

Given minimum and maximum possible integer values for the time delays of t_5 and t_7 (the green periods), denoted as θ_5^{min}, θ_7^{min}, θ_5^{max} and θ_7^{max} respectively, a finite set of possible control values is defined:

$$CS = \{(\theta_5, \theta_7) \in \mathbb{N} \times \mathbb{N} | \theta_5^{min} \leq \theta_5 \leq \theta_5^{max}, \theta_7^{min} \leq \theta_7 \leq \theta_7^{max}\} \tag{6.9}$$

Next, given the initial queue lengths ($\mathbf{m}_0[p_1]$ and $\mathbf{m}_0[p_2]$) and a fixed time horizon $\mathcal{T}$, for each pair $(\theta_5, \theta_7) \in CS$, the following cost function is computed:

$$J(\mathcal{T}, \theta_5, \theta_7) = \frac{1}{\mathcal{T}} \int_0^{\mathcal{T}} \mathbf{w} \cdot \begin{bmatrix} \mathbf{m}[p_1] \\ \mathbf{m}[p_2] \end{bmatrix} \cdot d\tau \tag{6.10}$$

where $\mathbf{w}$ is a positive row vector representing some optimization weights. Finally, the cost values thus obtained are compared, and so, the minimum of them determines the optimal control policy $(\theta_5^{opt}, \theta_7^{opt})$ to be applied.

Note that $(\theta_5^{opt}, \theta_7^{opt})$ may not be the optimal values at the steady state. Nevertheless, given the current estimates of the state ($\mathbf{m}_0[p_1]$ and $\mathbf{m}_0[p_2]$), $(\theta_5^{opt}, \theta_7^{opt})$ minimizes the average vehicle delay over an interval of time starting at the present time and looking $\mathcal{T}$ time units into the future (like in *model predictive controllers*). Furthermore, note that the *cycle time* is not fixed a priori, since it depends on the values obtained for $(\theta_5^{opt}, \theta_7^{opt})$.

The main drawback of the previous approach is the high computational cost, since the cost function is evaluated for each possible combination for the values of (θ_5, θ_7), rather than optimizing by using programming techniques. Nevertheless, the computation of J (6.10) can be achieved very efficiently by computing in parametric form (but off-line) the incremental cost $J(\tau + \Delta\tau) - J(\tau)$, during a time interval $\Delta\tau$ that the system remains in the same discrete state, for each possible discrete state.

For instance, consider the system as in fig. 6.8. Given the rates $\{\lambda_1, \lambda_2, \lambda_3, \lambda_4\}$ for $\{t_1, t_2, t_3, t_4\}$, time delays $(\theta_5, \theta_6, \theta_7, \theta_8) = (20, 5, 40, 5)$ seconds for $\{t_5, t_6, t_7, t_8\}$, and delays $(\theta_9, \theta_{10}) = (10, 30)$ seconds for $\{t_9, t_{10}\}$, the system will remain at the same discrete state during $\Delta\tau = min(\theta_5, \theta_9) = 10$ seconds (i.e., the minimum time delay of those discrete transitions that are enabled at the current discrete state). During such time $\Delta\tau$, the queues will change, i.e., the marking at p_1 and p_2, but this evolution is deterministic and can be computed in parametric form.

In particular, it is easy to prove that, given initial values $\mathbf{m}_0[p_1]$ and $\mathbf{m}_0[p_2]$, after $\Delta\tau$ time units

during which the discrete state remains at $\mathbf{m}[p_e] = 1$ and $\mathbf{m}[p_5] = 1$, the variables are:

$$\begin{aligned}\mathbf{m}[p_1](\Delta\tau) &= \begin{cases} (\lambda_1 - \lambda_2) \cdot \Delta\tau + \mathbf{m}_0[p_1] & \text{if } \Delta\tau \leq \tau_c \\ \frac{\lambda_1}{\lambda_2} + \left[1 - \frac{\lambda_1}{\lambda_2}\right] e^{-\lambda_2(\tau - \tau_c)} & \text{if } \Delta\tau > \tau_c \end{cases} \\ \mathbf{m}[p_2](\Delta\tau) &= \lambda_3 \cdot \Delta\tau + \mathbf{m}_0[p_2]\end{aligned} \tag{6.11}$$

where $\tau_c = (1 - \mathbf{m}_0[p_1])/(\lambda_1 - \lambda_2)$ is the time needed for the first queue to reach the value of 1 (according to the ISS, if the first queue $\mathbf{m}[p_1]$ is larger than 1 then transition t_2 is constrained by p_5, so this queue decreases according to a constant speed, but if the queue is lower than 1 then t_2 is constrained by p_1 and so, in this case, it decreases with a speed that depends on the queue's current value). Furthermore, the increment of the cost function defined as

$$\Delta J = \int_0^{\Delta\tau} \mathbf{w} \cdot \begin{bmatrix} \mathbf{m}[p_1] \\ \mathbf{m}[p_2] \end{bmatrix} \cdot d\tau = w_1 \int_0^{\Delta\tau} \mathbf{m}[p_1] d\tau + w_2 \int_0^{\Delta\tau} \mathbf{m}[p_2] d\tau \tag{6.12}$$

can be easily computed by using, for this discrete state, the following expressions:

$$\int_0^{\Delta\tau} \mathbf{m}[p_1] d\tau = \frac{(\lambda_1 - \lambda_2)}{2} \Delta\tau^2 + \mathbf{m}_0[p_1] \Delta\tau \tag{6.13}$$

if $\Delta\tau \leq \tau_c$. For the case in which $\Delta\tau > \tau_c$ then

$$\int_0^{\Delta\tau} \mathbf{m}[p_1] d\tau = \frac{(\lambda_1 - \lambda_2)}{2} \Delta\tau^2 + \mathbf{m}_0[p_1] \Delta\tau + \frac{\lambda_1}{\lambda_2}(\Delta\tau - \tau_c) + \left[\frac{\lambda_1}{\lambda_2^2} - \frac{1}{\lambda_2}\right] \left[e^{\lambda_2(\tau_c - \Delta\tau)} - 1\right] \tag{6.14}$$

and in both cases

$$\int_0^{\Delta\tau} \mathbf{m}[p_2] d\tau = \frac{\lambda_3}{2} \Delta\tau^2 + \mathbf{m}_0[p_2] \Delta\tau \tag{6.15}$$

By following a similar reasoning, expressions for $\mathbf{m}[p_1](\Delta\tau)$, $\mathbf{m}[p_2](\Delta\tau)$ and ΔJ can be obtained for all the different discrete states. Therefore, the computation of the cost function for a given pair (θ_5, θ_7) can be quickly achieved by following a discrete-event simulation algorithm:

Algorithm 6.2. Computation of the optimization cost for a traffic light policy for the model of fig. 6.8.

Initialize $\tau = 0, J_{ac} = 0$
While $\tau \leq \mathcal{T}$ (time horizon) **do**
  Compute the remaining time at the current discrete state: $\Delta\tau$.
  Compute the queues at $\tau + \Delta\tau$, i.e., $\mathbf{m}[p_1](\tau + \Delta\tau)$ and $\mathbf{m}[p_2](\tau + \Delta\tau)$,
  by using the expressions obtained off-line (6.11).
  Compute ΔJ, by usingthe expressions obtained off-line (6.12).
  Add the incremental cost: $J_{ac} = J_{ac} + \Delta J$.
  Update the time: $\tau = \tau + \Delta\tau$.
  Fire the enabled discrete transition.
end While
Compute the total cost as: $J(\tau) = \frac{1}{\tau} \cdot J_{ac}$

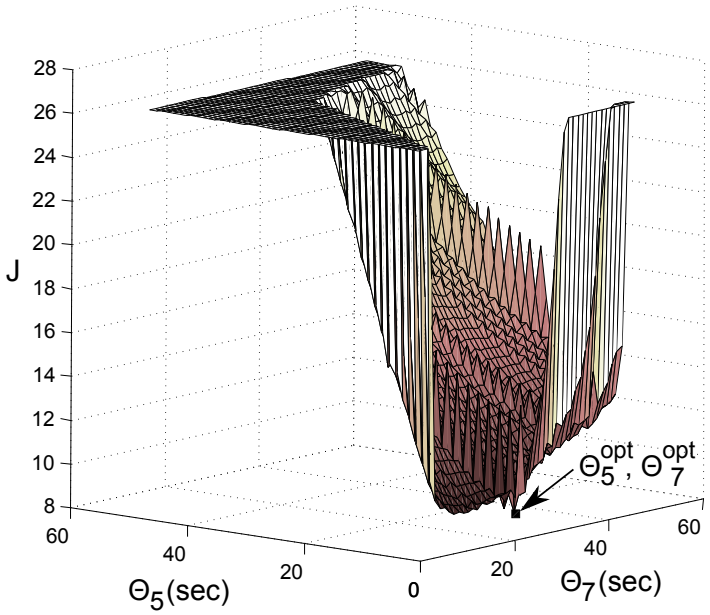

Fig. 6.9: Computation of optimal switching delays: $(\theta_5^{opt}, \theta_7^{opt}) = (4, 27)$ sec. with $J = 7.18$.

In this way, denoting as $\#_{events}$ the number of discrete events that occur during the horizon $\mathcal{T}$ (i.e., changes in the traffic light signal and in the incoming flow condition), the complexity of this algorithm is linear on the product $\#_{events} \cdot (\theta_5^{max} - \theta_5^{min}) \cdot (\theta_7^{max} - \theta_7^{min})$. Note that the complexity does not depend on the number of cars crossing the intersection neither on the magnitude of the flow.

For instance, fig. 6.9 shows the results obtained for the system of fig. 6.8 with rates $[1, 3, 1, 3]$ for $\{t_1, t_2, t_3, t_4\}$, delays $[10, 30]$ seconds for $\{t_9, t_{10}\}$ and $[5, 5]$ seconds for $\{t_6, t_8\}$, weights $\mathbf{w} = [1, 1]$ and a time horizon $\mathcal{T} = 1200$ seconds. Note that the minimum value for this, i.e., the optimal switching delays, is unique (the dashed square: $(\theta_5^{opt}, \theta_7^{opt}) = (4, 27)$ with $J = 7.18$). Note also in fig. 6.9 that the cost function is not convex, then, a gradient-based optimization may not compute the optimal value. Nevertheless, the algorithm introduced before does compute the optimal, since it evaluates the cost function for each possible combination (θ_5, θ_7). For this experiment, a CPU with a Intel Core 2 Duo at 2GHz has spent 84 seconds for computing the optimal value, which is considerably lower than the time horizon $\mathcal{T} = 1200$ seconds.

6.3.3 Controlling 1-intersection in a traffic network

This subsection is devoted to advance some ideas leading to a control strategy for urban traffic networks. The goal here is to use the optimization algorithm previously introduced in a MPC scheme. Then, the green periods of one intersection will be computed on-line, reducing thus its average queue lengths. This strategy can be extended in order to simultaneously control several interconnected intersection in a distributed way, nevertheless, that is beyond the scope of this work.

The proposed example is shown in fig. 6.10. This system consists of 2 intersections connected by a link (one-way street). The first intersection is modeled as in fig. 6.6, i.e., the incoming flows occur with

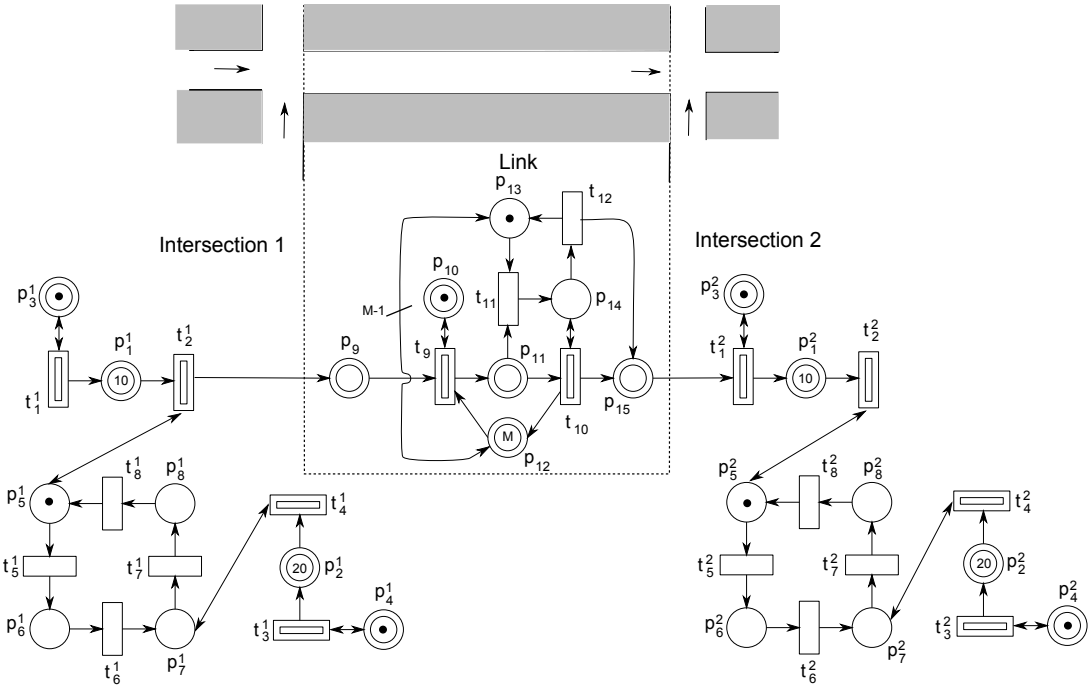

Fig. 6.10: PN model of 2 intersections connected by a link.

constant rates. The output flow of one direction is connected to a second intersection by a link, which introduces a pure delay. The subnet $\{p_9, p_{10}, p_{11}, p_{12}, p_{13}, p_{14}, t_9, t_{10}, t_{11}, t_{12}\}$ defines such link, in which transitions $\{t_{11}, t_{12}\}$ are discrete and $\{t_9, t_{10}\}$ are continuous. This link model works as follows: when a burst is departing from Intersection 1, whose output transition is t_2^1, tokens flow to p_9 and then through t_9 into place p_{11}, where they are accumulated, enabling at the same time t_{11}. After θ_{11} time units, t_{11} is fired (θ_{11} is the time needed by the leading vehicle of the burst leaving p_1^1 to reach the downstream intersection), marking p_{12}, and enabling t_{10}, so that the burst is free to follow its way towards the Intersection 2 (i.e., from p_{11} to place p_{14} and then to p_1^2, which is the queue at the second intersection). After the last token has left p_{11} (the last car has left the link), t_{12} is enabled and then it is fired, resetting the initial condition of this part of the model.

The dynamic behavior of the second intersection can be represented by means of the model of fig. 6.8, since the incoming flow through t_1^2 occurs in bursts, while the incoming flow through t_3^2 occurs with a constant rate. In this way, transitions $\{t_1^2, t_2^2, t_3^2, t_4^2\}$ and places $\{p_1^2, p_2^2, p_4^2\}$ of fig. 6.10 correspond to $\{t_1, t_2, t_3, t_4\}$ and $\{p_1, p_2, p_4\}$ of fig. 6.8, respectively (in the same order). In a similar way, the nodes modeling the traffic light of the second intersection in fig. 6.10 $\{p_5^2, t_5^2, p_6^2, t_6^2, p_7^2, t_7^2, p_8^2, t_8^2\}$ correspond to nodes $\{p_5, t_5, p_6, t_6, p_7, t_7, p_8, t_8\}$ in fig. 6.8. The information about arriving bursts (i.e., delays of $\{t_9, t_{10}\}$ and marking of $\{p_e, p_{ne}\}$ in fig. 6.8) is not directly available from the 2-intersections model, thus it must be obtained by off-line computation or on-line estimation.

It is assumed that the switching delays of the traffic light for the first intersection are fixed. The goal in this example is to compute on-line the switching delays of the second traffic light, showing that the model for 1-intersection of fig. 6.8 can capture the interactions with neighbor intersections in a urban network. A model predictive controller is implemented for this, by using the optimization algorithm

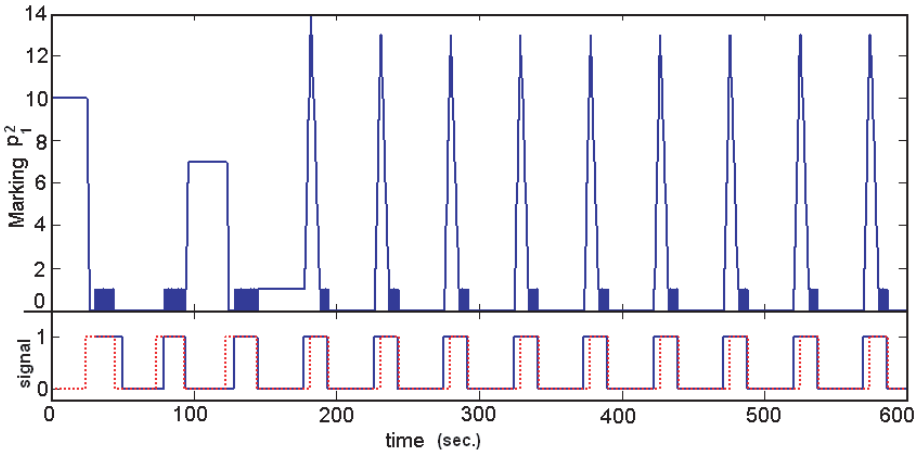

Fig. 6.11: Marking of queues at the second intersection (fig. 6.10) under control, and signals of the green period (dashed line) and arriving bursts (solid line).

introduced in the previous subsection. Let us describe this:

I. The parameters of the arriving bursts from Intersection 1 are estimated. These parameters are incorporated into the 1-intersection model of fig. 6.8 (that represents Intersection 2). The other rates and markings are given by the corresponding ones of Intersection 2.

II. The optimization algorithm introduced in the previous section is used for computing on-line the optimal switching delays for the local traffic light, using a fixed finite horizon $\mathcal{T}$.

III. Those switching delays are applied to the system.

IV. After a fixed time $\mathcal{T}_{upd}$ (updating time), lower than the horizon $\mathcal{T}$, return to the step 1, i.e., estimate again the parameters of incoming bursts and compute and apply again the corresponding optimal switching delays. While the time horizon $\mathcal{T}$ can be large enough to consider a few traffic-light cycles, the updating time $\mathcal{T}_{upd}$ must be small enough in order to update the estimation of the incoming bursts, and thus, to compute again the optimal switching delays with the most accurate available information.

Since the rates of the transitions of Intersection 1 are assumed to be fixed and known, then the bursty arrival stream to Intersection 2 is periodic, meaning that its parameters are constant and can be computed off-line. Nevertheless, in a general urban traffic network where the switching delays of several traffic lights are being adjusted, the bursts' parameters are variable and it is required to estimate them in real time. The synthesis of such an estimator is left for a future work. In order to consider the general case, step 4 in the previous control procedure states that the estimation, optimization and modification of the traffic light periods have to be iterated periodically.

This control strategy was applied to the hybrid model of fig. 6.10. Delays for the first traffic light $\{t_5^1, t_6^1, t_7^1, t_8^1\}$ are $(20, 5, 20, 4)$ (in the same order). Delays for the Intersection 1 $\{t_1^1, t_2^1, t_3^1, t_4^1\}$ were $(1, 1/3, 1/3, 1/5)$ seconds, for the second intersection $\{t_1^2, t_2^2, t_3^2, t_4^2\}$ were $(1/3, 1/5, 1, 1/3)$ seconds, while delays for the link $\{t_9, t_{10}, t_{11}, t_{12}\}$ were $(1/10, 1/3, 30, 1/3)$ seconds (the link delay is $\theta_{11} = 30$ seconds).

The initial queues were given by $(10, 20)$ for $\{p_1^1, p_2^1\}$ and $\{p_1^2, p_2^2\}$, respectively. During the experiment, the control law was applied to Intersection 2, while the periods for the traffic light of Intersection 1 remained fixed. The optimal control law was computed and applied each 5 seconds (the computation of the control law takes 3.62 seconds on a CPU with Intel Core 2 Duo at 2.00GHz each time it is computed), with an horizon of 110 seconds. The parameters of arriving bursts were obtained from an estimation procedure (not described in this work, but these can be easily computed off-line for this example). The results are shown in fig. 6.11. The marking at p_1^2 corresponds to the queue with bursty incoming flow. The square signals in the lower part of fig. 6.11 correspond to the green period (dashed line) of the traffic light for that queue and the arriving bursts (solid line, cars are added to the queue when this signal is 1). As it can be seen, the controller synchronized the green period with the incoming bursts in order to induce a green wave, reducing thus the queue at p_1^2 as much as possible. The value obtained for the cost function (defined as in (6.10) with $\mathbf{w} = [1, 1]$ and $\mathcal{T} = 600$ seconds) was 11.59, which is considerably lower than the value for the system with fixed switching times 16.59 (without control, those fixed switching times were computed by minimizing (6.8) assuming constant arrival rates).

6.4 Conclusions on control implementation

In this chapter, a control structure has been provided for the interpretation of a control law, designed for a TCPN system, into the corresponding MPN one. The resulting scheme constitutes a tool for controlling the average marking of a MPN system by means of applying additional delays to the controllable transitions, rejecting unexpected perturbations, i.e., for controlling the performance of the original stochastic Petri net.

Firstly, this control strategy has been applied for the stock level control of a Kanban-based automotive assembly line. The results obtained are positive, showing the feasibility of the control scheme proposed. Nevertheless, it is required that the control law designed for the TCPN system be robust enough, since the MPN system is interpreted as a TCPN with state and output perturbations. Furthermore, the covariance matrices of the EKF need to be suitably adjusted in order to obtain a good closed-loop performance. It is left for future research a formal analysis on the close-loop stability of the proposed approach.

Secondly, a different control problem was considered, introducing a hybrid PN model for intersections in an urban traffic network. Large urban traffic systems can be modeled by interconnecting several of these intersection models with delay lines modeling the roads linking them. It was shown that, the simplicity of the intersection model leads to simulation runs that are so fast that it is possible to compare the effect of different scenarios for the switching times of the traffic light. Accordingly, a model predictive feedback control law, that selects the best future scenario after each update of the (estimated) state, leads to a significant improvement in the performance (w.r.t. an open-loop strategy) of a traffic intersection in an urban network, since the model captures the information required for creating green waves. It is left for a future research, the extension of the introduced control law in order to simultaneously control, in a *distributed* way, several traffic lights of interconnected intersections.

General conclusions

A timed continuous Petri net under infinite server semantics can be considered as a relaxed version of the corresponding *Markovian* (discrete) Petri net.

By using TCPNs for the analysis of MPNs, an interesting advantage is found: the possibility of the application of techniques and concepts developed in the Control Theory for continuous-sate systems, like the synthesis of performance controllers and observers, the analysis of stability, etc. In this way, the fluidization represents a bridge between particular classes of continuous-state systems and discrete event ones.

Through this dissertation, a theoretical framework has been provided for the use of TCPNs for the synthesis of performance controllers for MPNs. In a first step, the approximation between a MPN and its corresponding TCPN has been studied. Later, it has been analyzed some qualitative properties of the TCPN model: the connection between timing, liveness and boundedness; and controllability. In a third step, three control law structures have been proposed for TCPNs, considering a set-point control problem. Finally, it has been illustrated how a control law derived for the TCPN can be applied to the original MPN, leading to a performance controller for the discrete event system. The obtained results are described with more detail in the following:

• **Approximation between TCPNs and MPNs** (Chapter 2). Approximation errors appear due to synchronizations: rendez-vous and weighted arcs (in non-ordinary nets). In fact, a perfect match is obtained for ordinary Join-free nets. For non-ordinary Join free models, assuming liveness and asymptotic stability, approximation errors are ultimately bounded. That result is extended to non Join-free nets, under the assumption that the system evolves inside one region with a high probability. In order to improve the approximation when the system evolves in several regions, the TCPN model is enriched by adding white gaussian *noise* to the transitions' flow, obtaining a new stochastic continuous model TnCPN. Assuming liveness and ergodicity, the pdf of the marking of the TnCPN may approximate that of the MPN. The larger the MPN's enabling degrees during the most probable trajectories, the better the approximation. This result has been extended to partially relaxed models, i.e., hybrid Petri nets. Nevertheless, the approximation provided by hybrid systems is not always better than that provided by continuous systems, particularly when continuous places barely enable discrete transitions. For this reason, having a large number of enabled servers in the transitions is desirable for a good approximation (specially for continuous transitions having output weighted arcs and discrete transitions being enabled by continuous places).

• **Connection between the timing, liveness and boundedness in TCPNs** (Chapter 3). In continuous models, the timing constraints may enforce the system to (eventually) behave as conservative and/or consistent when the autonomous continuous PN does not exhibit these properties. The existence of a timing that induces such behavior has been studied for general nets and for particular subclasses as well. This has been approached by defining two algebraic timing-dependent properties: λ-consistency and λ-conservativeness. It has been proved that, if the system is λ-consistent and all the minimal

siphons are initially marked, then the TCPN becomes live. This represents a connection between an algebraic property and a behavioral one. At a dynamical level, such timing dependent property can be interpreted as the existence of invariants where the system is live. Based on this, a couple of sufficient conditions for avoiding non-live equilibrium markings, and sufficient conditions for reaching them, have been introduced. Furthermore, algorithms, devoted to compute a timing s.t. the TCPN is live and bounded, have been provided.

• **Controllability for TCPNs** (Chapter 4). TCPNs are not controllable under the classical controllability concept used for linear continuous-state systems, since the marking is restricted to an invariant set (denoted as $Class(\mathbf{m}_0)$) determined by the P-flows. Furthermore, in TCPNs the only allowed control action is the reduction of the flow of certain controllable transitions (i.e., a local reduction of the activity in the system), leading to relevant input constraints. For these reasons, a *local* controllability concept has been proposed, taking into account the input constraints. For models in which control actions can be applied to all transitions, the controllability over the relative interior set of $Class(\mathbf{m}_0)$ is guaranteed iff the system is consistent, obtaining thus a purely structural characterization of controllable models. Moreover, the system is controllable over the complete $Class(\mathbf{m}_0)$ iff additionally no siphon is empty in this set. The controllability analysis for systems with uncontrollable transitions is much more complex. In this case, TCPNs are frequently not controllable over $Class(\mathbf{m}_0)$. Thus, the controllability analysis is restricted to subsets of potential equilibrium markings (where the system can be stabilized). For a single marking region (or configuration, where the system behaves linearly), a sufficient and necessary condition for controllability over equilibrium markings have been obtained. Furthermore, given a connected union of sets of equilibrium markings belonging to different regions, the system is controllable over the complete union if it is controllable over each of the component-subsets. In this case, the controllability depends not only on the structure of the net but also on the timing.

• **Synthesis of controllers for TCPNs** (Chapter 5). The goal of the control problem considered here consists in driving the system towards a desired target marking. It has been firstly addressed the control problem for systems in which all the transitions are controllable. Regarding this, an affine centralized control law has been derived for TCPNs. The application of the control scheme is achieved in polynomial time. Nevertheless, the complexity appears during the synthesis, since the required computation of the vertices of the polytope ($Class(\mathbf{m}_0)$) is not polynomial. In order to deal with such complexity, specially for systems having a large net structure, those results have been extended in order to provide a modular-coordinated control strategy. The resulting scheme consists of a set of affine local controllers and a coordinator that receives and sends information to the local controllers. Next, the control problem for system with uncontrollable transitions has been considered for the centralized case, by adopting a more classical approach: a linear state-feedback control law based on pole-assignment techniques. The implementation of the resulting control law consists of the computation of a suitable gain matrix for each region, and the resolution of a LPP during its application for computing suitable intermediate markings that guarantee the boundedness of the input, obtaining thus a piecewise-linear constrained control structure. For the three control structures introduced in this work, feasibility and convergence have been demonstrated.

• **Implementation of controllers designed for TCPNs into the corresponding MPNs** (Chapter 5). A control law designed for a TCPN system can be applied into the corresponding MPN one. An estimator-based control structure has been provided for this purpose. The continuous control

law is thus transformed into the application of additional delays to the controllable transitions in order to enforce a desired performance in the *original* stochastic Petri net. This control strategy was applied for the stock level control of a Kanban-based automotive assembly line. As a second application example, the optimization problem of traffic lights in urban traffic systems has been addressed by using hybrid PN models for the intersections, and a model predictive control strategy for an on-line optimization. Further research is required for the evaluation of the performance of this approach in large traffic networks.

Despite the broad results that can be found in the literature for continuous Petri nets, and the analysis introduced in this dissertation, there are several interesting questions that remain open. Let us mention a few of them:

• The approximation analysis may be extended to wider classes of time interpreted discrete PNs, for instance, to deterministically T-timed Petri nets with single server semantics. Another interesting issue is the modification of the semantics in order to improve the approximation, as mentioned in Subsection 2.5.2.

• Regarding controllability, there are some questions concerning the case of uncontrollable transitions. For instance, the connexity of the set of equilibrium marking is still unknown for the general case, which is important for the controllability analysis over the union of different regions. Furthermore, an efficient technique for the analysis of reachability between regions is required, since the number of these increases exponentially w.r.t. the number of synchronizations (rendez-vous). Moreover, the connection between the controllability property and the net structure is not completely understood for systems with uncontrollable transitions.

• There is still a lack of control synthesis procedures for systems with uncontrollable transitions. In particular, the problem of transferring the system through regions (configurations) is difficult to address. According to the control scheme proposed in Chapter 5, the control law derived for the continuous PN can be finally applied to the corresponding MPN, which is seen as the continuous model under state and output perturbations. In this sense, it becomes particularly relevant the development of *robust* control structures for TCPNs with noise.

• For the synthesis of performance controllers for MPNs via TCPNs, a closed-loop stability analysis is still missing. In Chapter 2 it was proved that the marking's pdf of the MPN can be approximated by that of the TCPN with white noise, what leads to the use of an extended Kalman filter in order to obtain an estimation of the average behavior of the MPN. Nevertheless, such approximation is, in general, not perfect. Furthermore, the control laws to be applied are derived for the TCPN without noise, assuming a perfect knowledge of the state. In this way, it should be desirable to enjoy of a sort of Separation Principle (providing sufficient conditions for closed-loop stability, when the controller and the observer/estimator are independently synthesized) for TCPNs, in order to formalize the application of TCPN controllers into the original MPN system.

From a more general perspective, it seems interesting to extend the results obtained in this work to hybrid Petri nets, since these models exhibit an interesting expressiveness power. An example of this was shown in Chapter 6, by modeling intersections in urban traffic networks, allowing the on-line optimization of the traffic lights.

This dissertation has illustrated a particular potential application for fluid relaxations in the analysis

and synthesis in PNs. In this way, the fluidization seems a promising approach and opens wide possibilities for addressing different problems, like state-estimation, performance evaluation, on-line optimization, etc., from a powerful perspective.

Bibliography

[Alla and David, 1988] Alla, H. and David, R. (1988). Modelling of production systems by continuous Petri nets. In *3rd International Conference on CAD/CAM Robotics and Factories of the Future*, Berlin, Germany.

[Alla and David, 1998] Alla, H. and David, R. (1998). Continuous and hybrid Petri nets. *Journal of Circuits, Systems and Computers*, 8(1):159–188.

[Altman et al., 2001] Altman, E., Jimnez, T., and Koole, G. (2001). On the comparison of Queueing Systems with their Fluid limits. *Probability in the Engineering and Informational Sciences*, 15:165–178.

[Amer-Yahia et al., 1996] Amer-Yahia, C., Zerhouni, N., El-Moudni, A., and Ferney, M. (1996). State variable decription and controllability of a class of continuous Petri nets. In *IEEE International Symposium on Circuits and Systems*, volume 3, pages 68–71.

[Amrah et al., 1997] Amrah, A., Zerhouni, N., and El-Moudni, A. (1997). Control of discrete event systems modelled by continuous Petri nets: case of opened assembly manufacturing lines. In *IEEE International Conference on Robotics and Automation*.

[Amrah et al., 1998] Amrah, A., Zerhouni, N., and El-Moudni, A. (1998). On the control of manufacturing lines modelled by controlled continuous Petri nets. *International Journal of Systems Science*, 29(2):127–137.

[Apaydin-Ozkan et al., 2009] Apaydin-Ozkan, H., Júlvez, J., Mahulea, C., and Silva, M. (2009). An efficient heuristics for minimum time control of continuous Petri nets. In *3rd IFAC Conference on Analysis and Design of Hybrid Systems, ADHS09*.

[Apaydin-Ozkan et al., 2010] Apaydin-Ozkan, H., Júlvez, J., Mahulea, C., and Silva, M. (2010). A control method for timed distributed continuous Petri nets. In *American Control Conference 2010*, Baltimore, Maryland, USA. IEEE Press.

[Balbo and Silva, 1998] Balbo, G. and Silva, M. (1998). *Performance Models for Discrete Event Systems with Synchronizations: Formalisms and Analysis Techniques*. KRONOS.

[Balduzzi et al., 2001] Balduzzi, F., Giua, A., and Seatzu, C. (2001). Modelling manufacturing systems with first-order hybrid Petri nets. *International Journal of Production Research, Special Issue on Modeling, Specification and Analysis of Manufacturing Systems*, 39(2):225–282.

[Balduzzi et al., 2000] Balduzzi, F., Menga, G., and Giua, A. (2000). First-order hybrid Petri nets: a model for optimization and control. *IEEE Transactions on Robotics and Automation*, 16(4):382–399.

[Bazzan, 2005] Bazzan, A. (2005). A distributed approach for coordination of traffic signals. *Autonomous Agents and Multi-Agent Systems*, 10(1):131–164.

[Bemporad et al., 1999] Bemporad, A., Ferrari-Trecate, G., and Morari, M. (1999). Observability and controllability of piecewise affine and hybrid systems. In *38th IEEE Conference on Decision and Control*.

[Bemporad et al., 2002] Bemporad, A., Morari, M., Dua, V., and Pistikopoulos, E. N. (2002). The explicit linear quadratic regulator for constrained systems. *Automatica*, 38(1):3–20.

[Brammer, 1972] Brammer, R. (1972). Controllability in linear autonomous systems with positive controllers. *SIAM Journal Control*, 10(2):329–353.

[Brams, 1983] Brams, G. (1983). *Réseaux de Petri: Théorie et pratique*. Masson.

[Camlibel, 2007] Camlibel, M. (2007). Popov-belevitch-hautus type controllability tests for linear complementarity systems. *Systems and Control Letters*, 56(5):381–387.

[Camponagara and Kraus, 2003] Camponagara, E. and Kraus, W. (2003). Distributed learning agents in urban traffic control. In *Progress in artificial intelligence (6th EPIA)*.

[Champagnat et al., 1998] Champagnat, R., Esteban, P., Pingaud, H., and Valette, R. (1998). Modeling and simulation of a hybrid system through pr/tr pn-dae model. In *Proceedings of ADPM98*, pages 131–137.

[Chen, 1984] Chen, C. (1984). *Linear system theory and design*. Oxford University Press, New York.

[Chen and Mandelbaum, 1991] Chen, H. and Mandelbaum, A. (1991). Discrete flow networks: Bottleneck analysis and fluid approximations. *Mathematical Operations Research*, 16:408–446.

[Colom and Silva, 1991] Colom, J. M. and Silva, M. (1991). Improving the linearly based characterization of P/T nets. *Adavances in Petri nets 1990*, *483 of Lecture Notes in Computer Science*:113–145.

[Dai, 1995] Dai, J. G. (1995). On positive Harris recurrence of multiclass queuing networks: A unified approach via fluid limit models. *The Annals of Applied Probability*, 5(1):49–77.

[David and Alla, 1987] David, R. and Alla, H. (1987). Continuous Petri Nets. In *8th European Workshop on Application and Theory of Petri Nets*, pages 275–294, Zaragoza, Spain.

[David and Alla, 1990] David, R. and Alla, H. (1990). Autonomous and timed continuous Petri Nets. In *11th International Conference on Application and Theory of Petri Nets*, pages 367–386, Paris, France.

[David and Alla, 2010] David, R. and Alla, H. (2010). *Continuous and Hybrid Petri Nets, 2^{nd} ed.* Springer, Berlin.

[Demongodin et al., 1993] Demongodin, I., Audry, N., and Prunet, F. (1993). Batches Petri nets. In *IEEE conference on Systems, Man and Cybernetics, 'Systems engineering in the service of humans'*, pages 607–617.

[Dotoli et al., 2006] Dotoli, M., Fanti, M. P., and Meloni, C. (2006). A signal timing plan formulation for urban traffic control. *Control Engineering Practice*, 14:1297–1311.

[Dub et al., 2002] Dub, M., Pipan, G., and Hanzálek, Z. (2002). Stock optimization of a kanban-based assembly line. In *12th International Conference on Flexible Automation & Intelligent Manufacturing*.

[Ezpeleta et al., 1993] Ezpeleta, J., Couvreur, J., and Silva, M. (1993). A new technique for finding a generating family of siphons, traps and st-components. application to colored Petri nets. *Advances in Petri nets 1993, 674 of Lecture Notes in Computer Science*:126–147.

[Ezzine and Haddad, 1989] Ezzine, J. and Haddad, A. H. (1989). Controllability and observability of hybrid systems. *International Journal of Control*, 49(6):2045–2055.

[Florin and Natkin, 1985] Florin, G. and Natkin, S. (1985). *Les réseaux de Petri stochastiques: Théorie, Techniques de calcul, applications*. thèse de Doctorat d'Etat. Technical report, Université P. et M. Curie.

[Fukuda, 2000] Fukuda, K. (2000). Frequently asked questions in polyhedral computation. Technical report, Zürich, http://www.ifor.math.ethz.ch/∼fukuda/polyfaq/polyfaq.html

[Genrich and Lautenbach, 1981] Genrich, H. J. and Lautenbach, K. (1981). System modelling with high-level Petri nets. *Theoretical Computer Science*, 13(1):109–135.

[Giua et al., 1992] Giua, A., DiCesare, F., and Silva, M. (1992). Generalized mutual exclusion constraints on nets with uncontrollable transitions. In *IEEE International Conference on Systems, Man, and Cybernetics*.

[Giua et al., 2000] Giua, A., Furcas, R., Piccaluga, A., and Seatzu, C. (2000). Modeling and control of inventory management policies using first-order hybrid Petri nets. In *4th International Conference Automation of Mixed Processes: Hybrid Dynamical Systems*, pages 273–278.

[Grewal and Andrews, 2001] Grewal, M. S. and Andrews, A. P. (2001). *Kalman Filtering, Theory and Practice Using MatLab*. Wiley-Interscience Publication USA.

[Habets et al., 2006] Habets, L. C. G. J. M., Collins, P. J., and van Schuppen, J. H. (2006). Reachability and control synthesis for piecewise-affine hybrid systems on simplices. *IEEE Transactions on Automatic Control*, 51:938–948.

[Habets and van Schuppen, 2001] Habets, L. C. G. J. M. and van Schuppen, J. H. (2001). A controllability results for piecewise-linear hybrid systems. In *European Control Conference*, pages 3871–3873.

[Habets and van Schuppen, 2004] Habets, L. C. G. J. M. and van Schuppen, J. H. (2004). A control problem for affine dynamical systems on a full-dimensional polytope. *Automatica*, 40:21–35.

[Heemels et al., 2008] Heemels, W. P. M. H., Lazar, M., van de Wouw, N., and Pavlov, A. (2008). Observer-based control of discrete-time piecewise affine systems: exploiting continuity twice. In *IEEE Conference on Decision and Control*.

[Hennequin et al., 1999] Hennequin, S., Lefebvre, D., and El-Moudni, A. (1999). Fuzzy control of variable speed continuous Petri nets. In *38th IEEE Conference on Decision and Control*.

[Hillston, 2005] Hillston, J. (2005). Fluid Flow Approximation of PEPA models. In *QEST*, pages 33–43.

[Holloway et al., 1997a] Holloway, L. E., Krogh, B. H., and Giua, A. (1997a). A survey of Petri net methods for controlled discrete event systems. *Journal of Discrete Event Dynamic Systems*, 9(2):151–190.

[Holloway et al., 1997b] Holloway, L. E., Krogh, B. H., and Giua, A. (1997b). A survey of Petri nets methods for controlled discrete event systems. *Journal of Discrete Event Dynamic Systems*, 7(2):151–190.

[Hunt et al., 1982] Hunt, P. B., Robertson, D. I., Bretherton, R. D., and Royle, M. C. (1982). The scoot online traffic signal optimization technique. *Traffic Engineering and Control*, 23:190–192.

[Iordache and Antsaklis, 2006] Iordache, M. V. and Antsaklis, P. J. (2006). *Supervisory control of concurrent systems*. Birkhäuser, Boston.

[Jensen, 1981] Jensen, K. (1981). Coloured Petri nets and the invariant method. *Theoretical Computer Science*, 14:317–336.

[Jiménez et al., 2005] Jiménez, E., Júlvez, J., Recalde, L., and Silva, M. (2005). On controllability of timed continuous Petri net systems: the join free case. In *44th IEEE Conference on Decision and Control (Joint CDC-ECC), Seville, Spain*.

[Jing et al., 2008a] Jing, X., Recalde, L., and Silva, M. (2008a). Tracking control of join-free timed continuous Petri net systems under infinite servers semantics. *Journal of Discrete Event Dynamic Systems*, 18(2):263–283.

[Jing et al., 2008b] Jing, X., Recalde, L., and Silva, M. (2008b). Tracking control of timed continuous Petri net systems under infinite servers semantics. In *IFAC World Congress*.

[Júlvez et al., 2008] Júlvez, J., Jiménez, E., Recalde, L., and Silva, M. (2008). On Observability and Design of Observers inTimed Continuous Petri Net Systems. *IEEE Transactions on Automation Science and Engineering*, 5(3):532–537.

[Júlvez et al., 2005] Júlvez, J., Recalde, L., and Silva, M. (2005). Steady state performance evaluation of continuous mono-T-semiflow Petri nets. *Automatica*, 41(4):605–616.

[Júlvez et al., 2006] Júlvez, J., Recalde, L., and Silva., M. (2006). Deadlock-freeness analysis of continuous mono-t-semiflow Petri nets. *IEEE Transactions on Automatic Control*, 51:1472–1781.

[Kara et al., 2009] Kara, R., Ahmane, M., Loiseau, J. J., and Djennoune, S. (2009). Constrained regulation of continuous Petri nets. *Nonlinear Analysis: Hybrid Systems*, 3(4):738–748.

[Kara et al., 2006] Kara, R., Djennoune, S., and Loiseau, J. J. (2006). State feedback control for the manufacturing systems modeled by continuous Petri nets. In *Information Control Problems in Manufacturing (INCOM)*.

[Khalil, 2002] Khalil, H. K. (2002). *Nonlinear Systems, Third Edition*. Prentice-Hall.

[Kloetzer et al., 2010] Kloetzer, M., Mahulea, C., Belta, C., and Silva, M. (2010). An automated framework for formal verification of timed continuous Petri nets. *IEEE Transactions on Industrial Informatics*, 6(3):460–471.

[Kurtz, 1970] Kurtz, T. (1970). Solutions of ordinary differential equations as limits of pure jump Markov processes. *Journal of Applied Probability*, 7(1):49–58.

[Lefeber and Rooda, 2006] Lefeber, E. and Rooda, J. E. (2006). Controller design for switched linear systems with setups. *Physica A*, 363:48–61.

[Lefebvre, 1999] Lefebvre, D. (1999). Feedback control designs for manufacturing systems modelled by continuous Petri nets. *International Journal of Systems Science*, 30(6):591–600.

[Lefebvre et al., 2007] Lefebvre, D., Catherine, D., Leclerq, E., and Druaux, F. (2007). Some contributions with Petri nets for the modelling, analysis and control of HDS. In *International Conference on Hybrid Systems and Applications*, volume 1, pages 451–465.

[Lefebvre et al., 2010] Lefebvre, D., Leclerq, E., Akchioui, N. E., Khalij, L., and Cursi, E. D. (2010). A geometric approach for the homothetic approximation of stochastic Petri nets. In *10th IFAC Workshop on Discrete Event Systems*.

[Lefebvre et al., 2009] Lefebvre, D., Leclerq, E., Khalij, L., Cursi, E. D., and Akchioui, N. E. (2009). Approximation of MTS stochastic Petri nets steady state by means of continuous Petri nets: A numerical approach. In *3rd IFAC Conference on Analysis and Design of Hybrid Systems*.

[Levine, 1996] Levine, W. S. (1996). *The Control Handbook*. CRC Press.

[Liberzon, 2004] Liberzon, D. (2004). Common lyapunov functions and gradient algorithms. *IEEE Transactions on Automatic Control*, 49(6):990–994.

[Lowrie, 1982] Lowrie, P. R. (1982). Scats principles, methodologies, algorithm. In *IEE Conference on Road traffic Signal*, pages 67–70.

[Mahulea et al., 2008a] Mahulea, C., Giua, A., Recalde, L., Seatzu, C., and Silva, M. (2008a). Optimal model predictive control of timed continuous Petri nets. *IEEE Transactions on Automatic Control*, 53(7):1731–1735.

[Mahulea et al., 2008b] Mahulea, C., Ramírez-Treviñ, A., Recalde, L., and Silva, M. (2008b). Steady state control reference and token conservation laws in continuous Petri net systems. *IEEE Transactions on Automation Science and Engineering*, 5(2):307–320.

[Mahulea et al., 2009] Mahulea, C., Recalde, L., and Silva, M. (2009). Basic server semantics and performance monotonicity of continuous Petri nets. *Journal of Discrete Event Dynamic Systems*, 19(2):189–212.

[Mahulea et al., 2010] Mahulea, C., Recalde, L., and Silva, M. (2010). Observability of continuous Petri nets with infinite server semantics. *Nonlinear Analysis: Hybrid Systems*, 4(2):219–232.

[Marsan et al., 1984] Marsan, M. A., Balbo, G., and Conte, G. (1984). A class of generalized stochastic Petri nets for the performance evaluation of multiprocessor systems. *ACM Transactions on Computer Systems*, 2(2):93–122.

[Marsan et al., 1995] Marsan, M. A., Balbo, G., Conte, G., Donatelli, S., and Franceschinis, G. (1995). *Modelling with generalized stochastic Petri nets*. John Wiley and Sons.

[Merlin and Farber, 1976] Merlin, P. M. and Farber, D. J. (1976). Recoverability of communication protocols: Implications of a theoretical study. *IEEE Transactions on Communications*, 24(9):1036–1043.

[Molloy, 1982] Molloy, M. K. (1982). Performance analysis using stochastic Petri nets. *IEEE Transactions on Computers*, 31(9):913–917.

[Murata, 1989] Murata, T. (1989). Petri nets: Properties, analysis and applications. *Proceeding of the IEEE*, 77(4):541–580.

[Papoulis, 1984] Papoulis, A. (1984). *Probability, Random Variables, and Stochastic Processes*. McGraw-Hill.

[Paulraj and Sumathi, 2010] Paulraj, S. and Sumathi, P. (2010). A comparative study of redundant constraints identification methods in linear programing problems. *Mathematical problems in engineering, doi:10.1155/2010/723402*.

[Petri, 1962] Petri, C. A. (1962). Kommunikation mit Automaten. Technical report, Bonn: Institut für instrumentelle mathematik, Schriften des IIM Nr. 2.

[Petri, 1966] Petri, C. A. (1966). Kommunikation mit Automaten. Technical report, Suplement 1 to Technical report RADC-TR-65-337. Translation by C.F. Greene.

[Phillips and Nagle, 1984] Phillips, C. and Nagle, T. (1984). *Digital control system analysis and design*. Prentice-Hall.

[Porche et al., 1996] Porche, I., Sampath, M., Sengupta, R., Chen, Y., and Lafortune, S. (1996). A decentralized scheme for real-time optimization of traffic signals. In *IEEE International Conference on Control Applications*.

[Ramchandani, 1974] Ramchandani, C. (1974). Analysis of asynchronous concurrent systems by timed Petri nets, phD Thesis. Technical report, MIT, Cambridge, MA.

[Recalde et al., 2010] Recalde, L., Haddad, S., and Silva, M. (2010). Continuous Petri nets: Expressive power and decidability issues. *International Journal of Foundations of Computer Science*, 21(2):235–256.

[Recalde and Silva, 2001] Recalde, L. and Silva, M. (2001). Petri nets fluidification revisited: Semantics and steady state. *European Journal of Automation APII-JESA*, 35(4):435–449.

[Recalde et al., 1999] Recalde, L., Teruel, E., and Silva, M. (1999). Autonomous Continuous P/T systems. *Application and Theory of Petri Nets, 1639 of Lecture Notes in Computer Science*:107–126.

[Silva, 1993] Silva, M. (1993). *Introducing Petri nets, In Practice of Petri Nets in Manufacturing*. Chapman & Hall.

[Silva and Recalde, 2002] Silva, M. and Recalde, L. (2002). Petri nets and integrality relaxations: A view of continuous Petri nets. *IEEE Transactions on Systems, Man, and Cybernetics*, 32(4):314–327.

[Silva and Recalde, 2004] Silva, M. and Recalde, L. (2004). On fluidification of Petri net models: from discrete to hybrid and continuous models. *Annual Reviews in Control*, 28(2):253–266.

[Silva et al., 1998] Silva, M., Teruel, E., and Colom, J. M. (1998). Linear algebraic and linear programming techniques for the analysis of P/T net systems. *Lectures in Petri Nets. I: Basic Models*, *1491 of Lecture Notes in Computer Science*:309–373.

[Sun and Zheng, 2001] Sun, Z. and Zheng, D. (2001). On stabilization of switched linear control systems. *IEEE Transactions on Automatic Control*, 46(2):291–295.

[Teruel et al., 1997] Teruel, E., Colom, J. M., and Silva, M. (1997). Choice-free Petri nets: A model for deterministic concurrent systems with bulk services and arrivals. *IEEE Transactions on Systems, Man, and Cybernetics*, 27(1):73–83.

[Toshihiko, 2003] Toshihiko, O. (2003). Optimization control of traffic flow in urban road networks. *Matsushita Technical Journal*, 49(3):239–244.

[Trivedi and Kulkarni, 1993] Trivedi, K. and Kulkarni, V. G. (1993). Fspns: Fluid Stochastic Petri nets. *Application and Theory of Petri Nets*, *691 of Lecture Notes in Computer Science*:24–31.

[USDOT, 2005] USDOT Federal Highway Administration (2005). *Traffic Control Systems Handbook*.

[van den Berg et al., 2004] van den Berg, M., Schutterand, B. D., Hegyi, A., and Hellendoorn, J. (2004). Model predictive control of mixed urban and freeway networks. In *83rd annual meeting of Transportation Research Board*.

[Vázquez, 2010] Vázquez, C. R. (2010). ISS Hybrid Petri net simulator. Technical report, Universidad de Zaragoza.

[Vázquez et al., 2008] Vázquez, C. R., Mangini, A. M., Mihalache, A. M., Recalde, L., and Silva, M. (2008). Timing and deadlock-freeness in continuous Petri nets. In *17th IFAC World Congress*.

[Vázquez et al., 2008a] Vázquez, C. R., Ramírez, A., Recalde, L., and Silva, M. (2008a). On controllability of timed continuous Petri nets. *Hybrid Systems: Computational and Control*, *4981 of Lecture Notes in Computer Science*:528–541.

[Vázquez et al., 2008b] Vázquez, C. R., Recalde, L., and Silva, M. (2008b). Stochastic–continuous state approximation of Markovian Petri net systems. In *47th IEEE Conference on Decision and Control*.

[Vázquez and Silva, 2009a] Vázquez, C. R. and Silva, M. (2009a). Hybrid Petri nets as an approximation to Markovian Petri nets. In *3rd IFAC Conference on Analysis and Design of Hybrid Systems*.

[Vázquez and Silva, 2009b] Vázquez, C. R. and Silva, M. (2009b). Performance control of Markovian Petri nets via fluid models: A stock-level control example. In *5th IEEE Conference on Automation Science and Engineering (IEEE CASE)*.

[Vázquez and Silva, 2009c] Vázquez, C. R. and Silva, M. (2009c). Piecewise-linear constrained control for timed continuous Petri nets. In *48th IEEE Conference on Decision and Control*.

[Vázquez and Silva, 2010] Vázquez, C. R. and Silva, M. (2010). Timing-dependent boundedness and liveness in continuous Petri nets. In *10th International Workshop on Discrete Event Systems (WODES)*, Berlin, Germany.

[Vázquez and Silva, 2011] Vázquez, C. R. and Silva, M. (2011). Timing and liveness in continuous Petri nets. *Automatica*, 47:283–290.

[Vázquez et al., 2010] Vázquez, C. R., Sutarto, H. Y., Boel, R., and Silva, M. (2010). Hybrid Petri net model of a traffic intersection in an urban network. In *2010 IEEE Multiconference on Systems and Control*, Yokohama, Japan.

[Vázquez et al., 2011] Vázquez, C. R., van Schuppen, J. H., and Silva, M. (to be held on August, 2011). A modular-coordinated control for continuous Petri nets. In *18th IFAC World Congress*.

[Wang et al., 2010] Wang, L., Mahulea, C., Júlvez, J., and Silva, M. (2010). Minimum-time control for structurally persistent continuous Petri nets. In *IEEE Conference on Decision and Control*.

[Xie and Wang, 2002] Xie, G. and Wang, L. (2002). Controllability and stabilization of switched linear systems. *Systems and Control Letters*, 48(2):135–155.

[Xu and Xie, 2005] Xu, J. and Xie, L. (2005). Null controllability of discrete-time planar bimodal piecewise linear systems. *International Journal of Control*, 78(18):1486–1496.

[Zerhouni and Alla, 1990] Zerhouni, N. and Alla, H. (1990). Dynamic analysis of manufacturing systems using continuous Petri nets. In *IEEE International Conference on Robotics and Automation*.

[Zimmermann and Knoke, 2007] Zimmermann, A. and Knoke, M. (2007). Timenet 4.0 user manual. Technical report, Technische Universität Berlin.

APPENDIX

Appendix A

ISS hybrid Petri nets simulator

The approximation of the marking of Markovian PN's, provided by the corresponding TCPN, was studied in Chapter 2. Accordingly, the existence of syncronizations: rendez-vous and weighted arcs, introduce approximation errors, nevertheless, assuming liveness and stability, such errors are ultimately bounded.

Later, in order to improve the approximation when the system evolves through several regions, a new stochastic continuous model TnCPN was defined. The approximation provided by this model was also analyzed, obtaining a similar kind of results, i.e., under certain liveness and stability assumptions, the approximation errors are ultimately bounded. In such case, the approximation holds not only for the average marking, but also for the probability distribution. In a third step, a *partial relaxation* of a MPN leads to a hybrid Petri net model MHPN. It was shown that the approximation provided by such hybrid systems is not always better than those provided by fully continuous net models. For this reason, different results were introduced, which may lead to provided sufficient conditions for an effective approximation.

Despite the formal results obtained in Chapter 2, from a practical point of view, there are interesting remaining questions. For instance, given a particular MPN system and its corresponding relaxations (TCPN, TnCPN, MHPN), how accurate is the approximation provided? is it possible to compute bounds for the errors? does the approximation holds for a different timing?

These are difficult questions, and unfortunately, no general answers have been found until now. Nevertheless, under the assumption of liveness and ergodicity (stability), valid information can be obtained from several simulations, obtaining thus a practical way for deciding if, given a particular MPN, its relaxation provide a good approximation. For this reason, a simulator was developed in order to compare the steady and transient behavior of either discrete, continuous or hybrid Petri nets under infinite server semantics. This appendix will present such a simulator, which is available in http://webdiis.unizar.es/∼cvazquez/ together with a user's manual [Vázquez, 2010].

A.1 Simulation algorithm

In this section, a basic algorithm for simulating a *Markovian hybrid Petri net* is introduced. In a general timing interpretation of a discrete PN, the marking does not provide all the information required for determining the future evolution of the system, i.e., it is not the full *state* of the system. It is also required some information about the time at which each active server will be fired, which in this work

is called *clock*. In a MPN (here under infinite server semantics), *one* clock variable per transition is enough (because the minimum of n exponentially distributed r.v.'s with a parameter λ_i is equal to an exponentially distributed r.v. with parameter $n \cdot \lambda_i$), meaning the time at which the following firing occurs. By using these variables and the marking, it is possible to simulate a MPN by using either an event-driven simulation or a time-driven one. Even if the event-driven approach is more efficient (because the marking and clocks are updated at only few time instants, when a firing occurs), in this work a time-driven one will be adopted with a fixed sampling (time increments). The reason for this is the continuous dynamics in hybrid models, which are difficult to simulate in an event-driven scheme, but easy to handle in a time-driven one (just by using its discrete-time state equation), specially when gaussian noise is added to the transitions, since this is defined based on a discrete-time evolution.

Algorithm A.1. Simulating a MHPN.

$\tau := \tau_0$
$\mathbf{M} := \mathbf{M}_0$
clocks $:= \mathbf{0}$
while $\tau \leq$ total simulation time
    $\tau := \tau + \Delta\tau$
    % Firing the discrete transitions %
    for all $t_j \in T^d$ to be fired (i.e, $\forall t_j \in T^d$ s.t. $clocks_j \leq \tau$) **do**
        define $\Delta\boldsymbol{\sigma} \in \mathbb{N}^{|T|}$ with null entries, excepting $\Delta\sigma_j := 1$
        $\mathbf{M} := \mathbf{M} + \mathbf{C} \cdot \Delta\boldsymbol{\sigma}$
        for all $t_i \in T^d$
            compute $Enab(t_i, \mathbf{M})$
            if t_i is not enabled **then** $clocks_i := \infty$
            elseif t_i is enabled and either $t_i = t_j$ or it is newly enabled **then**
                get $\theta \in \mathbb{R}_{>0}$ from an exponential p.d.f with parameter:
                $$\lambda_i \cdot Enab(t_i, \mathbf{M})$$
                $clocks_i := \tau + \theta$
            end if
        end for
    end for
    % Firing the continuous transitions%
    $\Delta\mathbf{w} := \mathbf{0}$
    for all $t_i \in T$ **do**
        if $t_i \in T^d$ **then** $\Delta w_i := 0$
        elseif $t_i \in T^{c,d}$ **then** $\Delta w_i := \lambda_i \cdot enab_i(\mathbf{M})\Delta\tau$
        elseif $t_i \in T^{c,n}$ **then**
            get $noise \in \mathbb{R}_{>0}$ from a normal pdf with zero mean and variance:
            $$\lambda_i \cdot enab_i(\mathbf{M})\Delta\tau$$
            $\Delta w_i := \lambda_i \cdot enab_i(\mathbf{M})\Delta\tau + noise$
        end if

end for
$\mathbf{M} = \mathbf{M} + \mathbf{C} \cdot \Delta\mathbf{w}$
% Actualize the clocks of the discrete transitions %
for all $t_i \in T^d$
compute $Enab(t_i, \mathbf{M})$
if t_i is not enabled **then** $clocks_i := \infty$
elseif t_i is enabled and either $t_i = t_j$ or it is newly enabled **then**
get $\theta \in \mathbb{R}_{>0}$ from an exponential p.d.f with parameter:
$\lambda_i \cdot Enab(t_i, \mathbf{M})$
$clocks_i := \tau + \theta$
end if
end for
end while

The previous algorithm simulates a MHPN in which white noise can be added to the continuous transitions. These are classified as discrete (T^d, with exponential delays and ISSS), continuous ($T^{c,d}$, deterministic under ISS) and continuous with white noise added to the flow ($T^{c,n}$).

Note that, the firing of the continuous transitions is achieved after the firing of the discrete ones. The reason for this is that, in the continuous-time model, the firing of the discrete transitions do not consume time (is instantaneous), thus, if there is a conflict between a continuous and a discrete transition (that has to be fired), the discrete transition is always fired. Furthermore, after the firing of the continuous transitions it is required to update again the clocks, since the firing of the continuous transitions can change the enabling degree of the discrete ones. Previous algorithm can be extended for simulating different kind of timings at the discrete transitions. For instance, suppose that $t_i \in T^d$ fires with a constant delay θ_i (with 1-server semantics), then, when the corresponding clock ($clock_i$) is updated, the value $\tau + \theta_i$ is assigned instead of obtaining a value from an exponential pdf (nevertheless, in this case a conflict resolution policy must be implemented).

A.2 Simulator and interface

The algorithm described in the previous section (with the option of defining discrete transitions with constant delays) is implemented in the m-file *fSimRoutine.m*, in order to use it in MatLab. A graphical Interface is also implemented with the name *ISS_HybPN*. In this section, the use of the Interface for the hybrid simulator is described.

First, in order to use the Interface, call it from the Command Window in MatLab by typing ISS_HybPN.

A.2.1 Introducing the parameters of the PN

The parameters of the PN required for the Simulator are (see fig. A.1): the incidence matrix **C**, the precondition matrix **Pre**, the initial marking $\mathbf{M}_0$ and the mean time delays, which is a vector having as

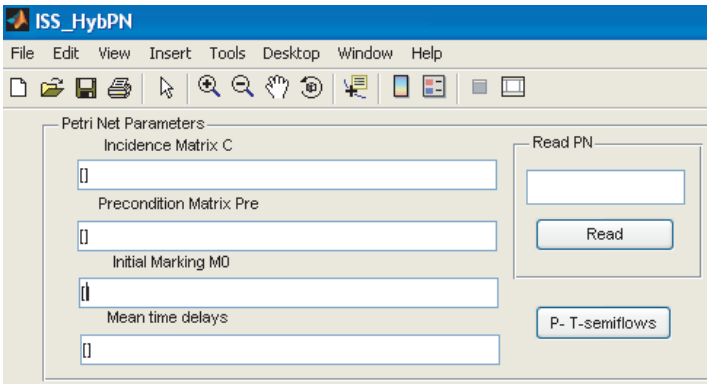

Fig. A.1: Introducing the parameters of the PN.

entries the inverse of the values of $\boldsymbol{\lambda}$ (it can be computed in MatLab as $\mathbf{delaym} = \mathbf{ones}(nt, 1)./\boldsymbol{\lambda}$, where nt is the number of transitions and $\boldsymbol{\lambda}$ is a column vector). These values can be typed directly on the Interface, following the standard matrix format in MatLab (for instance, $[1, -1; -1, 1]$). Furthermore, if those matrices have been defined previously in the current Workspace, they can be called on the Interface by typing the name of the variables. For instance, if the matrix $\mathbf{C}$ was previously defined in the Workspace as the variable $\mathbf{C} = [1, -1; -1, 1]$, then it is only required to type $\mathbf{C}$ on the Interface (it is case sensitive).

It is also possible to load the values of a net from the files generated by Softwares *PMEdit* (graphical editor of PN) and *TimeNet* [Zimmermann and Knoke, 2007]. In order to do this, just click the button *Read* (fig. A.1) on the Interface and select the desired file. It is also possible to load the values from a *.mat file, which is the format used by MatLab for saving the data of the workspace.

Once the incidence matrix is properly defined, the Interface allows to select the *kind of PN*. Three options are allowed in a first glance: *Continuous ISS* (i.e., a TCPN), *Discrete ISS exp* (i.e, a MPN) and *Hybrid*. When the *Hybrid* option is selected, each transition can be defined independently as either discrete or continuous, by selecting the desired transitions in the pop-up menu (fig. A.2(a)). Actually, there are 5 different options:

1. *Discrete 1-server constant*, it fires with a constant delay equal to the corresponding *mean delay* (fig. A.2(a)).

2. *Discrete ISS expected delay*, it fires with a deterministic delay $\theta = (\lambda \cdot Enab(t, \mathbf{m}))^{-1}$, which is the expected value of the stochastic delay under ISS.

3. *Discrete ISS Exponential*, as in a MPN.

4. *Continuous ISS*, as in a TCPN.

5. *Continuous ISS with noise*, as in a TnCPN.

After introducing the Incidence matrix, it is possible to compute the *T- P-semiflows*, by pressing the corresponding button. The results will appear on the command window.

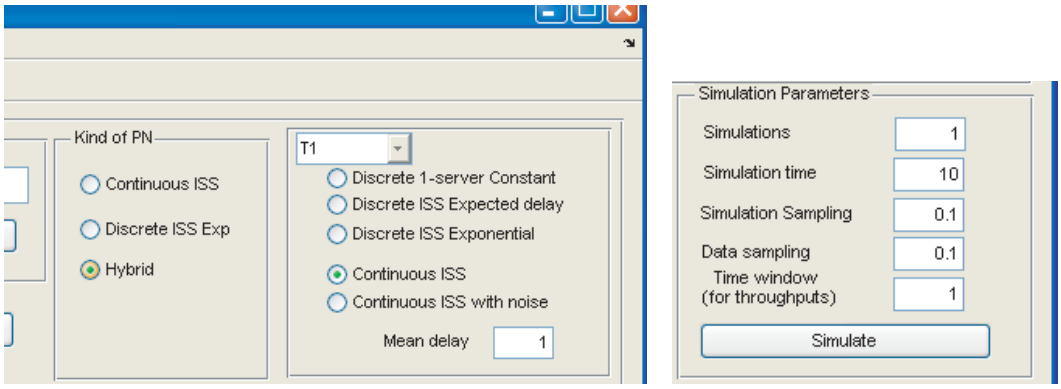

(a) (b)

Fig. A.2: (a) Selecting the kind of PN, and defining the timing of each transition. (b) Introducing the Simulation Parameters.

A.2.2 Introducing the simulation parameters and simulating

The following step is to introduce the simulation parameters. Let us remark that the simulation is achieved in discrete time with a fixed sampling time, independently of the kind of Petri net. Then, the parameters required for the simulation are (see fig. A.2(b)):

1. *Simulations*, the number of simulations required. This value is meaningless for deterministic systems (for instance, a TCPN). Nevertheless, for stochastic systems, like a MPN, the Simulator will simulate the system several times (the number specified at this entry), and only the average and variances information of all the realizations thus obtained will be available. If only one realization is required then set this entry as 1.

2. *Simulation time*, the total simulation time.

3. *Simulation sampling*, the fixed sampling time $\Delta\tau$.

4. *Data sampling*, the sampling time for recording data, for instance, if a value of 1 is defined it means that only each 1 second the data is recorded and it will be available for plotting it. The simulation is faster when this number is large.

5. *Time window*, this is the time window (interval) used for computing the throughputs of discrete transitions, for instance, if a value of 5 is defined, the throughput of t_i at time instant 10 is computed as the number of firings of t_i during the last 5 seconds (in the interval $(5, 10]$) divided by 5.

After defining all the system and simulation parameters, the button *Simulate* (fig. A.2(b)) have to be pressed for simulating. If an error is produced due to some bad definition of the PN parameters, a message pointing out the error will appear on the Interface and the command window, otherwise, the message *SIMULATION IN PROGRESS..* will appear until finishing the simulation. During the process, the number of simulations done will appear on the command window, and at the end, the final values for the average markings and throughputs will also appear on this.

A.2.3 Plotting results

After obtaining a successful simulation, the average marking, throughputs and marking variances trajectories can be plotted. In order to do that, first define the information to plot and after that push the button *Plot*. For instance, in fig. A.3 it appears the average marking trajectories of places p_1 and p_2 (denoted as M(P1) and M(P2)). This information is indicated on the Interface at the entry *Marking Averages to Plot* having a value of [1 2], meaning p_1 and p_2. In the same figure it is also plotted the Throughput of t_1 (in this case the flow, since the system simulated is a TCPN), which is denoted as Thr(T1). This information is indicated at the entry *Throughputs to Plot* with a value of [1]. Entry *Marking Variances to Plot* is used for indicating the places whose marking variances are required to be plotted (instantaneous variance of the marking of the corresponding places, computed with the data obtained from several simulations indicated at the entry *Simulations* in fig. A.2(b)). After pressing *Plot*, the final values of the curves plotted can be seen on the Interface, for instance, in fig. A.3 it appears the *Final value* of M(P1), which is 3.666.

If other curves are desired to be plotted, it is not required to simulate again the system (unless a new system or realization is desired). In such case just define the required curves at the entries *Marking Averages to Plot*, *Throughputs to Plot* and *Marking Variances to Plot*, and push the button *Plot* again. The check box *Hold on* can be used for plotting curves without erasing the previous ones. This option is particularly useful for comparing data of different systems, for instance, for comparing the average marking of a MPN with the corresponding TCPN.

All the figure tools are also available on the Interface, in order to modify the appearance of the curves. By saving the current figure (at the menu, file/save as..) the data and curves are saved, and so they can be loaded in the next session just by opening the corresponding figure file (at the menu, file/open). It is advised to save the figure using always a different name. Moreover, by pressing *Plot==>Figure*, the current curves are plotted in a new window.

By pressing *Data==> WS*, the data of the curves currently plotted and the system and simulation parameters are stored in the current workspace. This function is useful in order to manipulate the data on the command window, or to save the data in a *.mat file.

A.2.4 Example

Consider the MPN system of fig. 5.7(a) with $\mathbf{M} = [10, 0, 30, 0, 10, 0]^T$ and $\boldsymbol{\lambda} = [1, 1, 1, 2]$. Suppose that it is required to know if this system accepts a reasonable fluidization. One way for doing that is to simulate the MPN several times and also the corresponding TCPN and then to compare the average trajectories of both systems.

In this case, the system parameters to be introduced on the Interface are:

1. Incidence Matrix:
   $[-1, 1, 0, 0; 1, -1, 0, 0; 0, -1, 1, 0; 0, 1, -1, 0; 0, 0, -1, 1; 0, 0, 1, -1]$.
2. Precondition Matrix: $[1, 0, 0, 0; 0, 1, 0, 0; 0, 1, 0, 0; 0, 0, 1, 0; 0, 0, 1, 0; 0, 0, 0, 1]$.
3. Initial Marking M0: $[10; 0; 30; 0; 10; 0]$.
4. Mean time delays: $[1; 1; 1; 1/2]$ (remember that these values are the inverse of those of $\boldsymbol{\lambda}$).

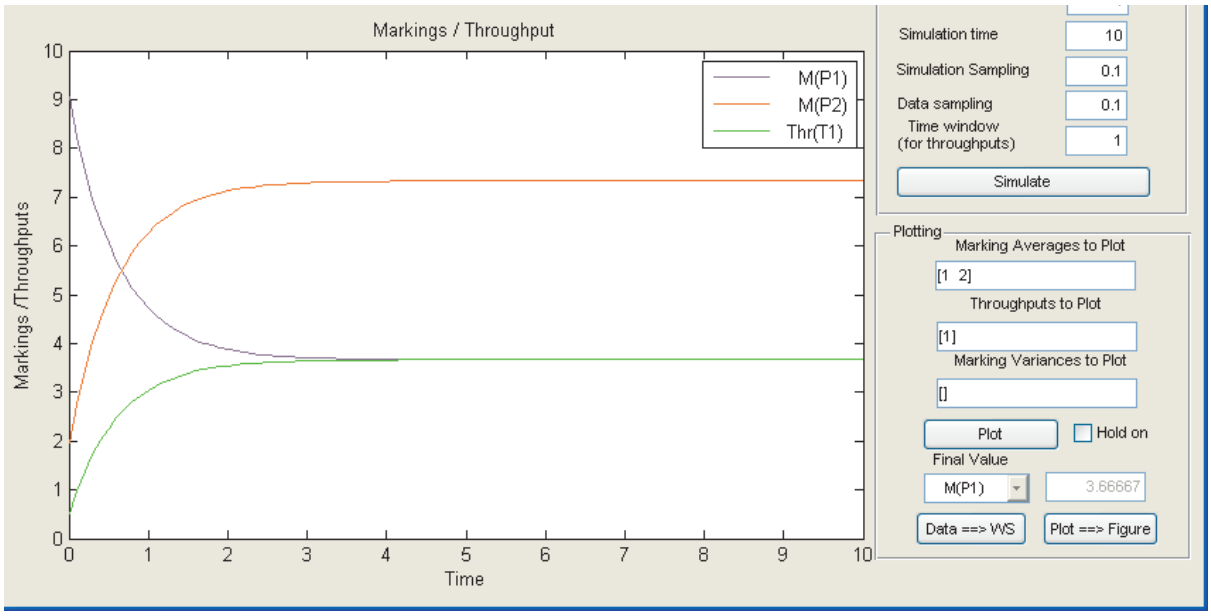

Fig. A.3: Plotting results after a simulation.

First, let us simulate the MPN. Then, select the *kind of PN* as *Discrete ISS exp*. The simulation parameters are defined as: *Simulations* 100 (for simulating the MPN a hundred of times and plotting the average trajectory), *Simulation time* 10, *Simulation sampling* 0.1, *Data sampling* 0.1 and *Time window* 1. After setting these parameters, push the button *Simulate*. A text *SIMULATION IN PROGRESS...* should appear on the Interface, while on the command window the progress of the simulation is indicated (it should appear: Simulation 10 of 100, Simulation 20 of 100, etc). When the simulations have been done, the text *Simulation done* substitutes the previous one.

Now, since the system has 3 P-semiflows, the markings of only 3 places is required for determining the whole marking of the system. Let us take p_1, p_3 and p_5. Then, in order to plot the average markings at those places, set the value [1 3 5] at the entry *Marking Averages to Plot*, and push the button *Plot*. The average marking trajectories of the MPN system are now shown on the Interface.

In order to simulate the corresponding TCPN system, just change the entry at *kind of PN* as *Continuous ISS* and push the button *Simulate* again. In this case, the simulator will simulate the PN only once, since a TCPN is deterministic. Then, after a short time, the text *Simulation done* will appear on the Interface. Since it is desired to plot the marking trajectories but without erasing the previous ones, first check the box *Hold on*. After that, push the button *Plot*. Fig. A.4 shows the results thus obtained. Labels M(P1), M(P3) and M(P5) correspond to the first plotting, i.e., the MPN, while labels 2-M(P1),2-M(P3) and 2-M(P5) correspond to the second one, i.e., the TCPN. As it can be seen, the continuous marking approximates well the average marking of the MPN, then, it can be concluded that the system of fig. 5.7(a) accepts a reasonable fluidization.

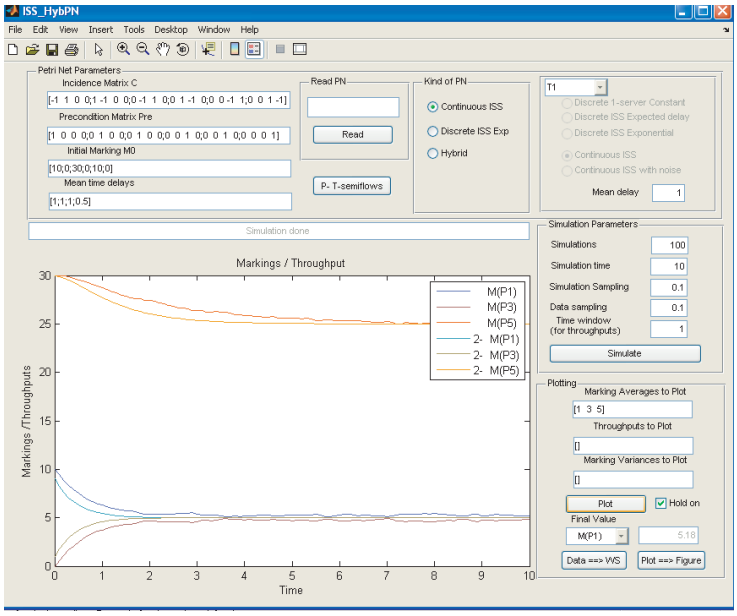

Fig. A.4: Results obtained after simulating the system of fig. 5.7(a) as both MPN and TCPN.

A.2.5 Simulation script

The core of the simulation is the algorithm previously described. Even if the Interface allows certain flexibility, it could be desired to elaborate more complex simulation routines, for instance, for simulating a system with different timings $\boldsymbol{\lambda}$ and after that, plotting the steady state values thus obtained. In such case, the Interface may not be useful enough, and an algorithm that uses the core of the simulator has to be implemented.

For such case, it is only required to use the file *fSimRoutine.m*, which is actually the simulator routine. In order to learn how this file can be called from other m-file, an script is also included in the package: *Script_Simulator.m*. This script shows how to call the *fSimRoutine.m*. It also calls the plotting routine *fPlotRoutine.m*, which could be interesting for understanding the structure of the output of the Simulator.

A.3 HybNet block for Simulink

In the Simulator package, the folder *Simulink_files* contains the file *Simulink_HybPN.mdl*, which is a model file for Simulink. This model may be useful for designing and implementing different functions and systems that interact with a hybrid Petri net. For instance, in order to implement a control law for a TCPN system.

Fig. A.5 shows the model of *Simulink_HybPN.mdl*. The upper part is actually the model. The signals in this part of the system are the instantaneous marking of the PN. Block *Hybrid_PN* is the subsystem shown in the lower dashed square. The simulation model was designed in order to work in discrete time with a fixed time step, then, make sure that the correct settings are defined (at the menu, Simulation/Configuration Parameters, Type: Fixed-step).

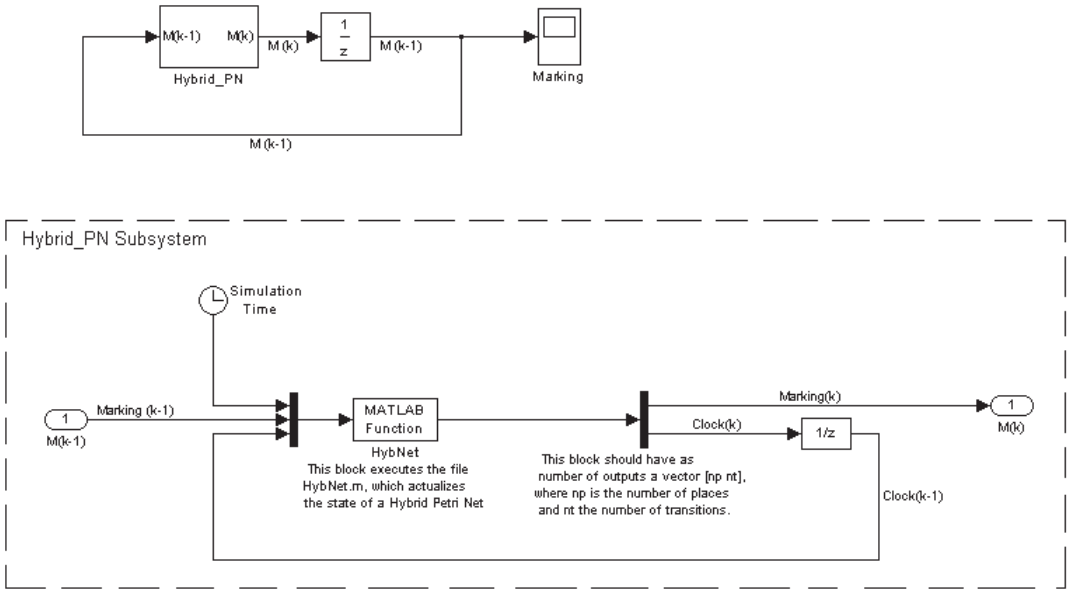

Fig. A.5: Simulink_HybPN model.

In order to load the parameters of the net, it is required to open the m-file *HybNet.m*, which is called by the function-block *HybNet* in the subsystem *Hybrid_PN*. The code of this file is similar to the algorithm described in Section A.1 (for simulating a MHPN), but without the *while* loop. In *HybNet.m*, the data required is the Incidence matrix **C**, the Precondition Matrix **Pre**, the Mean time delays **delaym** (a column vector), the vector **type**, the sampling time dt and the total simulation time $tsim$. These variables are the same required for the Interface (described in the previous section), excepting the vector **type**, which is a column vector that specifies the type of each transition. There are 5 kind of transitions, that were described in the previous section. The corresponding entries in the type vector are:

1. *Discrete 1-server constant*, 'd0'.
2. *Discrete ISS expected delay*, 'd1'.
3. *Discrete ISS Exponential*, 'd2'.
4. *Continuous ISS*, 'c1'.
5. *Continuous ISS with noise*, 'c2'.

For instance, for a MPN system with 3 transitions, the type vector should be type=['d2';'d2';'d2']. The initial condition is defined at the unit delay block of the main system (block $\frac{1}{z}$ at the upper part of fig. A.5).

It is important to make sure that the sampling time be the same than that specified in the Configuration Parameters (at the menu, Simulation/Configuration Parameters, Fixed-step size). Furthermore, it is required to open the Properties window of the Demux Block of the lower subsystem (the bar acting as a demultiplexor in the lower dashed square in fig. A.5), and to set the number of outputs as [np nt], where np is the number of places and nt is the number of inputs.

After modifying the required elements, the model is ready to be simulated.

Appendix B

Complementary results on fluidization

B.1 Error introduced by $\Delta\tau$

In Proposition 1.6, a difference equation that approximates the behavior of the MPN model was introduced. There, the number of firings during a time step $\Delta\tau$ was approximated by a vector of r.v.'s $\Delta\boldsymbol{\sigma}(\mathbf{F}_k\Delta\tau)$ having Poisson pdfs with parameters $\mathbf{F}_k\Delta\tau$. In this section, it is proved that the errors introduced by such approximation can be arbitrarily bounded, by choosing a small enough sampling $\Delta\tau$.

Proposition B.1. *Consider a bounded MPN. For a given transition t_i, denote as $\#\sigma_i$ a r.v. that represents the number of firings of t_i during $[\tau_0, \tau_0 + \Delta\tau)$. Define a r.v. $\Delta\sigma_i$ having a Poisson pdf with parameter $\boldsymbol{\lambda}_i Enab(t_i, \tau_0)\Delta\tau$. Then, the absolute error $|Prob(\#\sigma_i = a) - Prob(\Delta\sigma_i = a)|$, for an arbitrary value $a \in \mathbb{N}$, is upper bounded by a monotonic function of $\Delta\tau$, i.e., the smaller $\Delta\tau$ the lower the upper bound for the error. Furthermore, at the limit $\Delta\tau \to 0$ such error is null.*

Proof. Let us denote with $Enab(t_i, \tau) = Enab(t_i, \tau_0)$ (resp. $Enab(t_i, \tau) \neq Enab(t_i, \tau_0)$), the event: t_i has a constant (resp. has not a constant) enabling degree during $[\tau_0, \tau_0 + \Delta\tau)$. Then, by conditional probabilities:

$$\begin{aligned} &Prob(\#\sigma_i = a) = \\ &\quad Prob(\#\sigma_i = a | Enab(t_i, \tau) = Enab(t_i, \tau_0)) \cdot Prob(Enab(t_i, \tau) = Enab(t_i, \tau_0)) + \\ &\quad Prob(\#\sigma_i = a | Enab(t_i, \tau) \neq Enab(t_i, \tau_0)) \cdot Prob(Enab(t_i, \tau) \neq Enab(t_i, \tau_0)) \end{aligned}$$

Denoting as $\Delta\sigma_i$ a r.v. having a Poisson pdf with parameter $\boldsymbol{\lambda}_i Enab(t_i, \tau_0)\Delta\tau$, then $Prob(\#\sigma_i = a | Enab(t_i, \tau) = Enab(t_i, \tau_0)) = Prob(\Delta\sigma_i = a)$, $\forall a \in \mathbb{N}$, as it was explained in the proof of Proposition 1.6. The error in the probability computation due to assuming the number of active servers of t_i as constant during $\Delta\tau$ is defined, for each probable value a, as $\epsilon_i(a) = Prob(\#\sigma_i = a) - Prob(\Delta\sigma_i = a)$. Then, by using previous equations, it can be obtained:

$$\begin{aligned} |\epsilon_i(a)| &= |Prob(\#\sigma_i = a | Enab(t_i, \tau) \neq Enab(t_i, \tau_0)) - Prob(\Delta\sigma_i = a)| \\ &\qquad \cdot Prob(Enab(t_i, \tau) \neq Enab(t_i, \tau_0)) \\ &\leq Prob(Enab(t_i, \tau) \neq Enab(t_i, \tau_0)) \end{aligned} \tag{B.1}$$

The enabling degree of t_i remains constant during $[\tau_0, \tau_0 + \Delta\tau)$ if none transition fires during such time interval.

Let us analyze a particular transition t_j. Suppose that t_j is enabled at τ_0 and denote as $\tau_0 + \theta(t_j)$ the time instant of the next firing of t_j, starting form τ_0. Then t_j does not fire during $[\tau_0, \tau_0 + \Delta\tau)$ if $\theta(t_j) \geq \Delta\tau$. Since $\theta(t_j)$ is exponentially distributed with parameter $\lambda_j Enab(t_j, \tau_0)$, then $Prob(\theta(t_j) \geq \Delta\tau) = 1 - Prob(\theta(t_j) < \Delta\tau) = e^{-\lambda_j Enab(t_j,\tau_0)\Delta\tau}$. Moreover, the assumption of boundedness implies that $\forall t_j \in T$, $\exists Enab_j$ s.t. $Enab_j \geq Enab(t_j, \tau)$. In this way, denoting as $[\lambda Enab]_{max}$ the maximum value in the set $\{\lambda_j Enab_j | t_j \in T\}$, then $e^{-\lambda_j Enab(t_j,\tau_0)\Delta\tau} \geq e^{-[\lambda Enab]_{max}\Delta\tau}$. Therefore, the probability that t_j does not fire during $[\tau_0, \tau_0 + \Delta\tau)$ is given by $Prob(\theta(t_j) \geq \Delta\tau) \geq e^{-[\lambda Enab]_{max}\Delta\tau}$. This expression holds for any transition t_j.

Now, $Prob(Enab(t_i, \tau) = Enab(t_i, \tau_0))$ is equal or larger than the probability that none transition fires during $[\tau_0, \tau_0 + \Delta\tau)$, given by $\prod_{\forall t_j \in T} Prob(\theta(t_j) \geq \Delta\tau) \geq \prod_{\forall t_j \in T} e^{-[\lambda Enab]_{max}\Delta\tau} = e^{-\alpha\Delta\tau}$, where $\alpha = |T|[\lambda Enab]_{max}$. Then, $Prob(Enab(t_i, \tau) \neq Enab(t_i, \tau_0)) \leq 1 - e^{-\alpha\Delta\tau}$. Finally, according to (B.1):

$$|\epsilon_i(a)| \leq 1 - e^{-\alpha\Delta\tau} \tag{B.2}$$

Previous equality means that the error of using $\Delta\sigma_i$ as an approximation of $\#\sigma_i$ is upper bounded by a monotonic function of $\Delta\tau$. Then, the lower the value of $\Delta\tau$, the lower the error. Furthermore, it is not difficult to see from (B.2) that $lim_{\Delta\tau \to 0} |\epsilon_i(a)| = 0$. Moreover, given a desired bound ϵ^B, a sampling $\Delta\tau \leq ln\left[(1 - \epsilon^B)^{-\alpha}\right]$ guarantees $|\epsilon_i(a)| \leq \epsilon^B$, $\forall a \in \mathbb{N}$. This means that the error bound can be arbitrarily reduced by suitably choosing $\Delta\tau$. In our experience, considering $[\lambda Enab]_{max}$ the maximum value in the set $\{\lambda_j Enab_j | t_j \in T\}$, a sampling obtained by $\Delta\tau = 0.1/(|T|[\lambda Enab]_{max})$ is small enough to provide a good approximation (so, the probability that the enabling degree remains constant during $\Delta\tau$ is larger than $e^{-0.1} = 0.90$). ∎

B.2 Computation of the ultimate bound of the approximation error in Join-Free nets

Let us recall a result related to stability with non-vanishing perturbations [Khalil, 2002] (page 347):
Lemma 9.2 Consider a nonlinear system under perturbations:

$$\dot{\mathbf{x}} = \mathbf{f}(\tau, \mathbf{x}) + \mathbf{g}(\tau, \mathbf{x}) \tag{B.3}$$

where $\dot{\mathbf{x}} = \mathbf{f}(\tau, \mathbf{x})$ *denotes the nominal behavior and* $\mathbf{g}(\tau, \mathbf{x})$ *is the system's perturbation.*
Let $\mathbf{x} = \mathbf{0}$ *be an exponentially stable equilibrium point of the nominal system. Let* $V(\tau, \mathbf{x})$ *be a Lyapunov function of the nominal system that satisfies*

$$c_1\|\mathbf{x}\|^2 \leq V(\tau, \mathbf{x}) \leq c_2\|\mathbf{x}\|^2$$
$$\frac{\delta V}{\delta \tau} + \frac{\delta V}{\delta \mathbf{x}}\mathbf{f}(\tau, \mathbf{x}) \leq -c_3\|\mathbf{x}\|^2$$
$$\|\frac{\delta V}{\delta \mathbf{x}}\| \leq c_4\|\mathbf{x}\|^2$$

in $[0, \inf) \times D$, *where* $D = \{\mathbf{x} \in \mathbb{R}^n | \|\mathbf{x}\| < r\}$ *(here* $||\cdot||$ *denotes the euclidian norm). Suppose the perturbation term* $\mathbf{g}(\tau, \mathbf{x})$ *satisfies* $\|\mathbf{g}(\tau, \mathbf{x})\| \leq \delta < (c_3/c_4)(c_1/c_2)^{1/2}\theta r$, *for all* $\tau \geq 0$, $\mathbf{x} \in D$, *and some positive constant* $\theta < 1$. *Then, for all* $\|\mathbf{x}(\tau_0)\| < (c_1/c_2)^{1/2} r$, *the solution* $\mathbf{x}(\tau)$ *of the perturbed system satisfies*

$$\|\mathbf{x}(\tau)\| \leq s e^{-\gamma(\tau-\tau_0)}\|x(\tau_0)\|, \qquad \forall \tau_0 \leq \tau \leq \tau_0 + \mathcal{T}$$

and $\|\mathbf{x}(\tau)\| \leq \beta$, $\forall \tau \geq \tau_0 + \mathcal{T}$, *for some finite* $\mathcal{T}$, *where*

$$s = \sqrt{\frac{c_2}{c_1}}, \qquad \gamma = \frac{(1-\theta)c_3}{2c_2}, \qquad \beta = \frac{c_4}{c_3}\sqrt{\frac{c_2}{c_1}}\frac{\delta}{\theta}$$

Let us compute then the ultimate bounded for the approximation error in a Join-Free net.

The approximation error is given by (2.5), where the nominal system is (in discrete-time) $\boldsymbol{\varepsilon}_{k+1} = [\mathbf{I} + \mathbf{C\Lambda\Pi}\Delta\tau]\,\boldsymbol{\varepsilon}_k$ and the perturbation is $\mathbf{C\Lambda} \cdot E\{\mathbf{b}_k\}\Delta\tau$.

It is known that in PN's, P-flows induce conservative marking laws, what leads to state invariants and zero-valued poles. Nevertheless, since $\mathbf{M}_0 = \mathbf{m}_0$ then $\mathbf{B}_y^T\boldsymbol{\varepsilon}_k = \mathbf{0}$ (because $\mathbf{B}_y^T\mathbf{M}_k = \mathbf{B}_y^T\mathbf{M}_0 = \mathbf{B}_y^T\mathbf{m}_0 = \mathbf{B}_y^T\mathbf{m}_0$), then the projection of $\boldsymbol{\varepsilon}_k$ in the modes associated to those zero-valued poles is null. This implies that there exists a reduced-order model that describes the dynamic behavior of the approximation error, in which those zero-valued poles are removed (see, for instance, the proof of Proposition 3.22). Such model can be expressed as:

$$\boldsymbol{\varepsilon}'_{k+1} = \mathbf{Z}\left[\mathbf{I} + \mathbf{C\Lambda\Pi}\Delta\tau\right]\mathbf{A}\boldsymbol{\varepsilon}'_k + \mathbf{ZC\Lambda} \cdot E\{\mathbf{b}_k\}\Delta\tau \tag{B.4}$$

where $\boldsymbol{\varepsilon}'_k = \mathbf{Z}\boldsymbol{\varepsilon}_k$ with $\mathbf{Z}$ a matrix s.t. $\left[\mathbf{Z}^T, \mathbf{B}_y^T\right]^T$ has full rank, while $\mathbf{A}$ is a matrix s.t. $\left[\mathbf{Z}^T, \mathbf{B}_y^T\right]^T\mathbf{A} = [\mathbf{I}, \mathbf{0}]^T$. Furthermore, $\boldsymbol{\varepsilon}'_k = \mathbf{0}$ iff $\boldsymbol{\varepsilon}_k = \mathbf{0}$. This model can be represented in continuous time as:

$$\dot{\boldsymbol{\varepsilon}'} = \mathbf{ZC\Lambda\Pi A}\boldsymbol{\varepsilon}' + \mathbf{ZC\Lambda} \cdot E\{\mathbf{b}^c(\tau)\} \tag{B.5}$$

where $\mathbf{b}^c(\tau) = \mathbf{b}_k$ during $k\Delta\tau + \tau_0 \leq \tau < (k+1)\Delta\tau + \tau_0$.

In this way, if the steady state reached in the PN model is unique for any initial marking in $Class(\mathbf{m}_0)$, then $\boldsymbol{\varepsilon}' = \mathbf{0}$ in (B.5) is asymptotically stable. Now, let us apply Lemma 9.2 to this error model.

Assume that $\boldsymbol{\varepsilon}' = \mathbf{0}$ in (B.5) is asymptotically stable. Then, since this model is linear and time invariant there exists a Lyapunov function $V = \boldsymbol{\varepsilon'}^T\mathbf{P}\boldsymbol{\varepsilon}'$, s.t. $\mathbf{P}\left[\mathbf{ZC\Lambda\Pi A}\right] + \left[\mathbf{ZC\Lambda\Pi A}\right]^T\mathbf{P} = -\mathbf{Q}$, where $\mathbf{P}$ and $\mathbf{Q}$ are positive definite matrices. In such case, it can be proved that (see, for instance, example 9.1, page 342 in [Khalil, 2002])

$$\begin{gathered}\lambda_{min}(\mathbf{P})\|\boldsymbol{\varepsilon}'\|^2 \leq V(\boldsymbol{\varepsilon}') \leq \lambda_{max}(\mathbf{P})\|\boldsymbol{\varepsilon}'\|^2 \\ \frac{\delta V}{\delta t} + \frac{\delta V}{\delta \boldsymbol{\varepsilon}'}\mathbf{f}(\boldsymbol{\varepsilon}') \leq -\lambda_{min}(\mathbf{Q})\|\boldsymbol{\varepsilon}'\|^2 \\ \|\frac{\delta V}{\delta \boldsymbol{\varepsilon}'}\| \leq 2\lambda_{max}(\mathbf{P})\|\boldsymbol{\varepsilon}'\|^2\end{gathered}$$

for all $\boldsymbol{\varepsilon}' \in \mathbb{R}^n$, where $\lambda_{max}(\cdot)$ and $\lambda_{min}(\cdot)$ denote the minimum and maximum eigenvalues of the corresponding matrix. Furthermore, the perturbation fulfills $\|\mathbf{ZC\Lambda} \cdot E\{\mathbf{b}^c(\tau)\}\| \leq \|\mathbf{ZC\Lambda}\|\|E\{\mathbf{b}^c(\tau)\}\| \leq \|\mathbf{ZC\Lambda}\|\sqrt{|T|}$ (where $|T|$ is the number of transitions), which is a constant value (given a vector $\mathbf{1}$ of length

$|T|$ whose elements are 1's, then $||T|| = \sqrt{|T|}$, furthermore, since $E\{\mathbf{b}^c(\tau)\} \leq \mathbf{1}$ then $||E\{\mathbf{b}^c(\tau)\}|| \leq \sqrt{|T|}$). Therefore, all the conditions of Lemma 9.2 are fulfilled, with constants

$$c_1 = \lambda_{min}(\mathbf{P}), \quad c_2 = \lambda_{max}(\mathbf{P}), \quad c_3 = \lambda_{min}(\mathbf{Q})$$
$$c_4 = 2\lambda_{max}(\mathbf{P}), \quad \delta = \|\mathbf{ZC\Lambda}\|\sqrt{|T|}$$

Furthermore, defining r large enough, θ can be settled as any value in $(0, 1)$. Then, according to this lemma, the ultimate bound for the transformed error $\boldsymbol{\varepsilon}'(\tau)$ can be computed as: $\beta = \frac{2\lambda_{max}(\mathbf{P})}{\lambda_{min}(\mathbf{Q})}\sqrt{\frac{\lambda_{max}(\mathbf{P})}{\lambda_{min}(\mathbf{P})}} \cdot \frac{\|\mathbf{ZC\Lambda}\|\sqrt{|T|}}{\theta}$, with $\theta \in (0, 1)$ (a value close to 1 leads a smaller bound). Finally, it can be shown that $\mathbf{A}\boldsymbol{\varepsilon}'_k = \boldsymbol{\varepsilon}_k$, which implies $\|\mathbf{A}\|\|\boldsymbol{\varepsilon}'_k\| \geq \|\mathbf{A}\boldsymbol{\varepsilon}'_k\| = \|\boldsymbol{\varepsilon}_k\|$. Combining this equation with the value for β obtained before, it can be concluded that there exists some time instant $\mathcal{T} = \tau_0 + \eta\Delta\tau$ s.t.

$$\|\boldsymbol{\varepsilon}_k\| \leq \|\mathbf{A}\|\frac{2\lambda_{max}(\mathbf{P})}{\lambda_{min}(\mathbf{Q})}\sqrt{\frac{\lambda_{max}(\mathbf{P})}{\lambda_{min}(\mathbf{P})}}\frac{\|\mathbf{ZC\Lambda}\|\sqrt{|T|}}{\theta}$$

for all $k \geq \eta$. Note that the bound for $\|\boldsymbol{\varepsilon}_k\|$ depends on the timed net $\langle \mathbf{C}, \boldsymbol{\lambda} \rangle$, but not in the initial marking $\mathbf{M}_0 = \boldsymbol{\mu}_0$.

B.3 Lemmas for the approximation analysis

Lemma B.2. *Consider a live and ergodic MPN system with an initial deterministic marking* $\mathbf{M}_0 = q \cdot \mathbf{M}_0^r$. *Consider the evolution of the system with a sampling* $\Delta\tau = \Delta\tau^r/q$ *during a fix number of time steps* n. *Assume that, for the most probable evolutions of the system, all the transitions are enabled. Then, the larger the parameter* q, *the closer is* $\sum_{k=0}^{n-1} \Delta\boldsymbol{\sigma}(\mathbf{F}_k\Delta\tau)$ *to* $Poisson(n \cdot \mathbf{F}_0^r\Delta^r\tau)$, *where* $\mathbf{F}_0^r\Delta^r\tau = \Lambda\Pi(\mathbf{M}_0^r)\mathbf{M}_0^r\Delta^r\tau$.

Proof. This lemma is a particular case of Lemma B.4, defined for hybrid Petri nets. In this way, that lemma proves this one, just considering $T = T^d$, i.e., ignoring the parts concerning variables $\mathbf{m}_k$, $\mathbf{f}_k$ and $\Delta\mathbf{w}_k$.

Lemma B.3. *Consider a TnCPN system with an initial deterministic marking* $\mathbf{m}_0 = q \cdot \mathbf{m}^r$. *Assume that there are not non-live equilibrium markings in* $Class(\mathbf{m}_0)$. *Consider the evolution of the system in discrete time with a sampling* $\Delta\tau = \Delta\tau^r/q$ *during a fix number of time steps* n. *Assume that, for the most probable evolutions of the system, all the transitions are enabled. Then, the larger the parameter* q, *the closer is* $\sum_{i=0}^{n-1} \Delta\mathbf{w}_{k+i}$ *to* $Normal(n \cdot \mathbf{f}_0\Delta\tau, n \cdot \mathbf{f}_0\Delta\tau)$.

Proof. This lemma is a particular case of Lemma B.4, defined for hybrid Petri nets. Then, for this proof consider that of B.4 with $T = T^c$, ignoring the parts concerning variables $\mathbf{M}_k$, $\mathbf{F}_k$ and $\Delta\boldsymbol{\sigma}(\cdot)_k$.

Lemma B.4. *Consider a live and ergodic MnHPN system with an initial deterministic marking* $\mathbf{M}_0^h = q \cdot \mathbf{M}_0^{h,r}$. *Consider the evolution of the system with a sampling* $\Delta\tau = \Delta\tau^r/q$ *during a fix number of time steps* n. *Assume that, for the most probable evolutions of the system, all the transitions are enabled. Then, the larger the parameter* q, *the closer is* $\sum_{k=0}^{n-1} \Delta\boldsymbol{\sigma}(\mathbf{F}_k^d\Delta\tau)$ *and* $\sum_{k=0}^{n-1} \Delta\mathbf{w}_k$ *to* $Poisson(n\,\mathbf{F}_0^{d,r}\Delta^r\tau)$ *and* $Normal(n\,\mathbf{f}_0\Delta\tau)$, *respectively, where* $\mathbf{F}_0^{d,r}\Delta^r\tau = \boldsymbol{\Lambda}^d\boldsymbol{\Pi}^d(\mathbf{M}_0^r)\mathbf{M}_0^r\Delta^r\tau$.

Proof. This proof is split in two different parts. In the first one, it will be demonstrated, by following an inductive reasoning, that for any time step $k \in \{1, 2, .., n\}$ it holds:

a) $\mathbf{F}_k^d \Delta\tau$ and $\mathbf{f}_k \Delta\tau$ monotonically converge to constant values $\mathbf{F}_0^r \Delta^r\tau$ and $\mathbf{f}_0 \Delta\tau$, respectively, when $q \to \infty$ (intuitively, $\mathbf{F}_k^d$ and $\mathbf{f}_k$ increase when $q \to \infty$, but $\Delta\tau$ decreases in a similar proportion).

b) $|\mathbf{M}_{k+1}^h - \mathbf{M}_k^h|/q$ is upper bounded by a monotonically decreasing function that converges to $\mathbf{0}$ when $q \to \infty$.

According to this, for a large enough q, it is reasonable to assume $\mathbf{F}_k^d \Delta\tau \simeq \mathbf{F}_0^{d,r} \Delta^r\tau$ and $\mathbf{f}_k \Delta\tau \simeq \mathbf{f}_0 \Delta\tau$, $\forall k \in \{1, 2, ..., n\}$.
In the second part, by using the previous result and the fact that $\mathbf{F}_0^{d,r} \Delta^r\tau$ and $\mathbf{f}_0 \Delta\tau$ are constant, it will be proved that $\sum_{k=0}^{n-1} \Delta\boldsymbol{\sigma}(\mathbf{F}_k^d \Delta\tau) \sim Poisson\{n \cdot \mathbf{F}_0^{d,r} \Delta^r\tau\}$ and $\sum_{k=0}^{n-1} \Delta\mathbf{w}_k \sim Normal\{n \cdot \mathbf{f}_0 \Delta\tau\}$.

Before starting the proof, let us introduce the vector function $\Delta\boldsymbol{\sigma}^{max}(\mathbf{v})$: $\mathbb{R}_{\geq 0}^{|T|} \to \mathbb{N}^{|T|}$; which is defined by elements as: $\Delta\sigma_j^{max}(\mathbf{v}) = min(a)$ s.t. $e^{-v_j} \sum_{i=0}^{a} v_j^i/i! \geq 0.99$. In this way, $\Delta\boldsymbol{\sigma}^{max}(\mathbf{v}) \geq Poisson(\mathbf{v})$ with a probability larger than 0.99. It can be demonstrated (by checking that the partial derivative of $e^{-v_j} \sum_{i=0}^{a} v_j^i/i!$ is negative) that $\Delta\boldsymbol{\sigma}^{max}(\mathbf{v})$ is a monotonically increasing function. Similarly, the following function is defined $\Delta\mathbf{w}^{max}(\mathbf{v}) = \mathbf{v} + 3\sqrt{\Delta\tau\mathbf{v}}$ in such a way that $\Delta\mathbf{w}^{max}(\mathbf{v}) \geq Normal(\mathbf{v})$ (where the square root operator is interpreted as componentwise) with a probability larger that 0.997.

Part 1. Let us start with the inductive part of the proof:
I) For the initial time step. Substituting $\Delta\tau = \Delta^r\tau/q$ and $\mathbf{M}_0^h = q \cdot \mathbf{M}_0^{h,r}$ in $\mathbf{F}_0^d \Delta\tau = \boldsymbol{\Lambda}^d \lfloor \boldsymbol{\Pi}^d(\mathbf{M}_0^h) \mathbf{M}_0^h \rfloor \Delta\tau$, it is obtained $\mathbf{F}_0^d(q)\Delta\tau = \boldsymbol{\Lambda}^d \boldsymbol{\Pi}^d(\mathbf{M}_0^{h,r}) \mathbf{M}_0^{h,r} \Delta^r\tau + \boldsymbol{\Lambda}^d \boldsymbol{\Pi}^d(\mathbf{M}_0^{h,r}) \Delta^r\tau \mathbf{b}_0/q$. Note that $\mathbf{F}^d(\cdot)$ has been denoted as a function of q, in order to make explicit the influence of this variable. According to this, $\mathbf{F}_0^d(q)\Delta\tau$ monotonically converges to the constant value $\mathbf{F}_0^{d,r} \Delta^r\tau = \boldsymbol{\Lambda}^d \boldsymbol{\Pi}^d(\mathbf{M}_0^{h,r}) \mathbf{M}_0^{h,r} \Delta^r\tau$ when $q \to \infty$. Thus, statement (a) is proved for $k = 0$. Now, by definition $\Delta\boldsymbol{\sigma}^{max}(\mathbf{F}_0^d(q)\Delta\tau) \geq \Delta\boldsymbol{\sigma}(\mathbf{F}_0^d \Delta\tau)$ with probability "almost 1" .
Similarly, $\Delta\mathbf{w}^{max}(\mathbf{f}_0) \geq \Delta\mathbf{w}_0$ with probability almost 1. Then, defining $\delta_o^1 = \mathbf{M}_1^h - \mathbf{M}_0^h$, from (2.26) it is obtained $|\delta_0^1| \leq |\mathbf{C}|[(\Delta\boldsymbol{\sigma}^{max}(\Delta\mathbf{F}_0^d(q)))^T, (\Delta\mathbf{w}^{max}(\mathbf{f}_0))^T]^T$. Moreover, since $\mathbf{F}_0^d(q)\Delta\tau$ monotonically converges to the constant value $\mathbf{F}_0^{d,r} \Delta^r\tau$ then $\Delta\boldsymbol{\sigma}^{max}(\mathbf{F}_0^d(q)\Delta\tau)$ monotonically converges to a constant value $\Delta\boldsymbol{\sigma}^{max}(\mathbf{F}_0^{d,r} \Delta^r\tau)$. On the other hand, $\Delta\mathbf{w}^{max}(\mathbf{f}_0)$ is already constant. Thus, the upper bound for $|\mathbf{M}_1^h - \mathbf{M}_0^h|/q$ monotonically converges to $\mathbf{0}$ when $q \to \infty$, i.e., statement (b).

II) For the time step k, assume that the function $\mathbf{F}_k^d(q)\Delta\tau$ is upper (resp. lower) bounded by a monotonically decreasing (resp. increasing) function of q, denoted as $\Delta\mathbf{F}_k^{max}(q)$ (resp. $\Delta\mathbf{F}_k^{min}(q)$) that converges to $\mathbf{F}_0^{d,r} \Delta^r\tau$.
Similarly, assume that $\mathbf{f}_k(q)\Delta\tau$ is upper (resp. lower) bounded by a monotonically decreasing (resp. increasing) function of q, denoted as $\Delta\mathbf{f}_k^{max}(q)$ (resp. $\Delta\mathbf{f}_k^{min}(q)$) that converges to $\mathbf{f}_0 \Delta\tau$, i.e., statement (a).
Assume that $|\delta_k^{k+1}|/q = |\mathbf{M}_{k+1}^h - \mathbf{M}_k^h|/q$ is upper bounded by
$|\mathbf{C}|[(\Delta\boldsymbol{\sigma}^{max}(\Delta\mathbf{F}_k^{max}(q)))^T, (\Delta\mathbf{w}^{max}(\Delta\mathbf{f}_k^{max}))^T]^T/q$ that monotonically converges to $\mathbf{0}$, i.e., statement (b).

III) Proving properties for the time step $k+1$. By definition of $\mathbf{F}^d(\cdot)$ and using the property $\forall \mathbf{\Pi}^d_j$, $\mathbf{\Pi}^d(\mathbf{M}^h_k)\mathbf{M}^h_k \leq \mathbf{\Pi}^d_j\mathbf{M}^h_k$, it can be obtained: $[\mathbf{F}^d_{k+1}\Delta\tau - \mathbf{F}^d_k\Delta\tau] \leq \mathbf{\Lambda}^d\mathbf{\Pi}^d(\mathbf{M}^h_k)[\mathbf{M}^h_{k+1} - \mathbf{M}^h_k]\Delta\tau +$ $\mathbf{\Lambda}^d\mathbf{\Pi}^d(\mathbf{M}^h_k)\Delta\tau\mathbf{1}$ (where $\mathbf{1}$ denotes a vector whose elements are 1's). Similarly, $\mathbf{\Lambda}^d\mathbf{\Pi}^d(\mathbf{M}^h_{k+1})[\mathbf{M}^h_{k+1} - \mathbf{M}^h_k]\Delta\tau - \mathbf{\Lambda}^d\mathbf{\Pi}^d(\mathbf{M}^h_{k+1})\Delta\tau\mathbf{1} \leq [\mathbf{F}^d_{k+1}\Delta\tau - \mathbf{F}^d_k\Delta\tau]$. By using previous expressions, it can be proved that $\Delta\mathbf{F}^{max}_{k+1}(q) = \Delta\mathbf{F}^{max}_k(q) + [\mathbf{\Lambda}^d\mathbf{\Pi}^d(\mathbf{M}^h_k)\delta^{k+1}_k\Delta^r\tau + \mathbf{\Lambda}^d\mathbf{\Pi}^d(\mathbf{M}^h_k)\Delta^r\tau\mathbf{1}]/q$ is an upper bound for $\mathbf{F}^d_{k+1}(q)\Delta\tau$. By the induction hypothesis related to $\Delta\mathbf{F}^{max}_k(q)$ and δ^{k+1}_k, it can be proved that $\Delta\mathbf{F}^{max}_{k+1}(q)$ is a monotonically decreasing function of q that converges to $\Delta\mathbf{F}^{max}_k(q)$, which by hypothesis converges to $\mathbf{F}^{d,r}_0\Delta^r\tau$. In a similar way, it can be proved that $\Delta^{min}\mathbf{F}^d_{k+1}(q) = \Delta\mathbf{F}^{min}_k(q) - [\mathbf{\Lambda}^d\mathbf{\Pi}^d(\mathbf{M}^h_{k+1})\delta^{k+1}_k\Delta^r\tau + \mathbf{\Lambda}^d\mathbf{\Pi}^d(\mathbf{M}^h_{k+1})\Delta^r\tau\mathbf{1}]/q$ is a lower bound for $\mathbf{F}^d_{k+1}(q)\Delta\tau$, and this is a monotonically increasing function of q that converges to $\mathbf{F}^{d,r}_0\Delta^r\tau$.
A similar reasoning holds for the continuous transitions, proving that $\Delta\mathbf{f}^{max}_{k+1}(q) = \Delta\mathbf{f}^{max}_k(q) +$ $[\mathbf{\Lambda}^c\mathbf{\Pi}^c(\mathbf{m}_k)\delta^{k+1}_k\Delta^r\tau]/q$ is an upper bound for $\Delta\mathbf{f}_{k+1}$, and that $\Delta\mathbf{f}^{max}_{k+1}(q)$ is a monotonically decreasing function of q that converges to $\Delta\tau\mathbf{f}_0$. Thus, statement (a) is proved.
Next, since $\Delta\boldsymbol{\sigma}^{max}(\cdot)$ is a monotonically increasing function, then $\Delta\boldsymbol{\sigma}^{max}(\Delta\mathbf{F}^{max}_{k+1}(q))$ is a monotonically decreasing function of q that converges to $\Delta\boldsymbol{\sigma}^{max}(\mathbf{F}^{d,r}_0\Delta^r\tau)$. Furthermore, by definition $\Delta\boldsymbol{\sigma}(\mathbf{F}^d_{k+1}(q)\Delta\tau)$ $\leq \Delta\boldsymbol{\sigma}^{max}(\mathbf{F}^d_{k+1}(q)\Delta\tau)$ with probability "almost 1" .
Similarly, for the continuous transitions, $|\Delta\mathbf{w}_k| \leq \Delta\mathbf{w}^{max}(\Delta\mathbf{f}^{max}_{k+1}(q))$, where $\Delta\mathbf{w}^{max}(\Delta\mathbf{f}^{max}_{k+1}(q))$ is a monotonically decreasing function of q that converges to $\Delta\mathbf{w}^{max}(\Delta\tau\mathbf{f}_0) = \Delta\mathbf{w}^{max}_0$.
Then, by using (2.26), the difference $\delta^{k+2}_{k+1} = \mathbf{M}^h_{k+2} - \mathbf{M}^h_{k+1}$ fulfills

$$|\delta^{k+2}_{k+1}| \leq |\mathbf{C}|[(\Delta\boldsymbol{\sigma}^{max}(\Delta F^{max}_{k+1}(q)))^T, (\Delta\mathbf{w}^{max}(\Delta\mathbf{f}^{max}_{k+1}(q)))^T]^T$$

Moreover, vectors $\Delta\boldsymbol{\sigma}^{max}(\Delta\mathbf{F}^{max}_{k+1}(q))$ and $\Delta\mathbf{w}^{max}(\Delta\mathbf{f}^{max}_{k+1}(q))$ monotonically converges to the constant values $\Delta\boldsymbol{\sigma}^{max}(\mathbf{F}^{d,r}_0\Delta^r\tau)$ and $\Delta\mathbf{w}^{max}_0$, respectively. Therefore, the upper bound for $|\mathbf{M}^h_{k+2} - \mathbf{M}^h_{k+1}|/q = |\delta^{k+2}_{k+1}|/q$ monotonically converges to $\mathbf{0}$ when $q \to \infty$, thus statement (b) is proved.

According to this inductive reasoning, the difference between $\mathbf{F}^d_k\Delta\tau$ and $\mathbf{F}^{d,r}_0\Delta^r\tau$ and between $\mathbf{f}_k\Delta\tau$ and $\mathbf{f}_0\Delta\tau$, for each time step $k \in \{1, 2, ..., n\}$, is lower and upper bounded by functions that monotonically converge to $\mathbf{0}$ when $q \to \infty$. Roughly speaking, there always exists a large enough q s.t. it is reasonable to assume $\mathbf{F}^d_k\Delta\tau \simeq \mathbf{F}^{d,r}_0\Delta^r\tau$ and $\mathbf{f}_k\Delta\tau \simeq \mathbf{f}_0\Delta\tau$, $\forall k \in \{1, 2, ..., n\}$.

Part 2. Consider a particular discrete transition $t_j \in T^d$. In terms of conditional probabilities, the probability that $\Delta\sigma_j(F^d_{k,j}\Delta\tau) = a$, for a fix natural number a, can be expressed as:

$$\begin{aligned} Prob\{\Delta\sigma_j(F^d_{k,j}\Delta\tau) = a\} = Prob\{\Delta\sigma_j(F^{d,r}_{0,j}\Delta^r\tau) = a\} + \\ \textstyle\sum_{b\in\mathbb{S}}\Big[Prob\{\Delta\sigma_j(b) = a\} - Prob\{\Delta\sigma_j(F^{d,r}_{0,j}\Delta^r\tau) = a\}\Big] \cdot Prob\{F^d_{k,j}\Delta\tau = b\} \end{aligned} \tag{B.6}$$

where $\mathbb{S}$ denotes the set of possible values for $F^d_{k,j}\Delta\tau$ different than $F^{d,r}_{0,j}\Delta^r\tau$. According to the inductive reasoning previously introduced, with probability "almost 1" , $F^d_{k,j}\Delta\tau - F^{d,r}_{0,j}\Delta^r\tau$ is upper and lower bounded by monotonic functions that converge to 0 when $q \to \infty$. This means that for the most probable values b that $F^d_{k,j}\Delta\tau$ can take, the difference $b - F^{d,r}_{0,j}\Delta^r\tau$ is lower and upper bounded by monotonic

functions of q that converges to 0. Then, by using the fact that $Prob\{\Delta\sigma_j(b) = a\} = b^a e^{-b}/a!$ is a continuous function of b, it follows that the difference $Prob\{\Delta\sigma_j(b) = a\} - Prob\{\Delta\sigma_j(F_{0,j}^{d,r}\Delta^r\tau) = a\}$ can be lower and upper bounded by functions of q that converges to 0 when $q \to \infty$. Therefore, according to (B.6) and generalizing to all the discrete transitions, it can be concluded that $\Delta\boldsymbol{\sigma}(\mathbf{F}_k^d\Delta\tau)$ converges to $\Delta\boldsymbol{\sigma}(\mathbf{F}_0^{d,r}\Delta^r\tau) \sim Poisson(\mathbf{F}_0^{d,r}\Delta^r\tau)$ when $q \to \infty$.
A similar reasoning holds for the continuous transitions. Proving that, for each continuous transition $t_j \in T^c$, $Prob\{\Delta w_{k,j} \leq a\}$ converges to $Prob\{\Delta w_{0,j} \leq a\}$ when $q \to 0$. Generalizing this to all the continuous transitions, it can be concluded that the larger q, the closer is the distribution of $\Delta\mathbf{w}_k$ to that of $\Delta\mathbf{w}_0 \sim Normal(\Delta\mathbf{w}_0)$.

Finally, since $\Delta\boldsymbol{\sigma}(\mathbf{F}_k^d\Delta\tau) \sim \Delta\boldsymbol{\sigma}(\mathbf{F}_{k+1}^d\Delta\tau) \sim Poisson(\mathbf{F}_0^{d,r}\Delta^r\tau)$ for large values of q, and $\mathbf{F}_0^{d,r}\Delta^r\tau$ is a constant value, then $\Delta\boldsymbol{\sigma}(\mathbf{F}_k^d\Delta\tau)$ is stochastically independent of $\Delta\boldsymbol{\sigma}(\mathbf{F}_{k+1}^d\Delta\tau)$. Therefore, since the previous reasoning is valid for any time step $k \in \{0, 1, ..., n\}$, and the sum of independent Poisson distributed r.v.'s is also a Poisson distributed r.v. whose parameter is the sum of the parameters of the summands, then $\sum_{k=0}^{n-1}\Delta\boldsymbol{\sigma}(\mathbf{F}_k^d\Delta\tau) \sim Poisson\{n \cdot \mathbf{F}_0^{d,r}\Delta^r\tau\}$. Similarly for the continuous transitions, $\Delta\mathbf{w}_k$ is stochastically independent of $\Delta\mathbf{w}_{k+1}$. Since the sum of independent normally distributed r.v.'s is also a normally distributed r.v. whose parameter (mean and variance) is the sum of the parameters of the summands, then $\sum_{k=0}^{n-1}\Delta\mathbf{w}_k \sim Normal\{n\mathbf{f}_0\Delta\tau, n\mathbf{f}_0\Delta\tau\}$. ∎

Appendix C

Complementary results on controllability and control

C.1 Algorithms for controllability analysis

Algorithm 4.1. Computation of a generator $\mathbf{G}_i$.

For each $t_j \in T_c = \{t_{c_1}, ..., t_{c_{|T_c|}}\}$ do

Compute a solution $\mathbf{d}_j$ for:

$$\begin{bmatrix} \mathbf{C\Lambda\Pi}_i \\ \mathbf{B}_y^T \end{bmatrix} \mathbf{d}_j = \begin{bmatrix} [\mathbf{C}]^j \\ \mathbf{0} \end{bmatrix}$$

If there exists such a solution $\mathbf{d}_j$ **then** add it as a column of $\mathbf{G}_i$

end for

Compute a basis $\mathbf{D}$ for the right annuler of

$$\begin{bmatrix} \mathbf{C\Lambda\Pi}_i \\ \mathbf{B}_y^T \end{bmatrix} \mathbf{D} = \mathbf{0}$$

If $\mathbf{D} \neq \mathbf{0}$ then add the columns of $\mathbf{D}$ to $\mathbf{G}_i$ (i.e., $\mathbf{G}_i$ has the form $[\mathbf{d}_{c_1}, ..., \mathbf{d}_{c_{|T_c|}}, \mathbf{D}]$).
If $\mathbf{G}_i$ does not have full column rank **then** remove linearly dependent columns until obtaining a full column rank matrix.

Proof. Consider two equilibrium markings $(\mathbf{m}_1, \mathbf{u}_1)$ and $(\mathbf{m}_2, \mathbf{u}_2)$ that belong to E_i. Then, by definition, $\mathbf{C\Lambda\Pi}_i\mathbf{m}_1 - \mathbf{Cu}_1 = \mathbf{0}$ and $\mathbf{C\Lambda\Pi}_i\mathbf{m}_2 - \mathbf{Cu}_2 = \mathbf{0}$. Combining these two equations with $\mathbf{B}_y^T\mathbf{m}_1 = \mathbf{B}_y^T\mathbf{m}_2$ it is obtained:

$$\begin{bmatrix} \mathbf{C\Lambda\Pi}_i \\ \mathbf{B}_y^T \end{bmatrix} (\mathbf{m}_1 - \mathbf{m}_2) = \begin{bmatrix} \mathbf{C} \\ \mathbf{0} \end{bmatrix} (\mathbf{u}_1 - \mathbf{u}_2) \tag{C.1}$$

Without loss of generality assume that the first k columns of $\mathbf{C}$ are related to the controllable

transitions. In this way, $\exists \boldsymbol{\alpha}$ s.t. $\mathbf{C}(\mathbf{u}_1 - \mathbf{u}_2) = \mathbf{C}[\mathbf{e}_1, ..., \mathbf{e}_k]\boldsymbol{\alpha}$ where $\mathbf{e}_j$ is the j-th column of the unity matrix of dimension $|T|$. Furthermore, assume that these k columns are linearly independent (otherwise it is always possible to remove the linearly dependent columns, i.e., $\forall \boldsymbol{\alpha}$, $\exists \boldsymbol{\alpha'}$ s.t. $\mathbf{C}[\mathbf{e}_1, ..., \mathbf{e}_k]\boldsymbol{\alpha} = \mathbf{C}[\mathbf{e}'_1, ..., \mathbf{e}'_r]\boldsymbol{\alpha}'$, where $\mathbf{C}[\mathbf{e}'_1, ..., \mathbf{e}'_r]$ are the r linearly independent columns of $\mathbf{C}[\mathbf{e}_1, ..., \mathbf{e}_k]$). Let us prove by contradiction that, given $\mathbf{C}(\mathbf{u}_1 - \mathbf{u}_2) = \mathbf{C}[\mathbf{e}_1, ..., \mathbf{e}_k]\boldsymbol{\alpha}$ then $\forall j$ s.t. $\alpha_j \neq 0$ $\exists \mathbf{d}_j \neq \mathbf{0}$ that fulfills (4.1). In this way, suppose that $\exists j$ s.t. $\alpha_j \neq 0$ and $[[\mathbf{C}]^{j\,T}, \mathbf{0}^T]^T \notin span\left\{\left[(\mathbf{C}\boldsymbol{\Lambda}\boldsymbol{\Pi}_i)^T, \mathbf{B}_y\right]^T\right\}$. Then, since the columns of $\mathbf{C}[\mathbf{e}_1, ..., \mathbf{e}_k]$ are linearly independent, for any $(\mathbf{m}_1 - \mathbf{m}_2)$ and $\{\alpha_1, .., \alpha_k\}$ it fulfills

$$\begin{bmatrix} \mathbf{C}\boldsymbol{\Lambda}\boldsymbol{\Pi}_i \\ \mathbf{B}_y^T \end{bmatrix}(\mathbf{m}_1 - \mathbf{m}_2) - \begin{bmatrix} [\mathbf{C}]^1 & ... & [\mathbf{C}]^{j-1} & [\mathbf{C}]^{j+1} & ... & [\mathbf{C}]^k \\ \mathbf{0} & ... & \mathbf{0} & \mathbf{0} & ... & \mathbf{0} \end{bmatrix} \begin{bmatrix} \alpha_1 \\ \vdots \\ \alpha_{j-1} \\ \alpha_{j+1} \\ \vdots \\ \alpha_k \end{bmatrix} \neq \begin{bmatrix} \mathbf{C}_j \\ \mathbf{0} \end{bmatrix} \alpha_j$$

which is equivalent to $\left[(\mathbf{C}\boldsymbol{\Lambda}\boldsymbol{\Pi}_i)^T, \mathbf{B}_y\right]^T(\mathbf{m}_1 - \mathbf{m}_2) \neq \left[\mathbf{C}^T, \mathbf{0}^T\right]^T(\mathbf{u}_1 - \mathbf{u}_2)$, but this is a contradiction. Therefore, given $\mathbf{C}(\mathbf{u}_1 - \mathbf{u}_2) = \mathbf{C}[\mathbf{e}_1, ..., \mathbf{e}_k]\boldsymbol{\alpha}$ then $\forall j$ s.t. $\alpha_j \neq 0$ $\exists \mathbf{d}_j \neq \mathbf{0}$ that fulfills (4.1). In this way,

$$\begin{bmatrix} \mathbf{C} \\ \mathbf{0} \end{bmatrix}(\mathbf{u}_1 - \mathbf{u}_2) = \begin{bmatrix} \mathbf{C} \\ \mathbf{0} \end{bmatrix} \begin{bmatrix} \mathbf{e}_1 & ... & \mathbf{e}_k \end{bmatrix} \boldsymbol{\alpha} = \begin{bmatrix} \mathbf{C}\boldsymbol{\Lambda}\boldsymbol{\Pi}_i \\ \mathbf{B}_y^T \end{bmatrix} \begin{bmatrix} \mathbf{d}_1 & ... & \mathbf{d}_k \end{bmatrix} \boldsymbol{\alpha} \tag{C.2}$$

Now, it is very classical the fact that $\forall \mathbf{x}$ s.t. $\mathbf{A}\mathbf{x} = \mathbf{b}$, it exists γ s.t. $\mathbf{x} = \mathbf{x}_p + \mathbf{K}_A \cdot \gamma$, where $\mathbf{x}_p$ is a particular solution and $\mathbf{K}_A$ is a basis for the kernel of $\mathbf{A}$. Using this idea, $(\mathbf{m}_1 - \mathbf{m}_2)$ in (C.1) and $\begin{bmatrix} \mathbf{d}_1 & ... & \mathbf{d}_k \end{bmatrix} \boldsymbol{\alpha}$ in (C.2) are particular solutions of the same algebraic problem, while $\mathbf{D}$ is a basis for the kernel of $\left[(\mathbf{C}\boldsymbol{\Lambda}\boldsymbol{\Pi}_i)^T, \mathbf{B}_y\right]^T$. Then, $\exists \boldsymbol{\gamma}$ s.t. $(\mathbf{m}_1 - \mathbf{m}_2) = \begin{bmatrix} \mathbf{d}_1 & ... & \mathbf{d}_k \end{bmatrix} \boldsymbol{\alpha} + \mathbf{D}\boldsymbol{\gamma}$. Therefore, $(\mathbf{m}_1 - \mathbf{m}_2)$ is in the span of $\mathbf{G}_i = \begin{bmatrix} \mathbf{d}_1 & ... & \mathbf{d}_k & \mathbf{D} \end{bmatrix}$. Finally, $\mathbf{G}_i$ is minimal because of the fourth step of the algorithm. Therefore, $\mathbf{G}_i$ thus computed is a generator. ∎

Algorithm C.1. Computation of T_{cf}^i providing that $int\{\Re_i\} \cap E_i^+ \neq \emptyset$.

Compute a suitable equilibrium marking $\mathbf{m}^q \in int\{\Re_i\} \cap E_i^+$ and its equilibrium input $\mathbf{u}^q$, by solving the following LPP:

max	ε subject to	
	$\mathbf{m}^q \geq \mathbf{0}$, $\mathbf{u}^q \geq \mathbf{0}$, $\varepsilon \geq 0$	
	$\mathbf{B}_y^T(\mathbf{m}^q - \mathbf{m}_0) = \mathbf{0}$	$\{\mathbf{m}^q \in Class(\mathbf{m}_0)\}$
	$\mathbf{C}\boldsymbol{\Lambda}\boldsymbol{\Pi}_i\mathbf{m}^q = \mathbf{C}\mathbf{u}^q$	$\{Equilibrium\ marking\}$
	$u_j^q = 0 \quad \forall t_j \in T_{nc}$	$\{Uncontrollable\ transitions\}$
	$\boldsymbol{\Lambda}\boldsymbol{\Pi}_i\mathbf{m}^q - \mathbf{u}^q \geq \varepsilon \cdot \mathbf{1}$	$\{Nonnegative\ flow\}$
	$[\boldsymbol{\Pi}_j - \boldsymbol{\Pi}_i]\mathbf{m}^q \geq \mathbf{0}$ and	$\{\mathbf{m}^q \in \Re_i\}$
	$[1, ..., 1][\boldsymbol{\Pi}_j - \boldsymbol{\Pi}_i]\mathbf{m}^q \geq \varepsilon$, $\forall \boldsymbol{\Pi}_j \neq \boldsymbol{\Pi}_i$	$\{Interior\ of\ \Re_i\}$

---

if $\varepsilon \leq 0$ **then** $int\{\Re_i\} \cap E_i^+ = \emptyset$ and the algorithm **ends**
else
  initialize $T_{cf}^i = \emptyset$
  for each $t_j \in T_c$
    if $u_j^q > 0$ **then** include t_j in T_{cf}^i
    else
      if there exists solution $\mathbf{d}_j$ in (4.1) **then** include t_j in T_{cf}^i, **end if**
    end if
  end for
  set $T_{cp}^i = T - T_{cf}^i$
end if

Proof. First, let us show that the first LPP computes an equilibrium marking in $int\{\Re\} \cap E_i^+$. In this way, $\mathbf{m}^q \geq \mathbf{0}$ and $\mathbf{B}_y^T(\mathbf{m}^q - \mathbf{m}_0) = \mathbf{0}$ are fulfilled iff $\mathbf{m}^q \in Class(\mathbf{m}_0)$. Moreover, $\mathbf{m}^q \in \Re_i$ is equivalent to $\forall j\ (\mathbf{\Pi}_j - \mathbf{\Pi}_i)\mathbf{m}^q \geq \mathbf{0}$. Furthermore, $\mathbf{m}^q$ is an equilibrium marking iff $\mathbf{C\Lambda\Pi}_i\mathbf{m}^q = \mathbf{Cu}^q$, where $\mathbf{u}^q$ is s.b., which is defined as $\mathbf{\Lambda\Pi}_i\mathbf{m}^q \geq \mathbf{u}^q \geq \mathbf{0}$ and $\forall t_j \in T_{nc}\ u_j^q = 0$. Moreover, by definition, $\mathbf{m}^q$ belongs to E_i iff it is an equilibrium marking in $\Re_i$. Therefore, if $\exists \varepsilon \geq 0$ fulfilling all the constraints then $\mathbf{m}^q \in E_i$, otherwise $E_i = \emptyset$. Furthermore, $\mathbf{m}^q \in E_i^+$ iff $\mathbf{\Lambda\Pi}_i\mathbf{m}^q - \mathbf{u}^q \geq \varepsilon \cdot \mathbf{1}$ and $\varepsilon > 0$. While conditions $\forall j\ [1, ..., 1](\mathbf{\Pi}_j - \mathbf{\Pi}_i)\mathbf{m}^q \geq \varepsilon$ with $\varepsilon > 0$ and $(\mathbf{\Pi}_j - \mathbf{\Pi}_i)\mathbf{m}^q \geq \mathbf{0}$ are equivalent to $\forall j\ (\mathbf{\Pi}_j - \mathbf{\Pi}_i)\mathbf{m}^q \gneq \mathbf{0}$, meaning that $\mathbf{m}^q \in int\{\Re_i\}$ (the equality holds only on the borders between regions). Therefore, if the LPP computes a $\varepsilon > 0$ then $\mathbf{m}^q \in int\{\Re\} \cap E_i^+$. Otherwise, such equilibrium marking does not exist, so $int\{\Re\} \cap E_i^+ = \emptyset$.

Next, assume that an equilibrium marking $\mathbf{m}^q \in int\{\Re_i\} \cap E_i^+$ has been computed. According to the definition of T_{cf}^i, $t_j \in T_{cf}^i$ iff $\exists \mathbf{m}^{q'} \in E_i$ s.t. $u_j^{q'} > 0$. Thus, if $u_j^q > 0$ then $t_j \in T_{cf}^i$ (second step of the algorithm). Now, if $\exists t_j$ s.t. $u_j^q = 0$ and $\exists \mathbf{d}_j$ solution of (4.1), then $\exists \alpha > 0$ small enough s.t. the marking $\mathbf{m}^{q'} = \mathbf{m}^q + \alpha\mathbf{d}_j$ will belong to E_i (because $\mathbf{m}^q \in int\{\Re_i\}$) and its equilibrium input $\mathbf{u}^{q'} = \mathbf{u}^q + \alpha\mathbf{e}_j$ will fulfill $u_j^{q'} > 0$. In such case t_j also belongs to T_{cf}^i (third step of the algorithm).

Finally, let us show that if $u_j^q = 0$ and $\nexists \mathbf{d}_j$ solution of (4.1) then $t_j \notin T_{cf}^i$. For this, consider any $\mathbf{m}^{q'} \in E_i$. Then, $\exists \gamma$ s.t. $(\mathbf{m}^{q'} - \mathbf{m}^q) = \mathbf{G}_i\gamma$. Assume that the first k transitions correspond to the controllable ones. Let us define the matrix $\mathbf{G}_i'$, of dimension $|P| \times k$, s.t. the j-th column of this matrix is $\mathbf{d}_j$ (the solution of (4.1)) if it exists, otherwise it is $\mathbf{0}$. In this way, since all the columns of $\mathbf{G}_i$ are included in $[\mathbf{G}_i', \mathbf{D}]$, then $\exists \gamma', \eta$ s.t. $(\mathbf{m}^{q'} - \mathbf{m}^q) = \mathbf{G}_i\gamma = [\mathbf{G}_i', \mathbf{D}][(\gamma')^T, (\eta)^T]^T$. Furthermore, by definition

$$\begin{bmatrix} \mathbf{C\Lambda\Pi}_i \\ \mathbf{B}_y^T \end{bmatrix} \cdot \begin{bmatrix} \mathbf{G}_i' & \mathbf{D} \end{bmatrix} = \begin{bmatrix} \mathbf{C} \\ \mathbf{0} \end{bmatrix} \cdot \begin{bmatrix} \mathbf{e}_1' & ... & \mathbf{e}_k' \end{bmatrix}$$

where $\mathbf{e}_j'$ is the j-th vector of the unity matrix of dimension $|T|$ if $\exists \mathbf{d}_j$, otherwise $\mathbf{e}_j' = \mathbf{0}$. Thus, since $(\mathbf{m}^{q'} - \mathbf{m}^q) = [\mathbf{G}_i', \mathbf{D}][(\gamma')^T, (\eta)^T]^T$, by using (C.1) (with $(\mathbf{m}^{q'} - \mathbf{m}^q)$ instead of $(\mathbf{m}_1 - \mathbf{m}_2)$) it can be obtained $(\mathbf{u}^{q'} - \mathbf{u}^q) = [\mathbf{e}_1', .., \mathbf{e}_k']\,\gamma'$. Therefore, if for some $t_j \in T_c$ it does not exist solution for $\mathbf{d}_j$, then $\mathbf{e}_j' = \mathbf{0}$, meaning that $(u_j^{q'} - u_j^q) = 0$. If additionally $u_j^q = 0$ then $u_j^{q'} = 0$. Finally, since this occurs for any $\mathbf{m}^{q'} \in E_i$ then $t_j \notin T_{cf}^i$. ∎

Algorithm C.2. Computation of an equilibrium marking $\mathbf{m}^q \in E_1^* \cap E_2^*$.

Solve the following LPP:

max	ε subject to	
	$\mathbf{m}^q \geq \mathbf{0}$, $\mathbf{u}^q \geq \mathbf{0}$, $\varepsilon \geq 0$	
	$\mathbf{B}_y^T(\mathbf{m}^q - \mathbf{m}_0) = \mathbf{0}$	$\{\mathbf{m}^q \in Class\{\mathbf{m}_0\}\}$
	$\mathbf{C\Lambda\Pi}_1\mathbf{m}^q = \mathbf{Cu}^q$	$\{Equilibrium\ marking\}$
	$\mathbf{\Lambda\Pi}_1\mathbf{m}^q - \mathbf{u}^q \geq \varepsilon \cdot \mathbf{1}$	$\{Nonnegative\ flow\}$
	$u_j^q \geq \varepsilon \quad \forall t_j \in T_{cf}^i$	$\{Positive\ fully\ controllable\ inputs\}$
	$u_j^q = 0 \quad \forall t_j \in T_{nc}$	$\{Uncontrollable\ transitions\}$
	$\mathbf{\Pi}_1\mathbf{m}^q = \mathbf{\Pi}_2\mathbf{m}^q$	$\{Border\ marking\}$
	$\mathbf{\Pi}_1\mathbf{m}^q \leq \mathbf{\Pi}_j\mathbf{m}^q\ \forall j$	$\{\mathbf{m}^q \in \Re_1\}$

---

if $\varepsilon > 0$ **then** $\mathbf{m}^q \in E_1^* \cap E_2^*$
else $E_1^* \cap E_2^* = \emptyset$ (in the case $\varepsilon = 0$ it means that $\mathbf{m}^q \in E_1 \cap E_2$ but still $E_1^* \cap E_2^* = \emptyset$).

Proof. First, $\mathbf{m}^q \geq \mathbf{0}$ and $\mathbf{B}_y^T(\mathbf{m}^q - \mathbf{m}_0) = \mathbf{0}$ are fulfilled iff $\mathbf{m}^q \in Class(\mathbf{m}_0)$. Moreover, $\mathbf{m}^q \in \Re_1$ is equivalent to $\forall j\ \mathbf{\Pi}_1\mathbf{m}^q \leq \mathbf{\Pi}_j\mathbf{m}^q$. Furthermore, $\mathbf{m}^q$ is an equilibrium marking iff $\mathbf{C\Lambda\Pi}_1\mathbf{m}^q = \mathbf{Cu}^q$, where $\mathbf{u}^q$ is s.b., which is defined as $\mathbf{\Lambda\Pi}_1\mathbf{m}^q \geq \mathbf{u}^q \geq \mathbf{0}$ and $\forall t_j \in T_{nc}$, $u_j = 0$. Moreover, by definition, $\mathbf{m}^q$ belongs to E_1 iff it is an equilibrium marking in $\Re_1$. Therefore, if $\exists \varepsilon \geq 0$ fulfilling all the constraints then $\mathbf{m}^q \in E_1$, otherwise $E_1 = \emptyset$. Additionally, given $\mathbf{m}^q \in E_1$, $\mathbf{m}^q \in E_1 \cap E_2$ iff $\mathbf{\Pi}_1\mathbf{m}^q = \mathbf{\Pi}_2\mathbf{m}^q$.

Furthermore, $\mathbf{m}^q \in E_1^*$ iff $\mathbf{\Lambda\Pi}_1\mathbf{m}^q - \mathbf{u}^q \geq \varepsilon \cdot \mathbf{1}$, $u_j^q \geq \varepsilon \quad \forall t_j \in T_{cf}^i$ and $\varepsilon > 0$. This condition also implies $\mathbf{m}^q \in E_2^*$, providing $\mathbf{\Pi}_1\mathbf{m}^q = \mathbf{\Pi}_2\mathbf{m}^q$. Therefore, if the LPP computes $\varepsilon > 0$ then $\mathbf{m}^q \in E_1^* \cap E_2^*$. Otherwise, such equilibrium marking does not exist, so $E_1^* \cap E_2^* = \emptyset$. ∎

C.2 On the product $\mathbf{v}^T\mathbf{e}^{\mathbf{A}\tau}\mathbf{b}$

In this appendix, a couple of propositions will be provided regarding the sign of the product $\mathbf{v}^T\mathbf{e}^{\mathbf{A}\tau}\mathbf{b}$. For this, some basic concepts about the Jordan block form of a square matrix $\mathbf{A}$, and some matrices and vectors, will be firstly introduced.

Jordan block form: Given a real-valued square matrix $\mathbf{A}$, there exists a real-valued transformation matrix $\mathbf{Q}$ s.t. $\mathbf{J} = diag(\mathbf{J}_1, \mathbf{J}_2, .., \mathbf{J}_r) = \mathbf{Q}^{-1}\mathbf{A}_i\mathbf{Q}$ is in the so called Jordan block form, where each block is associated to either a real eigenvalue or to a pair of conjugated complex eigenvalues (see, for instance, [Chen, 1984]), having the form:

$$\text{if } s_i \in \mathbb{R},\ \mathbf{J}_i = \begin{bmatrix} s_i & 1 & 0 & ... & 0 \\ 0 & s_i & 1 & ... & 0 \\ \vdots & \vdots & \vdots & & \vdots \\ 0 & 0 & 0 & ... & s_i \end{bmatrix}, \quad \text{if } s_i = \alpha \pm i\beta \in \mathbb{C},\ \mathbf{J}_i = \begin{bmatrix} \mathbf{D} & \mathbf{I} & \mathbf{0} & ... & \mathbf{0} \\ \mathbf{0} & \mathbf{D} & \mathbf{I} & ... & \mathbf{0} \\ \vdots & \vdots & \vdots & & \vdots \\ \mathbf{0} & \mathbf{0} & \mathbf{0} & ... & \mathbf{D} \end{bmatrix} \tag{C.3}$$

$$\text{where } \mathbf{D} = \begin{bmatrix} \alpha & -\beta \\ \beta & \alpha \end{bmatrix}$$

In this work, it will be assumed that the blocks are ordered according to the real part of its eigenvalues, i.e., $Real(s_1) \geq Real(s_2) \geq ... \geq Real(s_r)$.

Property C.1. Given a Jordan block $\mathbf{J}_j$, the exponential matrix $e^{\mathbf{J}_j\tau}$ is given by

$$\begin{aligned}
&\text{if } s_j \in \mathbb{R},\ e^{\mathbf{J}_j\tau} = e^{s_j\tau}\begin{bmatrix} 1 & \tau & ... & \frac{\tau^{m_j-1}}{(m_j-1)!} \\ 0 & 1 & ... & \frac{\tau^{m_j-2}}{(m_j-2)!} \\ \vdots & \vdots & & \vdots \\ 0 & 0 & ... & 1 \end{bmatrix}, \\
&\text{if } s_j \in \mathbb{C},\ e^{\mathbf{J}_j\tau} = e^{\alpha\tau} diag(\mathbf{W}(\tau))\begin{bmatrix} \mathbf{I} & \mathbf{I}\tau & ... & \mathbf{I}\frac{\tau^{m_j-1}}{(m_j-1)!} \\ \mathbf{0} & \mathbf{I} & ... & \mathbf{I}\frac{\tau^{m_j-2}}{(m_j-2)!} \\ \vdots & \vdots & & \vdots \\ \mathbf{0} & \mathbf{0} & ... & \mathbf{I} \end{bmatrix}, \\
&\text{where } s_j = \alpha \pm i\beta \text{ and } \mathbf{W}(\tau) = \begin{bmatrix} cos(\beta\tau) & -sin(\beta\tau) \\ sin(\beta\tau) & cos(\beta\tau) \end{bmatrix}
\end{aligned} \tag{C.4}$$

Additional definitions:

• Let $\mathbf{b}'_j$ be the restriction of $\mathbf{b}' = \mathbf{Q}^{-1}\mathbf{b}$ to the corresponding elements of $\mathbf{J}_j$, so $\mathbf{b}'^T = [\mathbf{b}'^T_1, ..., \mathbf{b}'^T_r]$. The components of $\mathbf{b}'_j$ are denoted as follows: for $s_j \in \mathbb{R}$, $\mathbf{b}'^T_j = [b^j_1, ..., b^j_{m_j}]$ with b^j_l being scalars; for $s_j \in \mathbb{C}$, $\mathbf{b}'^T_j = [\mathbf{b}^j_1, .., \mathbf{b}^j_{m_j}]$ with $\mathbf{b}^j_l$ being two-element row vectors. Then, for each block, consider the matrix $\overline{\mathbf{b}_j}$ and vector $\boldsymbol{\alpha}_j(\tau)$ defined as:

$$\forall s_j \in \mathbb{R}: \quad \overline{\mathbf{b}_j} = \begin{bmatrix} b^j_{m_j} & \mathbf{0} & ... & \mathbf{0} \\ b^j_{m_j-1} & b^j_{m_j} & ... & \mathbf{0} \\ \vdots & \vdots & & \vdots \\ b^j_1 & b^j_2 & ... & b^j_{m_j} \end{bmatrix},$$

$$\boldsymbol{\alpha}_j(\tau) = e^{s_j\tau}\begin{bmatrix} \tau^{m_j-1} & \tau^{m_j-2} & ... & 1 \end{bmatrix},$$

$$\forall s_j \in \mathbb{C}: \quad \overline{\mathbf{b}_j} = \begin{bmatrix} |\mathbf{b}^j_{m_j}| & \mathbf{0} & ... & \mathbf{0} \\ |\mathbf{b}^j_{m_j-1}| & |\mathbf{b}^j_{m_j}| & ... & \mathbf{0} \\ \vdots & \vdots & & \vdots \\ |\mathbf{b}^j_1| & |\mathbf{b}^j_2| & ... & |\mathbf{b}^j_{m_j}| \end{bmatrix} diag\left(\begin{bmatrix} 1 & 1 \\ 1 & 1 \end{bmatrix}\right),$$

$$\boldsymbol{\alpha}_j(\tau) = e^{Real(s_j)\tau}\begin{bmatrix} \tau^{m_j-1} & \tau^{m_j-2} & ... & 1 \end{bmatrix}$$

• Define a matrix S as follows:
If all the entries in $\boldsymbol{\alpha}(\tau) = [\boldsymbol{\alpha}_1(\tau), ..., \boldsymbol{\alpha}_r(\tau)]$, related to real eigenvalues, are different then $\mathbf{S} = \mathbf{I}$. Otherwise, consider $\widehat{\boldsymbol{\alpha}}(\tau)$, defined as the vector resulting from eliminating the repetitive entries in $\boldsymbol{\alpha}(\tau)$ related to real eigenvalues. Matrix $\mathbf{S}$ is then defined by merging, in the unity matrix $\mathbf{I}$, the rows that correspond to repetitive entries in $\boldsymbol{\alpha}(\tau)$ associated to real eigenvalues (for instance, if $\alpha_1(\tau) = \alpha_2(\tau)$ are

associated to a real eigenvalue, then the row vector $[1, 1, 0, .., 0]$ appears in $\mathbf{S}$).

• Vector $\mathbf{a} = first(\mathbf{S} \cdot diag([\overline{\mathbf{b}_1}, \overline{\mathbf{b}_2}, .., \overline{\mathbf{b}_r}]) \cdot \mathbf{S}^T)$ is defined as a row vector where each kth component $[\mathbf{a}]_k$ is equal to the first non-null entry of the kth column of the argument matrix $\mathbf{S} \cdot diag([\overline{\mathbf{b}_1}, \overline{\mathbf{b}_2}, .., \overline{\mathbf{b}_r}]) \cdot \mathbf{S}^T$.

• Vector $\hat{\mathbf{a}}$ is a row vector of length $2n$ defined by pairs of components as follows:

$$\forall l \in \{1, ..., n\},\ [[\hat{\mathbf{a}}]_{2l-1}, [\hat{\mathbf{a}}]_{2l}] = \begin{cases} [[\mathbf{a}]_l, -[\mathbf{a}]_l] & \text{if } [\mathbf{Q}^{-1}]_l \text{ is associated to a real eigenvalue} \\ [[\mathbf{a}]_l, [\mathbf{a}]_l] & \text{if } [\mathbf{Q}^{-1}]_l \text{ is associated to a complex eigenvalue} \end{cases}$$

• $\mathbf{H}(\mathbf{Q}, \mathbf{b})$ is a matrix built with row vectors $\mathbf{h}^k$, defined for each positive entry of $\hat{\mathbf{a}}$ (i.e, for each $[\hat{\mathbf{a}}]_k > 0$) as follows: $\forall l \in \{1, .., 2n\}$,

$$\left[\mathbf{h}^k\right]_l = \begin{cases} 1 & \text{if } l = k \\ -\infty & \text{if } [\hat{\mathbf{a}}]_l < 0 \text{ and either } (k \text{ is odd and } l < k) \text{ or } (k \text{ is even and } l < k-1) \\ 0 & \text{otherwise} \end{cases}$$

Example 4.5 in Chapter 4 illustrates the definitions of the matrices and vectors previously introduced.

Proposition C.2. *Let* $\mathbf{v}$ *and* $\mathbf{b}$ *be arbitrary column vectors of length* n*. Then,* $lim_{\tau\to\infty}\mathbf{v}^T\mathbf{e}^{\mathbf{A}\tau}\mathbf{b} \leq 0$ *iff* $\exists\mathbf{v}''$ *s.t.*

$$\begin{aligned} &\mathbf{S}\mathbf{Q}^T \cdot \mathbf{v} = diag([1, -1]) \cdot \mathbf{v}'' \\ &\mathbf{v}'' \geq \mathbf{0} \\ &\mathbf{H}(\mathbf{Q}, \mathbf{b})\mathbf{v}'' \leq \mathbf{0} \end{aligned} \tag{C.5}$$

Proof. The proof is split $\mathbf{e}^{\mathbf{A}\tau}$ it will be proven that $lim_{\tau\to\infty}\mathbf{v}^T\mathbf{e}^{\mathbf{A}\tau}\mathbf{b} \leq 0$ iff the first non-null product $[\mathbf{a}]_l[\mathbf{Q}^T\mathbf{v}]_l$ is negative and $[\mathbf{Q}^T]_l$ is associated to a real-eigenvalue. In the second part, this condition will be expressed as the linear inequality $\mathbf{H}(\mathbf{Q}, \mathbf{b})\mathbf{v}'' \leq \mathbf{0}$ s.t. $\mathbf{v}'' \geq \mathbf{0}$ and $\mathbf{S}\mathbf{Q}^T \cdot \mathbf{v} = diag([1, -1]) \cdot \mathbf{v}''$.

Part 1. By definition $\mathbf{v}^T\mathbf{e}^{\mathbf{A}\tau}\mathbf{b} = \mathbf{v}'^T\mathbf{e}^{\mathbf{J}\tau}\mathbf{b}'$, where $\mathbf{v}'^T = \mathbf{v}^T\mathbf{Q}$. Furthermore, since the Jordan form is diagonal by blocks then $\mathbf{v}'^T\mathbf{e}^{\mathbf{J}\tau}\mathbf{b}' = \sum_{j=1}^{r}\mathbf{v}_j'^T\mathbf{e}^{\mathbf{J}_j\tau}\mathbf{b}_j'$, where $\mathbf{v}_j'$ denotes the restriction of $\mathbf{v}'$ to the elements corresponding to $\mathbf{J}_j$. Let us consider now a block associated to a real eigenvalue s_j. By using (C.4) and denoting $\mathbf{v}_j'^T = [v_1'^j, .., v_{m_j}'^j]$ and $\mathbf{b}_j'^T = [b_1^j, ..., b_{m_j}^j]$, the product $\mathbf{v}_j'^T e^{\mathbf{J}_j\tau}\mathbf{b}_j'$ can be expressed as

$$\begin{aligned} \mathbf{v}_j'^T\mathbf{e}^{\mathbf{J}_j\tau}\mathbf{b}_j' &= e^{s_j\tau}\left[\tfrac{\tau^{m_j-1}}{(m_j-1)!}, \tfrac{\tau^{m_j-2}}{(m_j-2)!}, ..., 1\right] \cdot \begin{bmatrix} b_{m_j}^j & \mathbf{0} & ... & \mathbf{0} \\ b_{m_j-1}^j & b_{m_j}^j & ... & \mathbf{0} \\ \vdots & \vdots & & \vdots \\ b_1^j & b_2^j & ... & b_{m_j}^j \end{bmatrix} \cdot \begin{bmatrix} v_1'^j \\ v_2'^j \\ \vdots \\ v_{m_j}'^j \end{bmatrix} \\ &= \boldsymbol{\alpha}_j(\tau) \cdot \overline{\mathbf{b}_j} \cdot \mathbf{v}_j' \end{aligned} \tag{C.6}$$

Note that the terms in (C.6) are ordered in such a way that the first of them are dominant (of larger magnitude) when $\tau \to \infty$. For instance, if $b_{m_j}^j v_1'^j < 0$ (or $b_{m_j}^j v_1'^j > 0$) then, independently of the other values of $\mathbf{v}_j'$ and $\mathbf{b}_j'$, $lim_{\tau\to\infty}\mathbf{v}_j'^T e^{\mathbf{J}_j\tau}\mathbf{b}_j' < 0$ (or > 0, respectively). In fact, it is not difficult to see from (C.6) that the sign of $lim_{\tau\to\infty}\mathbf{v}_j'^T e^{\mathbf{J}_j\tau}\mathbf{b}_j'^T$ is equal to the sign of $[\overline{\mathbf{b}_j}]_{m,k}[\mathbf{v}_j']_k$, where $[\mathbf{v}_j']_k$ is the first non-null element of $\mathbf{v}_j'$ and $[\overline{\mathbf{b}_j}]_{m,k}$ is the first non-null element of the kth column of $\overline{\mathbf{b}_j}$. This information is resumed by the vector $\mathbf{a}_j = first(\overline{\mathbf{b}_j})$, by keeping the first non-null entries of the columns of $\overline{\mathbf{b}_j}$.

Let us consider now a block $\mathbf{J}_j$ associated to a complex eigenvalue. By using (C.4), the product $\mathbf{v}_j'^T e^{\mathbf{J}_j\tau}\mathbf{b}_j'$ can be expressed as

$$\begin{aligned}\mathbf{v}_j'^T\mathbf{e}^{\mathbf{J}_j\tau}\mathbf{b}_j' &= e^{\alpha_j\tau}\left[\tfrac{\tau^{m_j-1}}{(m_j-1)!},...,1\right]\cdot\begin{bmatrix}\mathbf{b}_{m_j}^j & \mathbf{0} & ... & \mathbf{0}\\ \mathbf{b}_{m_j-1}^j & \mathbf{b}_{m_j}^j & ... & \mathbf{0}\\ \vdots & \vdots & & \vdots\\ \mathbf{b}_1^j & \mathbf{b}_2^j & ... & \mathbf{b}_{m_j}^j\end{bmatrix}\cdot diag(\mathbf{W}(\tau)^T)\cdot\begin{bmatrix}v_1'^j\\ \vdots\\ v_{m_j-1}'^j\\ v_{m_j}'^j\end{bmatrix}\\ &= \boldsymbol{\alpha}_j(\tau)\cdot\overline{\mathbf{b}_j^w}(\tau)\cdot\mathbf{v}_j'\end{aligned} \tag{C.7}$$

where $\mathbf{b}_l^j$ are two-element row vectors s.t. $\mathbf{b}_j'^T=[\mathbf{b}_1^j,..,\mathbf{b}_{m_j}^j]$. Note that the terms in (C.7) are oscillatory ($\mathbf{W}(\tau)$ is defined in (C.4), being clearly oscillatory), meaning that, if the product $\mathbf{v}_j^T e^{\mathbf{J}_j\tau_1}\mathbf{b}_j'<0$ (or >0) at some time τ_1, then there exists $\tau_2>\tau_1$ s.t. $\mathbf{v}_j^T e^{\mathbf{J}_j\tau_2}\mathbf{b}_j^T>0$ (<0, respectively). In this sense, for blocks associated to complex eigenvalues, the relevant information for deciding the contribution of $\mathbf{v}_j'^T\mathbf{e}^{\mathbf{J}_j\tau}\mathbf{b}_j'$, to the sign of $lim_{\tau\to\infty}\mathbf{v}'^T\mathbf{e}^{\mathbf{J}\tau}\mathbf{b}'$, is which of the entries of $\overline{\mathbf{b}_j^w}(\tau)\mathbf{v}_j'$ are non-null (at some time). Since $\overline{\mathbf{b}_j^w}(\tau)$ is time-dependent, let us consider the following upper bound:

$$\begin{aligned}\mathbf{v}_j'^T\mathbf{e}^{\mathbf{J}_j\tau}\mathbf{b}_j' &\le e^{\alpha_j\tau}\left[\tfrac{\tau^{m_j-1}}{(m_j-1)!},...,1\right]\cdot\begin{bmatrix}|\mathbf{b}_{m_j}^j| & \mathbf{0} & ... & \mathbf{0}\\ |\mathbf{b}_{m_j-1}^j| & |\mathbf{b}_{m_j}^j| & ... & \mathbf{0}\\ \vdots & \vdots & & \vdots\\ |\mathbf{b}_1^j| & |\mathbf{b}_2^j| & ... & |\mathbf{b}_{m_j}^j|\end{bmatrix}\cdot diag\left(\begin{bmatrix}1 & 1\\ 1 & 1\end{bmatrix}\right)\cdot|\mathbf{v}_j'|\\ &= \boldsymbol{\alpha}_j(\tau)\cdot\overline{\mathbf{b}_j}\cdot|\mathbf{v}_j'|\end{aligned} \tag{C.8}$$

This expression provides a properly thin upper-bound. In fact, $\forall\tau\ge0$, $\mathbf{v}_j'^T\mathbf{e}^{\mathbf{J}_j\tau}\mathbf{b}_j'=0$ iff $[1,..,1]\cdot\overline{\mathbf{b}_j}\cdot|\mathbf{v}_j'|=0$. Then, the vectors $\mathbf{a}_j=first(\overline{\mathbf{b}_j})$ and $|\mathbf{v}_j'|$ provide the information of what entries of $\overline{\mathbf{b}_j^w}(\tau)\mathbf{v}_j'$ are null for all time, i.e., $\forall\tau\ge0$, $\mathbf{v}_j'^T\mathbf{e}^{\mathbf{J}_j\tau}\mathbf{b}_j'=0$ iff $\mathbf{a}_j\cdot|\mathbf{v}_j'|=0$.

Now, let us consider all the Jordan blocks. Combining them we obtain:

$$\mathbf{v}'^T\mathbf{e}^{\mathbf{J}\tau}\mathbf{b}'=\sum_{j=1}^{r}\mathbf{v}_j'^T\mathbf{e}^{\mathbf{J}_j\tau}\mathbf{b}_j'=[\boldsymbol{\alpha}_1(\tau),\boldsymbol{\alpha}_2(\tau),...,\boldsymbol{\alpha}_r(\tau)]\cdot\begin{bmatrix}\overline{\mathbf{b}_1^*} & \mathbf{0} & ... & \mathbf{0}\\ \mathbf{0} & \overline{\mathbf{b}_2^*} & ... & \mathbf{0}\\ \vdots & \vdots & & \vdots\\ \mathbf{0} & \mathbf{0} & ... & \overline{\mathbf{b}_r^*}\end{bmatrix}\cdot\begin{bmatrix}\mathbf{v}_1'\\ \mathbf{v}_2'\\ \vdots\\ \mathbf{v}_r'\end{bmatrix} \tag{C.9}$$

where $\overline{\mathbf{b}_j^*}=\overline{\mathbf{b}_j}$ if $s_j\in\mathbb{R}$ while $\overline{\mathbf{b}_j^*}=\overline{\mathbf{b}_j^w}(\tau)$ if $s_j\in\mathbb{C}$.

The vector $\vec{\mathbf{a}}=[\mathbf{a}_1,..,\mathbf{a}_r]$ keeps the first non-null entries of the columns of $diag([\overline{\mathbf{b}_1},..,\overline{\mathbf{b}_r}])$, i.e., the key information of this matrix for deciding the sign of $\mathbf{v}_j'^T\mathbf{e}^{\mathbf{J}_j\tau}\mathbf{b}'$ in the limit $\tau\to\infty$. On the other hand, since the Jordan blocks are ordered according to the real part of their corresponding eigenvalues (from the largest to the lowest), then the entries of $\boldsymbol{\alpha}(\tau)=[\boldsymbol{\alpha}_1(\tau),\boldsymbol{\alpha}_2(\tau),...,\boldsymbol{\alpha}_r(\tau)]$ are also ordered from the largest to the lowest when $\tau\to\infty$. Remember that in complex-eigenvalue blocks the non-null entries of the product $[\overline{\mathbf{b}_j^*}]^l[\mathbf{v}_j]_l$ oscillate, being negative and positive at different times; while for real-eigenvalue blocks the sign of the entries of $[\overline{\mathbf{b}_j^*}]^l[\mathbf{v}_j]_l$ remain constant, so, these are required in order to make the

sign of $\mathbf{v}_j'^T\mathbf{e}^{\mathbf{J}_j\tau}\mathbf{b}_j'$ to be constant at the limit $\tau \to \infty$.

Let us suppose that the entries of $\boldsymbol{\alpha}(\tau)$, related to real eigenvalues, are different. In this way, denoting as l the first index s.t. $\vec{a}_l v_l' \neq 0$, $lim_{\tau\to\infty}\mathbf{v}_j'^T\mathbf{e}^{\mathbf{J}_j\tau}\mathbf{b}_j' \leq 0$ iff $\vec{a}_l v_l' < 0$ and v_l' is associated to a real-eigenvalue block (otherwise stated, $[\mathbf{Q}^T]_l$ is associated to a real-eigenvalue since $v_l' = [\mathbf{Q}^T]_l\mathbf{v}$).

Nevertheless, it may occur the case that the entry of $\boldsymbol{\alpha}(\tau)$ that corresponds to $\vec{a}_l$, let us say $\alpha_k(\tau)$, is not unique, e.g., if $\alpha_k(\tau) = \alpha_{k+1}(\tau)$ (this may occur, for instance, if there are repetitive eigenvalues but associated to the same number of different eigenvectors). In such case, there could be more entries in $\vec{\mathbf{a}}$ with the same importance than $\vec{a}_l$ (in our exemple, the sign of $lim_{\tau\to\infty}\mathbf{v}_j'^T\mathbf{e}^{\mathbf{J}_j\tau}\mathbf{b}_j'$ would be negative if $\vec{a}_l v_l' + \vec{a}_{l+1}v_{l+1}' < 0$, because $\vec{a}_l$ and $\vec{a}_{l+1}$ are associated with $\alpha_k(\tau)$ and $\alpha_{k+1}(\tau)$, which are equal). In order to overcome this situation, the vector $\hat{\boldsymbol{\alpha}}(\tau)$ is defined by eliminating from $\boldsymbol{\alpha}(\tau)$ the repetitive undesired entries. Similarly, the matrix $\mathbf{S}$ is defined in such a way that the entries in $diag([\overline{\mathbf{b}_1}, .., \overline{\mathbf{b}_r}])$, corresponding to the repetitive elements in $\boldsymbol{\alpha}(\tau)$, appear summed in the product $\mathbf{S}\cdot diag([\overline{\mathbf{b}_1}, .., \overline{\mathbf{b}_r}])\cdot\mathbf{S}^T$. Thus, $\mathbf{a}$ as defined above overcomes this situation. Accordingly, the vector $\hat{\mathbf{v}} = \mathbf{S}\mathbf{v}'$ resumes the information of $\mathbf{v}'$ that corresponds to those entries in $\mathbf{a}$.

Part 2. Previous condition can be rephrased as follows:

Condition 1. - $\forall m$ s.t. either ($a_m\hat{v}_m > 0$ and $\hat{v}_m$ is associated to a real-eigenvalue) or ($a_m\hat{v}_m \neq 0$ and $\hat{v}_m$ is associated to a complex-eigenvalue), $\exists k < m$ s.t. $a_k\hat{v}_k < 0$ and $\hat{v}_k$ is associated to a real-eigenvalue.

Now, let us consider the auxiliary variable $\mathbf{v}'' \geq \mathbf{0}$ s.t. $\hat{\mathbf{v}} = diag([1,-1])\mathbf{v}''$ (note that $\forall\hat{\mathbf{v}}\ \exists\mathbf{v}''$ that fulfills this equality, but this is not unique). Let us also consider the vector $\mathbf{a}^* = [\mathbf{a}_1^*, ..., \mathbf{a}_r^*]$, where $\mathbf{a}_j^* = -\mathbf{a}_j$ if the jth block is associated to a real eigenvalue, and $\mathbf{a}_j^* = \mathbf{a}_j$ if the jth block is associated to a complex eigenvalue. Note that the entries of $\hat{\mathbf{v}}$ are associated to pairs in $\mathbf{v}''$, i.e., $\hat{v}_j = v''_{2j-1} - v''_{2j}$. In this way, the vector $\hat{\mathbf{a}}$ is equivalent to $\hat{\mathbf{a}} = [a_1, a_1^*, a_2, a_2^*, .., a_n, a_n^*]$, where each pair $\hat{a}_{2j-1} = a_j$ and $\hat{a}_{2j} = a_j^*$ is associated to each entry a_j. Accordingly, *Condition 1* is equivalent to

Condition 2. - $\exists\mathbf{v}'' \geq \mathbf{0}$ with $\hat{\mathbf{v}} = diag([1,-1])\mathbf{v}''$ fulfilling: $\forall m$ s.t. either ($\hat{a}_m v_m'' > 0$ and v_m'' is associated to a real-eigenvalue) or ($\hat{a}_m v_m'' \neq 0$ and v_m'' is associated to a complex-eigenvalue), $\exists k$ s.t. $\hat{a}_k v_k'' < 0$ and v_k'' is associated to a real-eigenvalue and either (m is odd and $k < m$) or (m is even and $k < m-1$).

Note that $k < m$ is not enough in case m is even because v''_{m-1} and v_m'' are associated to the same $\hat{v}_{(m/2)}$, $a_{(m/2)}$ and $\alpha_{m/2}(\tau)$ (thus the sign of $\hat{a}_{m-1}v''_{m-1}$ is not predominant over the sign of $\hat{a}_m v_m''$ when $\tau\to\infty$). Moreover, $\hat{\mathbf{a}}$ and $\mathbf{v}''$ have very useful properties: $\mathbf{v}'' \geq \mathbf{0}$ and $\hat{a}_m v_m'' \geq 0$ for all v_m'' associated to a complex-eigenvalue. Therefore, *Condition 2* is simplified as:

Condition 3. - $\exists\mathbf{v}'' \geq \mathbf{0}$ with $\hat{\mathbf{v}} = diag([1,-1])\mathbf{v}''$ fulfilling: $\forall m$ s.t. $\hat{a}_m > 0$ and $v_m'' > 0$, $\exists k$ s.t. $\hat{a}_k < 0$ and $v_k'' > 0$ and either (m is odd and $k < m$) or (m is even and $k < m-1$).

Finally, consider the matrix $\mathbf{H}(\mathbf{Q},\mathbf{b})$, built with all the row vectors $\mathbf{h}^m$ as defined above. Given a particular entry $\hat{a}_m > 0$, there exists an associated row $\mathbf{h}^m$ in $\mathbf{H}$. In this, the entry $\hat{a}_m > 0$ is represented in $\mathbf{h}^m$ as 1, being its unique positive entry. The negative entries $\hat{a}_k < 0$ represented in $[\mathbf{h}^m]_k$, as $-\infty$, are those associated with a $\alpha_{(k/2)}(\tau)$ larger than $\alpha_{(m/2)}(\tau)$ when $\tau\to\infty$ (or $\alpha_{(k-1)/2}(\tau)$ if k is odd and/or $\alpha_{(m-1)/2}(\tau)$ if m is odd, but still $\alpha_{(k-1)/2}(\tau) < \alpha_{(m-1)/2}(\tau)$ when $\tau\to\infty$). Then, assuming $v_m'' > 0$, the inequality $\mathbf{h}^m\mathbf{v}'' \leq \mathbf{0}$ holds iff $\exists k$ s.t. $\hat{a}_k < 0$ and $v_k'' > 0$ and either (m is odd and $k < m$) or (m is even and $k < m-1$). Since this reasoning holds for each $\hat{a}_m > 0$, defined for each positive entry of $\hat{\mathbf{a}}$, *Condition 3* is satisfied (equivalently *Condition 1* and thus $lim_{\tau\to\infty}\mathbf{v}'^T\mathbf{e}^{\mathbf{J}\tau}\mathbf{b}' \leq 0$) iff $\mathbf{H}(\mathbf{Q},\mathbf{b})\mathbf{v}'' \leq \mathbf{0}$.

∎

Proposition C.3. *Given a matrix* $\mathbf{B}$ *of dimension* $n \times q$*, there exists a row vector* $\mathbf{w}$ *s.t.* $\mathbf{w}^T\mathbf{e}^{\mathbf{A}\tau}\mathbf{B} \leq \mathbf{0}$*,* $\forall\tau$*, and* $\mathbf{w}^T\mathbf{G} \neq \mathbf{0}$ *iff* $\exists\mathbf{v}'' \neq \mathbf{0}$ *s.t.*

$$\begin{aligned} &\mathbf{v}^T\mathbf{G} \neq \mathbf{0} \\ &\mathbf{v}'' \geq \mathbf{0} \\ &\mathbf{v}^T\mathbf{B} \leq \mathbf{0} \\ &\mathbf{S}\mathbf{Q}^T \cdot \mathbf{v} = diag([1,-1]) \cdot \mathbf{v}'' \\ \forall j \in \{1,..,q\}, \quad &\mathbf{H}(\mathbf{Q},[\mathbf{B}]^j)\mathbf{v}'' \leq \mathbf{0} \end{aligned} \tag{C.10}$$

Proof. Firstly, according to Proposition C.2, conditions $\mathbf{v}'' \geq \mathbf{0}$, $\mathbf{S}\mathbf{Q}^T \cdot \mathbf{v} = diag([1,-1]) \cdot \mathbf{v}''$ and $\mathbf{H}(\mathbf{Q},[\mathbf{B}]^j)\mathbf{v}'' \leq \mathbf{0}$ are fulfilled iff $\mathbf{v}^T\mathbf{e}^{\mathbf{A}\tau}[\mathbf{B}]^j \leq \mathbf{0}$ in the limit $\tau \to \infty$. Since this condition is required $\forall j \in \{1,..,t\}$, then it is equivalent to $\mathbf{v}^T\mathbf{e}^{\mathbf{A}\tau}\mathbf{B} \leq \mathbf{0}$ in the limit $\tau \to \infty$. Moreover, $\mathbf{v}^T\mathbf{B} \leq \mathbf{0}$ holds iff $\mathbf{v}^T\mathbf{e}^{\mathbf{A}\tau}\mathbf{B} \leq \mathbf{0}$ for $\tau = 0$. Let us demonstrate in the sequel that $\exists\mathbf{v}$ s.t. $\mathbf{v}^T\mathbf{e}^{\mathbf{A}\tau}\mathbf{B} \leq \mathbf{0}$ for $\tau = 0$ and in the limit $\tau \to \infty$ iff $\exists\mathbf{w}$ s.t. $\mathbf{w}^T\mathbf{e}^{\mathbf{A}\tau}\mathbf{B} \leq \mathbf{0}$ $\forall\tau$.

(Necessity) If $\nexists\mathbf{v}$ that fulfills $\mathbf{v}^T\mathbf{e}^{\mathbf{A}\tau}\mathbf{B} \leq \mathbf{0}$ for $\tau = 0$ and in the limit $\tau \to \infty$ then clearly $\nexists\mathbf{w}$ s.t. $\mathbf{w}^T\mathbf{e}^{\mathbf{A}\tau}\mathbf{B} \leq \mathbf{0}$ $\forall\tau \geq 0$.

(Sufficiency) For the other implication, let us firstly consider a column $\mathbf{b}$ of matrix $\mathbf{B}$. Assume that $\exists\mathbf{v}$ s.t. $\mathbf{v}^T\mathbf{e}^{\mathbf{A}\tau}\mathbf{b} \leq \mathbf{0}$ for $\tau = 0$ and in the limit $\tau \to \infty$. According to (C.9), (C.6) and (C.7), the product $\mathbf{v}^T\mathbf{e}^{\mathbf{A}\tau}\mathbf{b}$ can be expressed as

$$\begin{aligned} \mathbf{v}^T\mathbf{e}^{\mathbf{A}\tau}\mathbf{b} &= \textstyle\sum_{j=1}^{r} \mathbf{v}_j'^T\mathbf{e}^{\mathbf{J}_j\tau}\mathbf{b}_j' = \sum_{\forall j|s_j\in\mathbb{R}} \mathbf{v}_j'^T\mathbf{e}^{\mathbf{J}_j\tau}\mathbf{b}_j' + \sum_{\forall j|s_j\in\mathbb{C}} \mathbf{v}_j'^T\mathbf{e}^{\mathbf{J}_j\tau}\mathbf{b}_j' \\ &\leq \textstyle\sum_{\forall j|s_j\in\mathbb{R}} \boldsymbol{\alpha}_j(\tau)\overline{\mathbf{b}_j}\mathbf{v}_j' + \sum_{\forall j|s_j\in\mathbb{C}} \boldsymbol{\alpha}_j(\tau)\overline{\mathbf{b}_j}\mathbf{v}_j' \end{aligned} \tag{C.11}$$

where $\boldsymbol{\alpha}(\tau) = [\boldsymbol{\alpha}_1(\tau),..,\boldsymbol{\alpha}_r(\tau)]$ is a vector whose entries are time-functions of the kind $\alpha_l(\tau) = \tau^{m_l}e^{s_j\tau}$ (thus they are positive and monotonic). By definition, the entries of $\boldsymbol{\alpha}(\tau)$ are ordered s.t. the first of them become larger than the others when $\tau \to \infty$ (let us assume, without loss of generality, that $\mathbf{S} = \mathbf{I}$), then, $\forall j > s$ $\exists\boldsymbol{\alpha}^{max} > \mathbf{0}$ s.t. $\frac{\alpha_j(\tau)}{\alpha_s(\tau)} \leq \alpha_j^{max}$ $\forall\tau$. On the other hand, for Proposition C.2 it has been demonstrated that, if $\mathbf{v}^T\mathbf{e}^{\mathbf{A}\tau}\mathbf{b} \leq \mathbf{0}$ in the limit $\tau \to \infty$ then the first block j, s.t. $\overline{\mathbf{b}_j}\mathbf{v}_j' \neq \mathbf{0}$, is related to a real eigenvalue and the first entry of $\overline{\mathbf{b}_j}\mathbf{v}_j'$ is negative (let us denote the corresponding global index of such entry of $\mathbf{v}'$ as f, and let d be the index of the corresponding entry in $\boldsymbol{\alpha}(\tau)$). In this way, $\boldsymbol{\alpha}(\tau)\cdot\overline{\mathbf{b}}_f\, v_f' = \alpha_d(\tau)[\overline{\mathbf{b}}]_{d,f}v_f' + \sum_{\forall i\in\{d+1,..,n\}} \alpha_i(\tau)[\overline{\mathbf{b}}]_{i,f}v_f'$. Defining a slightly different $\mathbf{v}''$ s.t. $\overline{\mathbf{b}}_j\cdot\mathbf{v}_j'' \leq \mathbf{0}$ and $v_f'' = v_f'$ (which can always be defined according to (C.6)), then $\boldsymbol{\alpha}(\tau)\cdot\overline{\mathbf{b}}_f\, v_f'' \leq \alpha_d(\tau)[\overline{\mathbf{b}}]_{d,f}v_f''$.

Then, defining $\mathbf{w}' = \mathbf{v}' + \beta\mathbf{v}''$ and using (C.11) it can be obtained

$$\begin{aligned} \mathbf{w}'^T\mathbf{e}^{\mathbf{J}\tau}\mathbf{b}' &= \mathbf{v}'^T\mathbf{e}^{\mathbf{J}\tau}\mathbf{b}' + \beta\mathbf{v}''^T\mathbf{e}^{\mathbf{J}\tau}\mathbf{b}' \leq \alpha_d(\tau)[\overline{\mathbf{b}}]_{d,f}v_f' \\ &\quad + \textstyle\sum_{\forall j\in\{f,..,n\}} \sum_{\forall i\in\{d+1,..,n\}} \alpha_i(\tau)[\overline{\mathbf{b}}]_{i,j}v_j' + \beta\alpha_d(\tau)[\overline{\mathbf{b}}]_{d,f}v_f'' \\ &\leq \alpha_s(\tau)\left(-(\beta+1)|[\overline{\mathbf{b}}]_{d,f}v_f'| + \textstyle\sum_{\forall j\in\{f,..,n\}} \sum_{\forall i\in\{d+1,..,n\}} \alpha_s^{max}|[\overline{\mathbf{b}}]_{i,j}v_j'|\right) \end{aligned}$$

Note that, by chosing a large enough $\beta^* > 0$, the previous inequality can be made negative $\forall\tau > 0$. In that case, the vector $\mathbf{w} = (\mathbf{Q}^T)^{-1}\mathbf{w}'$ fulfills $\mathbf{w}^T\mathbf{e}^{\mathbf{A}\tau}\mathbf{b} = \mathbf{w}'^T\mathbf{e}^{\mathbf{J}\tau}\mathbf{b}' \leq \mathbf{0}$ $\forall\tau > 0$.

This reasoning can be generalized to several vectors $[\mathbf{b}^1,..,\mathbf{b}^q] = \mathbf{B}$. In this case, for each vector $\mathbf{b}^i$ it is possible to have a different dominant component v_{f_i}' and $\alpha_{d_i}(\tau)$ associated to a different Jordan

block j_i. In any case, for each $\mathbf{b}^i$ it is possible to define a vector $\mathbf{v}''^i$ as defined before (whose non-null components are those related to the block j_i), and add them to the premilinarily solution $\mathbf{v}'$, so $\mathbf{w}' = \mathbf{v}' + \sum_{\forall i \in 1,..,t} \beta_i^* \mathbf{v}''^i$. In order to show that there always exist proper values for β_i, let us assume, without loss of generality, that $j_1 > j_2 > ... > j_t$. In this way, a component $\beta_{i+1}^* \mathbf{v}''^{i+1}$ is s.t. $\boldsymbol{\alpha}(\tau) \cdot \overline{\mathbf{b}^i} \cdot \mathbf{v}''^{i+1} = \mathbf{0}$ (equivalently, $(\mathbf{v}''^{i+1})^T \mathbf{e}^{\mathbf{J}\tau} \mathbf{b}^{i\prime} = \mathbf{0}$), because the rows of $\overline{\mathbf{b}^i}$ related to blocks lower than j_i are null (remember that j_i is the dominant block, i.e., the first for which $\overline{\mathbf{b}^i}_{j_i} \cdot \mathbf{v}'_{j_i}$ is not null) while the vector $\mathbf{v}''^{i+1}$ is defined in such a way that its non-null components are related to some of those indexes ($j_{i+1} < j_i$). Therefore, by following a procedure of t steps, each β_i^* can be computed s.t. $\mathbf{w}' = \mathbf{v}' + \sum_{\forall p \in 1,..,i} \beta_p^* \mathbf{v}''^p$ fulfills $\mathbf{w}' \mathbf{e}^{\mathbf{J}\tau} \mathbf{b}'_i \leq \mathbf{0}\ \forall \tau > 0$, starting from $i = 1$ until $i = t$.

Finally, $\mathbf{v}^T \mathbf{G} \neq \mathbf{0}$ is equivalent to $\mathbf{v}'^T \mathbf{Q}^{-1} \mathbf{G} \neq \mathbf{0}$. In such case, by thinking in a t-steps procedure as above, $\forall i$ it is always possible to find $\beta_i \geq \beta_i^*$ s.t. $\mathbf{w}'^T \mathbf{Q}^{-1} \mathbf{G} = \mathbf{v}'^T \mathbf{Q}^{-1} \mathbf{G} + (\sum_{p \in \{1,..,i\}} \beta_p (\mathbf{v}''^p)^T) \cdot \mathbf{Q}^{-1} \mathbf{G} \neq \mathbf{0}$. Therefore, defining $\mathbf{w} = (\mathbf{Q}^T)^{-1} \mathbf{w}'$ it follows $\mathbf{w}^T \mathbf{G} \neq \mathbf{0}$ and $\mathbf{w}^T \mathbf{e}^{\mathbf{A}\tau} \mathbf{B} \leq \mathbf{0}\ \forall \tau$. ∎

C.3 Additional algorithms for coordinated control

The computation of $\mathbf{m}_f^B$, achieved during the control synthesis stage in Procedure 5.2 (Section 5.3), can be done by setting any $\mathbf{m}_f^B$ fulfilling two linear constraints (so it can be computed in polynomial time): i) $\mathbf{m}_f^B > \mathbf{1}\epsilon$, ii) $\mathbf{B}_y^T[B]\mathbf{m}_f^B = \mathbf{B}_y^T[B]\mathbf{m}_0^B + \sum \mathbf{B}_y^T[P^i](\mathbf{m}_0^i - \mathbf{m}_f^i)$. This equality constraint is equivalent to $\mathbf{B}_y^T \mathbf{m}_f = \mathbf{B}_y^T \mathbf{m}_0$, where $\mathbf{m}_f$ is the global final marking. In this way, $\mathbf{m}_f \in Class_\epsilon(\mathbf{m}_0)$. Thus, since the net is consistent, $\mathbf{m}_f$ is reachable.

On the other hand, the computation of $\eta_{x_j}^i$, η_w^i, η_d^i, η_T^i and ψ in Procedure 5.2 is equivalent to solve: maximum α s.t. $\mathbf{a}\alpha \leq \mathbf{b}$, with $\mathbf{a}, \mathbf{b} \geq \mathbf{0}$. For computing this, define the set of indices $S = \{i | [\mathbf{a}]_i > 0\}$. Next, if there exists a solution, this is given by $\alpha = min\{[\mathbf{b}]_i / [\mathbf{a}]_i | i \in S\}$.

The computation of $\mathbf{d}^i$ and $\boldsymbol{\gamma}$ in Procedure 5.2 is equivalent to the problem of solving $\mathbf{x} > \mathbf{0}$ s.t. $\mathbf{A}\mathbf{x} = \mathbf{b}$, assuming that there exists a solution and $\exists \mathbf{a} > \mathbf{0}$ s.t. $\mathbf{A}\mathbf{a} = \mathbf{0}$. For the computation of $\mathbf{d}^i$ and $\boldsymbol{\gamma}$, the matrices that are represented by $\mathbf{A}$ are fixed. On the contrary, the vectors represented by $\mathbf{b}$ *change* during the evolution of the system.

Algorithm C.3. Computation of $\mathbf{x} > \mathbf{0}$ s.t. $\mathbf{A}\mathbf{x} = \mathbf{b}$.

Computation off-line:

Compute permutation matrices $\mathbf{P}_1$ and $\mathbf{P}_2$ so

$$\mathbf{P}_1 \mathbf{A} \mathbf{P}_2 = \begin{bmatrix} \mathbf{A}_{11} & \mathbf{A}_{12} \\ \mathbf{A}_{21} & \mathbf{A}_{22} \end{bmatrix},$$

$\mathbf{A}_{11}$ is invertible and has the same rank, ρ, that $\mathbf{A}$.

Operation on-line:

I . **Define** $\mathbf{b}' = \mathbf{P}_1^{-1} \mathbf{b}$ and $\mathbf{b}'_1$ as the vector built with the first ρ elements of $\mathbf{b}'$.

II . **Compute** $\mathbf{x}^p = \mathbf{P}_2 \cdot [(\mathbf{A}_{11}^{-1}\mathbf{b}'_1)^T, \mathbf{0}^T]^T$.

III. **Take** any scalar $\alpha > |min(\mathbf{x}'./\mathbf{a})|$ (where the division of vectors is element-wise), **then** $\mathbf{x} = \mathbf{x}^p + \alpha\mathbf{a} > \mathbf{0}$ and it is a solution for $\mathbf{Ax} = \mathbf{b}$.

Proof. Since $\exists \mathbf{x}^p$ s.t. $\mathbf{Ax}^p = \mathbf{b}$, then $\exists \mathbf{x}' = \mathbf{P}_2^{-1}\mathbf{x}^p$ s.t. $\mathbf{P}_1\mathbf{AP}_2\mathbf{x}' = \mathbf{b}'$, where $\mathbf{b}' = \mathbf{P}_1\mathbf{b}$. On the other hand, the rows of $[\mathbf{A}_{21}, \mathbf{A}_{22}]$ are linear combinations of those of $[\mathbf{A}_{11}, \mathbf{A}_{12}]$. Combining these two facts, $\mathbf{x}'$ that fulfills $[\mathbf{A}_{11}, \mathbf{A}_{12}]\mathbf{x}' = \mathbf{b}'_1$ is also a solution for $\mathbf{P}_1\mathbf{AP}_2\mathbf{x}' = \mathbf{b}'$. Then, $\mathbf{x}' = [(\mathbf{A}_{11}^{-1}\mathbf{b}'_1)^T, \mathbf{0}^T]^T$ is a particular solution of $\mathbf{P}_1\mathbf{AP}_2\mathbf{x}' = \mathbf{b}'$, and so, $\mathbf{x}^p = \mathbf{P}_2\mathbf{x}'$ is a particular solution for $\mathbf{Ax}^p = \mathbf{b}$. Finally, given α s.t. $\alpha\mathbf{a} > |\mathbf{x}'|$ and $\mathbf{Aa} = \mathbf{0}$, then $\mathbf{x} = \mathbf{x}^p + \alpha\mathbf{a}$ is a positive solution for $\mathbf{Ax}^p = \mathbf{b}$. ∎

Note that $\mathbf{b}'$ and $\mathbf{x}^p$ are just evaluations, while for α it is only required to find the minimum element of a vector, so the complexity is linear in the number of elements of $\mathbf{x}$.